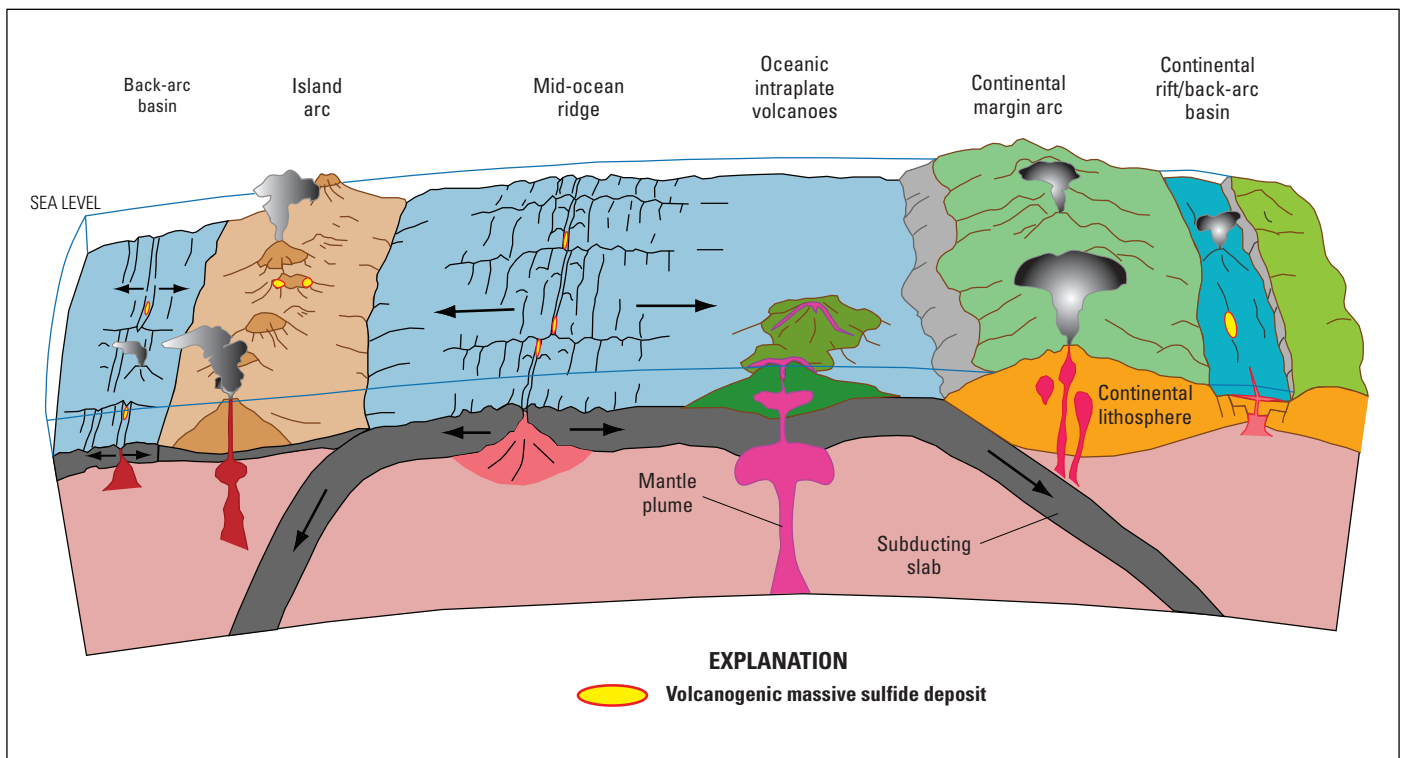


Volcanogenic Massive Sulfide Occurrence Model



Scientific Investigations Report 2010–5070–C

Volcanogenic Massive Sulfide Occurrence Model

Edited by W.C. Pat Shanks III and Roland Thurston

Scientific Investigations Report 2010–5070–C

U.S. Department of the Interior
U.S. Geological Survey

U.S. Department of the Interior
KEN SALAZAR, Secretary

U.S. Geological Survey
Marcia K. McNutt, Director

U.S. Geological Survey, Reston, Virginia: 2012

For more information on the USGS—the Federal source for science about the Earth, its natural and living resources, natural hazards, and the environment, visit <http://www.usgs.gov> or call 1-888-ASK-USGS.

For an overview of USGS information products, including maps, imagery, and publications, visit <http://www.usgs.gov/pubprod>

To order this and other USGS information products, visit <http://store.usgs.gov>

Any use of trade, product, or firm names is for descriptive purposes only and does not imply endorsement by the U.S. Government.

Although this report is in the public domain, permission must be secured from the individual copyright owners to reproduce any copyrighted materials contained within this report.

Suggested citation:

Shanks, W.C. Pat, III, and Thurston, Roland, eds., 2012, Volcanogenic massive sulfide occurrence model: U.S. Geological Survey Scientific Investigations Report 2010-5070-C, 345 p.

Contents

1. Introduction

| | |
|-----------------------|---|
| Overview..... | 5 |
| Scope | 5 |
| Purpose..... | 6 |
| References Cited..... | 7 |

2. Deposit Type and Associated Commodities

| | |
|--|----|
| Name and Synonyms..... | 15 |
| Brief Description | 15 |
| Associated Deposit Types | 15 |
| Primary and Byproduct Commodities..... | 16 |
| Example Deposits..... | 16 |
| References Cited..... | 19 |

3. Historical Evolution of Descriptive and Genetic Knowledge and Concepts

| | |
|--|----|
| Hydrothermal Activity and Massive Sulfide Deposit Formation on the Modern Seafloor | 27 |
| References Cited..... | 31 |

4. Regional Environment

| | |
|--|----|
| Geotectonic Environment..... | 37 |
| Mid-Ocean Ridges and Mature Back-Arc Basins (Mafic-Ultramafic Lithologic Association)..... | 37 |
| Sediment-Covered Ridges and Related Rifts (Siliciclastic-Mafic Lithologic Association)..... | 39 |
| Intraoceanic Volcanic Arcs and Related Back-Arc Rifts (Bimodal-Mafic Lithologic Association)..... | 41 |
| Continental Margin Arcs and Related Back-Arc Rifts (Bimodal-Felsic and Felsic- Siliciclastic Lithologic Associations) | 42 |
| Temporal (Secular) Relations..... | 43 |
| Duration of Magmatic-Hydrothermal System and Mineralizing Processes | 43 |
| Relations to Structures | 45 |
| Relations to Igneous Rocks..... | 49 |
| Flow Lithofacies Association | 50 |
| Volcaniclastic Lithofacies Association | 50 |
| Relations to Sedimentary Rocks | 52 |
| Relations to Metamorphic Rocks..... | 52 |
| References Cited..... | 53 |

5. Physical Volcanology of Volcanogenic Massive Sulfide Deposits

| | |
|---|----|
| Introduction..... | 65 |
| Role of Water in Submarine Volcanism..... | 68 |
| Classification System..... | 68 |
| Flow Lithofacies Associations | 69 |

| | |
|---|----|
| Mafic-Ultramafic Volcanic Suite (Primitive Intraoceanic Back-Arc or Fore-Arc Basins or Oceanic Ridges) | 72 |
| Pillow Lava Flows in Mafic-Ultramafic Associations | 72 |
| Bimodal-Mafic Volcanic Suite (Incipient-Rifted Intraoceanic Arcs) | 75 |
| Effusive Dominated Subaqueous Calderas in the Bimodal-Mafic Associations | 75 |
| Felsic Lobe-Hyaloclastite Flows in Bimodal-Mafic Associations | 77 |
| Other Silicic Flows and Domes in Bimodal-Mafic Associations | 80 |
| Bimodal-Felsic Type (Incipient-Rifted Continental Margin Arcs and Back Arcs)..... | 83 |
| Explosive Dominated Submarine Calderas in Bimodal-Felsic Associations | 83 |
| Volcaniclastic Lithofacies Associations | 85 |
| Sedimentary Lithofacies Associations | 85 |
| Siliciclastic-Felsic Volcanic Suite (Mature Epicontinental Margin Arcs and Back Arcs) | 87 |
| Siliciclastic-Mafic Volcanic Suite (Rifted Continental Margin, Intracontinental Rift, or Sedimented Oceanic Ridge) | 88 |
| Subvolcanic Intrusions | 91 |
| Summary and Conclusions..... | 94 |
| References Cited..... | 95 |

6. Physical Description of Deposit

| | |
|--|-----|
| Definition | 105 |
| Dimensions in Plan View | 105 |
| Size of Hydrothermal System Relative to Extent of Economically Mineralized Rock..... | 105 |
| Vertical Extent | 105 |
| Form/Shape..... | 106 |
| Host Rocks | 108 |
| References Cited..... | 108 |

7. Geophysical Characteristics of Volcanogenic Massive Sulfide Deposits

| | |
|-----------------------------|-----|
| Introduction..... | 117 |
| Electrical Signature | 117 |
| Magnetic Signature..... | 118 |
| Gravity Signature | 123 |
| Radiometric Signature | 125 |
| Seismic Techniques..... | 125 |
| Concealed Deposits..... | 127 |
| Conclusions..... | 129 |
| References Cited..... | 129 |

8. Hypogene Ore Characteristics

| | |
|-------------------------------|-----|
| Mineralogy | 137 |
| Mineral Assemblages | 137 |
| Paragenesis | 139 |
| Zoning Patterns..... | 139 |
| Textures and Structures | 139 |
| Grain Size | 143 |
| References Cited..... | 143 |

9. Hypogene Gangue Characteristics

| | |
|---------------------------|-----|
| Mineralogy | 151 |
| Mineral Assemblages | 151 |
| Paragenesis | 151 |
| Zoning Patterns | 151 |
| Grain Size | 152 |
| References Cited..... | 152 |

10. Exhalites

| | |
|---|-----|
| Geometry and Spatial Distribution | 159 |
| Mineralogy and Zoning | 160 |
| Protoliths | 161 |
| Geochemistry..... | 161 |
| References Cited..... | 161 |

11. Hydrothermal Alteration

| | |
|--|-----|
| Relations among Alteration, Gangue, and Ore | 169 |
| Mineralogy, Textures, and Rock Matrix Alteration..... | 170 |
| Mineral Assemblages and Zoning Patterns | 170 |
| Alteration in Modern Seafloor Volcanogenic Massive Sulfide Systems | 170 |
| Alteration Zoning in Ancient Volcanogenic Massive Sulfide Deposits | 173 |
| Lateral and Vertical Dimensions | 175 |
| Alteration Intensity | 175 |
| References Cited..... | 178 |

12. Supergene Ore and Gangue Characteristics

| | |
|--|-----|
| Mineralogy and Mineral Assemblages | 185 |
| Paragenesis and Zoning Patterns..... | 185 |
| Textures, Structures, and Grain Size | 187 |
| References Cited..... | 189 |

13. Weathering Processes

| | |
|--|-----|
| Mineralogic Reactions to Establish Process | 195 |
| Geochemical Processes..... | 196 |
| Factors Controlling Rates of Reaction..... | 198 |
| Effects of Microclimate and Macroclimate | 199 |
| Effects of Hydrologic Setting | 199 |
| References Cited..... | 200 |

14. Geochemical Characteristics

| | |
|--|-----|
| Trace Elements and Element Associations | 207 |
| Zoning Patterns | 207 |
| Fluid-Inclusion Thermometry and Geochemistry | 211 |
| Stable Isotope Geochemistry | 215 |
| $\delta^{18}\text{O}$ and δD | 215 |

| | |
|---|-----|
| $\delta^{34}\text{S}$ | 216 |
| $\delta^{11}\text{B}$, $\delta^{64}\text{Cu}$, $\delta^{66}\text{Zn}$, $\delta^{57}\text{Fe}$, $\delta^{82}\text{Se}$ | 216 |
| Radiogenic Isotope Geochemistry..... | 220 |
| References Cited..... | 222 |

15. Petrology of Associated Igneous Rocks

| | |
|---|-----|
| Importance of Igneous Rocks to Deposit Genesis..... | 231 |
| Rock Names..... | 231 |
| Rock Associations | 231 |
| Mafic-Ultramafic Association | 231 |
| Siliciclastic-Mafic Association | 232 |
| Bimodal-Mafic Association | 232 |
| Bimodal-Felsic Association..... | 233 |
| Siliciclastic-Felsic Association | 234 |
| Mineralogy..... | 234 |
| Textures and Structures | 234 |
| Petrochemistry | 235 |
| Major-Element Geochemistry..... | 235 |
| Trace-Element Geochemistry | 235 |
| Isotope Geochemistry..... | 242 |
| Radiogenic Isotopes..... | 242 |
| MORB, OIB, BABB, IAB, and Related Volcanics | 242 |
| Strontium, Neodymium, Lead..... | 242 |
| Traditional Stable Isotopes..... | 243 |
| Deuterium/Hydrogen | 243 |
| $^{18}\text{O}/^{16}\text{O}$ | 246 |
| $\delta^{34}\text{S}$ | 252 |
| Depth of Emplacement..... | 252 |
| References Cited..... | 256 |

16. Petrology of Sedimentary Rocks Associated with Volcanogenic Massive Sulfide Deposits

| | |
|---|-----|
| Importance of Sedimentary Rocks to Deposit Genesis..... | 267 |
| Rock Names..... | 268 |
| Mineralogy..... | 269 |
| Textures | 269 |
| Grain Size | 269 |
| Environment of Deposition | 269 |
| References Cited..... | 271 |

17. Petrology of Metamorphic Rocks Associated with Volcanogenic Massive Sulfide Deposits

| | |
|--|-----|
| Importance of Metamorphic Rocks to Deposit Genesis | 279 |
| Rock Names..... | 281 |
| Mineralogy and Mineral Assemblages..... | 281 |
| Deformation and Textures | 284 |

| | |
|---|-----|
| Grain Size | 284 |
| Examples of Information Gained from Study of Metamorphic Rocks Associated with Volcanogenic Massive Sulfide Deposits | 285 |
| References Cited..... | 285 |
| 18. Theory of Deposit Formation | |
| Ore Deposit Types..... | 293 |
| Sources of Metals and Other Ore Components..... | 293 |
| Sources of Ligands Involved in Ore Component Transport | 294 |
| Sources of Fluids Involved in Ore Component Transport..... | 295 |
| Chemical Transport and Transfer Processes | 295 |
| Fluid Drive Including Thermal, Pressure, and Geodynamic Mechanisms | 296 |
| Character of Conduits/Pathways that Focus Ore-Forming Fluids | 298 |
| Nature of Traps and Wallrock Interaction that Trigger Ore Precipitation..... | 298 |
| Structure and Composition of Residual Fluid Outflow Zones | 298 |
| References Cited..... | 298 |
| 19. Exploration-Resource Assessment Guides | |
| Geological | 309 |
| Geochemical..... | 309 |
| Isotopic | 311 |
| Geophysical | 311 |
| Attributes Required for Inclusion in Permissive Tracts at Various Scales | 312 |
| Factors Influencing Undiscovered Deposit Estimates (Deposit Size and Density) | 312 |
| References Cited..... | 313 |
| 20. Geoenvironmental Features | |
| Weathering Processes | 323 |
| Sulfide Oxidation, Acid Generation, and Acid Neutralization Processes | 323 |
| Metal Cycling Associated with Efflorescent Sulfate Salts | 324 |
| Secondary Precipitation of Hydroxides and Hydroxysulfates | 324 |
| Pre-Mining Baseline Signatures in Soil, Sediment, and Water | 324 |
| Past and Future Mining Methods and Ore Treatment | 325 |
| Volume of Mine Waste and Tailings | 327 |
| Mine Waste Characteristics | 327 |
| Mineralogy | 327 |
| Acid-Base Accounting..... | 328 |
| Element Mobility Related to Mining in Groundwater and Surface Water..... | 330 |
| Pit Lakes | 334 |
| Ecosystem Issues | 335 |
| Human Health Issues | 335 |
| Climate Effects on Geoenvironmental Signatures | 335 |
| References Cited..... | 336 |
| 21. Knowledge Gaps and Future Research Directions | |
| Supergiant Deposit Formation Processes | 345 |

| | |
|--|-----|
| Mapping at Regional and Quadrangle Scales | 345 |
| New Modeling of Fluid Flow and Mineralization | 345 |
| Causes of Temporal and Spatial Localization and Preservation of Deposits | 345 |
| New Methods of Prospection for Concealed Deposits..... | 345 |

Figures

| | |
|---|----|
| 2-1. Grade and tonnage of volcanogenic massive sulfide deposits..... | 16 |
| 2-2. Map showing locations of significant volcanogenic massive sulfide deposits in the United States..... | 17 |
| 3-1. Map of seafloor tectonic boundaries, metalliferous sediment distribution, locations of seafloor hydrothermal vents and deposits, and distribution of U.S. Exclusive Economic Zones | 28 |
| 3-2. Representative examples of large seafloor massive sulfide deposits | 30 |
| 4-1. Schematic diagram showing volcanogenic massive sulfide deposits in divergent and convergent plate tectonic settings | 38 |
| 4-2. Schematic diagram showing proposed hydrothermal fluid flow at a fast-spreading ridge..... | 38 |
| 4-3. Structural map of the Gulf of California showing the extent of newly accreted oceanic crust in extensional basins along an extension of the East Pacific Rise..... | 40 |
| 4-4. Histograms showing number of volcanogenic massive sulfide deposits and contained metal of Cu+Zn+Pb in million tonnes..... | 44 |
| 4-5. Schematic diagram showing examples of the different structural settings of hydrothermal vents relative to faults and breakdown regions..... | 46 |
| 4-6. Model for fluid circulation and types of hydrothermal venting related to the development of detachment faults along slow-spreading mid-ocean ridges..... | 47 |
| 4-7. Conceptual diagram showing the evolution of a caldera-related submarine magmatic-hydrothermal system | 48 |
| 4-8. Composite stratigraphic sections illustrating flow, volcanoclastic, and sediment dominated lithofacies that host volcanogenic massive sulfide deposits..... | 51 |
| 5-1. Graphic representations of the lithological classification used in this study | 66 |
| 5-2. Genetic classification of volcanic deposits erupted in water and air | 67 |
| 5-3. Physical conditions for volcanic eruptions..... | 70 |
| 5-4. Diagrams showing different types of genetically related and nonrelated volcanic rocks and processes..... | 71 |
| 5-5. Tectonics and stratigraphy of mafic-ultramafic volcanogenic massive sulfide deposits | 73 |
| 5-6. Series of figures highlighting environment and features of pillow lavas..... | 74 |
| 5-7. Composite stratigraphic sections for various areas hosting volcanogenic massive sulfide mineralization in the bimodal mafic suite | 76 |
| 5-8. Paleogeographic reconstruction of the evolution of the Normetal caldera from a subaqueous shield volcano to a piston-type caldera | 78 |
| 5-9. Features associated with bimodal mafic association, specifically the felsic lobe hyaloclastite facies..... | 79 |
| 5-10. Volcanic domes common in a siliciclastic felsic suite | 81 |
| 5-11. Schematic evolution of the Bald Mountain sequence | 82 |

| | | |
|-------|--|-----|
| 5-12. | Products of explosive dominated submarine calderas in bimodal-felsic volcanic suite..... | 86 |
| 5-13. | Schematic cross section of the Rio Tinto mine, Iberian Pyrite Belt deposit, showing location of the volcanogenic massive sulfide deposit and sediment-sill complexes..... | 88 |
| 5-14. | Composite stratigraphic sections for various areas hosting volcanogenic massive sulfide mineralization in the siliciclastic felsic association | 89 |
| 5-15. | Generalized stratigraphic sections for volcanogenic massive sulfide mineralization in a siliciclastic mafic suite..... | 90 |
| 5-16. | Physical parameters and controls on volcanism..... | 92 |
| 5-17. | Schematic of a volcanic section hosting volcanogenic massive sulfide showing relative positions of subvolcanic intrusions..... | 93 |
| 5-18. | Geologic map of the Archean Noranda camp showing the volcanogenic massive sulfide deposits underlain by the Flavrian-Powell subvolcanic intrusive complex | 94 |
| 6-1. | Different forms and styles of volcanogenic massive sulfide deposits | 107 |
| 7-1. | Schematic diagram of the modern Trans-Atlantic Geothermal sulfide deposit on the Mid-Atlantic Ridge, depicting a cross section of a volcanogenic massive sulfide deposit with concordant semi-massive to massive sulfide lens underlain by a discordant stockwork vein system and associated alteration halo | 118 |
| 7-2. | Selected airborne geophysical surveys for Bathurst mining camp..... | 122 |
| 7-3. | Gravity model showing that an excess mass in the crust contributes to the gravity field and produces a positive anomaly or gravity high..... | 123 |
| 7-4. | Geological and geophysical maps of the area containing the Armstrong B massive sulfide deposit, Bathurst mining camp, New Brunswick, with geophysical profiles across the deposit..... | 124 |
| 7-5. | Schematic diagram showing airborne and ground radiometric surveys..... | 126 |
| 7-6. | Velocity values of various rock types and ore minerals plotted against their density with lines of constant acoustic impedance overlain within field..... | 127 |
| 7-7. | Seismic reflection profiles through volcanogenic massive sulfide deposits | 128 |
| 8-1. | Examples of paragenetic sequences in volcanogenic massive sulfide deposits | 140 |
| 8-2. | Idealized massive sulfide lens illustrating zonation features for hypogene ore minerals..... | 141 |
| 8-3. | Comparative hypogene mineral zonation | 142 |
| 10-1. | Simplified cross sections of volcanogenic massive sulfide deposits showing different types and morphologies of exhalites | 160 |
| 11-1. | Representative cross sections of alteration related to hydrothermal activity or fossil hydrothermal activity on the modern seafloor | 172 |
| 11-2. | Representative examples of alteration zoning in volcanogenic massive sulfide deposits | 174 |
| 11-3. | Fluid flow modeling showing water/rock ratios during hydrothermal circulation | 176 |
| 11-4. | Geochemical techniques for quantifying hydrothermal alteration effects..... | 177 |
| 12-1. | Sequence of supergene mineralization summarized from volcanogenic massive sulfide deposits in the Bathurst mining camp..... | 188 |
| 14-1. | Idealized cross sections through the two main stages of growth of a massive sulfide chimney | 209 |

| | | |
|-------|--|-----|
| 14-2. | Idealized cross section through the Trans-Atlantic Geothermal hydrothermal field based on Alvin dive observations and Ocean Drilling Program drilling during Leg 158 | 210 |
| 15-1. | Schematic diagram showing the principal components and processes involved in the production of island-arc and back-arc volcanics that are major lithostratigraphic units associated with volcanogenic massive sulfide deposits | 233 |
| 15-2. | Two classifications of common igneous rocks..... | 237 |
| 15-3. | The use of trace-element abundances and trace-element ratios as proxies for the subduction input to the overlying mantle preserved in the mantle partial melts that form island-arc and back-arc volcanics | 241 |
| 15-4. | Trace-element patterns for several types of volcanics from modern tectonic environments that are commonly associated with volcanogenic massive sulfide deposits | 242 |
| 15-5. | Frequency distributions of copper in various modern volcanics. | 243 |
| 15-6. | Relationships between strontium, neodymium, and lead isotopes in a variety of mid-ocean ridge basalts and oceanic island basalts | 244 |
| 15-7. | Strontium, neodymium, and lead isotopic variability in island-arc basalt volcanics and back-arc basin basalt volcanics | 245 |
| 15-8. | Hydrogen and oxygen isotopic composition of various types of terrestrial waters | 246 |
| 15-9. | Oxygen isotopic composition of various lithologic units relative to mid-ocean ridge basalt | 251 |
| 17-1. | Pressure/temperature diagram showing the principal eight metamorphic facies; the Al_2SiO_5 polymorphs kyanite, andalusite, and sillimanite and the three major types of pressure/temperature facies series..... | 281 |
| 18-1. | Reaction progress diagram showing mineral stabilities and amounts formed as 350 °C East Pacific Rise hot spring water mixes progressively with cold (2 °C) bottom seawater | 296 |
| 18-2. | Schematic cross section of typical mid-ocean ridge crustal architecture..... | 297 |
| 20-1. | Geochemical data for waters associated with unmined massive sulfide deposits..... | 326 |
| 20-2. | Geochemical data for major constituents in mine drainage associated with massive sulfide deposits | 332 |
| 20-3. | Geochemical data for minor constituents in mine drainage associated with massive sulfide deposits. | 333 |
| 20-4. | Geochemical data for dissolved metals in drainage associated with massive sulfide deposits | 334 |

Tables

| | | |
|------|---|-----|
| 1-1. | Classification systems for volcanogenic massive sulfide deposits..... | 6 |
| 2-1. | Examples of deposit types with lithologic associations, inferred tectonic settings, and possible modern seafloor analogs..... | 18 |
| 5-1. | Comparison of some important properties of water versus air and their effects on eruptions | 68 |
| 5-2. | Comparison of some important environmental factors for subaqueous and subaerial eruptions..... | 69 |
| 7-1. | Utility of geophysical techniques in exploration of volcanogenic massive sulfide deposits | 119 |

| | | |
|-------|--|-----|
| 7-2. | Physical properties of common rock ore minerals and ore-related minerals | 120 |
| 7-3. | Massive sulfide ore mineral density and magnetic susceptibility. | 123 |
| 8-1. | Hypogene ore mineralogy of ancient volcanogenic massive sulfide deposits..... | 138 |
| 8-2. | Examples of hypogene mineral zonation patterns in selected volcanogenic massive sulfide deposits | 141 |
| 11-1. | Diagnostic minerals in hydrothermally altered volcanogenic massive sulfide deposits at different metamorphic grades | 171 |
| 12-1. | Mineral assemblages of supergene environments in selected volcanogenic massive sulfide deposits. | 186 |
| 12-2. | Mineralogy of supergene sulfide zones and gossans..... | 187 |
| 14-1. | Modern and ancient volcanogenic massive sulfide deposits with high sulfidation state minerals | 208 |
| 14-2. | Fluid inclusion thermometry and chemical compositions for selected volcanogenic massive sulfide deposits | 212 |
| 14-3. | Some transitional metal isotope ratios in volcanogenic massive sulfide deposits and related rocks..... | 218 |
| 14-4. | Lead isotopic composition of selected volcanogenic massive sulfide deposits..... | 221 |
| 15-1. | Major and trace element composition of major minerals observed in igneous rocks associated with modern seafloor massive sulfides in a variety of settings | 235 |
| 15-2. | Common textures observed in pristine igneous rocks associated with modern seafloor massive sulfides | 236 |
| 15-3. | Average major element composition of basaltic rocks associated with volcanogenic massive sulfide deposits | 238 |
| 15-4. | Major element compositions of various volcanic rock series associated with volcanogenic massive sulfide deposits | 239 |
| 15-5. | Hydrogen isotope compositions of ore and alteration fluids, whole rocks, and minerals for selected volcanogenic massive sulfide deposits | 247 |
| 15-6. | Selected oxygen isotope studies of volcanic rocks hosting volcanogenic massive sulfide deposits | 253 |
| 15-7. | Whole rock $\delta^{18}\text{O}$ values for lithostratigraphic units associated with volcanogenic massive sulfide deposits | 254 |
| 17-1. | Characteristic minerals for principal rock composition types in the various metamorphic facies..... | 280 |
| 17-2. | Diagnostic mineralogy and major-element geochemistry of greenschist- and granulite-grade metamorphosed alteration products associated with volcanogenic massive sulfide deposits | 282 |
| 20-1. | Selected common mineralogical characteristics of volcanogenic massive sulfide deposits with a comparison to sedimentary-exhalative deposits..... | 329 |
| 20-2. | Environmental guidelines relevant to mineral deposits | 331 |

Abbreviations Used in This Report

Units of Measure

| | | | |
|----------------|----------------------------------|-----|----------------|
| °C | degree Celcius | W | watt |
| μg | microgram | wt% | weight percent |
| b.y. | billion years (interval of time) | yr | year |
| Bt | billion metric tons | | |
| cm | centimeter | | |
| E _n | oxidation/reduction potential | | |
| g | gram | | |
| Ga | giga-annum (age) | | |
| Hz | hertz | | |
| J | joule | | |
| K | kelvin | | |
| ka | kilo-annum (age) | | |
| kg | kilogram | | |
| km | kilometer | | |
| L | liter | | |
| m | meter | | |
| m.y. | million years (interval of time) | | |
| Ma | mega-annum (age) | | |
| mbsf | meters below sea floor | | |
| mg | milligram | | |
| mGal | milligal | | |
| mM | millimolar | | |
| mmol | millimole | | |
| MPa | megapascal | | |
| mPa | millipascal | | |
| mS | millisiemen | | |
| Mt | million metric tons | | |
| nT | nanotesla | | |
| Pa | pascal | | |
| ppm | parts per million | | |
| s | second | | |
| t | ton | | |
| T, temp. | temperature | | |
| vol% | volume percent | | |

Elements

| | | | |
|----|-----------|----|-----------|
| Ag | silver | Si | silicon |
| Al | aluminum | Sn | tin |
| As | arsenic | Sr | strontium |
| Au | gold | Ta | tantalum |
| B | boron | Te | tellurium |
| Ba | barium | Th | thorium |
| Be | beryllium | Ti | titanium |
| Bi | bismuth | Tl | thallium |
| Br | bromine | U | uranium |
| C | carbon | V | vanadium |
| Ca | calcium | W | tungsten |
| Cd | cadmium | Y | yttrium |

| | | | |
|----|------------|----|-----------|
| Ce | cerium | Yb | ytterbium |
| Cl | chlorine | Zn | zinc |
| Co | cobalt | Zr | zirconium |
| Cr | chromium | | |
| Cs | cesium | | |
| Cu | copper | | |
| Eu | europium | | |
| F | fluorine | | |
| Fe | iron | | |
| Ga | gallium | | |
| Gd | gadolinium | | |
| Ge | germanium | | |
| H | hydrogen | | |
| He | helium | | |
| Hf | hafnium | | |
| Hg | mercury | | |
| In | indium | | |
| K | potassium | | |
| La | lanthanum | | |
| Li | lithium | | |
| Lu | lutetium | | |
| Mg | magnesium | | |
| Mn | manganese | | |
| Mo | molybdenum | | |
| N | nitrogen | | |
| Na | sodium | | |
| Nb | niobium | | |
| Nd | neodymium | | |
| Ni | nickel | | |
| O | oxygen | | |
| Os | osmium | | |
| P | phosphorus | | |
| Pb | lead | | |
| Rb | rubidium | | |
| Re | rhenium | | |
| S | sulfur | | |
| Sb | antimony | | |
| Sc | scandium | | |
| Se | selenium | | |
| Si | silicon | | |
| Sn | tin | | |
| Sr | strontium | | |
| Ta | tantalum | | |
| Te | tellurium | | |
| Th | thorium | | |
| Ti | titanium | | |
| Tl | thallium | | |
| U | uranium | | |

1. Introduction

By W.C. Pat Shanks III and Randolph A. Koski

1 of 21

Volcanogenic Massive Sulfide Occurrence Model

Scientific Investigations Report 2010–5070–C

U.S. Department of the Interior
U.S. Geological Survey

U.S. Department of the Interior
KEN SALAZAR, Secretary

U.S. Geological Survey
Marcia K. McNutt, Director

U.S. Geological Survey, Reston, Virginia: 2012

For more information on the USGS—the Federal source for science about the Earth, its natural and living resources, natural hazards, and the environment, visit <http://www.usgs.gov> or call 1-888-ASK-USGS.

For an overview of USGS information products, including maps, imagery, and publications, visit <http://www.usgs.gov/pubprod>

To order this and other USGS information products, visit <http://store.usgs.gov>

Any use of trade, product, or firm names is for descriptive purposes only and does not imply endorsement by the U.S. Government.

Although this report is in the public domain, permission must be secured from the individual copyright owners to reproduce any copyrighted materials contained within this report.

Suggested citation:

Shanks III, W.C. Pat, and Koski, R.A., 2012, Introduction in volcanogenic massive sulfide occurrence model: U.S. Geological Survey Scientific Investigations Report 2010-5070 -C, chap. 1, 4 p.

Contents

| | |
|-----------------------|---|
| Overview..... | 5 |
| Scope | 5 |
| Purpose..... | 6 |
| References Cited..... | 7 |

Table

| | |
|--|---|
| 1-1. Classification systems for volcanogenic massive sulfide deposits..... | 6 |
|--|---|

1. Introduction

By W.C. Pat Shanks III and Randolph A. Koski

Overview

Volcanogenic massive sulfide (VMS) deposits, also known as volcanic-hosted massive sulfide, volcanic-associated massive sulfide, or seafloor massive sulfide deposits, are important sources of copper, zinc, lead, gold, and silver (Cu, Zn, Pb, Au, and Ag). These deposits form at or near the seafloor where circulating hydrothermal fluids driven by magmatic heat are quenched through mixing with bottom waters or porewaters in near-seafloor lithologies. Massive sulfide lenses vary widely in shape and size and may be podlike or sheet-like. They are generally stratiform and may occur as multiple lenses.

Volcanogenic massive sulfide deposits range in size from small pods of less than a ton (which are commonly scattered through prospective terrains) to supergiant accumulations like Rio Tinto (Spain), 1.5 Bt (billion metric tons); Kholodrina (Russia), 300 Mt (million metric tons); Windy Craggy (Canada), 300 Mt; Brunswick No. 12 (Canada), 230 Mt; and Ducktown (United States), 163 Mt (Galley and others, 2007). Volcanogenic massive sulfide deposits range in age from 3.55 Ga (billion years) to zero-age deposits that are actively forming in extensional settings on the seafloor, especially mid-ocean ridges, island arcs, and back-arc spreading basins (Shanks, 2001; Hannington and others, 2005). The widespread recognition of modern seafloor VMS deposits and associated hydrothermal vent fluids and vent fauna has been one of the most astonishing discoveries in the last 50 years, and seafloor exploration and scientific studies have contributed much to our understanding of ore-forming processes and the tectonic framework for VMS deposits in the marine environment.

Massive ore in VMS deposits consists of >40 percent sulfides, usually pyrite, pyrrhotite, chalcopyrite, sphalerite, and galena; non-sulfide gangue typically consists of quartz, barite, anhydrite, iron (Fe) oxides, chlorite, sericite, talc, and their metamorphosed equivalents. Ore composition may be Pb-Zn-, Cu-Zn-, or Pb-Cu-Zn-dominated, and some deposits are zoned vertically and laterally.

Many deposits have stringer or feeder zones beneath the massive zone that consist of crosscutting veins and veinlets of sulfides in a matrix of pervasively altered host rock and gangue. Alteration zonation in the host rocks surrounding the deposits are usually well-developed and include advanced

argillic (kaolinite, alunite), argillic (illite, sericite), sericitic (sericite, quartz), chloritic (chlorite, quartz), and propylitic (carbonate, epidote, chlorite) types (Bonnet and Corriveau, 2007).

An unusual feature of VMS deposits is the common association of stratiform “exhalative” deposits precipitated from hydrothermal fluids emanating into bottom waters. These deposits may extend well beyond the margins of massive sulfide and are typically composed of silica, iron, and manganese oxides, carbonates, sulfates, sulfides, and tourmaline.

Scope

This VMS deposit model is designed to supercede previous models developed for the purpose of U.S. Geological Survey (USGS) mineral resource assessments (Cox, 1986; Cox and Singer, 1986; Singer, 1986a, 1986b; Taylor and others, 1995). Because VMS deposits exhibit a broad range of geological and geochemical characteristics, a suitable classification system is required to incorporate these variations into the mineral deposit model. Cox and Singer (1986) grouped VMS deposits into (1) a Cyprus subtype associated with marine mafic volcanic rocks, (2) a Besshi subtype associated with clastic terrigenous sediment and marine mafic volcanic rocks, and (3) a Kuroko subtype associated with marine felsic to intermediate volcanic rocks (table 1–1). This terminology was developed earlier by Sawkins (1976) on the basis of probable tectonic settings for each deposit type. Volcanogenic massive sulfide deposits have also been classified according to base metal (Cu-Zn-Pb) ratios (Hutchinson, 1973; Franklin and others, 1981) and ratios of precious metals (Au-Ag) to base metals (Poulsen and Hannington, 1995) in massive sulfides.

More recent attempts to classify VMS deposit types have emphasized compositional variations in associated volcanic and sedimentary host rocks (Barrie and Hannington, 1999; Franklin and others, 2005; Galley and others, 2007). The advantage of these classification schemes is a closer link between tectonic setting and lithostratigraphic assemblages and an increased predictive capability during field-based studies. The lithology-based typology of Galley and others (2007) is shown in table 1–1 with approximate equivalencies to the categories of Cox and Singer (1986). The lithologic groups correlate with tectonic settings as follows: (1) mafic

Table 1–1. Classification systems for volcanogenic massive sulfide deposits.

| Cox and Singer (1986) | Galley and others (2007) | Mosier and others (2009) | This report |
|--------------------------|-----------------------------|-----------------------------|----------------------|
| Kuroko | Felsic-siliciclastic | Felsic | Siliciclastic-felsic |
| | Bimodal-felsic ¹ | | Bimodal-felsic |
| | Bimodal-mafic | Bimodal-mafic | Bimodal-mafic |
| Besshi | Pelitic-mafic | Mafic | Siliciclastic-mafic |
| Cyprus | Back-arc mafic | | Mafic-ultramafic |

¹ Includes hybrid bimodal-felsic group of Galley and others (2007).

rocks with mid-ocean ridges or mature intraoceanic back arcs; (2) pelitic-mafic rocks with sediment-covered back arcs; (3) bimodal-mafic rocks with rifted intraoceanic volcanic arcs; (4) bimodal-felsic rocks with continental margin arcs and back arcs; and (5) felsic-siliciclastic rocks with mature epicontinental back arcs. A sixth group listed by Galley and others (2007), hybrid bimodal-felsic, is treated here as part of the bimodal-felsic group.

In developing grade and tonnage models for 1,090 VMS deposits, Mosier and others (2009) found no significant differences between grade and tonnage curves for deposits hosted by pelite-mafic and back-arc-mafic rocks and for deposits hosted by felsic-siliciclastic and bimodal-felsic rocks, resulting in their threefold classification of mafic, bimodal-mafic, and felsic subtypes (table 1–1). For the mineral deposit model described in this report, however, the compositional variations in sequences of volcanic rocks and the occurrence of sedimentary rocks in stratigraphic sequences containing VMS deposits are important variables in the identification of geologic and tectonic settings. Furthermore, bimodal volcanic assemblages and presence of sedimentary deposits are discernible map features useful in the assessment of mineral resources. Therefore, we have adopted a fivefold classification slightly modified from Galley and others (2007) for use throughout this report (table 1–1). We prefer the term “siliciclastic-felsic” to “felsic-siliciclastic” because of the abundance of volcanoclastic and epiclastic sediment relative to felsic volcanic rocks in this group of deposits (for example, Iberian Pyrite Belt; Carvalho and others, 1999). This usage is consistent with Franklin and others (2005). The term “siliciclastic-mafic” is used because it encompasses the broader range of noncarbonate sedimentary rocks such as graywackes, siltstones, and argillites associated with this type of VMS deposit (Slack, 1993). Finally, the modified term “mafic-ultramafic” includes both back-arc and mid-ocean ridge environments and acknowledges recently discovered massive sulfide deposits along the Mid-Atlantic Ridge, in which serpentized peridotites are present in the footwall (for example, Rainbow vent field; Marques and others, 2007).

Purpose

The main purpose of this model is to provide the basis for the VMS component of the next National Assessment of undiscovered mineral resources in the United States. The three-part quantitative assessment strategy employed by the USGS (Singer, 1995, 2007; Cunningham and others, 2008) includes (1) delineation of permissive tracts for VMS deposits, (2) selection of grade-tonnage models appropriate for evaluating each tract, and (3) estimation of the number of undiscovered deposits in each tract. Hence, accurate and reliable data on VMS deposits, especially host lithology, tectonic setting, structure, ore-gangue-alteration mineralogy, geochemical and geophysical signatures, theory of deposit formation, and geoenvironmental features, are critical to the assessment methodology.

We believe that geologic information and quantitative data presented in this report are sufficient to identify permissive tracts for VMS deposits and to guide experts in estimating the number of undiscovered deposits in the permissive tracts. In addition, we have tried to provide comprehensive information to aid in assigning deposits from a tract to a specific deposit model type (siliciclastic-felsic, bimodal-felsic, bimodal-mafic, siliciclastic-mafic, and mafic-ultramafic) so that the correct grade-tonnage curve(s) can be used in assessing undiscovered deposits.

Beyond its importance in the National assessment, we believe that an updated VMS deposit model will be useful to exploration geologists, students and teachers of economic geology, and researchers interested in understanding the origin of this important deposit type in the context of earth history and plate tectonics. Among the latter group is a large international group of scientists studying the distribution, characteristics, and origin of VMS deposits on the modern seafloor.

References Cited

- Barrie, C.T., and Hannington, M.D., 1999, Classification of volcanic-associated massive sulfide deposits based on host-rock composition, *in* Barrie, C.T., and Hannington, M.D., eds., *Volcanic-associated massive sulfide deposits—Processes and examples in modern and ancient settings: Reviews in Economic Geology*, v. 8, p. 1–11.
- Bonnet, A.-L., and Corriveau, L., 2007, Alteration vectors to metamorphosed hydrothermal systems in gneissic terranes, *in* Goodfellow, W.D., ed., *Mineral deposits of Canada—A synthesis of major deposit-types, district metallogeny, the evolution of geological provinces, and exploration methods: Geological Association of Canada, Mineral Deposits Division, Special Publication No. 5*, p. 1035–1049.
- Carvalho, D., Barriga, F.J.A.S., and Munha, J., 1999, Bimodal-siliciclastic systems—The case of the Iberian Pyrite Belt, *in* Barrie, C.T., and Hannington, M.D., eds., *Volcanic-associated massive sulfide deposits—Processes and examples in modern and ancient settings: Reviews in Economic Geology*, v. 8, p. 375–408.
- Cox, D.P., 1986, Descriptive model of Besshi massive sulfide, *in* Cox, D.P., and Singer, D.A., eds., *Mineral deposit models: U.S. Geological Survey Bulletin 1693*, p. 136–138.
- Cox, D.P., and Singer, D.A., 1986, Mineral deposit models: U.S. Geological Survey Bulletin 1693, 379 p.
- Cunningham, C.G., Zappettini, E.O., Waldo, V.S., Celada, C.M., Quispe, J., Singer, D.A., Briskey, J.A., Sutphin, D.M., Gajardo M., M., Diaz, A., Portigliati, C., Berger, V.I., Carrasco, R., and Schulz, K.J., 2008, Quantitative mineral resource assessment of copper, molybdenum, gold, and silver in undiscovered porphyry copper deposits in the Andes Mountains of South America: U.S. Geological Survey Open-File Report 2008–1253, 282 p.
- Franklin, J.M., Gibson, H.L., Jonasson, I.R., and Galley, A.G., 2005, Volcanogenic massive sulfide deposits, *in* Hedenquist, J.W., Thompson, J.F.H., Goldfarb, R.J., and Richards, J.P., eds., *Economic Geology 100th anniversary volume, 1905–2005: Littleton, Colo., Society of Economic Geologists*, p. 523–560.
- Franklin, J.M., Lydon, J.M., and Sangster, D.F., 1981, Volcanic-associated massive sulfide deposits, *in* Skinner, B.J., ed., *Economic Geology 75th anniversary volume, 1905–1980: Littleton, Colorado, The Economic Geology Publishing Company*, p. 485–627.
- Galley, A.G., Hannington, M., and Jonasson, I., 2007, Volcanogenic massive sulphide deposits, *in* Goodfellow, W.D., ed., *Mineral deposits of Canada—A synthesis of major deposit-types, district metallogeny, the evolution of geological provinces, and exploration methods: Geological Association of Canada, Mineral Deposits Division, Special Publication 5*, p. 141–161.
- Hannington, M.D., de Ronde, C.E.J., and Petersen, S., 2005, Sea-floor tectonics and submarine hydrothermal systems, *in* Hedenquist, J.W., Thompson, J.F.H., Goldfarb, R.J., and Richards, J.P., eds., *Economic Geology 100th anniversary volume 1905–2005: Littleton, Colorado, Society of Economic Geologists*, p. 111–141.
- Hutchinson, R.W., 1973, Volcanogenic sulfide deposits and their metallogenic significance: *Economic Geology*, v. 68, p. 1223–1246.
- Marques, A.F.A., Barriga, F.J.A.S., and Scott, S.D., 2007, Sulfide mineralization in an ultramafic-rock hosted seafloor hydrothermal system—From serpentinization to the formation of Cu-Zn-(Co)-rich massive sulfides: *Marine Geology*, v. 245, p. 20–39.
- Mosier, D.L., Berger, V.I., and Singer, D.A., 2009, Volcanogenic massive sulfide deposits of the world—Database and grade and tonnage models: U.S. Geological Survey Open-File Report 2009–1034, 50 p.
- Poulsen, H., and Hannington, M., 1995, Auriferous volcanogenic sulfide deposits, *in* Eckstrand, O.R., Sinclair, W.D., and Thorpe, R.I., eds., *Geology of Canadian mineral deposit types: Geological Survey of Canada, Geology of Canada no. 8; Geological Society of America, Decade of North American Geology v. P1*, p. 183–196.
- Sawkins, F.J., 1976, Massive sulphide deposits in relation to geotectonics, *in* Strong, D.F., ed., *Metallogeny and plate tectonics: Geological Association of Canada, Special Paper 14*, p. 221–240.
- Shanks, W.C., III, 2001, Stable isotopes in seafloor hydrothermal systems—Vent fluids, hydrothermal deposits, hydrothermal alteration, and microbial processes, *in* Valley, J.W., and Cole, D.R., eds., *Stable isotope geochemistry: Reviews in Mineralogy and Geochemistry*, v. 43, p. 469–525.
- Singer, D.A., 1986a, Descriptive model of Cyprus massive sulfide, *in* Cox, D.P., and Singer, D.A., eds., *Mineral deposit models: U.S. Geological Survey Bulletin 1693*, p. 131–135.

8 1. Introduction to Volcanogenic Massive Sulfide Occurrence Model

Singer, D.A., 1986b, Descriptive model of Kuroko massive sulfide, *in* Cox, D.P., and Singer, D.A., eds., Mineral deposit models: U.S. Geological Survey Bulletin 1693, p. 189–197.

Singer, D.A., 1995, World-class base and precious metal deposits—A quantitative analysis: *Economic Geology*, v. 90, p. 88–104.

Singer, D.A., 2007, Short course introduction to quantitative mineral resource assessments: U.S. Geological Survey Open-File Report 2007–1434, 13 p.

Slack, J.F., 1993, Descriptive and grade-tonnage models for Besshi-type massive sulphide deposits, *in* Kirkham, R.V., Sinclair, W.D., Thorpe, R.I., and Duke, J.M., eds., Mineral deposit modeling: Geological Association of Canada Special Paper 40, p. 343–371.

Taylor, C.D., Zierenberg, R.A., Goldfarb, R.J., Kilburn, J.E., Seal, R.R., II, and Kleinkopf, M.D., 1995, Volcanic-associated massive sulfide deposits, *in* du Bray, E.A., ed., Preliminary compilation of descriptive geoenvironmental mineral deposit models: U.S. Geological Survey Open-File Report 95–851, p. 137–144.

2. Deposit Type and Associated Commodities

By Randolph A. Koski and Dan L. Mosier

2 of 21

Volcanogenic Massive Sulfide Occurrence Model

Scientific Investigations Report 2010–5070–C

U.S. Department of the Interior
U.S. Geological Survey

U.S. Department of the Interior
KEN SALAZAR, Secretary

U.S. Geological Survey
Marcia K. McNutt, Director

U.S. Geological Survey, Reston, Virginia: 2012

For more information on the USGS—the Federal source for science about the Earth, its natural and living resources, natural hazards, and the environment, visit <http://www.usgs.gov> or call 1-888-ASK-USGS.

For an overview of USGS information products, including maps, imagery, and publications, visit <http://www.usgs.gov/pubprod>

To order this and other USGS information products, visit <http://store.usgs.gov>

Any use of trade, product, or firm names is for descriptive purposes only and does not imply endorsement by the U.S. Government.

Although this report is in the public domain, permission must be secured from the individual copyright owners to reproduce any copyrighted materials contained within this report.

Suggested citation:

Koski, R.A., and Mosier, D.L., 2012, Deposit type and associated commodities in volcanogenic massive sulfide occurrence model: U.S. Geological Survey Scientific Investigations Report 2010-5070 -C, chap. 2, 8 p

Contents

| | |
|--|----|
| Name and Synonyms..... | 15 |
| Brief Description | 15 |
| Associated Deposit Types | 15 |
| Primary and Byproduct Commodities..... | 16 |
| Example Deposits..... | 16 |
| References Cited..... | 19 |

Figures

| | |
|---|----|
| 2-1. Grade and tonnage of volcanogenic massive sulfide deposits | 16 |
| 2-2. Map showing locations of significant volcanogenic massive sulfide deposits in the United States | 17 |

Table

| | |
|---|----|
| 2-1. Examples of deposit types with lithologic associations, inferred tectonic settings, and possible modern seafloor analogs..... | 18 |
|---|----|

2. Deposit Type and Associated Commodities

By Randolph A. Koski and Dan L. Mosier

Name and Synonyms

The type of deposit described in this document is referred to as volcanogenic massive sulfide (VMS). This terminology has been in use for more than 35 years (Hutchinson, 1973) and embraces the temporal and spatial association of sulfide mineralization with submarine volcanic processes. Similar terms for VMS deposits recorded in the literature include volcanogenic sulfide, volcanic massive sulfide, exhalative massive sulfide, volcanic-exhalative massive sulfide, submarine-exhalative massive sulfide, volcanic-hosted massive sulfide, volcanic-sediment-hosted massive sulfide, volcanic-associated massive sulfide, and volcanophile massive sulfide deposits. In some earlier studies, the terms cupreous pyrite and stratabound pyrite deposits were used in reference to the pyrite-rich orebodies hosted by ophiolitic volcanic sequences in Cyprus and elsewhere (Hutchinson, 1965; Gilmour, 1971; Hutchinson and Searle, 1971). More recently, the term polymetallic massive sulfide deposit has been applied by many authors to VMS mineralization on the modern seafloor that contains significant quantities of base metals (for example, Herzig and Hannington, 1995, 2000). Other commonly used names for VMS deposit subtypes such as Cyprus type, Besshi type, Kuroko type, Noranda type, and Urals type are derived from areas of extensive mining activities.

Brief Description

Volcanogenic massive sulfide deposits are stratabound concentrations of sulfide minerals precipitated from hydrothermal fluids in extensional seafloor environments. The term volcanogenic implies a genetic link between mineralization and volcanic activity, but siliciclastic rocks dominate the stratigraphic assemblage in some settings. The principal tectonic settings for VMS deposits include mid-oceanic ridges, volcanic arcs (intraoceanic and continental margin), back-arc basins, rifted continental margins, and pull-apart basins. The composition of volcanic rocks hosting individual sulfide deposits range from felsic to mafic, but bimodal mixtures are not uncommon. The volcanic strata consist of massive and pillow lavas, sheet flows, hyaloclastites, lava breccias, pyroclastic deposits, and volcanoclastic sediment. Deposits range

in age from Early Archean (3.55 Ga) to Holocene; deposits are currently forming at numerous localities in modern oceanic settings.

Deposits are characterized by abundant Fe sulfides (pyrite or pyrrhotite) and variable but subordinate amounts of chalcopyrite and sphalerite; bornite, tetrahedrite, galena, barite, and other mineral phases are concentrated in some deposits. Massive sulfide bodies typically have lensoidal or sheetlike forms. Many, but not all, deposits overlie discordant sulfide-bearing vein systems (stringer or stockwork zones) that represent fluid flow conduits below the seafloor. Pervasive alteration zones characterized by secondary quartz and phyllosilicate minerals also reflect hydrothermal circulation through footwall volcanic rocks. A zonation of metals within the massive sulfide body from Fe+Cu at the base to Zn+Fe±Pb±Ba at the top and margins characterizes many deposits. Other features spatially associated with VMS deposits are exhalative (chemical) sedimentary rocks, subvolcanic intrusions, and semi-conformable alteration zones.

Associated Deposit Types

Associations with other types of mineral deposits formed in submarine environments remain tentative. There is likely some genetic kinship among VMS deposits, Algoma-type iron formations (Gross, 1980, 1996; Cannon, 1986), and volcanogenic manganese deposits (Mosier and Page, 1988). Sedimentary-exhalative (SEDEX) deposits have broadly similar morphological features consistent with syngenetic formation in extensional submarine environments, but their interpreted paleotectonic settings (failed intracratonic rifts and rifted Atlantic-type continental margins), hydrothermal fluid characteristics (concentrated NaCl brines), absence or paucity of volcanic rocks, and association with shale and carbonate rocks distinguish them from VMS deposits (Leach and others, 2005).

The recognition of high-sulfidation mineralization and advanced argillic alteration assemblages at hydrothermal discharge zones in both modern and ancient submarine oceanic arc environments has led to the hypothesis (Sillitoe and others, 1996; Large and others, 2001) that a transitional relationship exists between VMS and epithermal (Au-Ag) types of mineral deposits. Galley and others (2007) include epithermal-style

mineralization in the hybrid bimodal-felsic subtype of their VMS classification.

A rather enigmatic type of Co-, As-, and Cu-rich massive sulfide mineralization in serpentinized ultramafic rocks of some ophiolite complexes (for example, Troodos and Bou Azzer) has been attributed to magmatic (syn- or post-ophiolite emplacement) and serpentinization processes (Panayiotou, 1980; Page, 1986; Leblanc and Fischer, 1990; Ahmed and others, 2009). Recent discoveries at slow-rate spreading axes of the Mid-Atlantic Ridge reveal that high-temperature hydrothermal fluids are precipitating Cu-Zn-Co-rich massive sulfide deposits on substrates composed of serpentinized peridotite (for example, Rainbow vent field; Marques and others, 2007). Based on these modern analogs, it is suggested that Co-Cu-As mineralization in ultramafic rocks of ophiolites may in fact belong to the spectrum of VMS deposits.

Primary and Byproduct Commodities

Volcanogenic massive sulfide deposits are a major global source of copper, lead, zinc, gold, and silver. Figure 2-1 illustrates the broad ranges in combined base-metal concentrations (Cu+Zn+Pb) and tonnages for more than 1,000 VMS deposits

worldwide. Although generally present as trace constituents, a number of other elements are of interest as economically recoverable byproducts or environmental contaminants: arsenic, beryllium, bismuth, cadmium, cobalt, chromium, gallium, germanium, mercury, indium, manganese, molybdenum, nickel, selenium, tin, tellurium, and platinum group metals.

Example Deposits

Worldwide, there are nearly 1,100 recognized VMS deposits including more than 100 in the United States and 350 in Canada (Galley and others, 2007; Mosier and others, 2009). Locations of significant VMS deposits in the United States are plotted on a geologic base map from the National Atlas of the United States in figure 2-2. Selected representatives of this deposit type, grouped according to their lithologic associations, are presented in table 2-1 along with inferred tectonic settings (modified from Franklin and others, 2005) and possible modern analogs.

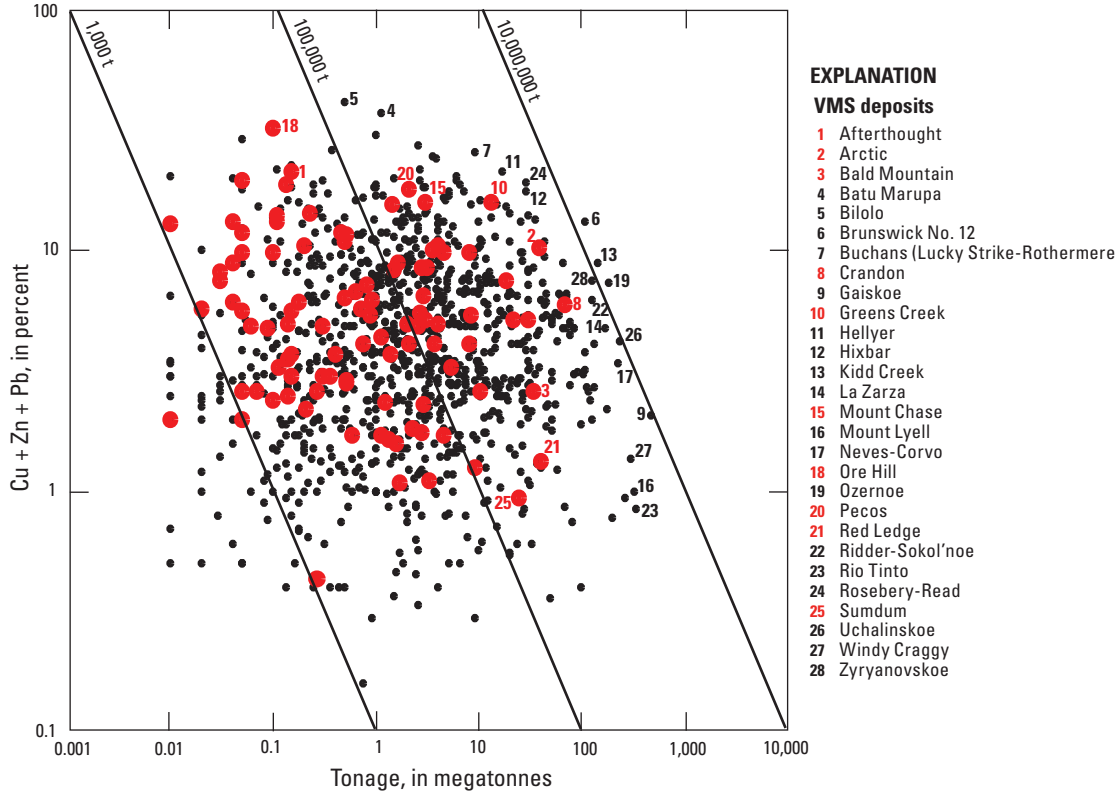


Figure 2-1. Grade and tonnage of volcanogenic massive sulfide deposits. Data are shown for 1,021 deposits worldwide. U.S. deposits are shown as red dots. Data from Mosier and others (2009) (Cu, copper; Zn, zinc; Pb, lead).

LOCATIONS OF SIGNIFICANT US VOLCANOGENIC MASSIVE SULFIDE DEPOSITS



Figure 2-2. Locations of significant volcanogenic massive sulfide deposits in the United States.

Table 2–1. Examples of deposit types with lithologic associations, inferred tectonic settings, and possible modern seafloor analogs.

| Examples of ancient deposits | Lithologic associations | Inferred tectonic settings | Possible modern analogs | References |
|--|-------------------------|--|--|---|
| Rio Tinto (Spain); Brunswick 12 (Canada); Stekenjokk (Sweden); Delta (USA); Bonfield (USA) | Siliciclastic-felsic | Mature epicontinental margin arc and back arc | | <u>Ancient deposits:</u> Tornos (2006); Goodfellow and others (2003); Grenne and others (1999); Dashevsky and others (2003); Dusel-Bacon and others (2004) |
| Hanaoka (Japan); Eskay Creek (Canada); Rosebery (Australia); Tambo Grande (Peru); Arctic (USA); Jerome (USA) | Bimodal-felsic | Rifted continental margin arc and back arc | Okinawa Trough; Woodlark Basin; Manus Basin | <u>Ancient deposits:</u> Ohmoto and Skinner (1983); Barrett and Sherlock (1996); Large and others (2001); Steinmüller and others, 2000; Schmidt (1986); Gustin (1990) <u>Modern analogs:</u> Binns and others (1993); Halbach and others (1993); Binns and Scott (1993) |
| Horne (Canada); Komsomolskoye (Russia); Bald Mountain (USA); Crandon (USA) | Bimodal-mafic | Rifted immature intraoceanic arc | Kermadec Arc; Izu-Bonin Arc; Mariana Arc | <u>Ancient deposits:</u> Gibson and others (2000); Prokin and Buslaev (1999); Schulz and Ayuso (2003); Lambe and Rowe (1987) <u>Modern analogs:</u> Wright and others (1998); Glasby and others (2000); Hannington and others (2005) |
| Windy Craggy (Canada); Besshi (Japan); Ducktown (USA); Gossan Lead (USA); Beatson (USA) | Siliciclastic-mafic | Rifted continental margin; sedimented oceanic ridge or back arc; intracontinental rift | Guaymas Basin; Escanaba Trough; Middle Valley; Red Sea | <u>Ancient deposits:</u> Peter and Scott (1999); Banno and Sakai (1989); Stephens and others (1984); Gair and Slack (1984); Crowe and others (1992); <u>Modern analogs:</u> Koski and others (1985); Zierenberg and others (1993); Goodfellow and Franklin (1993); Shanks and Bischoff (1980) |
| Skouriotissa (Cyprus); Lasail (Oman); Lokken (Norway); Betts Cove (Canada); Bou Azzer (Morocco); Turner-Albright (USA) | Mafic-ultramafic | Intraoceanic back-arc or fore-arc basin; oceanic ridge | Lau Basin; North Fiji Basin; Trans-Atlantic Geothermal (TAG) field; Rainbow vent field | <u>Ancient deposits:</u> Constantinou and Govett (1973); Alabaster and Grenne and others (1999); Stephens and others (1984); Upadhyay and Strong (1973); Leblanc and Fischer (1990); Zierenberg and others (1988) <u>Modern analogs:</u> Fouquet and others (1993); Kim and others (2006); Rona and others (1993); Marques and others (2007) |

References Cited

- Ahmed, A.H., Arai, S., and Ikenne, M., 2009, Mineralogy and paragenesis of the Co-Ni arsenide ores of Bou Azzer, Anti-Atlas, Morocco: *Economic Geology*, v. 104, p. 249–266.
- Alabaster, T., and Pearce, J.A., 1985, The interrelationship between magmatic and ore-forming hydrothermal processes in the Oman ophiolite: *Economic Geology*, v. 80, p. 1–16.
- Banno, S., and Sakai, C., 1989, Geology and metamorphic evolution of the Sanbagawa metamorphic belt, Japan, in Daly, J.S., Cliff, R.A., and Yardley, B.W.D., eds., *Evolution of metamorphic belts*: Geological Society of London Special Publication 43, p. 519–532.
- Barrett, T.J., and Sherlock, R.L., 1996, Geology, litho-geochemistry and volcanic setting of the Eskay Creek Au-Ag-Cu-Zn deposit, northwestern British Columbia: *Exploration and Mining Geology*, v. 5, p. 339–368.
- Binns, R.A., and Scott, S.D., 1993, Actively forming polymetallic sulfide deposits associated with felsic volcanic rocks in the eastern Manus back-arc basin, Papua New Guinea: *Economic Geology*, v. 88, p. 2222–2232.
- Binns, R.A., Scott, S.D., Bogdanov, Y.A., Lisitzin, A.P., Gordeev, V.V., Gurvich, E.G., Finlayson, E.J., Boyd, T., Dotter, L.E., Wheller, G.E., and Muravyev, K.G., 1993, Hydrothermal oxide and gold-rich sulfate deposits of Franklin Seamount, western Woodlark Basin, Papua New Guinea: *Economic Geology*, v. 88, p. 2122–2153.
- Cannon, W.F., 1986, Descriptive model of Algoma Fe, in Cox, D.P., and Singer, D.A., eds., *Mineral deposit models*: U.S. Geological Survey Bulletin 1693, p. 198.
- Constantinou, G., and Govett, G.J.S., 1973, Geology, geochemistry and genesis of Cyprus sulfide deposits: *Economic Geology*, v. 68, p. 843–858.
- Crowe, D.E., Nelson, S.W., Brown, P.E., Shanks, W.C., III, and Valley, J.W., 1992, Geology and geochemistry of volcanogenic massive sulfide deposits and related igneous rocks, Prince William Sound, south-central Alaska: *Economic Geology*, v. 87, p. 1722–1746.
- Dashevsky, S.S., Schaefer, C.F., Hunter, E.N., 2003, Bedrock geologic map of the Delta mineral belt, Tok mining district, Alaska: Alaska Division of Geological and Geophysical Surveys Professional Report 122, 122 p., 2 pls., scale 1:63,360.
- Dusel-Bacon, C., Wooden, J.L., and Hopkins, M.J., 2004, U-Pb zircon and geochemical evidence for bimodal mid-Paleozoic magmatism and syngenetic base-metal mineralization in the Yukon-Tanana terrane, Alaska: *Geological Society of America Bulletin*, v. 116, p. 989–1015.
- Fouquet, Y., von Stackelberg, U., Charlou, J.-L., Erzinger, J., Herzig, P.M., Muhe, R., and Wiedicke, M., 1993, Metallogenesis in back-arc environments—The Lau basin example: *Economic Geology*, v. 88, p. 2154–2181.
- Franklin, J.M., Gibson, H.L., Jonasson, I.R., and Galley, A.G., 2005, Volcanogenic massive sulfide deposits, in Hedenquist, J.W., Thompson, J.F.H., Goldfarb, R.J., and Richards, J.P., eds., *Economic Geology 100th anniversary volume, 1905–2005*: Littleton, Colo., Society of Economic Geologists, p. 523–560.
- Gair, J.E., and Slack, J.F., 1984, Deformation, geochemistry, and origin of massive sulfide deposits, Gossan Lead district, Virginia: *Economic Geology*, v. 79, p. 1442–1478.
- Galley, A.G., Hannington, M., and Jonasson, I., 2007, Volcanogenic massive sulphide deposits, in Goodfellow, W.D., ed., *Mineral deposits of Canada: A synthesis of major deposit-types, district metallogeny, the evolution of geological provinces, and exploration methods*: Geological Association of Canada, Mineral Deposits Division, Special Publication 5, p. 141–161.
- Gibson, H.L., Kerr, D.J., and Cattalani, S., 2000, The Horne Mine: Geology, history, influence on genetic models, and a comparison to the Kidd Creek Mine: *Exploration and Mining Geology*, v. 9, p. 91–111.
- Gilmour, P., 1971, Strata-bound massive pyritic sulfide deposits—A review: *Economic Geology*, v. 66, p. 1239–1249.
- Glasby, G.P., Iizasa, K., Yuasa, M., and Usui, A., 2000, Submarine hydrothermal mineralization on the Izu-Bonin arc, south of Japan—An overview: *Marine Georesources and Geotechnology*, v. 18, p. 141–176.
- Goodfellow, W.D., and Franklin, J.M., 1993, Geology, mineralogy, and chemistry of sediment-hosted clastic massive sulfides in shallow cores, Middle Valley, northern Juan de Fuca Ridge: *Economic Geology*, v. 88, p. 2037–2068.
- Goodfellow, W.D., McCutcheon, S.R., and Peter, J.M., 2003, Introduction and summary of findings, in Goodfellow, W.D., McCutcheon, S.R., and Peter, J.M., eds., *Massive sulfide deposits of the Bathurst mining camp, New Brunswick, and northern Maine*: *Economic Geology Monograph* 11, p. 1–16.
- Grenne, T., Ihlen, P.M., and Vokes, F.M., 1999, Scandinavian Caledonide metallogeny in a plate tectonic perspective: *Mineralium Deposita*, v. 34, p. 422–471.
- Gross, G.A., 1980, A classification of iron formations based on depositional environments: *Canadian Mineralogist*, v. 18, p. 215–222.

20 2. Deposit Type and Associated Commodities

- Gross, G.A., 1996, Algoma-type iron-formation, in Eckstrand, O.R., Sinclair, W.D., and Thorpe, R.I., eds., *Geology of Canadian mineral deposit types: Geological Survey of Canada, Geology of Canada no. 8; Geological Society of America, Decade of North American Geology v. P1*, p. 66–73.
- Gustin, M.S., 1990, Stratigraphy and alteration of the host rocks, United Verde massive sulfide deposit, Jerome, Arizona: *Economic Geology*, v. 85, no. 1, p. 29–49.
- Halbach, P., Pracejus, B., and Maerten, A., 1993, Geology and mineralogy of massive sulfide ores from the central Okinawa Trough, Japan: *Economic Geology*, v. 88, p. 2210–2225.
- Hannington, M.D., de Ronde, C.E.J., and Petersen, S., 2005, Sea-floor tectonics and submarine hydrothermal systems, in Hedenquist, J.W., Thompson, J.F.H., Goldfarb, R.J., and Richards, J.P., eds., *Economic geology 100th anniversary volume 1905–2005*: Littleton, Colo., Society of Economic Geologists, p. 111–141.
- Herzig, P.M., and Hannington, M.D., 1995, Polymetallic massive sulfides at the modern seafloor—A review: *Ore Geology Reviews*, v. 10, p. 95–115.
- Herzig, P.M., and Hannington, M.D., 2000, Polymetallic massive sulfides and gold mineralization at mid-ocean ridges and in subduction-related environments, in Cronan, D.S., ed., *Handbook of marine mineral deposits: Boca Raton, Fla., CRC Press Marine Science Series*, p. 347–368.
- Humphris, S.E., Herzig, P.M., Miller, D.J., Alt, J.C., Becker, K., Brown, D., Brugmann, G., Chiba, H., Fouquet, Y., Gemmell, J.B., Guerin, G., Hannington, M.D., Holm, N.G., Honnorez, J.J., Iturrino, G.J., Knott, R., Ludwig, R., Nakamura, K., Petersen, S., Reysenbach, A.L., Rona, P.A., Smith, S., Sturz, A.A., Tivey, M.K., and Zhao, X., 1995, The internal structure of an active sea-floor massive sulphide deposit: *Nature*, v. 377, no. 6551, p. 713–716.
- Hutchinson, R.W., 1965, Genesis of Canadian massive sulphides reconsidered by comparison to Cyprus deposits: *Canadian Mining and Metallurgical Bulletin*, v. 58, p. 972–986.
- Hutchinson, R.W., 1973, Volcanogenic sulfide deposits and their metallogenic significance: *Economic Geology*, v. 68, p. 1223–1246.
- Hutchinson, R.W., and Searle, D.L., 1971, Stratabound pyrite deposits in Cyprus and relations to other sulphide ores: *Society of Mining Geologists of Japan, Special Issue 3*, p. 198–205.
- Kim, J., Lee, I., Halbach, P., Lee, K.-Y., Ko, Y.-T., and Kim, K.-H., 2006, Formation of hydrothermal vents in the North Fiji Basin—Sulfur and lead isotope constraints: *Chemical Geology*, v. 233, p. 257–275.
- Koski, R.A., Lonsdale, P.F., Shanks, W.C., III, Berndt, M.E., and Howe, S.S., 1985, Mineralogy and geochemistry of a sediment-hosted hydrothermal sulfide deposit from the Southern Trough of Guaymas Basin, Gulf of California: *Journal of Geophysical Research*, v. 90, p. 6695–6707.
- Lambe, R.N., and Rowe, R.G., 1987, Volcanic history, mineralization, and alteration of the Crandon massive sulfide deposit, Wisconsin: *Economic Geology*, v. 82, p. 1204–1238.
- Large, R.R., McPhie, J., Gemmell, J.B., Herrmann, W., and Davidson, G.J., 2001, The spectrum of ore deposit types, volcanic environments, alteration halos, and related exploration vectors in submarine volcanic successions: Some examples from Australia: *Economic Geology*, v. 96, p. 913–938.
- Leach, D.L., Sangster, D.F., Kelley, K.D., Large, R.R., Garven, G., Allen, C.R., Gutzmer, J., and Walters, S., 2005, Sediment-hosted lead-zinc deposits—A global perspective, in Hedenquist, J.W., Thompson, J.F.H., Goldfarb, R.J., and Richards, J.P., eds., *Economic Geology 100th anniversary volume*, p. 561–607.
- Leblanc, M., and Fischer, W., 1990, Gold and platinum group elements in cobalt arsenide ores—Hydrothermal concentration from a serpentinite source-rock: *Mineralogy and Petrology*, v. 42, p. 197–209.
- Marques, A.F.A., Barriga, F.J.A.S., and Scott, S.D., 2007, Sulfide mineralization in an ultramafic-rock hosted seafloor hydrothermal system—From serpentinitization to the formation of Cu-Zn-(Co)-rich massive sulfides: *Marine Geology*, v. 245, p. 20–39.
- Mosier, D.L., Berger, V.I., and Singer, D.A., 2009, Volcanogenic massive sulfide deposits of the world: Database and grade and tonnage models: U.S. Geological Survey Open-File Report 2009–1034, 50 p.
- Mosier, D.L., and Page, N.J., 1988, Descriptive and grade-tonnage models of volcanogenic manganese deposits in oceanic environments: A modification: *U.S. Geological Survey Bulletin* 1811, 28 p.
- Ohmoto, H., and Skinner, B.J., eds., 1983, *The Kuroko and related volcanogenic massive sulfide deposits: Economic Geology Monograph* 5, 604 p.

- Page, N.J., 1986, Descriptive model of Limassol Forest Co-Ni, in Cox, D.P., and Singer, D.A., eds., *Mineral deposit models*: U.S. Geological Survey Bulletin 1693, p. 45.
- Panayiotou, A., 1980, Cu-Ni-Co-Fe sulphide mineralization, Limassol Forest, Cyprus, in Panayiotou, A., ed., *Ophiolites—International Ophiolite Symposium, Cyprus, 1979*, Proceedings: Republic of Cyprus, Geological Survey Department, p. 102–116.
- Peter, J.M., and Scott, S.D., 1988, Mineralogy, composition, and fluid-inclusion microthermometry of seafloor hydrothermal deposits in the Southern Trough of Guaymas Basin, Gulf of California: *Canadian Mineralogist*, v. 26, p. 567–587.
- Peter, J.M., and Scott, S.D., 1999, Windy Craggy, northwestern British Columbia—The world's largest Besshi-type deposit, in Barrie, C.T., and Hannington, M.D., eds., *Volcanic-associated massive sulfide deposits—Processes and examples in modern and ancient settings: Reviews in Economic Geology*, v. 8, p. 261–295.
- Prokin, V.A., and Buslaev, F.P., 1999, Massive copper-zinc deposits in the Urals: *Ore Geology Reviews*, v. 14, p. 1–69.
- Rona, P.A., Hannington, M.D., Raman, C.V., Thompson, G., Tivey, M.K., Humphris, S.E., Lalou, C., and Petersen, S., 1993, Active and relict seafloor hydrothermal mineralization at the TAG hydrothermal field, Mid-Atlantic Ridge: *Economic Geology*, v. 88, p. 1989–2017.
- Schmidt, J.M., 1986, Stratigraphic setting and mineralogy of the Arctic volcanogenic massive sulfide prospect, Ambler District, Alaska: *Economic Geology*, v. 81, p. 1619–1643.
- Schulz, K.J., and Ayuso, R.A., 2003, Lithogeochemistry and paleotectonic setting of the Bald Mountain massive sulfide deposit, northern Maine, in Goodfellow, W.D., McCutcheon, S.R., and Peter, J.M., eds., *Massive sulfide deposits of the Bathurst mining camp, New Brunswick, and northern Maine*: *Economic Geology Monograph* 11, p. 79–109.
- Shanks, W.C., III, and Bischoff, J.L., 1980, Geochemistry, sulfur isotope composition, and accumulation rates of Red Sea geothermal deposits: *Economic Geology*, v. 75, p. 445–459.
- Sillitoe, R.H., Hannington, M.D., and Thompson, J.F.H., 1996, High sulfidation deposits in the volcanogenic massive sulfide environment: *Economic Geology*, v. 91, p. 204–212.
- Steinmüller, K., Abad, N.C., and Grant, B., 2000, Volcanogenic massive sulphide deposits in Peru, in Sherlock, R.L., and Logan, M.A., eds., *Volcanogenic massive sulphide deposits of Latin America: Geological Association of Canada Special Publication No. 2*, p. 423–437.
- Stephens, M.B., Swinden, H.S., and Slack, J.F., 1984, Correlation of massive sulfide deposits in the Appalachian-Caledonian orogen on the basis of paleotectonic setting: *Economic Geology*, v. 79, p. 1442–1478.
- Tornos, F., 2006, Environment of formation and styles of volcanogenic massive sulfides—The Iberian Pyrite Belt: *Ore Geology Reviews*, v. 28, p. 259–307.
- Upadhyay, H.D., and Strong, D.F., 1973, Geological setting of the Betts Cove copper deposits, Newfoundland—An example of ophiolite sulfide mineralization: *Economic Geology*, v. 68, p. 161–167.
- Wright, I.C., de Ronde, C.E.J., Faure, K., and Gamble, J.A., 1998, Discovery of hydrothermal sulfide mineralization from southern Kermadec arc volcanoes (SW Pacific): *Earth and Planetary Science Letters*, v. 164, p. 335–343.
- Zierenberg, R.A., Koski, R.A., Morton, J.L., Bouse, R.M., and Shanks, W.C., III, 1993, Genesis of massive sulfide deposits on a sediment-covered spreading center, Escanaba trough, southern Gorda Ridge: *Economic Geology*, v. 88, p. 2069–2098.
- Zierenberg, R.A., Shanks, W.C., III, Seyfried, W.E., Jr., Koski, R.A., and Strickler, M.D., 1988, Mineralization, alteration, and hydrothermal metamorphism of the ophiolite-hosted Turner-Albright sulfide deposit, southwestern Oregon: *Journal of Geophysical Research*, v. 93, p. 4657–4674.

3. Historical Evolution of Descriptive and Genetic Knowledge and Concepts

By W.C. Pat Shanks III

3 of 21

Volcanogenic Massive Sulfide Occurrence Model

Scientific Investigations Report 2010–5070–C

U.S. Department of the Interior
U.S. Geological Survey

U.S. Department of the Interior
KEN SALAZAR, Secretary

U.S. Geological Survey
Marcia K. McNutt, Director

U.S. Geological Survey, Reston, Virginia: 2012

For more information on the USGS—the Federal source for science about the Earth, its natural and living resources, natural hazards, and the environment, visit <http://www.usgs.gov> or call 1-888-ASK-USGS.

For an overview of USGS information products, including maps, imagery, and publications, visit <http://www.usgs.gov/pubprod>

To order this and other USGS information products, visit <http://store.usgs.gov>

Any use of trade, product, or firm names is for descriptive purposes only and does not imply endorsement by the U.S. Government.

Although this report is in the public domain, permission must be secured from the individual copyright owners to reproduce any copyrighted materials contained within this report.

Suggested citation:

Shanks III, W.C. Pat, 2012, Historical evolution of descriptive and genetic knowledge and concepts in volcanogenic massive sulfide occurrence model: U.S. Geological Survey Scientific Investigations Report 2010-5070-C, chap. 3, 6 p.

Contents

Hydrothermal Activity and Massive Sulfide Deposit Formation on the Modern Seafloor27
References Cited.....31

Figures

3-1. Map of seafloor tectonic boundaries, metalliferous sediment distribution, locations of seafloor hydrothermal vents and deposits, and distribution of U.S. Exclusive Economic Zones28
3-2. Representative examples of large seafloor massive sulfide deposits30

3. Historical Evolution of Descriptive and Genetic Knowledge and Concepts

By W.C. Pat Shanks III

Massive sulfide deposits of base metal sulfides are among the earliest metallic ore deposits known and extracted because of their high grade, strong contrast with country rocks, iron staining and gossans at the surface, and their relatively simple mining and extraction. However, understanding the timing and mode of emplacement of these deposits proved much more difficult, and it was not until the second half of the twentieth century that several lines of evidence, not the least being the discovery of hydrothermal activity on the modern seafloor, conspired to convince researchers and explorationists that these deposits form syngenetically at or slightly beneath the seafloor by hydrothermal exhalative processes.

Most workers in the nineteenth century believed massive sulfide deposits, including many that would later be recognized as VMS deposits, formed by fissure-filling and (or) selective hydrothermal replacement. The source of the fluids was controversial, with some researchers favoring lateral-secretion from country rocks and some favoring fluids from granitoid intrusives (Stanton, 1984). Emmons (1909) studied so-called segregated vein deposits in the Appalachians from Newfoundland to Georgia and established that many of the deposits were formed prior to regional metamorphism. He noted the complete gradation from schistose country rock to sulfide-schist laminations to massive sulfide, and concluded that the country rock and interbedded and massive ore are all of the same age. Despite these seminal observations and interpretations, most workers accepted epigenetic theories, and even Emmons switched to a selective-replacement theory for Ducktown ores (Emmons and Laney, 1911). The work of Lindgren (1913) emphasized magmatic hydrothermal replacement theories and was very influential, especially in North America.

In the 1950s, discoveries of stratiform volcanic-hosted massive sulfides in the Bathurst area of New Brunswick opened the door for syngenetic interpretations (Stanton, 1959). These ideas coincided with the emergence of the exhalative theory as applied to massive sulfide deposits of the Norwegian and Irish Caledonides (Oftedahl, 1958; Dunham, 1964).

Though still controversial in some quarters, the modern era of studies of volcanic exhalative massive sulfides emerged in the 1960s through a combination of new discoveries and new exposures, improved radiometric dating, fluid inclusion studies, new stable and radiogenic isotope studies, work

on continental hot springs (White and others, 1963), and, in particular, discovery of modern seafloor hydrothermal activity (Miller and others 1966; Bischoff, 1969; Edmond and others, 1979; Hekinian and others, 1980; Spiess and others, 1980).

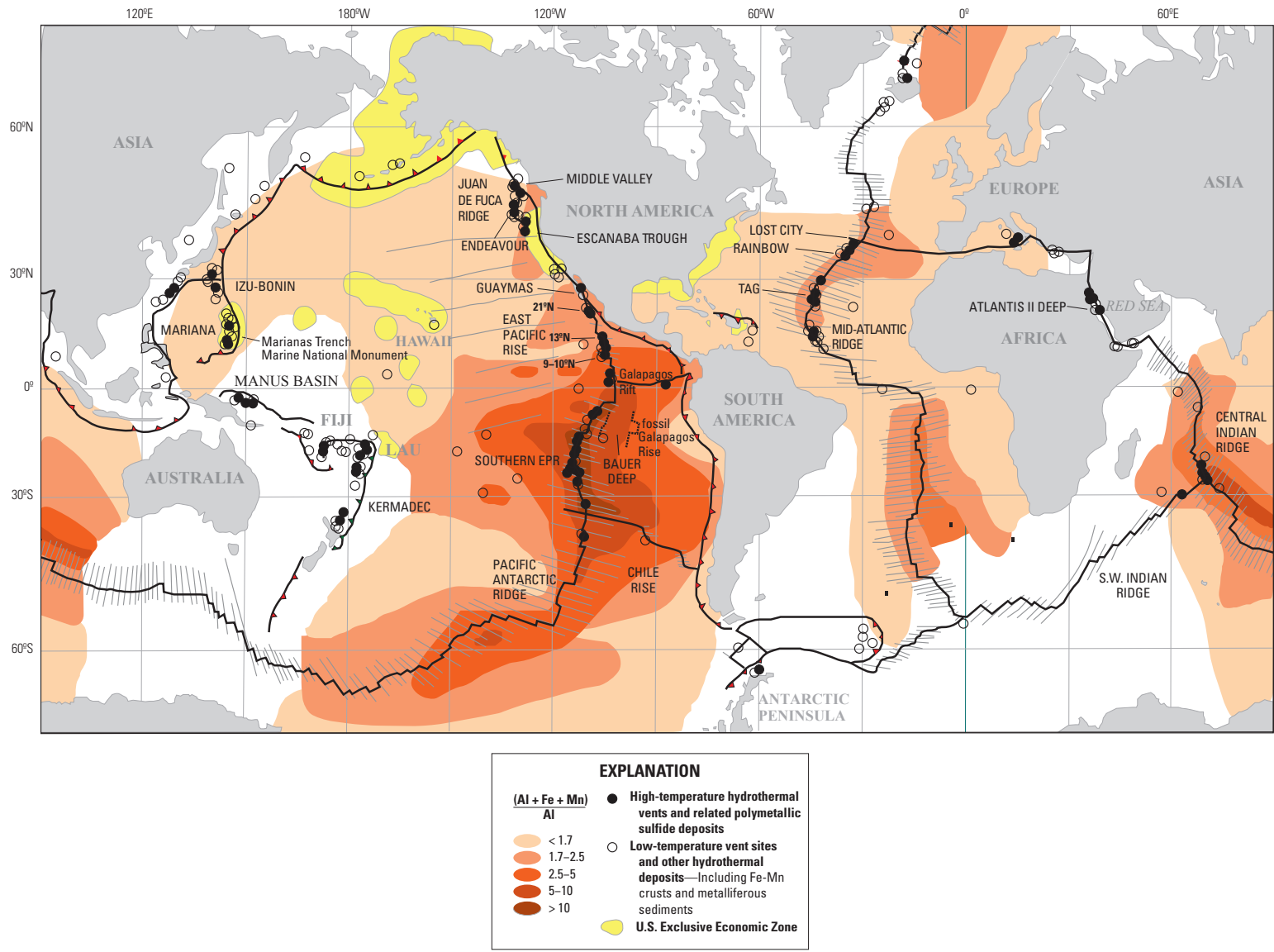
Hydrothermal Activity and Massive Sulfide Deposit Formation on the Modern Seafloor

The recognition of abundant and widespread hydrothermal activity and associated unique lifeforms on the ocean floor is one of the great scientific discoveries of the latter half of the twentieth century. Studies of seafloor hydrothermal processes led to advances in understanding fluid convection and the cooling of the ocean crust, the origin of greenstones and serpentinites, and the origin of stratiform and statabound massive sulfide deposits. Suggestions of possible submarine hydrothermal activity date from the late 1950s when a number of investigators debated the importance of “volcanic emanations” as a factor in the widespread occurrence of manganese nodules and other ferromanganese oxide deposits on the seafloor. For example, Arrhenius and Bonatti (1965), in their classic paper “Neptunism and Vulcanism in the Oceans,” stated the following:

The origin of authigenic minerals on the ocean floor has been extensively discussed in the past with emphasis on two major processes: precipitation from solutions originating from submarine eruptions, and slow precipitation from sea water of dissolved elements, originating from weathering of continental rocks. It is concluded that in several marine authigenic mineral systems these processes overlap. (p. 7)

Boström and Peterson (1966), in another classic paper, published evidence for extensive and widespread Fe-rich metalliferous sediments on the seafloor with a distribution strongly correlated with the mid-ocean ridges (fig. 3–1). They stated:

On the very crest of the East Pacific Rise, in equatorial latitudes—particularly 12° to 16°S, the sediments are enriched in Fe, Mn, Cu, Cr, Ni, and Pb.



Distribution of Seafloor Metalliferous Sediment, Massive Sulfide Deposits, and Hydrothermal Vents

Modified after Hannington and others (2007) and Bostrom and others (1969)

Figure 3-1. Map of seafloor tectonic boundaries, metalliferous sediment distribution (modified from Boström and Peterson, 1966), locations of seafloor hydrothermal vents and deposits (modified from Hannington and others, 2005), and distribution of U.S. Exclusive Economic Zones. [Al, aluminum; Fe, iron; Mn, manganese]

The correlation of these areas of enrichment to areas of high heat flow is marked. It is believed that these precipitates are caused by ascending solutions of deep-seated origin, which are probably related to magmatic processes at depth. The Rise is considered to be a zone of exhalation from the mantle of the earth, and these emanations could serve as the original enrichment in certain ore forming processes. (p. 1258)

At about the same time, the discovery of hot brine pools on the floor of the Red Sea (fig. 3-1) indicated the possibility of direct precipitation of metalliferous sediments (fig. 3-2) from hydrothermal brines on the seafloor (Miller and others, 1966; Bischoff, 1969, Hackett and Bischoff, 1973). This discovery more than any other resulted in a revolution in the field of ore genesis and a reassessment of the origin of massive sulfide deposits.

Following the Red Sea discoveries, several lines of evidence from mid-ocean ridge studies and laboratory experiments on basalt-seawater reaction (Bischoff and Dickson, 1975) indicated that seawater circulation through and reaction with ocean crust, owing to convective heating by subseafloor magma chambers, played a dominant role in the formation of ore-depositing fluids. These investigations set the stage for the discoveries of active hydrothermal vents and related sulfide deposits on mid-ocean ridges, island-arc volcanoes, and back-arc spreading centers. Active and inactive hydrothermal vent systems and hydrothermal deposits on the modern seafloor are more abundant than anticipated, especially considering that only a small percentage of the ocean ridge and convergent margins have been explored in detail. Over 300 sites with evidence of significant past or present seafloor hydrothermal activity are now known (Hannington and others, 2005).

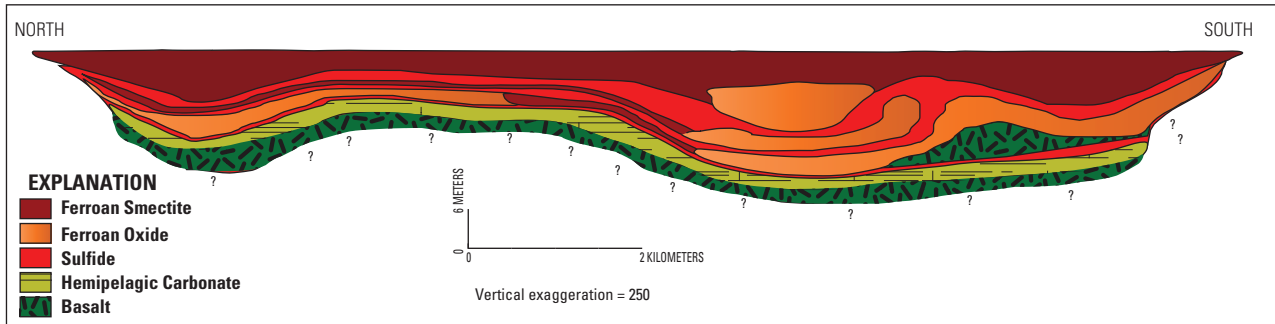
In addition to the Red Sea brine deposits, several large (millions of tons), high-metal-grade deposits are now known

on the mid-ocean ridges (fig. 3-2), including the Trans-Atlantic Geotraverse (TAG) site on the Mid-Atlantic Ridge (Humphris and others, 1995), the Middle Valley site (Zierenberg and others, 1998) on the northernmost Juan de Fuca Ridge, and the 12°43' N site slightly east of the East Pacific Rise (Fouquet and others, 1996).

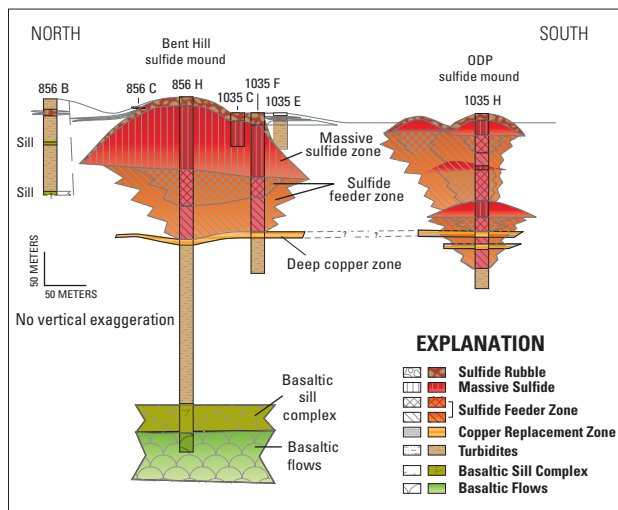
In the back-arc extensional environment of eastern Manus Basin, massive sulfide deposits with high concentrations of Cu, Zn, Au, Ag, Pb, As, Sb (antimony), and Ba (fig. 3-2) are hosted by calc-alkaline rocks ranging in composition from basalt to rhyolite. These deposits have been sampled and drilled for exploration purposes (Binns and Scott, 1993), and high grades and significant tonnages have spurred some companies to complete environmental studies, and develop seafloor mining technology, and seek permits in anticipation of mining (Herzig, 1999; Baker and German, 2007; Kunzig, 2009). All of these studies confirm the interpretation of a genetic kinship between modern seafloor deposits and ancient VMS deposits.

Studies of deposits on the continents have proceeded in concert with seafloor discoveries. Applications of chemical and isotopic methods, interpretations of physical volcanology and tectonic settings, and increasingly sophisticated fluid inclusion studies have improved understanding. The recognition of ophiolites as fossil oceanic crust formed at seafloor spreading centers (Gass, 1968) was accompanied by the realization that associated massive sulfide deposits were syngenetic with their host volcanic strata (Hutchinson, 1965; Constantinou and Govett, 1973). Studies of Kuroko deposits in Japan established them as volcanic exhalative in origin (Lambert and Sato, 1974; Ohmoto and Takahashi, 1983). Besshi-type deposits were recognized as deformed stratiform deposits (Fox, 1984; Slack, 1993), and deposits from Archean and Proterozoic greenstone belts, especially in northern Ontario, were recognized as volcanogenic (Gilmour, 1965; Franklin and others, 1981).

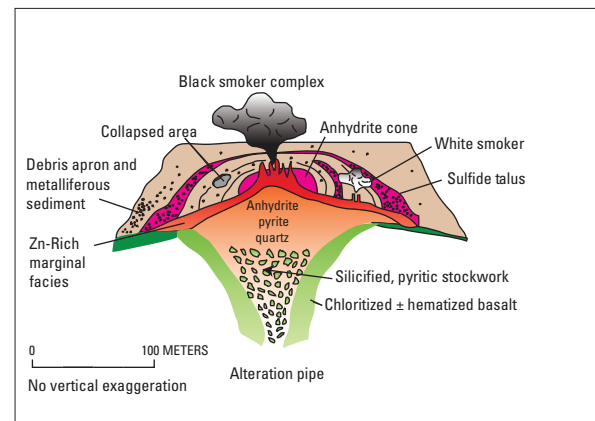
A. Mineralogic Facies of Metalliferous Sediment beneath the Atlantis II Deep Brine Pool, Red Sea



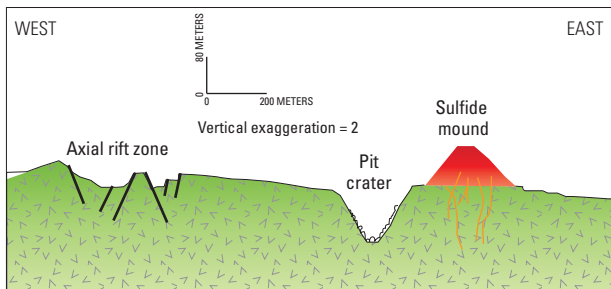
B. Middle Valley Massive Sulfide System



C. TAG Sulfide-Sulfate Mound, Mid-Atlantic Ridge



D. 12°43'N EPR sulfide mound



E. Solara-1 massive sulfide deposit, Eastern Manus Basin

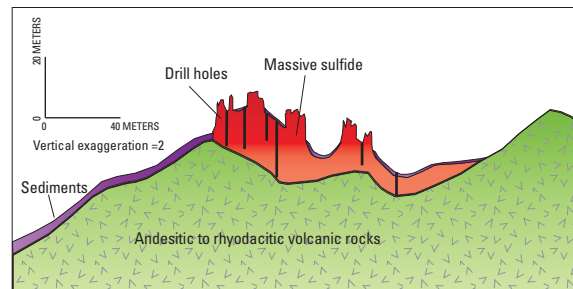


Figure 3–2. Representative examples of large seafloor massive sulfide deposits. *A*, Cross-section of metalliferous mud facies, Atlantis II Deep, Red Sea (after Hackett and Bischoff, 1973). *B*, Cross-section of Bent Hill and Ocean Drilling Program (ODP) mound massive sulfide deposits, Middle Valley, Juan de Fuca Ridge (after Zierenberg and others, 1998). *C*, Trans-Atlantic Geothermal (TAG) sulfate-sulfide mound, Mid-Atlantic Ridge (after Hannington and others, 1998). *D*, 13°N sulfide mound, East Pacific Rise (after Fouquet and others, 1996). *E*, Solara-1 massive sulfide deposit, eastern Manus Basin (after Baker and German, 2007).

References Cited

- Arrhenius, G., and Bonatti, E., 1965, Neptunism and volcanism in the ocean, *in* Sears, M., ed., *Progress in oceanography*: Oxford, Pergamon, p. 7–22.
- Baker, M., and German, C., 2007, Going for Gold! Who will win the race to exploit ores from the deep?: *Ocean Challenge*, v. 16, p. 10–17.
- Binns, R.A., and Scott, S.D., 1993, Actively forming polymetallic sulfide deposits associated with felsic volcanic rocks in the eastern Manus back-arc basin, Papua New Guinea: *Economic Geology*, v. 88, no. 8, p. 2222–2232.
- Bischoff, J.L., 1969, Red Sea geothermal brine deposits—Their mineralogy, chemistry, and genesis, *in* Degens, E.T., and Ross, D.A., eds., *Hot brines and recent heavy metal deposits in the Red Sea*: New York, Springer Verlag, p. 368–401.
- Bischoff, J.L., and Dickson, F.W., 1975, Sea water-basalt interaction at 200°C and 500 bars—Implications for origin of sea-floor heavy-metal deposits and regulation of sea water chemistry: *Earth and Planetary Science Letters*, v. 25, no. 3, p. 385–397.
- Boström, K., and Peterson, M.N.A., 1966, Precipitates from hydrothermal exhalations on the East Pacific Rise: *Economic Geology*, v. 61, p. 1258–1265.
- Boström, K., Peterson, M.N.A., Joensuu, O., and Fisher, D.E., 1969, Aluminum-poor ferromanganous sediments on active ocean ridges: *Journal of Geophysical Research*, v. 74, p. 3261–3270.
- Constantinou, G., and Govett, G.J.S., 1973, Geology, geochemistry and genesis of Cyprus sulfide deposits: *Economic Geology*, v. 68, p. 843–858.
- Dunham, K.C., 1964, Neptunist concepts in ore genesis: *Economic Geology*, v. 59, p. 1–21.
- Edmond, J.M., Measures, C., McDuff, R.E., Chan, L., Collier, R., Grant, B., Gordon, L.I., and Corliss, J., 1979, Ridge crest hydrothermal activity and the balances of the major and minor elements in the ocean—The Galapagos data: *Earth and Planetary Science Letters*, v. 46, p. 1–18.
- Emmons, W.H., 1909, Some regionally metamorphosed ore deposits and the so-called segregated veins: *Economic Geology*, v. 4, p. 755–781.
- Emmons, W.H., and Laney, F.B., 1911, Preliminary report on the mineral deposits of Ducktown, Tennessee, *in* Paige, S., ed., *Contributions to economic geology, 1910—Part I. Metals and nonmetals except fuels—Copper*: U.S. Geological Survey Bulletin 470–C, p. 151–172.
- Fouquet, Y., Knott, R., Cambon, P., Fallick, A., Rickard, D., and Desbruyeres, D., 1996, Formation of large sulfide mineral deposits along fast spreading ridges—Example from off-axial deposits at 12°43'N on the East Pacific Rise: *Earth and Planetary Science Letters*, v. 144, no. 1–2, p. 147–162.
- Fox, J.S., 1984, Besshi-type volcanogenic sulphide deposits—A review: *Canadian Institute of Mining and Metallurgy Bulletin*, v. 77, no. 864, p. 57–67.
- Franklin, J.M., Lydon, J.M., and Sangster, D.F., 1981, Volcanic-associated massive sulfide deposits, *in* Skinner, B.J., ed., *Economic Geology 75th anniversary volume, 1905–1980*: Littleton, Colo., Economic Geology Publishing Company, p. 485–627.
- Gass, I.G., 1968, Is the Troodos massif of Cyprus a fragment of Mesozoic ocean floor?: *Nature*, v. 220, no. 5162, p. 39–42.
- Gilmour, P., 1965, The origin of massive sulphide mineralization in the Noranda district, northwestern Quebec: *Geological Association of Canada Proceedings*, v. 16, p. 63–81.
- Hackett, J.P., Jr., and Bischoff, J.L., 1973, New data on the stratigraphy, extent, and geologic history of the Red Sea geothermal deposits: *Economic Geology*, v. 68, no. 4, p. 553–564.
- Hannington, M.D., Galley, A.G., Herzig, P.M., and Petersen, S., 1998, Comparison of the TAG mound and stockwork complex with Cyprus-type massive sulfide deposits, *in* Herzig, P.M., Humphris, S.E., Miller, D.J., and Zierenberg, R.A., eds., *Proceedings of the Ocean Drilling Program, Scientific Results*, v. 158, p. 389–415.
- Hannington, M.D., de Ronde, C.E.J., and Petersen, S., 2005, Sea-floor tectonics and submarine hydrothermal systems, *in* Hedenquist, J.W., Thompson, J.F.H., Goldfarb, R.J., and Richards, J.P., eds., *Economic geology 100th anniversary volume 1905–2005*: Littleton, Colo., Society of Economic Geologists, p. 111–141.
- Hekinian, R., Fevrier, M., Bischoff, J.L., Picot, P., and Shanks, W.C., 1980, Sulfide deposits from the East Pacific Rise near 21°N: *Science*, v. 207, no. 4438, p. 1433–1444.

- Herzig, P.M., 1999, Economic potential of sea-floor massive sulphide deposits—Ancient and modern: *Philosophical Transactions of the Royal Society of London*, v. 357, p. 861–875.
- Humphris, S.E., Herzig, P.M., Miller, D.J., Alt, J.C., Becker, K., Brown, D., Brugmann, G., Chiba, H., Fouquet, Y., Gemmell, J.B., Guerin, G., Hannington, M.D., Holm, N.G., Honnorez, J.J., Iturrino, G.J., Knott, R., Ludwig, R., Nakamura, K., Petersen, S., Reysenbach, A.L., Rona, P.A., Smith, S., Sturz, A.A., Tivey, M.K., and Zhao, X., 1995, The internal structure of an active sea-floor massive sulphide deposit: *Nature*, v. 377, no. 6551, p. 713–716.
- Hutchinson, R.W., 1965, Genesis of Canadian massive sulphides reconsidered by comparison to Cyprus deposits: *Canadian Mining and Metallurgical Bulletin*, v. 58, p. 972–986.
- Kunzig, R., 2009, Can giant robots successfully mine the mile-deep seafloor?—The economic collapse threatens the long-held dream of underwater mining: *Discover Magazine*, 4 May 2009, 6 p.
- Lambert, I.B., and Sato, T., 1974, The Kuroko and associated ore deposits of Japan—A review of their features and metallogenesis: *Economic Geology*, v. 69, p. 1215–1236.
- Lindgren, W., 1913, *Mineral deposits*: New York, McGraw-Hill Book Company, 883 p.
- Miller, A.L., Densmore, C.D., Degens, E.T., Hathaway, J.C., Manheim, F.T., McFarlin, P.F., Pocklington, R., and Jokela, A., 1966, Hot brines and recent iron deposits of the Red Sea: *Geochimica et Cosmochimica Acta*, v. 30, p. 341–359.
- Oftedahl, C., 1958, A theory of exhalative-sedimentary ores: *Geologiska Föreningens I Stockholm Förhandlingar*, v. 80, no. 492, p. 1–19.
- Ohmoto, H., and Takahashi, T., 1983, Geological setting of the Kuroko deposits, Japan—Part III. Submarine calderas and kuroko genesis, in Ohmoto, H., and Skinner, B.J., eds., *The Kuroko and related volcanogenic massive sulfide deposits*: *Economic Geology Monograph* 5, p. 39–54.
- Slack, J.F., 1993, Descriptive and grade-tonnage models for Besshi-type massive sulphide deposits, in Kirkham, R.V., Sinclair, W.D., Thorpe, R.I., and Duke, J.M., eds., *Mineral deposit modeling*: Geological Association of Canada Special Paper 40, p. 343–371.
- Spiess, F.N., Macdonald, K.C., Atwater, T., Ballard, R., Carranza, A., Cordoba, D., Cox, C., Diaz Garcia, V.M., Francheteau, J., Guerrero, J., Hawkins, J., Haymon, R., Hessler, R., Juteau, T., Kastner, M., Larson, R., Luyendyk, B., Macdougall, J.D., Miller, S., Normark, W., Orcutt, J., and Rangin, C., 1980, East Pacific Rise—Hot springs and geophysical experiments: *Science*, v. 207, no. 4438, p. 1421–1433.
- Stanton, R.L., 1959, Mineralogical features and possible mode of emplacement of the Brunswick Mining and Smelting orebodies, Gloucester County, N.B.: *Canadian Institute of Mining and Metallurgy Transactions*, v. 62, p. 631–643.
- Stanton, R.L., 1984, Investigations of the Appalachian-Caledonide ore province and their influence on the development of stratiform ore genesis theory—A short historical review: *Economic Geology*, v. 79, p. 1428–1441.
- White, D.E., Anderson, E.T., and Grubbs, D.K., 1963, Geothermal brine well—Mile deep drill hole may tap ore-bearing magmatic water and rocks undergoing metamorphism: *Science*, v. 139, p. 919–922.
- Zierenberg, R.A., Fouquet, Y., Miller, D.J., Bahr, J.M., Baker, P.A., Bjerksgarden, T., Brunner, C.A., Duckworth, R.C., Gable, R., Gieskes, J.M., Goodfellow, W.D., Groeschel-Becker, H.M., Guerin, G., Ishibashi, J., Iturrino, G.J., James, R.H., Lackschewitz, K.S., Marquez, L.L., Nehlig, P., Peter, J.M., Rigsby, C.A., Schultheiss, P.J., Shanks, W.C., III, Simoneit, B.R.T., Summit, M., Teagle, D.A.H., Urbat, M., and Zuffa, G.G., 1998, The deep structure of a sea-floor hydrothermal deposit: *Nature*, v. 392, no. 6675, p. 485–488.

4. Regional Environment

By Klaus J. Schulz

4 of 21

Volcanogenic Massive Sulfide Occurrence Model

Scientific Investigations Report 2010–5070–C

U.S. Department of the Interior
U.S. Geological Survey

U.S. Department of the Interior
KEN SALAZAR, Secretary

U.S. Geological Survey
Marcia K. McNutt, Director

U.S. Geological Survey, Reston, Virginia: 2012

For more information on the USGS—the Federal source for science about the Earth, its natural and living resources, natural hazards, and the environment, visit <http://www.usgs.gov> or call 1-888-ASK-USGS.

For an overview of USGS information products, including maps, imagery, and publications, visit <http://www.usgs.gov/pubprod>

To order this and other USGS information products, visit <http://store.usgs.gov>

Any use of trade, product, or firm names is for descriptive purposes only and does not imply endorsement by the U.S. Government.

Although this report is in the public domain, permission must be secured from the individual copyright owners to reproduce any copyrighted materials contained within this report.

Suggested citation:

Schulz, K.J., 2012, Regional environment in volcanogenic massive sulfide occurrence model: U.S. Geological Survey Scientific Investigations Report 2010-5070 -C, chap. 4, 24 p.

Contents

| | |
|--|----|
| Geotectonic Environment..... | 37 |
| Mid-Ocean Ridges and Mature Back-Arc Basins (Mafic-Ultramafic Lithologic Association)..... | 37 |
| Sediment-Covered Ridges and Related Rifts (Siliciclastic-Mafic Lithologic Association)..... | 39 |
| Intraoceanic Volcanic Arcs and Related Back-Arc Rifts (Bimodal-Mafic Lithologic Association)..... | 41 |
| Continental Margin Arcs and Related Back-Arc Rifts (Bimodal-Felsic and Felsic-Siliciclastic Lithologic Associations)..... | 42 |
| Temporal (Secular) Relations..... | 43 |
| Duration of Magmatic-Hydrothermal System and Mineralizing Processes..... | 43 |
| Relations to Structures..... | 45 |
| Relations to Igneous Rocks..... | 49 |
| Flow Lithofacies Association..... | 50 |
| Volcaniclastic Lithofacies Association..... | 50 |
| Relations to Sedimentary Rocks..... | 52 |
| Relations to Metamorphic Rocks..... | 52 |
| References Cited..... | 53 |

Figures

| | |
|---|----|
| 4-1. Schematic diagram showing volcanogenic massive sulfide deposits in divergent and convergent plate tectonic settings..... | 38 |
| 4-2. Schematic diagram showing proposed hydrothermal fluid flow at a fast- spreading ridge..... | 38 |
| 4-3. Structural map of the Gulf of California showing the extent of newly accreted oceanic crust in extensional basins along an extension of the East Pacific Rise..... | 40 |
| 4-4. Histograms showing number of volcanogenic massive sulfide deposits and contained metal of Cu+Zn+Pb in million tonnes..... | 44 |
| 4-5. Schematic diagram showing examples of the different structural settings of hydrothermal vents relative to faults and breakdown regions..... | 46 |
| 4-6. Model for fluid circulation and types of hydrothermal venting related to the development of detachment faults along slow-spreading mid-ocean ridges..... | 47 |
| 4-7. Conceptual diagram showing the evolution of a caldera-related submarine magmatic-hydrothermal system..... | 48 |
| 4-8. Composite stratigraphic sections illustrating flow, volcaniclastic, and sediment dominated lithofacies that host volcanogenic massive sulfide deposits..... | 51 |

4. Regional Environment

By Klaus J. Schulz

Geotectonic Environment

Volcanogenic massive sulfide (VMS) deposits are formed in marine tectonic settings where a strong spatial and temporal relationship exists between magmatism, seismicity, and high-temperature hydrothermal venting. These settings include extensional oceanic seafloor spreading ridges, volcanic arcs (oceanic and continental margin), and related back-arc basin environments (fig. 4–1). In addition, extensional environments may form in post-accretion and (or) successor arc settings (rifted continental margins and strike-slip basins). Volcanogenic massive sulfide deposits in Proterozoic and Phanerozoic sequences can generally be assigned to specific plate tectonic regimes, with all but the siliciclastic-felsic type represented by modern analogs (table 2–1). However, the assignment of deposits in Archean terranes is less certain, as the role of conventional plate tectonic systems in early earth history continues to be debated (Condie and Pease, 2008). Thus, although Archean VMS deposits can be classified by the relative amounts of associated mafic, felsic, and sedimentary rock, such classification does not necessarily correspond to modern plate tectonic settings. However, because plate tectonic processes appear to have operated at least since the Paleoproterozoic and possibly earlier, the geotectonic environments of VMS deposits are described below in the context of modern plate tectonic regimes.

In the modern oceans, the majority of known hydrothermal activity is located along mid-ocean ridges (65 percent), with the remainder in back-arc basins (22 percent), along volcanic arcs (12 percent), and on intraplate volcanoes (1 percent) (Baker and German, 2004; Hannington and others, 2004), but this distribution is likely biased by ridge-centric exploration driven by programs such as Ridge and InterRidge. In contrast, most VMS deposits preserved in the geologic record appear to have formed in extensional oceanic and continental volcanic arc and back-arc settings like the Miocene Japan arc–back-arc system and the modern Okinawa Trough and Lau and Manus Basins (Allen and others, 2002; Franklin and others, 2005). The general paucity in the geologic record of VMS deposits that formed on mid-ocean ridges likely reflects subduction and recycling of ocean floor crust since at least the Paleoproterozoic; the crust of the present ocean floor is no older than 180 million years (m.y.).

Although VMS deposits formed on mid-ocean ridges are rarely preserved in the geologic record, study of the volcanic, tectonic, and hydrothermal processes occurring at modern ridge crests forms much of the basis for current models of VMS-forming hydrothermal systems (Hannington and others, 2005). High-temperature (350 °C) black smoker vents, first discovered on the East Pacific Rise in 1979 (Francheteau and others, 1979; Speiss and others, 1980), are the most recognizable features of seafloor hydrothermal activity and are most common on intermediate- to fast-spreading mid-ocean ridges. Studies of black smokers continue to provide important information on the geodynamic and chemical processes that lead to the formation of seafloor hydrothermal systems; however, because of their inaccessibility, important questions about their formation and evolution remain, including the three dimensional structure of seafloor hydrothermal systems and the source(s) of heat driving high-temperature fluid circulation. These aspects of VMS-forming systems, as well as the regional architecture of the volcanic sequences hosting deposits, are more easily investigated through detailed and regional-scale studies of ancient VMS environments (for example, Galley, 2003). However, interpretations of the setting of ancient VMS deposits can be difficult, particularly when they are present in tectonically deformed slivers in an orogen.

The tectonic settings described below represent end-member types; many natural settings are transitional in some respects between these settings (for example, a volcanic arc and related back-arc basin may change laterally from continental to oceanic).

Mid-Ocean Ridges and Mature Back-Arc Basins (Mafic-Ultramafic Lithologic Association)

The present global mid-ocean ridge system forms a submarine mountain range more than 50,000 kilometers (km) long and that averages about 3,000 meters (m) above the abyssal seafloor. Different types of ridges are discriminated on the basis of spreading rate and morphology, which vary in response to regional tectonic stresses and rates of magma supply (Sinha and Evans, 2004; Hannington and others, 2005). These factors also influence the size and vigor of hydrothermal convection systems on ridges, and there is a general positive correlation between increasing spreading rate and the

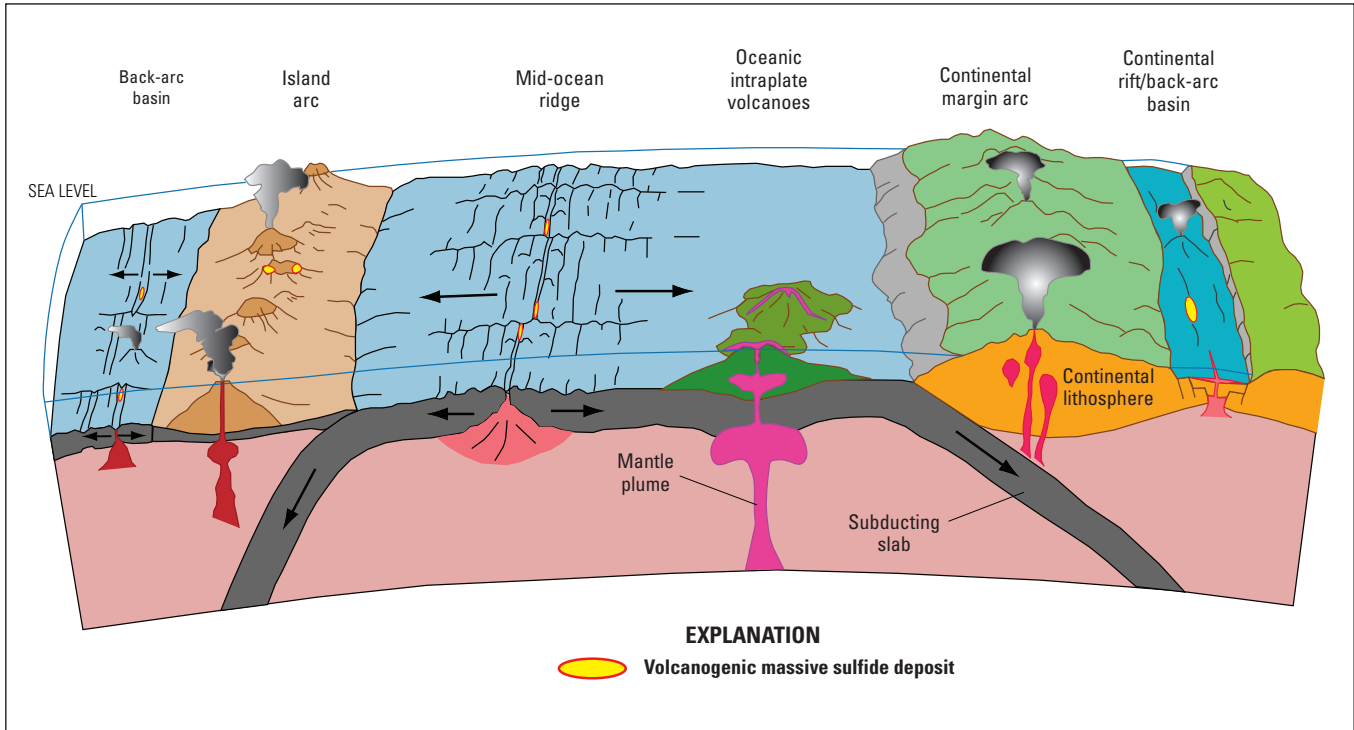


Figure 4-1. Schematic diagram showing volcanogenic massive sulfide deposits in divergent (mid-ocean ridge and back-arc basin) and convergent (subduction related island arc and continental margin arc) plate tectonic settings. Modified from Schmincke (2004) and Galley and others (2007).

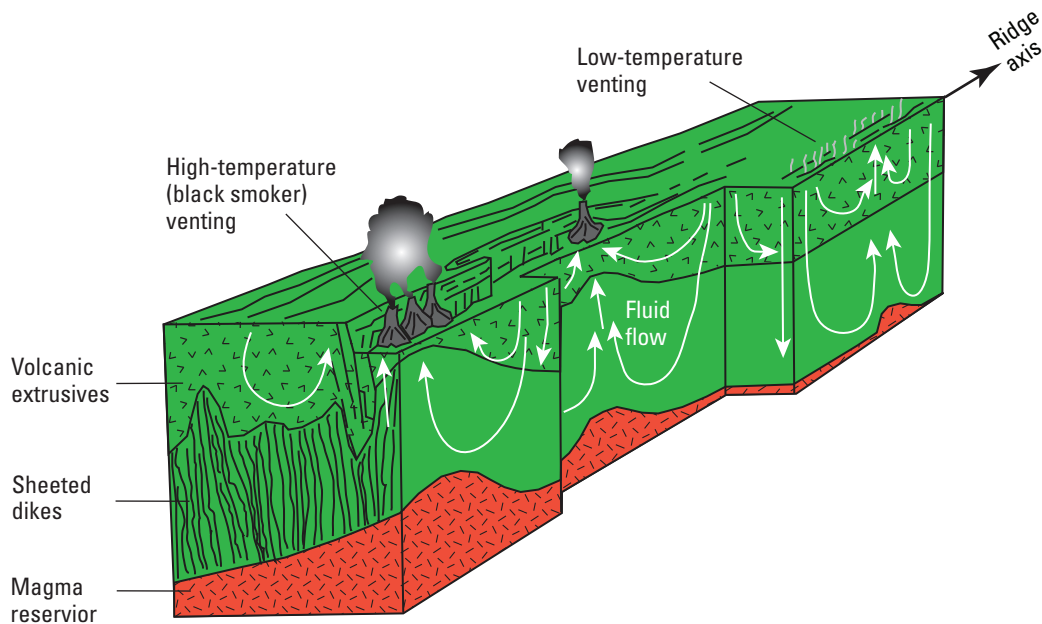


Figure 4-2. Schematic diagram showing proposed hydrothermal fluid flow at a fast-spreading ridge (for example, East Pacific Rise). Note that high-temperature (black smoker) vents occur above shallower segments of the axial magma reservoir. Modified from Haymon and others (1991).

incidence of hydrothermal venting (Baker and others, 1996; Baker, 2009).

At fast-spreading centers (full spreading rates of 6 to ≥ 10 centimeters per year [cm/yr]) such as the East Pacific Rise, high-temperature fluids circulate to relatively shallow depths (1–2 km) (fig. 4–2), owing to the intermittent presence of magma in shallow subaxial chambers, and venting correlates closely with the areas of most recent volcanic eruptions. However, the deposits formed on fast-spreading centers tend to be small (less than a few thousand tons) because frequent eruptions tend to disrupt the flow of hydrothermal fluids and bury sulfide accumulations, and because the vent complexes are rapidly displaced from their heat source by the fast spreading rate (Hannington and others, 2005). Intermediate-rate spreading centers (4–6 cm/yr), such as the Juan de Fuca and Gorda Ridge systems and the Galapagos Rift in the eastern Pacific Ocean, are characterized by lower rates of magma supply, deeper axial valleys, and greater structural control on hydrothermal fluid upflow than at fast-spreading ridges. Intermediate-rate spreading centers have some of the largest known vent fields, with venting commonly focused along the rift valley walls or in axial fissure zones. For example, the Endeavour segment of the Juan de Fuca Ridge has 50–100 black smokers located in six evenly spaced vent fields, 2–3 km apart, along a 15-km segment of the axial valley (Delaney and others, 1992; Kelley and others, 2001). Slow-spreading ridges (1–4 cm/yr) like the Mid-Atlantic Ridge between 13° and 15°N, are characterized by low rates of magma supply and only intermittent local eruptions of basalt. These ridges show evidence of vigorous tectonic extension characterized by large amounts of rotation on normal faults and exposures of intrusive gabbros and serpentinized ultramafic rocks in core complexes formed by detachment faulting (Escartin and others, 2008; Smith and others, 2008). At several locations along the Mid-Atlantic Ridge, black smokers and massive sulfide deposits, some characterized by enrichments in Ni, Co, and platinum group elements, occur on top of serpentinized ultramafic rocks representing exposed mantle (Krasnov and others, 1995; Bogdanov and others, 1997; McCaig and others, 2007). As shown by the TAG hydrothermal field on the Mid-Atlantic Ridge, large, long-lived hydrothermal systems can develop on slow-spreading ridges (Kleinrock and Humphris, 1996; Humphris and Tivey, 2000; Petersen and others, 2000).

Because ocean basins and their contained ridges compose more of the Earth's surface (approx. 48 percent) than any other crustal type, submarine volcanic rocks are the most widespread and abundant near-surface igneous rocks on Earth, and about 80 percent or more of these rocks are basalt generated at mid-ocean ridges. Basalts that form mid-ocean ridge crust (MORB) are dominantly subalkaline tholeiitic basalt characterized by depletions in thorium (Th), uranium (U), alkali metals, and light rare earth elements (NMORB; Viereck and others, 1989) relative to ocean island and continental basalts and have distinctive isotopic characteristics (Hofmann, 2003). Some intermediate- and slow-spreading centers have more evolved magma compositions (ferrobasalt and andesite) that reflect fractional crystallization, magma mixing, and (or) local crustal assimilation at shallow to intermediate depths

(Perfit and others, 1999). In addition, some spreading centers (for example, portions of the Juan de Fuca Ridge system) also have enriched tholeiitic basalts (EMORB) with elevated concentrations of incompatible trace elements (for example, Ba, Cs [cesium], Rb [rubidium], Th, U, K [potassium], light rare earths); these enrichments also may be reflected in the composition of hydrothermal fluids and sulfide deposits at these locations (Hannington and others, 2005). Although most ancient ocean floor appears to have been subducted over time, rare obducted remnants, such as the Ordovician Bay of Islands ophiolite in Newfoundland (Bédard and Hébert, 1996), are present in some orogens. However, most ophiolites are fragments of extensional arc and back-arc basins formed in supra-subduction zone settings (Pearce, 2003). Although few ancient examples of VMS deposits formed on mid-ocean ridges are known, those formed at spreading centers in suprasubduction zone settings (mafic-ultramafic association) include deposits in the Troodos complex, Cyprus (for example, Mavrovouni deposit; Galley and Koski, 1999); the Oman ophiolite, Oman (for example, Lasail deposit; Alabaster and Pearce, 1985); the Løkken ophiolite in central Norway (for example, Løkken deposit; Grenne, 1989); the Betts Cove ophiolite, Newfoundland (for example, Betts Cove deposit; Sangster and others, 2007); and the Josephine ophiolite, Orogen (for example, Turner Albright deposit; Zierenberg and others, 1988).

Sediment-Covered Ridges and Related Rifts (Siliciclastic-Mafic Lithologic Association)

Active spreading centers that become proximal to continental margins through subduction of ocean crust (Juan de Fuca and Gorda Ridge systems), ridge propagation and development of a continental margin rift (East Pacific Rise in the Gulf of California) (fig. 4–3), or more complex plate tectonic processes (Red Sea) can experience high rates of sedimentation by major rivers involving hemipelagic muds and (or) clastic sediments derived from adjacent continental crust. Today, about 5 percent of the world's active spreading centers are covered by sediment from nearby continental margins, including portions of the Juan de Fuca and Gorda Ridges in the northeast Pacific and the northern East Pacific Rise in the Gulf of California (Hannington and others, 2005). The high rates of sedimentation at these sites (10–100 cm/1,000 yr versus 1 cm/1,000 yr in the open ocean) result in thick sedimentary sequences that provide an effective density barrier to the eruption of relatively dense basalt on the seafloor. As a result, volcanic eruptions are rare at sedimented ridges, but subseafloor intrusions forming sill-sediment complexes are common (Einsele, 1985). Venting of high temperature hydrothermal fluids may occur around the margins of the buried sills, as in Middle Valley, the Escanaba Trough, and the Guaymas Basin today (Hannington and others, 2005). Although the sills may be partly responsible for driving hydrothermal circulation, high-temperature fluids mainly appear to originate in the volcanic basement where they are intercepted

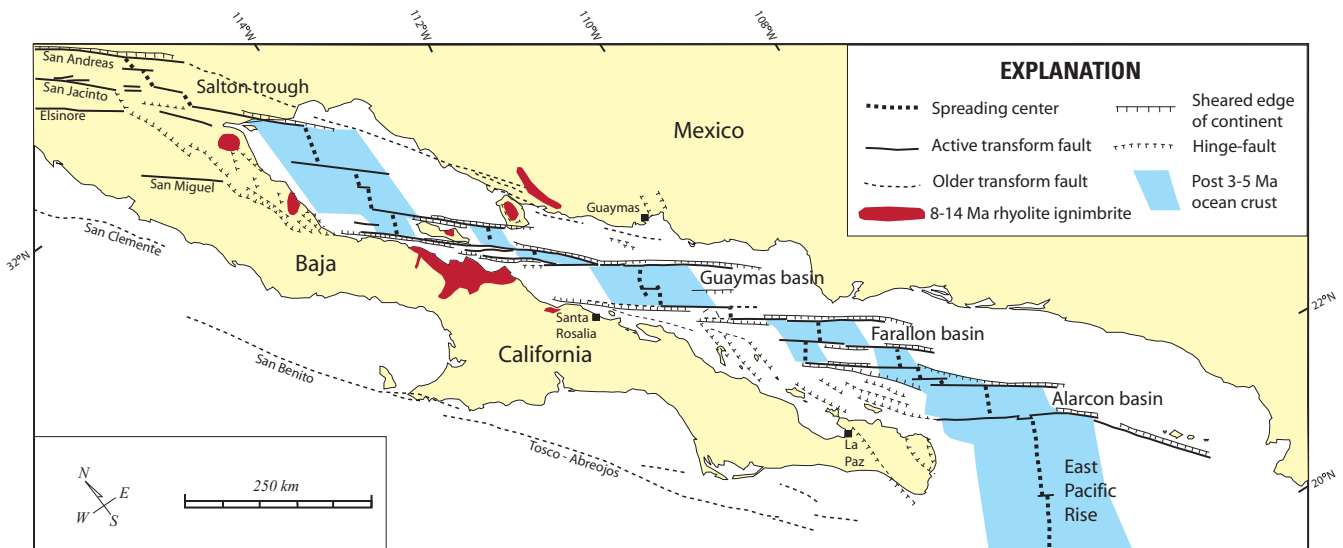


Figure 4-3. Structural map of the Gulf of California showing the extent of newly accreted oceanic crust in extensional basins (for example, Alarcon, Farallon, and Guaymas basins) along an extension of the East Pacific Rise. Massive sulfide mineralization is present in the Guaymas basin (Lonsdale and Becker, 1985). Modified from Lonsdale (1989).

along their flow path by basement highs and focused upward along growth faults or buried intrusions. At these sites, metals may be mainly deposited below the seafloor by replacement of the host sediment, resulting in sulfide deposits that are typically larger than deposits formed on bare mid-ocean ridges (Hannington and others, 2005). Also, because the high-temperature fluids may interact with continentally-derived clastic sediments as well as ocean crust, the sulfide deposits formed at sediment-covered ridges typically have different proportions of base and precious metals, particularly higher Pb and Ag contents (Franklin and others, 2005; Hannington and others, 2005). In some cases where rifting has resulted from propagation of an oceanic spreading axis into continental crust or from upwelling of the asthenosphere (for example, Red Sea), peralkaline rhyolites and transitional or alkaline basalts may be present in addition to the subalkaline suite (Barrett and MacLean, 1999).

Examples of ancient VMS deposits that appear to have formed in a sediment-covered ridge setting include the Triassic Windy Craggy deposit, Canada (Peter and Scott, 1999); the late Paleozoic Besshi deposit, Japan (Slack, 1993); the Neoproterozoic Ducktown deposit, United States (Slack, 1993); and the Miocene Beatson deposit, United States (Crowe and others, 1992).

Intraoceanic Volcanic Arcs and Related Back-Arc Rifts (Bimodal-Mafic Lithologic Association)

Volcanic arcs are curved chains of volcanoes that are convex toward the adjacent oceanic basin and separated from it by a deep submarine trench. Intraoceanic arcs have oceanic crust on either side and may overlie older arc volcanics, remnants of oceanic crust, and intrusive mafic-ultramafic bodies. Early intraoceanic arc volcanism is typically tholeiitic low-titanium (Ti) island-arc basalt and boninite (high-magnesium [Mg] andesite) (Stern and Bloomer, 1992; Pearce and Peate, 1995), but the summit calderas of the largest volcanoes commonly contain more silicic low-K volcanic rocks, including relatively abundant rhyolite pumice and postcaldera dacite-rhyolite lava domes (Fiske and others, 2001; Smith and others, 2003; Graham and others, 2008). Recent studies of several intraoceanic arcs in the western Pacific show that the overall volcanism is bimodal, with 30–50 percent of arc construction being dacitic to rhyolitic (≥ 63 weight percent [wt%] SiO_2) (Graham and others, 2008). As the arcs evolve, volcanism tends to become more andesitic and calc-alkaline. The tholeiitic island-arc basalts are mostly high-aluminum (Al) (≥ 16.5 wt% Al_2O_3) and are the product of partial melting of the mantle caused by the addition of H_2O and other volatiles to the sub-arc mantle through dehydration of subducting sediments and hydrated oceanic crust. The basalts differ from MORB by having (1) higher and more variable H_2O contents, (2) enrichments of large ion lithophile elements such as Cs, Rb, K, Ba, Pb, and Sr (strontium), and (3) relative depletions in high field strength

elements, particularly Nb (niobium) and Ta (tantalum) (Pearce and Peate, 1995). These compositional characteristics are broadly consistent with the selective transport of elements by aqueous fluids derived from subducting sediments and oceanic crust. The felsic volcanic rocks associated with these intraoceanic arc volcanoes are generally highly vesicular and glassy, indicating degassing at depth and rapid cooling after mainly pyroclastic eruption during caldera formation (Graham and others, 2008). In addition, wide-angle seismic studies of some arcs indicate midcrustal layers with distinctive P-wave velocities that are interpreted as felsic intrusions (Crawford and others, 2003; Kodaira and others, 2007). The large volumes of silicic rocks present in intraoceanic arcs as well as their compositional heterogeneity, even from the same center, suggest that the silicic magmas are the result of dehydration melting of underplated arc material (Smith and others, 2003; Tamura and others, 2009).

Intraoceanic back-arc basins (regions of extension at convergent plate margins where rifting and, in some cases, seafloor spreading develops in the overriding plate) typically develop during periods of oceanward migration and sinking of the subducting plate (that is, slab rollback) and may accompany or follow episodes of arc extension and rifting (Clift and others, 1994; Marsaglia, 1995). The early rift phase of back-arc basin formation is characterized by development of structural grabens separated along strike by chains of volcanoes and structural highs (Taylor and others, 1991). Volcanism is bimodal, with predominantly basalt lava flows and cones and minor dacite and rhyolite lava flows in submarine calderas. Large quantities of volcanoclastic sediment derived from adjacent arc volcanoes may be deposited in the developing back-arc grabens (Clift and others, 1994). As extension continues and back-arc basins mature, seafloor spreading may commence with development of a spreading center similar to a mid-ocean ridge. Volcanism along the back-arc basin spreading center is tholeiitic basalt similar to MORB but is typically characterized by enrichments in large ion lithophile elements (for example, Cs, Rb, Ba, Th) and relative depletions in high field strength elements, particularly Nb and Ta (Pearce and Stern, 2006). These compositional attributes are attributed to interaction between the mantle and a component derived from the subducting slab of the arc system. The subduction signature of the back-arc basin basalts (BABB) tends to be greatest early in the evolution of the basin, when the spreading center is in closest proximity to the arc, and tends to diminish as the basin grows (Hawkins, 1995). High-temperature hydrothermal vents are commonly associated with back-arc volcanoes and spreading centers (Hannington and others, 2005).

The classic examples of modern intraoceanic arc-back-arc systems are the Izu-Bonin-Mariana arc and back-arc trough and the Lau Basin and Tonga-Kermadec arc and back-arc basin in the western Pacific (R.N. Taylor and others, 1992; Ewart and others, 1998). In both arc systems, early arc volcanism consists of low-K basaltic pillow lavas, hyaloclastite, and interbedded calcareous sediments. These rocks are overlain by strata cones consisting of basalt to andesite lavas and

volcaniclastic deposits (Smith and others, 2003). Some larger volcanoes have experienced explosive caldera-forming eruptions involving dacitic to rhyolitic pyroclastics that occurred at depths of at least 1,500 m (see Fiske and others, 2001; Smith and others, 2003). High-temperature hydrothermal venting is present in many of the calderas (de Ronde and others, 2003) and is typically localized along caldera walls or on postcaldera felsic domes (Fiske and others, 2001; Wright and others, 2002). The venting generally occurs at shallower water depths than that on mid-ocean ridges or back-arc spreading centers (Hannington and others, 2005), resulting in widespread boiling and hydrothermal fluids venting at generally lower temperatures. In addition, the presence of sulfur-rich fumaroles and low-pH vent fluids provides evidence of the direct input of magmatic volatiles to the hydrothermal fluids. At least some of these intraoceanic arc hydrothermal systems appear to be transitional to magmatic-hydrothermal systems in subaerial arc volcanoes and are characterized by distinctive polymetallic sulfides and Au-Ag-barite-rich deposits (Hannington and others, 1999).

High-temperature hydrothermal vents are present in the back-arc basins associated with both the Izu-Bonin-Mariana and Tonga-Kermadec arc systems. In the Mariana Trough, high-temperature hydrothermal activity occurs both at an axial volcano along the back-arc spreading center and at a number of back-arc volcanoes immediately behind the arc front (Ishibashi and Urabe, 1995; Stuben and others, 1995). In the Lau Basin behind the Tonga arc, black smoker activity resembling typical mid-ocean ridge hydrothermal vents occurs on the northern Lau spreading center and is hosted by typical MORB basalt. In contrast, vent activity in the south Lau Basin is hosted mainly by arclike andesite and deposits contain abundant barite, as well as much higher Pb, As, Sb, Ag, and Au (Hannington and others, 1999). The north to south change in the nature of back-arc magmatism and black smoker activity in the Lau Basin corresponds with (1) a significant change in width of the basin from about 600 km in the north to only about 200 km in the south, (2) a decrease in the spreading rate from about 10 cm/yr in the north to about 4 cm/yr in the south, (3) a decrease in axial water depth from 2,300–2,400 m in the north to about 1,700 m in the south, and (4) a decrease in the distance of the back-arc spreading center to the active arc, which approaches to within about 20 km of the arc in the southern part of the basin (Hannington and others, 2005).

Although high-temperature hydrothermal vents and massive sulfide deposits are present in some volcanoes at the front of intraoceanic arcs, these deposits are expected to be relatively small because of smaller hydrothermal circulation cells related to small, shallow magma chambers beneath the summit calderas of the stratovolcanoes (Hannington and others, 2005). The presence of abundant pyroclastic deposits formed during explosive eruption events in these submarine arc volcanoes (Fiske and others, 1998, 2001) also suggests that the hydrothermal systems would experience frequent disruptions. In addition, shallow water depths and lower confining pressures at the summits of these arc volcanoes can result in

subseafloor boiling and development of vertically extensive stockwork mineralization rather than development of large seafloor massive sulfide deposits. From recent studies of intraoceanic volcanic arcs and related back-arc rift systems, as well as from comparisons with the geologic record, it appears that the potential for the formation of large massive sulfide deposits is greatest behind the arc (that is, associated with arc rifting and back-arc development) rather than at the volcanic front (Hannington and others, 2005).

Ancient examples of VMS deposits that are interpreted to have formed in intraoceanic volcanic arc–back-arc settings include the Archean Kidd Creek deposit, Canada (Barrie and others, 1999); the Paleoproterozoic Crandon deposit, United States (DeMott, 1994); the Ordovician Bald Mountain deposit, United States (Schulz and Ayuso, 2003); the Permo-Triassic Kutcho Creek deposit, Canada (Barrett and others, 1996); and the Jurassic-Cretaceous Canatuan deposit, Philippines (Barrett and MacLean, 1999).

Continental Margin Arcs and Related Back-Arc Rifts (Bimodal-Felsic and Felsic-Siliciclastic Lithologic Associations)

Submarine magmatic arcs and related back-arc basins that develop in a basement of extended continental crust, pre-existing arc crust, or entirely in a basement of continental crust (continental margin arc–back-arc system) are characterized by increased amounts of felsic volcanic rocks and more complex chemistry of both arc and back-arc magmas, which can range from MORB-like basalt compositions to medium and high-K calc-alkaline and shoshonitic andesite, dacite, and rhyolite (Barrett and MacLean, 1999). In addition, there can be considerable overlap of magma sources, which can result in arclike magmas being erupted in the back-arc region. Particularly in continental margin arcs and back-arcs, the abundance of felsic volcanic rocks may reflect both greater extents of fractional crystallization of magmas trapped in thickened crust and direct partial melting of continental crust. Because of their proximity to continental crust, continental margin arc–back-arc systems also can receive large amounts of siliceous clastic sediment.

The modern Okinawa Trough and Ryukyu arc south of Japan are examples of a continental back-arc rift and margin arc, respectively. In this region, oblique northward subduction of the Philippine Sea plate has led to development of a back-arc basin that varies in width from about 230 km in the north to only 60–100 km in the south. In the north, the basin is characterized by diffuse extensional faulting and water depths of only a few hundred meters. In contrast, the central part of the Okinawa Trough consists of several en echelon grabens 50–100 km long and 10–20 km wide at water depths up to 2,300 m. The variation in depth and style of rifting corresponds with major differences in crustal thickness, which ranges from 30 km in the north to only 10 km in the south (Sibuet and others, 1995). Also varying from north to south is the thickness of sedimentary cover, which is up to 8 km in the

north but only about 2 km in the south. The individual grabens in the central Okinawa Trough contain a number of volcanic ridges or elongate volcanoes composed of a bimodal calc-alkaline suite of vesicular basalt, andesite, and rhyolite (Shinjo and Kato, 2000). Hydrothermal activity is widespread around the volcanic ridges, but the largest vent field (JADE) is located in a structural depression (Izena cauldron) floored by basalt and andesite with local dacite and rhyolite lava domes and a cover of rhyolite pumice and mudstone (Halbach and others, 1989). Polymetallic sulfides in the JADE field are distinctly rich in Pb, As, Sb, Hg, Ag, Au, and Ba (Halbach and others, 1993).

Ancient examples of VMS deposits that are interpreted to have formed in continental margin arc-back-arc settings include the Miocene Kuroko deposits in Japan (Ohmoto and Skinner, 1983); the Ordovician Brunswick No. 12 and other deposits in the Bathurst mining camp, Canada (Goodfellow and McCutcheon, 2003); the Jurassic Eskay Creek deposit, Canada (Barrett and Sherlock, 1996); and deposits in the Devonian-Mississippian Bonnifield district, United States (Dusel-Bacon and others, 2004).

Temporal (Secular) Relations

Volcanogenic massive sulfide deposits have formed in extensional submarine volcanic settings that range in age from Paleoproterozoic (3.55 Ga) to Recent, with deposits actively forming today at mid-ocean ridges and oceanic volcanic arcs and back-arc basins. However, deposits are not uniformly distributed through time but are concentrated particularly in late Archean (2.85–2.60 Ga), Paleoproterozoic (2.0–1.7 Ga), Neoproterozoic (900–700 Ma), Cambro-Ordovician (550–450 Ma), Devonian-Mississippian (400–320 Ma), and Early Jurassic to Recent (200–0 Ma) subaqueous volcanic sequences (fig. 4-4A; see also Galley and others, 2007). Similarly, the total tonnage and contained metal content of VMS deposits are concentrated in late Archean (2.85–2.60 Ga), Paleoproterozoic (2.0–1.7 Ga), lower Paleozoic (550–450 Ma), upper Paleozoic (400–320 Ma), and Early Jurassic to Recent (200–0 Ma) sequences (fig. 4-4H). Deposits less than 15 Ma (middle Miocene) are almost all associated with modern ocean settings (Franklin and others, 2005; Mosier and others, 2009), due to limited obduction of younger marine volcanosedimentary sequences onto the continents. The heterogeneous temporal distribution of VMS deposits can be ascribed to the balance between a deposit's formation under specific conditions in particular geodynamic settings and its preservation once formed (Groves and Bierlein, 2007). Most VMS deposits preserved in the geologic record formed in subduction-related oceanic and continental volcanic arc and back-arc settings, and their temporal distribution corresponds closely with periods of major ocean-closing and terrane accretion following the breakup of large continents (Barley and Groves, 1992; Titley, 1993; Groves and others, 2005). However, it is likely that most VMS deposits have been lost from the geologic record either by oxidation at the seafloor or through

accretion, uplift, and erosion in marginal orogenic belts during supercontinent assembly (Barley and Groves, 1992; Groves and others, 2005).

The different VMS deposit types also show temporal variations in abundance (figs. 4-4C-G). Deposits in the bimodal-mafic association are most common in the Archean and Paleoproterozoic, but they are also important constituents in the Mesozoic and Cenozoic. In contrast, deposits in the mafic-ultramafic association are almost all Paleozoic and younger, except for a small group of Paleoproterozoic deposits (fig. 4-4G), reflecting the subduction of most ancient ocean floor along convergent margins. The siliciclastic-mafic and felsic-siliciclastic deposits are mainly Mesozoic, while bimodal-felsic deposits are more evenly distributed although less common in the Precambrian. These variations in deposit types over time also reflect fundamental changes in tectonic style through time, as well as differences in preservation of different tectonic settings (Franklin and others, 2005; Groves and others, 2005). The relatively rare occurrence in the early Precambrian of both siliciclastic-mafic and felsic-siliciclastic deposit types suggests that extensional continent margin tectonic settings were less common during the early evolution of the Earth.

Duration of Magmatic-Hydrothermal System and Mineralizing Processes

Volcanogenic massive sulfide deposits are the product of volcanically generated hydrothermal systems developed at a specific time interval or intervals in the evolution of submarine volcanic sequences. Structural, lithostratigraphic, and geochemical characteristics of these submarine volcanic sequences indicate that they formed during periods of extension. In most arc-related settings, peak extension or rifting is short lived and often marked by the occurrence of high silica volcanic rocks (dacite to rhyolite) and their intrusive equivalents. It is during these short lived periods of extension, typically lasting less than 2 to 3 m.y., that VMS deposits are formed (Franklin and others, 2005).

Two major factors help control the fluid flow, discharge duration, and life span of a VMS-forming hydrothermal system (Schardt and Large, 2009): (1) the nature, depth, and size of the heat source, and (2) the temporal permeability distribution in the rock units and faults. The results of recent numerical computer simulations of ancient and modern VMS systems (see review in Schardt and Large, 2009) suggest that the duration of significant hydrothermal fluid discharge ($T > 150^\circ\text{C}$) can last anywhere from 400 years to $>200,000$ years. These results are comparable to average radiometric dates determined for modern seafloor hydrothermal systems ($<1,000$ to about 250,000 years; Lalou and others, 1995; Scott, 1997). Numerical computer simulations conducted by Schardt and Large (2009) suggest that in a hydrothermal fluid with seawater salinity, 10 parts per million (ppm) Zn+Cu, and a

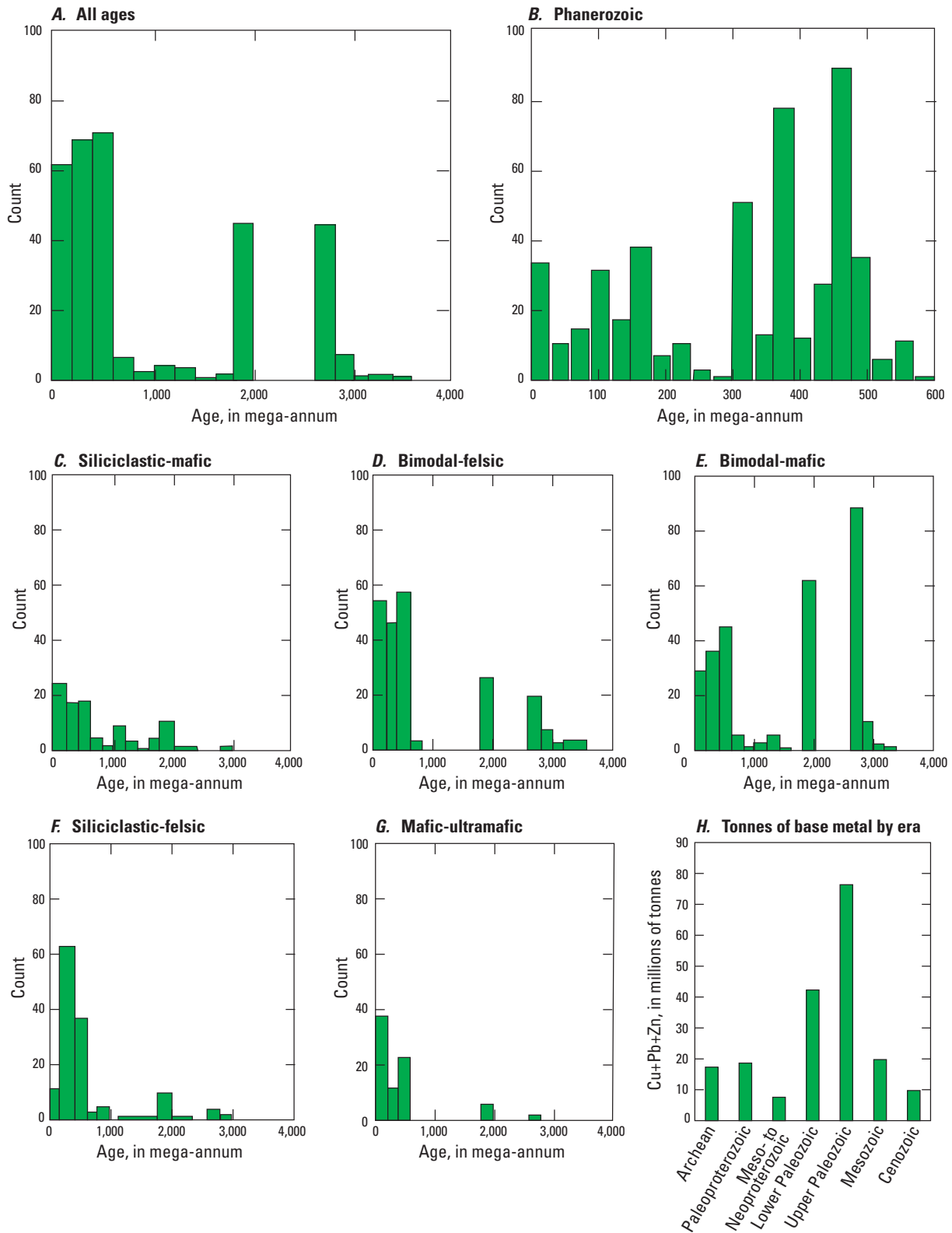


Figure 4-4. Histograms showing (A–G) number of volcanogenic massive sulfide deposits and (H) tonnage of contained metal of Cu + Zn + Pb in million tonnes versus age in million years. Data revised from Mosier and others, 2009. [Cu, copper; Pb, lead; Zn, zinc]

deposition efficiency greater than 10 percent, an average VMS deposit (1.2 Mt total metal) could form within a time frame of less than 5,000 years to as long as 14,000 years, depending on geologic conditions such as temperature and depth of the heat source. Fluids carrying lower amounts of metals are unlikely to deposit sufficient base metals to form an average size deposit, whereas a lower deposition efficiency (<10 percent) would require a much longer time to form such a deposit. Formation of a giant (>1.7 Mt Zn or 2 Mt Cu total metal) and supergiant deposit (>12 Mt Zn or 24 Mt Cu total metal) requires (a) a fluid with a higher metal content in solution (>10 ppm), (b) a deposition efficiency exceeding 10 percent, and (or) (c) a longer time to accumulate sufficient metals. Higher salinity hydrothermal fluids have increased metal-carrying capacity and would improve chances of forming a large base metal deposit.

Studies of the TAG hydrothermal field, located on the slow-spreading Mid-Atlantic Ridge at 26°N, have shown that activity began about 100,000 to 150,000 years ago with low-temperature fluids forming stratiform Mn-oxide deposits (Lalou and others, 1995). High-temperature hydrothermal events, which first started about 100,000 years ago in the Mir zone within the TAG field, have been episodic and generally followed periods of basalt extrusion at an adjacent pillow lava dome. The correlation between the hydrothermal and volcanic events supports the interpretation that episodic intrusions at the volcanic center supplied the heat to drive episodic hydrothermal activity at the adjacent TAG sulfide mound (Rona and others, 1993). The radiometric studies at the TAG field show that hydrothermal venting may be reactivated in the same area and that periods of activity and quiescence may alternate with a periodicity of thousands of years (Lalou and others, 1995).

Relations to Structures

Many VMS deposits occur in clusters or districts about 40 km in diameter that contain about a dozen relatively evenly spaced deposits, one or more of which contains more than half of the district's resources (Sangster, 1980). Controls on the localization of VMS deposits mainly involve volcanic and synvolcanic features. Such features include, but are not limited to, calderas, craters, grabens, and domes; faults and fault intersections; and seafloor depressions or local basins. Identification of these types of controls is generally limited to relatively undeformed deposits with minimal or no postore structural overprint.

In most cases, localization of sulfide mineralization involved structural preparation of a plumbing system including the development of permeable conduits for metalliferous hydrothermal fluids. Faults show the most fracturing around fault tip-lines (breakdown regions), the curvilinear trace of the fault termination, where stresses associated with the displacement gradient are concentrated and drive crack propagation into non-fractured rock (Curewitz and Karson, 1997). Where two or more fault tip-lines are in close proximity, the

individual breakdown regions merge, forming a single, modified breakdown region. Curewitz and Karson (1997) have shown that the structural setting of hydrothermal vents varies based on the geometry of the fault system and the mechanisms that create and maintain permeable pathways for fluid flow (fig. 4–5). Their global survey of hydrothermal vents showed that 78 percent are near faults and 66 percent of the vents at mid-ocean ridges are in fault interaction areas (Curewitz and Karson, 1997). Detailed studies along both fast-spreading mid-ocean ridges (for example, Haymon and others, 1991) and slow-spreading ridges (for example, Kleinrock and Humphris, 1996) confirm the prevalence of hydrothermal venting in areas of fault interaction. In addition, recent studies near slow- and ultraslow-spreading segments of the Mid-Atlantic Ridge have shown that high-temperature black smoker fluids have been focused above low-angle detachment faults (fig. 4–6; McCaig and others, 2007). Intense metasomatic and isotopic alteration in the fault rocks along these detachment structures show that large volumes of fluid have been focused along them resulting in potentially long-lived hydrothermal systems and large massive sulfide deposits (Lalou and others, 1995; McCaig and others, 2007).

The preferential alignment of ancient VMS deposits and their proximity to volcanic vent areas and synvolcanic faults demonstrates a pronounced structural control on their location (for example, Hokuroku district; Scott, 1980). The orientation of synvolcanic faults in extensional environments is controlled by the direction of least principal stress during periods of extension and volcanism (Cox and others, 2001). The principal extensional direction can be subhorizontal and perpendicular to the rift axis or, in more complex cases such as transtensional rifts, oriented oblique to the rift axis (Kleinrock and others, 1997). The synvolcanic faults provide loci for magma migration as well as for hydrothermal fluid discharge. Features useful in identifying synvolcanic faults in ancient volcanic sequences (Franklin and others, 2005) include: (1) local discontinuities in the stratigraphy of footwall sections; (2) diachronous wedges of talus; (3) debris flows that thicken or terminate over a short lateral distance; (4) transgressive alteration zones; (5) synvolcanic dikes and dike swarms, particularly those that terminate in either cryptodomes or at intra-volcanic sedimentary horizons; (6) the location of felsic lava flows, domes, and cryptodomes marking a volcanic center; and (7) the preferential alignment of volcanic vents.

Volcanic collapse structures in submarine settings are mainly calderas, craters, and grabens. For example, recent studies along the Izu-Bonin arc-back-arc system in the western Pacific Ocean have discovered several moderate- to deep-water calderas characterized by rhyolite pumice (Fiske and others, 1998, 2001; Yuasa and Kano, 2003) and hydrothermal massive sulfide mineralization (Ishibashi and Urabe, 1995; Iizasa and others, 1999). Studies have interpreted submarine calderas to be settings for several ancient VMS deposits and districts, based on comparisons with the settings of modern seafloor hydrothermal systems. (see Ohmoto, 1978; Stix and others, 2003; Mueller and others, 2009). Ancient VMS

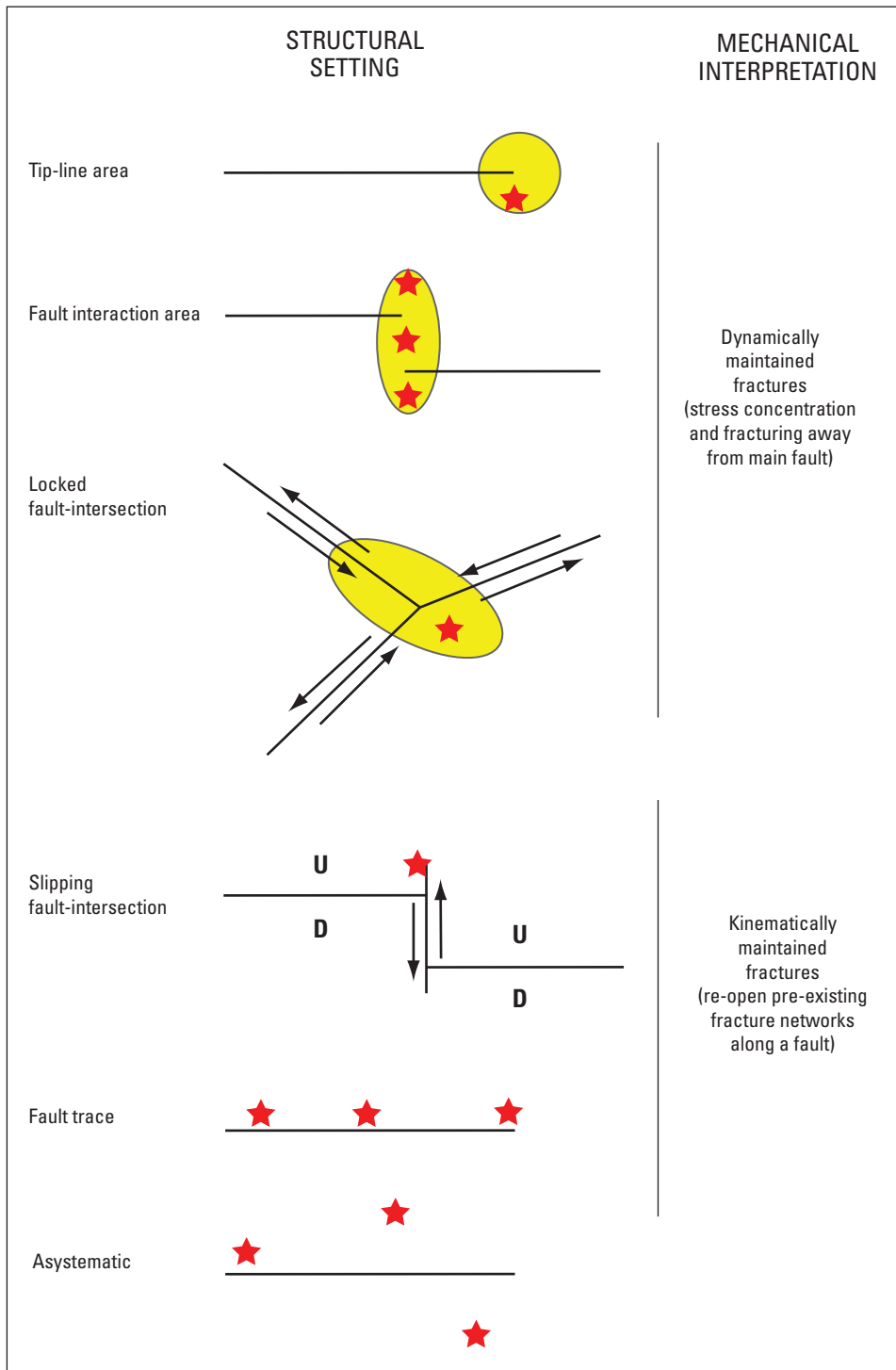


Figure 4-5. Schematic diagram showing examples of the different structural settings of hydrothermal vents (red stars) relative to faults (straight lines) and breakdown regions (yellow shaded areas). In the upper three examples, vents are located in areas of stress concentration and are fracturing away from the main fault (dynamically maintained fractures), while in the next three examples the vents are located along the fault in re-opened, pre-existing fracture networks (kinematically maintained fractures). After Curewitz and Karson (1997).

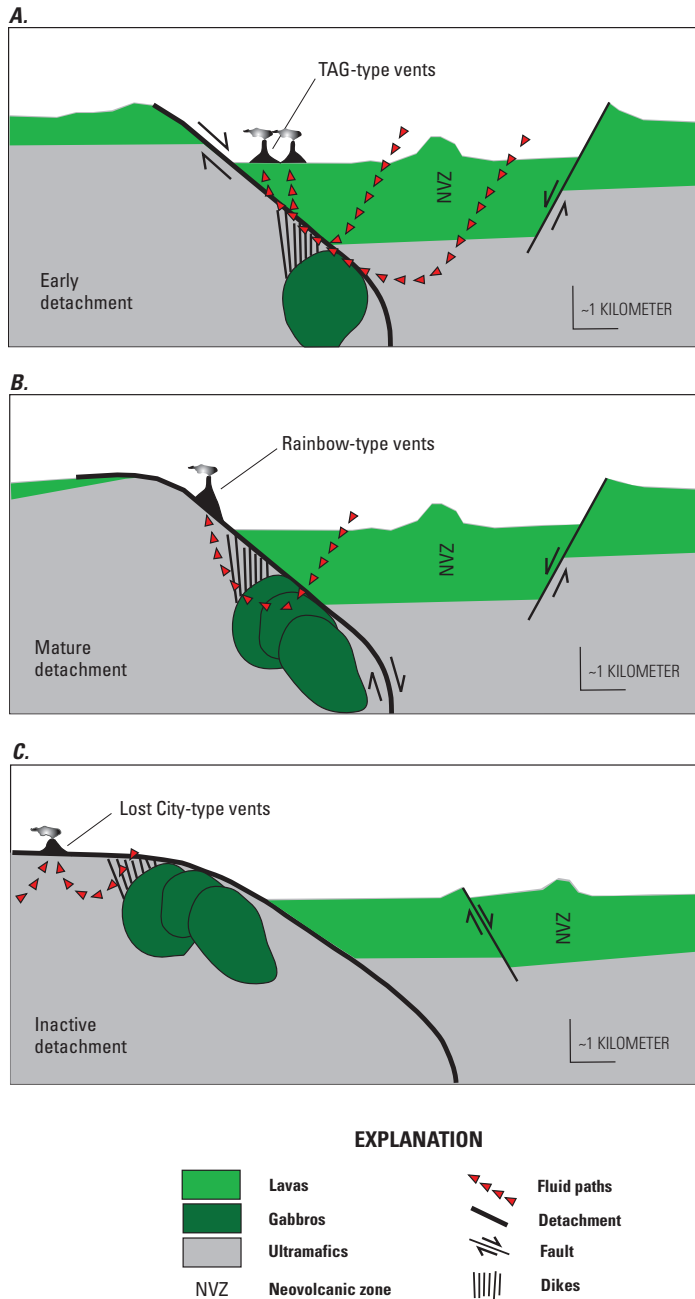


Figure 4-6. Model for fluid circulation and types of hydrothermal venting related to the development of detachment faults along slow-spreading mid-ocean ridges. Modified from McCaig and others (2007). [TAG, Trans-Atlantic Geothermal]

deposits that have interpreted caldera structure settings include those of the Hokuroku district in Japan (Scott, 1980; Ohmoto and Takahashi, 1983), the Sturgeon Lake district in Ontario (Morton and others, 1991; Hudak and others, 2003; Mumin and others, 2007), and the Hunter Mine Group in the Noranda district in Quebec (Mueller and Mortensen, 2002; Mueller and others, 2009). Possible structural controls within such caldera settings include ring faults and their intersections with regional arc or back-arc faults, hinge faults along asymmetric trapdoor-type collapse structures, and volcanic domes and their margins. A volcanic-related graben was evoked by Slack and others (2003) and Busby and others (2003) as having controlled the location and geometry of the thick, bowl-shaped Bald Mountain deposit in Maine. In the Noranda district of Quebec, some massive sulfide orebodies such as Millenbach are localized within former volcanic vents on a series of structurally-aligned rhyolite domes (Knuckey and others, 1982; Gibson and Galley, 2007). A detailed structural analysis by Mumin and others (2007) of VMS deposits within the south Sturgeon Lake caldera, Ontario, showed that massive sulfides occur preferentially along faults and fissures related to the formation of synvolcanic rifts and grabens. The types and styles of favorable structures reflect: (1) the composition, competency, and alteration of the host rocks; (2) the history of synvolcanic tectonism including extension-related collapse; and (3) orthogonal faulting and shearing. In the Golden Grove deposit, Western Australia, a synvolcanic growth fault is inferred by Sharpe and Gemmell (2002) to coincide with the highest grades of Cu (\pm Au) and the thickest zones of massive sulfide, magnetite, and footwall feeder zone mineralization.

The spatial-temporal conditions that control the formation of submarine calderas also may largely determine the size and location of contained VMS deposits (Stix and others, 2003). Field studies and experimental work show that two main types of faults develop during caldera collapse: (1) inner faults, which generally dip outward and accommodate the majority of displacement, and (2) outer, inward-dipping faults associated with late-stage peripheral extension, normal faulting, and down sagging as the caldera collapses (Stix and others, 2003; Kennedy and others, 2004). In areas of extension and transtension, the main caldera faults may not be circular, but instead may be significantly more asymmetric (Kennedy and others, 2004). When these linear and arcuate structures intersect, the resulting fracture system is better developed than in other areas of the caldera and therefore forms particularly favorable sites for hydrothermal circulation and the formation of mineral deposits. In addition, asymmetric calderas formed by subsidence either as a trapdoor along a single hinge fault or as a series of blocks (Heiken and others, 1986; Wohletz and Heiken, 1992) appear to provide structural settings that are particularly favorable for the formation of certain VMS deposits (Mueller and others, 2009). The formation of VMS deposits appears favored

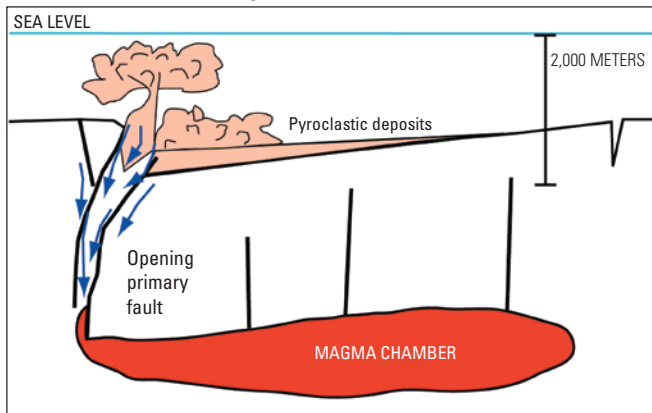
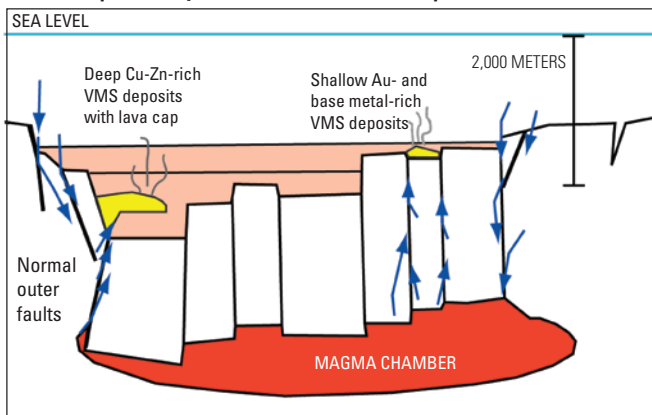
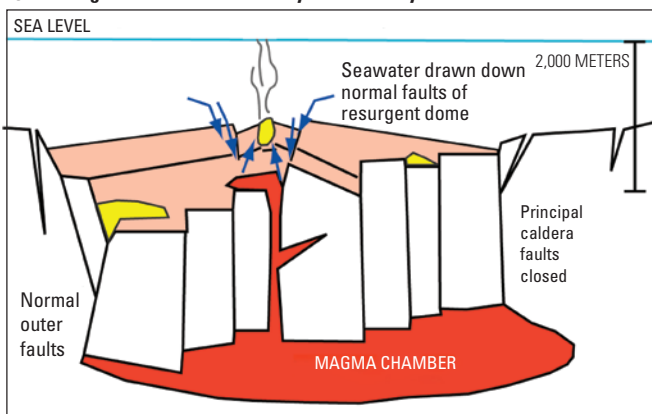
A. Influx of seawater along primary caldera fault**B. Development of hydrothermal cells and VMS deposits****C. Resurgent dome and shallow hydrothermal system**

Figure 4-7. (left) Conceptual diagram showing the evolution of a caldera-related submarine magmatic-hydrothermal system. *A*, Asymmetric collapse of the caldera allows influx of seawater along opening caldera margin fault; erupted pyroclastic deposits pond within the developing asymmetric basin. *B*, Cold seawater flows downward along outer inward-dipping faults, while hot mineralizing fluids move up along a series of outward-dipping faults resulting from piecemeal caldera collapse. As a result, massive sulfide deposits can form in a number of locations and possible water depths within the caldera. *C*, Caldera resurgence, related to renewed magmatism and intrusion into roof rocks above the main magma chamber, is accompanied by the formation of tensional faults as the center of the caldera is uplifted. This permits additional hydrothermal fluid circulation and formation of additional massive sulfide deposits in the central parts of the caldera. Modified from Stix and others (2003). [VMS, volcanogenic massive sulfide; Au, gold; Cu, copper; Zn, zinc]

at two stages of caldera formation (fig. 4-7): (1) during and immediately after caldera collapse and (2) during post-caldera resurgence accompanying re-injections of magma at shallow depth. During the initial subsidence of an asymmetric caldera, a magmatic-hydrothermal system is opened and exposed along the main outward-dipping caldera faults (fig. 4-7A). This opening promotes greater magma degassing and provides opportunity for large influxes of seawater or local meteoric water that may interact directly with the magma reservoir. Over time, the initially deep hydrothermal system migrates upward along inner caldera faults, while simultaneously the hydrothermal system is recharged through the peripheral faults (fig. 4-7B). Metals may be supplied to the hydrothermal fluid directly by magma degassing and by high-temperature leaching from the volcanic rocks. The largest VMS deposits are generally developed in porous pyroclastic deposits adjacent to caldera-bounding faults (Stix and others, 2003; Mueller and others, 2009). During post-caldera resurgence, the injection of new magma can cause uplift of the caldera floor and reactivation of the hydrothermal system as open fluid pathways develop along tensional faults (fig. 4-7C).

Summit calderas on submarine arc-front volcanoes are generally relatively small (<10 km across) and are expected to have only small hydrothermal systems and correspondingly small but potentially high grade massive sulfide deposits (Hannington and others, 2005). However, recent surveys in the western Pacific have shown that such calderas and associated hydrothermal activity are much more common than previously recognized (de Ronde and others, 2007). In addition, calderas are rarely simple constructions because, over time, they can evolve into composite structures, including nested or overlapping caldera complexes (Mueller and others, 2009). In the geologic record, such complex calderas can host major massive sulfide resources (Mueller and others, 2009; Pearson

and Daigneault, 2009). In general, calderas on intraoceanic arc volcanoes are smaller than those developed on continental-margin arc volcanoes (Smith, 1979).

Structural controls also have been proposed for VMS deposits that lack definitive evidence of a caldera setting. For example, in back-arc areas where the crust is actively rifting, large seafloor depressions or cauldrons may develop, such as the DESMOS cauldron in the eastern Manus Basin and the Izena cauldron in the Okinawa Trough (Hannington and others, 2005). The DESMOS cauldron in the eastern Manus Basin north of New Britain is located in extended crust between ridges of vesicular calc-alkaline basalt to rhyolite volcanic rocks. Hydrothermal venting occurs along a 10-km strike length, and drilling has recovered sulfide-impregnated volcanoclastic rocks from the top of a ridge to 380 m below the seafloor. In the central part of the Okinawa Trough, back-arc volcanism and hydrothermal activity occurs within several en echelon grabens. The individual grabens are 50–100 km long, 10–20 km wide, and contain a number of volcanic ridges or elongate volcanoes comprising bimodal vesicular calc-alkaline basalt, andesite, and rhyolite. Hydrothermal activity occurs on or adjacent to the volcanic ridges with the largest vent field (JADE) located in a 5×6-km-wide and 300-m-deep structural depression known as the Izena cauldron. Other examples include the Tambo Grande deposit in Peru, attributed by Tegart and others (2000) to localization in structurally-bound troughs and second-order grabens, and the San Nicolás deposit in Mexico, where syndepositional faults and the steep flank of a rhyolite dome appear to have focused massive sulfide mineralization, according to Johnson and others (2000).

One indirect structural control for VMS deposits is their proximity to large subvolcanic sills, occurring as much as 2,000 m in the footwall of some deposits, which not only provide significant heat to drive hydrothermal systems, but also can increase fracturing of host volcanic strata and focus hydrothermal fluids towards the seafloor (see Galley, 2003; Carr and Cathless, 2008). Heat flow data for modern submarine systems in Guaymas Basin, Gulf of California, further suggest that the hydrothermal fluids are localized in fractures within the sills and along their margins (Lonsdale and Becker, 1985). Finite element modeling to simulate the deposit size and spatial distribution of VMS deposits above the Bell River Complex in the Matagami District in Quebec (Carr and Cathless, 2008) shows that a simple dependence of host rock permeability on temperature localizes hydrothermal upwelling above the intrusive complex and produces a spatial pattern and range of vented fluid volumes similar to that found in the Matagami District. Similarly, three-dimensional modeling of the structure and dynamics of mid-ocean ridge hydrothermal systems has demonstrated that convection cells self-organize into pipeline upflow zones spaced at regular distances of roughly 500 m surrounded by narrow zones of focused and relatively warm downflow (Coumou, and others, 2008). These results closely approximate the regularly spaced high-temperature vents of the Main Endeavour Field on the Juan de Fuca Ridge (Tivey and Johnson, 2002).

Other depositional controls relate mainly to paleotopography. Seafloor depressions, regardless of origin, serve as local basins for the deposition of both chemically and mechanically deposited sulfides. Chemically-precipitated sulfides preferentially accumulate in topographically low areas, especially in cases where the vent fluids are high-salinity brines that are denser than ambient seawater, forming local metalliferous brine pools (see Large, 1992; Solomon, 2008). Seafloor depressions also localize clastic sulfides eroded from sulfide-rich chimneys, mounds, and other edifices. In many deposits, these sulfides consist of sand- to silt-sized polymictic grains that preserve graded bedding and other sedimentary features. Rarely, VMS-derived debris flows contain cobble- to boulder-size clasts of massive sulfide that accumulated in elongate channels that extend as much as 1 km or more along strike from their in situ source, such as in the high-grade, transported orebodies at Buchans, Newfoundland, Canada (Walker and Barbour, 1981; Binney, 1987).

Relations to Igneous Rocks

Volcanogenic massive sulfide deposits form at or near the seafloor in extensional geodynamic settings in spatial, temporal, and genetic association with contemporaneous volcanism. The deposits are often directly hosted by, or occur in, volcanic-dominated sequences, but they also can occur in sediment-dominated sequences in association with periods of volcanic-intrusive activity. In mafic-dominated juvenile environments (for example, mafic-ultramafic, bimodal-mafic, and siliciclastic-mafic lithologic associations), VMS deposits are associated with boninite and low-Ti island-arc tholeiite, mid-ocean ridge basalt (MORB), or back-arc basin basalt (BABB) (Barrett and MacLean, 1999). Felsic rocks in mafic-dominated juvenile settings are typically tholeiitic and relatively depleted in trace elements (Barrett and MacLean, 1999; Hart and others, 2004). In environments associated with continental crust and typically dominated by felsic magmatism (for example, bimodal-felsic and felsic-siliciclastic lithologic associations), VMS-associated mafic rocks can include tholeiitic, calc-alkaline, and alkaline basalts and andesites, with the felsic rocks typically ranging from calc-alkaline dacite-rhyolite to trace element enriched peralkaline compositions (Lentz, 1998; Barrett and MacLean, 1999; Hart and others, 2004). The major relationships between volcanic activity and VMS deposits include: (1) controls on the localization of deposits in volcanic and synvolcanic structures and lithologic units (Gibson and others, 1999); (2) production of high rates of heat advection to the near surface environment that drives seawater convection and fluid-rock interaction in footwall rocks (Schardt and Large, 2009); and (3) contributions of metals and sulfur through reaction of footwall rocks with convecting fluid and (or) directly from magmatic-hydrothermal fluids (de Rhonde, 1995; Yang and Scott, 1996; Franklin and others, 2005; Yang and Scott, 2006).

Studies of modern hydrothermal activity on mid-ocean spreading centers of all spreading rates demonstrate that high-temperature vent fields are almost universally associated with the presence of magma; “hot rock” or nonmagmatic heat sources appear insufficient to generate high-temperature hydrothermal activity (Baker, 2009). In ancient volcanic sequences, composite synvolcanic intrusions are often present in the footwall below VMS deposits and are taken to represent the heat engine that initiated and sustained the subseafloor hydrothermal activity that formed the deposits (Galley, 2003, and references therein). At ocean spreading-ridge settings magma may rise to within a few thousand meters of the seafloor and form elongate gabbroic sills that parallel the seafloor-spreading axis (Stinton and Detrick, 1992; Perk and others, 2007). In settings with pre-existing ocean floor and arc crust, mafic magmas may underplate the crust and produce intermediate to felsic partial melts that form bimodal intrusive/extrusive assemblages (Lentz, 1998). The resulting composite (gabbro-diorite-tonalite-thronthjemite) intrusive complexes may rise to within 2–3 km of the seafloor, while underplating and extension in thicker (20–30 km) crust may result in mid-crustal intrusions (Galley, 2003). Gibson and others (1999) note that, in ancient VMS-hosting sequences, synvolcanic intrusions can be recognized by: (1) their sill-like, composite nature; (2) weak or absent contact metamorphic aureole; (3) similar composition to rocks of the host volcanic sequence; (4) similar, but commonly younger, age; (5) the presence of hydrothermal alteration assemblages similar to those in the host volcanic rocks; and (6) the presence of base metal (Cu, Mo) and (or) gold mineralization.

Volcanogenic massive sulfide deposits bear a close relation to the volcanic lithofacies association that hosts them (Gibson and others, 1999); the rocks of the footwall (and immediate hanging wall) record the environment in which the deposits form and the environment that influenced the deposit morphology, mechanisms of sulfide accumulation and composition, and geometry and mineralogy of alteration assemblages (Gibson and others, 1999; Franklin and others, 2005). In addition, hanging-wall strata provide a record of the duration and termination of the mineralization event and indicate how the deposit was preserved. Three end member lithofacies subdivisions have been defined by Franklin and others (2005) (fig. 4–8): (1) flow lithofacies association, (2) volcanoclastic lithofacies association, and (3) sedimentary lithofacies association (discussed under the “Relations to Sedimentary Rocks” section, this chapter). The associations can be further subdivided into mafic and felsic subtypes, based on the dominant composition of the volcanic rocks.

Flow Lithofacies Association

Flow-dominated successions include coherent ultramafic (komatiitic), mafic, and (or) felsic lava flows and domes and their associated autoclastic deposits (autobreccia, hyaloclastite, and their redeposited equivalents) (fig. 4–8). Synvolcanic

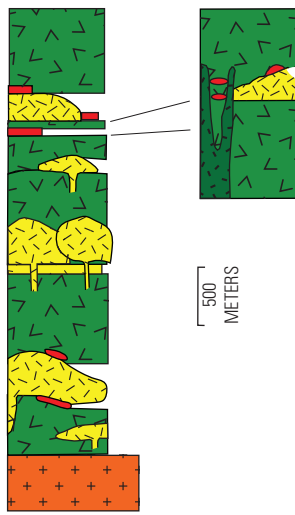
intrusions are common and include dikes, sills, and occasionally cryptodomes (and associated peperite). Volcanoclastic rocks are a minor component and typically consist of redeposited hyaloclastite breccia and some primary pyroclastic deposits. Minor amounts of sedimentary rocks may be present and typically consist of carbonaceous argillite and immature volcanic-derived wacke, minor carbonate, and minor chemical sediments (exhalite, iron-formation).

Flow-dominated successions form volcanic complexes composed of single or composite submarine shield-like volcanoes constructed through effusive eruption processes at depths generally greater than 1,000 m (Gibson and others, 1999). In these successions, VMS deposits typically occur at breaks in volcanism, which can be marked by local or laterally extensive sulfidic, water-laid tuff, and (or) chemical sedimentary units (exhalite horizons). Because the host rocks are relatively impermeable, ascending hydrothermal fluids are focused along permeable zones and sulfide precipitation occurs at and immediately below the seafloor. Resulting regional semiconformable alteration is focused on areas of high permeability such as flow contacts, flow breccias, amygdules, and synvolcanic faults (Gibson and others, 1999). The sulfide deposits grow through the processes of chimney growth, collapse, replacement of chimney debris, and finally renewed chimney growth (Hannington and others, 1995) to form classic mound or lens-shaped deposits above a stringer or stockwork sulfide zone. Volcanogenic massive sulfide deposits that form in mafic flow-dominated successions tend to be Cu-rich, while those in felsic successions tend to be Cu-Zn±Pb-rich. Examples of VMS deposits in the flow lithofacies association include deposits forming on modern mid-ocean spreading ridges (Hannington and others, 1995), ophiolite-hosted deposits (Galley and Koski, 1999), and intracaldera deposits in the Archean Noranda Camp (Mueller and others, 2009).

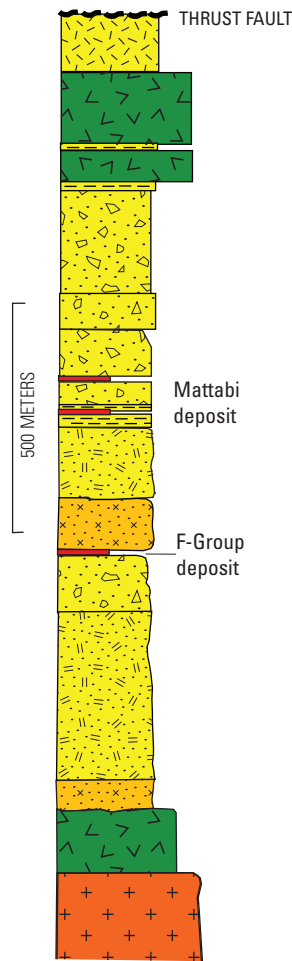
Volcanoclastic Lithofacies Association

Volcanoclastic-dominated successions are largely composed of pyroclastic and syneruptive redeposited pyroclastic and epiclastic deposits, along with subordinate coherent mafic and felsic lava flows and domes (±autobreccia, hyaloclastite, and their redeposited equivalents), cryptodomes with associated peperite and (or) fluidal breccia, and lesser synvolcanic dikes, sills, and clastic sedimentary rocks (fig. 4–8). The clastic sedimentary rocks, which commonly occur within the hanging wall sequence, are typically carbonaceous argillite, immature epiclastic volcanic wacke, and carbonate units. The dominance of pyroclastic rocks in this lithofacies suggests explosive eruptions in relatively shallow (<1,000 m) water volcanic environments characterized by the construction of central volcanic complexes with one or more submarine volcanoes (Gibson and others, 1999). The occurrence of thick, localized successions of juvenile volcanoclastic rocks in the upper or central parts of the sequence suggests emplacement within large subsidence structures or calderas (Busby and

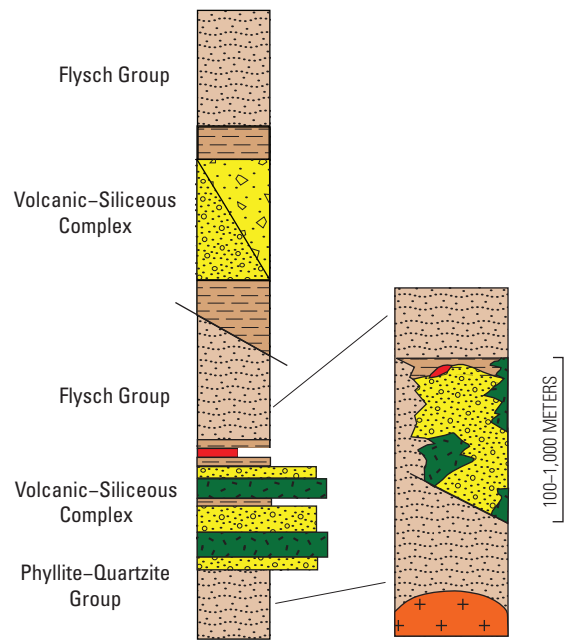
Flow lithofacies association
Noranda Camp



Volcaniclastic lithofacies association
Sturgeon Lake District







Sedimentary lithofacies association
Iberian Pyrite Belt








EXPLANATION

Flows and intrusions

-  Rhyolite flow/dome/cryptodome
-  Basalt-andesite flow
-  Basalt-andesite sill/dike
-  Pre-tectonic-syntectonic intrusion

Volcaniclastic deposits

-  Felsic pumice-rich deposit (±crystals, lithics)
-  Felsic lithic-rich deposit (±crystals, pumice)
-  Mafic scoria to lithic-rich deposit (±crystals)
-  Ash-sized and crystal-rich deposit (felsic)
-  Plane bedding

Sedimentary deposits


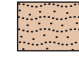

-  Massive sulfide
-  Siliciclastics
-  Mudstone, argillite

Figure 4-8. Composite stratigraphic sections illustrating flow, volcaniclastic, and sediment dominated lithofacies that host volcanogenic massive sulfide deposits. Modified from Franklin and others (2005).

others, 2003; Hudak and others, 2003; Mueller and others, 2009). Volcaniclastic lithofacies associations are common in bimodal-mafic, bimodal-felsic, and felsic-siliciclastic associations.

Initial hydrothermal discharge in volcaniclastic-dominated successions occurs over a larger area than in flow-dominated successions, with relatively unfocused discharge occurring from numerous coalescing hydrothermal vents that are sometimes confined to linear, fault-controlled depressions or grabens (Gibson and others, 1999). Sulfide precipitation commonly occurs within pore spaces of the highly permeable volcaniclastic footwall as unfocused ascending hydrothermal fluid is cooled by interaction with trapped and entrained seawater. This results in the replacement of the volcaniclastic rocks and formation of tabular or sheet-like, largely seafloor replacement VMS deposits. With continued hydrothermal circulation, zone refining processes can lead to replacement of early-formed pyrite and pyrite-sphalerite mineralization by higher-temperature chalcopyrite and sphalerite-chalcopyrite assemblages (Eldridge and others, 1983). In addition, because some volcaniclastic-dominated successions develop in shallow water settings, the resulting VMS deposits may show similarities with subaerial epithermal deposits, including more Au-rich compositions and advanced argillic-type alteration zones, represented in ancient deposits by aluminum-silicate alteration assemblages or K-bearing assemblages (sericite, K-feldspar) (Gibson and others, 1999; Hannington and others, 1999e).

Examples of VMS deposits associated with volcaniclastic lithofacies association include the Horne, Gallen, and Mobern deposits, Noranda Camp, Canada (Mueller and others, 2009); the Matabi deposit, Sturgeon Lake Camp, Canada (Morton and others, 1991; Hudak and others, 2003); the Garpenberg and Zinkgruvan deposits, Bergslagen District, Sweden (Allen and others, 1996); the Rosebery and Hercules deposits, Tasmania (McPhie and Allen, 1992); and the Bald Mountain deposit, United States (Busby and others, 2003).

Relations to Sedimentary Rocks

Sediment-dominated successions that host VMS deposits consist of two distinct facies: (1) a siliciclastic facies composed predominantly of wacke, sandstone, siltstone, argillite, and locally iron formation or Fe-Mn-rich argillite, and (2) a pelitic facies with argillite, carbonaceous argillite, siltstone, marl, and carbonate (bioclastic and chemical) (Franklin and others, 2005). Also present in these sediment-dominated successions are subordinate coherent mafic and (or) felsic lava flows, domes, cryptodomes, and associated autobreccia, hyaloclastite, and peperite, or voluminous felsic volcaniclastic units with subordinate felsic lava flows, domes, and cryptodomes (fig. 4–8). In some sedimentary successions, the dominant volcanic component may be synvolcanic dikes, sills, and cryptodomes. The VMS deposits are spatially associated with complex volcanic centers developed in smaller subsidence structures located within larger sediment-filled

extensional basins; however, the immediate host rocks may be either sedimentary or volcanic. Like some VMS deposits formed in volcaniclastic-dominated successions, deposits in sediment-dominated successions may form just below the seafloor through precipitation in pore spaces and replacement of the sedimentary rocks. This kind of formation may be aided by the presence of a cap layer of silica, carbonate, or sulfide acting as a physical barrier to ascending hydrothermal fluids. In sedimentary successions dominated by terrigenous clastic sedimentary rocks in continental rifts and back-arc basins, the VMS deposits generally contain significant Pb and Ag (Zn-Pb-Cu-Ag deposits) (Franklin and others, 2005). Ancient examples of VMS deposits in sediment-dominated successions include the Brunswick No. 12 deposit, Bathurst mining camp, Canada (Goodfellow and McCutcheon, 2003); Windy Craggy deposit, Canada (Peter and Scott, 1999); and deposits in the Iberian Pyrite Belt, Spain and Portugal (Carvalho and others, 1999).

Iron formations and other hydrothermally precipitated chemical sediments (for example, chert, jasper, Fe-Mn-rich sediment) commonly display a spatial and temporal association with VMS deposits (Spry and others, 2000) and are particularly well developed and laterally extensive in sediment-dominated successions that formed in continental rift and back-arc settings (for example, Bathurst mining camp, Canada). These “exhalites” typically occur in the immediate vicinity of the sulfide deposit and can be at the same stratigraphic horizon, or slightly lower or higher (Peter, 2003). Jaspers (hematitic cherts) commonly form thin, localized caps over VMS deposits, while in other districts relatively thin (<2 m thick) iron formations can form laterally extensive marker horizons that interconnect (in time and space) several massive sulfide deposits. These thinly bedded to laminated rocks are dominantly precipitated from submarine hydrothermal fluids, but they also contain contributions from clastic detritus (for example, Al, Ti) and seawater. Use of iron formation as a stratigraphic guide in the exploration for VMS deposits has met with variable success. A positive europium (Eu) anomaly in iron formation is taken to reflect high-temperature fluid venting and may serve as a guide to mineralization in some districts (Peter, 2003). In addition, mineralogical variations from oxide through carbonate to sulfide within regionally extensive iron formations may indicate proximity to more focused, higher temperature hydrothermal vent complexes (Galley and others, 2007), although subsequent metamorphism often overprints primary mineralogy.

Relations to Metamorphic Rocks

Volcanogenic massive sulfide deposits are syngenetic deposits and are not directly related to metamorphic processes. However, the stratified, district-scale semi-conformable alteration that typically develops from seafloor hydrothermal convection above cooling sill complexes can produce alteration mineral assemblages that mimic those produced by

regional metamorphism (Spooner and Fyfe, 1973; Alt, 1995; Hannington and others, 2003). The resulting alteration mineral assemblages can vary from amphibolite-facies assemblages (for example, Fe-Ca-rich amphibole, clinozoisite, Ca-plagioclase, magnetite) directly above the intrusions through Na-Ca-rich greenschist facies assemblages (for example, albite, quartz, chlorite, actinolite, epidote) to zeolite-clay and related subgreenschist facies mineral assemblages (for example, K-Mg-rich smectites, mixed-layer chlorites, K-feldspar) closer to the seafloor (Galley and others, 2007). In addition, some VMS deposits formed in shallow water settings are characterized by proximal aluminum silicate alteration of their footwall rocks. As described by Bonnet and Corriveau (2007), regional metamorphism of the hydrothermal alteration zones related to massive sulfide formation can produce distinctive mineral assemblages and rock types that can serve as guides to mineralization in ancient volcano-plutonic terranes (for example, hydrothermal aluminum silicate alteration can give rise to sillimanite-kyanite-quartz-biotite-cordierite-garnet assemblages at upper amphibolite-granulite metamorphism).

Prograde metamorphism of massive sulfides also produces changes (Marshall and others, 2000), including: (1) grain-size coarsening of the base metal sulfides; (2) conversion of pyrite to pyrrhotite and generation of pyrrhotite through sulfidation of Fe in other minerals above the greenschist-amphibolite facies boundary; (3) a progressive increase in the FeS content of sphalerite as well as chalcopyrite exsolution from sphalerite; (4) the formation of zinc spinel, zincian staurolite, and Pb-rich feldspar at upper amphibolite-granulite facies conditions; (5) the release of gold from pyrite and its partitioning between electrum and chalcopyrite; (6) release of other trace elements included or nonstoichiometrically substituted in base metal sulfides; and (7) the partitioning of trace elements between equilibrium sulfide pairs. Some of these prograde metamorphic effects can be reversed under appropriate retrograde processes (for example, pyrrhotite can undergo sulfidation to pyrite). In addition, deformation accompanying metamorphism can result in mobilization and redistribution of massive sulfide mineralization (Marshall and Gilligan, 1993; Marshall and others, 2000), including the separation of more ductile minerals, such as galena and sphalerite, from more brittle sulfide minerals, such as pyrite.

References Cited

- Alabaster, T., and Pearce, J.A., 1985, The interrelationship between magmatic and ore-forming hydrothermal processes in the Oman ophiolite: *Economic Geology*, v. 80, p. 1–16.
- Allen, R.L., Lundstrom, I., Ripa, M., Simeonov, A., and Christofferson, H., 1996, Facies analysis of a 1.9 Ga continental margin, back-arc, felsic province with diverse Zn-Pb-Ag (Cu-Au) sulfide and Fe oxide deposits, Bergslagen Region, Sweden: *Economic Geology*, v. 91, p. 979–1008.
- Allen, R.L., Weihed, P., and Team, G.V.R.P., 2002, Global comparisons of volcanic-associated massive sulphide districts, *in* Blundell, D.J., Neubauer, F., and Von Quadt, A., eds., *The Timing and Location of Major Ore Deposits in an Evolving Orogen*: Geological Society, London, Special Publication 204, p. 13–37.
- Alt, J.C., 1995, Subseafloor processes in mid-ocean ridge hydrothermal systems, *in* Humphris, S.E., Zierenberg, R.A., Mullineaux, L.S., and Thomas, R.E., eds., *Seafloor hydrothermal systems—Physical, chemical, biological, and geological interactions*: American Geophysical Union, Geophysical Monograph 91, p. 85–114.
- Baker, E.T., 2009, Relationships between hydrothermal activity and axial magma chamber distribution, depth, and melt content: *Geochemistry Geophysics Geosystems*, v. 10, Q06009, 15 p., doi.10.1029/2009GC002424.
- Baker, E.T., and German, C.R., 2004, On the global distribution of hydrothermal vent sites, *in* Lowell, R.P., Seewald, J., Metaxa, A., and Perfit, M., eds., *Magma to Microbe—Modeling Hydrothermal Processes at Oceanic Spreading Centers*: American Geophysical Union Geophysical Monograph 148, p. 1–18.
- Baker, E.T., Chen, Y.J., and Phipps Morgan, J., 1996, The relationship between near-axis hydrothermal cooling and the spreading rate of mid-ocean ridges: *Earth and Planetary Science Letters*, v. 142, p. 137–145.
- Barley, M.E., and Groves, D.I., 1992, Supercontinent cycles and the distribution of metal deposits through time: *Geology*, v. 20, p. 291–294.
- Barrett, T.J., and MacLean, W.H., 1999, Volcanic sequences, lithogeochemistry, and hydrothermal alteration in some bimodal volcanic-associated massive sulfide deposits, *in* Barrie, C.T., and Hannington, M.D., eds., *Volcanic-associated massive sulfide deposits—Processes and examples in modern and ancient settings*: *Reviews in Economic Geology*, v. 8, p. 101–131.
- Barrett, T.J., and Sherlock, R.L., 1996, Geology, lithogeochemistry and volcanic setting of the Eskay Creek Au-Ag-Cu-Zn deposit, northwestern British Columbia: *Exploration and Mining Geology*, v. 5, p. 339–368.
- Barrett, T.J., Thompson, J.F.H., and Sherlock, R.L., 1996, Stratigraphic, lithogeochemical and tectonic setting of the Kutcho Creek massive sulfide deposit, northwestern British Columbia: *Exploration and Mining Geology*, v. 5, p. 309–338.
- Barrie, C.T., Hannington, M.D., and Bleeker, W., 1999, The giant Kidd Creek volcanic-associated massive sulfide deposit, Abitibi Subprovince, Canada, *in* Barrie, C.T., and Hannington, M.D., eds., *Volcanic-associated massive sulfide deposits—Processes and examples in modern and ancient settings*: *Reviews in Economic Geology*, v. 8, p. 247–259.

- Bédard, J.H., and Hébert, R., 1996, The lower crust of the Bay of Islands ophiolite in Canada—Petrology, mineralogy, and the importance of syntaxis in magmatic differentiation in ophiolites and at ocean ridges: *Journal of Geophysical Research*, v. 101, p. 25,105–25,124.
- Binney, W.P., 1987, A sedimentological investigation of Maclean channel transported sulfide ores, *in* Kirkham, R.V., ed., *Buchans geology, Newfoundland: Geological Survey of Canada Paper 86-24*, p. 107–147.
- Bogdanov, Y.A., Bortnikov, N.S., Vikent'ev, I.V., Gurvich, E.G., and Sagalevich, A.M., 1997, A new type of modern mineral-forming systems—Black smokers of the hydrothermal field at 14°45'N latitude, Mid-Atlantic Ridge: *Geology of Ore Deposits*, v. 39, p. 68–90.
- Bonnet, A.-L., and Corriveau, L., 2007, Alteration vectors to metamorphosed hydrothermal systems in gneissic terranes, *in* Goodfellow, W.D., ed., *Mineral Resources of Canada—A Synthesis of Major Deposit-Types, District Metallogeny, the Evolution of Geological Provinces, and Exploration Methods: Geological Association of Canada, Mineral Deposits Division, Special Publication No. 5*, p. 1035–1050.
- Busby, C.J., Kessel, L., Schulz, K.J., Foose, M.P., and Slack, J.F., 2003, Volcanic setting of the Ordovician Bald Mountain massive sulfide deposit, northern Maine, *in* Goodfellow, W.D., McCutcheon, S.R., and Peter, J.M., eds., *Volcanogenic massive sulfide deposits of the Bathurst district, New Brunswick, and northern Maine: Economic Geology Monograph 11*, p. 219–244.
- Carr, P.M., and Cathless, L.M., III, 2008, On the size and spacing of volcanogenic massive sulfide deposits within a district with application to the Matagami District, Quebec: *Economic Geology*, v. 103, p. 1395–1409.
- Carvalho, D., Barriga, F.J.A.S., and Munhá, J., 1999, Bimodal siliciclastic systems—The case of the Iberian Pyrite Belt, *in* Barrie, C.T., and Hannington, M.D., eds., *Volcanic-associated massive sulfide deposits—Processes and examples in modern and ancient settings: Reviews in Economic Geology*, v. 8, p. 375–408.
- Clift, P.D., and ODP Leg 135 Scientific Party, 1994, Volcanism and sedimentation in a rifting island-arc terrain: An example from Tonga, SW Pacific, *in* Smellie, J.L., ed., *Volcanism Associated with Extension at Consuming Plate Margins: Geological Society, London, Special Publication 81*, p. 29–51.
- Condie, K.C., and Pease, V., editors, 2008, When did plate tectonics begin on planet Earth?: *Geological Society of America Special Paper 440*, 294 p.
- Coumou, D., Driesner, T., and Heinrich, C.A., 2008, The structure and dynamics of mid-ocean ridge hydrothermal systems: *Science*, v. 321, p. 1825–1828.
- Cox, S.F., Knackstedt, M.A., and Braun, J., 2001, Principles of structural control on permeability and fluid flow in hydrothermal systems: *Reviews in Economic Geology*, v. 14, p. 1–24.
- Crawford, W.C., Hildebrand, J.A., Dorman, L.M., Webb, S.C., and Wiens, D.A., 2003, Tonga Ridge and Lau Basin crustal structure from seismic refraction data: *Journal of Geophysical Research*, v. 108(B4), 2195, 19 p., doi:10.1029/2001JB001435.
- Crowe, D.E., Nelson, S.W., Brown, P.E., Shanks, W.C., III, and Valley, J.W., 1992, Geology and geochemistry of volcanogenic massive sulfide deposits and related igneous rocks, Prince William Sound, south-central Alaska: *Economic Geology*, v. 87, p. 1,722–1,746.
- Curewitz, D., and Karson, J.A., 1997, Structural settings of hydrothermal outflow—Fracture permeability maintained by fault propagation and interaction: *Journal of Volcanology and Geothermal Research*, v. 79, p. 149–168.
- de Ronde, C.E.J., 1995, Fluid chemistry and isotopic characteristics of seafloor hydrothermal systems and associated VMS deposits: potential for magmatic contributions, *in* Thompson, J.F.H., ed., *Magma, fluids and ore deposits: Ottawa, Ontario, Mineralogical Association of Canada Short Course Series*, p. 479–510.
- de Ronde, C.E.J., Massoth, G.J., Baker, E.T., and Lupton, J.E., 2003, Submarine hydrothermal venting related to volcanic arcs, *in* Simmons, S.F., and Graham, I.J., eds., *Volcanic, geothermal and ore-forming fluids: Rulers and witnesses of processes within the Earth: Society of Economic Geologists Special Publication 10*, p. 91–109.
- de Ronde, C.E.J., Baker, E.T., Massoth, G.J., Lupton, J.E., Wright, I.C., Sparks, R.J., Bannister, S.C., Reyners, M.E., Walker, S.L., Greene, R.R., Ishibashi, J., Faure, K., Resing, J.A., and Lebon, G.T., 2007, Submarine hydrothermal activity along the mid-Kermadec Arc, New Zealand—Large-scale effects on venting: *Geochemistry, Geophysics, Geosystems*, v. 8, Q07007, 27 p., doi:10.1029/2006GC001495.
- Delaney, J.R., Robigou, V., McDuff, R.E., and Tivey, M.K., 1992, Geology of a vigorous hydrothermal system on the Endeavour segment, Juan de Fuca Ridge: *Journal of Geophysical Research*, v. 97, p. 19,663–19,682.
- DeMatties, T.A., 1994, Early Proterozoic volcanogenic massive sulfide deposits in Wisconsin: An overview: *Economic Geology*, v. 89, p. 1122–1151.
- Dusel-Bacon, C., Wooden, J.L., and Hopkins, M.J., 2004, U-Pb zircon and geochemical evidence for bimodal mid-Paleozoic magmatism and syngenetic base-metal mineralization in the Yukon-Tanana terrane, Alaska: *Geological Society of America Bulletin*, v. 116, p. 989–1015.

- Einsele, G., 1985, Basaltic sill-sediment complexes in young spreading centers—Genesis and significance: *Geology*, v. 13, p. 249–252.
- Eldridge, C.S., Barton, P.B., and Ohmoto, H., 1983, Mineral textures and their bearing on the formation of the Kuroko orebodies, *in* Ohmoto, H., and Skinner, B.J., eds., *The Kuroko and related volcanogenic massive sulfide deposits: Economic Geology Monograph 5*, p. 241–281.
- Escartin, J., Smith, D.K., Cann, J., Schouten, H., Langmuir, C.H., and Escrig, S., 2008, Central role of detachment faults in accretion of slow-spreading oceanic lithosphere: *Nature*, v. 455, p. 790–795.
- Ewart, A., Collerson, K.D., Regelous, M., Wendt, J.I., and Niu, Y., 1998, Geochemical evolution within the Tonga-Kermadec-Lau arc-back-arc systems—The role of varying mantle wedge composition in space and time: *Journal of Petrology*, v. 39, p. 331–368.
- Fiske, R.S., Cashman, C.V., Shibata, A., and Watanabe, K., 1998, Tephra dispersal from Myojinsho, Japan, during its shallow submarine eruption of 1952/1953: *Bulletin of Volcanology*, v. 59, p. 262–275.
- Fiske, R.S., Naka, J., Iizasa, K., Yuasa, M., and Klaus, A., 2001, Submarine silicic caldera at the front of the Izu-Bonin Arc, Japan—Voluminous seafloor eruptions of rhyolite pumice: *Geological Society of America Bulletin*, v. 113, p. 813–824.
- Francheteau, J., Needham, H.D., Choukroune, P., Juteau, J., Seguret, M., Ballard, R.D., Fox, P.J., Normark, W., Carranza, A., Cordoba, A., Guerrero, J., Rangin, C., Bougault, H., Cambon, P., and Hekinina, R., 1979, Massive deep sea sulfide ore deposit discovered on the East Pacific Rise: *Nature*, v. 277, p. 523–528.
- Franklin, J.M., Gibson, H.L., Jonasson, I.R., and Galley, A.G., 2005, Volcanogenic massive sulfide deposits, *in* Hedenquist, J.W., Thompson, J.F.H., Goldfarb, R.J., and Richards, J.P., eds., *Economic Geology 100th anniversary volume, 1905–2005*: Littleton, Colo., p. 523–560.
- Galley, A.G., 1993, Characteristics of semi-conformable alteration zones associated with volcanogenic massive sulfide districts: *Journal of Geochemical Exploration*, v. 48, p. 175–200.
- Galley, A.G., 2003, Composite synvolcanic intrusions associated with Precambrian VMS-related hydrothermal systems: *Mineralium Deposita*, v. 38, p. 443–473.
- Galley, A.G., and Koski, R.A., 1999, Setting and characteristics of ophiolite-hosted volcanogenic massive sulfide deposits, *in* Barrie, C.T., and Hannington, M.D., eds., *Volcanic-Associated Massive Sulfide Deposits—Processes and Examples in Modern and Ancient Settings*, p. 215–236.
- Galley, A.G., Hannington, M.D., and Jonasson, I.R., 2007, Volcanogenic Massive Sulfide Deposits, *in* Goodfellow, W.D., ed., *Mineral deposits of Canada—A synthesis of major deposit-types, district metallogeny, the evolution of geological provinces, and exploration methods*: Geological Association of Canada, Mineral Deposits Division, Special Publication No. 5, p. 141–161.
- Gibson, H.L., and Galley, A.G., 2007, Volcanogenic massive sulfide deposits of the Archean, Noranda district, Quebec, *in* Goodfellow, W.D., ed., *Mineral deposits of Canada—A synthesis of major deposit-types, district metallogeny, the evolution of geological provinces, and exploration methods*: Geological Association of Canada, Mineral Deposits Division, Special Publication No. 5, p. 533–552.
- Gibson, H.L., Morton, R.L., and Hudak, G.J., 1999, Submarine volcanic processes, deposits and environments favorable for the location of volcanic-associated massive sulfide deposits, *in* Barrie, C.T., and Hannington, M.D., eds., *Volcanic-associated massive sulfide deposits—Processes and examples in modern and ancient settings*: *Reviews in Economic Geology*, v. 8, p. 13–51.
- Goodfellow, W.D., and McCutcheon, S.R., 2003, Geologic and genetic attributes of volcanic sediment-hosted massive sulfide deposits of the Bathurst Mining Camp, northern New Brunswick—A synthesis, *in* Goodfellow, W.D., McCutcheon, S.R., and Peter, J.M., eds., *Massive sulfide deposits of the Bathurst Mining Camp, New Brunswick, and northern Maine*: *Economic Geology Monograph 11*, p. 79–109.
- Graham, I.J., Reyes, A.G., Wright, I.C., Peckett, K.M., Smith, I.E.M., and Arculus, R.J., 2008, Structure and petrology of newly discovered volcanic centers in the northern Kermadec-southern Tofa arc, South Pacific Ocean: *Journal of Geophysical Research*, v. 113, B08S02, 24 p., doi:10.1029/2007JB005453.
- Grenne, T., 1989, The feeder-zone to the Lokken ophiolite-hosted massive sulphide deposit and related mineralizations in the central Norwegian Caledonides: *Economic Geology*, v. 84, p. 2173–2195.
- Groves, D.I., and Bierlein, F.P., 2007, Geodynamic settings of mineral deposit systems: *Journal of the Geological Society of London*, v. 164, p. 19–30.
- Groves, D.I., Vielreicher, R.M., Goldfarb, R.J., and Condie, K.C., 2005, Controls on the heterogeneous distribution of mineral deposits through time, *in* MacDonald, I., Boyce, A.J., Butler, I.B., Herrington, R.J., and Polya, D., eds., *Mineral deposits and earth evolution*: Geological Society of London, Special Publication 248, p. 71–101.

- Halbach, P., Nakamura, K., Washner, M., Lange, J., Sakai, H., Kaselitz, L., Hansen, R.-D., Yamano, M., Post, J., Prause, B., Seifert, R., Michaelis, W., Teichmann, F., Kinoshita, M., Marten, A., Ishibashi, J., Czerwinski, S., and Blum, N., 1989, Probable modern analogue of Kuroko-type massive sulfide deposits in the Okinawa trough back-arc basin: *Nature*, v. 338, p. 496–499.
- Halbach, P., Pracejus, B., and Marten, A., 1993, Geology and mineralogy of massive sulfide ores from the central Okinawa trough: *Economic Geology*, v. 88, p. 2,210–2,225.
- Hannington, M.D., de Ronde, C.E., and Petersen, S., 2005, Sea-floor tectonics and submarine hydrothermal systems, in Hedenquist, J.W., Thompson, J.F.H., Goldfarb, R.J., and Richards, J.P., eds., *Economic Geology 100th anniversary volume, 1905–2005*: Littleton, Colo., p. 111–141.
- Hannington, M.D., Jonasson, I.R., Herzig, P.M., and Petersen, S., 1995, Physical and chemical processes of seafloor mineralization at Mid-Ocean Ridges, in Humphris, S.E., Zierenberg, R.A., Mullineaux, L.S., and Thomas, R.E., eds., *Seafloor hydrothermal systems—Physical, chemical, biological, and geological interactions*: American Geophysical Union, *Geophysical Monograph* 91, p. 115–157.
- Hannington, M.D., Petersen, S., Herzig, P.M., and Jonasson, I.R., 2004, A global database of seafloor hydrothermal systems, including a digital database of geochemical analyses of seafloor polymetallic sulfides: *Geological Survey of Canada Open File* 4598, CD-ROM.
- Hannington, M.D., Poulsen, K.H., Thompson, J.F.H., and Siliteo, R.H., 1999, Volcanogenic gold in the massive sulfide environment, in Barrie, C.T., and Hannington, M.D., eds., *Volcanic-associated massive sulfide deposits—Processes and examples in modern and ancient settings*: *Reviews in Economic Geology*, v. 8, p. 325–356.
- Hannington, M.D., Santaguida, F., Kjarsgaard, I.M., and Cathless, L.M., 2003, Regional greenschist facies hydrothermal alteration in the central Blake River Group, western Abitibi subprovince, Canada: *Mineralium Deposita*, v. 38, 393–422.
- Hart, T.R., Gibson, H.L., and Leshner, C.M., 2004, Trace element geochemistry and petrogenesis of felsic volcanic rocks associated with volcanogenic massive Cu-Zn-Pb sulfide deposits: *Economic Geology*, v. 99, p. 1003–1013.
- Haymon, R.M., Fornari, D.J., Edwards, M.H., Carbotte, S., Wright, D., and MacDonald, K.C., 1991, Hydrothermal vent distribution along the East Pacific Rise crest (9°09' - 54°N) and its relationship to magmatic and tectonic processes on fast-spreading mid-ocean ridges: *Earth and Planetary Sciences*, v. 104, p. 513–534.
- Hawkins, J.W., Jr., 1995, The geology of the Lau basin, in Taylor, B., ed., *Backarc Basins—Tectonics and magmatism*: New York, Plenum Press, p. 63–138.
- Heiken, G., Goff, F., Stix, J., Tamanyu, S., Shafiqullah, M., Garcia, S., and Hagan, R., 1986, Intracaldera volcanic activity, Toledo caldera and embayment, Jemez Mountains, New Mexico: *Journal of Geophysical Research*, v. 91, p. 1799–1815.
- Hofmann, A.W., 2003, Sampling mantle heterogeneity through oceanic basalts—Isotopes and trace elements: *Treatise on Geochemistry*, v. 2, p. 61–101.
- Hudak, G.J., Mortan, R.L., Franklin, J.M., and Peterson, D.M., 2003, Morphology, distribution, and estimated eruption volumes for intracaldera tuffs associated with volcanic-hosted massive sulfide deposits in the Archean Sturgeon Lake Caldera Complex, Northwestern Ontario, in White, J.D.L., Smellie, J.L., and Clague, D.A., eds., *Explosive subaqueous volcanism*: American Geophysical Union, *Geophysical Monograph* 140, p. 345–360.
- Humphris, S.E., and Tivey, M.K., 2000, A synthesis of geological and geochemical investigations of the TAG hydrothermal field: Insights into fluid flow and mixing processes in a hydrothermal system, in Dilek, Y., Moorse, E., Elthon, D., and Nicholas, A., eds., *Ophiolites and oceanic crust—New insights from field studies and the ocean drilling program*: Geological Society of America Special Paper 349, p. 213–236.
- Iizasa, K., Fiske, R.S., Ishizuka, O., Yuasa, M., Hashimoto, J., Ishibashi, J., Naka, J., Horii, Y., Fujiwara, Y., Imai, A., and Koyama, S., 1999, A Kuroko-type polymetallic sulfide deposit in a submarine caldera: *Science*, v. 283, p. 975–977.
- Ishibashi, J., and Urabe, T., 1995, Hydrothermal activity related to arc-backarc magmatism in the Western Pacific, in Taylor, B., ed., *Backarc basins—Tectonics and magmatism*: New York, Plenum Press, p. 451–495.
- Johnson, B.J., Montante-Martínez, J.A., Canela-Barboza, M., and Danielson, T.J., 2000, Geology of the San Nicolás deposit, Zacatecas, Mexico, in Sherlock, R.L., and Logan, M.A.V., eds., *Volcanogenic massive sulphide deposits of Latin America*: Geological Association of Canada, Mineral Deposits Division Special Publication 2, p. 71–85.
- Kelley, D.S., Delaney, J.R., and Yoerger, D.A., 2001, Geology and venting characteristics of the Mothra hydrothermal field, Endeavour segment, Juan de Fuca Ridge: *Geology*, v. 29, p. 385–491.
- Kennedy, B., Stix, J., Vallance, J.W., Lavallée, Y., and Longpré, M.-A., 2004, Controls on caldera structure—Results from analogue sandbox modeling: *Geological Society of America Bulletin*, v. 116, p. 515–524.
- Kleinrock, M.C., and Humphris, S.E., 1996, Structural control on sea-floor hydrothermal activity at the TAG active mound: *Nature*, v. 382, p. 149–153.

- Kleinrock, M.C., Tucholke, B.E., Lin, J., and Tivey, M.A., 1997, Fast rift propagation at a slow-spreading ridge: *Geology*, v. 25, p. 639–642.
- Kodaira, S., Sato, T., Takahashi, N., Miura, S., Tamura, Y., Tatsumi, Y., and Kaneda, Y., 2007, New seismological constraints on growth of continental crust in the Izu-Bonin intra-oceanic arc: *Geology*, v. 35, p. 1031–1034.
- Krasnov, S.G., Proroshina, I.M., and Cherkashev, G.A., 1995, Geological setting of high-temperature hydrothermal activity and massive sulfide formation on fast and slow-spreading ridges, *in* Parson, L.M., Walker, C.L., and Dixon, D.R., eds., *Hydrothermal Vents and Processes*: Geological Society of London, Special Publication 87, p. 17–32.
- Knuckey, M.J., Comba, C.D.A., and Riverin, G., 1982, Structure, metal zoning and alteration at the Millenbach deposit, Noranda, Quebec, *in* Hutchinson, R.W., Spence, C.D., and Franklin, J.M., eds., *Precambrian sulphide deposits*: Geological Association of Canada Special Paper 25, p. 255–295.
- Lalou, C., Reyss, J-L., Brichet, E., Rona, P.A., and Thompson, G., 1995, Hydrothermal activity on a 10⁵-year scale at a slow-spreading ridge, TAG hydrothermal field, Mid-Atlantic Ridge 26°N: *Journal of Geophysical Research*, v. 100, p. 17855–17862.
- Large, R.R., 1992, Australian volcanic-hosted massive sulfide deposits: Features, styles, and genetic models: *Economic Geology*, v. 87, p. 471–510.
- Lentz, D.R., 1998, Petrogenetic evolution of felsic volcanic sequences associated with Phanerozoic volcanic-hosted massive sulfide systems—The role of extensional geodynamics: *Ore Geology Reviews*, v. 12, p. 289–327.
- Lonsdale, P., 1989, Geology and tectonic history of the Gulf of California, *in* Winterer, E.L., Hussong, D.M., and Decker, R.W., eds., *The Eastern Pacific Ocean and Hawaii*: Geological Society of America, Decade of North America Geology, v. N, p. 499–521.
- Lonsdale, P., and Becker, K., 1985, Hydrothermal plumes, hot springs, and conductive heat flow in the Southern Trough of Guaymas Basin: *Earth and Planetary Sciences*, v. 73, p. 211–225.
- Marsaglia, K.M., 1995, Interarc and backarc basins, *in* Busby, C.J., and Ingersoll, R.V., eds., *Tectonics of sedimentary basins*: Cambridge, Mass., Blackwell Science, p. 299–329.
- Marshall, B., and Gilligan, L.B., 1993, Remobilization, syn-tectonic processes and massive sulfide deposits: *Ore Geology reviews*, v. 8, p. 39–64.
- Marshall, B., Vokes, F.M., and Larocque, A.C.L., 2000, Regional metamorphic remobilization: Upgrading and formation of ore deposits, *in* Spry, P.G., Marshall, B., and Vokes, F.M., eds., *Metamorphosed and metamorphic ore deposits: Reviews in Economic Geology*, v. 11, p. 19–38.
- McCaig, A.M., Cliff, R.A., Escartin, J., Fallick, A.E., and MacLeod, C.J., 2007, Oceanic detachment faults focus very large volumes of black smoker fluids: *Geology*, v. 35, p. 935–938.
- McPhie, J., and Allen, R.L., 1992, Facies architecture of mineralized submarine volcanic sequences: Cambrian Mount Read Volcanics, Western Tasmania: *Economic Geology*, v. 87, p. 587–596.
- Morton, R.L., Walker, J.S., Hudak, G.J., and Franklin, J.M., 1991, The early development of an Archean submarine caldera complex with emphasis on the Mattabi ash-flow tuff and its relationship to the Mattabi massive sulfide deposit: *Economic Geology*, v. 86, p. 1002–1011.
- Mosier, D.L., Berger, V.I., and Singer, D.A., 2009, Volcanogenic massive sulfide deposits of the world—Database and grade and tonnage models: U.S. Geological Survey Open-File Report 2009–1034, 46 p.
- Mueller, W.U., and Mortensen, J., 2002, Age constraints and characteristics of subaqueous volcanic construction, the Archean Hunter Mine Group, Abitibi greenstone belt: *Precambrian Research*, v. 115, p. 119–152.
- Mueller, W.U., Stix, J., Corcoran, P.I., and Daigneault, R., 2009, Subaqueous calderas in the Archean Abitibi greenstone belt: An overview and new ideas: *Ore Geology Reviews*, v. 35, p. 4–46.
- Mumin, A.H., Scott, S.D., Somarin, A.K., and Oran, K.S., 2007, Structural controls on massive sulfide deposition and hydrothermal alteration in the South Sturgeon Lake caldera, Northwestern Ontario: *Exploration and Mining Geology*, v. 16, p. 83–107.
- Ohmoto, H., 1978, Submarine calderas: A key to the formation of volcanogenic massive sulfide deposits: *Mining Geology*, v. 28, p. 219–231.
- Ohmoto, H., and Skinner, B.J., eds., 1983, *The Kuroko and related volcanogenic massive sulfide deposits*: Economic Geology Monograph 5, 604 pp.
- Ohmoto, H., and Takahashi, T., 1983, Part III. Submarine calderas and Kuroko genesis, *in* Ohmoto, H., and Skinner, B.J., eds., *The Kuroko and related volcanogenic massive sulfide deposits*: Economic Geology Monograph 5, p. 39–54.

- Pearce, J.A., 2003, Supra-subduction zone ophiolites: The search for modern analogues, *in* Dilek, Y., and Newcomb, S., eds., *Ophiolite concept and the evolution of geological thought: Geological Society of America Special Paper 373*, p. 269–293.
- Pearce, J.A., and Peate, D.W., 1995, Tectonic implications of the composition of volcanic arc magmas: *Annual Review of Earth and Planetary Sciences*, v. 23, p. 251–285.
- Pearce, J.A., and Stern, R.J., 2006, Origin of back-arc basin magmas: Trace element and isotope perspective, *in* Christie, D.M., Fisher, C.R., Lee, S.-M., and Givens, S., eds., *Back-arc spreading systems—Geological, Biological, Chemical, and Physical Interactions: American Geophysical Union Geophysical Monograph 166*, p. 63–86.
- Pearson, V., and Daigneault, R., 2009, An Archean megacaldera complex—The Blake River Group, Abitibi greenstone belt: *Precambrian Research*, v. 168, p. 66–82.
- Perfit, M.R., Ridley, W.I., and Jonasson, I.R., 1999, Geologic, petrologic, and geochemical relationships between magmatism and massive sulfide mineralization along the eastern Galapagos spreading center, *in* Barrie, C.T., and Hannington, M.D., eds., *Volcanic-associated massive sulfide deposits—Processes and examples in modern and ancient settings: Reviews in Economic Geology*, v. 8, p. 75–100.
- Perk, N.W., Coogan, L.A., Karson, J.A., Klein, E.M., and Hanna, H.D., 2007, Petrology and geochemistry of primitive lower oceanic crust from Pito Deep—Implications for the accretion of the lower crust at the Southern East Pacific Rise: *Contributions to Mineralogy and Petrology*, v. 154, p. 575–590.
- Peter, J.M., 2003, Ancient iron-rich metalliferous sediments (iron formations): Their genesis and use in exploration for strataform base metal sulphide deposits, with examples from the Bathurst Mining Camp, *in* Lentz, D.R., ed., *Geochemistry of sediments and sedimentary rocks—Evolutionary considerations to mineral deposit-forming environments: Geological Association of Canada, GEOText 4*, p. 145–173.
- Peter, J.M., and Scott, S.D., 1999, Windy Craggy, northwestern British Columbia: The world's largest Besshi-type deposit, *in* Barrie, C.T., and Hannington, M.D., eds., *Volcanic-associated massive sulfide deposits—Processes and examples in modern and ancient settings: Reviews in Economic Geology*, v. 8, p. 261–295.
- Petersen, S., Herzig, P.M., and Hannington, M.D., 2000, Third dimension of a presently forming VMS deposit: TAG hydrothermal mound, Mid-Atlantic Ridge, 26°N: *Mineralium Deposita*, v. 35, p. 233–259.
- Rona, P.A., Hannington, M.D., Raman, C.V., Thompson, G., Tivey, M.K., Humphris, S., and Lalou, C., 1993, Active and relict seafloor hydrothermal mineralization at the TAG hydrothermal field, Mid Atlantic Ridge: *Economic Geology*, v. 88, p. 1989–2017.
- Sangster, D.F., 1980, Quantitative characteristics of volcanogenic massive sulphide deposits—Part I. Metal content and size distribution of massive sulphide deposits in volcanic centres: *Canadian Institute of Mining and Metallurgy Bulletin*, v. 73, no. 814, p. 74–81.
- Sangster, A.L., Douma, S.L., and Lavigne, J., 2007, Base metal and gold deposits of the Betts Cove Complex, Baie Verte Peninsula, Newfoundland, *in* Goodfellow, W.D., ed., *Mineral deposits of Canada—A synthesis of major deposit-types, district metallogeny, the evolution of geological provinces, and exploration methods: Geological Association of Canada, Mineral Deposits Division, Special Publication 5*, p. 703–721.
- Schardt, C., and Large, R.R., 2009, New insights into the genesis of volcanic-hosted massive sulfide deposits on the seafloor from numerical modeling studies: *Ore Geology Reviews*, v. 35, p. 333–351.
- Schmincke, H.-U., 2004, *Volcanism: Berlin, Springer*, 324 p.
- Schulz, K.J., and Ayuso, R.A., 2003, Litho-geochemistry and paleotectonic setting of the Bald Mountain massive sulfide deposit, northern Maine, *in* Goodfellow, W.D., McCutcheon, S.R., and Peter, J.M., eds., *Massive sulfide deposits of the Bathurst Mining Camp, New Brunswick, and northern Maine: Economic Geology Monograph 11*, p. 79–109.
- Scott, S.D., 1980, Geology and structural control of Kuroko-type massive sulfide deposits: *Geological Association of Canada Special Paper 20*, p. 705–721.
- Scott, S.D., 1997, Submarine hydrothermal systems and deposits, *in* Barnes, H.L., ed., *Geochemistry of hydrothermal ore deposits: New York, Wiley and Sons*, p. 797–875.
- Sharpe, R., and Gemmel, J.B., 2002, The Archean Cu-Zn magnetite-rich Gossan Hill volcanic-hosted massive sulfide deposit, Western Australia—Genesis of a multistage hydrothermal system: *Economic Geology*, v. 97, p. 517–539.
- Shinjo, R., and Kato, Y., 2000, Geochemical constraints on the origin of bimodal magmatism at the Okinawa trough, and incipient back-arc basin: *Lithos*, v. 54, p. 117–137.
- Sibuet, J.-C., Hsu, S.-K., Shyn, C.-T., and Liu, C.-S., 1995, Structural and kinematic evolution of the Okinawa trough backarc basin, *in* Taylor, B., ed., *Backarc basins—Tectonics and Magmatism: New York, Plenum Press*, p. 343–378.

- Sinha, M.C., and Evans, R.L., 2004, Geophysical constraints upon the thermal regime of ocean crust, *in* German, C.R., and others, eds., *Mid-ocean ridges—Hydrothermal interactions between the lithosphere and oceans: American Geophysical Union Geophysical Monograph 148*, p. 19–62.
- Slack, J.F., 1993, Descriptive and grade-tonnage models for Besshi-type massive sulfide deposits, *in* Kirkham, R.V., Sinclair, W.D., Thorpe, R.I., and Duke, J.M., eds., *Mineral deposit models: Geological Association of Canada Special Paper 40*, p. 343–371.
- Slack, J.F., Foose, M.P., Flohr, M.J.K., Scully, M.V., and Belkin, H.E., 2003, Exhalative and seafloor replacement processes in the formation of the Bald Mountain massive sulfide deposit, northern Maine, *in* Goodfellow, W.D., McCutcheon, S.R., and Peter, J.M., eds., *Volcanogenic massive sulfide deposits of the Bathurst district, New Brunswick, and northern Maine: Economic Geology Monograph 11*, p. 513–548.
- Smith, D.K., Escartin, J., Schouten, H., and Cann, J.R., 2008, Fault rotation and core complex formation—Significant processes in seafloor formation at slow-spreading mid-ocean ridges (Mid-Atlantic Ridge, 13°–15°N): *Geology Geophysics Geosystems*, v. 9, Q03003, 23 p., doi:10.1029/2007GC001699.
- Smith, I.E.M., Worthington, T.J., Stewart, R.B., Price, R.C., and Gamble, J.A., 2003, Felsic volcanism in the Kermadec arc, SW Pacific—Crustal recycling in an oceanic setting, *in* Larter, R.D., and Leet, P.T., eds., *Intra-oceanic subduction systems—Tectonic and magmatic processes: Geological Society of London, Special Publication 219*, p. 99–118.
- Smith, R.L., 1979, Ash-flow magmatism, *in* Chapin, C.E., and Elston, W.E., eds., *Ash-flow tuffs: Geological Society of America Special Paper 180*, p. 5–27.
- Solomon, M., 2008, Brine pool deposition for the Zn-Pb-Cu massive sulphide deposits of the Bathurst mining camp, New Brunswick, Canada. I. Comparisons with the Iberian pyrite belt: *Ore Geology Reviews*, v. 33, p. 329–351.
- Spiess, F.N., Macdonald, K.C., Atwater, T., Ballard, R., Carranza, A., Cordoba, D., Cox, C., Diaz Garcia, V.M., Francheteau, J., Guerrero, J., Hawkins, J., Haymon, R., Hessler, R., Juteau, T., Kastner, M., Larson, R., Luyendyk, B., Macdougall, J.D., Miller, S., Normark, W., Orcutt, J., and Rangin, C., 1980, East Pacific Rise—Hot springs and geophysical experiments: *Science*, v. 207, no. 4438, p. 1421–1433.
- Spooner, E.T.C., and Fyfe, W.S., 1973, Seafloor metamorphism, heat and mass transfer: *Contribution to Mineralogy and Petrology*, v. 42, p. 287–304.
- Spry, P.G., Peter, J.M., and Slack, J.F., 2000, Meta-exhalites as exploration guides to ore, *in* Spry, P.G., Marshall, B., and Vokes, F.M., eds., *Metamorphosed and metamorphic ore deposits: Reviews in Economic Geology*, v. 11, p. 163–201.
- Stern, R.J., and Bloomer, S.H. 1992, Subduction zone infancy: Examples from the Eocene Izu-Bonin-Mariana and Jurassic California: *Geological Society of America Bulletin*, v. 104, p. 1621–1636.
- Stinton, J.M., and Detrick, R.S., 1992, Mid-ocean ridge magma chambers: *Journal of Geophysical Research*, v. 97, p. 197–216.
- Stix, J., Kennedy, B., Hannington, M., Gibson, H., Fiske, R., Mueller, W., and Franklin, J., 2003, Caldera-forming processes and the origin of submarine volcanogenic massive sulfide deposits: *Geology*, v. 31, p. 375–378.
- Stuben, D., Neumann, T., Taibi, N.E., and Glasby, G.P., 1995, Variations in hydrothermal activity at the Mariana arc backarc spreading center at 18°13'N between 1987 and 1990: *Chemie der Erde*, v. 55, p. 61–79.
- Taylor, B., Klaus, A., Brown, G.R., and Moore, G.F., 1991, Structural development of Sumisu Rift, Izu-Bonin arc: *Journal of Geophysical Research*, v. 96, p. 16,113–16,129.
- Taylor, R.N., Murton, B.J., and Nesbitt, R.W., 1992, Chemical transects across intra-oceanic arcs: Implications for tectonic setting of ophiolites, *in* Parson, L.M., Murton, B.J., and Browning, P., eds., *Ophiolites and their modern oceanic analogues: Geological Society of London, Special Publication 60*, p. 117–132.
- Tamura, Y., Gill, J.B., Tollstrup, D., Kawabata, H., Shukuno, H., Chnag, Q., Miyazaki, T., Takahashi, T., Hirahara, Y., Kodaira, S., Ishizuka, O., Suzuki, T., Kido, Y., Fiske, R.S., and Tatsumi, Y., 2009, Silicic magmas in the Izu-Bonin oceanic arc and implications for crustal evolution: *Journal of Petrology*, v. 50, p. 685–723.
- Tegart, P., Allen, G., and Carstensen, A., 2000, Regional setting, stratigraphy, alteration and mineralization of the Tambo Grande VMS district, Piura Department, northern Peru, *in* Sherlock, R.L., and Logan, M.A.V., eds., *Volcanogenic massive sulphide deposits of Latin America: Geological Association of Canada, Mineral Deposits Division, Special Publication 2*, p. 375–405.
- Titley, S.R., 1993, Relationship of stratabound ores with tectonic cycles of the Phanerozoic and Proterozoic: *Precambrian Research*, v. 61, p. 295–322.
- Tivey, M.A., and Johnson, H.P., 2002, Crustal magnetization reveals subsurface structure of Juan de Fuca Ridge hydrothermal vent fields: *Geology*, v. 30, p. 979–982.

Viereck, L.G., Flower, M.F.J., Hertogen, J., Scmincke, H.-U., and Jenner, G.A., 1989, The genesis and significance of N-MORB sub-types: Contributions to Mineralogy and Petrology, v. 102, p. 112–126.

Walker, P.N., and Barbour, D.M., 1981, Geology of the Buchans ore horizon breccias, *in* Swanson, E.A., Strong, D.F., and Thurlow, J.G., eds., The Buchans orebodies—Fifty years of geology and mining: Geological Association of Canada Special Paper 22, p. 161–185.

Wohletz, K., and Heiken, G., 1992, Volcanology and geothermal energy: Berkeley, University of California Press, 432 p.

Wright, I.C., Stoffers, P., Hannington, M., de Ronde, C.E.J., Herzig, P., Smith, I.E.M., and Browne, P.R.L., 2002 Towed-camera investigations of shallow-intermediate water-depth submarine basaltic stratavolcanoes of the southern Kermadec arc, New Zealand: Marine Geology, v. 185, p. 207–218.

Yang, K., and Scott, S.D., 1996, Possible contribution of a metal-rich magmatic fluid to a seafloor hydrothermal system: Nature, v. 383, p. 420–423.

Yang, K., and Scott, S.D., 2006, Magmatic fluids as a source of metals in seafloor hydrothermal systems, *in* Christie, D.M., Fisher, C.R., Lee, S-M, and Givens, S., eds., Back-arc spreading systems—Geological, biological, chemical, and physical interactions: American Geophysical Union Geophysical Monograph 166, p. 163–184.

Yuasa, M., and Kano, K., 2003, Submarine silicic calderas on the northern Shichito-Iwojima Ridge, Izu-Ogasawara (Bonin) arc, Western Pacific, *in* White, J.D.L., Smellie, J.L., and Clague, D.A., eds., Explosive subaqueous volcanism: American Geophysical Union, Geophysical Monograph 140, p. 231–243.

Zierenberg, R.A., Shanks, W.C., III, Seyfried, W.E., Jr., Koski, R.A., and Strickler, M.D., 1988, Mineralization, alteration, and hydrothermal metamorphism of the ophiolite-hosted Turner-Albright sulfide deposit, southwestern Oregon: Journal of Geophysical Research., v. 93, p. 4657–4674.

5. Physical Volcanology of Volcanogenic Massive Sulfide Deposits

By Lisa A. Morgan and Klaus J. Schulz

5 of 21

Volcanogenic Massive Sulfide Occurrence Model

Scientific Investigations Report 2010–5070–C

U.S. Department of the Interior
U.S. Geological Survey

U.S. Department of the Interior
KEN SALAZAR, Secretary

U.S. Geological Survey
Marcia K. McNutt, Director

U.S. Geological Survey, Reston, Virginia: 2012

For more information on the USGS—the Federal source for science about the Earth, its natural and living resources, natural hazards, and the environment, visit <http://www.usgs.gov> or call 1-888-ASK-USGS.

For an overview of USGS information products, including maps, imagery, and publications, visit <http://www.usgs.gov/pubprod>

To order this and other USGS information products, visit <http://store.usgs.gov>

Any use of trade, product, or firm names is for descriptive purposes only and does not imply endorsement by the U.S. Government.

Although this report is in the public domain, permission must be secured from the individual copyright owners to reproduce any copyrighted materials contained within this report.

Suggested citation:

Morgan, L.A., and Schulz, K.J., 2012, Physical volcanology of volcanogenic massive sulfide deposits in volcanogenic massive sulfide occurrence model: U.S. Geological Survey Scientific Investigations Report 2010-5070 -C, chap. 5, 36 p.

Contents

| | |
|---|----|
| Introduction..... | 65 |
| Role of Water in Submarine Volcanism..... | 68 |
| Classification System..... | 68 |
| Flow Lithofacies Associations..... | 69 |
| Mafic-Ultramafic Volcanic Suite (Primitive Intraoceanic Back-Arc or Fore-Arc Basins or Oceanic Ridges) | 72 |
| Pillow Lava Flows in Mafic-Ultramafic Associations | 72 |
| Bimodal-Mafic Volcanic Suite (Incipient-Rifted Intraoceanic Arcs) | 75 |
| Effusive Dominated Subaqueous Calderas in the Bimodal-Mafic Associations | 75 |
| Felsic Lobe-Hyaloclastite Flows in Bimodal-Mafic Associations | 77 |
| Other Silicic Flows and Domes in Bimodal-Mafic Associations | 80 |
| Bimodal-Felsic Type (Incipient-Rifted Continental Margin Arcs and Back Arcs)..... | 83 |
| Explosive Dominated Submarine Calderas in Bimodal-Felsic Associations | 83 |
| Volcaniclastic Lithofacies Associations | 85 |
| Sedimentary Lithofacies Associations..... | 85 |
| Siliciclastic-Felsic Volcanic Suite (Mature Epicontinental Margin Arcs and Back Arcs) | 87 |
| Siliciclastic-Mafic Volcanic Suite (Rifted Continental Margin, Intracontinental Rift, or Sedimented Oceanic Ridge) | 88 |
| Subvolcanic Intrusions | 91 |
| Summary and Conclusions..... | 94 |
| References Cited..... | 95 |

Figures

| | |
|---|----|
| 5-1. Graphic representations of the lithological classification used in this study | 66 |
| 5-2. Genetic classification of volcanic deposits erupted in water and air..... | 67 |
| 5-3. Physical conditions for volcanic eruptions..... | 70 |
| 5-4. Diagrams showing different types of genetically related and nonrelated volcanic rocks and processes..... | 71 |
| 5-5. Tectonics and stratigraphy of mafic-ultramafic volcanogenic massive sulfide deposits..... | 73 |
| 5-6. Series of figures highlighting environment and features of pillow lavas..... | 74 |
| 5-7. Composite stratigraphic sections for various areas hosting volcanogenic massive sulfide mineralization in the bimodal mafic suite | 76 |
| 5-8. Paleogeographic reconstruction of the evolution of the Normetal caldera from a subaqueous shield volcano to a piston-type caldera | 78 |
| 5-9. Features associated with bimodal mafic association, specifically the felsic lobe hyaloclastite facies..... | 79 |
| 5-10. Volcanic domes common in a siliciclastic felsic suite..... | 81 |
| 5-11. Schematic evolution of the Bald Mountain sequence | 82 |
| 5-12. Products of explosive dominated submarine calderas in bimodal-felsic volcanic suite..... | 86 |

| | | |
|-------|---|----|
| 5-13. | Schematic cross section of the Rio Tinto mine, Iberian Pyrite Belt deposit, showing location of the volcanogenic massive sulfide deposit and sediment-sill complexes..... | 88 |
| 5-14. | Composite stratigraphic sections for various areas hosting volcanogenic massive sulfide mineralization in the siliciclastic felsic association | 89 |
| 5-15. | Generalized stratigraphic sections for volcanogenic massive sulfide mineralization in a siliciclastic mafic suite..... | 90 |
| 5-16. | Physical parameters and controls on volcanism..... | 92 |
| 5-17. | Schematic of a volcanic section hosting volcanogenic massive sulfide showing relative positions of subvolcanic intrusions..... | 93 |
| 5-18. | Geologic map of the Archean Noranda camp showing the volcanogenic massive sulfide deposits underlain by the Flavrian-Powell subvolcanic intrusive complex | 94 |

Tables

| | | |
|------|--|----|
| 5-1. | Comparison of some important properties of water versus air and their effects on eruptions | 68 |
| 5-2. | Comparison of some important environmental factors for subaqueous and subaerial eruptions..... | 69 |

5. Physical Volcanology of Volcanogenic Massive Sulfide Deposits

By Lisa A. Morgan and Klaus J. Schulz

Introduction

Volcanogenic massive sulfide (VMS) deposits form at or near the seafloor in a variety of marine volcano-tectonic terranes (fig. 5–1). These deposits form from a spectrum of volcanic and hydrothermal processes (fig. 5–2), include a broad range of chemical compositions, occur in a variety of tectonic settings, and commonly display marked contrasts in physical characteristics between the ore body and its host rock. Volcanogenic massive sulfide deposits are enriched in Cu, Pb, Zn, Au, and Ag and are significant global sources of these elements. Approximately 1,100 VMS deposits have been identified worldwide with a total estimated resource of about 10 Bt (billion tons) (Mosier and others, 2009).

A highly effective approach in understanding the origin and evolution of VMS deposits is the application of physical volcanology, the study of eruption dynamics and emplacement processes responsible for the resultant deposit(s). Physical volcanology is especially useful in hydrothermally altered and metamorphosed volcanic terranes. In general, physical volcanology is used (1) to identify the products and deposits associated with volcanic eruptions; (2) to understand the complex mechanisms associated with eruptions; (3) to comprehend mechanisms of emplacement and post-emplacement processes of the deposits; and (4) to recognize volcanic terranes by their geomorphology (Gibson and others, 1999; Gibson, 2005).

Physical volcanology is important in the classification of VMS deposits (McPhie and others, 1993; Gibson and others, 1999) (fig. 5–2). The controls on whether an eruption is explosive or effusive include the magma composition, volatile content, eruption rate, viscosity, and ambient conditions, especially the presence of external water and ambient pressure (Cas and Wright, 1987; Cas, 1992). The reconstruction of volcanic history through facies analyses and stratigraphic correlation permits the paleogeographic and geotectonic environment of older volcanic terranes to be revealed. This provides a framework to understand the controls for localization of mineralization. Recognition of distinctive volcanic facies and facies associations is critical to reconstructing the original facies architecture of the system (McPhie and Allen, 1992). Techniques such as geologic mapping, stratigraphic and facies analyses, geochemical and geophysical fingerprinting, and interpretation of core samples help define the specific

volcanic-tectonic setting and contribute to the identification of distinct volcanic environments that are favorable for the formation of VMS deposits. This approach enhances predictive capability and provides a basis for establishing criteria for exploration.

We use the classification system of Franklin and others (2005) and Galley and others (2007), recognizing five lithostratigraphic deposit types and associated tectonic terranes in which VMS deposits form (fig. 5–1). This classification scheme considers the entire stratigraphic sequence or volcano-sedimentary cycle within a district (Franklin and others, 2005). Each sequence is bounded either by faults, disconformities, or unconformities marking a significant break in the stratigraphic record (Franklin and others, 2005). Deposits within a specific district are confined to a limited volcanic episode or stratigraphic interval (Franklin, 1996), usually lasting <2 m.y. These deposits form in terranes at different levels of maturity in their evolution and include (fig. 5–1 inset):

1. primitive intraoceanic back arc, fore-arc basin, or oceanic ridge producing a mafic-ultramafic suite typified by ophiolite sequences containing <10 percent sediment (for example, Cyprus, Oman) (Franklin and others, 2005) (fig. 5–1);
2. incipient-rifted intraoceanic arcs producing a bimodal-mafic suite typified by lava flows and <25 percent felsic strata (for example, Noranda, Ural Mountains);
3. incipient-rifted continental margin arc and back arc producing a bimodal-felsic suite, typified by 35–70 percent felsic volcanoclastic strata (for example, Skellefte, Tasmania, Jerome);
4. mature epicontinental margin arc and back arc producing a siliciclastic-felsic suite dominated by continent-derived sedimentary and volcanoclastic strata (for example, Iberia, Bathurst); and
5. rifted continental margin or intracontinental rift or sedimented oceanic ridge producing a siliciclastic-mafic suite typified by subequal amounts of pelite and basalt (for example, Windy Craggy, Besshi).

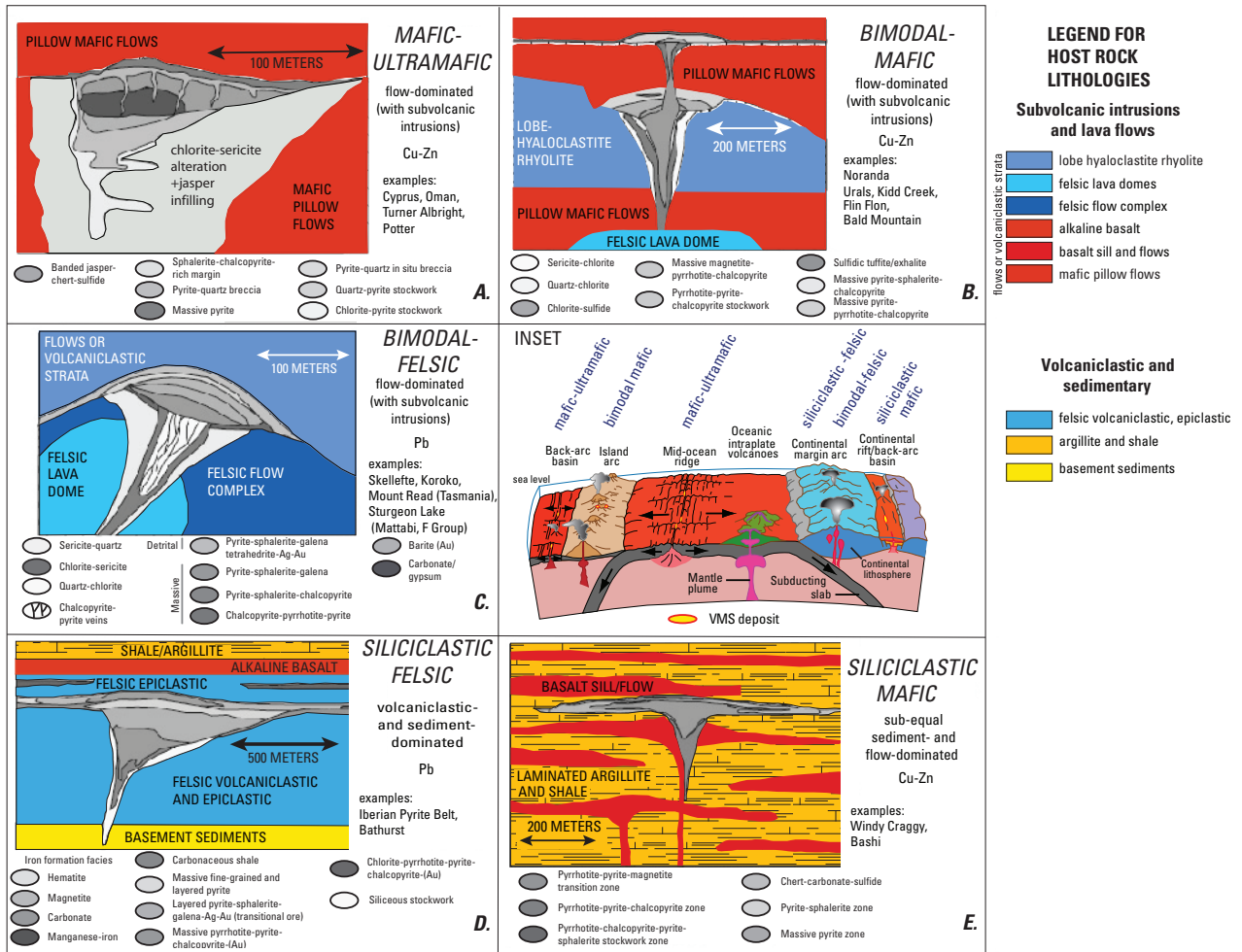


Figure 5-1. Graphic representations of the lithological classification used in this study (modified from Barrie and Hannington, 1999, by Franklin and others, 2005). Emphasized here in color (red generally for mafic compositions, blue generally for felsic compositions) are the volcanic, volcanoclastic, or sediment host rocks for each lithofacies unit; examples of associated VMS deposits are represented in shades of gray and are listed. The inset (from fig. 4-2, this volume) identifies the tectonic environment for each volcanic terrane; the individual type of associated lithofacies is shown as larger italicized letters above their respective terranes. Modified from Galley and others (2005). [Ag, silver; Au, gold; Cu, copper; Pb, lead; Zn, zinc]

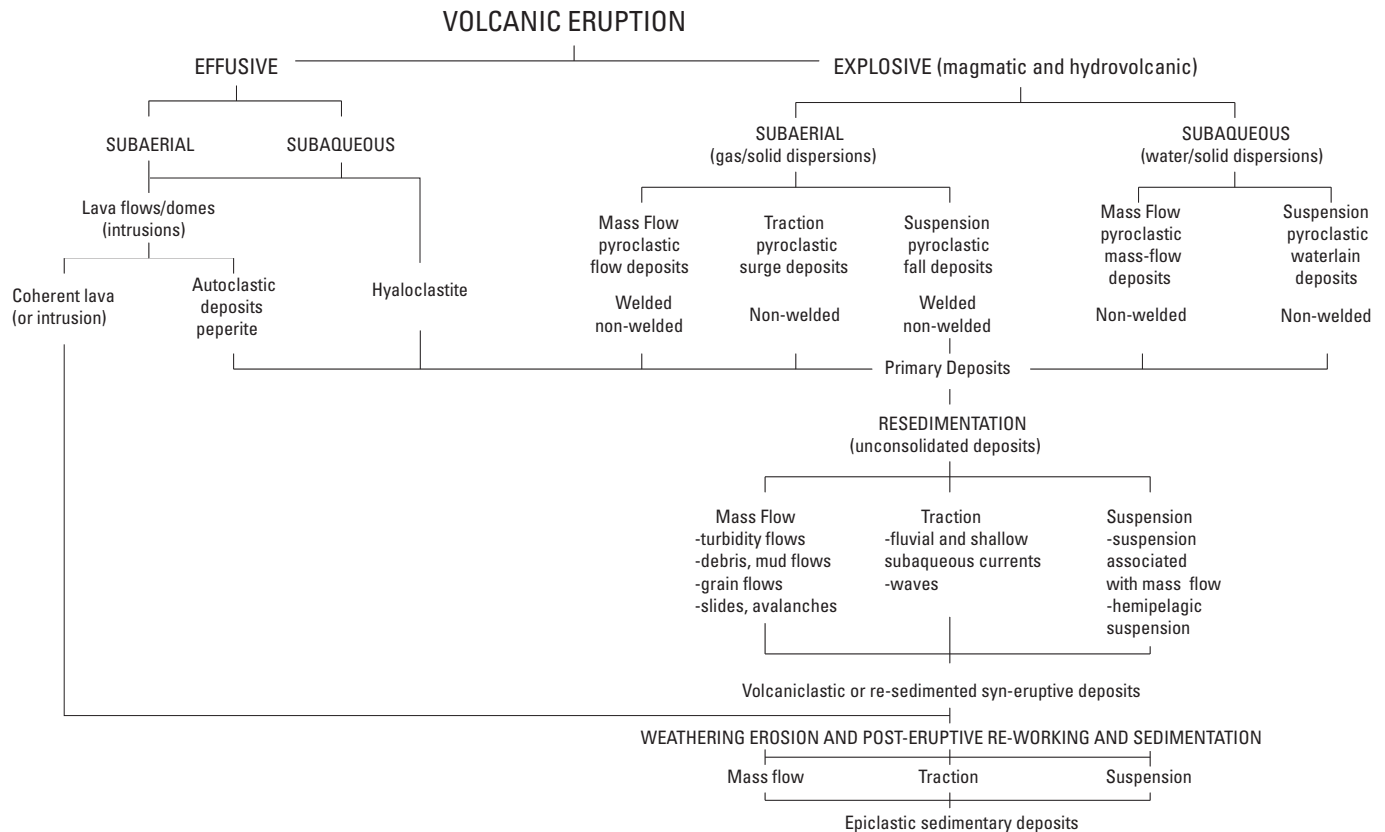


Figure 5-2. Genetic classification of volcanic deposits erupted in water and air (from Gibson and others, 1999).

The mafic-ultramafic, bimodal-mafic, and siliciclastic-mafic volcanic suites are associated with ocean-ocean subduction-related processes and represent various stages in the evolution of arc development (Franklin and others, 2005). Bimodal-felsic and siliciclastic-felsic volcanic suites are associated with continental margins to back-arc environments. These suites were developed in submarine environments where about 85 percent of all volcanism on Earth occurs (White and others, 2003). Tables 5-1 and 5-2 consider the differences for sub-aerial volcanic deposits versus those emplaced in subaqueous environments, prime locales for VMS deposition.

Volcanogenic massive sulfide mineralization occurs in two main types of volcanic deposit associations, each of which may contain subordinate sedimentary lithofacies: lava flow-dominated lithofacies associations and volcanoclastic-dominated lithofacies associations. These associations are suggested to correspond in general to deposits that formed in deep water versus shallow water volcanic environments, respectively (Gibson and others, 1999) (fig. 5-3A). A third lithofacies type that hosts or is associated with VMS mineralization is sediment dominated (see fig. 4-8).

Volcanic processes and deposits have a major influence on modifying their physical environments (for example, water depth, elevation, gradient, and relief) (McPhie and Allen, 1992) (fig. 5-3). Explosive volcanism can occur suddenly and

can erupt large volumes of pyroclastic material resulting in abnormal sedimentation rates, changes in drainage patterns, and deposition of lateral facies that represent contrasting emplacement processes. Of all rock types, volcanic rocks have the largest range of physical properties, including density, porosity, permeability, and chemical stability. Post-emplacment processes such as vitrification, devitrification, quenching, welding, degassing, and alteration impose additional variability in the diversity and properties of rock types. Volcanic rocks can be emplaced at extremely high and low temperatures and in dry and wet forms. Discharge rate and magma composition control the shapes and dimensions of lava flows (Walker, 1992).

The bulk density of overlying host strata and the density of magmas that intrude the sequence influence the type of volcanism and whether lavas are emplaced on the surface, intrude into wet sediment and mix to create peperite, intrude into the sediments as invasive flows, or are emplaced as shallow dikes and sills never reaching the surface. Multiple and overlapping volcanic events may be contemporaneous but not genetically related (fig. 5-4), and thus it is critical in establishing the volcanic history of the terrane that the different volcanic environments responsible for emplacement of specific volcanic deposits are understood and can be identified (McPhie and Allen, 1992; McPhie and others, 1993).

Table 5–1. Comparison of some important properties of air versus water and their effects on eruptions. Note the similar values for the viscosity of steam and the values for heat capacity to those of air. Heat capacity per volume for both air and steam is much lower than that of water; the values in the table are heat capacity per kilogram. Thermal conductivity of water is about 20 times that of air, but steam has a thermal conductivity almost 50 times that of water.

[Source: White, 2003. kg/m³, kilogram per cubic meters; mPa•s, millipascal-second; J/kg•K, joule per kilogram-Kelvin; W/m•K, watt per meter-Kelvin; °C, degree Celsius; K, Kelvin; STP, standard conditions for temperature and pressure]

| Air | Water (*steam) |
|---|--|
| Density | |
| 1.239 kg/m ³ (cold dry air at sea level) decreases with altitude | 1,000 kg/m ³ (fresh water, standard conditions) 1,025 kg/m ³ (typical surface seawater) |
| Viscosity | |
| 0.0179 mPa•s (millipascal) at 15°C, STP | 1.00 mPa•s (millipascal) at 20°C, STP * 0.01 mPa•s (millipascal) saturated steam, STP |
| Specific heat capacity | |
| 1,158 J/kg•K (at 300 K) | 4,148.8 J/kg•K (liquid water at 20°C) * 1,039.2 J/kg•K (water vapor at 100°C) |
| Thermal conductivity | |
| 0.025 W/m•K (air at sea level) | 0.56 W/m•K (liquid water at 273 K) * 27.0 (water vapor at 400 K) ** 2.8 (ice at 223 K) |

Role of Water in Submarine Volcanism

Water plays an important role in controlling and influencing the physical nature of volcanism. Over two thirds of the Earth's surface is below sea level and, as recent submarine investigations reveal, volcanism is more common on the seafloor than in the subaerial environment (Fisher and others, 1997). Until recently, few eruptions on the seafloor have been witnessed, but those that have been witnessed on the seafloor (Chadwick and others, 2008) have provided new and insightful observations (Kessel and Busby, 2003; Cashman and others, 2009; Chadwick and others, 2009). Much remains to be learned about the effects of ambient water and hydrostatic pressure on volcanic eruptions in deep marine environments (fig. 5–2; tables 5–1, 5–2) (see also Busby, 2005; Clague and others, 2009).

The environment of formation for all VMS deposits is subaqueous and, thus, water strongly influences subsequent volcanic processes and the physical nature of rock created. Water creates a very different set of conditions for submarine volcanism compared to more frequently observed subaerial volcanism. In the submarine environment, ambient temperatures may be at near-freezing temperatures; pressures can range up to 500 bars (approximately 5000 m water depth) or more (McBirney, 1963). Water can be locally heated by lava and change rapidly from a liquid phase to a vapor phase, resulting in a sudden increase in total volume.

Classification System

Figure 5–1 highlights the volcanic and sedimentary rock types for each major VMS deposit subtype in the classification system used. The volcanic deposits can be subdivided and grouped into two primary environments: (1) those dominated by high-level dikes, sills, cryptodomes, and lava flows (fig. 5–1-A, B, C), and (2) those dominated by volcanoclastic and sedimentary sequences (fig. 5D, E). The following is a summary of the physical volcanological characteristics for each of the lithostratigraphic types and associated tectonic terranes linked with VMS deposition. The focus of this chapter is on the specific terranes and specific volcanic-related deposits that are common to VMS terranes. As such, in regard to volcanic and sedimentary rocks, only those rock types that are typical to VMS deposits are discussed, including pillow basalts and other flow forms in deep water environments, lobe-hyaloclastite rhyolite, felsic lava domes, felsic flow complexes, pyroclastic deposits, flow- or volcanoclastic-dominated sequences, terrigenous clastic sediments, and shale/argillitic sequences. Subvolcanic intrusions, mapped as deep crustal bodies and plutons, provide the major sustained heat sources for VMS mineralization and are discussed at the end of this chapter.

Table 5-2. Comparison of some important environmental factors for subaqueous and subaerial eruptions.

[Source: White, 2003]

| Phenomenon | Subaqueous | Effect (± trend) | Subaerial | Effect |
|---|---|--|---|--|
| Steam from interaction with magma, hot particles, and (or) as magmatic volatile | Ubiquitously formed above critical depths by interaction of magma with ambient water, films on hot clasts, from magma at shallower than critical depths | Expansion (may be violent), high buoyancy, low heat capacity compared to water, steam formation suppressed with depth; disappears at ~3 km in seawater | Steam from interaction with magma only in “wet” sites, steam in eruption plume also from heating of air entrained, and from magma | Expansion (may be violent), buoyant when hot, condensing water alters particle transport properties (for example, adhesion) heat capacity similar to air |
| Pressure | Hydrostatic pressure | Damps expansion of steam from boiling and of magmatic gases; in combination with cooling, condenses gas in eruption plumes to produce aqueous plumes or currents; effect increases strongly with depth | Atmospheric pressure | Allows expansion of gases; eruption plumes are at maximum pressure near vent exit, and pressure decreases gradually with height in atmosphere |
| Thermal behavior | High heat capacity | Rapid cooling of magma, hot rock (but see steam, above) can cause fragmentation by granulation | Low heat capacity | Slow cooling of magma, hot rock; granulation not effective, but dynamothermal spalling for some lavas |
| Rheology | High density, high viscosity | Low clast settling velocities, slower movement or expansion of plumes, currents; hot particles may be temporarily buoyant, and some pumice persistently buoyant; gas-supported currents require very high particle concentrations to remain negatively buoyant | Low density, low viscosity | High clast settling velocities, granular collisions more important in transport; all clasts more dense than atmosphere at all times; gas-supported currents negatively buoyant even at low to moderate particle concentrations |

Flow Lithofacies Associations

Essential elements in the lithofacies classification include (1) coherent lava flows and domes of several compositions ranging from ultramafic to mafic to felsic; (2) possible associated autoclastic deposits (autobreccia, hyaloclastite, and redeposited equivalents) (Franklin and others, 2005); and (3) possible hosting of synvolcanic intrusions, including sills, dikes, and less commonly, cryptodomes. Minor amounts of volcanoclastic rocks are associated with some VMS deposits

and range from redeposited autobreccia to primary pyroclastic deposits. Sedimentary rocks such as carbonaceous argillite, minor carbonate, immature volcanoclastic wacke, and exhalite (Franklin and others, 2005) may occur with the flow lithofacies. The flow lithofacies associations, dominated by lava flows, domes, and synvolcanic intrusions, are controlled by effusive eruptive processes. The eruptive sources for these effusive lavas and subvolcanic intrusions are commonly single or composite submarine volcanoes fed by subvolcanic dikes, sills, and cryptodomes. In some cases, VMS deposits occur in the capping caldera(s) or synvolcanic graben(s).

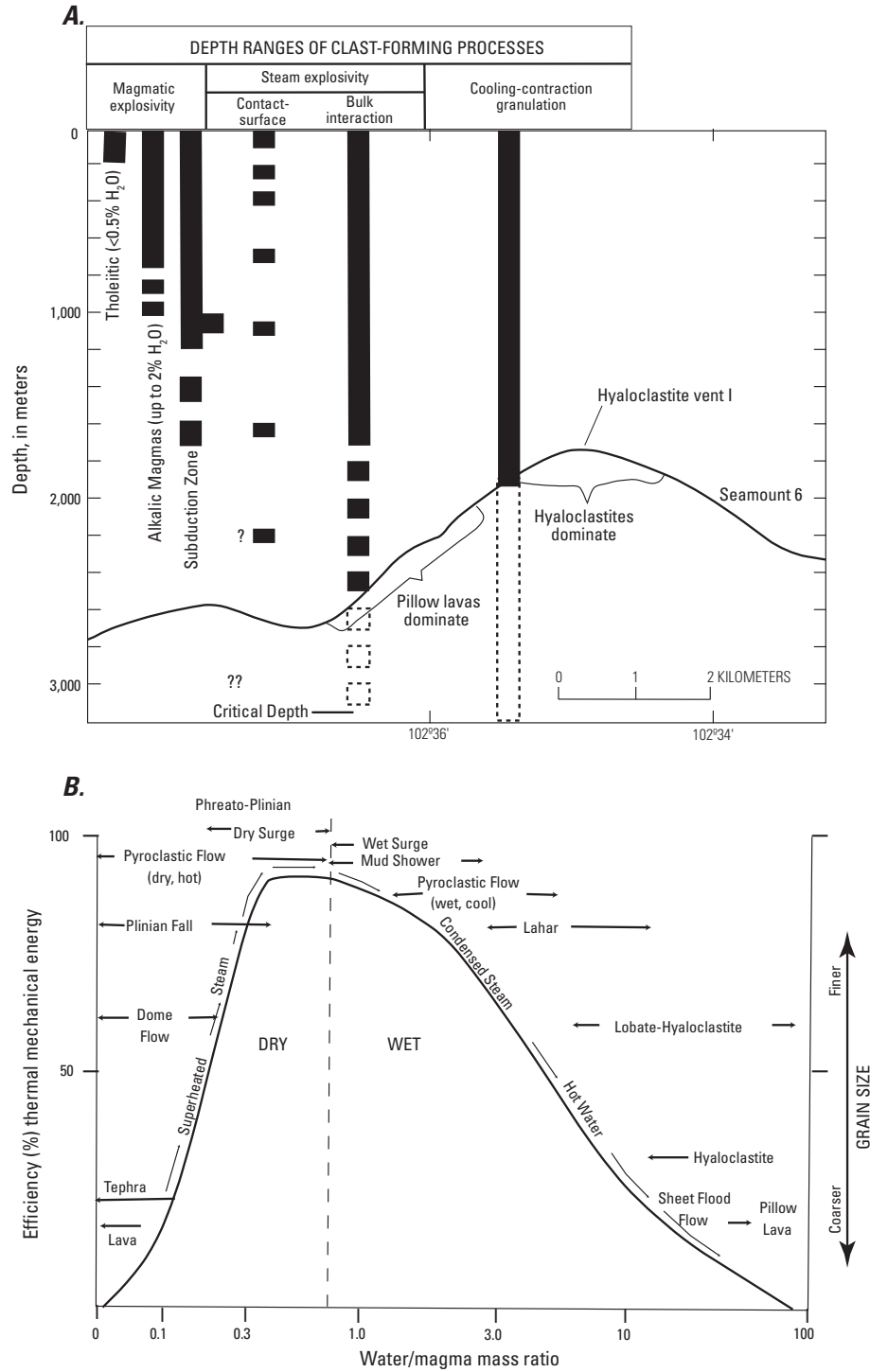


Figure 5-3. Physical conditions for volcanic eruptions. *A*, General geologic setting, conditions, and environment for magma and lava emplacement in submarine seamounts (from Head and Wilson, 2003). The cross section shown is for Seamount 6 (Eastern Pacific Ocean) but is assumed to be exemplary of conditions and observations on other seamounts (data from Smith and Batiza, 1989). Also shown are the ranges in depth of various clast-forming processes on the seafloor (from Kokelaar, 1986). *B*, Water/magma ratio versus deposit type and efficiency of fragmentation (from Gibson and others, 1999; after Wohletz and Sheridan, 1983; Wohletz, 1986; Wohletz and Heiken, 1992)

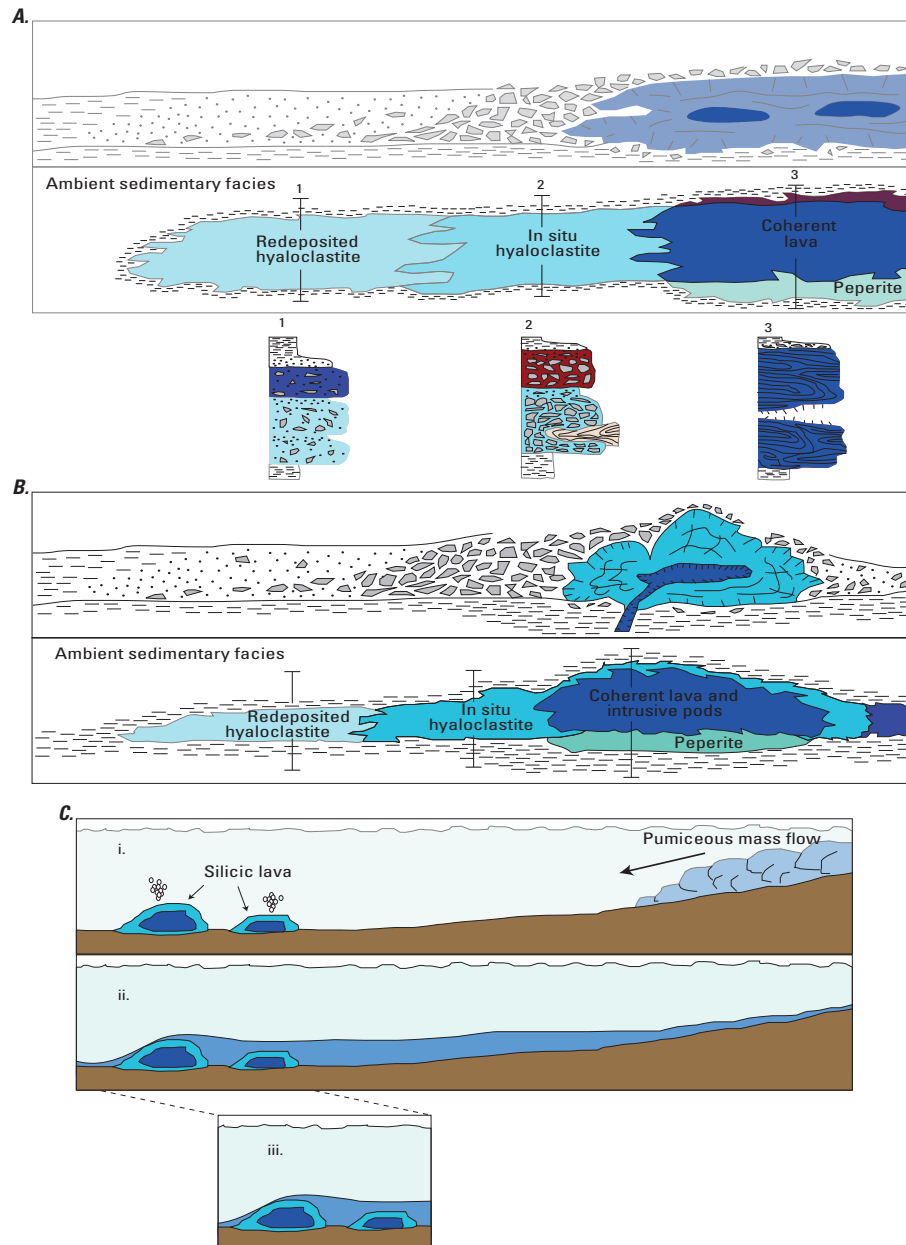


Figure 5-4. Diagrams showing different types of genetically related and nonrelated volcanic rocks and processes. *A*, Schematic cross sections through a submarine lava flow showing the character and arrangement of contemporaneous volcanic facies that develop in association with the emplacement of these lavas. Sections marked 1, 2, and 3 on the facies diagrams are defined by stratigraphic sections located between the facies diagrams. Each section shows genetically related facies that are markedly different in lithologic character, texture, and internal organization. After McPhie and others (2003). *B*, Schematic cross sections through a submarine dome showing the character and arrangement of contemporaneous volcanic facies that develop in association with the emplacement of these lavas. Sections marked 1, 2, and 3 on the facies diagrams below *A* are defined by stratigraphic sections located between the facies diagrams. Each section shows genetically related facies that are markedly different in lithologic character, texture, and internal organization. After McPhie and others (2003). *C*, Sketches illustrating penecontemporaneous, laterally equivalent volcanic facies that are not genetically related. (a) A subaqueous silicic lava dome with a brecciated carapace is emplaced and contributes considerable relief to the sea floor landscape. Pyroclastic mass flows sourced elsewhere sweep into the basin. (b) The pyroclastic mass flows are deposited as a widespread sheet and fill the topography created by the lava dome and breccia and basin. (c) The background sedimentary facies encloses the two genetically distinct volcanic facies that are directly juxtaposed and emplaced contemporaneously. From McPhie and Allen (1992).

Mafic-Ultramafic Volcanic Suite (Primitive Intraoceanic Back-Arc or Fore-Arc Basins or Oceanic Ridges)

Mafic-ultramafic suites formed during much of the Archean and Proterozoic when it is hypothesized that mantle plume activity dominated formation of Earth's early crust. Numerous incipient rifting events formed basins characterized by thick ophiolite sequences (Galley and others, 2007). A generalized stratigraphic section through an ophiolite (fig. 5-5) has (1) a series of effusive flows, mostly pillow lavas, with minimal interflow volcanoclastic material and <5 percent felsic volcanic rocks (Franklin and others, 2005) above (2) a thick section of synvolcanic intrusions in the form of sheeted dikes. These associations are typical mafic volcanic successions that form at fast ocean spreading centers or in incipient back- or fore-arc environments. This mafic succession continues downward into (3) a thick sequence of layered gabbros (representative of the crystallized magma chamber) and peridotite (representative of the depleted upper mantle beneath the magma chamber). The ultramafic suite of rocks may form in slow to ultraslow spreading environments where classic crustal successions are absent.

In deep water marine rift environments, eruptions producing pillow lava flows occur along fissures and at point sources (Cas, 1992). Such edifices include elongate shield volcanoes (fig. 5-6A), small isolated lava mounds, and lava lakes where the pillowed flows are ponded in fault blocks within and adjacent to the ridge axis (Gibson and others, 1999; Gibson, 2005). Such edifices have been identified as hosts to VMS deposits, such as the copper-rich ophiolite-hosted Cyprus deposits (Gibson and others, 1999) (fig. 5-1A).

Pillow Lava Flows in Mafic-Ultramafic Associations

Pillow lavas are among the most common volcanic rocks on Earth (Walker, 1992), having formed in underwater environments as sets of bulbous, tubular, or spherical lobes of lava fed by an interconnected system of lava tubes or channels. Pillow lavas can form in any subaqueous environment regardless of depth; they are common in deep marine environments, in glaciated environments as subglacial eruptions, and in shallow water environments such as lakes, rivers, and near-shore marine environments (Fridleifsson and others, 1982). Subaqueous development of bulbous forms by the inflation of a chilled skin that accommodates additional injections of magma is an essential attribute to pillow lava formation (Walker, 1992). Pillow lavas are produced by the rupture and subsequent piling up of individual pillow lobes; each lobe has a thick skin with a thin selvage of quenched glass (figs. 5-6B, C, D). Small mafic pillow lava lobes tend to be circular in cross section and flatten as their dimension increases, most likely under the influence of gravity (Cousineau and Dimroth, 1982). Each lobe has a convex upper surface and a base that

is either flat or concave upward, the shape commonly being a cast of the underlying pillow form. As such, pillow lavas in basaltic and andesitic flows have a distinctive and easily identifiable morphology (Gibson and others, 1999). The size of individual pillows is a function of magma viscosity; andesite pillows are usually larger than basaltic pillows and frequently have a "breadcrusted" outer surface texture. The aspect ratio (horizontal/vertical ratio) of pillow lobes varies with andesitic lavas plotting at the upper end of the spectrum and basaltic lobes at the lower end, a relationship inferred to relate to viscosity (Walker, 1992).

A pillow lava flow is fed by an interconnected system of lava tubes or open channels that are branching and intertwined. Stratigraphic analyses of Archean submarine basalt flows often show a sequence with massive flows at the base grading upward to pillow lavas and a carapace of pillow breccias (Dimroth and others, 1978, 1985). Mapping suggests that pillows form by a budding and branching process (fig. 5-6D) (Moore, 1975; Dimroth and others, 1978; Walker, 1992; Goto and McPhie, 2004). Dimroth and others (1978) propose that massive lavas form by the surging advance of hot, low-viscosity lavas. Pillow lavas form at the distal end of the flow front and have lower temperatures and higher viscosities than in their massive equivalent. The decrease in temperature and increase in viscosity results in a decrease in the velocity of the flow (Walker, 1992). Most pillow mounds form not because of decrease in temperature or viscosity but because of the decrease in the supply of magma, that is, flow rate. In general, given a constant viscosity, the formation of pillow mounds is principally a function of flow rate. As the pile of pillow lobes form, fresh magma oozes through ruptures in pre-existing lobes and the pillow pile grows in this manner. Proximal pillow lavas tend to have larger pillows than distal equivalents (fig. 5-6A). This flow process forms steep-sided ridges or mounds that can be tens of meters thick, commonly called "haystacks." Mega-pillows, up to tens of meters in diameter, have been identified in the upper and capping parts of pillow lava flows and are interpreted to be possible master channels by which fresh lava was transported from the vent to the advancing flow front (Walker, 1992). Features, dimensions, and structures associated with pillow lobes and lavas can be used to infer flow direction and source area.

The subaerial equivalents of pillow flows are tube-fed pahoehoe lava flows. Both lava flow types are interpreted to be the products of sustained eruptions at low effusion rates. The confirmation that pillow lavas and pahoehoe lavas form by similar mechanisms came with direct observations of subaqueous lava deltas associated with eruptions into the sea from Kilauea in 1972 and 1974 (Moore, 1975). Low effusion rates allow for a thick skin to form on the exterior of lava lobes or toes and contribute to insulation of the lobe interior, allowing the interior to remain hotter and more fluid. Most pillow lava lobes are dense throughout but may contain vesicles arranged in a radial pattern in the upper sections of individual lobes due to exsolution and trapping of magmatic gases. Degassing contributes somewhat to inflation of the interior and the overall

Mafic-ultramafic

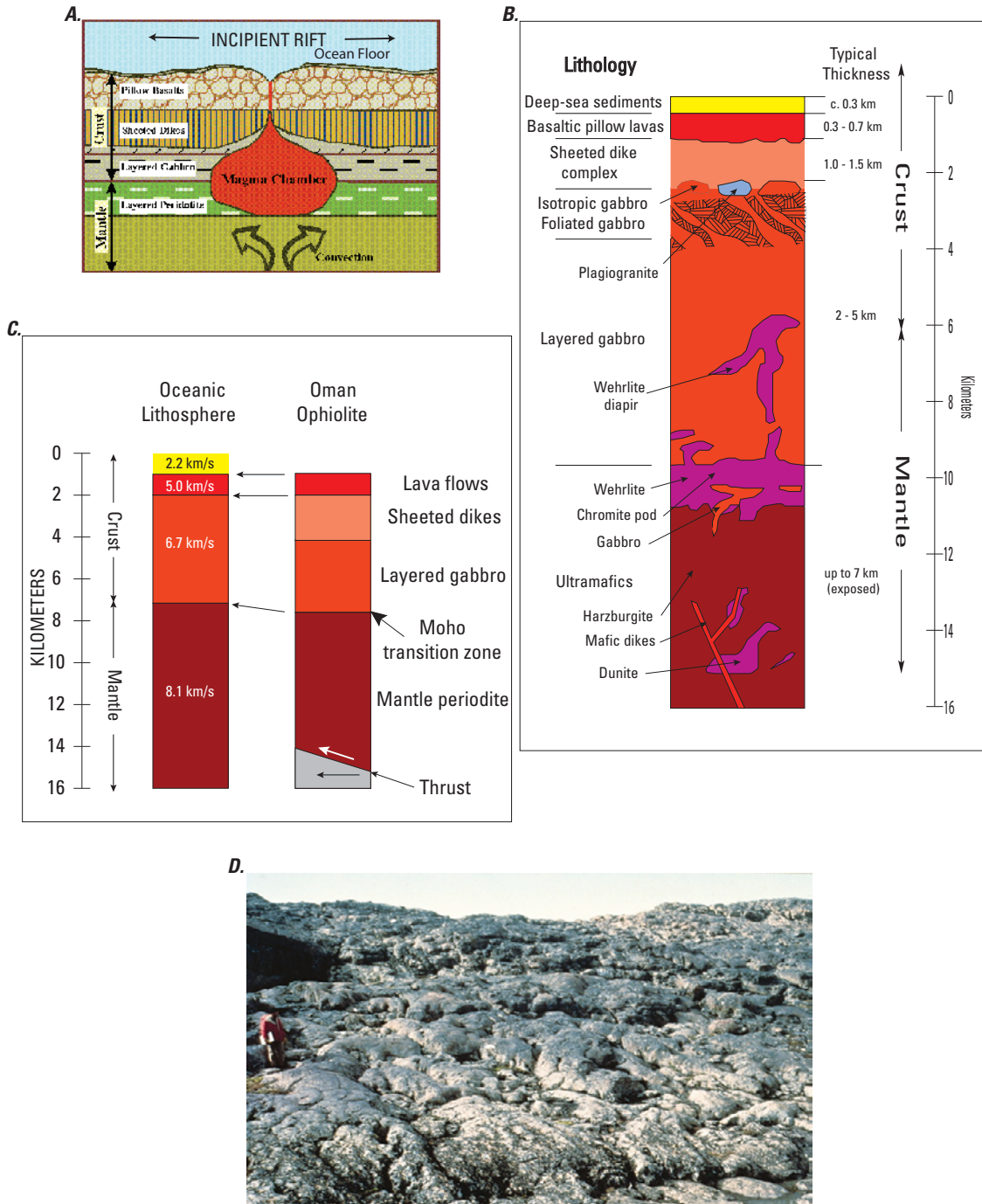


Figure 5-5. Tectonic setting and stratigraphy of mafic-ultramafic volcanogenic massive sulfide deposits. **A.** Generalized diagram showing the tectonic setting for mafic-ultramafic lithofacies (modified from Galley and Koski, 1999). The sheeted dikes and upper pillow basalt flows represent magma in transit to or on the surface whereas the layered gabbro and peridotite represent different parts of the upper mantle magma chamber, namely the crystallized magma and the depleted upper mantle under the magma chamber, respectively. **B.** Generalized stratigraphic column with associated typical thicknesses of an ophiolite sequence showing the main stratigraphic components <http://www.geol.lsu.edu/henry/Geology3041/lectures/13MOR/MOR.htm>; **C.** Comparison of the oceanic lithosphere with the Oman Ophiolite, the largest ophiolite sequence in the world (modified from http://geogroup.seg.org/oman_ophiolite.htm); **D.** Photograph of a 2-Ga ophiolite in Quebec, Canada showing basaltic pillow lava surface (from <http://www.earth.northwestern.edu/people/seth/107/Ridges/ophiolite.htm>). (Harper, G.D., 1984).

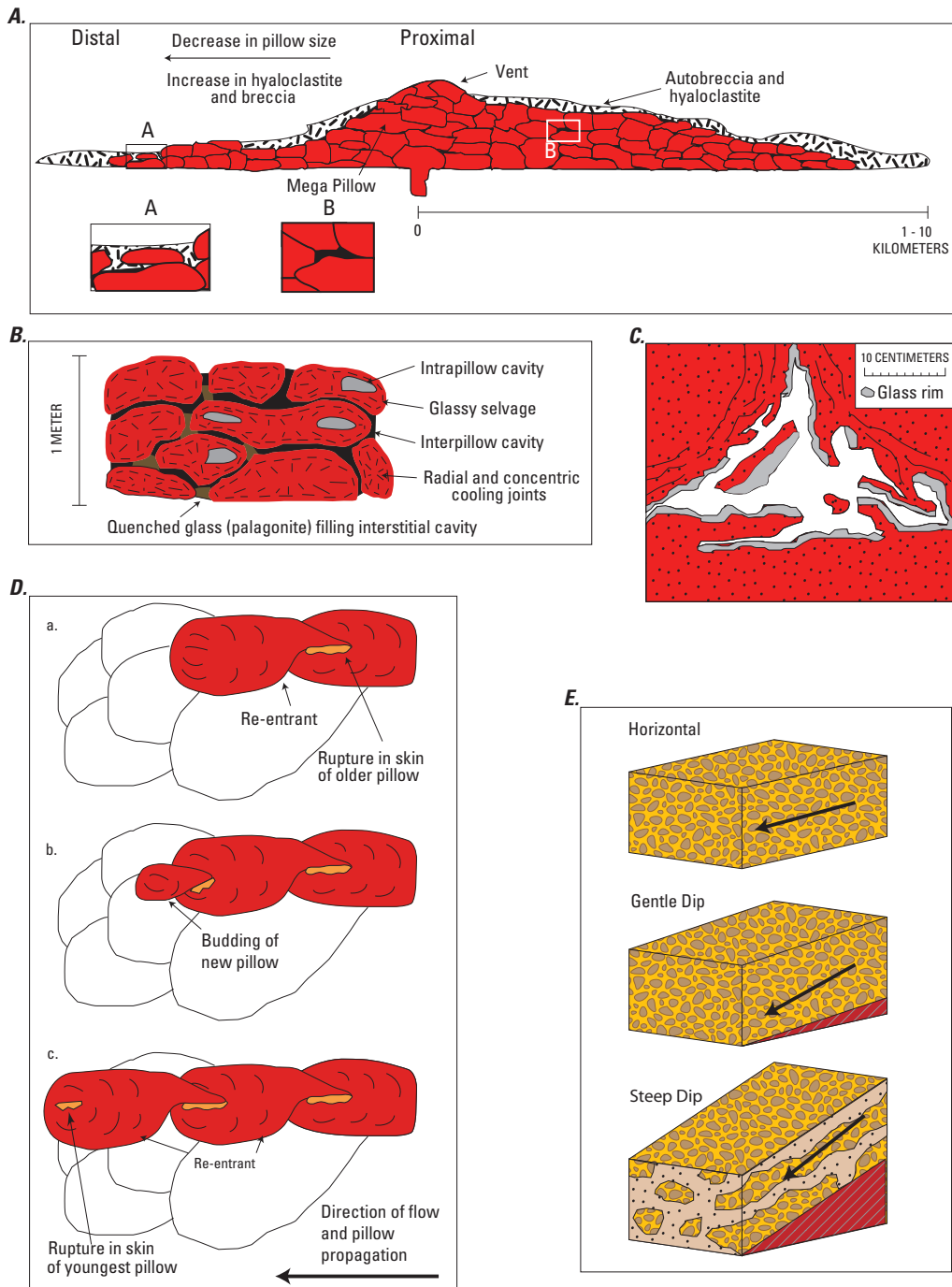
Mafic-Ultramafic Pillow Lava Flows

Figure 5-6. Series of figures highlighting features of mafic-ultramafic pillow lava flows. *A*, Idealized cross section through a pillow (tube-fed) basalt-andesite flow showing flow morphology and structures typical of proximal and distal facies. Inset *A* illustrates autobrecciation of pillows; inset *B* illustrates densely packed pillows surrounding a mega-pillow or lava tube. Vertical exaggeration is approx. 3x. From Gibson and others (1999). *B*, Detail of pillows. In cross section, pillows can vary from 10 cm spheres to large forms several meters across; they are usually several tens of centimeters in diameter. From Cas and Wright (1988); modified from Hargreaves and Ayres (1979). *C*, Close-up sketch of pillow lavas showing glassy rims or selvages spalling off, creating fine-grained material. From Walker (1992). *D*, Cross section illustrating development of re-entrant selvages by budding of a new pillow. After Hargreaves and Ayres (1979). *E*, Schematic block diagrams illustrating the morphological changes of pillow flows with change in slope. Modified from Walker (1992).

pillow form (Walker, 1992). The exterior skin on each pillow is quenched, preventing coalescence into a massive form (fig. 5–6*B*). Slope angle also exerts control on the size and aspect ratio of pillows (see Ross and Zierenberg, 1994) (fig. 5–6*E*).

Pillow flows of basaltic composition are relatively small in size, are typically smooth surfaced, and are inferred to have inflated mainly by stretching of their skin (Walker, 1992). Gibson and others (1999) subdivided pillow lavas into two units: a pillow lava unit and a less abundant pillow breccia unit. A cross section of a pillow lava sequence shows densely packed “pillows” separated by thin glassy selvages and hyaloclastite breccia (fig. 5–4*B*, fig. 5–6*B*). The lava flow advances as a prograding pillow delta fed by bifurcating and meandering tubes that feed a variable supply of magma to the flow front; this is reflected in the variable dimensions of individual pillows. Proximity to source vent and sequence in eruption interval also contribute to the physical form of the flow. Monolithic breccias at the top and terminus of a pillow lava and occurring between pillows are interpreted as autobreccias and represent in situ fragmentation of pillows, pillow budding, spalling of lobes, gravitational collapse on steep slopes, and later granulation of sideromelane pillow crusts.

Komatiites are magnesium-rich volcanic rocks that are found as lava flows, tuffs, hyaloclastites, and autobreccias (Gibson and others, 1999). Ultramafic (>18 percent MgO) komatiitic flows are interpreted as lavas erupted at high temperatures (1,400–1,700 °C) and very low viscosities (Huppert and Sparks, 1985), the latter factor contributing to the extensive aerial extent and sheet-like form of komatiitic flows. The high temperatures permit the flows to melt and thermally erode their bases and deepen their flow channels. Huppert and Sparks (1985) showed that komatiitic melts have Reynolds numbers in excess of the critical value of 2,000 and are replaced by turbulent flow, which would also enhance thermal erosion and contribute to heat loss and high cooling rates. While association of VMS deposition in komatiitic flows is uncommon, komatiitic flows are exposed at the base of the volcanic succession at the Kidd Creek district in Ontario, Canada. Whether they somehow contributed to the giant VMS complex at Kidd Creek is unknown, as the komatiites are separated from the VMS deposits by about 350 m of overlying strata containing rhyolitic domes, cryptodomes, and volcanoclastic rocks (Prior, 1996; Barrie and Hannington, 1999). Small VMS deposits are associated with tholeiitic and komatiitic basalts in the Kidd-Munro assemblage.

As shown in figure 5–1*A*, VMS bodies may be completely enclosed by mafic pillow flows above sheeted dikes. Thick (approx. 0.4 km average) sections (figs. 5–5*A–C*) of sheeted dikes are present below the typical pillow lava flow-dominated sequence in ophiolites. Sheeted dikes represent the conduits transporting magma to the surface to pillow flows. Typical mineralization in the dikes is limited and most of the massive sulfide mineralization is localized in the pillowed lavas.

Bimodal-Mafic Volcanic Suite (Incipient-Rifted Intraoceanic Arcs)

Intraoceanic rifted bimodal arcs make up approximately 17,000 linear km (40 percent) of the global volcanic arc system. Volcanism mostly occurs on the seafloor; however, occasionally the upper part of the volcanic edifice becomes emergent and forms islands (Leat and Larter, 2003). In contrast to subduction systems at continental margins, the intraoceanic subduction systems generally have a shorter history of subduction and are distinct in that magmas are not contaminated by ancient sialic crust and have little or no continental component. Intraoceanic arcs form on oceanic crust produced either at mid-ocean ridges or in back-arc spreading centers and erupt a predominantly basalt bimodal volcanic suite that can contain up to 25 percent felsic lava flows and domes. Intraoceanic arc volcanism is truly bimodal. Basaltic and basalt andesitic mafic lavas are dominant; subordinate units include silicic lavas. Intermediate composition volcanic rocks (such as andesite) are essentially absent from these terranes.

Volcanic products are lava flow dominated and include basaltic pillow and massive lava flows, felsic lavas flows, and felsic domes (figs. 5–1*B*, 5–7). Summit calderas, typically 3–7 km in diameter, are common in bimodal-mafic volcanic systems (Leat and Larter, 2003). Ancient and modern subaqueous calderas have been identified in shallow and deep marine environments and are primary hosts of VMS deposits (for example, Gibson and Watkinson, 1990; Syme and Bailes, 1993). Calderas are volcano-tectonic collapse structures that form because of the evacuation of voluminous amounts of high-level magma (Mueller and others, 2009). Volcanism associated with caldera formation can be dominated by either effusive eruptions (producing lobe-hyaloclastite flows, domes, blocky lavas, or shallow intrusions) or explosive activity (producing pyroclastic flow, surge, and fall deposits).

Effusive Dominated Subaqueous Calderas in the Bimodal-Mafic Associations

In bimodal mafic systems, subaqueous calderas form at the summit of long-lived fissure-fed shield volcanoes, have a variety of shapes and aspect ratios, and vary in their level of complexity (Franklin and others, 2005). These collapse structures can cover up to tens of square kilometers. The stratigraphic sequences from these systems contain compositionally and texturally diverse lavas and volcanoclastic rocks, reflecting a broad spectrum of eruption styles and emplacement processes (McPhie and Allen, 1992).

The subaqueous Hunter Mine caldera in the Archean Abitibi greenstone belt is a 5–7-kilometer-wide felsic-filled caldera that developed over a 6 m.y. time span (Mueller and others, 2009) and is presented as one example of an effusive-dominated caldera forming system. Caldera formation was followed by renewed rifting and the emplacement of massive and pillowed komatiitic lavas. Silicified mudstone, banded

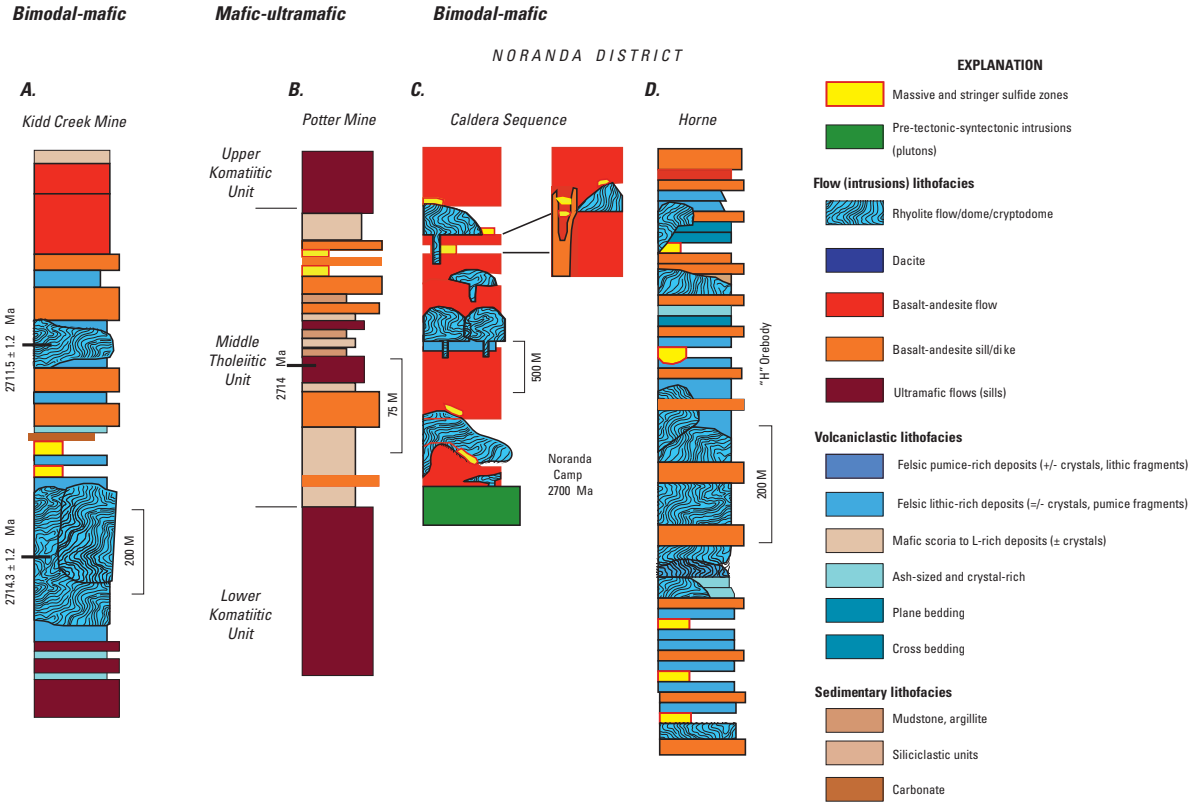


Figure 5-7. Composite stratigraphic sections for various areas hosting volcanogenic massive sulfide mineralization in the bimodal mafic suite. A–B, Kidd Creek Mine and Potter Mine contain both flow and volcaniclastic lithofacies assemblages. At Potter Mine, rhyolitic flows and volcaniclastic units are absent; abundant basaltic pyroclastic strata are present. From Gibson and Gamble (2000); geochronology from Bleeker and Parrish (1996). C–D, Schematic stratigraphic sections from the Noranda District through intracaldera flow-dominated lithofacies (C) and the rhyolitic volcaniclastic-dominated lithofacies succession that hosts the Horne deposit (D) is located along the southern structural margin of the Noranda caldera (modified after Gibson, 2005). From Franklin and others (2005). The Noranda District is considered to be bimodal mafic. (Ma, mega-annum)

iron formation, bedded felsic hyaloclastite, and abundant Bouma sequences on depositional contacts above komatiitic flows testify to submarine volcanism occurring at >500 m water depth (Mueller and others, 2009). Caldera formation in the Hunter Mine caldera was complex, involving at least two caldera-forming events separated in time by the intrusion of a gabbroic sill. The 5–7-km-wide caldera contains numerous synvolcanic faults and fractures; vertical offsets can be as much as 20 m (Mueller and others, 2009). The initial caldera formational stage included emplacement of three distinct lithofacies: (1) felsic lavas, domes, and autoclastic breccias (about 70 percent); (2) subaqueous pyroclastic deposits and reworked equivalents (Mueller and others, 2009); and (3) a 5– to 7-km-wide section of north-trending rhyolitic dikes that can be traced for several kilometers, representing the final lithofacies. A shallow, intracaldera, 1-km-thick gabbroic sill was subsequently emplaced during a period of tectonic extension, possibly associated with caldera resurgence (Wharton and others, 1994). The formation of a second caldera was marked by a trend toward more mafic-dominated magmatism. Three distinct lithofacies also are associated with the second caldera-forming stage: (1) felsic and mafic lava flows and domes, (2) volcanoclastic rocks and banded iron-formations, and (3) mafic dikes and sills.

Further evidence for long-lived multiphase caldera formation has been documented at the Normetal caldera, Quebec, where Mueller and others (2009) identified 5 stages of caldera formation and infill (fig. 5–8). Here, the volcanic sequence began with emplacement of primarily basaltic and basalt andesitic massive and pillow flows in water depths in excess of 500 m. Later dacite lavas were emplaced near the summit of the shield volcano. In stage 2, caldera formation followed with emplacement of rhyolitic lavas and volcanoclastic material. Later in stage 3, andesite-dacite flows and breccias and thick rhyolite flows were emplaced as individual volcanic centers. The fourth stage was constructive with the emplacement of high-level rhyolite endogenous domes. Deposition of deep-water volcanoclastic turbidites and shale sedimentation followed and represents a period of deconstruction and partial collapse of the volcanic edifice. The final phase of volcanic activity included emplacement of mafic and felsic flows with tuff, lapilli tuff, and lapilli tuff breccia (Mueller and others, 2008, 2009).

Volcanoclastic units are subordinate in the bimodal-mafic environment, but both mafic and felsic volcanoclastic rocks with sedimentary rocks including immature wacke, sandstone, argillite, and debris flows occur locally (fig. 5–7) (Franklin and others, 2005). The effusive nature of the dominant lava flow lithofacies associations suggest eruptive sources such as single and composite shield-like volcanoes fed by subvolcanic dikes, sills, and cryptodomes.

Up to 25 percent of the lavas erupted in young, intra-oceanic arcs are subaqueous felsic lobe-hyaloclastite flows, cryptodomes (shallow subvolcanic intrusions), and blocky lavas and domes; all are associated with VMS deposits in ancient associations (fig. 5–8) (Gibson and others, 1999;

Gibson, 2005; Mueller and others, 2008, 2009). Occasionally, the lavas form broad shield forms with slopes up to 15°. Commonly, the felsic lavas are hundreds of meters thick, have flowed up to 10 km from source, and have steep flow fronts (up to 40°) (Cas, 1992). One such felsic lava in a mafic-bimodal suite has been mapped in an Archean volcanic complex at the Noranda district in northwestern Quebec. Here the cauldron or rift graben is underlain by a large multiphase subvolcanic intrusive complex. The complex is dominated by mafic flows into which discrete felsic dome complexes have been emplaced along synvolcanic fault systems. In the Noranda cauldron, these faults are defined by dike swarms associated with the underlying subvolcanic system (Gibson and Galley, 2007) which fed the eruptions. The felsic lobe-hyaloclastite flow best typifies felsic lavas found in mafic-bimodal complexes.

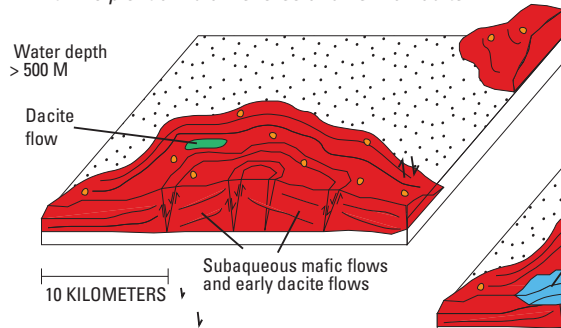
Felsic Lobe-Hyaloclastite Flows in Bimodal-Mafic Associations

Felsic lobe-hyaloclastite flows in the Noranda complex are interpreted as fissure-fed systems that formed gentle sloped (10–20°) shield volcanoes or plateaus as much as 500 m high with individual lava flows restricted to <5 km from their vents (Gibson and Watkinson, 1990). The flows formed domes or “lobes” that vented from their summits above the sediment-water interface and above their feeding fissures, which preferentially follow synvolcanic faults (fig. 5–9). The lobes are irregular or podiform in shape, may be up to tens of meters in diameter, and may show a distinct lithologic zonation described by Cas (1992).

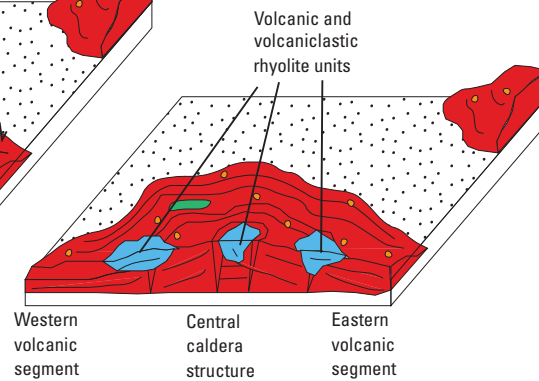
Three primary facies (massive, lobe-hyaloclastite, and breccia) are associated with felsic lobe-hyaloclastite flows and relate to distance from the vent (fig. 5–9) (Gibson and others, 1999). Each facies represents a continuum in the evolution of textures and structures in response to cooling and quench fragmentation during the eruption of lava into water. Massive facies are proximal flows and are represented by lobes >100 m in length composed of massive, flow-banded, and brecciated lava. At or next to the vent, the massive facies are dome-like. The lobes in massive facies typically have columnar, jointed, and glassy interiors which grade outward into chilled, flow-banded, and amygdaloidal vitrophyric exteriors. The lobe-hyaloclastite facies consists of irregular lobes, 2 to 100 m in length, engulfed by hyaloclastite and brecciated flow-banded lava (fig. 5–9A). Hyaloclastite refers to the clastic aggregate that forms through non-explosive fragmentation and disintegration of quenched lavas and intrusions (Rittman, 1962; Yamagishi, 1987; McPhie and others, 1993). The breccia facies is distal and composed of a poorly sorted carapace breccia and a crudely layered to redeposited flank breccia (Gibson and others, 1999). At these distal exposures, lobes appear to physically range from in situ fractured clasts of “jigsaw-fit” obsidian to obsidian hyaloclastite breccias with rotated clasts (fig. 5–9A) (Cas, 1992). Each facies is interpreted as

Bimodal-mafic dominated**evolution of Normetal caldera**

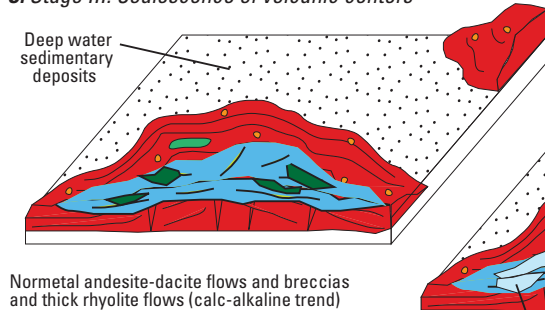
A. Stage I: Broad subaqueous shield volcano construction with incipient annular reverse and normal faults



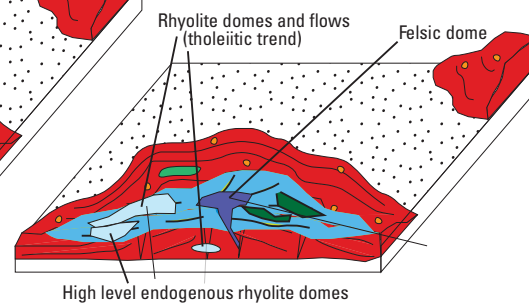
B. Stage II: Formation of individual felsic volcanic centers



C. Stage III: Coalescence of volcanic centers

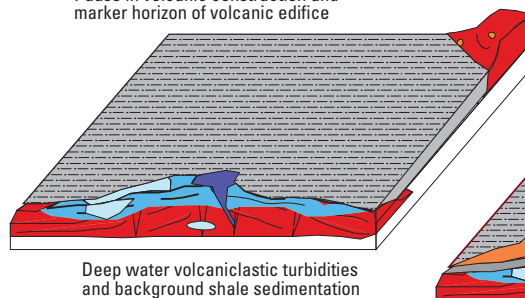


D. Stage IV: Effusive volcanism and high level dome emplacement



E. Volcaniclastic sedimentation

Pause in volcanic construction and marker horizon of volcanic edifice



F. Stage V: Final volcanism and VMS mineralization

Mafic and felsic flows with tuff, lapilli tuff, and lapilli tuff breccias

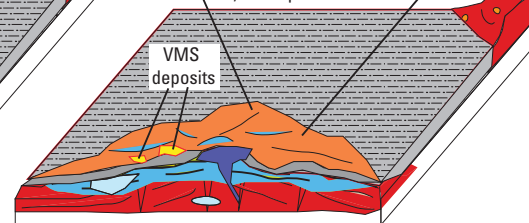


Figure 5-8. Paleogeographic reconstruction of the bimodal-mafic dominated evolution of the Normetal caldera from a subaqueous shield volcano to a piston-type caldera. *A*, Stage I. Broad subaqueous shield volcano construction with incipient annular reverse and normal faults. *B*, Stage II. Formation of individual felsic volcanic centers. *C*, Stage III. Coalescence of volcanic centers. *D*, Stage IV. Effusive volcanism and high level dome emplacement. *E*, Volcaniclastic sedimentation. *F*, Stage V. Mine sequence. From Mueller (2008).

**Bimodal-mafic dominated
felsic lobe hyaloclastite facies**

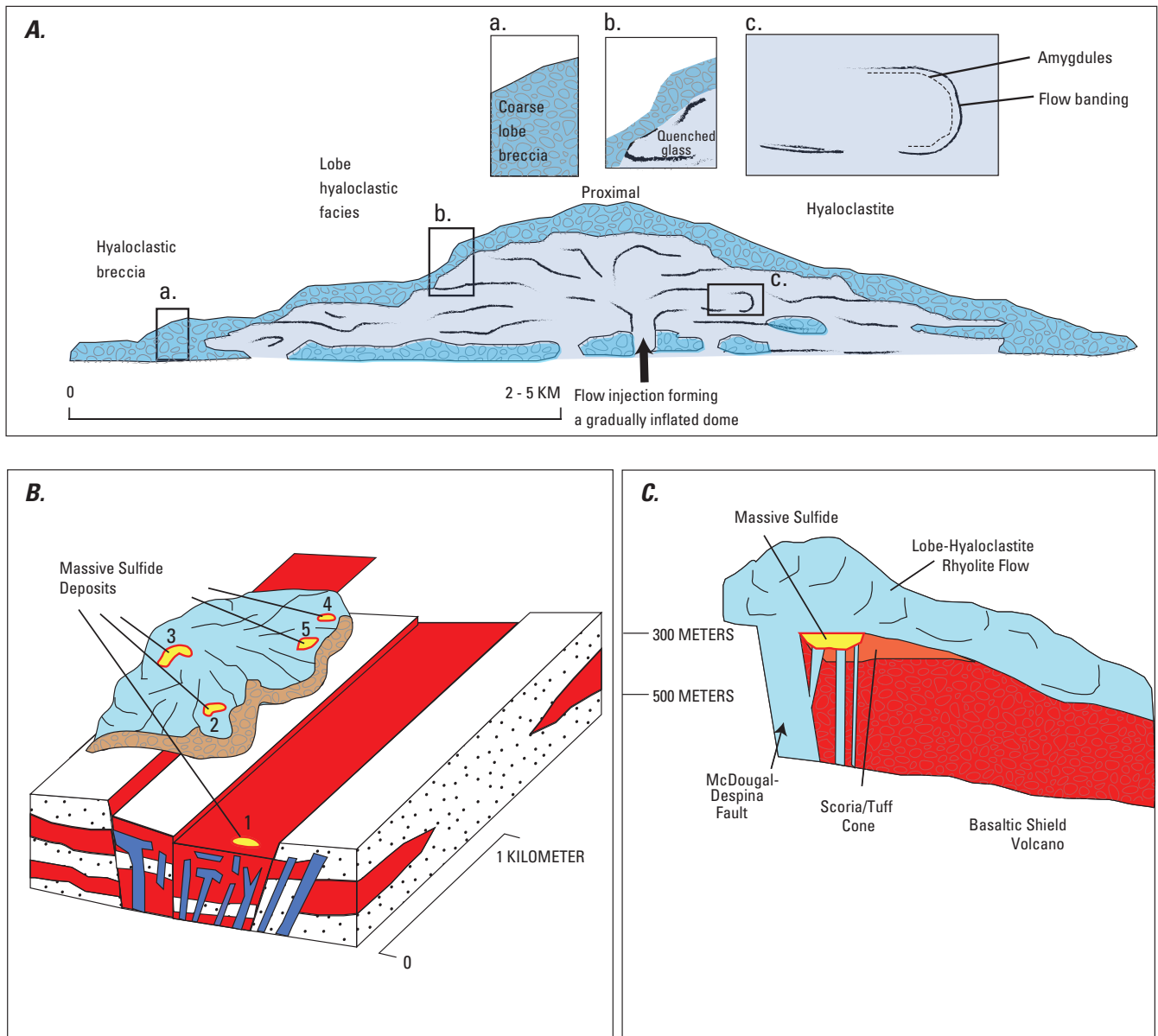


Figure 5-9. Features associated with bimodal-mafic association, specifically the felsic lobe hyaloclastite facies. **A**, Schematic cross section through a rhyolitic lobe-hyaloclastite flow showing flow morphology and structures typical of proximal and distal facies (modified after Gibson and Watkinson, 1990). **B**, Oblique perspective of the Noranda complex showing the volcanic reconstruction of contemporaneous rhyolitic and basaltic andesite flows of the Amulet Formation within a graben or fissure defined by massive flows and dikes of the Old Waite Paleofissure. The volcanogenic massive sulfide (VMS) deposits, marked by red-rimmed yellow blobs, are localized within and along the fissure and are associated with both the rhyolitic and andesitic basalt flows; numbers 1-5 correspond to VMS deposits (from Dimroth and others, 1985; Gibson and Watkinson, 1990). **C**, Cross section perspective through the McDougal-Despina fault, the feeder dike, and relationships between the lobe-hyaloclastite flow, the massive sulfide deposit, and the shield volcano and tuff cone.

representing a continuum in the evolution of textures and structures formed in response to cooling and quench fragmentation during the eruption of lava into water.

The massive facies lack hyaloclastite, which suggests a general lack of interaction with water. Rather, this facies most likely evolved by successive injections of magma lobes into a gradually inflating dome. Individual lobes are identified by stringers of amygdules and flow-banded margins (fig. 5–9A, inset c) (Gibson and others, 1999) and a lack of glassy selvages. In contrast, flowing lava in contact with water forms glass-like selvages on exterior lobes, which reflect rapid quenching (Gibson and others, 1999). These glass selvages are the source for the fine-grained clastic materials that form the hyaloclastite component of the lobe-hyaloclastite facies (Gibson and Galley, 2007).

The breccia subfacies is composed of matrix-supported hyaloclastite that has formed through quench fragmentation and contains clasts of flow-banded and massive felsic lava lobe fragments. Two subfacies of the breccia facies have been recognized: carapace breccia, which covers the flow, and hyaloclastite breccia, which forms at the distal edges and perimeter of the flow. The carapace breccia phase contains chaotically distributed clasts of flow-banded felsic flows. Here, the absence of bedding and grading and a lack of broken crystals indicate an origin derived through autobrecciation, which involves the non-explosive fragmentation of flowing lava (McPhie and others, 1993). The more distal breccia subfacies is the flank breccia (fig. 5–9A) and consists of clast-supported beds of coarse lobe fragments in a fine-grained hyaloclastite matrix (Gibson and others, 1999) interbedded with plane-bedded hyaloclastite deposits. The areal extent and volume of flank breccias are limited and represent the outer-most part of the lobe-hyaloclastite flow where slumping and later redeposition of autobreccia and hyaloclastite as subaqueous mass flow deposits are controlled by the low relief and gentle slope of the flows.

Quaternary, subglacial lobe-hyaloclastic flows of dacite and rhyolite composition in Iceland have similar characteristics as those found in the geologic record (Furnes and others, 1980). In the Iceland flows, however, some are associated with pumiceous hyaloclastite containing gray pumice and obsidian fragments that may have been emplaced as Surtseyian or Subplinian to Plinian eruptions (Furnes and others, 1980). Furnes and others (1980) interpret these flows as being emplaced in a shallow (<200 m) subglacial lake. The lack of pumiceous hyaloclastite in subaqueous lobe-hyaloclastite flows observed in the geologic record may be a function of their emplacement in deeper water (Gibson and others, 1999).

Lobe-hyaloclastite flows have many of the same physical characteristics as tube-fed pahoehoe or pillow lavas and are interpreted as being the silicic analogue for the better-known mafic process. Lobe-hyaloclastite flows advance in tube fed systems but because of higher viscosity and lower temperatures develop somewhat different morphologies. These lobes look very similar to basaltic pillow lavas but are developed on a much larger scale. In comparing the physical characteristics

of the flow lobes in the massive facies with flow lobes contained in the breccia facies, both have very similar textures, structures, and amygdule content, suggesting that the hyaloclastitic matrix and glass selvages had excellent thermal insulating properties which protected and preserved these features (Gibson and Galley, 2007).

The felsic lobe-hyaloclastite flows represent the later and more evolved stages of submarine basaltic fissure vent systems, which form large shield volcanoes on the ocean floor. In ophiolite complexes, such as Oman and Semail, lobe-hyaloclastite flows are volumetrically small and occur in the upper mafic volcanic sequences of these complexes. Often, collapse calderas occur at the summit of large shield volcanoes and are filled by fissure-fed lobe-hyaloclastite flows emplaced as isolated domes; the lobe-hyaloclastite flow is the dominant lava flow morphology for felsic lavas in these subaqueous environments. In the upper sections of the Oman ophiolite complex, the fissures feeding the felsic lobe-hyaloclastite flows are oriented perpendicular to the inferred orientation of the spreading ridge (Gibson and others, 1999). It should be noted that VMS deposits in both intraoceanic arcs (where mafic-bimodal volcanic suites are the dominant lithofacies) and in continental arc and back-arc terranes (where felsic-bimodal volcanic suites dominate) form a variety of lithofacies within each individual complex.

Other Silicic Flows and Domes in Bimodal-Mafic Associations

Small-volume silicic lava flows and domes often are emplaced as endogenous domes immediately above feeding fissures and flow as viscous blocky lava flows <2 km from their vents. Like their subaerial equivalents, these flows have steep flow fronts (20–70°), a rugged form, and develop into a proximal and distal facies (Gibson and others, 1999) (fig. 5–10). In the submarine setting, three facies develop: a massive central facies, a carapace breccia facies, and a distal flank facies, similar in nature as described above for felsic lobe-hyaloclastite flows (Gibson and others, 1999). At the Millenbach-D68 lava dome in the Noranda cauldron complex, Quebec, Canada, 15 VMS deposits are associated with silicic flows immediately above their feeding vent fissures, which later acted as the conduits for ascending hydrothermal fluids. Figure 5–10 identifies these facies.

Another bimodal mafic VMS deposit, Bald Mountain (Maine, USA), formed in deep marine, rift-controlled basins or calderas (Busby and others, 2003). The 5-km-thick volcanic sequence was deposited in three major episodes (fig. 5–11). An early volcanic episode during rapid extension was dominated by a high rate of eruption of basaltic flows and development of breccia hyaloclastites. This episode was followed by an ignimbrite-producing, caldera-forming episode and development of VMS mineralization and a final episode that included eruption of rhyolitic lavas and emplacement of subvolcanic intrusions (Busby and others, 2003; Goodfellow and others, 2003).

Siliciclastic Felsic Domes

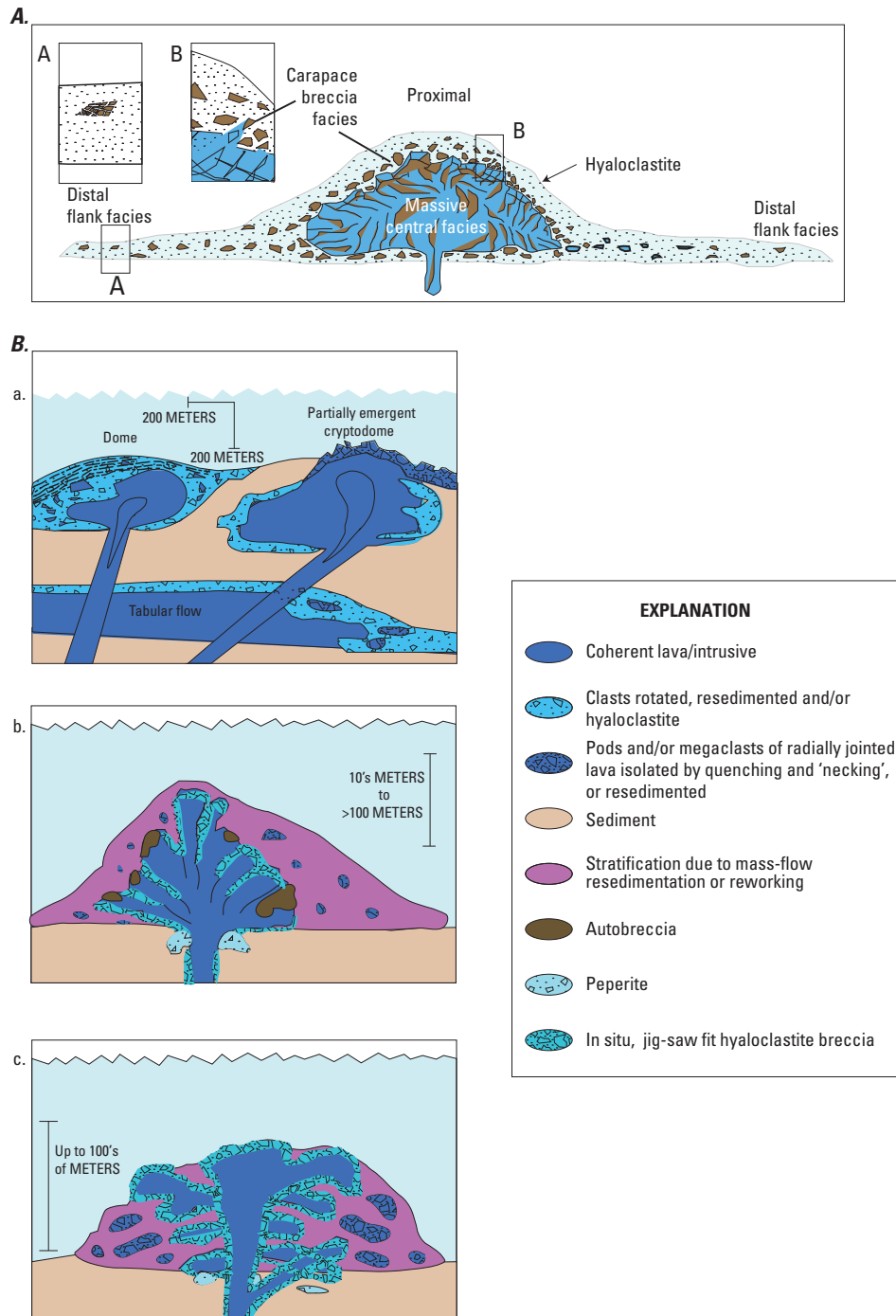


Figure 5-10. Volcanic domes common in a siliciclastic felsic suite. *A*, Schematic cross-section through a blocky rhyolitic flow depicting flow morphology and structures common for proximal and distal facies (after Gibson, 1990). *B*, Silicic lavas can be divided into three main types. (a) Various forms of silicic submarine lavas and intrusive domes (from Allen, 1988). (b) Schematic representation of the internal form and facies of a vent-top silicic submarine dome (after Pilchler, 1965; Yamagishi, 1987). (c) Schematic sketch of the internal form and facies of a subaqueous lava lobe-hyaloclastite complex (after de Rosen-Spense and others, 1980; Furnes and others, 1980; Yamagishi and Dimroth, 1985). From Cas (1992).

Bimodal-felsic dominated

(No Scale Implied)

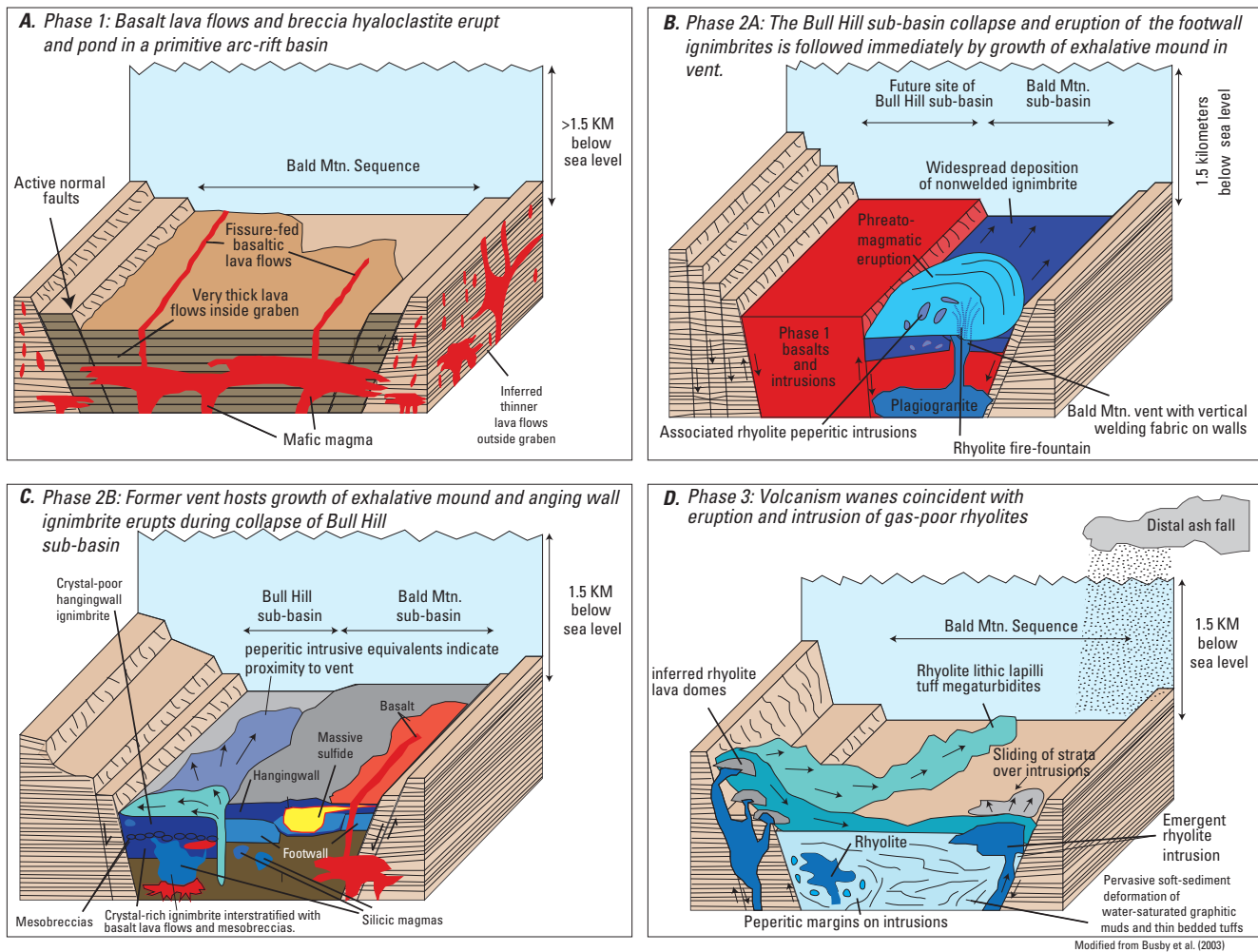


Figure 5-11. Schematic evolution of the bimodal-felsic dominated Bald Mountain sequence. (Cross sections are based on data presented in Busby and others, 2003.) *A*, Phase 1. Outpouring and ponding of basalt lava flows and breccia hyaloclastite in a primitive arc basin. *B*, Phase 2A. The collapse of Bald Mountain sub-basin and eruption of footwall ignimbrite was followed immediately by volcanogenic massive sulfide (VMS) mineralization of an exhalative mound within the vent structure. *C*, Phase 2B. As the Bull Hill sub-basin collapsed, the pyroclastic flow forming the hangingwall ignimbrite erupted. *D*, Phase 3. The waning stages of volcanism were represented by the eruption of gas-poor rhyolites emplaced as lobe-hyaloclastite flow capping VMS mineralization. Modified from Busby and others (2003).

Major breaks in volcanic activity allowed for the deposition of laminated carbonaceous interbedded mudstones. Based on fluid inclusion data from the VMS deposit (Foley, 2003) and sedimentologic features in the deposits at Bald Mountain, Busby and others (2003) suggest that the entire 5-km-thick section of the Bald Mountain sequence was emplaced in very deep water at submarine depths in excess of 1,450 m.

Bimodal-Felsic Type (Incipient-Rifted Continental Margin Arcs and Back Arcs)

Modern continental margin arcs and related back arcs have a global length of approximately 25,600 km (Von Huene and Scholl, 1991) and are hosts to felsic volcanic rocks (35–70 percent total volume of volcanic strata), mafic volcanic rocks (20–50 percent total volume of the volcanic strata), and about 10 percent terrigenous sediment (Franklin and others, 2005). Modern examples include the Okinawa Trough, the Woodlark Basin, and the Manus Basin (table 2–1). In these environments, submarine felsic volcanoclastics and lavas dominate with subordinate volumes of basaltic and (or) basalt andesitic flows, dikes, and sills (Franklin and others, 2005). This association hosts some of the most economically significant VMS deposits (Galley and others, 2007) that have developed in a variety of lithofacies (Franklin and others, 2005). Magmas in these environments are strongly influenced, both physically and chemically, by continental crust and include a broad spectrum of compositions including basalts, basaltic andesites, andesites, dacites, and rhyolites. Volcanism in the early stages of development of a continental arc may begin in a subaqueous environment (such as at Manus and Woodlark Basins). The volcanic systems and the subduction process here often have a prolonged history and continue to develop into large, massive subaerial volcanoes. The subaerial felsic-bimodal volcanic suite contributes clastic volcanic material that has been fragmented and dispersed by any transporting agent, deposited in any environment. This clastic material may be mixed in any significant portion with non-volcanic fragments into the subaqueous environment and redeposited as volcanoclastic material (Fisher and Schmincke, 1984).

Volcanism in incipient-rifted continental margin arcs and back arcs is focused at newly formed rifts. Volcanism begins with emplacement of basaltic massive and pillow lavas, forming large submarine shield volcanoes. As the magmatic system evolves, volcanism becomes more silicic, gas-rich, and explosive and the resulting subaqueous eruptions have abundant pyroclastic material. The explosive activity is interspersed with effusion of lava flows and domes and intrusions of dikes and sills feeding individual eruptions. Interspersed with constructional volcanic processes are those processes associated with structural or magmatic collapse of the volcanic edifices, including debris flows, pyroclastic fall and flow deposits, mud flows, and lava domes, some of which are subaerial and eventually contribute to the subaqueous bimodal-felsic stratigraphic sequences.

Submarine calderas form in either shallow or deep marine environments and develop on both stratovolcanoes and composite volcanoes through large-scale pyroclastic eruptions. Consequently, pyroclastic lithofacies are an important component of the bimodal felsic suite. Pyroclastic lithologies are composed of magmatic ash and pumice, crystal fragments, and lithic clasts derived from the vent wall or incorporated from the underlying terrain during flow.

In the submarine environment, most volcanoclastic material is pyroclastic; however, fragmental material is also derived from autobrecciation, quench fragmentation, pyroclast fragmentation, and resedimentation (Cas, 1992). Physical characteristics of pyroclastic deposits vary between subaerial and submarine settings. In the subaerial environment, Plinian eruption columns are responsible for large pyroclastic-fall deposits and typically are accompanied by pyroclastic flows. Clast size in subaerial pyroclastic fall deposits vary systematically with distance from eruptive source and are a function of eruption column conditions, grain size, density of the various sized clasts, and prevailing wind direction (Walker, 1971; Sparks and others, 1973; Gibson, 2005). In contrast, the eruptive columns of explosive submarine eruptions can be completely subaqueous or become subaerial as a function of eruption intensity and water depth. Consequently, size sorting may involve both water and air. In comparison to subaerial deposits, subaqueous pyroclastic deposits are generally better sorted, are more limited in their aerial distribution, and are typically enriched in crystals and fragments at their base, with finer and ash-rich deposits at their tops. Like their subaerial equivalents, clast size and thickness of deposit varies systematically with distance from eruptive source. The subaerial component of the submarine eruption can produce large volumes of fine ash and cold pumice that are removed by flotation so that the resultant submarine deposits near the edifice may be pumice-depleted. (Gibson, 2005).

Explosive Dominated Submarine Calderas in Bimodal-Felsic Associations

The history of a well-studied and well-exposed Archean caldera is preserved in a 2- to 4-km-thick intracaldera volcanic sequence from the Sturgeon Lake caldera, Canada. The 30-km-wide Sturgeon Lake caldera has a 1- to 2-km-thick sequence of volcanoclastic debris and subaqueous pyroclastic density flow deposits (Mueller and others, 2008) that overlie a thick (approx. 2 km) tonalite-diorite sill-like body. Caldera development advanced in four stages. Stage 1 was a shield-building phase that involved primarily mafic lavas with subordinate felsic breccia and volcanoclastite. Stage 2 was characterized by further caldera collapse associated with the emplacement of 650–1,300-m thick of pyroclastic deposits. This stage contains caldera wall collapse breccias, ignimbrites, bedded tuffs, and lapilli tuffs. Further caldera collapse is recognized in Stage 3 and is associated with the eruption of andesitic and dacitic flows, emplacement of endogenous

domes, and deposition of banded iron formation and volcanoclastic debris. Intra-caldera deposits were dominated by thick, pillowed andesitic flows and felsic lava domes. The final phase of caldera formation (Stage 4) was marked by the emplacement of basaltic andesite flows and volcanoclastic rocks filling the last remnants of the caldera (Mueller and others, 2008).

Estimates of water depths in which subaqueous explosive eruptions can occur are controversial (McBirney, 1963; Pecover and others, 1973; Sparks and Huang, 1980; Burnham, 1983; Kokelaar, 1986; Wohletz, 1986; Cas and Wright, 1987; Cas, 1992). McBirney (1963) noted that the critical point and specific volume changes of pure water control the depth at which submarine explosive eruptions can occur (fig. 5–3A). The critical point of water is defined as the pressure at which water is incompressible and the properties of vapor and liquid are indistinguishable (Cas, 1992). For pure water, the critical point is 216 bars (2.16×10^7 pascals [Pa]); for sea water with 3.5 percent NaCl, the critical point is 315 bars (3.15×10^7 Pa) (Sourirajan and Kennedy, 1962; Cas and Wright, 1988; Cas, 1992); thus, given the pressure gradient of water of approximately 1 bar (10^5 Pa) per 10 m water depth, the depth of the critical point in pure water is about 2,160 m and in seawater is about 3,150 m. These critical point depths represent maxima for subaqueous explosive activity because at greater depths magmatic water and heated seawater would be incapable of expansion (Cas, 1992). For most magmas, the practical maximum depths of explosive eruptions range between 500 and 1,000 m, and generally less than that because these are the depths at which a range of silicate melts become vapor-saturated (McBirney, 1963). Pecover and others (1973) estimated the maximum depth for hydrovolcanic eruptions is less than 700 m.

Recently, several pumice beds in the Izu-Bonin arc (Japan) and the Lau Basin near Tonga have been discovered at depths greater than 1,500 m (Cashman and Fiske, 1991; Fiske and others, 2001), which suggests that pumice erupted from relatively shallow submarine continental-arc and back-arc volcanoes can be redistributed into deeper water. The bulk density of dry, cold pumice is about 0.6 grams per cubic centimeter (g/cm^3), so subaerial pumice will float. However, hot (>700 °C) pumice erupted subaqueously will become saturated in the underwater eruptive column and sink to the seafloor (Whitham and Sparks, 1986). Pumice produced during submarine pyroclastic eruptions has a bulk density between 1.1 and 1.4 g/cm^3 (Kato, 1987) because air in vesicles is displaced by steam, which condenses on cooling and forms a partial vacuum or negative pressure that draws in the surrounding water and saturates the pumice fragments. Interconnected vesicles further enhance water saturation (Cashman and Fiske, 1991). In submarine explosive eruptions, vesicles are formed by exsolving magmatic gases (H_2O , H_2S , CO_2 , CO, and H) and have no component of air. If the pumice cools quickly, it will be saturated before reaching the surface of the sea and will sink and be deposited on the seafloor.

Few submarine explosive eruptions have been witnessed. Four submarine volcanic eruptions from >100 m depths have been documented as later evolving into subaerial eruptions (Mastin and Witter, 2000). The plume of ejecta from the recently witnessed submarine explosive eruption of NW Rota-1 (517 m below the surface) in April 2006 ascended less than 100 m above the vent and did not breach the ocean surface. The maximum depth from which submarine pyroclastic material can reach the ocean surface remains unknown (Chadwick and others, 2008). The top of the eruption column of many deep marine eruptions is severely influenced by the drag on the particles imposed by seawater; thus, the vertical momentum will rapidly decrease with height above the vent. The containment of erupted pyroclastic material results in a large volume of pyroclastic transport downslope and deposition on the lower slopes of the volcanic edifice, as observed at NW Rota-1 (Chadwick and others, 2008).

Recent (April 2006 and April 2009) explosive submarine eruptions at a depth of 550–560 m on NW Rota-1 volcano in the Marianas Arc were witnessed and recorded using a submersible remotely operated vehicle (Chadwick and others, 2008, 2009). The NW Rota-1 volcano, one of many volcanoes located in this intraoceanic subduction zone where underwater volcanoes outnumber their subaerial counterparts 5:1 (Bloomer and others, 1989; Stern and others, 2003; Embley and others, 2004; Chadwick and others, 2008), is a basalt to basaltic andesite steep-sided cone. Its summit depth is at 517 m below sea level (bsl) and its base is at 2,800 m bsl; it has a diameter of 16 km (Chadwick and others, 2008). Previous eruptions at NW Rota-1 volcano were briefly witnessed in 2004 and 2005 but in April 2006 observations made over a week-long period showed that the eruption evolved from an effusive phase that culminated in explosive bursts of glowing red lavas ejected by rapidly expanding gases (Chadwick and others, 2008). Video footage and hydrophones allowed for correlation between observations and digital acoustic data. The eruptive style is akin to subaerial Strombolian activity driven by ascending pockets of magmatic gases that result in periodic phases of explosive activity. In the case of NW Rota-1, the primary magmatic gas that causes explosive activity is interpreted as H_2O , which has the highest potential for rapid thermal expansion at magmatic temperatures (Chadwick and others, 2008). In contrast, CO_2 is assumed to be relatively passive and rises as clear bubbles from explosive bursts (Chadwick and others, 2008). Syneruptive sulfur gases, mainly SO_2 , were also released as clouds of molten sulfur that dropped as beads to the ocean floor. As noted, water is the dominant gas at NW Rota-1 and is driving the explosive nature of this eruption. This type of volcanism is surmised to be common for intraoceanic arcs.

Exposures of submarine pyroclastic deposits in the Mio-Pliocene Shirahama Group, Izu Peninsula, Japan, a submerged continental arc, give insight into submarine volcanism at 3–6 Ma (Cashman and Fiske, 1991). The volcanic sequence is represented by a basal pyroclastic debris flow, a transition

zone, and a capping fall-deposit zone. The lower pyroclastic debris flow contains clasts of andesite with chilled margins; analyses of their thermal remanent magnetism indicates that they were hot (approximately 450 °C) when emplaced. Grain-size decreases systematically upward from the pyroclastic debris flow to the capping fall deposit. All units are extremely depleted in material with grain sizes less than 1 mm (figs. 5–12A, B) and are interpreted as being from the same eruption (Cashman and Fiske, 1991). The fall deposit contains lithic fragments, pumice fragments, and broken crystals and has a striking size bimodality; the pumice fragments are five to ten times larger than the lithic fragments. In a subaerial setting, the density difference between dry pumice (0.6 g/cm³) and lithic fragments (2.4 g/cm³) produces a 2:1 to 3:1 pumice diameter to lithic diameter ratio. In contrast, saturated pumice in a submarine eruption has a higher bulk density (1.1–1.3 g/cm³). The small density difference between saturated pumice and seawater results in reduced terminal velocities and produces hydraulically equivalent pumice and lithic fragments that have diameter ratios of 5:1 to 10:1 (Cashman and Fiske, 1991). Cashman and Fiske (1991) plotted terminal velocity values versus spherical diameter and showed that, theoretically, submarine fall deposits can be distinguished from subaerial fall deposits by the diameter ratios between pumice and lithic fragments.

Insight into the evolution of a submarine siliceous caldera and its associated deep-water pyroclastic deposits is provided by the young (several thousand years) Myojin Knoll caldera located along the Izu-Bonin arc. The caldera has a flat floor 1,400 m below sea level with walls that are 500–900 m high (Fiske and others, 2001). An actively developing Kuroko-type VMS deposit, rich in Au and Ag, is located in the caldera wall. As depicted in figure 5–12C, five stages of volcanic evolution have been recognized. During the first stage a broad volcanic edifice was built, composed of individual rhyolite domes, lavas, and associated volcanoclastic material emplaced in a rift setting. The second stage was marked by the eruption of pumice from a central vent at about 600 m below sea level. The initial pumice eruption column rose nearly to sea level and subsequently sank, forming a broad apron of thick fall-out debris. At the climax of the eruption, but prior to caldera formation, the eruptive column breached the ocean surface, producing large rafts of floating pumice which may have been accompanied by hot pyroclastic flows. During stage three, large volumes of pumice flowed downslope as pyroclastic gravity flows as the slopes of the edifice steepened. Stage four was represented by caldera collapse due to large scale evacuation of magma and the generation of large volumes of hot, ash-laden water. The final stage was marked by the emplacement of silicic dome complexes within the floor of the caldera (Fiske and others, 2001). This evolutionary sequence provides important insights into interpreting the volcanic lithofacies observed in ancient VMS bimodal felsic associations.

Volcanoclastic-Lithofacies Associations

The volcanoclastic lithofacies are dominated by felsic volcanoclastic material with subordinate mafic and felsic domes and their associated autobreccia, hyaloclastite, and redeposited equivalents, cryptodomes, and minor synvolcanic intrusions such as sills, dikes, and minor clastic sedimentary rocks (Franklin and others, 2005). Sedimentary rocks such as carbonaceous argillite, immature epiclastic volcanic wacke, and carbonate (Franklin and others, 2005) are related to this lithofacies. The volcanoclastic lithofacies associations, the bulk of which is volcanoclastic material interspersed with lava flows, domes, and synvolcanic intrusions, have an origin controlled by explosive eruptive processes. Sources for volcanoclastic materials can be explosive, producing pyroclastic fall and flow deposits, syneruptive and redeposited (often interbedded with terrigenous materials), or post-eruptive. The overwhelming volcanoclastic component present in the volcanoclastic lithofacies is evidence of a volcanic architecture created by development of a central volcanic complex composed of single or composite submarine volcanoes (Franklin and others, 2005). The upper lithologies in this suite contain a very thick sequence of primary pyroclastic units that fill large collapse calderas. These lithologies are exposed in both the bimodal-mafic volcanic suite at the Sturgeon Lake caldera and the Hunter caldera, and the bimodal-felsic suite at the Roseberry and Hercules, Bald Mountain, and Bergslagen deposits. Some of these pyroclastic units are greater than 1 km in thickness, are areally extensive, and have volumes of as much as 50 km³.

Sedimentary-Lithofacies Associations

Terrigenous clastic sedimentary rocks, such as wacke, sandstone, siltstone, mudstone, and carbonaceous mudstone dominate the sedimentary lithofacies association. Subordinate rocks include chert, carbonate, marl, and iron formation (Franklin and others, 2005). Volcanogenic massive sulfide deposits are spatially associated with volcanic rocks, including mafic and felsic lava flows, domes, cryptodomes and associated autobreccia, hyaloclastite, and peperite. Volcanism may occur as synvolcanic intrusions where dikes, sills, and cryptodomes are emplaced into epiclastic sediments. A common theme in sediment-dominated successions is that the VMS deposits occur within small volcanic centers that occupy small subsidence structures; these, in turn, are located in a larger sediment-filled extensional basin (Franklin and others, 2005).

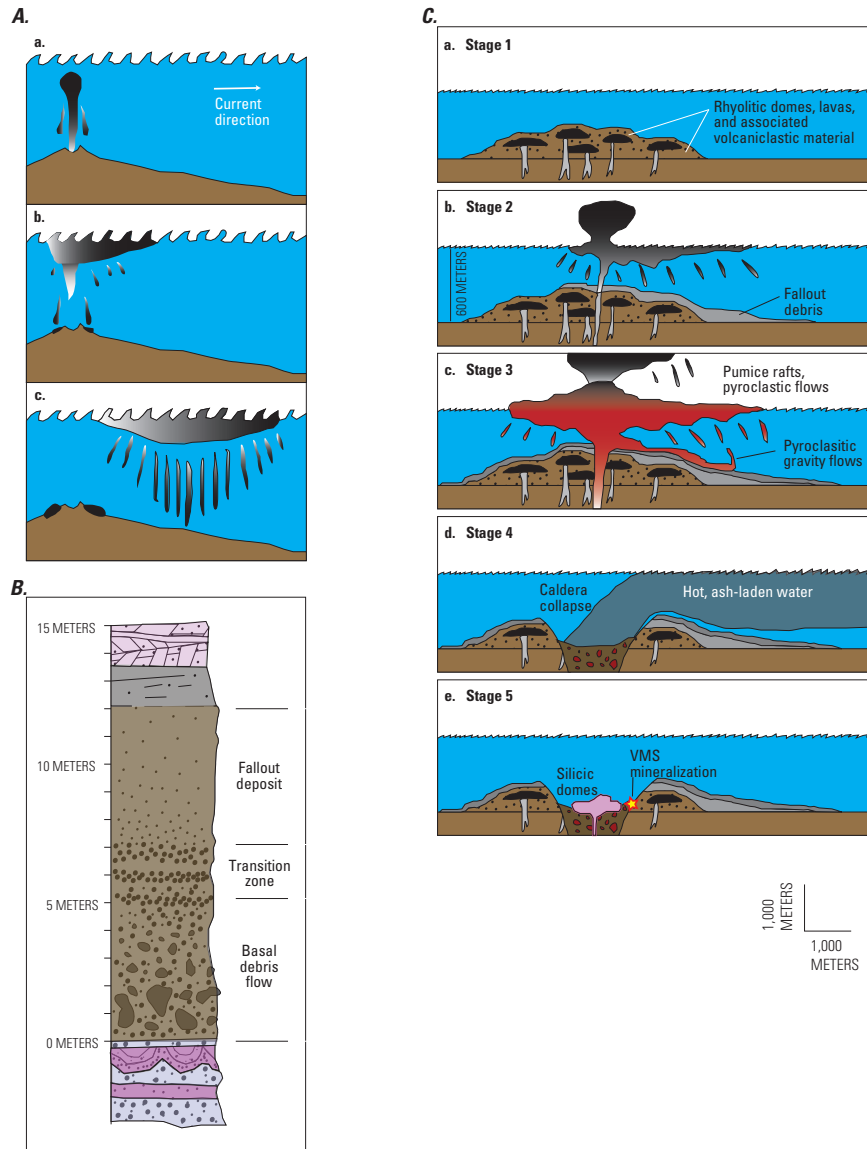


Figure 5-12. Products of explosive dominated submarine calderas in bimodal-felsic volcanic suite. **A**, Schematic representations of fallout from short-lived submarine eruption; arrow shows direction of current. (a) Particles with the highest terminal velocities fall from the margin of the rising eruption column and are deposited close to vent. (b) Eruption has ceased yet particles with lower terminal velocities begin to fall from base of expanding umbrella region. (c) The plume of fallout material drifts with the prevailing current off of the volcanic vent area; extensive fallout occurs from vestiges of laterally drifting umbrella region. From Cashman and Fiske (1991). **B**, Schematic stratigraphic section of a 12-m-thick sequence of pyroclastic material in the Japanese Shirahama Group that has three main facies and is interpreted as the product of a single submarine eruption. From Cashman and Fiske (1991). **C**, Stages in the development of the Myojin Knoll volcano and its caldera. (a) Stage 1. Rhyolitic domes (in black) and associated volcaniclastic deposits (random spot pattern) overlap to form an early volcano edifice. (b) Stage 2. Pre-caldera pumice erupts from summit, which had shoaled to 600 meters below sea level. The eruption column carries pumice to near sea level; however, most of the pumice sinks because of quick cooling and saturation of water and forms a thick sequence of fallout deposits that blanket older parts of the volcano. Larger pumice rises to the sea surface and slowly sinks away from the volcanic vent, resulting in deposits at the volcano that are somewhat pumice depleted. (c) Stage 3. Eruption continues and climaxes with the eruption column breaching the ocean surface. Huge volumes of floating pyroclastic rafts and pyroclastic flows are produced, resulting in the initial collapse of the caldera. (d) Stage 4. Caldera collapse and generation of hot ash-laden water. (e) Stage 5. Caldera begins to fill with post-caldera dome complexes emplaced on floor of the caldera; arrow points to the location of a volcanogenic massive sulfide deposit on the caldera wall. From Fiske and others (2001).

Siliciclastic-Felsic Volcanic Suite (Mature Epicontinental Margin Arcs and Back Arcs)

The siliciclastic-felsic association forms in mature epicontinental margin terranes and related back-arc settings (fig. 5-13A) (see Fig. 5-14A) (Franklin and others, 2005). About 80 percent of the strata are siliciclastic, the remainder being felsic volcanoclastic rocks with minor flows, domes, and subvolcanic intrusives. Mafic (alkaline to tholeiitic) flows and domes, sills, and volcanoclastic material can contribute up to about 10 percent of the total sequence (Franklin and others, 2005). Excellent examples of the siliciclastic-felsic assemblage are found in the Iberian Pyrite Belt in Spain and Portugal (Fig. 5-13) and the Bathurst district in Canada, as well as the Altai-Sayan region in Russia and Kazakhstan (fig. 5-14).

The Iberian Pyrite Belt hosts one of the largest concentrations of economic VMS deposits in volcano-sedimentary sequences of Upper Devonian to Lower Carboniferous age (Soriano and Marti, 1999). Volcanic rocks contribute only about 25 percent to the stratigraphic sequence but have greatly influenced mineralization. Rhyolitic pyroclastic and effusive deposits are intercalated with mudstone, which records a submarine, below-wave-base environment of deposition (fig. 5-13) (Rosa and others, 2008).

At the Neves Corvo deposit, volcanism began after a long period of volcanic quiescence. Several volcanic events record a 35-m.y. history of sedimentation interspersed with 3 major periods of volcanism spanning 22 m.y. (Rosa and others, 2008). The initial explosive volcanism generated at least two eruption-fed, thick, gravity flows of rhyolitic pumice-rich breccia, probably from multiple vents; an explosive origin is debatable (Soriano and Marti, 1999; Rosa and others, 2008). Lenses containing coarse fiamme (stretched and flattened pumice) in a laminated mudstone indicate that the pumice and mud particles were deposited at the same time. Sequences of fiamme, each ranging from 10 to 45 m in thickness, show no evidence for hot emplacement and, thus, deformation and flattening of the pumice is inferred to be diagenetic rather than hot welding and compaction (Rosa and others, 2008). A subsequent period of effusive, quench-fragmented rhyolitic volcanism from intra-basinal vents is intimately associated with and hosts VMS mineralization. These rhyolitic lavas range in thickness from about 250 m (presumably close to its source vent) to 85 m (at more distal locations). The lavas have coherent lobes and abundant rhyolitic hyaloclastites, a common submarine rhyolitic assemblage. A final volcanic event was explosive but minor compared to the earlier two events. In the Neves Corvo host succession, fourteen units are present: ten are volcanic and four are fine-grained sedimentary (Rosa and others, 2008).

The Rio Tinto area of the Iberian Pyrite Belt is a 1-km-thick volcano-sedimentary sequence, 80 percent of which is composed of high-level intrusions emplaced contemporaneously into wet mudstones (Boulter, 1993a, 1993b, 1996; Gibson and others, 1999). The intrusions grade upward from a 300-m-thick sequence of single and multiple doleritic sills

into a 600-m-thick sequence of rhyolitic sills in the upper 600 m (see fig. 5-14A). The peperitic lobes contain fragments of mudstone that penetrated the sills when the sill margins fragmented upon emplacement into the wet unconsolidated sediment. Some of the upper rhyolite sills surfaced into the subaqueous environment and resulted in explosive fragmentation and generation of sediment-bearing hyaloclastites. These deposits then were resedimented in fault-controlled basins (Gibson and others, 1999).

Many VMS deposits throughout the Iberian Pyrite Belt typify the siliciclastic-felsic association with two distinct sedimentary facies. One facies is a siliciclastic-dominated assemblage of wacke, sandstone, siltstone, and locally iron formation or Fe-Mn-rich argillite. The second facies is a pelitic-dominated assemblage of argillite, carbonaceous argillite, siltstone, marl, and carbonate (Franklin and others, 2005) (fig. 5-13B). Volcanogenic massive sulfide deposits in these terranes may be enclosed within hundreds of meters of sedimentary or epiclastic materials.

The Bathurst mining camp, part of the Bathurst Supergroup, New Brunswick, Canada, provides another excellent example of the siliciclastic-felsic association involving world-class VMS deposits (fig. 5-14B). Large volumes of mafic and felsic volcanic rocks are interspersed with sediments formed in a tectonically complex back-arc basin setting (van Staal and others, 2003). At Bathurst, forty-five volcanic sediment-hosted VMS deposits formed in a sediment-covered, back-arc continental rift, which was intensely deformed and metamorphosed from subsequent multiple collisional events (Goodfellow and McCutcheon, 2003; Franklin and others, 2005). The Bathurst Supergroup is divided into five major sedimentary-volcanic sequences that formed in different parts of the back-arc basin. Each sequence has a bimodal-felsic to mafic phase in varying proportions with subvolcanic intrusions, which are associated with thinning of the crust during rifting (Goodfellow and McCutcheon, 2003; Rogers and others, 2003; Rogers and van Staal, 2003). Each sequence begins with eruptions of silicic flows and submarine epiclastic, volcanoclastic, and pyroclastic deposits that range from dacite to rhyolite and contain aphyric to crystal-rich tuffs, hyaloclastite, autobreccias, and subvolcanic rhyolitic cryptodomes (Goodfellow and others, 2003). These tectonically complex sequences most likely formed in different rift basin settings and were later subducted (possibly obducted) and then structurally juxtaposed during the Late Ordovician to Late Silurian (Goodfellow and others, 2003; McNicoll and others, 2003; van Staal and others, 2003). Felsic magmatism was followed by VMS mineralization and later emplacement of alkaline and tholeiitic basaltic lava flows and hyaloclastites; this change in magmatic composition was associated with continued back-arc rifting. The progression in composition in the mafic magmas from alkaline to tholeiitic may reflect the transformation from a back-arc basin into oceanic marginal sea (van Staal and others, 2003), which also was marked by the cessation of felsic magmatism and the deposition of maroon-colored pelagic mudstone, siltstone, and chert intercalated with flows of alkaline basalt (Goodfellow and

Iberian Pyrite Belt

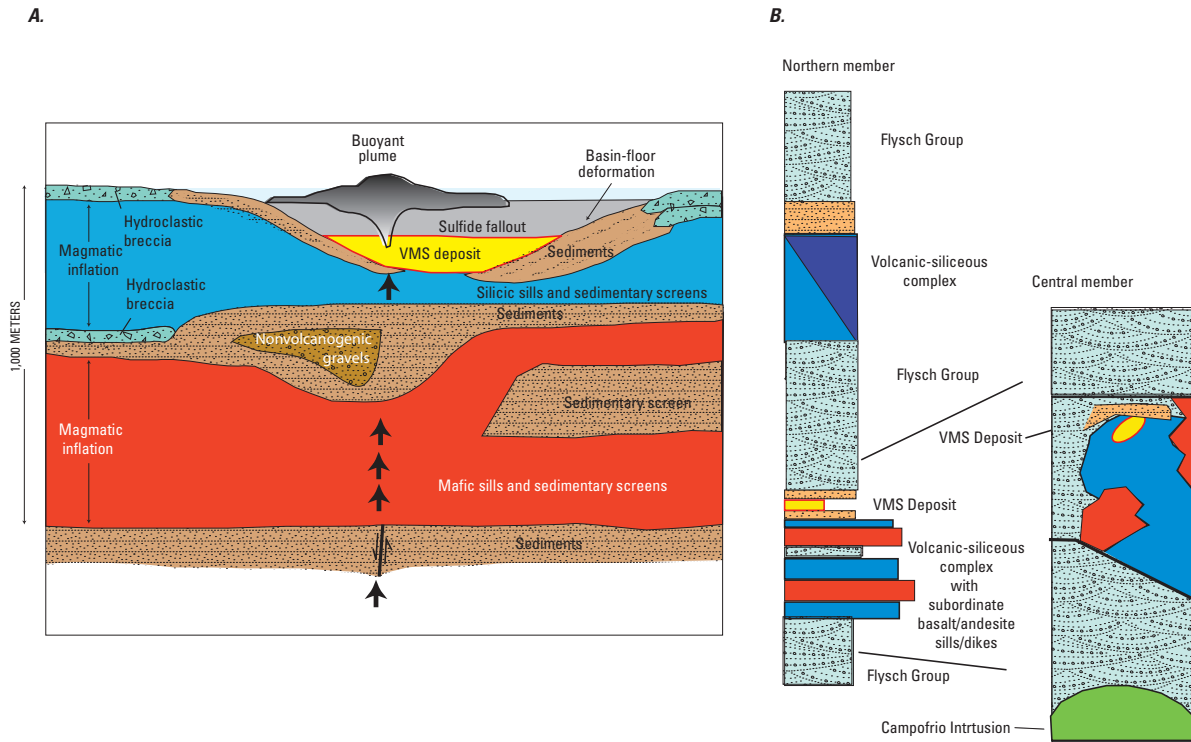


Figure 5-13. The Iberian Pyrite Belt, where volcanogenic massive sulfide mineralization has occurred in a siliciclastic-felsic suite, is shown in a schematic geologic cross section (A) and generalized stratigraphic sections (B). A, schematic cross section of the Rio Tinto mine showing the location of the volcanogenic massive sulfide deposit and sediment-sill complexes. After Boulter, 1993a. B, stratigraphic sections of the northern and central members of the Iberian Pyrite Belt. From Franklin and others (2005).

others, 2003). The textures and compositions of the sedimentary rocks indicate that the back-arc basins formed in varying water depths; some basins had shallow water submarine to subaerial environments whereas others were in much deeper marine environments (fig. 5-4C). Goodfellow and others (2003) note that Phanerozoic VMS deposits tend to be associated with sediments that formed under anoxic conditions and formed at times when ocean waters were rich in H_2O .

The Devonian rift-related Altai-Sayan region in Kazakhstan and Russia is another excellent example of VMS deposition associated with siliciclastic-felsic facies. Here, the base and top of the rift sequence are marked by regional unconformities. Siliclastic sediments constitute about 80% of the strata with felsic volcanoclastic rocks with minor flows, domes, and intrusive rocks contributing up to about 25% of the strata. Similar to other siliciclastic-felsic facies, mafic rocks of tholeiitic and alkaline lava flows, sills, and volcanoclastic making up less than 10% of strata (Fig. 5-14C).

Siliciclastic-Mafic Volcanic Suite (Rifted Continental Margin, Intracontinental Rift, or Sedimented Oceanic Ridge)

The siliciclastic-mafic association forms in continental margin arcs and related back-arc settings (Franklin and others, 2005) (fig. 5-1 inset). Basalt and pelitic sediments are subequal, or pelite may dominate. The volcanic component is primarily shallow synvolcanic basaltic sills that may make up about 25 percent of the entire sequence. Felsic volcanic rocks, if present, contribute <5 percent of the total succession (Franklin and others, 2005) (fig. 5-15).

An excellent example of the siliciclastic-mafic suite is Windy Craggy (fig. 5-15). Pelitic host rocks of the Windy Craggy deposit formed in a mature back-arc basin. The presence of only minor tuff beds coupled with the absence of any coarse-grained turbiditic sediments suggest that sedimentation

Siliciclastic felsic dominated

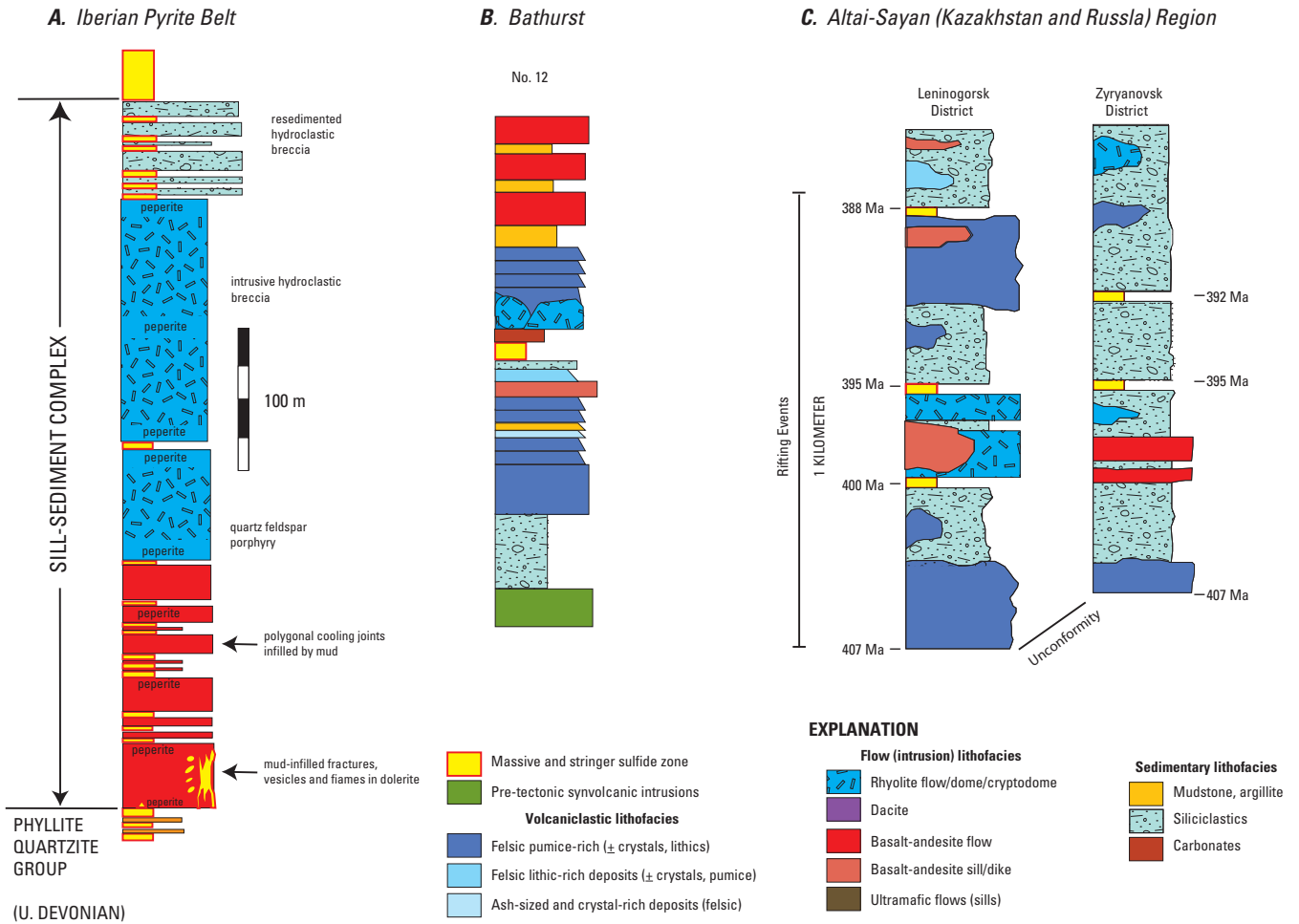


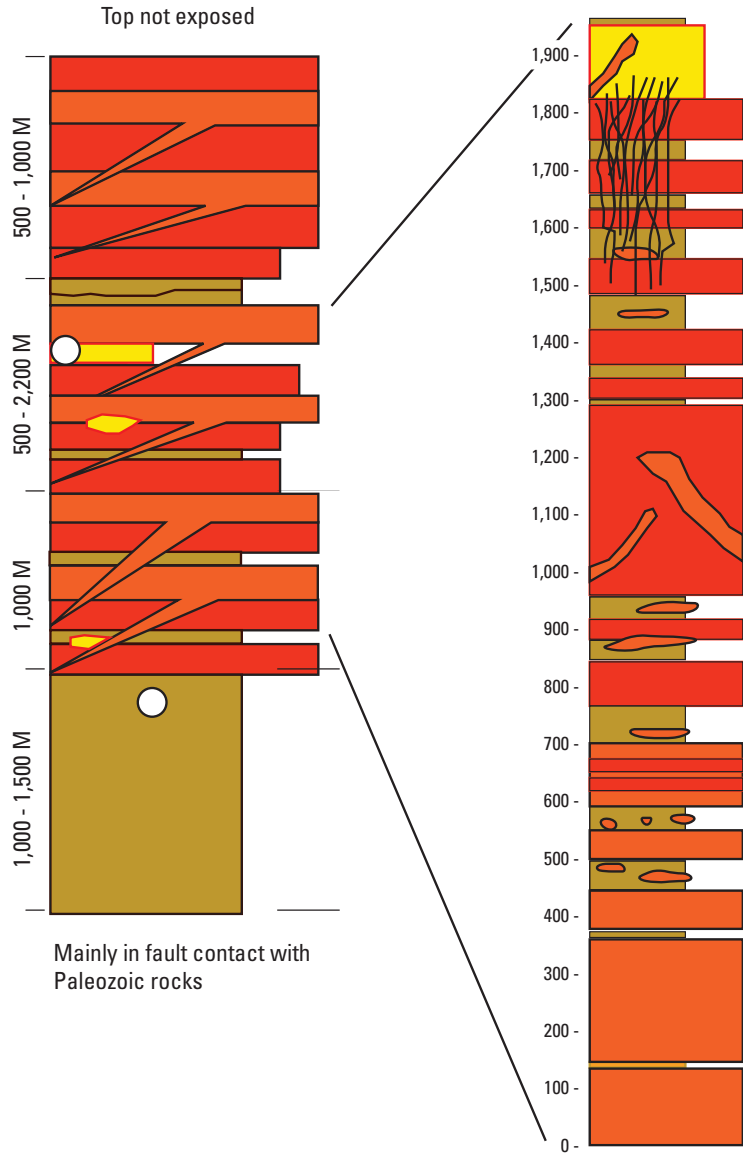
Figure 5-14. Composite stratigraphic sections for various areas hosting VMS mineralization in the siliciclastic-felsic dominated association. **A.** Generalized stratigraphic section through a sill-sediment complex in the Iberian Pyrite Belt. Note the abundance of peperite, polygonal cooling joints, and hydroclastic breccia indicative of the influential role of water and saturated sediments on emplacement of high-level intrusions. **B.** Generalized stratigraphic section at Bathurst no. 12. **C.** Generalized stratigraphic sections from the Altai-Sayan Region (Kazakhstan and Russia) showing the stratigraphic positions of significant VMS mineralization that are characteristic of siliciclastic-felsic dominated associations in the Leninogorsk and Zyryanovsk districts. From Frankin and others (2005).

Siliciclastic-mafic dominated

Windy Craggy (Canada)

Generalized Upper Triassic section of the Aisek-Tatshenshini area

Upper Triassic section of the Windy Craggy deposit



EXPLANATION

- Norian conodonts
- VMS Deposit
- || VMS Stringers

Flow (intrusion) lithofacies

- Basalt/andesite flow
- Basalt/andesite sill/dike

Sedimentary lithofacies

- Mudstone, argillite

Figure 5-15. Generalized stratigraphic sections from the Windy Craggy (Canada) district, an example of VMS mineralization in siliciclastic-mafic dominated terranes. Note the absence of volcanic units in the lower parts of the generalized section. Modified from van Staal and others (2005) and Carvalho and others (1999). From Franklin and other (2005).

occurred far from a clastic source, for example, a subaerial island arc (Klein, 1975; Peter and Scott, 1999). Mafic lava flows and synvolcanic sills are interspersed with carbonaceous argillites that host the VMS mineralization (Franklin and others, 2005). Primary textures in the silicified basalts have been obliterated by a mosaic of interlocking microcrystalline quartz with minor clusters of fine-grained chlorite (Peter and Scott, 1999). Franklin and others (2005) envisage a very shallow volcanic center developed near the seafloor where numerous high-level basaltic dikes, sills, and cryptodomes were emplaced into unconsolidated carbonaceous argillite.

In the mature back-arc basin setting, igneous activity is primarily subvolcanic and is the driver for VMS mineralization, even though the associated mafic suite may amount to only about 25 percent of the total sequence. As Moore (1970) noted, the volume of magma associated with subvolcanic intrusions exceeds the volume of magma erupted as lava flows or pyroclastic material by several orders of magnitude. Mapping of dikes and sills is important in determining their proximity to source. By plotting their density, thickness, location, orientation, and composition, a facies architecture can be determined. These data reveal processes that were operating prior to and during volcanism and may define the area of most intense VMS mineralization where the areas of highest heat flow and cross-stratal permeability may occur (Gibson and others, 1999; Gibson, 2005). Dikes and sills represent the magmatic conduits for the eruptions and commonly occur on faults. Dikes and sills are commonly reactivated structures for repeated injections of magma and later act as conduits for hydrothermal fluids (Gibson and others, 1999).

The ascent and emplacement of magma in the near surface are controlled by the bulk density and hydrostatic pressure of the magma compared with the bulk density of the country rocks and lithostatic pressure (fig. 5-16). Magma denser than its host tends to remain in the subsurface and be intruded as sills and dikes below the level of neutral buoyancy rather than erupt as lavas at the surface (Walker, 1989). In subaqueous settings, such as in a mature back-arc basin, thick accumulations of saturated unconsolidated sediments, whose wet density is generally less than 2.0 (fig. 5-16) (Moore, 1962), act as a perfect host for the emplacement of denser sills and dikes. Magmas are unlikely to erupt as lava flows in this sediment-dominated basin environment (McBirney, 1963; McPhie and others, 1993). Thick sequences of unconsolidated pelitic sediments are intercalated with volcanic intrusives and co-genetic related rocks, such as peperites (McPhie and others, 1993). The level of neutral buoyancy controls whether the magma will be emplaced as an intrusive or extrusive.

Quenched compositions of dikes and sills are identical to the lavas they fed. Dike swarms are commonly identified by evidence of multiple intrusions into the same structure. Contacts of intrusions into wet unconsolidated sediments show that the intrusions have quenched, locally thin, chilled contacts defined by peperite (McPhie and others, 1993). Feeder dikes can be subdivided into four different categories based on the character of their margins and associated hyaloclastite.

Yamagishi (1987, 1991) classifies apophyseal-type feeder dikes as those with bulbous or feeder-like protrusions into wet sediments; these break off into small concentric pillows. At the other end of the spectrum, massive feeder dikes are closely jointed and grade outward to angular fragment breccia and peperite (Yamagishi, 1987, 1991; McPhie and others, 1993). These are excellent conditions for VMS.

Subvolcanic Intrusions

Most volcanic-hosted massive sulfide districts form in proximal volcanic environments defined by vent to proximal facies volcanic sequences, with more than 75 percent of known deposits associated with felsic intrusive complexes (Franklin and others, 1981). In these settings, subvolcanic intrusions, representing the volcanic feeder system to the submarine volcanism, act as the thermal engine that drives hydrothermal convection cells that form VMS deposits on or near the seafloor (Galley, 2003). It is also inferred that shallow subvolcanic intrusions (2–5 km) may directly supply magmatic fluids and metals to the hydrothermal systems, particularly in the early stages of their development (Lydon, 1996; Yang and Scott, 1996; Hannington and others, 1999). Subvolcanic intrusions related to proximal facies volcanic sequences are one of the most important indicators of VMS potential (Franklin and others, 2005).

Subvolcanic intrusions can take four different forms representing different stages of magmatic activity and volcanism (fig. 5-17; Galley, 1996). The first is as large plutons or batholiths intruded 10–20 km below the seafloor, usually at or near the brittle-ductile transition zone in the crust (approximately the 450 °C isotherm) (A in fig. 5-17). These plutons are formed from primary melts from the mantle and (or) partial melts of the lower crust and represent lower magma chambers to the evolving volcanic system. However, such deep intrusions are unlikely to drive shallow hydrothermal convection because convection cells involving large amounts of seawater require relatively high permeability that can only be established within the zone of brittle deformation where open pore or fracture porosity can be maintained (Lydon, 1996).

The rise of magma batches from the lower magma chambers forms a second level of shallowly emplaced sills and stocks at depths generally less than 2–4 km (B in fig. 5-17). These intrusive phases tend to cluster asymmetrically below the eruptive centers in the comagmatic extrusive sequence. In most subvolcanic suites, the intrusive complexes are typically less than 2,000 m in width and commonly about 15–25 km in strike length (Franklin and others, 2005). The size of an intrusive complex is at least in part a function of the width, or diameter, of the volcanic subsidence structure under which it is emplaced (for example, Flavrian pluton, Noranda cauldron: Gibson and Watkinson, 1990; Beidelman Bay pluton, Sturgeon Lake caldera: Morton and others, 1991). In addition, the thickness of the intrusive complex appears to be directly related to the thickness of the overlying volcanic pile, although intrusion

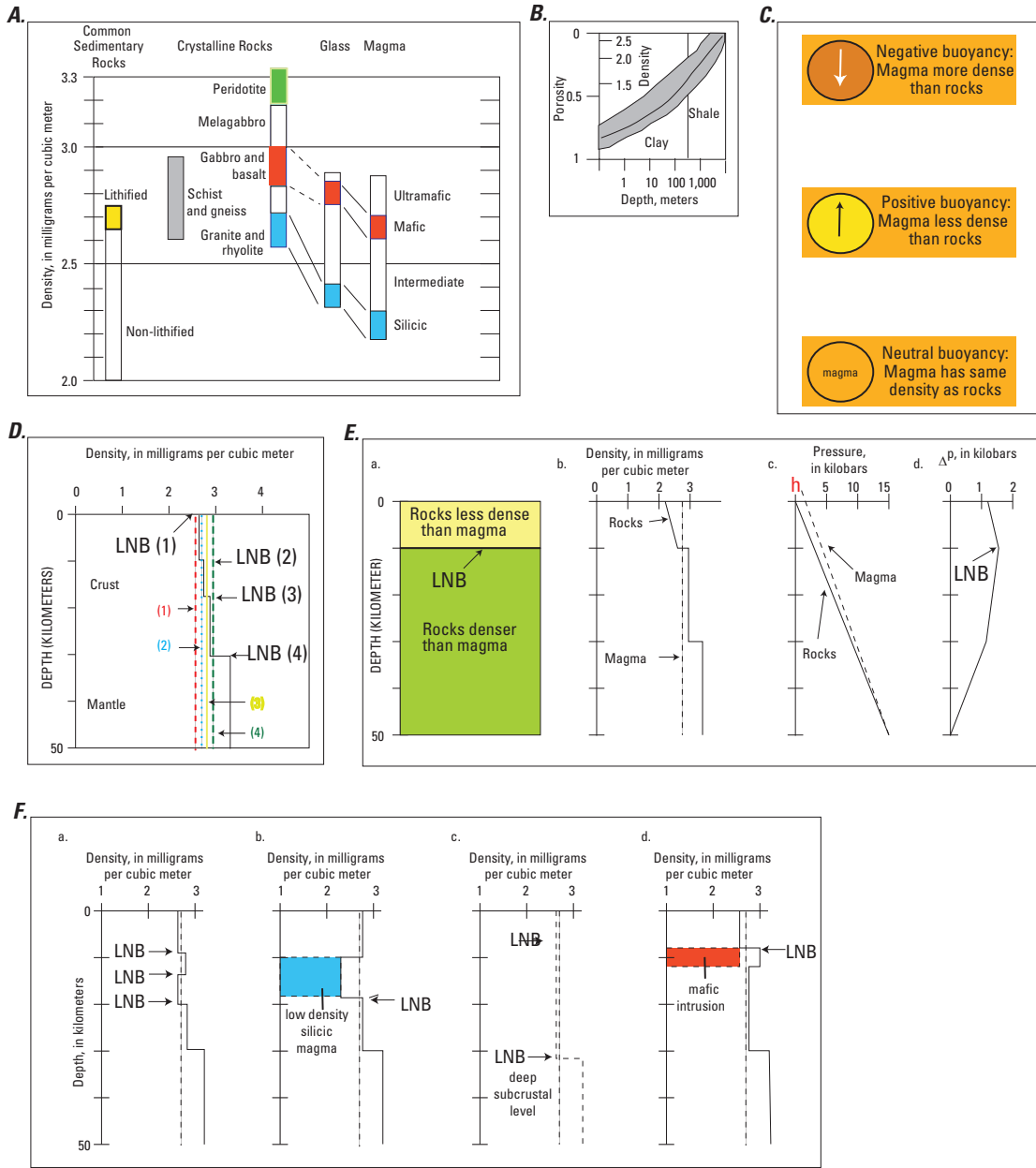


Figure 5-16. Physical parameters and controls on volcanism. *A*, Graph showing densities of common rock types and magmas of varying composition. *B*, Graph of porosity versus depth for young sediments; density increases and porosity decreases with increasing depth of burial. *C*, The net gravitational force (shown by arrow) exerted on magmas enclosed in less dense, denser, or equally dense rocks. *D*, Graph of the levels of neutral buoyancy (LNB) as a function of magma density for four different cases. *E*, Inferred behavior of mafic magma in a simple 2-layered crust. (a) Position of the idealized level of neutral buoyancy where intrusion is favored. (b) Graph of density versus depth profile for various crustal lithologies compared to a magma of uniform density. The cross-over point is the level of neutral buoyancy. (c) Graph of lithostatic pressure and magma hydrostatic pressure versus depth. Hydrostatic pressure is equal the lithostatic load pressure at an arbitrary 50 km depth. The difference (h) between the magma hydrostatic pressure and surface pressure determines the maximum height of h is the height to which hydrostatic pressure to which a volcano could be constructed and is usually reflected in the height of long-lasting lava lakes. (d) Difference between hydrostatic and lithostatic pressure, ΔP , reaches a maximum value at the level of neutral buoyancy. *F*, Graphs of specific examples of the levels of neutral buoyancy. (a) Several levels of neutral buoyancy resulting from country rocks of varying density. (b) Neutral buoyancy at the base of a low-density silicic magma body. (c) Neutral buoyancy at a deep subcrustal level. (d) Neutral buoyancy at the top of a mafic intrusion. From Walker (1989).

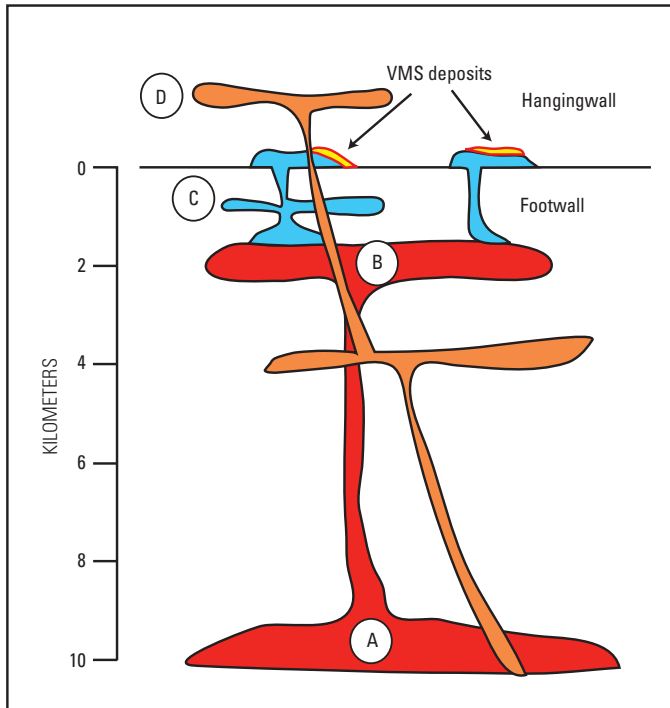


Figure 5-17. Schematic of a volcanic section hosting volcanogenic massive sulfide (VMS) showing relative positions of subvolcanic intrusions. *A*, Deep magma chamber with melts from mantle and/or lower crustal melting. *B*, High-level subvolcanic intrusive complex. *C*, Shallow sill-dike swarms feeding VMS-hosting rhyolites. *D*, Post-mineralization intrusions. After Galley (1996).

of post-VMS resurgent magmatic phases during hanging wall volcanic activity makes it difficult to quantify this relationship. Due to their shallow emplacement and composite nature (that is, long-lived), these intrusive complexes are often intimately associated with large-scale alteration systems and are proximal to massive sulfide horizons (Galley, 1996, 2003).

A third level of subvolcanic intrusion involves the largely vertical emplacement of dike swarms that are feeders to the overlying volcanic units (*C* in fig. 5-17). Often these dikes are localized along synvolcanic structures, such as caldera margins (Old Waite dike swarm, Noranda cauldron; Gibson and Watkinson, 1990) or spreading axes (sheeted dike swarms in ophiolites; Galley and Koski, 1999). In other cases they may form a series of sills and associated dikes such as the Powderhouse sill/dike swarm at Snow Lake, Canada (Bailes, 1988). These dike swarms are commonly characterized by a variety of compositions that can range from ultramafic to felsic, often representing a much wider variation than is present in either the host volcanic package or the underlying subvolcanic intrusions (Galley, 1996).

The fourth level of intrusions includes dikes and sills that represent feeders to the volcanic units in the hanging wall to the massive sulfide-bearing rocks. These dikes can cut the

shallow intrusive complexes, footwall dike swarms, and the VMS deposits along long-lived synvolcanic structures. In some cases (for example, Chisel Lake deposit, Snow Lake), these crosscutting dikes are altered where they transect the deposit's footwall alteration zone and have altered margins well up into the hanging wall, indicating that they were intruded into a still-active subsurface hydrothermal system (Galley and others, 1993). The recognition of discrete concentrations of sills and dikes within a volcanic package is important in identifying zones of long-lived synvolcanic extension along which VMS deposits can occur at several levels in the volcanic sequence.

Shallow level intrusive complexes emplaced in extensional regimes within oceanic arc environments (for example, nascent arc or primitive arc rifts) are characterized by low-alumina quartz diorite-tonalite-trondhjemite composition and are co-magmatic with the host volcanic strata (Leshner and others, 1986; Galley, 1996, 2003). These are the most common type of subvolcanic intrusive suites associated with clusters of VMS deposits, particularly in the Precambrian (>80 percent; Galley, 2003). Their high initial temperatures and relatively anhydrous composition allow the intrusions to rise rapidly to shallow crustal levels where an efficient transfer of heat from the magmas to the surrounding, fluid-rich volcanic pile results in convective hydrothermal fluid flow (Lydon, 1996). Well-described examples include the Archean Beidelman Bay intrusive complex, Sturgeon Lake caldera, Canada (Poulsen and Franklin, 1981; Morton and others, 1991); Archean Flavrian-Powell intrusion, Noranda cauldron, Canada (fig. 5-18) (Goldie, 1978; Gibson and Watkinson, 1990; Galley, 2003); and Paleoproterozoic Sneath Lake and Richard Lake intrusions, Snow Lake, Canada (Galley, 1996, 2003). In environments with continental crust (for example, epicontinental margin, continental-margin arc), intrusive complexes can include granodiorite, quartz monzonite, and granite (for example, Ordovician Bathurst camp, Canada: Whalen and others, 1998; Paleozoic Mount Read district: Large and others, 1996).

The interpretation that subvolcanic intrusions are the primary heat engines responsible for hydrothermal systems is supported by a number of observations (Galley, 2003; Franklin and others, 2005) including:

1. a close spatial relationship between subvolcanic intrusions and clusters of VMS deposits (fig. 5-18);
2. volcanic strata for several thousand meters above the intrusions containing a stratified, district-scale semi-conformable alteration zone defined by distinctive metasomatic mineral assemblages controlled in extent by the strike length of the underlying intrusion;

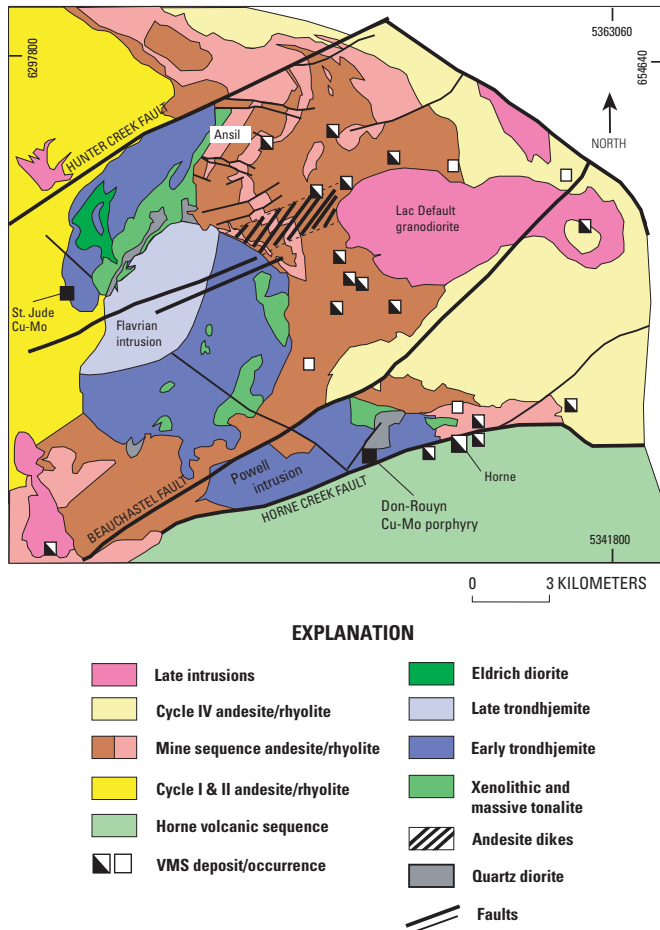


Figure 5-18. Geologic map of the Archean Noranda volcanogenic massive sulfide (VMS) camp showing the VMS deposits underlain by the Flavrian-Powell subvolcanic intrusive complex. After Galley (2003). [Cu, copper; Mo, molybdenum].

3. in some, the most intense alteration lying directly above and within the margin of the subvolcanic intrusions;
4. an apparent positive relationship between the aggregate massive sulfide tonnage in the host VMS district and the size of the associated subvolcanic intrusion for intrusions less than 60 km²; and
5. low whole-rock oxygen isotope values relative to unaltered rocks, providing quantitative evidence that the subvolcanic intrusions have reacted with hot, evolved seawater.

The identification of a subvolcanic intrusive complex is important for determining VMS potential and for defining exploration targets. Because the intrusive complexes are typically much larger than their comagmatic rhyolites that host VMS deposits, they provide a much larger target to identify prospective volcanic sequences. However, identifying the

intrusions can be difficult, particularly in orogenic belts where younger volcanic and tectonic-related intrusions occur, and the effects of deformation and metamorphism can be intense.

Three features of subvolcanic intrusive high-level intrusions are that they form the cores of early fold structures in deformed terranes, are grossly conformable with the host strata, and seldom have significant contact metamorphic haloes. Although sill-like in their overall morphology, these complexes typically consist of a series of stocks, sills, and dike swarms that were emplaced at about the same stratigraphic level within the volcanic sequence. They are commonly zoned, with more mafic hornblende-rich gabbroic, or dioritic, phases successively intruded by more felsic tonalite, trondhjemite, and granite stocks, sills, and dikes (fig. 5-18). Contacts between intrusive phases range from sharp to diffuse and transitional and provide evidence that intrusion of more felsic phases often occurred before full crystallization of the more mafic magma (Galley, 2003). Late-stage felsic intrusive phases (trondhjemites) also are often coarser grained than the early phases (Galley, 2003). This textural change may be an indication of a deeper emplacement depth and slower cooling for the felsic phases, perhaps as a result of thickening of the volcanic pile during the emplacement of the intrusive complex.

Evidence for rapid cooling of particularly the early intrusions through contact with a convecting external fluid is provided by the presence of a variety of disequilibrium textures such as complex compositional zonation of feldspars in mafic phases, myrmekitic textures, development of granophyre, acicular growth of pyroxene and amphibole, and the development of miarolitic cavities in the more felsic phases (Poulsen and Franklin, 1981; Galley, 2003). In addition, the presence of pegmatitic coronas around some xenoliths, abundant miarolitic cavities and (or) an increased volume of magmatic/hydrothermal alteration characterized by replacement and infilling by epidote, actinolite, quartz, albite, magnetite, and subordinate sulfide minerals provide evidence for the introduction into the cooling intrusions of seawater from external sources as well as possible devolatilization of the rapidly cooled magmas (Franklin and others, 2005). Various geochemical approaches can also help in the discrimination of synvolcanic intrusions from later tectonic and post-tectonic intrusions (Galley, 1996; Gaboury, 2006).

Summary and Conclusions

Volcanogenic massive sulfide mineralization occurs in a broad variety of submarine volcano-tectonic settings. Each setting has a distinctive suite of volcanically associated rocks that reflect a variety of volcanic, intrusive, and (or) sedimentological processes. Volcanogenic massive sulfide mineralization has five broad stratigraphic associations each with a distinctive volcanic lithofacies that falls into two broad subdivisions: (1) lithofacies developed by extrusive processes, as observed within the mafic-ultramafic association, the bimodal mafic association, and the bimodal felsic association; and

(2) lithofacies developed by primary and redeposited syn-eruptive pyroclastic deposits and subvolcanic intrusions, as observed within the siliciclastic-felsic association and the siliclastic-mafic association. The differences between the two may reflect deposition and emplacement in deep marine settings for the former subdivision versus shallower water environments for the latter subdivision. In addition, a hierarchy of architectural and lithofacies complexity ranges from the relatively simple siliciclastic-mafic association through the more complex mafic-ultramafic association to the highly complicated bimodal-mafic, bimodal-felsic, and siliciclastic-felsic associations (Gibson and others, 1999; Gibson, 2005). This hierarchy reflects the relative complexities of volcanic processes.

The application of physical volcanology is critical in characterizing terrane and interpreting the volcanic processes that accompany formation of VMS deposits. Thus, the key to understanding the dynamic environment of volcanism which localized VMS mineralization lies in the identification of volcanic lithofacies. A series of mafic pillow lavas overlying sheeted dikes above layered gabbro and mantle peridotite occur typically at mid-ocean ridge and mature back-arc environs. The ultramafic suite of rocks may form in slow to ultra-slow spreading environments where the classic penrose crustal successions are absent. However, back-arc basins may never develop spreading ridges, so that open-ocean crustal architecture does not develop. In this case, VMS mineralization here is hosted by pillow lavas. In incipient-rifted intraoceanic arcs, a bimodal-mafic assemblage records volcanism dominated by large subaqueous shield volcanoes with later developed summit calderas filled with silicic lavas; these also are found on the arc front (for example, Izu-Bonin arc; Fiske and others, 2001). Here, mafic pillow lavas overlie felsic domes or subvolcanic intrusions: rhyolitic lobe-hyaloclastite flows are found interbedded with the mafic pillow lavas. In contrast, incipient-rifted continental margin arc and back-arc settings produce a bimodal-felsic suite of primarily volcanic rocks dominated by explosive felsic volcanoclastic deposits intercalated with effusive lava flows. Mafic volcanism here is a subordinate component, and contributions from terrigenous sediments are minor but present. Mature epicontinental margin arcs and back arcs produce siliciclastic-felsic suite assemblages which reflect a prolonged history of sedimentation interspersed with silicic volcanism; mafic volcanism is rare and limited. Volcanic products include abundant pyroclastic flow and fall deposits, coarse turbidite deposits, sills, and subvolcanic intrusions. In rifted continental margin or intracontinental rift or sedimented oceanic ridges settings, the siliciclastic-mafic suite of rocks is dominated by fine-grained mudstones and argillites into which were intruded basaltic sills. These are simple subvolcanic settings but are host to some of the largest VMS deposits in the world. Each volcanic terrane produces a specific suite of lithofacies dependent on the tectonic setting.

Key elements in evaluating the prospectivity of ancient volcanic successions and VMS deposits appear to be deep-water sediments and lavas or shallow intrusions in an

extensional basin setting. While many explosive submarine calderas are host to VMS deposits, extensive VMS mineralization also occurs in autoclastic breccias and hyaloclastites that formed non-explosively.

References Cited

- Allen, R.L., 1988, False pyroclastic textures in altered silicic lavas, with implications for volcanic-associated mineralization: *Economic Geology*, v. 83, p. 1424–1446.
- Barrie, C.T., and Hannington, M.D., 1999, Classification of volcanic-associated massive sulfide deposits based on host-rock composition, *in* Barrie, C.T., and Hannington, M.D., eds., *Volcanic-associated massive sulfide deposits—Processes and examples in modern and ancient settings: Reviews in Economic Geology*, v. 8, p. 1–11.
- Bleeker, W., and Parrish, R.R., 1996, Stratigraphy and U-Pb zircon geochronology of Kidd Creek—Implications for the formation of giant volcanogenic massive sulfide deposits and the tectonic history of the Abitibi greenstone belt: *Canadian Journal of Earth Sciences*, v. 33, p. 1213–1321.
- Bloomer, S.H., Stern, R.J., and Smoot, N.C., 1989, Physical volcanology of the submarine Mariana and Volcano Arcs: *Bulletin of Volcanology*, v. 51, p. 210–224.
- Boulter, C.A., 1993a, Comparison of Rio Tinto, Spain, and Guaymas Basin, Gulf of California—An explanation of a supergiant massive sulfide deposit in an ancient sill-sediment complex: *Geology*, v. 21, no. 9, p. 801–804.
- Boulter, C.A., 1993b, High-level peperitic sills at Rio Tinto, Spain—Implications for stratigraphy and mineralization: *London, Institution of Mining and Metallurgy, Transactions*, v. 102, p. B30–B38.
- Boulter, C.A., 1996, Extensional tectonics and magmatism as drivers of convection leading to Iberian Pyrite Belt massive sulphide deposits?: *Journal of the Geological Society*, v. 153, no. 2, p. 181–184.
- Burnham, C.W., 1983, Deep submarine pyroclastic eruptions: *Economic Geology Monograph* 5, p. 142–148.
- Busby, C., 2005, Possible distinguishing characteristics of very deepwater explosive and effusive silicic volcanism: *Geology*, v. 33, p. 845–848.
- Busby, C.J., Kessel, L., Schulz, K.J., Foose, M.P., and Slack, J.F., 2003, Volcanic setting of the Ordovician Bald Mountain massive sulfide deposit, northern Maine: *Economic Geology Monograph* 11, p. 219–244.

- Carvalho, D., Barriga, F.J.A.S., and Munha, J., 1999, Bimodal siliciclastic systems—The case of the Iberian Pyrite Belt, *in* Barrie, C.T., and Hannington, M.D., eds., *Volcanic-associated massive sulfide deposits—Processes and examples in modern and ancient settings: Reviews in Economic Geology*, v. 8, p. 375–408.
- Cas, R.A.F., 1992, Submarine volcanism—Eruption styles, products, and relevance to understanding the host-rock successions to volcanic-hosted massive sulfide deposits: *Economic Geology*, v. 87, p. 511–541.
- Cas, R.A.F., and Wright, J.V., 1988, Volcanic successions—Modern and ancient. A geological approach to processes, products and successions: London, Unwin-Hyman, 528 p.
- Cashman, K.V., Chadwick, B., Fiske, R.S., and Deardorff, N., 2009, A comparison of eruption mechanisms in subaerial and submarine arc environments [abs.]: EOS, Transactions, American Geophysical Union, v. 90, no. 52, Fall meeting supplement, abstract V44B-01, p. 394.
- Cashman, K.V., and Fiske, R.S., 1991, Fallout of pyroclastic debris from submarine volcanic eruptions: *Science*, v. 253, no. 5017, p. 275–280.
- Chadwick, B., Dziak, R.P., Baker, E., Cashman, K.V., Embley, R.W., Ferrini, V., de Ronde, C.E., Butterfield, D.A., Deardorff, N., Haxel, J.H., Matsumoto, H., Fowler, M.J., Walker, S.L., Bobbitt, A.M., and Merle, S.G., 2009, Continuous, long-term, cyclic, varied eruptive activity observed at NW Rota-1 submarine volcano, Mariana Arc [abs.]: EOS, Transactions, American Geophysical Union, v. 90, no. 52, Fall meeting supplement, abstract V44B-03, p. 394.
- Chadwick, W.W., Jr., Cashman, K.V., Embley, R.W., Matsumoto, H., Dziak, R.P., de Ronde, C.E.J., Lau, T.K., Deardorff, N.D., and Merle, S.G., 2008, Direct video and hydrophone observations of submarine explosive eruptions at NW Rota-1 volcano, Mariana arc: *Journal of Geophysical Research*, v. 113, B08S10, 23 p., doi:10.1029/2007JB005215.
- Clague, D.A., Paduan, J.B., and Davis, A.S., 2009, Widespread strombolian eruptions of mid-ocean ridge basalt: *Journal of Volcanology and Geothermal Research*, v. 180, p. 171–188.
- Cousineau, P., and Dimroth, E., 1982, Interpretation of the relations between massive, pillowed and brecciated facies in an Archean submarine andesite volcano—Amulet Andesite, Rouyn-Noranda, Canada: *Journal of Volcanology and Geothermal Research*, v. 13, p. 83–102.
- de Rosen-Spense, A.P., Provost, G., Dimroth, E., Gochnauer, K., and Owen, V., 1980, Archean subaqueous felsic flows, Rouyn-Noranda, Quebec, Canada and their Quaternary equivalents: *Precambrian Research*, v. 12, p. 43–77.
- Dimroth, E., Cousineau, P., Leduc, M. and Sanschagrín, Y., 1978, Structure and organization of Archean subaqueous basalt flows, Rouyn-Noranda area, Quebec, Canada: *Canadian Journal of Earth Sciences*, v. 15, p. 902–918.
- Dimroth, E., Imreh, L., Cousineau, P., Leduc, M., and Sanschagrín, Y., 1985, Paleogeographic analysis of mafic submarine flows and its use in the exploration for massive sulfide deposits: Geological Society of Canada, Special Paper 28, p. 202–222.
- Embley, R.W., Baker, E.T., Chadwick, W.W., Jr., Lupton, J.E., Resing, J.A., Massoth, G.J., and Nakamura, K., 2004, Explorations of Mariana arc volcanoes reveal new hydrothermal systems: EOS, Transactions, American Geophysical Union, v. 85, no. 4, p. 37–40.
- Ewart, A., and Hawkesworth, C.J., 1987, The Pliocene-Recent Tonga-Kermadec arc lavas—Interpretation of new isotopic and rare earth data in terms of a depleted mantle source model: *Journal of Petrology*, v. 28, p. 495–530.
- Fisher, R.V., Heiken, G., and Hulen, J.B., 1997, *Volcanoes—Crucibles of change*: New Jersey, Princeton University Press, 317 p.
- Fisher, R.V., and Schmincke, H.U., 1984, *Pyroclastic rocks*: Berlin, Springer-Verlag, 472 p.
- Fiske, R.S., Naka, J., Iizasa, K., Yuasa, M., and Klaus, A., 2001, Submarine silicic caldera at the front of the Izu-Bonin Arc, Japan—Voluminous seafloor eruptions of rhyolite pumice: *Geological Society of America Bulletin*, v. 113, no. 7, p. 813–824.
- Franklin, J.M., 1996, Volcanic-associated massive sulphide base metals, *in* Eckstrand, O.R., Sinclair, W.D., and Thorpe, R.I., eds., *Geology of Canadian mineral deposit types*: Geological Survey of Canada, *Geology of Canada* no.8; Geological Survey of America, *Decade of North American Geology* v. P1, p. 158–183.
- Franklin, J.M., Gibson, H.L., Jonasson, I.R., and Galley, A.G., 2005, Volcanogenic massive sulfide deposits, *in* Hedenquist, J.W., Thompson, J.F.H., Goldfarb, R.J., and Richards, J.P., eds., *Economic Geology 100th anniversary volume, 1905–2005*: Littleton, Colo., Society of Economic Geologists, p. 523–560.
- Franklin, J.M., Lydon, J.M., and Sangster, D.F., 1981, Volcanic-associated massive sulfide deposits, *in* Skinner, B.J., ed., *Economic Geology 75th anniversary volume, 1905–1980*: Littleton, Colo., Economic Geology Publishing Company, p. 485–627.
- Fridleifsson, I.B., Furnes, H., and Atkins, F.B., 1982, Subglacial volcanic—On the control of magma chemistry on pillow dimensions: *Journal of Volcanology and Geothermal Research*, v. 13, p. 103–117.

- Furnes, H., Fridleifsson, I.B., and Atkins, F.B., 1980, Subglacial volcanics—On the formation of acid hyaloclastites: *Journal of Volcanology and Geothermal Research*, v. 8, p. 95–110.
- Gaboury, D., 2006, Geochemical approaches in the discrimination of synvolcanic intrusions as a guide for volcanogenic base metal exploration—An example from the Abitibi belt, Canada: *Applied Earth Sciences—Transactions of the Institution of Mining and Metallurgy section B*, v. 115, p. 71–79.
- Galley, A.G., 1996, Geochemical characteristics of subvolcanic intrusions associated with Precambrian massive sulfide deposits, *in* Wyman, D.A., ed., *Trace element geochemistry of volcanic rocks—Applications for massive sulfide exploration: Geological Association of Canada, Short Course Notes*, v. 12, p. 239–278.
- Galley, A.G., 2003, Composite synvolcanic intrusions associated with Precambrian VMS-related hydrothermal systems: *Mineralium Deposita*, v. 38, p. 443–473.
- Galley, A.G., Bailes, A.H., and Kitzler, G., 1993, Geological setting and hydrothermal evolution of the Chisel Lake and North Chisel Zn-Pb-Ag-Au massive sulphide deposit, Snow Lake, Manitoba: *Exploration and Mining Geology*, v. 2, p. 271–295.
- Galley, A.G., Hannington, M.D., and Jonasson, I.R., 2007, Volcanogenic massive sulphide deposits, *in* Goodfellow, W.D., ed., *Mineral deposits of Canada—A synthesis of major deposit-types, district metallogeny, the evolution of geological provinces, and exploration methods: Geological Association of Canada, Mineral Deposits Division, Special Publication 5*, p. 141–161.
- Galley, A.G., and Koski, R.A., 1999, Setting and characteristics of ophiolite-hosted massive sulfide deposits: *Reviews in Economic Geology*, v. 8, p. 445–473.
- Gibson, H.L., 2005, Volcano-hosted ore deposits, *in* Marti, J., and Ernst, G.G.J., eds., *Volcanoes and the environment: New York, Cambridge University Press*, p. 333–386.
- Gibson, H.L., and Galley, A.G., 2007, Volcanogenic massive sulphide deposits of the Archean, Noranda District, Quebec, *in* Goodfellow, W.D., ed., *Mineral deposits of Canada—A synthesis of major deposit-types, district metallogeny, the evolution of geological provinces, and exploration methods: Geological Association of Canada, Mineral Deposits Division, Special Publication 5*, p. 533–552.
- Gibson, H.L., and Gamble, A.P.D., 2000, A reconstruction of the volcanic environment hosting Archean seafloor and subseafloor VMS mineralization at the Potter Mine, Munro Township, Ontario, Canada, *in* Gemmel, J.B., and Pongratz, J., eds., *Volcanic environments and massive sulfide deposits: University of Tasmania, Australian Research Council, Center of Excellence in Ore Deposits (CODES) Special Publication 3*, p. 65–66.
- Gibson, H.L., Morton, R.L., and Hudak, G., 1999, Submarine volcanic processes, deposits, and environments favorable for the location of volcanic-associated massive sulfide deposits, *in* Barrie, C.T., and Hannington, M.D., eds., *Volcanic-associated massive sulfide deposits—Processes and examples in modern and ancient settings: Reviews in Economic Geology*, v. 8, p. 13–51.
- Gibson, H.L., and Watkinson, D.H., 1990, Volcanogenic massive sulphide deposits of the Noranda cauldron and shield volcano, Quebec, *in* Rive, M., Verpaelst, P., Gagnon, Y., Lulin, J.M., Riverin, G., and Simard, A., eds., *The north-western Quebec polymetallic belt—A summary of 60 years of mining exploration: Canadian Institute of Mining and Metallurgy Transactions special volume*, p. 119–132.
- Goldie, R.J., 1978, Magma mixing in the Flavrian pluton, Noranda area, Quebec: *Canadian Journal of Earth Sciences*, v. 15, p. 132–144.
- Goodfellow, W.D., and McCutcheon, S.R., 2003, Geological and genetic attributes of volcanic-associated massive sulfide deposits of the Bathurst mining camp, northern New Brunswick—A synthesis, *in* Goodfellow, W.D., McCutcheon, S.R., and Peter, J.M., eds., *Massive sulfide deposits of the Bathurst mining camp, New Brunswick, and northern Maine: Economic Geology Monograph 11*, p. 245–301.
- Goodfellow, W.D., McCutcheon, S.R., and Peter, J.M., 2003, Introduction and summary of findings, *in* Goodfellow, W.D., McCutcheon, S.R., and Peter, J.M., eds., *Massive sulfide deposits of the Bathurst mining camp, New Brunswick, and northern Maine: Economic Geology Monograph 11*, p. 1–16.
- Goto, Y., and McPhie, J., 2004, Morphology and propagation styles of Miocene submarine basaltic lava at Stanley, northwestern Tasmania, Australia: *Journal of Volcanology and Geothermal Research*, v. 130, p. 307–328.
- Hannington, M.D., Poulsen, K.H., Thompson, J.F.H., and Sillitoe, R.H., 1999, Volcanogenic gold in the massive sulfide environment, *in* Barrie, C.T., and Hannington, M.D., eds., *Volcanic-associated massive sulfide deposits—Processes and examples in modern and ancient settings: Reviews in Economic Geology*, v. 8, p. 325–356.

- Hargreaves, R., and Ayres, L.D., 1979, Morphology of Archean metabasalt flows, Utik Lake, Manitoba: *Canadian Journal of Earth Sciences*, v. 16, p. 1452–1466.
- Harper, G.D., 1984, The Josephine Ophiolite: *Geological Society of America Bulletin*, v. 95, p. 1009–1026.
- Head, J.W., III, and Wilson, Lionel, 2003, Deep submarine pyroclastic eruptions—Theory and predicted landforms and deposits: *Journal of Volcanology and Geothermal Research*, v. 121, p. 155–193.
- Huppert, H.E., and Sparks, S.J., 1985, Komatiites I—Eruption and flow: *Journal of Petrology*, v. 26, p. 694–725.
- Kato, Y., 1987, Woody pumice generated with submarine eruption: *Geological Society of Japan Journal*, v. 93, p. 11–20.
- Kessel, L.G., and Busby, C.J., 2003, Analysis of VHMS-hosting ignimbrites erupted at bathyal water depths (Ordovician Bald Mountain sequence, northern Maine), *in* White, J.D.L., Smelie, J.L., and Clague, D.A., eds., *Explosive subaqueous volcanism: American Geophysical Union, Geophysical Monograph 140*, p. 361–379.
- Klein, G., 1975, Depositional facies of Leg 30 DSDP sediment cores, *in* Andrews, J.E., and Packham, G., eds., *Initial reports of the Deep Sea Drilling Project: Washington, D.C., U.S. Government Printing Office*, p. 423–442.
- Kokelaar, P., 1986, Magma-water interactions in subaqueous and emergent basaltic volcanism: *Bulletin of Volcanology*, v. 48, no. 5, p. 275–289.
- Large, R.R., Doyle, M., Raymond, O., Cooke, D., Jones, A., and Heasman, L., 1996, Evaluation of the role of Cambrian granites in the genesis of world class VMS deposits in Tasmania: *Ore Geology Reviews*, v. 10, p. 215–230.
- Leat, P.T., and Larter, R.D., 2003, Intra-oceanic subduction systems—Introduction, *in* Larter, R.D., and Leat, P.T., eds., *Intra-oceanic subduction systems—Tectonic and magmatic processes: Geological Society Special Publication 219*, p. 1–18.
- Leshner, C.M., Goodwin, A.M., Campbell, I.H., and Gorton, M.P., 1986, Trace-element geochemistry of ore-associated and barren, felsic metavolcanic rocks in the Superior Province, Canada: *Canadian Journal of Earth Sciences*, v. 23, no. 2, p. 222–237.
- Lydon, J.W., 1996, Characteristics of volcanogenic massive sulfide deposits—Interpretations in terms of hydrothermal convection systems and magmatic hydrothermal systems: *Instituto Tecnológico Geomínero de España, Boletín Geológico y Minero*, v. 107, no. 3–4, p. 15–64.
- Mastin, L.G., and Witter, J.B., 2000, The hazards of eruptions through lakes and seawater: *Journal of Volcanology and Geothermal Research*, v. 97, p. 195–214.
- McBirney, A.R., 1963, Factors governing the nature of submarine volcanism: *Bulletin of Volcanology*, v. 26, p. 455–469.
- McNicoll, V.J., Whalen, J.B., and Stern, R.A., 2003, U-Pb geochronology of Ordovician plutonism, Bathurst mining camp, New Brunswick, *in* Goodfellow, W.D., McCutcheon, S.R., and Peter, J.M., eds., *Massive sulfide deposits of the Bathurst mining camp, New Brunswick, and northern Maine: Economic Geology Monograph 11*, p. 203–218.
- McPhie, J., and Allen, R.L., 1992, Facies architecture of mineralized submarine volcanic sequences—Cambrian Mount Read volcanics, western Tasmania: *Economic Geology*, v. 87, no. 3, p. 587–596.
- McPhie, J., Doyle, M., and Allen, R.L., 1993, *Volcanic textures—A guide to the interpretation of textures in volcanic rocks: Hobart, Tasmania, University of Tasmania, Centre for Ore Deposit and Exploration Studies*, 198 p.
- Moore, D.G., 1962, Bearing strength and other physical properties of some shallow and deep-sea sediments from the North Pacific: *Geological Society of America Bulletin*, v. 73, p. 1163–1166.
- Moore, J.G., 1970, Relationship between subsidence and volcanic load, Hawaii: *Bulletin of Volcanology*, v. 34, p. 526–576.
- Moore, J.G., 1975, Mechanism of formation of pillow lava: *American Scientist*, v. 63, p. 269–277.
- Morton, R.L., Walker, J.S., Hudak, G.J., and Franklin, J.M., 1991, The early development of an Archean submarine caldera complex with emphasis on the Mattabi ash-flow tuff and its relationship to the Mattabi massive sulfide deposit: *Economic Geology*, v. 86, p. 1002–1011.
- Mosier, D.L., Berger, V.I., and Singer, D.A., 2009, Volcanogenic massive sulfide deposits of the world; database and grade and tonnage models: U.S. Geological Survey Open-File Report 2009–1034, 46 p. (Also available at <http://pubs.usgs.gov/of/2009/1034/>.)
- Mueller, W.U., Stix, J.B., White, J.D.L., Corcoran, P.L., Lafrance, B., and Daigneault, R., 2008, Characterisation of Archean subaqueous calderas in Canada—Physical volcanology, carbonate-rich hydrothermal alteration and a new exploration model, *in* Gottsmann, J., and Marti, J., eds., *Caldera volcanism—Analysis, modeling, and response: Developments in Volcanology*, v. 10, p. 181–232.

- Mueller, W.U., Stix, J., Corcoran, P.L., and Daigneault, R., 2009, Subaqueous calderas in the Archean Abitibi greenstone belt—An overview and new ideas: *Ore Geology Reviews*, v. 35, p. 4–46.
- Pecover, R.S., Buchanan, D.J., and Ashby, D.E., 1973, Fuel-coolant interaction in submarine volcanism: *Nature*, v. 245, p. 307–308.
- Peter, J.M., and Scott, S.D., 1999, Windy Craggy, northwestern British Columbia—The world's largest Besshi-type deposit, *in* Barrie, C.T., and Hannington, M.D., eds., *Volcanic-associated massive sulfide deposits—Processes and examples in modern and ancient settings: Reviews in Economic Geology*, v. 8, p. 261–295.
- Pilcher, H., 1965, Acid hyaloclastites: *Bulletin of Volcanology*, v. 28, p. 283–310.
- Poulson, S.R., and Franklin, J.M., 1981, Copper and gold mineralization in an Archean trondhjemitic intrusion, Sturgeon Lake, Ontario: *Geological Survey of Canada Paper 81-1A*, p. 9–14.
- Rittman, A., 1962, *Volcanoes and their activity*: New York, Wiley, 305 p.
- Rogers, N., and van Staal, C.R., 2003, Volcanology and tectonic setting of the northern Bathurst Mining Camp—Part II. Mafic volcanic constraints on back-arc opening, *in* Goodfellow, W.D., McCutcheon, S.R., and Peter, J.M., eds., *Massive sulfide deposits of the Bathurst mining camp, New Brunswick, and northern Maine: Economic Geology Monograph 11*, p. 181–201.
- Rogers, N., van Staal, C.R., McNicoll, V., and Theriault, R., 2003, Volcanology and tectonic setting of the northern Bathurst mining camp—Part I. Extension and rifting of the Popelogan Arc, *in* Goodfellow, W.D., McCutcheon, S.R., and Peter, J.M., eds., *Massive sulfide deposits of the Bathurst mining camp, New Brunswick, and northern Maine: Economic Geology Monograph 11*, p. 157–179.
- Rosa, C.J.P., McPhie, J., Relvas, J.M.R.S., Pereira, Z., Oliveira, T., and Pacheco, N., 2008, Facies analyses and volcanic setting of the giant Neves Corvo massive sulfide deposit, Iberian Pyrite Belt, Portugal: *Mineralium Deposita*, v. 43, p. 449–466.
- Ross, S.L., and Zierenberg, R.A., 1994, Volcanic geomorphology of the SESCA and NESCA sites, Escanaba Trough, *in* Morton, J.L., Zierenberg, R.A., and Reiss, C.A., eds., *Geologic, hydrothermal, and biologic studies at Escanaba Trough, Gorda Ridge, offshore northern California: U.S. Geological Survey Bulletin 2022*, p. 223–240.
- Smith, T.L., and Batiza, R., 1989, New field and laboratory evidence for the origin of hyaloclastite flows on seamount summits: *Bulletin of Volcanology*, v. 51, p. 96–114.
- Soriano, C., and Marti, J., 1999, Facies analysis of volcano-sedimentary successions hosting massive sulfide deposits in the Iberian pyrite belt, Spain: *Economic Geology and the Bulletin of the Society of Economic Geologists*, v. 94, no. 6, p. 867–882.
- Sourirajan, S., and Kennedy, G.C., 1962, The system H₂O-NaCl at elevated temperatures and pressures: *American Journal of Science*, v. 260, p. 115–141.
- Sparks, R.S.J., Self, S., and Walker, G.P.L., 1973, Products of ignimbrite eruption: *Geology*, v. 1, p. 115–118.
- Sparks, R.S.J., and Huang, T.C., 1980, The volcanological significance of deep-sea ash layers associated with ignimbrites: *Geological Magazine*, v. 117, p. 425–436.
- Stern, R.J., Fouch, M.J., and Klempere, S.L., 2003, An overview of the Izu-Bonin-Mariana subduction factory, *in* Eiler, J., ed., *Inside the subduction factory: American Geophysical Union, Geophysical Monograph Series 138*, p. 175–222.
- van Staal, C.R., Wilson, R.A., Rogers, N., Fyffe, L.R., Langton, J.P., McCutcheon, S.R., McNicoll, V., and Ravenhurst, C.E., 2003, Geology and tectonic history of the Bathurst supergroup, Bathurst mining camp, and its relationships to coeval rocks in southwestern New Brunswick and adjacent Maine—A synthesis, *in* Goodfellow, W.D., McCutcheon, S.R., and Peter, J.M., eds., *Massive sulfide deposits of the Bathurst mining camp, New Brunswick, and northern Maine: Economic Geology Monograph 11*, p. 37–60.
- von Huene, R., and Scholl, D.W., 1991, Observations at convergent margins concerning sediment subduction, subduction erosion, and the growth of continental crust: *Reviews of Geophysics*, v. 29, no. 3, p. 279–316.
- Walker, G.P.L., 1971, Grain-size characteristics of pyroclastic deposits: *Journal of Geology*, v. 79, p. 696–714.
- Walker, G.P.L., 1989, Gravitational (density) controls on volcanism, magma chamber, and intrusions: *Australian Journal of Earth Sciences*, v. 36, p. 149–165.
- Walker, G.P.L., 1992, Morphometric study of pillow-size spectrum among pillow lavas: *Bulletin of Volcanology*, v. 54, p. 459–474.

- Whalen, J.B., Rogers, N., van Staal, C.R., Longstaffe, F.J., Jenner, G.A., and Winchester, J.A., 1998, Geochemical and isotopic (Nd,O) data from Ordovician felsic plutonic and volcanic rocks of the Miramichi Highlands—Petrogenetic and metallogenic implications for the Bathurst mining camp: *Canadian Journal of Earth Sciences*, v. 35, p. 237–252.
- Wharton, M.R., Hathway, B., and Colley, H., 1994, Volcanism associated with extension in an Oligocene-Miocene arc, southwestern Viti Levu, Fiji, *in* Smellie, J.L., ed., Volcanism associated with extension at consuming plate margins: Geological Society of London Special Publication 81, p. 95–114.
- White, J.D., Smellie, J.L., and Clague, D.A., 2003, Introduction—A deductive outline and topic overview of subaqueous explosive volcanism, *in* White, J., Smellie, J.L., and Clague, D., eds., Explosive subaqueous volcanism: American Geophysical Union, Geophysical Monograph Series 140, p. 1–23.
- Whitham, A.G., and Sparks, R.S.J., 1986, Pumice: *Bulletin of Volcanology*, v. 48, no. 4, p. 209–223.
- Wohletz, K.H., 1986, Explosive magma-water interactions—Thermodynamics, explosion mechanisms, and field studies: *Bulletin of Volcanology*, v. 48, no. 5, p. 245–264.
- Wohletz, K.H., and Sheridan, M.F., 1983, Hydrovolcanic explosions—Part II. Evolution of basaltic tuff rings and tuff cones: *American Journal of Science*, v. 283, no. 5, p. 385–413.
- Wohletz, K.H., and Heiken, G., 1992, *Volcanology and geothermal energy*: Berkeley, California, University of California Press, 432 p.
- Yamagishi, H., 1987, Studies on the Neogene subaqueous lavas and hyaloclastites in southwest Hokkaido: *Report of the Geological Survey of Hokkaido* 59, p. 55–117.
- Yamagishi, H., 1991, Morphological features of Miocene submarine coherent lavas from the “Green Tuff” basins—Examples from basaltic and andesitic rocks from the Shimokita Peninsula, northern Japan: *Bulletin of Volcanology*, v. 53, p. 173–181.
- Yamagishi, H., and Dimroth, E., 1985, A comparison of Miocene and Archean rhyolite hyaloclastites—Evidence for a hot and fluid lava: *Journal of Volcanology and Geothermal Research*, v. 23, p. 337–355.
- Yang, K., and Scott, S.D., 1996, Possible contribution of a metal-rich magmatic fluid to a seafloor hydrothermal system: *Nature*, v. 383, p. 420–423.

6. Physical Description of Deposit

By John F. Slack

6 of 21

Volcanogenic Massive Sulfide Occurrence Model

Scientific Investigations Report 2010–5070–C

U.S. Department of the Interior
U.S. Geological Survey

U.S. Department of the Interior
KEN SALAZAR, Secretary

U.S. Geological Survey
Marcia K. McNutt, Director

U.S. Geological Survey, Reston, Virginia: 2012

For more information on the USGS—the Federal source for science about the Earth, its natural and living resources, natural hazards, and the environment, visit <http://www.usgs.gov> or call 1-888-ASK-USGS.

For an overview of USGS information products, including maps, imagery, and publications, visit <http://www.usgs.gov/pubprod>

To order this and other USGS information products, visit <http://store.usgs.gov>

Any use of trade, product, or firm names is for descriptive purposes only and does not imply endorsement by the U.S. Government.

Although this report is in the public domain, permission must be secured from the individual copyright owners to reproduce any copyrighted materials contained within this report.

Suggested citation:

Morgan, L.A., and Schulz, K.J., 2012, Physical volcanology of volcanogenic massive sulfide deposits in volcanogenic massive sulfide occurrence model: U.S. Geological Survey Scientific Investigations Report 2010-5070-C, chap. 6, 8 p.

Contents

| | |
|--|-----|
| Definition | 105 |
| Dimensions in Plan View | 105 |
| Size of Hydrothermal System Relative to Extent of Economically Mineralized Rock..... | 105 |
| Vertical Extent | 105 |
| Form/Shape..... | 106 |
| Host Rocks | 108 |
| References Cited..... | 108 |

Figure

| | |
|--|-----|
| 6-1. Different forms and styles of volcanogenic massive sulfide deposits | 107 |
|--|-----|

6. Physical Description of Deposit

By John F. Slack

Definition

In the following description of VMS deposits and their physical features, a deposit is defined as a mineral occurrence that has sufficient size and grade(s) to be economically profitable to mine under favorable circumstances (Cox and others, 1986).

Dimensions in Plan View

Typical dimensions of VMS deposits are in the range of 100–500 m. Small deposits may be only tens of thousands of square meters in plan view, whereas giant deposits can have dimensions of several square kilometers. The unmined Windy Craggy deposit in British Columbia, Canada, at depth is approximately 200 m wide and 1.6 km long (Peter and Scott, 1999), with a dimension of 0.3 km²; the Kidd Creek orebody in Ontario, Canada, is approximately 500 m wide and at least 2,000 m long (down-dip mining extent) and has a minimum dimension, vertically restored, of 1.0 km² (Hannington and others, 1999). The Besshi deposit on Shikoku, Japan, is 3,500 m by 1,800 m, thus covering an area (reconstructed prior to deformation) of 6.3 km² (see Slack, 1993); the dimension of the original deposit, prior to erosion, was much greater. Such large variations in the dimensions of VMS deposits reflect diverse parameters, such as: the nature and duration of seafloor and subseafloor hydrothermal activity; seafloor topography; permeability of footwall strata; structural and (or) volcanic controls on mineralization; postore deformation including shearing, folding, and faulting; extent of erosional preservation; and mining cutoff grades.

Size of Hydrothermal System Relative to Extent of Economically Mineralized Rock

The diverse nature of VMS systems results in large size ranges for envelopes of altered rock surrounding economic orebodies. Highly focused fluid flow in some deposits has produced alteration of limited volumetric significance to

footwall stringer zones that typically contain only minor sulfides; hence, it is uneconomic to mine such deposits. However, many deposits have alteration haloes that in plan view extend well beyond the width of the orebody, including the Ordovician Brunswick No. 12 deposit in the Bathurst district of New Brunswick (Goodfellow and McCutcheon, 2003) and the Paleoproterozoic Chisel deposit in the Snow Lake district of Manitoba (Galley and others, 2007), where haloes are two or three times wider than the economic parts of the deposits. Even larger is the alteration zone surrounding the Western Tharsis deposits in Tasmania, Australia, being about 800 m in diameter compared to the maximum orebody width of about 150 m (Large and others, 2001). These dimensions do not consider the sizes of laterally extensive stratabound alteration zones, such as those occurring within footwall strata immediately below the sulfide ores, or in much deeper, so-called semi-conformable alteration zones that in some cases extend a kilometer or more from the projected economic margins of the deposit (Galley, 1993). Such zones may also occur in the stratigraphic hanging wall of deposits (for example, Noranda district), probably reflecting hydrothermal systems that were generated by synvolcanic but postore intrusions (see Franklin and others, 2005).

Vertical Extent

The nature of postore deformation determines whether the vertical extent of a VMS deposit is equivalent to its original stratigraphic thickness or its length. For relatively undeformed deposits, typical vertical extents (thicknesses) are on the order of tens of meters; extents of >250 m occur in a few deposits of this type, such as San Nicolás in Mexico, Tambo Grande in Peru, and Sibay in Russia (Johnson and others, 2000; Tegart and others, 2000; Herrington and others, 2005). The greatest vertical extents occur in tabular and sheetlike deposits that dip steeply to vertically, for which their extents reflect original deposit lengths and not thicknesses. Examples include the Besshi deposit in Japan (1,800 m; Sumitomo Metal Mining Company, Ltd., 1970) and the Kidd Creek orebody in Canada (>2,000 m; Hannington and others, 1999). Vertical extents of feeder zones also vary greatly, but they generally are less than 100 m, although some deposits have much thicker feeder zones (restored to predeformation geometries) on the

order of several hundred meters, such as Hellyer, Tasmania (Gemmell and Large, 1992), Podolsk, Russia (Herrington and others, 2005), and Rio Tinto, Spain (Tornos, 2006).

Form/Shape

The geometry of VMS deposits may preserve original hydrothermal shapes or alternatively reflect varying degrees of postore deformation such as folding, faulting, and shearing (see Large, 1992). In areas of no or minimal deformation, possible deposit forms include sheets, layers, lenses, mounds, pipes, and stockworks (fig. 6–1). Sheetlike deposits are characterized by high aspect ratios in which the lengths of sulfide zones exceed thicknesses by an order of magnitude or more. Examples include the Besshi deposit on Shikoku, Japan, which has approximate dimensions of 3,500×1,800 m and a typical thickness of <30 m (Slack, 1993, and references therein), and the Thalanga deposit in Queensland, Australia, having a strike length of approximately 3,000 m and a thickness of 10–20 m in most places (Berry and others, 1992). Such sheetlike geometries, where demonstrably not of deformational origin, may reflect:

- sulfide deposition in a brine pool,
- precipitation from dense high-salinity fluids that migrate to a topographic low,
- accumulation of clastic sulfides eroded from a topographically higher edifice of massive sulfide,
- near-vent (<500 m) precipitation from the buoyant part of a hydrothermal plume (Large and others, 2001; German and Von Damm, 2003),
- coalescence of originally isolated sulfide mounds by mineralization from multiple vent sites (Huston, 1990),
- subseafloor replacement of a permeable volcanic or sedimentary bed (Large, 1992), or
- extensive seafloor weathering of a former sulfide mound (Herrington and others, 2005).

Layers show broadly similar geometries. Lenses have shorter length to thickness ratios and in many cases display irregular shapes with tapered margins; a large deposit of this type is San Nicolás in Mexico, which is 900 m long, >200 m wide, and as much as 280 m thick (Johnson and others, 2000).

Sulfide mounds show a wide range of geometries, commonly with roughly equal widths and lengths (approx. 100–300 m) and much smaller thicknesses, such as the Millenbach deposit in the Noranda district of Quebec (Knuckey and others, 1982). Atypical geometries are those such as the roughly equidimensional massive sulfide mounds like the bowl-shaped Bald Mountain deposit in Maine, which is approximately 370×275 m in diameter and as much as 215 m thick (Slack and others, 2003), and the hourglass-shaped TG3 deposit at

Tambo Grande in Peru, which is approximately 500×350 m in diameter and up to about 250 m thick (Tegart and others, 2000). Such roughly equidimensional geometries likely reflect sulfide deposition within a confined space, such as volcanic craters or small grabens. Pipelike deposits, like those at Sibay in the South Urals of Russia (Herrington and others, 2005), Mount Morgan and Highway-Reward in Queensland, Australia (Messenger and others, 1997; Doyle and Huston, 1999), and Baiyinchang in Gansu Province, China (Hou and others, 2008), have thicknesses that are commonly greater than their diameters, typically as a result of subseafloor mineralization involving the replacement of permeable volcanic or sedimentary units by sulfides. The location and geometry of some pipelike deposits like Mount Morgan were controlled by synvolcanic growth faults (Taube, 1986). A modern analog is the Ocean Drilling Program (ODP) site at Middle Valley on the northern Juan de Fuca Ridge, where stacked sulfide mounds occur together with underlying alteration zones and a deep, epigenetic stratiform Cu zone (Zierenberg and others, 1998).

Stockworks generally occur in the stratigraphic footwall of sulfide-rich deposits and represent the feeder zone through which hydrothermal fluids rose towards the paleoseafloor (see Lydon, 1984; Franklin and others, 2005). Thicknesses vary from tens of meters to hundreds of meters in a few deposits. Where relatively undeformed, such stockworks commonly have an inverse funnel shape; others form a pipelike structure. Examples of classic VMS stockworks occur in the Kuroko, Noranda, Jerome, and Rio Tinto districts of Japan, Quebec, Arizona, and Spain, respectively (Franklin and others, 1981; Tornos, 2006; Gibson and Galley, 2007). Less commonly, stockworks are stacked and occur at two or more stratigraphic levels, such as in the Que River and Mount Lyell deposits in Tasmania, Australia (Large, 1992). Some stockworks have been selectively mined for copper, such as Jerome in Arizona (Gustin, 1990), Limni in Cyprus (Richards and others, 1989), and Rio Tinto in Spain (Nehlig and others, 1998). The stockwork of the giant Kidd Creek orebody in Canada is also economically important, as it has been mined for decades (see Hannington and others, 1999). Examples of modern stockworks that have been discovered on and beneath the seafloor include the Galapagos Rift (Ridley and others, 1994), Middle Valley (Zierenberg and others, 1998), and TAG (Petersen and others, 2000).

Deformed VMS deposits typically are folded, faulted, and (or) sheared. Folds within such deposits vary from broad open structures such as those at Eskay Creek, British Columbia, and Caribou, New Brunswick, Canada (Roth and others, 1998; Goodfellow, 2003), to isoclinally folded layers as at Tizapa, Mexico, and Kudz Ze Kayah, Yukon, Canada (Lewis and Rhys, 2000; Peter and others, 2007), to complexly folded lenses such as at Stekenjokk, Sweden, and Elizabeth, Vermont (Zachrisson, 1984; Slack and others, 2001). In the Bathurst district of New Brunswick, Canada, the sulfide deposits have undergone several periods of pervasive deformation, which is especially well-documented in the large Brunswick No. 12 and Heath Steele orebodies (van Staal and Williams, 1984; de Roo

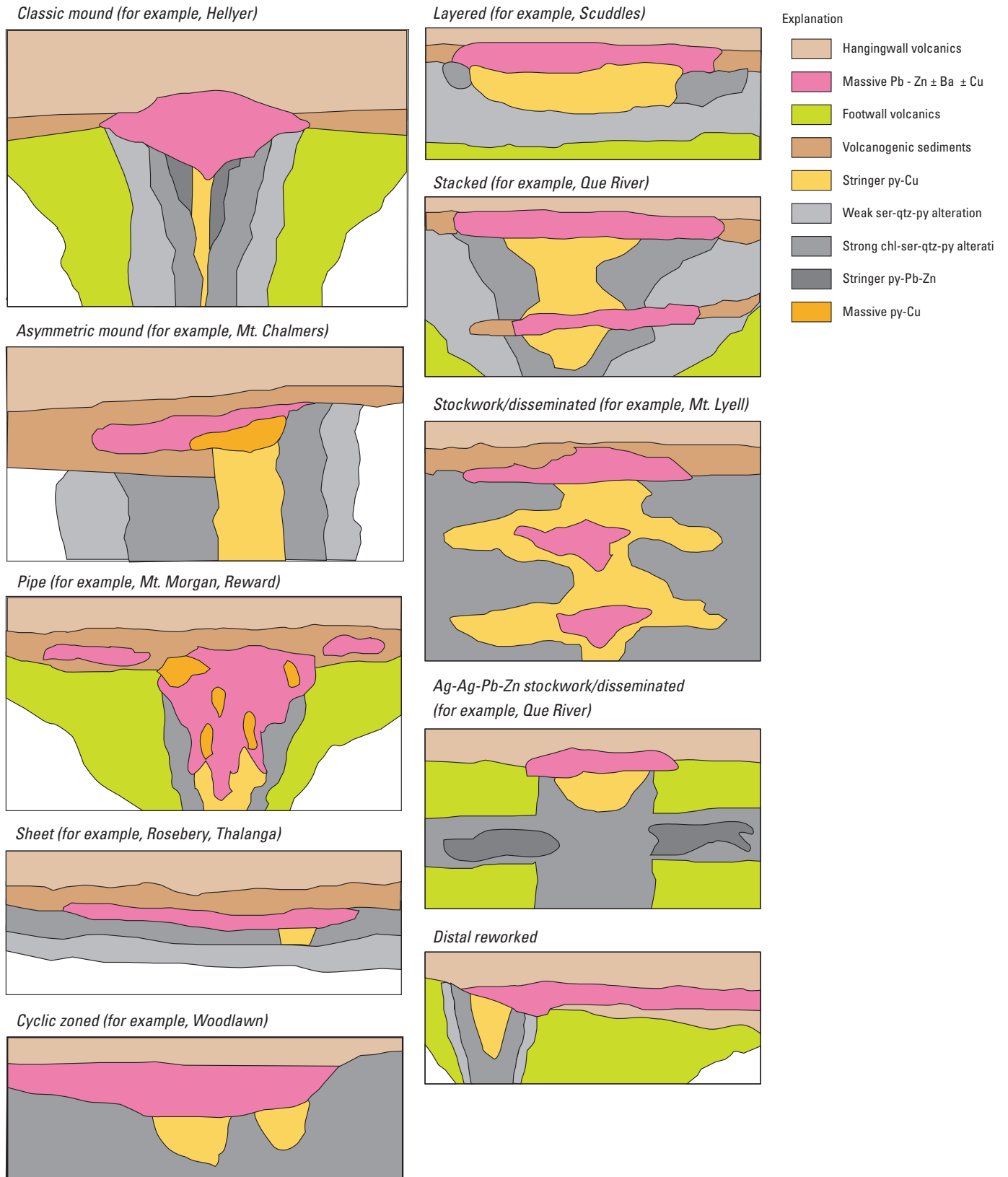


Figure 6-1. Different forms and styles of volcanogenic massive sulfide deposits (with example sites in parentheses). Modified from Large (1992). [Ag, silver; Ba, barium; Cu, copper; Pb, lead; Zn, zinc; chl, chlorite; py, pyrite; qtz, quartz; ser, sericite]

and others, 1991), including the remobilization of sulfides and formation of sulfide breccias (de Roo and van Staal, 2003). Map distributions of deformed deposits can be misleading because in some cases, like in the Ducktown district of Tennessee, what appears to be a simple pattern of one fold generation is actually an intensely folded and sheared group of deposits that experienced multiple deformational events (Slack, 1993, and references therein). Noteworthy are the thickened zones of massive sulfide that characteristically occur in the hinges of tight to isoclinal folds (for example, Brunswick No. 12; van Staal and Williams, 1984), which in many orebodies are of major economic importance.

Highly sheared deposits typically show elongate or dismembered shapes of sulfide bodies and (or) footwall stringer zones, both of which may be offset along shears or ductile faults. Examples include Brunswick No. 12, Ducktown, and Kristineberg in Sweden (van Staal and Williams, 1984; Slack, 1993; Årebäck and others, 2005). As a result of such shearing, and the development of transposed bedding in wall rocks and of complex fabrics within remobilized massive sulfides and feeder zones, it can be difficult to discern primary geometric relations between mineralized zones and volcanosedimentary host strata, including whether the deposits are syngenetic or epigenetic (van Staal and Williams, 1984; Marshall and Spry, 2000). Other products of extensive deformation of VMS deposits include the so-called “durchbewegung structure,” comprising fragments of rotated and typically rounded wall rocks in a sulfide-rich matrix, and features such as sulfide-rich veins, mylonites, and piercement cusps (see Marshall and Gilligan, 1989; Duckworth and Rickard, 1993; Marshall and others, 2000). Attenuation and thinning of deposits into the plane of foliation is common and can result in lateral distribution of compositional and mineralogical zoning patterns that were originally vertical, as for example the Silver Peak deposit in Oregon (Derkey and Matsueda, 1989) or many of the VMS deposits in the Foothill metavolcanic belt of California (Kemp, 1982).

Host Rocks

The volcanic and sedimentary rocks that typically host VMS deposits may include lavas, tuffs, shales, siltstones, and (or) sandstones and their metamorphosed equivalents. Sedimentary conglomerates are uncommon to rare. Coarse volcanic breccias and fragmental pyroclastic rocks are the host rocks to many deposits, reflecting proximity of hydrothermal vents to volcanic centers (see Franklin and others, 2005; Galley and others, 2007). In many cases, massive sulfide deposits occur along or near brecciated rhyolite domes, which are well documented in the footwall of many VMS camps such as the Hokoruko district of Japan (Ohmoto and Takahashi, 1983) and the Noranda district of Quebec (Gibson and Galley, 2007).

References Cited

- Årebäck, H., Barrett, T.J., Abrahamsson, S., and Fagerström, P., 2005, The Palaeoproterozoic Kristineberg VMS deposit, Skellefte district, northern Sweden—Part I. *Geology: Mineralium Deposita*, v. 40, p. 351–367.
- Berry, R.F., Huston, D.L., Stolz, A.J., Hill, A.P., Beams, S.D., Kuronen, U., and Taube, A., 1992, Stratigraphy, structure, and volcanic-hosted mineralization of the Mount Windsor subprovince, North Queensland, Australia: *Economic Geology*, v. 87, p. 739–763.
- Cox, D.P., Barton, P.R., and Singer, D.A., 1986, Introduction, in Cox, D.P., and Singer, D.A., eds., *Mineral deposit models: U.S. Geological Survey Bulletin 1693*, p. 1–10.
- de Roo, J.A., and van Staal, C.R., 2003, Sulfide remobilization and sulfide breccias in the Heath Steele and Brunswick deposits, Bathurst mining camp, New Brunswick, in Goodfellow, W.D., McCutcheon, S.R., and Peter, J.M., eds., *Massive sulfide deposits of the Bathurst mining camp, New Brunswick, and northern Maine: Economic Geology Monograph 11*, p. 479–496.
- de Roo, J.A., Williams, P.F., and Moreton, C., 1991, Structure and evolution of the Heath Steele base metal sulfide orebodies, Bathurst camp, New Brunswick, Canada: *Economic Geology*, v. 86, p. 927–943.
- Derkey, R.E., and Matsueda, H., 1989, Geology of the Silver Peak mine, a Kuroko-type deposit in Jurassic volcanic rocks, Oregon, U.S.A.: *Journal of the Mining College of Akita University*, ser. A, v. VII, no. 2, p. 99–123.
- Doyle, M.G., and Huston, D.L., 1999, The subsea-floor replacement origin of the Ordovician Highway-Reward volcanic-associated massive sulfide deposit, Mount Windsor subprovince, Australia: *Economic Geology*, v. 94, p. 825–843.
- Duckworth, R.C., and Rickard, D., 1993, Sulphide mylonites from the Renström VMS deposit, northern Sweden: *Mineralogical Magazine*, v. 57, p. 83–91.
- Franklin, J.M., Gibson, H.L., Jonasson, I.R., and Galley, A.G., 2005, Volcanogenic massive sulfide deposits, in Hedenquist, J.W., Thompson, J.F.H., Goldfarb, R.J., and Richards, J.P., eds., *Economic Geology 100th anniversary volume, 1905–2005*: Littleton, Colo., Society of Economic Geologists, p. 523–560.
- Galley, A.G., 1993, Characteristics of semi-conformable alteration zones associated with volcanogenic massive sulfide districts: *Journal of Geochemical Exploration*, v. 48, p. 175–200.

- Galley, A.G., Hannington, M., and Jonasson, I., 2007, Volcanogenic massive sulphide deposits, in Goodfellow, W.D., ed., *Mineral deposits of Canada—A synthesis of major deposit-types, district metallogeny, the evolution of geological provinces, and exploration methods*: Geological Association of Canada, Mineral Deposits Division, Special Publication 5, p. 141–161.
- Gemmell, J.B., and Large, R.R., 1992, Stringer system and alteration zones underlying the Hellyer volcanic-hosted massive sulfide deposit, Tasmania, Australia: *Economic Geology*, v. 87, p. 620–649.
- German, C.R., and Von Damm, K.L., 2003, Hydrothermal processes, in Elderfield, H., ed., *The oceans and marine geochemistry. Treatise on geochemistry*, v. 6: Amsterdam, Elsevier Ltd., p. 181–222.
- Gibson, H.L., and Galley, A.G., 2007, Volcanogenic massive sulphide deposits of the Archean, Noranda district, Québec, in Goodfellow, W.D., ed., *Mineral deposits of Canada—A synthesis of major deposit-types, district metallogeny, the evolution of geological provinces, and exploration methods*: Geological Association of Canada, Mineral Deposits Division, Special Publication 5, p. 533–552.
- Goodfellow, W.D., 2003, Geology and genesis of the Caribou deposit, Bathurst mining camp, New Brunswick, Canada, in Goodfellow, W.D., McCutcheon, S.R., and Peter, J.M., eds., *Volcanogenic massive sulfide deposits of the Bathurst mining camp, New Brunswick, and northern Maine*: *Economic Geology Monograph 11*, p. 327–360.
- Goodfellow, W.D., and McCutcheon, S.R., 2003, Geologic and genetic attributes of volcanic sediment-hosted massive sulfide deposits of the Bathurst Mining Camp, New Brunswick—A synthesis, in Goodfellow, W.D., McCutcheon, S.R., and Peter, J.M., eds., *Massive sulfide deposits of the Bathurst Mining Camp, New Brunswick, and northern Maine*: *Economic Geology Monograph 11*, p. 245–301.
- Gustin, M.S., 1990, Stratigraphy and alteration of the host rocks, United Verde massive sulfide deposit, Jerome, Arizona: *Economic Geology*, v. 85, no. 1, p. 29–49.
- Hannington, M.D., Barrie, C.T., and Bleeker, W., 1999, The giant Kidd Creek volcanogenic massive sulfide deposit, western Abitibi Subprovince, Canada—Summary and synthesis, in Hannington, M.D., and Barrie, C.T., eds., *The Giant Kidd Creek volcanogenic massive sulfide deposit, western Abitibi subprovince, Canada*: *Economic Geology Monograph 10*, p. 661–672.
- Herrington, R.J., Maslennikov, V., Zaykov, V., Seravkin, I., Kosarev, A., Buschmann, B., Orgeval, J.-J., Holland, N., Tesalina, S., Nimis, P., and Armstrong, R., 2005, Classification of VMS deposits—Lessons from the South Uralides: *Ore Geology Reviews*, v. 27, p. 203–237.
- Hou, Z.-Q., Zaw, K., Rona, P., Li, Y.-Q., Qu, X.-M., Song, S.-H., Peng, L., and Huang, J.-J., 2008, Geology, fluid inclusions, and oxygen isotope geochemistry of the Baiyinchang pipe-style volcanic-hosted massive sulfide Cu deposit in Gansu Province, northwestern China: *Economic Geology*, v. 103, p. 269–292.
- Huston, D.L., 1990, The stratigraphic and structural setting of the Balcooma volcanogenic massive sulphide lenses, northern Queensland: *Australian Journal of Earth Sciences*, v. 37, p. 423–440.
- Johnson, B.J., Montante-Martínez, J.A., Canela-Barboza, M., and Danielson, T.J., 2000, Geology of the San Nicolás deposit, Zacatecas, Mexico, in Sherlock, R.L., and Logan, M.A.V., eds., *Volcanogenic massive sulphide deposits of Latin America*: Geological Association of Canada, Mineral Deposits Division Special Publication 2, p. 71–85.
- Kemp, W.R., 1982, Petrochemical affiliations of volcanogenic massive sulfide deposits of the Foothill Cu-Zn belt, Sierra Nevada, California: Reno, Nev., University of Nevada at Reno, Ph.D. thesis, 493 p.
- Knuckey, M.J., Comba, C.D.A., and Riverin, G., 1982, Structure, metal zoning and alteration at the Millenbach deposit, Noranda, Quebec, in Hutchinson, R.W., Spence, C.D., and Franklin, J.M., eds., *Precambrian sulphide deposits*: Geological Association of Canada Special Paper 25, p. 255–295.
- Large, R.R., 1992, Australian volcanic-hosted massive sulfide deposits—Features, styles, and genetic models: *Economic Geology*, v. 87, p. 471–510.
- Large, R.R., McPhie, J., Gemmell, J.B., Herrmann, W., and Davidson, G.J., 2001, The spectrum of ore deposit types, volcanic environments, alteration halos, and related exploration vectors in submarine volcanic successions—Some examples from Australia: *Economic Geology*, v. 96, p. 913–938.
- Lewis, P.D., and Rhys, D.A., 2000, Geological setting of the Tizapa volcanogenic massive sulphide deposit, Mexico State, Mexico, in Sherlock, R.L., and Logan, M.A.V., eds., *Volcanogenic massive sulphide deposits of Latin America*: Geological Association of Canada, Mineral Deposits Division Special Publication 2, p. 87–112.
- Lydon, J.W., 1984, Volcanogenic massive sulphide deposits—Part 1. A descriptive model: *Geoscience Canada*, v. 11, p. 195–202.
- Marshall, B., and Gilligan, L.B., 1989, Durchbewegung structure, piercement cusps, and piercement veins in massive sulfide deposits—Formation and interpretation: *Economic Geology*, v. 84, p. 2311–2319.

- Marshall, B., and Spry, P.G., 2000, Discriminating between regional metamorphic remobilization and syntectonic emplacement in the genesis of massive sulfide ores: *Reviews in Economic Geology*, v. 11, p. 39–79.
- Marshall, B., Vokes, F.M., and Laroque, A.C.L., 2000, Regional metamorphic remobilization—Upgrading and formation of ore deposits, in Spry, P.G., Marshall, B., and Vokes, F.M., eds., *Metamorphic and metamorphogenic ore deposits: Reviews in Economic Geology*, v. 11, p. 19–38.
- Messenger, P.R., Golding, S.D., and Taube, A., 1997, Volcanic setting of the Mount Morgan Au-Cu deposit, central Queensland—Implications for ore genesis: *Geological Society of Australia Special Publication* 19, p. 109–127.
- Nehlig, P., Cassard, D., and Marcoux, E., 1998, Geometry and genesis of feeder zones of massive sulfide deposits—Constraints from the Rio Tinto ore deposit (Spain): *Mineralium Deposita*, v. 33, p. 137–149.
- Ohmoto, H., and Takahashi, T., 1983, Geological setting of the Kuroko deposits, Japan—Part III. Submarine calderas and kuroko genesis, in Ohmoto, H., and Skinner, B.J., eds., *The Kuroko and related volcanogenic massive sulfide deposits: Economic Geology Monograph* 5, p. 39–54.
- Peter, J.M., and Scott, S.D., 1999, Windy Craggy, northwestern British Columbia—The world's largest Besshi-type deposit, in Barrie, C.T., and Hannington, M.D., eds., *Volcanic-associated massive sulfide deposits—Processes and examples in modern and ancient settings: Reviews in Economic Geology*, v. 8, p. 261–295.
- Peter, J.M., Layton-Matthews, D., Piercey, S., Bradshaw, G., Paradis, S., and Boulton, A., 2007, Volcanic-hosted massive sulphide deposits of the Finlayson Lake district, Yukon, in Goodfellow, W.D., ed., *Mineral deposits of Canada—A synthesis of major deposit-types, district metallogeny, the evolution of geological provinces, and exploration methods: Geological Association of Canada Special Publication* 5, p. 471–508.
- Petersen, S., Herzig, P.M., and Hannington, M.D., 2000, Third dimension of a presently forming VMS deposit—TAG hydrothermal mound, Mid-Atlantic Ridge, 26°N: *Mineralium Deposita*, v. 35, p. 233–259.
- Richards, H.G., Cann, J.R., and Jensenius, J., 1989, Mineralogical zonation and metasomatism of the alteration pipes of Cyprus sulfide deposits: *Economic Geology*, v. 84, p. 91–115.
- Ridley, W.I., Perfit, M.R., Jonasson, I.R., and Smith, M.F., 1994, Hydrothermal alteration in oceanic ridge volcanics—A detailed study at the Galapagos fossil hydrothermal field: *Geochimica et Cosmochimica Acta*, v. 58, p. 2477–2494.
- Roth, T., Thompson, J.F.H., and Barrett, T.J., 1998, The precious metal-rich Eskay Creek deposit, northwestern British Columbia: *Reviews in Economic Geology*, v. 8, p. 367–384.
- Slack, J.F., 1993, Descriptive and grade-tonnage models for Besshi-type massive sulphide deposits, in Kirkham, R.V., Sinclair, W.D., Thorpe, R.I., and Duke, J.M., eds., *Mineral deposit modeling: Geological Association of Canada Special Paper* 40, p. 343–371.
- Slack, J.F., Foose, M.P., Flohr, M.J.K., Scully, M.V., and Belkin, H.E., 2003, Exhalative and seafloor replacement processes in the formation of the Bald Mountain massive sulfide deposit, northern Maine, in Goodfellow, W.D., McCutcheon, S.R., and Peter, J.M., eds., *Volcanogenic massive sulfide deposits of the Bathurst district, New Brunswick, and northern Maine: Economic Geology Monograph* 11, p. 513–548.
- Slack, J.F., Offield, T.W., Woodruff, L.G., and Shanks, W.C., III, 2001, Geology and geochemistry of Besshi-type massive sulfide deposits of the Vermont copper belt, in Hammarstrom, J.M., and Seal, R.R., II, eds., *Environmental geochemistry and mining history of massive sulfide deposits in the Vermont copper belt: Society of Economic Geologists Guidebook Series*, v. 35, part II, p. 193–211.
- Sumitomo Metal Mining Company, Ltd., 1970, Summary of the Besshi ore deposits [field guide], in IMA-IAGOD, 7th General Meeting, Tokyo and Kyoto, Japan, 1970, *Proceedings: International Mineralogical Association, International Association on the Genesis of Ore Deposits*, 16 p.
- Taube, A., 1986, The Mount Morgan gold-copper mine and environment, Queensland—A volcanogenic massive sulfide deposit associated with penecontemporaneous faulting: *Economic Geology*, v. 81, p. 1322–1340.
- Tegart, P., Allen, G., and Carstensen, A., 2000, Regional setting, stratigraphy, alteration and mineralization of the Tambo Grande VMS district, Piura Department, northern Peru, in Sherlock, R.L., and Logan, M.A.V., eds., *Volcanogenic massive sulphide deposits of Latin America: Geological Association of Canada, Mineral Deposits Division Special Publication* 2, p. 375–405.
- Tornos, F., 2006, Environment of formation and styles of volcanogenic massive sulfides—The Iberian Pyrite Belt: *Ore Geology Reviews*, v. 28, p. 259–307.
- van Staal, C.R., and Williams, P.F., 1984, Structure, origin, and concentration of the Brunswick 12 and 6 orebodies: *Economic Geology*, v. 79, p. 1669–1692.

Zachrisson, E., 1984, Lateral metal zonation and stringer zone development, reflecting fissure-controlled exhalations at the Stekenjokk-Levi strata-bound sulfide deposit, central Scandinavian Caledonides: *Economic Geology*, v. 79, p. 1643–1659.

Zierenberg, R.A., Fouquet, Y., Miller, D.J., Bahr, J.M., Baker, P.A., Bjerksgarden, T., Brunner, C.A., Duckworth, R.C., Gable, R., Gieskes, J.M., Goodfellow, W.D., Groeschel-Becker, H.M., Guerin, G., Ishibashi, J., Iturrino, G.J., James, R.H., Lackschewitz, K.S., Marquez, L.L., Nehlig, P., Peter, J.M., Rigsby, C.A., Schultheiss, P.J., Shanks, W.C., III, Simoneit, B.R.T., Summit, M., Teagle, D.A.H., Urvbat, M., and Zuffa, G.G., 1998, The deep structure of a sea-floor hydrothermal deposit: *Nature*, v. 392, no. 6675, p. 485–488.

7. Geophysical Characteristics of Volcanogenic Massive Sulfide Deposits

By Lisa A. Morgan

7 of 21

Volcanogenic Massive Sulfide Occurrence Model

Scientific Investigations Report 2010–5070–C

**U.S. Department of the Interior
U.S. Geological Survey**

U.S. Department of the Interior
KEN SALAZAR, Secretary

U.S. Geological Survey
Marcia K. McNutt, Director

U.S. Geological Survey, Reston, Virginia: 2012

For more information on the USGS—the Federal source for science about the Earth, its natural and living resources, natural hazards, and the environment, visit <http://www.usgs.gov> or call 1-888-ASK-USGS.

For an overview of USGS information products, including maps, imagery, and publications, visit <http://www.usgs.gov/pubprod>

To order this and other USGS information products, visit <http://store.usgs.gov>

Any use of trade, product, or firm names is for descriptive purposes only and does not imply endorsement by the U.S. Government.

Although this report is in the public domain, permission must be secured from the individual copyright owners to reproduce any copyrighted materials contained within this report.

Suggested citation:

Morgan, L.A., 2012, Geophysical characteristics of volcanogenic massive sulfide deposits in volcanogenic massive sulfide occurrence model: U.S. Geological Survey Scientific Investigations Report 2010-5070 -C, chap. 7, 16 p.

Contents

| | |
|-----------------------------|-----|
| Introduction..... | 117 |
| Electrical Signature | 117 |
| Magnetic Signature..... | 118 |
| Gravity Signature | 123 |
| Radiometric Signature | 125 |
| Seismic Techniques..... | 125 |
| Concealed Deposits..... | 127 |
| Conclusions..... | 129 |
| References Cited..... | 129 |

Figures

| | |
|---|-----|
| 7-1. Schematic diagram of the modern Trans-Atlantic Geothermal sulfide deposit on the Mid-Atlantic Ridge, depicting a cross section of a volcanogenic massive sulfide deposit with concordant semi-massive to massive sulfide lens underlain by a discordant stockwork vein system and associated alteration halo | 118 |
| 7-2. Selected airborne geophysical surveys for Bathurst mining camp..... | 122 |
| 7-3. Gravity model showing that an excess mass in the crust contributes to the gravity field and produces a positive anomaly or gravity high..... | 123 |
| 7-4. Geological and geophysical maps of the area containing the Armstrong B massive sulfide deposit, Bathurst mining camp, New Brunswick, with geophysical profiles across the deposit | 124 |
| 7-5. Schematic diagram showing airborne and ground radiometric surveys | 126 |
| 7-6. Velocity values of various rock types and ore minerals plotted against their density with lines of constant acoustic impedance overlain within field..... | 127 |
| 7-7. Seismic reflection profiles through volcanogenic massive sulfide deposits | 128 |

Tables

| | |
|--|-----|
| 7-1. Utility of geophysical techniques in exploration of volcanogenic massive sulfide deposits | 119 |
| 7-2. Physical properties of common rock ore minerals and ore-related minerals | 120 |
| 7-3. Massive sulfide ore mineral density and magnetic susceptibility. | 123 |

7. Geophysical Characteristics of Volcanogenic Massive Sulfide Deposits

By Lisa A. Morgan

Introduction

Volcanogenic massive sulfide (VMS) deposits typically have strong geophysical contrasts with their host rocks because of the substantial differences in physical and chemical properties between the deposits and the rock in which they form (Thomas and others, 2000). Such properties include density, magnetic intensity and susceptibility, gravity, electrical resistance, and acoustical velocity. Electrical self potential or transient responses to time-varying electromagnetic fields can also be used to detect buried sulfide deposits. Typically, the sulfide body is a concordant lens underlain by a discordant stockwork or stringer zone with vein-type sulfide mineralization (fig. 7-1) (Galley and others, 2007).

Based on the shape and depth of the ore body, the sulfide content in the ore produces significant geophysical signatures. As noted by Ford and others (2007), VMS deposits produce significant electromagnetic, gravimetric, and magnetic responses and thus provide great potential for geophysically detecting ore bodies (table 7-1). Geophysical surveys (fig. 7-2) have been employed successfully to identify ore bodies and are used at an early stage in exploration. For sulfide deposits, contrasts in magnetic, electromagnetic, and gravitational (density) properties become direct exploration vectors; gamma-ray spectroscopy provides an indirect technique based on chemical contrasts associated with near-surface alteration mostly as potassium enrichment or depletion within and surrounding the deposit (Thomas and others, 2000). As exploration for near-surface and surface base-metal deposits becomes more difficult, geophysical techniques are increasingly relied upon to identify areas of VMS mineralization (Bishop and Emerson, 1999).

The most common sulfide mineral in VMS deposits is pyrite, which is often associated with other sulfides such as pyrrhotite, chalcopyrite, sphalerite, and galena (Galley and others, 2007). Other possible nonsulfide minerals associated in VMS deposits include magnetite, hematite, and cassiterite; barite can be present as a gangue mineral. All these minerals have relatively high values of specific gravity (4.0–7.5 g/cm³; table 7-2), which is in strong contrast to the significantly lower densities measured in their sedimentary or volcanic host rocks. Thomas (2003) measured densities of 2.70–2.84 g/cm³ for the host rock at the Bathurst mining camp.

Electrical Signature

Electrical methods are highly effective in identifying VMS targets because they respond to the electrical conductivity of the rocks and minerals, which can vary by 20 orders of magnitude (Grant and West, 1965). Electrical methods are unique in being able to detect such a large range of magnitudes; no other physical property has such a wide range. Because of this large potential range in values, a variety of electrical techniques have been developed that capitalize on these differences, such as measurement of conductivity, resistivity (the inverse of conductivity), induced polarization, electromagnetism, and gamma ray spectra (table 7-1). Electrical methods are currently the most used technique in surveying for VMS deposits; a variety of survey types (for example, MegaTEM, Titan24, and borehole techniques) are pushing the limits of detectable depth ranges.

Volcanogenic massive sulfide deposits have high conductivities (fig. 7-2B) exceeding 500 mS/m (millisiemens per meter) and are similar in magnitude to graphite and saltwater (Ford and others, 2007). Compared to igneous and metamorphic rocks with typical conductivities of <1 mS/m and sedimentary rocks with conductivities from 1 to 500 mS/m, the contrast between VMS deposits and its host rock may be significant and can be a useful physical property. A complicating factor, however, may be introduced by a water-rich unit overlying the VMS ore body, as the content of water in a unit can substantially increase its conductivity; thus, such a unit could effectively mask the signal from the ore body. Anoxic sedimentary horizons that contain graphite or sulfide are also highly conductive and are difficult to distinguish from massive sulfide deposits. Some types of VMS deposits are typically associated with reducing sediments. Noneconomic pyrite-rich or pyrrhotite-rich deposits are not distinguishable from potentially economic deposits, so conductivity and other electromagnetic techniques are not fully definitive exploration tools in and of themselves.

Electrical resistivity surveys are useful in calculating the apparent resistivity of the subsurface at different depths resulting in the generation of cross sections of true resistivity (Ford and others, 2007). These can be used to produce three-dimensional geometries of ore bodies at depth. Resistivity surveys also are used to estimate the thickness of overburden, which

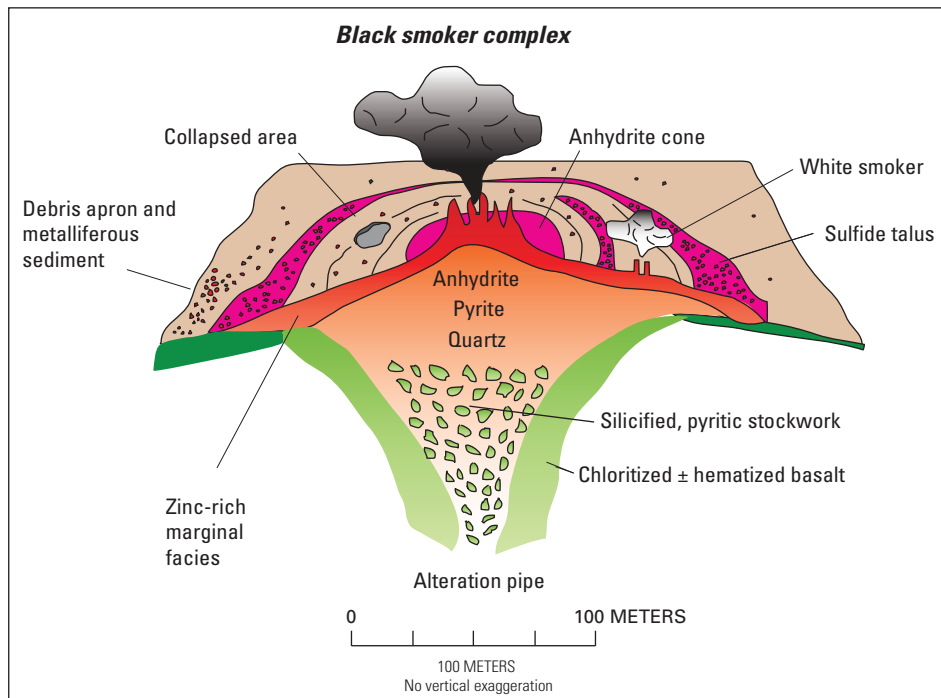


Figure 7-1. Schematic diagram of the modern Trans-Atlantic Geothermal (TAG) sulfide deposit on the Mid-Atlantic Ridge, depicting a cross section of a volcanogenic massive sulfide deposit with concordant semi-massive to massive sulfide lens underlain by a discordant stockwork vein system and associated alteration halo. From Hannington and others (1998) and Galley and others (2007). Modified from Hannington and others (2005).

then can be used to improve interpretation of ground gravity surveys (Ford and others, 2007). Conductivity, the inverse of resistivity, also can be used to map overburden.

Induced polarization (IP) surveys measure the chargeability of the ground and the time variance in the response of the electromagnetic field, which is related to ability of the material to retain electrical charges. Induced polarization surveys are very effective in detecting disseminated sulfide bodies. Typically, these sulfides occur in the altered halo surrounding the massive sulfide ore body and may be associated with clays, which also produce significant IP responses (Ford and others, 2007).

The techniques associated with electromagnetic (EM) surveys, collected both on ground and in air, are the most common electrical methods employed in mineral exploration. Electromagnetic techniques can directly detect conductive features such as base metal deposits where significant contrasts in conductivity values occur between the ore bodies and their resistive host rocks (Thomas and others, 2000). Values for the conductivity of soils, rocks, and ore bodies, measured in milliSiemens per meter, span several orders of magnitude ranging from 3.57×10^9 mS/m for graphite to 5×10^8 mS/m for pyrrhotite to 0.01 mS/m for gravel and sand (Thomas and others,

2000). Both airborne and ground electromagnetic techniques are effective in detecting massive sulfide mineralization, but only if the sulfide grains in the deposit are electrically connected (Dubé and others, 2007). In cases where sulfide grains are not electrically connected, such as in the disseminated sulfide stockwork below the main massive sulfide ore body, induced polarization can be successfully employed to detect these and other disseminated sulfides. As water content greatly influences the conductivity of the unit, Telford and others (1990) showed that the conductivity difference between a wet and a dry tuff differed by a factor of 100. Saturated overburden may produce conductivity values that effectively mask the EM of the VMS mineralization (Thomas and others, 2000).

Magnetic Signature

High-resolution magnetic data can be an excellent tool in identifying the broad geologic framework of an area and often show contrasting patterns that reflect differences in lithologic compositions, crustal structures, and type and degree of alteration. As one of the oldest geophysical exploration methods used in mineral exploration, the effectiveness of magnetic

Table 7-1. Utility of geophysical techniques in exploration of volcanogenic massive sulfide (VMS) deposits. O represent highly effective methods and X represent moderately effective methods.

[Source: Ford and others (2007)]

| Geophysical method | | |
|--------------------|----------------------|--------------|
| Air or ground | Application | VMS deposits |
| Electric | | |
| Air | Geological Framework | X |
| Ground | Direct Targeting | O |
| Electromagnetic | | |
| Air | Geological Framework | X |
| Air | Direct Targeting | O |
| Ground | Geological Framework | X |
| Ground | Direct Targeting | O |
| Magnetic | | |
| Air | Geological Framework | O |
| Air | Direct Targeting | O |
| Ground | Geological Framework | O |
| Ground | Direct Targeting | O |
| Gravity | | |
| Air | Geological Framework | X |
| Air | Direct Targeting | O |
| Ground | Geological Framework | X |
| Ground | Direct Targeting | O |
| Radiometric | | |
| Air | Geological Framework | O |
| Air | Direct Targeting | X |
| Ground | Geological Framework | X |
| Ground | Direct Targeting | X |
| Seismic | | |
| Ground | Geological Framework | X |
| Ground | Direct Targeting | X |

surveys depends on the presence of magnetite or other minerals with high values of magnetic susceptibility (fig. 7-2A; tables 7-2, 7-3). Metallic ore bodies are often identified by delineating magnetic anomalies.

Magnetic surveys measure the total magnetic intensity or strength of the Earth's field, measured in units of nanotesla (nT). The total field includes contributions imparted by the Earth's core, crust, and upper atmosphere; the resultant field subtracts contributions from the core and upper atmosphere leaving the crustal component which reflects both positive and negative values of crustal susceptibility. It is the total magnetic intensity of the crust that is referred to in discussing processed magnetic field data. A commonly applied derivative of the magnetic field data is the magnetic vertical gradient, measured in nanoteslas per meter (nT/m), which filters the magnetic data and emphasizes near-surface geological features. Compared to anomalies observed in total magnetic intensity maps, vertical gradient anomalies tend to be more confined and associated with closely spaced geological units that produce distinct magnetic anomalies (Thomas and others, 2000). Vertical gradient maps are commonly used to delineate VMS deposits (fig. 7-2).

Many sulfide minerals have high values of magnetic susceptibility resulting in prominent magnetic anomalies associated with VMS ore bodies. In some cases, the strong magnetic signature of a VMS deposit is associated with noneconomic mineralization. For example, a Cu-rich, chalcopyrite-bearing VMS deposit may have a strong magnetic anomaly due to its association with pyrrhotite, a highly magnetic but non-economic mineral (table 7-2). Very high values of magnetic susceptibility are measured in pyrrhotite ($3,200 \times 10^{-3}$ SI) and pyrite (5×10^{-3} SI), which is the most common mineral associated with VMS deposits. Compared to the lower values measured in most sedimentary and volcanic host rocks, this strong contrast in values results in positive magnetic anomalies in surveyed areas.

Other common sulfide minerals in VMS deposits, such as chalcopyrite, sphalerite and galena, have lower values of magnetic susceptibility that are similar to those found for their sedimentary and volcanic host rocks and thus do not contribute to any magnetic anomaly associated with the VMS ore body. Sphalerite has no salient geophysical properties that would allow its identification using routine geophysical techniques (Bishop and Emerson, 1999) and, in fact, detection of any Zn-bearing sulfides is difficult. Sphalerite, the most commonly mined Zn-bearing mineral, is not magnetic, is very resistive, and has a relatively low specific gravity. However, sphalerite rarely forms as an isolated sulfide as it is associated with galena, pyrite, pyrrhotite, and chalcopyrite (Bishop and Emerson, 1999). The fact that sulfides with high values of magnetic susceptibility are associated with VMS ore bodies facilitates their identification. Additionally, nonsulfide metallic minerals with high susceptibility values, such as magnetite ($5,500 \times 10^{-3}$ SI) and hematite (40×10^{-3} SI) (table 7-2), also are common in some massive sulfide deposits and contribute to the strong positive magnetic anomalies found associated with these ore bodies. Magnetite in VMS deposits typically occurs

120 7. Geophysical Characteristics of Volcanogenic Massive Sulfide Deposits

Table 7-2. Physical properties (density, magnetic susceptibility, electrical conductivity) of common rock ore minerals and ore-related minerals.

[Sources: Thomas and others (2000); Ford and others (2007). SI, International System of Units; g/cm³, gram per cubic centimeter; mS/m, millisiemens per meter]

| Rock type | Density (g/cc) | | | Magnetic (SI x 10 ⁻³) | | | Conductivity (mS/m) | | |
|---------------------------------|----------------|------|------|-----------------------------------|------|------|---------------------|-------|------|
| | Min. | Max. | Ave. | Min. | Max. | Ave. | Min. | Max. | Ave. |
| Sediments and sedimentary rocks | | | | | | | | | |
| Overburden | | | 1.92 | | | | | | |
| Soil | 1.2 | 2.4 | 1.92 | 0.01 | 1.26 | | | | |
| Clay | 1.63 | 2.6 | 2.21 | | | | 10 | 300 | |
| Glaciolacustrine clay | | | | | | 0.25 | 10 | 200 | |
| Gravel | 1.7 | 2.4 | 2 | | | | 0.1 | 2 | |
| Sand | 1.7 | 2.3 | 2 | | | | 0.1 | 2 | |
| Glacial till | | | | | | | 0.5 | 20 | |
| Saprolite (mafic) | | | | | | | 50 | 500 | |
| Saprolite (felsic) | | | | | | | 5 | 50 | |
| Sandstone | 1.61 | 2.76 | 2.35 | 0 | 20 | 0.4 | 1 | 200 | |
| Shale | 1.77 | 3.2 | 2.4 | 0.01 | 18 | 0.6 | 30 | 200 | |
| Argillite | | | | | | | 0.07 | 83.3 | |
| Iron formation | | | | | | | 0.05 | 3,300 | |
| Limestone | 1.93 | 2.9 | 2.55 | 0 | 3 | 0.3 | 0.001 | 1 | |
| Dolomite | 2.28 | 2.9 | 2.7 | 0 | 0.9 | 0.1 | 0.001 | 1 | |
| Conglomerate | | | | | | | 0.1 | 1 | |
| Greywacke | 2.6 | 2.7 | 2.65 | | | | 0.09 | 0.24 | |
| Coal | | | 1.35 | | | 0.03 | 2 | 100 | |
| Red sediments | | | 2.24 | 0.01 | 0.1 | | | | |
| Igneous rocks | | | | | | | | | |
| Rhyolite | | | 2.52 | 0.2 | 35 | | | | |
| Andesite | | | 2.61 | | | 160 | | | |
| Granite | | | 2.64 | | | 2.5 | | | |
| Granodiorite | | | 2.73 | | | | | | |
| Porphyry | | | 2.74 | | | 60 | | | |
| Quartz porphyry | | | | | | 20 | | | |
| Quartz diorite | | | 2.79 | | | | | | |
| Quartz diorite, dacite | | | | | | 83 | | | |
| Diorite | | | 2.85 | | | 85 | | | |
| Diabase | | | 2.91 | | | | | | |
| Olivine diabase | | | | | | 55 | | | |
| Basalt | | | 2.99 | | | 25 | | | |
| Gabbro | | | 3.03 | | | 70 | | | |
| Hornblende gabbro | | | 3.08 | | | 70 | | | |
| Peridotite | | | 3.15 | | | 250 | | | |
| Obsidian | | | 2.3 | | | | | | |
| Pyroxenite | | | 3.17 | | | 125 | | | |
| Monzonite | | | | | | 85 | | | |
| Acid igneous rocks | | | 2.61 | | | 8 | | | |
| Basic igneous rocks | | | 2.79 | | | 25 | | | |

Table 7-2. Physical properties (density, magnetic susceptibility, electrical conductivity) of common rock ore minerals and ore-related minerals.—Continued[Sources: Thomas and others (2000); Ford and others (2007). SI, International System of Units; g/cm³, gram per cubic centimeter; mS/m, millisiemens per meter]

| Rock type | Density (g/cc) | | | Magnetic (SI x 10 ⁻³) | | | Conductivity (mS/m) | | |
|-------------------|----------------|------|------|-----------------------------------|-------|-------|---------------------|------|------|
| | Min. | Max. | Ave. | Min. | Max. | Ave. | Min. | Max. | Ave. |
| Phonolite | | | 2.59 | | | | | | |
| Trachyte | | | 2.6 | | | 49 | | | |
| Nepheline syenite | | | 2.61 | | | | | | |
| Syenite | | | 2.77 | | | 49 | | | |
| Anorthosite | | | 2.78 | | | | | | |
| Norite | | | 2.92 | | | | | | |
| Metamorphic rocks | | | | | | | | | |
| Quartzite | | | 2.6 | | | 4 | | | |
| Schist | | | 2.64 | | | 1.4 | | | |
| Marble | | | 2.75 | | | | | | |
| Serpentine | | | 2.78 | | | | | | |
| Slate | | | 2.79 | | | 6 | | | |
| Gneiss | | | 2.8 | | | | | | |
| Amphibolite | | | 2.96 | | | 0.7 | | | |
| Eclogite | | | 3.37 | | | | | | |
| Granulite | | | 2.65 | | | | | | |
| Phyllite | | | 2.74 | | | | | | |
| Quartz slate | | | 2.77 | | | | | | |
| Chlorite schist | | | 2.87 | | | | | | |
| Skarn | 2.95 | 3.15 | | | | 2.5 | | | 1.25 |
| Hornfels | 2.9 | 3 | | | | 0.31 | | | 0.05 |
| Sulfide minerals | | | | | | | | | |
| Chalcopyrite | | | 4.2 | 0.02 | 0.4 | | 1.11 | 6.67 | |
| Galena | | | 7.7 | | | -0.03 | 1.11 | 1.47 | |
| Pyrite | | | 5 | 0.03 | 5.3 | | 1.67 | 8.33 | |
| Pyrrhotite | | | 5 | | 3,200 | | 6.25 | 5 | |
| Sphalerite | | | 3.75 | -0.03 | 0.75 | | 0.08 | 3.70 | |
| Other | | | | | | | | | |
| Magnetite | | | 5.04 | 1,000 | 5,700 | | | | |
| Graphite | | | 2.5 | -0.08 | 0.2 | | 1.01 | 3.57 | |

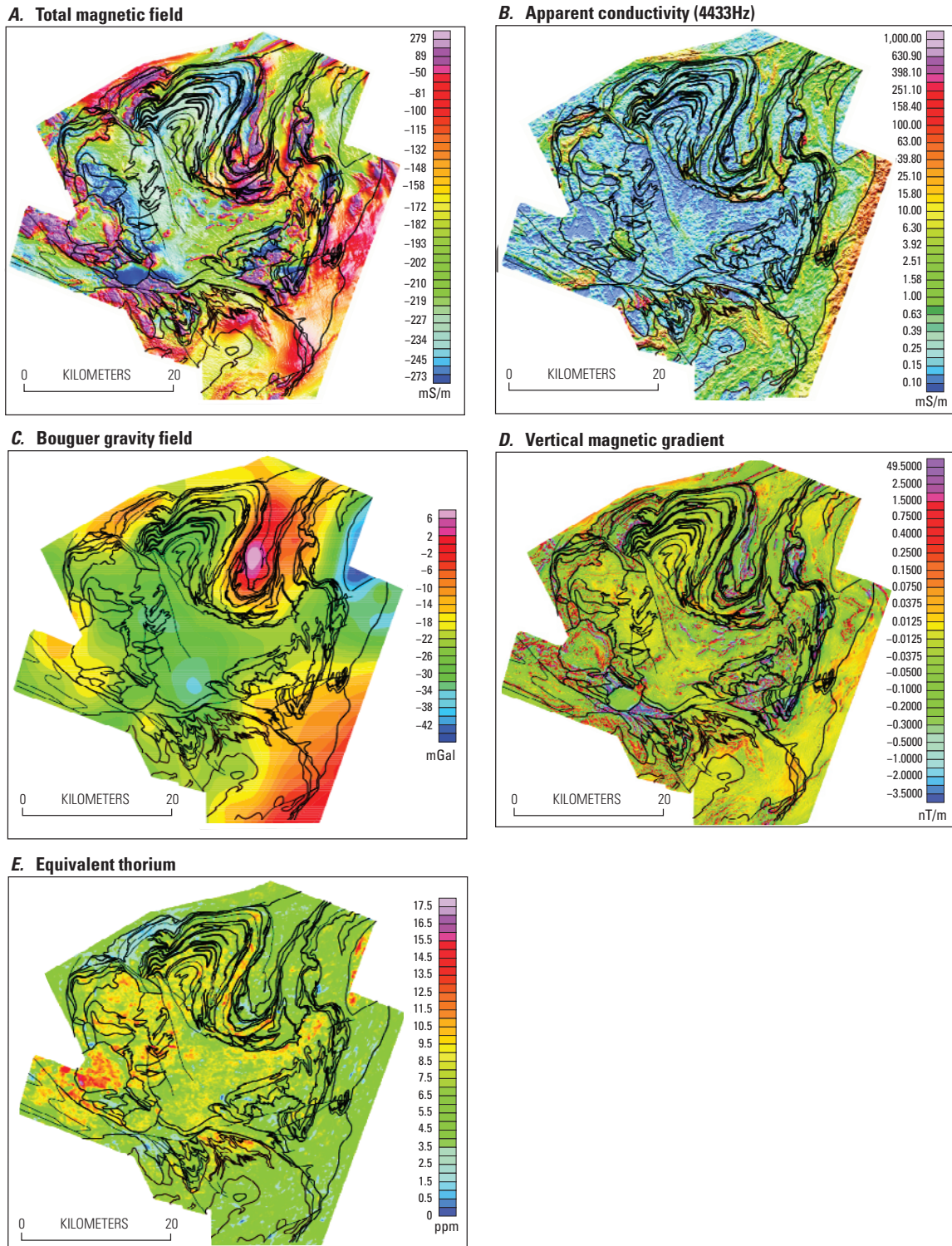


Figure 7-2. Selected airborne geophysical surveys for Bathurst mining camp. *A*, Map showing total magnetic intensity. Warm colors represent areas of high values of magnetic intensity, cooler colors denote low values of magnetic intensity. The areas with reddish and yellow coloration correlate to magnetite-bearing basalts (van Staal and others, 2003). *B*, High-frequency apparent conductivity map; areas of red and yellow represent black, sulfide-bearing shales and are quite conductive. *C*, Map showing Bouguer gravity field. *D*, Vertical magnetic gradient map emphasizing near-surface geologic features. *E*, Equivalent thorium map can be used to easily identify rocks with high concentrations of thorium (noted in red and yellow), such as granites and felsic volcanic rocks (van Staal and others, 2003). From Thomas and others (2000). [mS/m, milliSiemen per meter; mGal, milligal; nT/m, nanotesla per meter; ppm, part per million]

Table 7-3. Massive sulfide ore mineral density (g/cm³) and magnetic susceptibility (10⁻³ SI).

| Mineral | Density ¹ | Susceptibility ² |
|--------------|----------------------|-----------------------------|
| Barite | 4.5 | - |
| Chalcopyrite | 4.2 | 0.4 |
| Pyrite | 5.02 | 5 |
| Pyrrhotite | 4.62 | 3,200 |
| Sphalerite | 4 | 0.8 |
| Galena | 7.5 | -0.03 |
| Magnetite | 5.18 | 5,700 |
| Hematite | 5.26 | 40 |

¹Densities from Klein and Hurlbut (1985).²Susceptibilities from Hunt and others (1995).

in the core of the stockwork and central basal part of the overlying sulfide lens (Ford and others, 2007). Furthermore, magnetite and hematite are common minerals in iron-formation deposits that can be temporally and spatially associated with VMS deposits (Peter and others, 2003); high values of magnetic susceptibility for these minerals produce amplified magnetic anomalies.

At the Bathurst mining camp, Thomas (1997) measured values of magnetic susceptibility in host rocks that ranged from 0.1 to 1.1×10^{-3} SI. This strong contrast in values results in positive magnetic anomalies over the VMS ore body (fig. 7-2A) (Ford and others, 2007).

In other cases, hydrothermal alteration of footwall rocks beneath massive sulfide deposits may lead to the destruction of magnetic phases and results in anomalously low magnetic signals, much like the hydrothermal alteration zones around thermal basins in Yellowstone National Park (Finn and Morgan, 2002). Tivey and others (1993, 1996) conducted near-bottom magnetic surveys over the TAG massive sulfide deposit (fig. 7-1) and two other inactive sulfide mounds on the Mid-Atlantic Ridge using the submersible *Alvin*. They found small localized negative magnetic anomalies over individual sulfide deposits and a broader magnetic low zone not attributable to the small anomalies related to the mounds. They attribute the localized anomalies to destruction of magnetic minerals beneath the sulfide mounds in intense, focused hydrothermal up-flow zones. We note that alteration beneath the TAG massive sulfide deposit (fig. 7-1) has resulted in hematized basalts (Hannington and others, 1998); detailed studies of hydrothermal mineralogy have not identified any pyrrhotite or magnetite (Tivey and others, 1995). Geochemical and mineralogical observations are thus consistent with magnetic data indicating that strongly magnetic minerals are not present in the TAG sulfide deposit and hydrothermal alteration has apparently oxidized primary magnetite in the basalt host rocks. This apparent inconsistency with magnetic highs related to VMS deposits exposed on the continents could be due to

differing mineralogy or to the overall size of sulfide accumulations relative to the underlying alteration pipes.

Tivey and others (2003) conducted extensive deep-tow magnetometer surveys over the TAG area and concluded that the broad negative magnetic anomaly is due to the area's position on the hanging wall of a detachment fault that causes crustal thinning. They also suggest that the hanging wall of a long-lived detachment fault is a favorable site for hydrothermal vents that may form VMS deposits because of reactivation along the fault providing pathways for fluid flow.

Gravity Signature

Gravimetric surveys measure differences in units of milligals (mGal) in the Earth's gravity field, which is sensitive to variations in rock density (Ford and others, 2007). Gravimetric surveys can be used to detect excess mass (fig. 7-3), which may indicate a potential ore body at depth, and to estimate the size of the excess mass; gravimetric surveys can be used in conjunction with conductivity surveys in assessing whether a conductivity anomaly is due to a low-density graphite body at depth or a high-density sulfide mineralized zone (Thomas and others, 2000). As noted, the minerals found in VMS deposits have relatively high specific gravity values in marked contrast to lower specific gravity values measured in their sedimentary and volcanic host rocks. Gravity highs are typical in VMS terranes and center over the ore body (figs. 7-2C, 7-4).

In mineral exploration for massive sulfide deposits, gravity surveys generally follow other geophysical (magnetic, electrical, or electromagnetic) and geochemical surveys and are used to detect the excess mass of the ore body as well as determining its size and tonnage.

In the Iberian Pyrite Belt, the Las Cruces massive sulfide deposit, hosted in siliciclastic-felsic rock, originally was

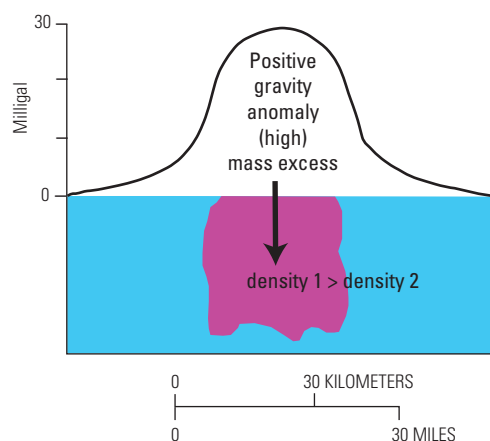
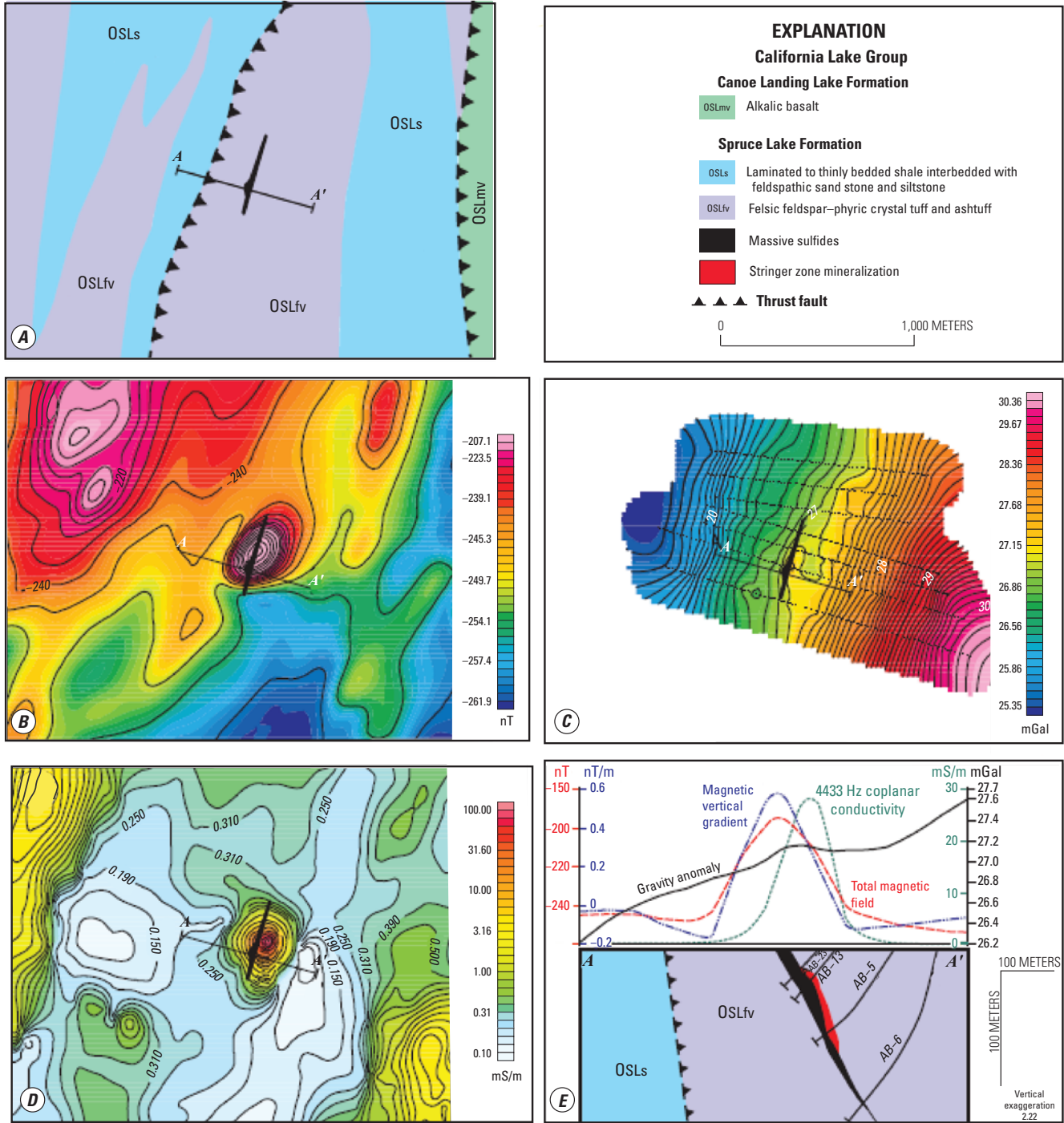


Figure 7-3. Gravity model showing that an excess mass in the crust contributes to the gravity field and produces a positive anomaly or gravity high. From Ford and others (2007).



discovered by a regional gravity survey (McIntosh and others, 1999) that indicated an extension of the Pyrite Belt lithologies beneath 120 m of cover. The 14.5-Mt deposit occurs in highly altered felsic to intermediate volcanic units with minor sedimentary rocks and is located in an industrialized zone within 18 km of Seville. The gravity survey was followed by IP (induced polarization) and TEM (transient electromagnetic) surveys that were effective in defining the extent of mineralization.

Gravimetry also played a critical role in identification of a pyrite ore body with associated polymetallic VMS deposit, the Lagoa Salgada ore body, in the tectonically complex Iberian Pyrite Belt of Portugal. Here the deposit is covered by a 128-m-thick cover of Tertiary strata and is associated with a 15-m-thick gossan (Oliveira and others, 1998). The VMS mineralization is somewhat variable and has significant values of Zn, Pb, Cu, As, Cd, Sn, Ag, Hg, and Au. The relatively dense ore body is hosted in a much less dense volcanoclastic-sedimentary host rock. The large contrast in density contributes to the large gravity anomaly. This anomaly has two main centers about 450 m apart and is strongly influenced by basement topography. Gravimetry has helped to delineate several structural alignments or faults and identify horst-graben structures (Oliveira and others, 1998) that potentially provide structural control on the localization of sulfide ore bodies.

Radiometric Signature

All rocks are naturally radioactive and contain various proportions of radioactive elements that can be measured in radiometric surveys (Thomas and others, 2000).

Gamma-ray spectrometry (fig. 7–5) measures discrete windows within the spectrum of gamma-ray energies, permitting measurement of the concentrations of individual radioelements, specifically potassium (K), uranium (U), and thorium (Th) (fig. 7–2E), through the detection of their shorter lived decay products. These measurements respond to sources from the top 20–60 cm of the Earth's surface and thus reflect only surficial geochemical conditions; the depth of features examined with gamma-ray spectrometry are much shallower in contrast to the depth of features measured below the mapped near-surface geology (tens to hundreds of meters) in other geophysical surveys, such as magnetic, electromagnetic, and gravity (Thomas and others, 2000). Tools for measuring radiation in bore holes allow the technique to be extended to the subsurface. Potassium, uranium, and thorium are measured in radiometric surveys because they are the principle elements contributing to natural radioactivity and are present in various concentrations in rocks and soils. Each element has distinct chemical properties that allow for characterization of normal and anomalous chemical and mechanical processes, which then can be further used to provide insight into ore-related processes (Ford and others, 2007). Potassium is present in most rocks and can be either significantly enriched or depleted by hydrothermal alteration. Uranium and thorium are present

in most rocks in minor abundances as relatively mobile and usually immobile elements, respectively (Thomas and others, 2000). Uranium mobility is strongly dependant on redox conditions and can thus be used to indicate favorable terrane for redox sensitive mineralization processes.

Gamma-ray spectrometry can be effective in geologic mapping and targeting mineralization, depending on several factors, including (1) where measurable differences in the radioactive element distributions can be related to differences in host rock lithologies, (2) where K content of the rock has been modified by alteration processes, and (3) where mineralization and alteration has affected surficial materials. Radioelement ratios of K, U, and Th can be applied to minimize the effects of moisture in soils, source geometry, and bedrock exposure. Preferential mobilization of individual radioelements in response to specific geochemical conditions allows the use of radioelement ratios as sensitive vectors in locating areas of mineralization (Thomas and others, 2000).

Alteration halos associated with VMS deposits also can contribute to their geophysical identification. As discussed by Shives and others (1997), K-altered mafic and felsic volcanic rocks are associated with a VMS deposit at Pilley's Island, Newfoundland, and produce strong airborne and ground gamma-ray spectrometry signatures (fig. 7–5).

At the Bathurst mining camp, distinctive trends in the abundances of K, U, and Th are apparent within and between the felsic volcanic and volcanoclastic rocks within the three geological groups surveyed (Shives and others, 2003). These trends reflect different primary lithochemical variations and subsequent seawater hydrothermal alteration and (or) greenschist overprints (Shives and others, 2003). While alkaline element mobility related to hydrothermal alteration and metamorphism affects the K value in these settings, concentrations of Th, a nonmobile element, can be compared with other high field strength immobile elements to aid in stratigraphic correlation and establishment of a stratigraphic framework. Radioactive element abundances can be used in distinguishing between individual formations and sometimes units within a formation; they also are very helpful as chemostratigraphic indicators (Shives and others, 2003). Mapping relative abundances of K, U, and Th in VMS terranes also is useful in delineating areas of hydrothermal alteration temporally and spatially associated with VMS mineralization (Shives and others, 2003).

Seismic Techniques

Geophysical exploration in crystalline crust for VMS deposits traditionally has been accomplished using potential field techniques that have the capability of penetrating only to 100–300 m in depth. Geophysical exploration for VMS deposits has not generally incorporated seismic techniques until recently. Because surface and near-surface VMS sources are depleted, modern exploration for VMS deposits must focus on identifying mineralization at greater depths, which

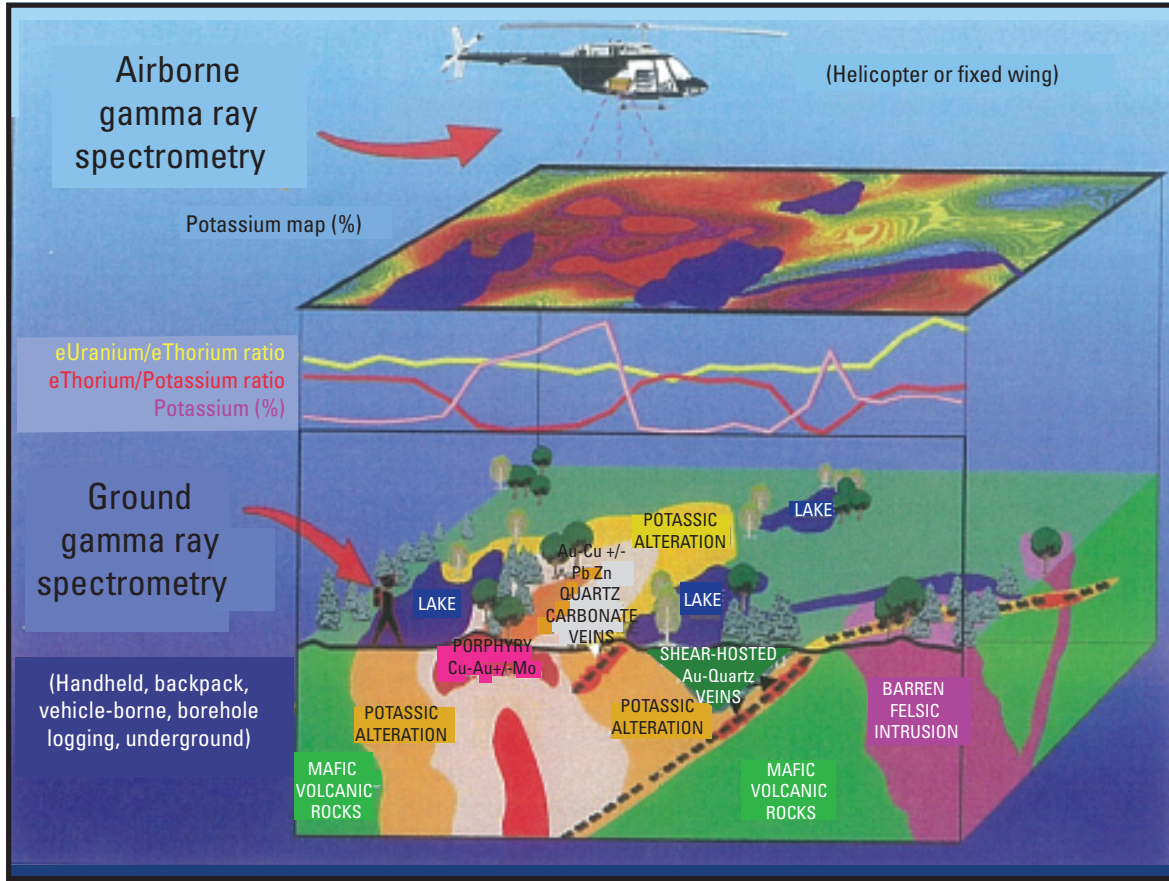


Figure 7-5. Schematic diagram showing airborne and ground radiometric surveys. From Ford and others (2007).

requires more sophisticated methodologies. Seismic tomography and reflection have been employed in detecting ore bodies (Elliot, 1967; Waboso and Mereu, 1978; Gustavsson and others, 1986; Goult, 1993; McGaughy and others, 1994); however, whether ore bodies can be directly imaged has been debated (Dahle and others, 1985). Salisbury and others (1996) measured the acoustic properties of ores and host rocks and showed that seismic reflection profiling is an effective technique in providing images of the regional structure in crystalline crust and also in delineating large VMS deposits (Milkerit and others, 1996). Furthermore, while surface seismic profiling is well suited for terrains with flat to moderate dips, Eaton and others (1996) and Salisbury and others (1996) show that in situations where steeply dipping or near vertical ore bodies are present, borehole seismic techniques can be used to successfully identify the ore body.

Seismic reflectivity is controlled by several factors, but one overriding factor is the difference in impedance between lithologies (Salisbury and others, 1996). Impedance is defined as the product of density and compressional wave velocity in a given material. Measurements of the specific gravities and velocities of common silicate rocks and ore minerals indicate

that ore minerals have significantly higher density values and a broad range of velocities, and therefore tend to have higher impedances than their host rocks. The difference in impedance value between the ore body and its host rock can be significant enough to result in high amplitude reflections and identification of the ore body (fig. 7-6) (Salisbury and others, 1996; Salisbury and Snyder, 2007).

Velocities of the most common sulfide minerals are quite variable and range from 8.04 km/s (kilometers per second) for pyrite to 4.68 km/s for pyrrhotite (Salisbury and others, 1996). In comparison, the measured densities are 5.02 g/cm³ (grams per cubic centimeter) for pyrite to 4.63 g/cm³ for pyrrhotite. As noted by Salisbury and others (1996), ore minerals associated with pyrite-dominated ores increase in velocity with increasing density whereas sphalerite-, chalcopyrite-, and pyrrhotite-dominated ores typically have velocity values that decrease with increasing density. This trend of decreasing values in velocity with increasing values in density is even more pronounced for mafic gangue with pyrrhotite (Salisbury and others, 1996). Host rock density values have a much narrower and lower range of density values and have a wide range of velocities (fig. 7-6).

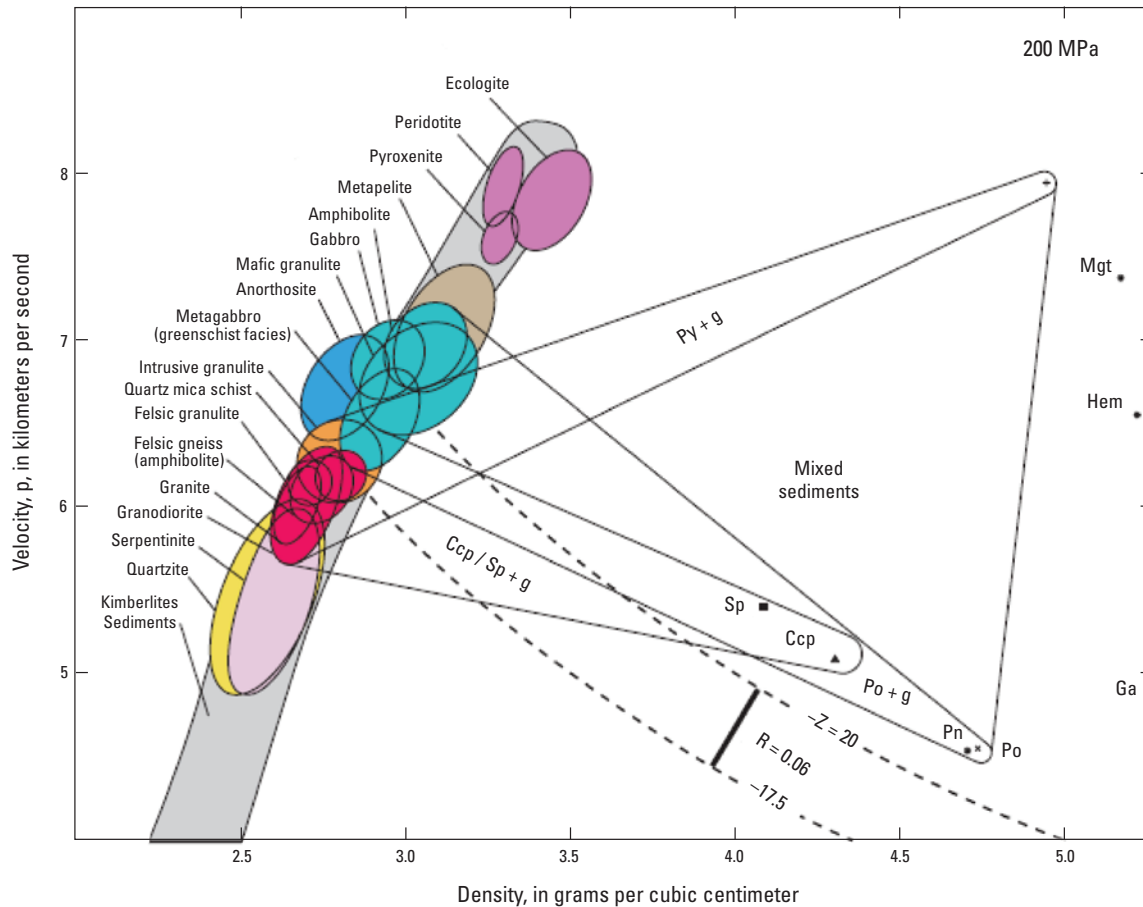


Figure 7-6. Velocity values of various rock types and ore minerals plotted against their density with lines of constant acoustic impedance (Z) overlain within field. Superimposed also is the Nafe-Drake curve (shown in gray) for common rock types at a standard confining pressure of 200 MPa (MegaPascals) (modified from Salisbury and others, 2003). Represented in graph are values for pyrite (Py), pentlandite (Pn), pyrrhothite (Po), chalcopyrite (Ccp), sphalerite (Sp), hematite (Hm), and magnetite (Mgt); also shown are fields for host rock-ore mixtures. Galena is off the scale shown, having a velocity of 3.7 km/s and a density of 7.5 g/cm³. As shown, a reflection coefficient (R) of 0.06 will give a strong reflection in contrasting lithologies. From Salisbury and Snyder (2007).

Successful seismic imaging of a zone of VMS mineralization is a function of the size, shape, and orientation/dip of the ore body and the acquisition parameters used in the seismic survey (Salisbury and others, 1996). Vertical seismic profiling uses existing deep boreholes as sites for acquisition (Eaton and others, 1996) of seismic data. Volcanogenic massive sulfide deposits are generally pyrite-dominated and, given their high acoustic impedances, are excellent candidates for high-resolution seismic exploration techniques (Bellefleur and others, 2004). Figure 7-7 shows a high-resolution seismic reflection profile through a VMS deposit at the Bathurst mining camp (Salisbury and Snyder, 2007).

Concealed Deposits

Geophysical surveys have been especially important in areas like northern Wisconsin where favorable volcanic terranes are covered by glacial debris. The Crandon deposit in Wisconsin, which is one of the largest VMS deposits in the United States at 68 Mt, and several other smaller deposits (Flambeau, Thornapple, Pelican, Lynne) were discovered using airborne aeromagnetic surveys with follow-up ground magnetic surveys, mapping, and drilling (Babcock, 1996). These types of surveys were particularly instrumental in the

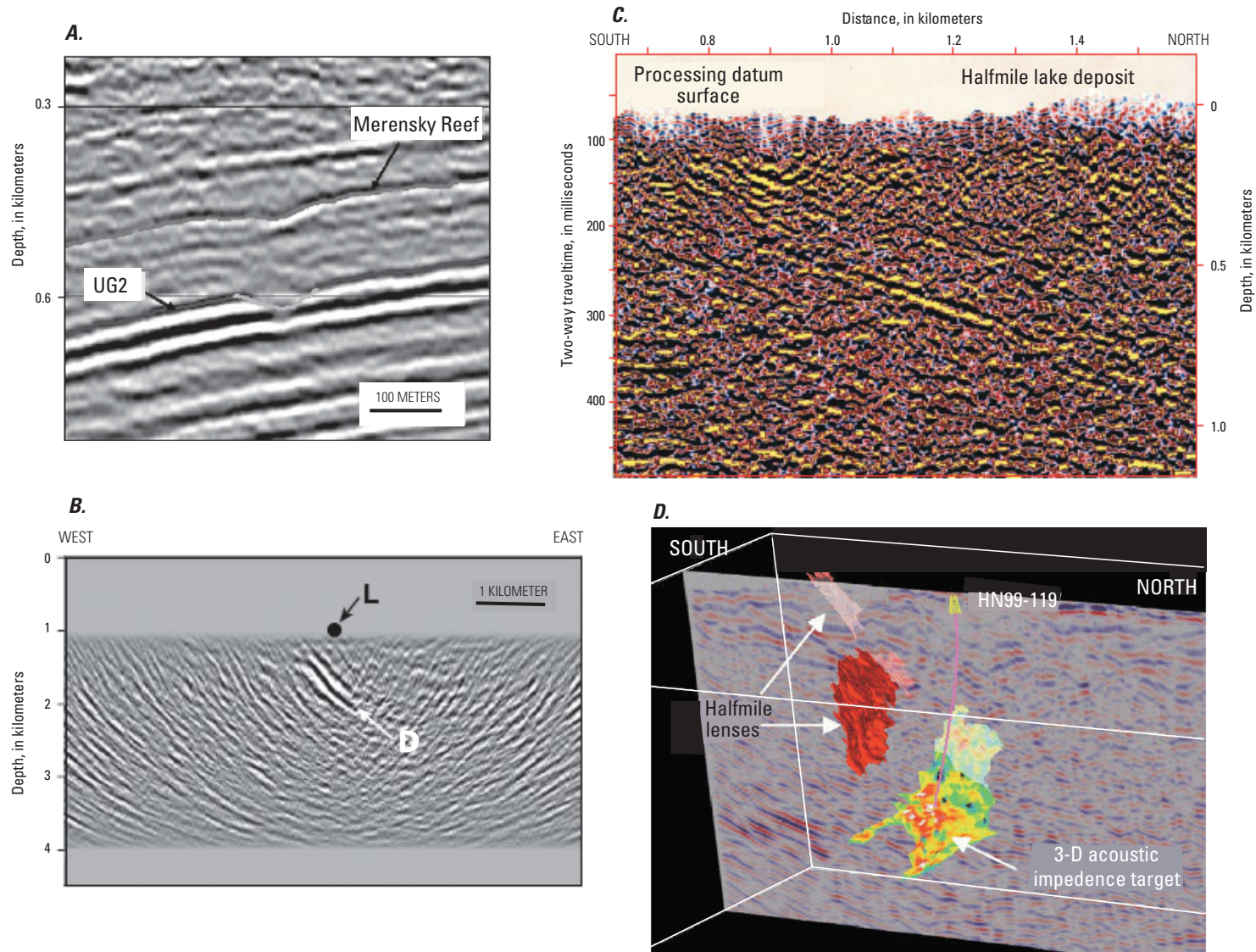


Figure 7-7. Seismic reflection profiles through volcanogenic massive sulfide (VMS) deposits. *A*, Seismic reflection profile showing a sulfide/platinoid-bearing Merensky Reef in the Bushveld Complex, South Africa; also shown (UG2) are strong reflectors representing a chromite layer in gabbroic cumulates. *B*, Three-dimensional seismic reflection profile over the Louvicourt VMS deposit, Val d’Or, Quebec. *L* shows location of the deposit; *D* is a reflection attributed to an alteration zone (modified from Adam and others, 2004; Salisbury and Snyder, 2007). *C*, Two-dimensional multichannel seismic image of the Halfmile Lake VMS deposit. *D*, Cross-section through a three-dimensional seismic cube showing the VMS deposit discovered using seismic methods at 1,300 m plus earlier discovered deposits at the Halfmile Lake VMS deposit. From Salisbury and Snyder (2007).

first discovery at Flambeau, as were the VMS mineral deposit models developed in the Canadian Archean and Proterozoic areas.

The giant Kidd Creek VMS deposit near Timmins, Ontario, was also a concealed deposit that was discovered in 1959 following airborne electromagnetic surveys. Follow-up surveys at the “Kidd 55” anomaly with ground geophysics and drilling discovered one of the largest deposits in the world (Hannington and others, 1999). In this case, the publication of Oftedahl’s classic 1958 paper “A theory of exhalative-sedimentary ores” greatly influenced thinking during the exploration program at Kidd Creek, and the refined mineral deposit occurrence perspective (we would now call it an occurrence model) was very important in the discovery.

Conclusions

Volcanogenic massive sulfide mineralization occurs in volcanic, volcanoclastic, and sedimentary rocks, units that generally form low- to moderate-density strata. Volcanogenic massive sulfide mineralization results in the precipitation of pyrite, pyrrhotite, chalcopyrite, sphalerite, and galena, all minerals with high density values. The marked contrasts between the physical properties of minerals formed in association with VMS mineralization and their host rocks make VMS deposits ideally suited for geophysical exploration. Geophysical surveys have played a critical role in mineral exploration (Bishop and Lewis, 1992). With depletion of VMS sources in surface or near-surface settings, exploration for VMS deposits must focus at much greater depths, which requires the more sophisticated techniques. Whereas potential field geophysical techniques have been highly successful in identifying VMS deposits at depths up to 300 m, high resolution seismic reflection profiling can target much greater depths and has been key in identifying VMS deposits at depths greater than those traditionally mined.

References Cited

- Adam, E., Milkereit, B., and Salmon, B., 2004, 3-D seismic exploration in the Val d’Or mining camp, Quebec, *in* Society of Exploration Geophysicists International Exposition and 74th annual meeting, Denver, Colo., 10–15 October 2004: Society of Exploration Geophysicists Technical Program Expanded Abstracts, v. 23, p. 1167–1170.
- Babcock, R.C., 1996, History of exploration for volcanogenic massive sulfides in Wisconsin, *in* LaBerge, G.L., ed., Volcanogenic massive sulfide deposits of northern Wisconsin—A commemorative volume, v. 2 of Institute on Lake Superior Geology 42d annual meeting, Cable, Wisc., 15–19 May 1996, Proceedings: St. Paul, Minn., The Institute, p. 1–15.
- Bellefleur, G., Muller, C., Snyder, D., and Matthews, L., 2004, Downhole seismic imaging of a massive sulphide ore body with mode-converted waves, Halfmile Lake, New Brunswick: *Geophysics*, v. 69, p. 318–329.
- Bishop, J.R., and Emerson, D.W., 1999, Geophysical properties of zinc-bearing minerals: *Australian Journal of Earth Sciences*, v. 46, p. 311–328.
- Bishop, J.R., and Lewis, R.J.G., 1992, Geophysical signatures of Australian volcanic-hosted massive sulfide deposits: *Economic Geology*, v. 87, p. 913–930.
- Dahle, A., Gjoystday, H., Grammelvedt, G., and Soyland, H.T., 1985, Application of seismic reflection methods for ore prospecting in crystalline rock: *First Break*, v. 3, no. 2, p. 9–16.
- Dubé, B., Gosselin, P., Mercier-Langevin, P., Hannington, M., and Galley, A., 2007, Gold-rich volcanogenic massive sulphide deposits, *in* Goodfellow, W.D., ed., Mineral deposits of Canada—A synthesis of major deposit-types, district metallogeny, the evolution of geological provinces, and exploration methods: Geological Association of Canada, Mineral Deposits Division, Special Publication 5, p. 75–94.
- Eaton, D., Guest, S., Milkereit, B., Bleeker, W., Crick, D., Schmitt, D., and Salisbury, M., 1996, Seismic imaging of massive Sulfide deposits—Part III. Borehole seismic imaging of near-vertical structures: *Economic Geology*, v. 91, p. 835–840.
- Elliot, C.L., 1967, Some applications of seismic refraction techniques in mining exploration, *in* Musgrave, A.W., ed., Seismic refraction prospecting: Tulsa, Okla., Society of Exploration Geophysicists, p. 522–538.
- Finn, C.A., and Morgan, L.A., 2002, High-resolution aeromagnetic mapping of volcanic terrain, Yellowstone National Park: *Journal of Volcanology and Geothermal Research*, v. 115, p. 207–231.
- Ford, K., Keating, P., and Thomas, M.D., 2007, Overview of geophysical signatures associated with Canadian ore deposits, *in* Goodfellow, W.D., ed., Mineral deposits of Canada—A synthesis of major deposit-types, district metallogeny, the evolution of geological provinces, and exploration methods: Geological Association of Canada, Mineral Deposits Division, Special Publication 5, p. 939–970.
- Galley, A.G., Hannington, M., and Jonasson, I., 2007, Volcanogenic massive sulphide deposits, *in* Goodfellow, W.D., ed., Mineral deposits of Canada—A synthesis of major deposit-types, district metallogeny, the evolution of geological provinces, and exploration methods: Geological Association of Canada, Mineral Deposits Division, Special Publication 5, p. 141–161.

- Goult, N.R., 1993, Controlled-source tomography for mining and engineering applications, *in* Iyer, H.M., and Hirahara, K., eds., *Seismic tomography—Theory and practice*: New York, Chapman and Hall, p. 797–813.
- Grant, F.S., and West, G.F., 1965, *Interpretation theory in applied geophysics*: New York, McGraw-Hill Books Company, 584 p.
- Gustavsson, M., Ivansson, S., Moren, P., and Pihl, J.L., 1986, Seismic borehole tomography—Measurement system and field studies: *Proceedings of the IEEE*, v. 74, no. 2, p. 339–346.
- Hannington, M.D., Barrie, C.T., and Bleeker, W., 1999, The giant Kidd Creek volcanogenic massive sulfide deposit, western Abitibi Subprovince, Canada—Summary and synthesis, *in* Hannington, M.D., and Barrie, C.T., eds., *The Giant Kidd Creek volcanogenic massive sulfide deposit, western Abitibi subprovince, Canada*: *Economic Geology Monograph 10*, p. 661–672.
- Hannington, M.D., Galley, A.G., Herzig, P.M., and Petersen, S., 1998, Comparison of the TAG mound and stockwork complex with Cyprus-type massive sulfide deposits, *in* Herzig, P.M., Humphris, S.E., Miller, D.J., and Zierenberg, R.A., eds., *TAG—Drilling an active hydrothermal system on a sediment-free slow-spreading ridge, site 957*: *Proceedings of the Ocean Drilling Program, Scientific Results*, v. 158, p. 389–415.
- Hunt, C.P., Moskowitz, B.M., and Banerjee, S.K., 1995, Magnetic properties of rocks and minerals, *in* Ahrens, T.J., ed., *Rock physics and phase relations—A handbook of physical constants*: American Geophysical Union, p. 189–204.
- Klein, C., and Hurlbut, C.S., 1985, *Manual of mineralogy* (after J.D. Dana): New York, John Wiley and Sons, 596 p.
- McGaughey, W.J., McCreary, R.G., Young, R.P., and Maxwell, S.C., 1994, Mining applications of seismic tomography: *Canadian Institute of Mining and Metallurgy Bulletin*, vol. 87, no. 977, p. 49–56.
- McIntosh, S.M., Gill, J.P., and Mountford, A.J., 1999, The geophysical response of the Las Cruces massive sulphide deposit: *Exploration Geophysics*, v. 30, no. 3–4, p. 123–133.
- Milkereit, B., Eaton, D., Wu, J., Perron, G., and Salisbury, M., 1996, Seismic imaging of massive Sulfide deposits—Part II. Reflection seismic profiling: *Economic Geology*, v. 91, p. 829–834.
- Oliveira, V., Matos, J., Bengala, M., Silva, N., Sousa, P., and Torres, L., 1998, Geology and geophysics as successful tools in the discovery of the Lagoa Salgada Orebody (Sado Tertiary Basin—Iberian Pyrite Belt), Grandola, Portugal: *Mineralium Deposita*, v. 33, p. 170–187.
- Peter, J.M., Kjarsgaard, I.M., and Goodfellow, W.D., 2003, Hydrothermal sedimentary rocks of the Heath Steele Belt, Bathurst mining camp, New Brunswick—Part 1. Mineralogy and mineral chemistry, *in* Goodfellow, W.D., McCutcheon, S.R., and Peter, J.M., eds., *Massive sulfide deposits of the Bathurst mining camp, New Brunswick, and northern Maine*: *Economic Geology Monograph 11*, p. 361–390.
- Salisbury, M., Milkereit, B., and Bleeker, W., 1996, Seismic imaging of massive sulfide deposits—Part I. Rock properties: *Economic Geology*, v. 91, p. 821–828.
- Salisbury, M., and Snyder, D., 2007, Applications of seismic methods to mineral exploration, *in* Goodfellow, W.D., ed., *Mineral deposits of Canada—A synthesis of major deposit-types, district metallogeny, the evolution of geological provinces, and exploration methods*: Geological Association of Canada, Mineral Deposits Division, Special Publication 5, p. 971–982.
- Shives, R.B.K., Charbonneau, B.W., and Ford, K.L., 1997, The detection of potassic alteration by gamma-ray spectrometry—Recognition of alteration related to mineralization, *in* Gubins, A.G., ed., *Geophysics and geochemistry at the millennium—Proceedings of Exploration 97, Fourth Decennial International Conference on Mineral Exploration*: Toronto, Prospectors and Developers Association of Canada, p. 741–752.
- Shives, R.B.K., Ford, K.L., and Peter, J.M., 2003, Mapping and exploration applications of gamma ray spectrometry in the Bathurst mining camp, northeastern New Brunswick, *in* Goodfellow, W.D., McCutcheon, S.R., and Peter, J.M., eds., *Massive sulfide deposits of the Bathurst mining camp, New Brunswick, and northern Maine*: *Economic Geology Monograph 11*, p. 819–840.
- Telford, W.M., Geldart, L.P., and Sheriff, R.E., 1990, *Applied geophysics* (2d ed.): Cambridge, Cambridge University Press, 770 p.
- Thomas, M.D., 1997, Gravity and magnetic prospecting for massive sulphide deposits—A short course sponsored under the Bathurst mining camp EXTECH II Initiative: Geological Survey of Canada Open File 3514, 66 p.

- Thomas, M.D., 2003, Gravity signatures of massive sulfide deposits, Bathurst mining camp, New Brunswick, Canada, *in* Goodfellow, W.D., McCutcheon, S.R., and Peter, J.M., eds., *Massive sulfide deposits of the Bathurst mining camp, New Brunswick, and northern Maine: Economic Geology Monograph 11*, p. 799–817.
- Thomas, M.D., Walker, J.A., Keating, P., Shives, R., Kiss, F., and Goodfellow, W.D., 2000, Geophysical atlas of massive sulphide signatures, Bathurst mining camp, New Brunswick: Geological Survey of Canada Open File 3887, 105 p.
- Tivey, M.A., Rona, P.A., and Kleinrock, M.C., 1996, Reduced crustal magnetization beneath relict hydrothermal mounds TAG hydrothermal field, Mid-Atlantic Ridge, 26°N: *Geophysical Research Letters*, v. 23, p. 3511–3514.
- Tivey, M.A., Rona, P.A., and Schouten, H., 1993, Reduced crustal magnetization beneath the active sulfide mound, TAG hydrothermal field, Mid-Atlantic Ridge at 26°N: *Earth and Planetary Science Letters*, v. 115, p. 101–115.
- Tivey, M.A., and Schouten, H., 2003, A near-bottom magnetic survey of the Mid-Atlantic Ridge axis at 26°N—Implications for the tectonic evolution of the TAG segment: *Journal of Geophysical Research*, v. 108, no. B5, 2277, 13 p., doi:10.1029/2002JB001967.
- Tivey, M.K., Humphris, S.E., Thompson, G., Hannington, M.D., and Rona, P.A., 1995, Deducing patterns of fluid flow and mixing within the TAG active hydrothermal mound using mineralogical and geochemical data: *Journal of Geophysical Research—Solid Earth*, v. 100, no. B7, p. 12527–12555.
- Tuach, J., Hewton, R.S., and Cavey, G., 1991, Exploration targets for volcanogenic, base-metal sulphide deposits on Pilely's Island, Newfoundland: *Ore Horizons*, v. 1, p. 89–98.
- van Staal, C.R., 1994, *Geology, Wildcat Brook, New Brunswick: Geological Survey of Canada*, scale 1:20 000.
- van Staal, C.R., Wilson, R.A., Rogers, N., Fyffe, L.R., Gower, S.J., Langton, J.P., McCutcheon, S.R., and Walker, J.A., 2003, A new geologic map of the Bathurst mining camp and surrounding areas—A product of integrated geological, geochemical, and geophysical data, *in* Goodfellow, W.D., McCutcheon, S.R., and Peter, J.M., eds., *Massive sulfide deposits of the Bathurst mining camp, New Brunswick, and northern Maine: Economic Geology Monograph 11*, p. 61–64.
- Waboso, C.E., and Mereu, R.F., 1978, The feasibility of delineating non-layered anomalous velocity zones by a combination of fan shooting and least-squares analysis: *Canadian Journal of Earth Sciences*, v. 15, no. 10, p. 1642–1652.

8. Hypogene Ore Characteristics

By Randolph A. Koski

8 of 21

Volcanogenic Massive Sulfide Occurrence Model

Scientific Investigations Report 2010–5070–C

U.S. Department of the Interior
U.S. Geological Survey

U.S. Department of the Interior
KEN SALAZAR, Secretary

U.S. Geological Survey
Marcia K. McNutt, Director

U.S. Geological Survey, Reston, Virginia: 2012

For more information on the USGS—the Federal source for science about the Earth, its natural and living resources, natural hazards, and the environment, visit <http://www.usgs.gov> or call 1-888-ASK-USGS.

For an overview of USGS information products, including maps, imagery, and publications, visit <http://www.usgs.gov/pubprod>

To order this and other USGS information products, visit <http://store.usgs.gov>

Any use of trade, product, or firm names is for descriptive purposes only and does not imply endorsement by the U.S. Government.

Although this report is in the public domain, permission must be secured from the individual copyright owners to reproduce any copyrighted materials contained within this report.

Suggested citation:

Koski, R.A., 2012, Hypogene ore characteristics in volcanogenic massive sulfide occurrence model: U.S. Geological Survey Scientific Investigations Report 2010-5070 -C, chap. 8, 10 p.

Contents

| | |
|-------------------------------|-----|
| Mineralogy | 137 |
| Mineral Assemblages | 137 |
| Paragenesis | 139 |
| Zoning Patterns | 139 |
| Textures and Structures | 139 |
| Grain Size | 143 |
| References Cited..... | 143 |

Figures

| | |
|---|-----|
| 8-1. Examples of paragenetic sequences in volcanogenic massive sulfide deposits | 140 |
| 8-2. Idealized massive sulfide lens illustrating zonation features for hypogene ore minerals..... | 141 |
| 8-3. Comparative hypogene mineral zonation | 142 |

Tables

| | |
|---|-----|
| 8-1. Hypogene ore mineralogy of ancient volcanogenic massive sulfide deposits..... | 138 |
| 8-2. Examples of hypogene mineral zonation patterns in selected volcanogenic massive sulfide deposits | 141 |

8. Hypogene Ore Characteristics

By Randolph A. Koski

Mineralogy

Although a detailed review of primary ore minerals in VMS deposits is beyond the scope of this report, a representative list of major, minor, and trace minerals culled from the literature is presented in table 8–1. The dominant ore mineralogy in most VMS deposits is relatively simple. In all deposit subtypes, the dominant sulfide mineral is pyrite or pyrrhotite. The next most abundant ore minerals, chalcopyrite and sphalerite, occur in variable amounts, and in a few deposits, one or the other or both occur in concentrations that exceed Fe sulfide content. The only other sulfide in the major mineral category is galena, which is concentrated in deposits associated with bimodal-felsic and siliciclastic-felsic rocks.

There are notable examples in which other ore minerals are abundant in VMS deposits. These include bornite at Kidd Creek (Hannington and others, 1999b) and Mount Lyell (Corbett, 2001); tetrahedrite, stibnite, and realgar in Au- and Ag-rich ores at Eskay Creek (Roth and others, 1999); arsenopyrite in Au-rich ore at Boliden (Weiher and others, 1996); and stannite and cassiterite in ore-grade tin mineralization at Neves Corvo and Kidd Creek (Hennigh and Hutchinson, 1999; Relvas and others, 2006). Table 8–1 includes a distinctive suite of Co- and Ni-bearing arsenides, sulfarsenides, and sulfides (for example, skutterudite, safflorite, cobaltite, löllingite, millerite, and pentlandite) that are rare in most VMS deposits, but relatively abundant in massive sulfide deposits associated with serpentized ultramafic rocks in ophiolitic terranes of Quebec (Auclair and others, 1993), Morocco (Ahmed and others, 2009), and Cyprus (Thalhammer and others, 1986), as well as metaperidotites of the Outokumpu mining district in Finland (Peltonen and others, 2008). Potentially analogous VMS deposits associated with serpentized ultramafic rocks on slow-spreading segments of the Mid-Atlantic Ridge (Rainbow, Logatchev) are also enriched in Co and Ni (Mozgova and others, 1999; Marques and others, 2006).

Although precious metals are an economically important commodity in many VMS deposits (Hannington and others, 1999c), they occur as volumetrically minor minerals. Visible gold is generally present as inclusions of native gold, electrum, or gold telluride minerals in major sulfide minerals, whereas silver occurs in Ag sulfides and sulfosalt minerals such as tetrahedrite and freibergite. In VMS-type mineralization on the modern seafloor, Au and Ag are most

enriched in extensional arc and back-arc settings (Herzig and Hannington, 2000), although the mineralogy of gold is not yet well established. Occurrences of native gold as inclusions in sphalerite and chalcopyrite are reported in massive sulfide samples from Lau Basin and eastern Manus Basin (Herzig and others, 1993; Moss and Scott, 2001). Gold is also concentrated in massive sulfide deposits in Escanaba Trough, a slow-spreading segment of the Gorda Ridge. There, Törmänen and Koski (2005) have reported an association of native gold, electrum, and maldonite (Au_2Bi) with a suite of sulfarsenide and bismuth minerals.

Mineral Assemblages

The mineral assemblages (and bulk chemical characteristics) of VMS deposits are directly related to the chemistry of ore-forming hydrothermal fluids that, in turn, reflect exchange reactions with wall rocks during fluid circulation. Thus, massive sulfide deposits formed in predominantly mafic rock environments are likely to have discrete mineralogical differences from deposits associated with sequences of predominantly felsic rocks. Furthermore, mineral assemblages are also influenced by fluids whose compositions are altered during passage through substantial thicknesses of arc- or continent-derived sediment. Whatever the source rocks, variations in mineralogy are often most obvious in the minor and trace mineral assemblages. A few examples are cited to illustrate variations in VMS mineral assemblages that correspond to a range of host-rock compositions.

Volcanogenic massive sulfide deposits occurring in mafic volcanic rocks are characterized by a major-mineral assemblage dominated by pyrite (much less frequently pyrrhotite or marcasite) along with variable but subordinate amounts of chalcopyrite and sphalerite (Galley and Koski, 1999). Other sulfide minerals are present in trace amounts, and more significantly, galena and base-metal sulfosalts are rare in all parts of these deposits. Deposits in siliciclastic-mafic environments have similar lead-poor mineral assemblages; however, pyrrhotite is more abundant relative to pyrite in some deposits (Slack, 1993; Peter and Scott, 1999). At the other end of the lithologic spectrum in which rhyolites and dacites are predominant, VMS deposits (such as Kuroko deposits) contain abundant and variable amounts of pyrite, chalcopyrite, and sphalerite, along with significant galena and tetrahedrite (Eldridge

Table 8–1. Hypogene ore mineralogy of volcanogenic massive sulfide deposits.

[Sources: Franklin and others, 1981; Large, 1992; Slack, 1993; Hannington and others, 1999a, c; Peter and Scott, 1999; Slack and others, 2003; Herrington and others, 2005; Koski and others, 2008; Peltonen and others, 2008; Ahmed and others, 2009]

| Major minerals | | Trace minerals (cont.) | |
|--------------------|--|------------------------|--|
| pyrite | FeS ₂ | freibergite | (Ag, Cu) ₁₂ (Sb, As) ₄ S ₁₃ |
| pyrrhotite | Fe _{1-x} S | germanite | Cu ₃ (Ge, Fe)(S, As) ₄ |
| chalcopyrite | CuFeS ₂ | gersdorffite | NiAsS |
| sphalerite | (Zn, Fe)S | glaucodot | (Co, Fe)AsS |
| galena | ZnS | gold | Au |
| Minor minerals | | gold tellurides | |
| marcasite | FeS ₂ | idaite | Cu ₅ FeS ₆ |
| magnetite | Fe ₃ O ₄ | hedleyite | Bi ₇ Te ₃ |
| cobaltite | (Co, Fe)AsS | hessite | Ag ₂ Te |
| arsenopyrite | FeAsS | löllingite | FeAs ₂ |
| tennantite | Cu ₁₂ As ₄ S ₁₃ | mackinawite | Fe ₁ +XS |
| tetrahedrite | Cu ₁₂ Sb ₄ S ₁₃ | millerite | NiS |
| Trace minerals | | mawsonite | Cu ₆ Fe ₂ SnS ₈ |
| acanthite | Ag ₂ S | molybdenite | MoS ₂ |
| argentite | Ag ₂ S | nickeline | NiAs |
| bismuth | Bi | pentlandite | (Fe, Ni) ₉ S ₈ |
| bismuthinite | Bi ₂ S ₃ | pyrargyrite | Ag ₃ SbS ₃ |
| bismuth tellurides | Bi ₂ Te ₃ | realgar | AsS |
| bornite | Cu ₅ FeS ₄ | rammelsbergite | NiAs ₂ |
| cubanite | CuFe ₂ S ₃ | roquesite | CuInS ₂ |
| boulangerite | Pb ₃ Sb ₄ S ₁₁ | rutile | TiO ₂ |
| bournonite | PbCuSbS ₃ | safflorite | CoAs ₂ |
| brannerite | UTi ₂ O ₆ | silver | Ag |
| bravoite | (Fe, Ni, Co)S ₂ | skutterudite | CoAs ₂₋₃ |
| carrolite | CuCo ₂ S ₄ | stannite | Cu ₂ FeSnS ₄ |
| cassiterite | SnO ₂ | stibnite | Sb ₂ S ₃ |
| cinnabar | HgS | stromeyerite | AgCuS |
| electrum | (Au, Ag) | tetradymite | Bi ₂ Te ₂ S |
| digenite | Cu ₉ S ₅ | valleriite | (Fe, Cu)S ₂ •(Mg, Al)(OH) ₂ |
| enargite | Cu ₃ As ₄ | wurtzite | ZnS |

and others, 1983). Deposits having this lithologic association often contain zones of ore with sulfide assemblages dominated by sphalerite and galena (for example, Rosebery; Smith and Huston, 1992), and in rare instances, ore mineral assemblages dominated by galena, tetrahedrite, realgar, and stibnite (Eskay Creek; Roth and others, 1999). Massive sulfide deposits in bimodal volcanic sequences can be expected to have sulfide mineral assemblages somewhat intermediate between mafic- and felsic-rock endmembers. Thus, the major mineral suite of pyrite, pyrrhotite, sphalerite, and chalcopyrite at Bald Mountain contains minor but significant galena and arsenopyrite mineralization within the orebody (Slack and others, 2003).

Paragenesis

Paragenesis, the sequence of mineral deposition, is complicated by replacement of early-formed minerals by new minerals as temperature conditions wax and wane during ongoing hydrothermal activity. Studies of contemporary “black smoker” massive sulfide chimneys and mounds on ocean ridges provide the best record of temporal mineralogical changes during formation of VMS deposits. Although mineral paragenesis will vary somewhat from deposit to deposit and within a given deposit, a generalized depositional sequence for major sulfide, sulfate, and silica minerals within a hypothetical sulfide chimney is shown in figure 8–1A (Hannington and others, 1995). At temperatures up to about 250 °C, barite, anhydrite, silica, sphalerite, and marcasite are precipitated. When temperature increases to about 350 °C, these minerals are replaced by pyrite, wurtzite, chalcopyrite, pyrrhotite, and isocubanite. An important aspect of this sequence is the replacement of original sulfides by Cu-Fe sulfides and pyrrhotite at high temperature. Sulfate and silicate mineral phases along with sphalerite and marcasite/pyrite are also deposited in late stages of mineralization as fluid temperatures decrease.

Mineral paragenesis for ancient VMS deposits can be much more complicated than that for the seafloor chimney cited above. A paragenetic diagram for the principal hypogene sulfide minerals (plus quartz) in the massive sulfide deposit at Bald Mountain is presented in figure 8–1B (Slack and others, 2003). The diagram for Bald Mountain illustrates a complex and repetitive pattern of sulfide mineral deposition during multiple stages of deposit formation. A noteworthy similarity between the Bald Mountain and seafloor chimney paragenesis, however, is the early Stage 1 deposition of pyrite, marcasite, sphalerite, and quartz followed by pyrrhotite and chalcopyrite replacement at higher temperatures in Stage 2. Numerous additional stages of mineral precipitation, mostly in the form of crosscutting veins, are superimposed on the massive pyrrhotite-chalcopyrite mineralization at Bald Mountain (Slack and others, 2003). The paragenesis of hypogene ore minerals in many ancient VMS deposits is further complicated by recrystallization and replacement during posthydrothermal metamorphism (for example, bornite ores at Kidd Creek; Hannington and others, 1999b).

Zoning Patterns

A deposit-scale zonation pattern in which the upper stockwork is dominated by chalcopyrite + pyrite ± magnetite, the basal part of the massive sulfide body is dominated by pyrite + chalcopyrite, and the upper and outer margins of the massive sulfide are dominated by sphalerite ± galena (± barite) has long been recognized in VMS systems (Lambert and Sato, 1974; Large, 1977; Eldridge and others, 1983). A highly idealized version of this zonation pattern (modified from Lydon, 1984)—including hypogene ore minerals in the massive sulfide lens and stockwork along with related stockwork alteration and peripheral sedimentary deposits—is illustrated in figure 8–2. This basic pattern of vertical zoning is best exhibited in well preserved deposits having bimodal-felsic or bimodal-mafic affinities (table 8–2) and has been attributed to sequential episodes of sulfide deposition and replacement within an intensifying geothermal system by Eldridge and others (1983) and Pisutha-Arnond and Ohmoto (1983). In their models, increasing fluid temperatures at the base of the growing ore lens result in chalcopyrite replacement of an earlier sulfide facies dominated by sphalerite, tetrahedrite, galena, and pyrite. The mobilized Zn and Pb migrate upward and reprecipitate as sphalerite and galena in cooler parts of the lens, resulting in the zonation of chalcopyrite and sphalerite (±galena) and Cu and Zn (±Pb) in many VMS deposits. The outward movement or “zone refining” of metals may also produce Au enrichment in sphalerite-rich zones of VMS deposits (Hannington and others, 1986; Large and others, 1989). Conversely, the very low base- and precious-metal concentrations in pyritic, ophiolite-hosted VMS deposits located in Cyprus and Oman may reflect the complete stripping or “over refining” of metals during sustained hydrothermal activity on the paleoseafloor (Hannington and others, 1998).

Deposit-scale zonation of Cu and Zn sulfides has also been described in massive sulfide mounds constructed on mid-ocean ridges (Embley and others, 1988; Fouquet and others, 1993). Perhaps the most distinctive example of Cu-Zn zoning is observed in individual high-temperature (>300 °C) black smoker chimneys (fig. 8–3) forming in contemporary ridge settings (Haymon, 1983; Goldfarb and others, 1983; Koski and others, 1994). In these examples, the precipitation of chalcopyrite and sphalerite is controlled by extreme temperature and chemical gradients operating at the centimeter scale.

Textures and Structures

Volcanogenic massive sulfide deposits span a continuum of physical attributes from massive ores composed of 100 percent sulfide minerals through semimassive ores that are mixtures of sulfides, gangue minerals, and host rock (volcanic or sedimentary) to increasingly sparse sulfide disseminated in wall rocks. This gradation may represent a vertical transition from seafloor (or near seafloor) mineralization to mineralization at depth within the feeder zone of the hydrothermal

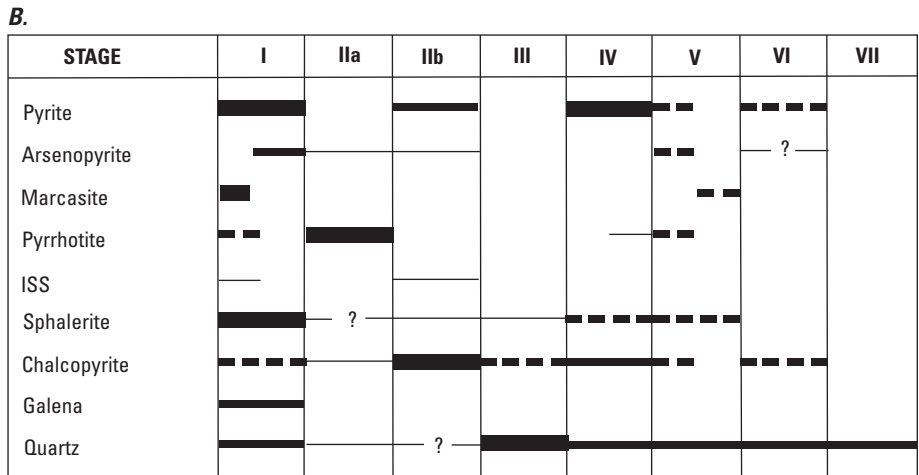
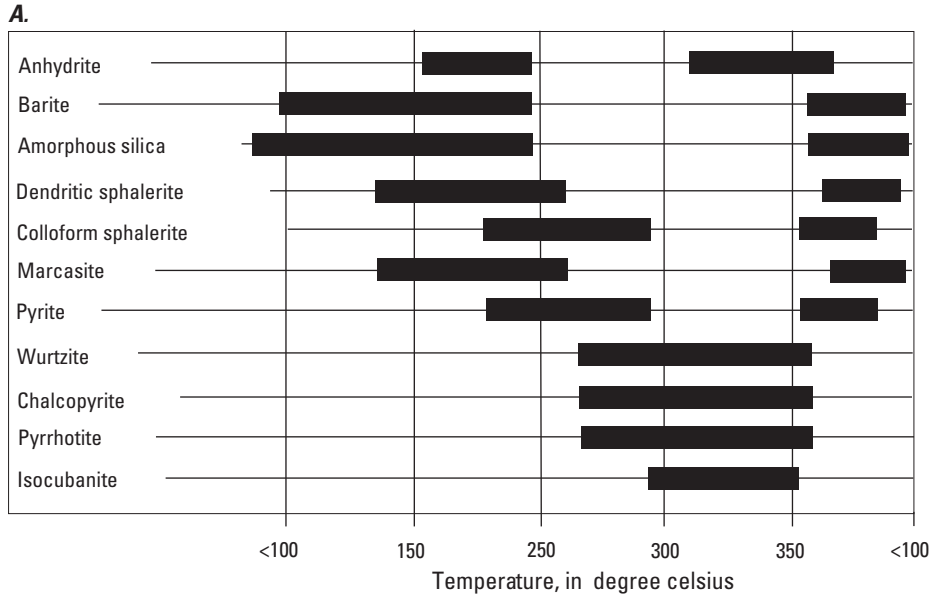


Figure 8-1. Examples of paragenetic sequences in volcanogenic massive sulfide deposits. *A*, Mineral paragenesis in hypothetical sulfide-sulfate-silica chimney. From Hannington and others (1995). During chimney growth, fluid temperatures increase to approximately 350 °C and then decrease as hydrothermal fluids mix with seawater. *B*, Paragenesis of hypogene sulfide minerals and quartz at Bald Mountain (Maine) massive sulfide deposit. After Slack and others (2003). Thickness of black bars represents relative proportions of minerals. [ISS, intermediate solid solution in the copper-iron-sulfur system]

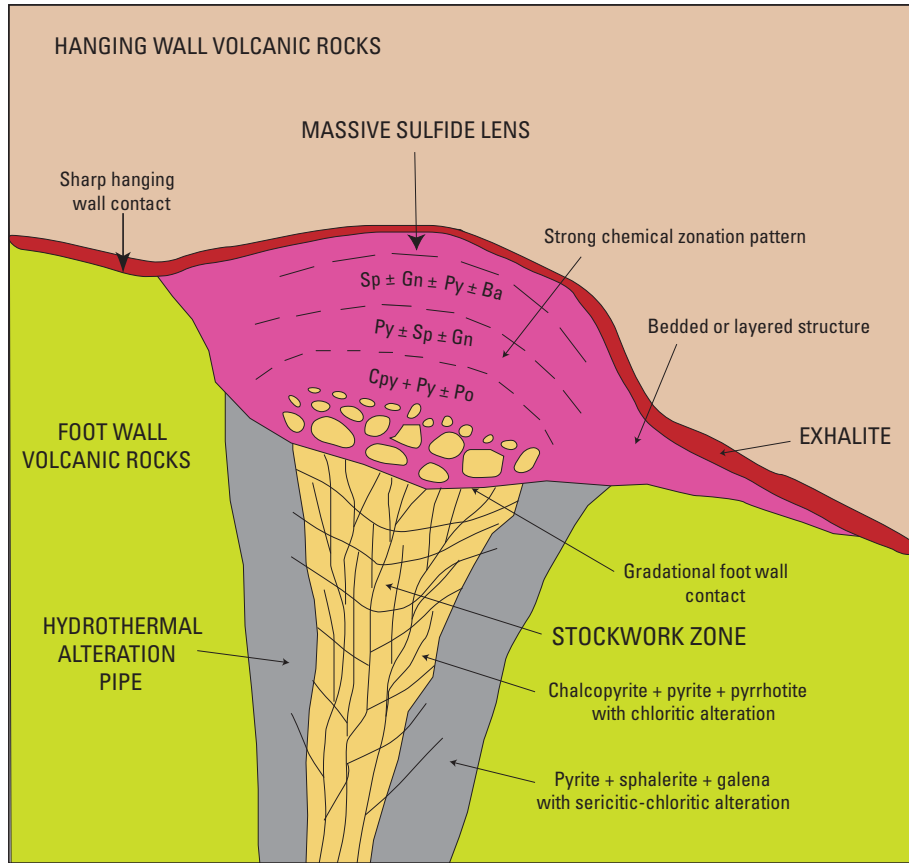


Figure 8-2. Idealized massive sulfide lens illustrating zonation features for hypogene ore minerals. Modified from Lydon (1984). [ba, barite; cpy, chalcopyrite; gn, galena; po, pyrrhotite; py, pyrite; sp, sphalerite]

Table 8-2. Examples of hypogene mineral zonation patterns in selected volcanogenic massive sulfide deposits.

[Cu, copper; Zn, zinc; ba, barite; bn, bornite; ch, chlorite; cp, chalcopyrite; gl, galena; mt, magnetite; po, pyrrhotite; py, pyrite; sp, sphalerite; ten, tennantite]

| Deposit or district | Mineral zonation | Reference |
|---------------------------------|--|----------------------------------|
| Hokuroku district (composite) | <p><u>Top to bottom:</u> Barite ore: ba > sulfides Massive black ore: sp + ba > py + gl Semiblack ore: sp + ba > py > cp Massive yellow ore: ch + py Powdery yellow ore: py > cp Massive pyrite ore: py >> cp >> sp</p> | Eldridge and others (1983) |
| Silver Peak (Oregon, USA) | <p><u>Top to bottom:</u> Barite ore: ba Black ore: py + bn + ten + sp + ba ± cp Yellow ore: py + cp + bn Friable yellow ore: py</p> | Derkey and Matsueda (1989) |
| Urals Cu-Zn deposit (composite) | <p><u>Top to bottom:</u> Outer/upper massive sulfide: sp + py ± cp ± ba ± gl Middle massive sulfide: cp + py Stockwork and basal massive sulfide: cp + py ± po ± mt</p> | Herrington and others (2005) |
| Bathurst camp (composite) | <p><u>Distal to proximal:</u> Bedded pyrite: py ± sp ± gl Bedded ores: py + sp + gl ± cp Ore-vent complex: po + mt + py + cp ± sp ± gl</p> | Goodfellow and McCutcheon (2003) |

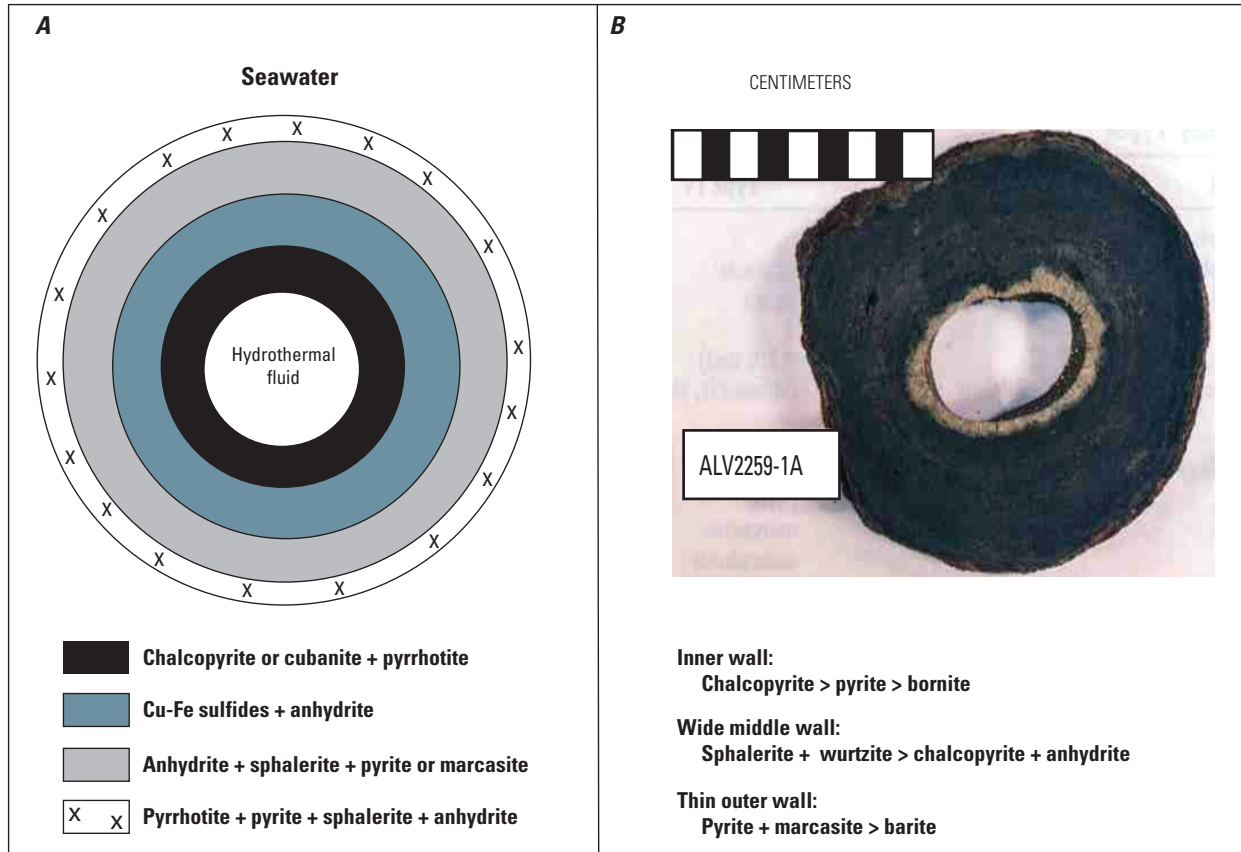


Figure 8-3. Comparative hypogene mineral zonation in (A) model of a 350°C “black smoker” chimney from the East Pacific Rise, 21°N (after Haymon, 1983), and (B) cross section of high temperature (approx. 310°C) chimney from Monolith Vent, southern Juan de Fuca Ridge (from Koski and others, 1994). Each chimney has an inner wall dominated by copper-iron sulfides, a middle wall containing abundant zinc sulfides, and an outer rind dominated by iron sulfides. [Cu, copper; Fe, iron]

system (for example, Turner-Albright; Zierenberg and others, 1988). Sulfide minerals also form veins (usually with quartz and other gangue minerals) cutting wall rock and earlier-formed massive sulfides, and many massive sulfide bodies are underlain by discordant vein networks (stockwork zones). Massive sulfides in many deposits are laterally gradational to bedded or layered sulfide deposits formed by mass wasting of the elevated mounds on the seafloor.

At the hand-specimen and thin section scale, massive sulfides are typically compact, fine-grained aggregates of intergrown sulfide minerals with irregular grain boundaries. More diagnostic primary textures in massive ores include idiomorphic crystals (for example, pyrite, pyrrhotite) projecting into cavities, colloform overgrowths (especially sphalerite, pyrite, and marcasite), framboidal and botryoidal pyrite, pseudomorphic replacement (for example, sulfate by pyrrhotite),

fine-scale replacement relationships (for example, chalcopyrite disease in sphalerite; Barton and Bethke, 1987), boxwork intergrowths, and internal mineral growth zoning (especially in Zn sulfides). Other common attributes of unmetamorphosed ores are high porosity and textural heterogeneity on the thin section scale. These types of primary textural features are especially well preserved in modern seafloor deposits (see Koski and others, 1984; Paradis and others, 1988; Hannington and others, 1995).

Textures and structures in ancient VMS deposits typically bear some overprint of postdepositional diagenesis and metamorphism. Metamorphism causes numerous textural changes including (1) recrystallization and increase in grain size, (2) development of porphyroblasts, (3) foliation and alignment of sulfide and gangue crystals, (4) 120° triple junction grain boundaries (annealing textures), (5) remobilization

of chalcopyrite, and (6) penetrative deformation (“durchbewegung” texture) of pyrrhotite and wall rock (Vokes, 1969; Franklin and others, 1981).

Most VMS deposits exhibit some form of primary structure. Fragmental and layered ores are prevalent structural characteristics at the deposit scale (see Spense, 1975; Slack and others, 2003; Tornos, 2006). In many cases, these features appear to result from mass wasting and flow from the steep flanks of sulfide mounds. Mass wasting and proximal sedimentation of hydrothermal debris from the TAG sulfide mound on the Mid-Atlantic Ridge represent a useful modern analog (Mills and Elderfield, 1995). Blocky, fragmental, and sandy zones also form distinctive internal structural features of well preserved massive sulfides (Constantinou, 1976; Eldridge and others, 1983; Lydon and Galley, 1986). Studies of contemporary seafloor sulfide mounds, especially the TAG site, indicate that these breccias formed by collapse of unstable sulfide chimneys on the mound surface as well as collapse following anhydrite dissolution in the core of the mound structure (Humphris and others, 1995; Petersen and others, 2000). Less common primary structures preserved in some VMS deposits include chimney fragments with fluid channelways (Oudin and Constantinou, 1984; Slack and others, 2003), fossils of hydrothermal vent fauna (Haymon and others, 1984; Little and others, 1999), and traces of microbial life forms (Juniper and Fouquet, 1988).

Grain Size

Volcanogenic massive sulfide deposits are typically fine grained. The range in grain sizes for the major hypogene sulfide minerals in unmetamorphosed massive sulfide deposits is approximately 0.1–1 millimeter (mm); accessory sulfides are considerably smaller in size. The grain size of gold minerals is smaller than that of major sulfides by more than one order of magnitude. In one example, the median size values for discrete gold grains (electrum) in eleven eastern Australian VMS deposits lie between 2.5 and 25 micrometers (mm) (Huston and others, 1992). In contrast, metamorphosed massive sulfides are coarser grained; sulfide grains in metamorphosed deposits commonly exceed 1 mm in diameter, and pyrite porphyroblasts up to 300 mm across occur in pyrrhotite-rich ores of the Ducktown mining district, Tennessee (Brooker and others, 1987).

References Cited

Ahmed, A.H., Arai, S., and Ikenne, M., 2009, Mineralogy and paragenesis of the Co-Ni arsenide ores of Bou Azzer, Anti-Atlas, Morocco: *Economic Geology*, v. 104, p. 249–266.

- Auclair, M., Gauthier, M., Trottier, J., Jébrak, M., and Chartrand, F., 1993, Mineralogy, geochemistry, and paragenesis of the Eastern Metals serpentinite-associated Ni-Cu-Zn deposit, Quebec Appalachians: *Economic Geology*, v. 88, p. 123–138.
- Barton, P.B., Jr., and Bethke, P.M., 1987, Chalcopyrite disease in sphalerite—Pathology and epidemiology: *American Mineralogist*, v. 72, p. 451–467.
- Brooker, D.D., Craig, J.R., and Rimstidt, J.D., 1987, Ore metamorphism and pyrite porphyroblast development at the Cherokee mine, Ducktown, Tennessee: *Economic Geology*, v. 82, p. 72–86.
- Constantinou, G., 1976, Genesis of conglomerate structure, porosity and collomorphic textures of the massive sulphide ores of Cyprus, in Strong, D.F., ed., *Metallogeny and plate tectonics: Geological Association of Canada Special Paper 14*, p. 187–210.
- Corbett, K.D., 2001, New mapping and interpretations of the Mount Lyell mining district, Tasmania—A large hybrid Cu-Au system with an exhalative Pb-Zn top: *Economic Geology*, v. 96, p. 1089–1122.
- Derkey, R.E., and Matsueda, H., 1989, Geology of the Silver Peak mine, a Kuroko-type deposit in Jurassic volcanic rocks, Oregon, U.S.A.: *Journal of the Mining College of Akita University*, ser. A, v. VII, no. 2, p. 99–123.
- Eldridge, C.S., Barton, P.B., Jr., and Ohmoto, H., 1983, Mineral textures and their bearing on formation of the Kuroko orebodies, in Ohmoto, H., and Skinner, B.J., eds., *The Kuroko and related volcanogenic massive sulfide deposits: Economic Geology Monograph 5*, p. 241–281.
- Embley, R.W., Jonasson, I.R., Perfit, M.R., Franklin, J.M., Tivey, M.A., Malahoff, A., Smith, M.F., and Francis, T.J.G., 1988, Submersible investigation of an extinct hydrothermal system on the Galapagos Ridge—Sulfide mounds, stockwork zone, and differentiated lavas: *Canadian Mineralogist*, v. 26, p. 517–539.
- Fouquet, Y., Wafic, A., Cambon, P., Mevel, C., Meyer, G., and Gente, P., 1993, Tectonic setting and mineralogical and geochemical zonation in the Snake Pit sulfide deposit (Mid-Atlantic Ridge at 23°N): *Economic Geology*, v. 88, p. 2018–2036.
- Franklin, J.M., Lydon, J.M., and Sangster, D.F., 1981, Volcanic-associated massive sulfide deposits, in Skinner, B.J., ed., *Economic Geology 75th anniversary volume, 1905–1980*: Littleton, Colo., Economic Geology Publishing Company, p. 485–627.

- Galley, A.G., and Koski, R.A., 1999, Setting and characteristics of ophiolite-hosted volcanogenic massive sulfide deposits, in Barrie, C.T., and Hannington, M.D., *Volcanic-associated massive sulfide deposits—Processes and examples in modern and ancient settings: Reviews in Economic Geology*, v. 8, p. 221–246.
- Goldfarb, M.S., Converse, D.R., Holland, H.D., and Edmond, J.M., 1983, The genesis of hot spring deposits on the East Pacific Rise, 21°N, in Ohmoto, H., and Skinner, B.J., eds., *The Kuroko and related volcanogenic massive sulfide deposits: Economic Geology Monograph 5*, p. 184–197.
- Goodfellow, W.D., and McCutcheon, S.R., 2003, Geologic and genetic attributes of volcanic sediment-hosted massive sulfide deposits of the Bathurst mining camp, New Brunswick—A synthesis, in Goodfellow, W.D., McCutcheon, S.R., and Peter, J.M., eds., *Massive sulfide deposits of the Bathurst mining camp, New Brunswick, and northern Maine: Economic Geology Monograph 11*, p. 245–301.
- Hannington, M.D., Bleeker, W., and Kjarsgaard, I., 1999a, Sulfide mineralogy, geochemistry, and ore genesis of the Kidd Creek deposit—Part I. North, central, and south orebodies, in Hannington, M.D., and Barrie, C.T., eds., *The giant Kidd Creek volcanogenic massive sulfide deposit, western Abitibi subprovince, Canada: Economic Geology Monograph 10*, p. 163–224.
- Hannington, M.D., Bleeker, W., and Kjarsgaard, I., 1999b, Sulfide mineralogy, geochemistry, and ore genesis of the Kidd Creek deposit—Part II. The bornite zone, in Hannington, M.D., and Barrie, C.T., eds., *The giant Kidd Creek volcanogenic massive sulfide deposit, western Abitibi subprovince, Canada: Economic Geology Monograph 10*, p. 225–266.
- Hannington, M.D., Galley, A.G., Herzig, P.M., and Petersen, S., 1998, Comparison of the TAG mound and stockwork complex with Cyprus-type massive sulfide deposits, in Herzig, P.M., Humphris, S.E., Miller, D.J., and Zierenberg, R.A., eds., *TAG—Drilling an active hydrothermal system on a sediment-free slow-spreading ridge, site 957: Proceedings of the Ocean Drilling Program, Scientific Results*, v. 158, p. 389–415.
- Hannington, M.D., Jonasson, I.R., Herzig, P.M., and Petersen, S., 1995, Physical and chemical processes of seafloor mineralization, in Humphris, S.E., Zierenberg, R.A., Mullineaux, L.S., and Thomson, R.E., eds., *Seafloor hydrothermal systems—Physical, chemical, biological, and geological interactions: American Geophysical Union Geophysical Monograph 91*, p. 115–157.
- Hannington, M.D., Peter, J.M., and Scott, S.D., 1986, Gold in sea-floor polymetallic sulfide deposits: *Economic Geology*, v. 81, p. 1867–1883.
- Hannington, M.D., Poulsen, K.H., Thompson, J.F.H., and Sillitoe, R.H., 1999c, Volcanogenic gold in the massive sulfide environment, in Barrie, C.T., and Hannington, M.D., eds., *Volcanic-associated massive sulfide deposits—Processes and examples in modern and ancient settings: Reviews in Economic Geology*, v. 8, p. 325–356.
- Haymon, R.M., 1983, Growth history of hydrothermal black smoker chimneys: *Nature*, 301, p. 695–698.
- Haymon, R.M., Koski, R.A., and Sinclair, C., 1984, Fossils of hydrothermal vent worms discovered in Cretaceous sulfide ores of the Samail ophiolite, Oman: *Science*, v. 223, p. 1407–1409.
- Hennigh, Q., and Hutchinson, R.W., 1999, Cassiterite at Kidd Creek—An example of volcanogenic massive sulfide-hosted tin mineralization, in Hannington, M.D., and Barrie, C.T., eds., *The giant Kidd Creek volcanogenic massive sulfide deposit, western Abitibi subprovince, Canada: Economic Geology Monograph 10*, p. 431–440.
- Herrington, R.J., Maslennikov, V., Zaykov, V., Seravkin, I., Kosarev, A., Buschmann, B., Orgeval, J.-J., Holland, N., Tesalina, S., Nimis, P., and Armstrong, R., 2005, Classification of VMS deposits—Lessons from the South Uralides: *Ore Geology Reviews*, v. 27, p. 203–237.
- Herzig, P.M., and Hannington, M.D., 2000, Polymetallic massive sulfides and gold mineralization at mid-ocean ridges and in subduction-related environments, in Cronan, D.S., ed., *Handbook of marine mineral deposits: Boca Raton, Fla., CRC Press Marine Science Series*, p. 347–368.
- Herzig, P.M., Hannington, M.D., Fouquet, Y., von Stackelberg, U., and Petersen, S., 1993, Gold-rich polymetallic sulfides from the Lau back arc and implications for the geochemistry of gold in sea-floor hydrothermal systems of the southwest Pacific: *Economic Geology*, v. 88, p. 2182–2209.
- Humphris, S.E., Herzig, P.M., Miller, D.J., Alt, J.C., Becker, K., Brown, D., Brugmann, G., Chiba, H., Fouquet, Y., Gemmell, J.B., Guerin, G., Hannington, M.D., Holm, N.G., Honnorez, J.J., Iturrino, G.J., Knott, R., Ludwig, R., Nakamura, K., Petersen, S., Reysenbach, A.L., Rona, P.A., Smith, S., Sturz, A.A., Tivey, M.K., and Zhao, X., 1995, The internal structure of an active sea-floor massive sulphide deposit: *Nature*, v. 377, no. 6551, p. 713–716.

- Huston, D.L., Bottrill, R.S., Creelman, R.A., Zaw, K., Ramsden, T.R., Rand, S.W., Gemmell, J.B., Jablonski, W., Sie, S.H., and Large, R.R., 1992, Geologic and geochemical controls on the mineralogy and grain size of gold-bearing phases, eastern Australian volcanic-hosted massive sulfide deposits: *Economic Geology*, v. 87, p. 542–563.
- Juniper, S.K., and Fouquet, Y., 1988, Filamentous iron-silica deposits from modern and ancient hydrothermal sites: *The Canadian Mineralogist*, v. 26, p. 859–869.
- Koski, R.A., Clague, D.A., and Oudin, E., 1984, Mineralogy and chemistry of massive sulfide deposits from the Juan de Fuca Ridge: *Geological Society of America Bulletin*, v. 95, p. 930–945.
- Koski, R.A., Jonasson, I.R., Kadko, D.C., Smith, V.K., and Wong, F.L., 1994, Compositions, growth mechanisms, and temporal relations of hydrothermal sulfide-sulfate-silica chimneys at the northern Cleft segment, Juan de Fuca Ridge: *Journal of Geophysical Research*, v. 99, p. 4813–4832.
- Koski, R.A., Munk, L., Foster, A.L., Shanks, W.C., III, and Stillings, L.L., 2008, Sulfide oxidation and distribution of metals near abandoned copper mines in coastal environments, Prince William Sound, Alaska, USA: *Applied Geochemistry*, v. 23, p. 227–254.
- Lambert, I.B., and Sato, T., 1974, The Kuroko and associated ore deposits of Japan—A review of their features and metallogenesis: *Economic Geology*, v. 69, p. 1215–1236.
- Large, R.R., 1977, Chemical evolution and zonation of massive sulfide deposits in volcanic terrains: *Economic Geology*, v. 72, p. 549–572.
- Large, R.R., 1992, Australian volcanic-hosted massive sulfide deposits—Features, styles, and genetic models: *Economic Geology*, v. 87, p. 471–510.
- Large, R.R., Huston, D.L., McGoldrick, P.J., Ruxton, P.A., and McArthur, G., 1989, Gold distribution and genesis in Australian volcanogenic massive sulfide deposits and their significance for gold transport models, in Keays, R.R., Ramsay, W.R.H., and Groves, D.I., eds., *The geology of gold deposits—The perspective in 1988*: *Economic Geology Monograph* 6, p. 520–535.
- Little, C.T.S., Cann, J.R., Herrington, R.J., and Morisseau, M., 1999, Late Cretaceous hydrothermal vent communities from the Troodos ophiolite, Cyprus: *Geology*, v. 27, p. 1027–1030.
- Lydon, J.W., 1984, Volcanogenic massive sulphide deposits—Part 1. A descriptive model: *Geoscience Canada*, v. 11, p. 195–202.
- Lydon, J.W., and Galley, A.G., 1986, Chemical and mineralogical zonation of the Mathiati alteration pipe, Cyprus, and its genetic significance, in Gallagher, M.J., Ixer, R.A., Neary, C.R., and Prichard, H.M., eds., *Metallogeny of basic and ultrabasic rocks*: London Institute of Mining and Metallurgy, p. 46–68.
- Marques, A.F.A., Barriga, F., Chavagnac, V., and Fouquet, Y., 2006, Mineralogy, geochemistry, and Nd isotope composition of the Rainbow hydrothermal field, Mid-Atlantic Ridge: *Mineralium Deposita*, v. 41, p. 52–67.
- Mills, R.A., and Elderfield, H., 1995, Hydrothermal activity and the geochemistry of metalliferous sediment, in Humphris, S.E., Zierenberg, R.A., Mullineaux, L.S., and Thomson, R.E., eds., *Seafloor hydrothermal systems—Physical, chemical, biological, and geological interactions*: American Geophysical Union, *Geophysical Monograph* 91, p. 392–407.
- Moss, R., and Scott, S.D., 2001, Geochemistry and mineralogy of gold-rich hydrothermal precipitates from the eastern Manus Basin, Papua New Guinea: *Canadian Mineralogist*, v. 39, p. 957–978.
- Mozgova, N.N., Efimov, A., Borodaev, Y.S., Krasnov, S.G., Cherkashov, G.A., Stepanova, T.V., and Ashadze, A.M., 1999, Mineralogy and chemistry of massive sulfides from the Logatchev hydrothermal field (14 degrees 45'N Mid-Atlantic Ridge): *Exploration and Mining Geology*, v. 8, p. 379–395.
- Oudin, E., and Constantinou, G., 1984, Black smoker chimney fragments in Cyprus sulphide deposits: *Nature*, v. 308, p. 349–353.
- Paradis, S., Jonasson, I.R., Le Cheminant, G.M., and Watkinson, D.H., 1988, Two zinc-rich chimneys from the Plume Site, southern Juan de Fuca Ridge: *Canadian Mineralogist*, v. 26, p. 637–654.
- Peltonen, P., Kontinen, A., Huhma, H., and Kuronen, U., 2008, Outokumpu revisited—New mineral deposit model for the mantle peridotite-associated Cu-Co-Zn-Ni-Ag-Au sulphide deposits: *Ore Geology Reviews*, v. 33, p. 559–617.
- Peter, J.M., and Scott, S.D., 1999, Windy Craggy, northwestern British Columbia—The world's largest Besshi-type deposit, in Barrie, C.T., and Hannington, M.D., eds., *Volcanic-associated massive sulfide deposits—Processes and examples in modern and ancient settings*: *Reviews in Economic Geology*, v. 8, p. 261–295.
- Petersen, S., Herzig, P.M., and Hannington, M.D., 2000, Third dimension of a presently forming VMS deposit—TAG hydrothermal mound, Mid-Atlantic Ridge, 26°N: *Mineralium Deposita*, v. 35, p. 233–259.

- Pisutha-Arnond, V., and Ohmoto, H., 1983, Thermal history and chemical and isotopic compositions of the ore-forming fluids responsible for the Kuroko massive sulfide deposits in the Hokuroku District of Japan, in Ohmoto, H., and Skinner, B.J., eds., *The Kuroko and related volcanogenic massive sulfide deposits: Economic Geology Monograph 5*, p. 523–558.
- Relvas, J.M.R.S., Barriga, J.A.S., Ferreira, A., Noiva, P.C., Pacheco, N., and Barriga, G., 2006, Hydrothermal alteration and mineralization in the Neves-Corvo volcanic-hosted massive sulfide deposit, Portugal—Part I. Geology, mineralogy, and geochemistry: *Economic Geology*, v. 101, p. 753–790.
- Roth, T., Thompson, J.F.H., and Barrett, T.J., 1999, The precious metal-rich Eskay Creek deposit, northwestern British Columbia, in Barrie, C.T., and Hannington, M.D., eds., *Volcanic-associated massive sulfide deposits—Processes and examples in modern and ancient settings: Reviews in Economic Geology*, v. 8, p. 357–373.
- Slack, J.F., 1993, Descriptive and grade-tonnage models for Besshi-type massive sulphide deposits, in Kirkham, R.V., Sinclair, W.D., Thorpe, R.I., and Duke, J.M., eds., *Mineral deposit modeling: Geological Association of Canada Special Paper 40*, p. 343–371.
- Slack, J.F., Foose, M.P., Flohr, M.J.K., Scully, M.V., and Belkin, H.E., 2003, Exhalative and seafloor replacement processes in the formation of the Bald Mountain massive sulfide deposit, northern Maine, in Goodfellow, W.D., McCutcheon, S.R., and Peter, J.M., eds., *Volcanogenic massive sulfide deposits of the Bathurst district, New Brunswick, and northern Maine: Economic Geology Monograph 11*, p. 513–548.
- Smith, R.N., and Huston, D.L., 1992, Distribution and association of selected trace elements at the Rosebery deposit, Tasmania: *Economic Geology*, v. 87, p. 706–719.
- Spence, C.D., 1975, Volcanogenic features of the Vauze sulfide deposit, Noranda, Quebec: *Economic Geology* v. 70, p. 102–114.
- Thalhammer, O., Stumpfl, E.F., and Panayiotou, A., 1986, Postmagmatic, hydrothermal origin of sulfide and arsenide mineralizations at Limassol Forest, Cyprus: *Mineralium Deposita*, v. 21, p. 95–105.
- Törmänen, T.O., and Koski, R.A., 2005, Gold enrichment and the Bi-Au association in pyrrhotite-rich massive sulfide deposits, Escanaba Trough, southern Gorda Ridge: *Economic Geology*, v. 100, p. 1135–1150.
- Tornos, F., 2006, Environment of formation and styles of volcanogenic massive sulfides—The Iberian Pyrite Belt: *Ore Geology Reviews*, v. 28, p. 259–307.
- Vokes, F.M., 1969, A review of the metamorphism of sulfide deposits: *Earth Science Reviews*, v. 5, p. 99–143.
- Weihed, J.B., Bergström, U., Billström, K., and Weihed, P., 1996, Geology, tectonic setting and origin of the PaleoProterozoic Boliden Au-Cu-As deposit, Skellefte District, northern Sweden: *Economic Geology*, v. 91, p. 1073–1097.
- Zierenberg, R.A., Shanks, W.C., III, Seyfried, W.E., Jr., Koski, R.A., and Strickler, M.D., 1988, Mineralization, alteration, and hydrothermal metamorphism of the ophiolite-hosted Turner-Albright sulfide deposit, southwestern Oregon: *Journal of Geophysical Research*, v. 93, p. 4657–4674.

9. Hypogene Gangue Characteristics

By John F. Slack

9 of 21

Volcanogenic Massive Sulfide Occurrence Model

Scientific Investigations Report 2010–5070–C

U.S. Department of the Interior
U.S. Geological Survey

U.S. Department of the Interior
KEN SALAZAR, Secretary

U.S. Geological Survey
Marcia K. McNutt, Director

U.S. Geological Survey, Reston, Virginia: 2012

For more information on the USGS—the Federal source for science about the Earth, its natural and living resources, natural hazards, and the environment, visit <http://www.usgs.gov> or call 1-888-ASK-USGS.

For an overview of USGS information products, including maps, imagery, and publications, visit <http://www.usgs.gov/pubprod>

To order this and other USGS information products, visit <http://store.usgs.gov>

Any use of trade, product, or firm names is for descriptive purposes only and does not imply endorsement by the U.S. Government.

Although this report is in the public domain, permission must be secured from the individual copyright owners to reproduce any copyrighted materials contained within this report.

Suggested citation:

Slack, J.F., 2012, Hypogene gangue characteristics in volcanogenic massive sulfide occurrence model: U.S. Geological Survey Scientific Investigations Report 2010-5070 -C, chap. 9, 4 p.

Contents

| | |
|--------------------------|-----|
| Mineralogy..... | 151 |
| Mineral Assemblages..... | 151 |
| Paragenesis..... | 151 |
| Zoning Patterns..... | 151 |
| Grain Size..... | 152 |
| References Cited..... | 152 |

9. Hypogene Gangue Characteristics

By John F. Slack

Mineralogy

All nonsulfide components of VMS deposits are generally considered to be gangue. In this section, discussion is limited to hypogene gangue minerals that occur within sulfide ore and sulfide-rich wall rocks, excluding occurrences in surrounding alteration zones. Minerals within this gangue category vary greatly depending on several factors including metamorphic grade, age, and geologic setting of the deposits (see Lydon, 1984; Franklin, 1993; Franklin and others, 2005). For deposits that occur at or below lower greenschist facies, the hypogene gangue may consist of quartz, carbonate, barite, white mica, and (or) chlorite, together with lesser amounts of magnetite, sodic plagioclase, epidote, tourmaline, analcime, and montmorillonite; fluorite, celsian, hyalophane; greenalite, stilpnomelane, hematite, anhydrite, and gypsum may be present locally. At higher metamorphic grades, chloritoid, garnet, amphibole, cordierite, gahnite, staurolite, kyanite, and andalusite are common gangue constituents, with minor rutile and (or) titanite occurring in places.

Ages of VMS deposits are linked broadly to the presence or absence of some gangue minerals. Notable among these is barite, which occurs in several Archean orebodies (Reynolds and others, 1975; Vearncombe and others, 1995; Li and others, 2004) but typically is absent in younger Precambrian deposits (for example, Franklin and others, 2005). Barite is relatively common in Phanerozoic deposits that contain abundant felsic volcanic rocks in footwall sequences, owing to generally high Ba concentrations in K-feldspar within such lithologies and their availability for leaching of this Ba by deeply circulating hydrothermal fluids. Anhydrite and gypsum occur in some weakly metamorphosed deposits, such as the Miocene Kuroko orebodies in Japan (Ogawa and others, 2007), but are generally unknown in more metamorphosed older deposits, mainly because of the retrograde solubility of anhydrite and its ease of dissolution by later fluids (see Hannington and others, 1995).

Mineral Assemblages

Assemblages of gangue minerals in VMS deposits vary widely as a function of several parameters such as fluid composition, fluid/rock ratio, P–T history, and postore

recrystallization. In the sulfide-rich zones of greenschist-facies deposits, common assemblages are quartz + chlorite + sericite ± carbonate ± barite ± albite; more strongly metamorphosed deposits may contain quartz + garnet + amphibole ± rutile as typical assemblages.

Paragenesis

The original hydrothermal paragenesis of gangue minerals is generally impossible to discern owing to postdepositional deformation and metamorphism. However, some well-preserved VMS deposits, at or below lower greenschist facies with minimal penetrative deformation, reveal apparently primary sequences of gangue mineralization. In the Ordovician Bald Mountain deposit in Maine, seven stages of mineralization have been recognized: early massive pyritic sulfide; massive pyrrhotite; vein quartz; massive pyrite, magnetite, and Fe-silicates; quartz-siderite-sulfide veins; and two sets of late quartz ± sulfide veins (Slack and others, 2003). Some VMS deposits of Silurian or Devonian age in the southern Urals of Russia preserve primary paragenetic relationships (Herrington and others, 2005). Gangue minerals in footwall feeder zones also may retain a premetamorphic paragenesis, such as at the Archean Kidd Creek deposit in Ontario (Slack and Coad, 1989; Hannington and others, 1999) and the Cambrian Hellyer deposit in Tasmania (Gemmell and Large, 1992). At the Archean Mons Cupri deposit in Western Australia, carbonate gangue occurs both in early and late assemblages, bracketing in time the deposition of semimassive sulfide (Huston, 2006).

Zoning Patterns

Mineralogical zoning is recognized in many VMS deposits (see Lydon, 1984, 1996; Franklin and others, 2005). Zoning of sulfide minerals is well documented, but gangue mineral zoning (excluding in exhalites) is seldom discussed. A few generalizations nevertheless can be made. First, in well-preserved Phanerozoic deposits, the gangue in cores of sulfide mounds is predominantly quartz, whereas the margins locally contain abundant barite and (or) anhydrite (Large, 1992; Galley and others, 2007). Chlorite and white mica may be concentrated in the lower or upper parts of sulfide mounds.

Carbonate minerals tend to be widely distributed, but in some deposits such as Ruttan in Manitoba occur preferentially in the stratigraphically higher parts of the sulfide zone (Barrie and others, 2005).

Grain Size

Gangue minerals show a range of grain sizes depending on the extent of post-depositional processes such as subsurface zone refining and metamorphic recrystallization. Typically, gangue minerals are less than 1 mm in maximum dimension. Although grain sizes typically are larger in more strongly deformed and metamorphosed VMS deposits, some ancient deposits below greenschist facies may contain gangue minerals as much as several centimeters in size. Much coarser grains are well documented in amphibolite- and granulite-facies deposits, where equant minerals like garnet and cordierite may be 5–8 cm in diameter, and prismatic minerals like amphibole and kyanite can be tens of centimeters long.

References Cited

- Barrie, C.T., Taylor, C., and Ames, D.E., 2005, Geology and metal contents of the Ruttan volcanogenic massive sulfide deposit, northern Manitoba, Canada: *Mineralium Deposita*, v. 39, p. 795–812.
- Franklin, J.M., 1993, Volcanic-associated massive sulphide deposits, *in* Kirkham, R.V., Sinclair, W.D., Thorpe, R.I., and Duke, J.M., eds., *Mineral deposit modeling: Geological Association of Canada Special Paper 40*, p. 315–334.
- Franklin, J.M., Gibson, H.L., Jonasson, I.R., and Galley, A.G., 2005, Volcanogenic massive sulfide deposits, *in* Hedenquist, J.W., Thompson, J.F.H., Goldfarb, R.J., and Richards, J.P., eds., *Economic Geology 100th anniversary volume, 1905–2005*: Littleton, Colo., Society of Economic Geologists, p. 523–560.
- Galley, A.G., Hannington, M., and Jonasson, I., 2007, Volcanogenic massive sulphide deposits, *in* Goodfellow, W.D., ed., *Mineral deposits of Canada—A synthesis of major deposit-types, district metallogeny, the evolution of geological provinces, and exploration methods*: Geological Association of Canada, Mineral Deposits Division, Special Publication 5, p. 141–161.
- Gemmell, J.B., and Large, R.R., 1992, Stringer system and alteration zones underlying the Hellyer volcanic-hosted massive sulfide deposit, Tasmania, Australia: *Economic Geology*, v. 87, p. 620–649.
- Hannington, M.D., Bleeker, W., and Kjarsgaard, I., 1999, Sulfide mineralogy, geochemistry, and ore genesis of the Kidd Creek deposit—Part II. The bornite zone, *in* Hannington, M.D., and Barrie, C.T., eds., *The giant Kidd Creek volcanogenic massive sulfide deposit, western Abitibi subprovince, Canada: Economic Geology Monograph 10*, p. 225–266.
- Hannington, M.D., de Ronde, C.E.J., and Petersen, S., 2005, Sea-floor tectonics and submarine hydrothermal systems, *in* Hedenquist, J.W., Thompson, J.F.H., Goldfarb, R.J., and Richards, J.P., eds., *Economic geology 100th anniversary volume 1905–2005*: Littleton, Colo., Society of Economic Geologists, p. 111–141.
- Herrington, R.J., Maslennikov, V., Zaykov, V., Seravkin, I., Kosarev, A., Buschmann, B., Orgeval, J.-J., Holland, N., Tesalina, S., Nimis, P., and Armstrong, R., 2005, Classification of VMS deposits—Lessons from the South Uralides: *Ore Geology Reviews*, v. 27, p. 203–237.
- Huston, D.L., 2006, Mineralization and regional alteration at the Mons Cupri stratiform Cu-Zn-Pb deposit, Pilbara Craton, Western Australia: *Mineralium Deposita*, v. 41, p. 17–32.
- Large, R.R., 1992, Australian volcanic-hosted massive sulfide deposits—Features, styles, and genetic models: *Economic Geology*, v. 87, p. 471–510.
- Li, J., Kusky, T., Niu, X., Jun, F., and Polat, A., 2004, Neoproterozoic massive sulfide of Wutai Mountain, North China—A black smoker chimney and mound complex within 2.50 Ga-old oceanic crust, *in* Kusky, T.M., ed., *Precambrian ophiolites and related rocks: Developments in Precambrian Geology*, v. 13, p. 339–362.
- Lydon, J.W., 1984, Volcanogenic massive sulphide deposits—Part 1. A descriptive model: *Geoscience Canada*, v. 11, p. 195–202.
- Lydon, J.W., 1996, Characteristics of volcanogenic massive sulfide deposits—Interpretations in terms of hydrothermal convection systems and magmatic hydrothermal systems: Instituto Tecnológico Geominero de Espana, *Boletín Geológico y Minero*, v. 107, no. 3–4, p. 15–64.
- Ogawa, Y., Shikazono, N., Ishiyama, D., Sato, H., Mizuta, T., and Nakano, T., 2007, Mechanisms for anhydrite and gypsum formation in the Kuroko massive sulfide-sulfate deposits, north Japan: *Mineralium Deposita*, v. 42, p. 219–233.
- Reynolds, D.G., Brook, A., Marshall, E., and Allchurch, P.D., 1975, Volcanogenic copper-zinc deposits in the Pilbara and Yilgarn blocks, *in* Knight, C.L., ed., *Economic geology of Australia and Papua New Guinea—Volume 1. Metals*: Australian Institute of Mining and Metallurgy, Monograph Series 5, p. 185–195.

- Slack, J.F., and Coad, P.R., 1989, Multiple hydrothermal and metamorphic events in the Kidd Creek volcanogenic massive sulphide deposit, Timmins, Ontario—Evidence from tourmalines and chlorites: *Canadian Journal of Earth Sciences*, v. 26, p. 694–715.
- Slack, J.F., Foose, M.P., Flohr, M.J.K., Scully, M.V., and Belkin, H.E., 2003, Exhalative and seafloor replacement processes in the formation of the Bald Mountain massive sulfide deposit, northern Maine, *in* Goodfellow, W.D., McCutcheon, S.R., and Peter, J.M., eds., *Volcanogenic massive sulfide deposits of the Bathurst district, New Brunswick, and northern Maine: Economic Geology Monograph 11*, p. 513–548.
- Vearncombe, S., Barley, M.E., Groves, D.I., McNaughton, N.J., Mikucki, E.J., and Vearncombe, J.R., 1995, 3.26 Ga black smoker-type mineralization in the Strelley belt, Pilbara Craton, Western Australia: *Journal of the Geological Society of London*, v. 152, p. 587–590.

10. Exhalites

By John F. Slack

10 of 21

Volcanogenic Massive Sulfide Occurrence Model

Scientific Investigations Report 2010–5070–C

U.S. Department of the Interior
U.S. Geological Survey

U.S. Department of the Interior
KEN SALAZAR, Secretary

U.S. Geological Survey
Marcia K. McNutt, Director

U.S. Geological Survey, Reston, Virginia: 2012

For more information on the USGS—the Federal source for science about the Earth, its natural and living resources, natural hazards, and the environment, visit <http://www.usgs.gov> or call 1-888-ASK-USGS.

For an overview of USGS information products, including maps, imagery, and publications, visit <http://www.usgs.gov/pubprod>

To order this and other USGS information products, visit <http://store.usgs.gov>

Any use of trade, product, or firm names is for descriptive purposes only and does not imply endorsement by the U.S. Government.

Although this report is in the public domain, permission must be secured from the individual copyright owners to reproduce any copyrighted materials contained within this report.

Suggested citation:

Slack, J.F., 2012, Exhalites in volcanogenic massive sulfide occurrence model: U.S. Geological Survey Scientific Investigations Report 2010-5070 -C, chap. 10, 6 p.

Contents

| | |
|---|-----|
| Geometry and Spatial Distribution | 159 |
| Mineralogy and Zoning | 160 |
| Protoliths | 161 |
| Geochemistry..... | 161 |
| References Cited..... | 161 |

Figure

| | |
|---|-----|
| 10-1. Simplified cross sections of volcanogenic massive sulfide deposits showing different types and morphologies of exhalites | 160 |
|---|-----|

10. Exhalites

By John F. Slack

Geometry and Spatial Distribution

The term exhalite refers to “exhalative” chemical sedimentary rock, following the first usage by Ridler (1971). Exhalites are stratiform beds or lenses of rock that are spatially associated with VMS deposits (Sangster, 1978; Franklin and others, 1981; Spry and others, 2000; Peter, 2003). Most workers consider exhalites to record the precipitation of mainly amorphous Fe ± Mn ± Si ± S ± Ba ± B phases from VMS-related hydrothermal vents and plumes (Peter and Goodfellow, 1996; Peter and others, 2003a; Grenne and Slack, 2005). Exhalites characteristically occur in proximal settings within hanging-wall strata above the sulfide deposits, and (or) as marginal aprons at approximately the same stratigraphic level. Distal exhalites, hundreds of meters or more along strike from VMS deposits, also may be present, although discerning their genetic relationship to specific sulfide horizons can be difficult. Less common are exhalites occurring in footwall sequences below the sulfide zones. Some siliceous beds such as the Main Contact Tuff in the Noranda district of Quebec (Kalogeropoulos and Scott, 1989) and the Key Tuffite in the Matagami district of Quebec (Liaghat and MacLean, 1992) have been interpreted as exhalites; however, based on studies of modern VMS systems, it is likely that these beds did not form by plume fallout but instead by widespread diffuse venting and related silicification of tuffaceous units on the seafloor or in the shallow subsurface.

Modern exhalites have been found in the vicinity of several VMS systems. Examples of proximal exhalites include those on the Mid-Atlantic Ridge (see Metz and others, 1988). Modern distal exhalites are represented by the Fe ± Mn sediments that surround many seafloor VMS deposits (TAG; German and others, 1993) and by far-field metalliferous sediments such as those in the Bauer Deep and on the East Pacific Rise (Heath and Dymond, 1977; Barrett and others, 1987; Hein and others, 1997; Koski and others, 2003b). In ancient settings, Algoma-type iron formations (Gross, 1996) likely formed through fallout from neutrally buoyant plumes in distal environments, relative to VMS systems, and are recognized in both Precambrian and Phanerozoic volcanic sequences (see Goodwin, 1973; Peter, 2003). Manganese-rich umbers like those in the Cretaceous ophiolite on Cyprus probably have a similar origin (Robertson and Hudson, 1973; Ravizza and others, 1999). A caveat here is that detrital sulfide-rich

turbidites or similar reworked sulfidic sediment, deposited far from a VMS deposit as on the modern Mid-Atlantic Ridge (Metz and others, 1988), does not reflect fallout from a hydrothermal plume.

Most exhalites are tabular in form and conformable to bedding within enclosing volcanic or sedimentary strata (Spry and others, 2000; Galley and others, 2007). Common thicknesses range from a few centimeters to as much as several meters. In many cases, proximal exhalites are thickest directly above sulfide zones and become progressively thinner with increasing distance from a deposit. Distal exhalites tend to have uniform thicknesses over strike lengths of tens to hundreds of meters, except in areas of inferred uneven seafloor topography and where affected by postdepositional faulting or folding. A very thick (20–30 m) proximal exhalite forms a tabular layer directly above pyritic massive sulfide at the Bald Mountain deposit in Maine, where a bowl-shaped graben structure promoted the accumulation of both thick sulfide zones and overlying Si-Fe deposits (Slack and others, 2003). At the United Verde deposit in the Jerome district, Arizona, an exhalative jasper approximately 30 m thick overlies the massive sulfide deposit (Lindberg, 2008, fig. 3). An even thicker exhalite occurs at the Baiyinchang deposit in western China, forming a mound-shaped lens 30–50 m thick above altered rocks in the hanging wall sequence (Hou and others, 2008). Such thick exhalites may have played an important role during evolution of some VMS deposits by confining heat and hydrothermal fluids in the subsurface, which in turn promoted subseafloor sulfide mineralization and related zone refining (Barriga and Fyfe, 1988; Slack and others, 2003). Based on modeling studies, Schardt and Large (2009) suggested that cap rocks aid in the formation of Zn-rich deposits by preventing the dissolution of anhydrite and Zn sulfides by late hydrothermal fluids. In some cases, siliceous cap rocks above VMS deposits did not form by exhalation onto the seafloor but instead by epigenetic replacement in the subsurface (Jones and others, 2006).

Strike lengths vary greatly depending on several factors, but in areas of good outcrop and (or) coverage by drill core, some exhalites are known to extend for several kilometers or more. Such laterally extensive exhalites are well documented in the Løkken district of central Norway, where beds of sulfide- and silicate-facies iron formation (“vasskis”) and jasper have been traced at the same stratigraphic levels for 3–5 km

(Grenne and Slack, 2005), as well as in the Bathurst district of New Brunswick, Canada, where some beds of oxide-carbonate-silicate iron formation extend >10 km along strike (Peter and Goodfellow, 1996). More commonly, however, field exposures limit the map continuity of exhalites to only a few hundred meters.

Mineralogy and Zoning

Diverse mineral facies of exhalites have been recognized, the most common of which are oxide, carbonate, sulfide, silicate, and sulfate, each being based on the predominant type of mineral component. Figure 10–1 shows simplified cross sections of VMS deposits and different types of related exhalites, their morphologies and facies, likely origins, and examples. Exhalites may be divided into the following types:

- oxide facies, consisting of jasper, hematite iron formation, and magnetite iron formation;
- carbonate facies, which includes one or more Fe-Mg-Ca-Mn carbonates such as siderite, ankerite, dolomite, calcite, rhodochrosite, and kutnahorite;
- silicate facies, comprising iron-rich minerals (such as greenalite and stilpnomelane), magnesian minerals (such as talc and chlorite), manganese-rich minerals (such as spessartine garnet), and boron-rich minerals (such as tourmaline);
- sulfide facies, chiefly composed of pyrite and (or) pyrrhotite with only minor base-metal sulfides (chalcopyrite, sphalerite, galena); and
- sulfate facies, which comprises barite and, in a limited number of deposits, anhydrite and gypsum.

Another facies type is chert and metachert, a widespread exhalite composed mainly of microcrystalline quartz that, in some deposits, forms a cap rock above the massive sulfide body (Gemmell and Large, 1992; Slack and others, 2003; Jones and others, 2006). Other exhalite facies that contain abundant fluorite, apatite, gahnite, or Zn-staurolite are uncommon to rare in the geologic record. Although proximal exhalites containing appreciable chalcopyrite and (or) sphalerite may occur within several hundred meters of a VMS deposit, because of chemical and hydrodynamic processes during plume fallout, distal pyrite- and pyrrhotite-rich sediments may instead be a reflection of euxinic (sulfidic) bottom waters (Grenne and Slack, 2005).

Vertical and lateral mineralogical zoning occurs in many exhalite units. Typical are multiple

layers or laminations composed of different proportions of hydrothermal components, in many cases intermixed or alternating with detrital material including pelagic clay and locally-derived volcanoclastic sediment. Layers may vary in thickness from <1 mm to as much as 1 m; many exhalites display fine-scale laminations of alternating mineral facies (see Spry and others, 2000; Peter and others, 2003b). Lateral zoning of minerals is not as well documented but is known in some districts, such as the Bathurst camp, New Brunswick, where siderite is most abundant near VMS deposits within a major iron formation unit of the Brunswick belt (Peter and Goodfellow, 1996), and a variety of constituents including carbonate, stilpnomelane, and apatite are most abundant in iron formations proximal to sulfide deposits of the Heath Steele belt (Peter and Goodfellow, 2003).

Base-metal sulfide minerals may show a zoning pattern in oxide-facies exhalites. Studies of modern seafloor precipitates from hydrothermal plumes indicate that proportions and grain sizes of such sulfides tend to decrease with increasing distance

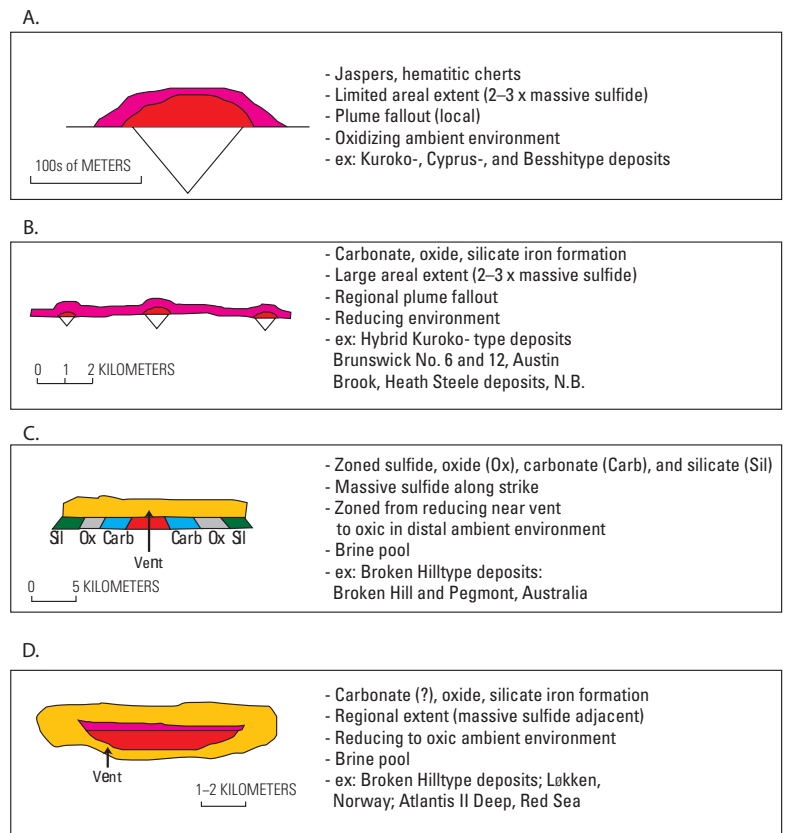


Figure 10–1. Simplified cross sections of volcanogenic massive sulfide deposits showing different types and morphologies of exhalites, with examples. *A*, Proximal jasper and hematitic chert overlying mound-like deposit. *B*, Proximal and distal (regionally extensive) iron formation occurring immediately above and along strike from deposits. *C*, Zoned iron formation, grading outward from inner sulfide-facies to carbonate-facies to oxide-facies to silicate-facies. *D*, Iron formation occurring immediately above a sheetlike deposit. Modified from Peter (2003).

from a vent site and that at distances of >1 km from a vent any sulfides present are volumetrically very minor in small grains <10 μm in diameter (Feely and others, 1994; German and Von Damm, 2003). Noteworthy are very large “superplumes” or “event plumes” in modern seafloor-hydrothermal systems (Baker, 1998), which could have formed widespread exhalite deposits in the ancient geologic record.

Protoliths

Owing to postdepositional effects of diagenesis and metamorphism, original hydrothermal components of exhalites may be largely or totally removed by such processes. In the case of oxide-facies iron formation, primary phases are widely believed to have been amorphous ferric-oxyhydroxide based on their occurrence in modern hydrothermal settings, including in plumes and plume-derived sediment (for example, Peter and others, 2003a). A similar precursor is inferred for the iron-rich component of jasper, with the quartz component being derived from amorphous silica of predominant seawater origin (Grenne and Slack, 2005). Crystalline hematite that occurs in ancient VMS-related jasper and iron formations is considered a product of diagenesis and (or) metamorphism, because in modern settings hematite only forms from moderate-temperature (>115 $^{\circ}\text{C}$) fluids (Hein and others, 2008), whereas in plume settings the ambient temperatures of iron precipitation are much lower (typically <10 $^{\circ}\text{C}$) and thus below the stability of hematite. Magnetite iron formation, where unrelated to diagenetic or metamorphic transformation of hematite, is likely to have originated by subseafloor alteration of primary ferric oxyhydroxide by nonredox processes (Ohmoto, 2003). Discerning the primary phase(s) in silicate-facies exhalites is more difficult because their stability is governed by a complex set of parameters including temperature, pH, $f\text{O}_2$, $f\text{CO}_2$, etc. (see Klein, 2005). Especially challenging is determining the protolith of spessartine-quartz rocks (coticles; Spry, 1990), which may have precursors of Mn-rich carbonate and clay, or Mn-oxyhydroxide and clay, depending on physicochemical conditions on and near the paleoseafloor (Slack and others, 2009, and references therein). Protoliths of various types of carbonate-, sulfide-, and sulfate-facies exhalites are generally considered to be similar or identical to the presently observed mineral assemblages for samples at or below lower greenschist grade metamorphic conditions.

Geochemistry

Many geochemical studies have been carried out on exhalites both to evaluate their origin and to determine possible use in mineral exploration. The former goal has focused recently on attempts to constrain the redox state of coeval bottom waters during deposition of protoliths to the exhalites (see Goodfellow and others, 2003), especially for Precambrian seafloor-hydrothermal systems (Slack and others, 2007,

2009). Exploration applications have been proposed by many workers, but few studies provide compelling guidelines, in part because of the need for extensive outcrops or drill cores in order to establish a thorough sampling distribution relative to a known hydrothermal source. Gale and others (1997) analyzed Archean exhalites in the Canadian shield for rare earth elements (REE) and suggested that the presence of positive Eu anomalies, in shale-normalized diagrams, indicates proximity to a VMS deposit. Detailed studies by Peter and Goodfellow (2003) showed that the highest Fe/Mn ratios in chlorite, stilpnomelane, siderite, and sphalerite along the Heath Steele belt occur near the B Zone sulfide deposit and that use of a hydrothermal sediment index, based on bulk compositions of exhalites, can be an effective guide to known sulfide mineralization. Grenne and Slack (2005) also showed that in seafloor-hydrothermal jaspers of the Løkken district, Norway, As/Fe and Sb/Fe ratios both decrease systematically away from an inferred major VMS vent site. Modern analogs of such Fe-Mn-Si exhalites show a range of bulk compositions including variations in REE and trace elements related to varying proportions of hydrothermal, hydrogenous, and detrital components (see Mills and Elderfield, 1995; Koski and others, 2003a).

References Cited

- Baker, E.T., 1998, Patterns of event and chronic hydrothermal venting following a magmatic intrusion—New perspectives from the 1996 Gorda Ridge eruption: *Deep-Sea Research, Part II*, v. 45, p. 2599–2618.
- Barrett, T.J., Taylor, P.N., and Lugowski, J., 1987, Metaliferous sediments from DSDP Leg 92, the East Pacific Rise transect: *Geochimica et Cosmochimica Acta*, v. 51, p. 2241–2253.
- Barriga, F.J.A.S., and Fyfe, W.S., 1988, Giant pyritic base-metal deposits—The example of Feitais (Aljustrel, Portugal): *Chemical Geology*, v. 69, p. 331–343.
- Feely, R.A., Massoth, G.J., Trefry, J.H., Baker, E.T., Paulson, A.J., and Lebon, G.T., 1994, Composition and sedimentation of hydrothermal plume particles from North Cleft segment, Juan de Fuca Ridge: *Journal of Geophysical Research*, v. 99B, p. 4985–5006.
- Franklin, J.M., Lydon, J.M., and Sangster, D.F., 1981, Volcanic-associated massive sulfide deposits, *in* Skinner, B.J., ed., *Economic Geology 75th anniversary volume, 1905–1980*: Littleton, Colo., Economic Geology Publishing Company, p. 485–627.
- Gale, G.H., Dabek, L.B., and Fedikow, M.A.F., 1997, The application of rare earth element analyses in the exploration for volcanogenic massive sulfide type deposits: *Exploration and Mining Geology*, v. 6, p. 233–252.

- Galley, A.G., Hannington, M., and Jonasson, I., 2007, Volcanogenic massive sulphide deposits, *in* Goodfellow, W.D., ed., Mineral deposits of Canada—A synthesis of major deposit-types, district metallogeny, the evolution of geological provinces, and exploration methods: Geological Association of Canada, Mineral Deposits Division, Special Publication 5, p. 141–161.
- Gemmell, J.B., and Large, R.R., 1992, Stringer system and alteration zones underlying the Hellyer volcanic-hosted massive sulfide deposit, Tasmania, Australia: *Economic Geology*, v. 87, p. 620–649.
- German, C.R., Higgs, N.C., Thomson, J., Mills, R., Elderfield, H., Blusztajn, J., Fleer, A.P., and Bacon, M.P., 1993, A geochemical study of metalliferous sediment from the TAG hydrothermal mound, 26°08'N, Mid-Atlantic Ridge: *Journal of Geophysical Research*, v. 98, p. 9683–9692.
- German, C.R., and Von Damm, K.L., 2003, Hydrothermal processes, *in* Elderfield, H., ed., The oceans and marine geochemistry. Treatise on geochemistry, v. 6: Amsterdam, Elsevier Ltd., p. 181–222.
- Goodfellow, W.D., Peter, J.M., Winchester, J.A., and van Staal, C.R., 2003, Ambient marine environment and sediment provenance during formation of massive sulfide deposits in the Bathurst mining camp—Importance of reduced bottom waters to sulfide precipitation and preservation, *in* Goodfellow, W.D., McCutcheon, S.R., and Peter, J.M., eds., Volcanogenic massive sulfide deposits of the Bathurst mining camp, New Brunswick, and northern Maine: *Economic Geology Monograph* 11, p. 129–156.
- Goodwin, A.M., 1973, Archean iron-formations and tectonic basins of the Canadian Shield: *Economic Geology*, v. 68, p. 915–933.
- Grenne, T., and Slack, J.F., 2005, Geochemistry of jasper beds from the Ordovician Løkken ophiolite, Norway—Origin of proximal and distal siliceous exhalites: *Economic Geology*, v. 100, p. 1511–1527.
- Gross, G.A., 1996, Algoma-type iron-formation, *in* Eckstrand, O.R., Sinclair, W.D., and Thorpe, R.I., eds., Geology of Canadian mineral deposit types: Geological Survey of Canada, Geology of Canada no. 8; Geological Society of America, Decade of North American Geology v. P1, p. 66–73.
- Heath, G.R., and Dymond, J., 1977, Genesis and transformation of metalliferous sediments from the East Pacific Rise, Bauer Deep, and Central Basin, Nazca plate: *Geological Society of America Bulletin*, v. 88, p. 723–733.
- Hein, J.R., Clague, D.A., Koski, R.A., Embley, R.W., and Dunham, R.E., 2008, Metalliferous sediment and a silica-hematite deposit within the Blanco Fracture Zone, northeast Pacific: *Marine Georesources and Geotechnology*, v. 26, p. 317–339.
- Hein, J.R., Koschinsky, A., Halbach, P., Manheim, F.T., Bau, M., Kang, J.-K., and Lubick, N., 1997, Iron and manganese oxide mineralization in the Pacific, *in* Nicholson, K., Hein, J.R., Bühn, B., and Dasgupta, S., eds., Manganese mineralization—Geochemistry and mineralogy of terrestrial and marine deposits: Geological Society of London Special Publication 119, p. 123–138.
- Hou, Z.-Q., Zaw, K., Rona, P., Li, Y.-Q., Qu, X.-M., Song, S.-H., Peng, L., and Huang, J.-J., 2008, Geology, fluid inclusions, and oxygen isotope geochemistry of the Baiyinchang pipe-style volcanic-hosted massive sulfide Cu deposit in Gansu Province, northwestern China: *Economic Geology*, v. 103, p. 269–292.
- Jones, S., Gemmell, J.B., and Davidson, G.J., 2006, Petrographic, geochemical, and fluid inclusion evidence for the origin of siliceous cap rocks above volcanic-hosted massive sulfide deposits at Myra Falls, Vancouver Island, British Columbia, Canada: *Economic Geology*, v. 101, p. 555–584.
- Kalogeropoulos, S.I., and Scott, S.D., 1989, Mineralogy and geochemistry of an Archean tuffaceous exhalite—The main contact tuff, Millenbach mine area, Noranda, Quebec: *Canadian Journal of Earth Sciences*, v. 26, p. 88–105.
- Klein, C., 2005, Some Precambrian banded iron-formations (BIFs) from around the world—Their age, geologic setting, mineralogy, metamorphism, geochemistry, and origin: *American Mineralogist*, v. 90, p. 1473–1499.
- Koski, R.A., Galley, A.G., and Hannington, M.D., 2003a, Ophiolite-hosted volcanogenic massive sulfide deposits—A view in 2003 [abs.]: Geological Society of America Abstracts with Programs, v. 35, p. 12.
- Koski, R.A., German, C.R., and Hein, J.R., 2003b, Fate of hydrothermal products from mid-ocean ridge hydrothermal systems—Near-field to global perspectives, *in* Halbach, P.E., Tunnicliffe, V., and Hein, J.R., eds., Energy and mass transfer in marine hydrothermal systems: Berlin, Dahlem University Press, p. 317–335.
- Liaghat, S., and MacLean, W.H., 1992, The Key Tuffite, Matagami mining district—Origin of the tuff components and mass changes: *Exploration and Mining Geology*, v. 1, p. 197–207.
- Lindberg, P.A., 2008, Early Proterozoic volcanogenic massive sulfide ore deposits, Jerome, Arizona, USA, *in* Spencer, J.E., and Tittley, S.R., eds., Ores and orogenesis—Circum-Pacific tectonics, geologic evolution, and ore deposits: Arizona Geological Society Digest 22, p. 601–610.

- Metz, S., Trefry, J.H., and Nelsen, T.A., 1988, History and geochemistry of a metalliferous sediment core from the Mid-Atlantic Ridge at 26°N: *Geochimica et Cosmochimica Acta*, v. 52, p. 2369–2378.
- Mills, R.A., and Elderfield, H., 1995, Rare earth element geochemistry of hydrothermal deposits from the active TAG mound, 26°N mid-Atlantic Ridge: *Geochimica et Cosmochimica Acta*, v. 59, p. 3511–3524.
- Ohmoto, H., 2003, Nonredox transformations of magnetite-hematite in hydrothermal systems: *Economic Geology*, v. 98, p. 157–161.
- Peter, J.M., 2003, Ancient iron formations—Their genesis and use in the exploration for stratiform base metal sulphide deposits, with examples from the Bathurst mining camp, *in* Lentz, D.R., ed., *Geochemistry of sediments and sedimentary rocks—Evolutionary considerations to mineral deposit-forming environments: Geological Association of Canada GEOTEXT 4*, p. 145–176.
- Peter, J.M., and Goodfellow, W.D., 1996, Mineralogy, bulk and rare earth element geochemistry of massive sulphide-associated hydrothermal sediments of the Brunswick horizon, Bathurst mining camp, New Brunswick: *Canadian Journal of Earth Sciences*, v. 33, p. 252–283.
- Peter, J.M., and Goodfellow, W.D., 2003, Hydrothermal sedimentary rocks of the Heath Steele belt, Bathurst mining camp, New Brunswick—Part 3. Application of mineralogy and mineral and bulk compositions to massive sulfide exploration, *in* Goodfellow, W.D., McCutcheon, S.R., and Peter, J.M., eds., *Massive sulfide deposits of the Bathurst mining camp, New Brunswick, and northern Maine: Economic Geology Monograph 11*, p. 417–433.
- Peter, J.M., Goodfellow, W.D., and Doherty, W., 2003a, Hydrothermal sedimentary rocks of the Heath Steele belt, Bathurst mining camp, New Brunswick—Part 2. Bulk and rare earth element geochemistry and implications for origin, *in* Goodfellow, W.D., McCutcheon, S.R., and Peter, J.M., eds., *Massive sulfide deposits of the Bathurst mining camp, New Brunswick, and northern Maine: Economic Geology Monograph 11*, p. 391–415.
- Peter, J.M., Kjarsgaard, I.M., and Goodfellow, W.D., 2003b, Hydrothermal sedimentary rocks of the Heath Steele belt, Bathurst mining camp, New Brunswick—Part 1. Mineralogy and mineral chemistry, *in* Goodfellow, W.D., McCutcheon, S.R., and Peter, J.M., eds., *Massive sulfide deposits of the Bathurst mining camp, New Brunswick, and northern Maine: Economic Geology Monograph 11*, p. 361–390.
- Ravizza, G., Sherrell, R.M., Field, M.P., and Pickett, E.A., 1999, Geochemistry of the Margi umbers, Cyprus, and the Os isotope composition of Cretaceous seawater: *Geology*, v. 27, p. 971–974.
- Ridler, R.H., 1971, Analysis of Archean volcanic basins in the Canadian Shield using the exhalite concept [abs.]: *Bulletin of the Canadian Institute of Mining and Metallurgy*, v. 64, no. 714, p. 20.
- Robertson, A.H.F., and Hudson, J.D., 1973, Cyprus umbers—Chemical precipitates on a Tethyan Ocean ridge: *Earth and Planetary Science Letters*, v. 18, p. 93–101.
- Sangster, D.F., 1978, Exhalites associated with Archean volcanogenic massive sulphide deposits: Perth, Australia, University of Western Australia, Geology Department and Extension Service Publication 2, p. 70–81.
- Schardt, C., and Large, R.R., 2009, New insights into the genesis of volcanic-hosted massive sulfide deposits on the seafloor from numerical modeling studies: *Ore Geology Reviews*, v. 35, p. 333–351.
- Slack, J.F., Foose, M.P., Flohr, M.J.K., Scully, M.V., and Belkin, H.E., 2003, Exhalative and seafloor replacement processes in the formation of the Bald Mountain massive sulfide deposit, northern Maine, *in* Goodfellow, W.D., McCutcheon, S.R., and Peter, J.M., eds., *Volcanogenic massive sulfide deposits of the Bathurst district, New Brunswick, and northern Maine: Economic Geology Monograph 11*, p. 513–548.
- Slack, J.F., Grenne, T., and Bekker, A., 2009, Seafloor-hydrothermal Si-Fe-Mn exhalites in the Pecos greenstone belt, New Mexico, and the redox state of ca. 1720 Ma deep seawater: *Geosphere*, v. 5, p. 1–13.
- Slack, J.F., Grenne, T., Bekker, A., Rouxel, O.J., and Lindberg, P.A., 2007, Suboxic deep seawater in the late Paleoproterozoic—Evidence from hematitic chert and iron formation related to seafloor-hydrothermal sulfide deposits, central Arizona, USA: *Earth and Planetary Science Letters*, v. 255, p. 243–256.
- Spry, P.G., 1990, The genetic relationship between cotocules and metamorphosed massive sulfide deposits, *in* Spry, P.G., and Bryndzia, L.T., eds., *Regional metamorphism of ore deposits and genetic implications: Utrecht, The Netherlands, VSP Publishers*, p. 49–75.
- Spry, P.G., Peter, J.M., and Slack, J.F., 2000, Meta-exhalites as exploration guides to ore, *in* Spry, P.G., Marshall, B., and Vokes, F.M., eds., *Metamorphosed and metamorphic ore deposits: Reviews in Economic Geology*, v. 11, p. 163–201.

11. Hydrothermal Alteration

By W.C. Pat Shanks III

11 of 21

Volcanogenic Massive Sulfide Occurrence Model

Scientific Investigations Report 2010–5070–C

U.S. Department of the Interior
U.S. Geological Survey

U.S. Department of the Interior
KEN SALAZAR, Secretary

U.S. Geological Survey
Marcia K. McNutt, Director

U.S. Geological Survey, Reston, Virginia: 2012

For more information on the USGS—the Federal source for science about the Earth, its natural and living resources, natural hazards, and the environment, visit <http://www.usgs.gov> or call 1-888-ASK-USGS.

For an overview of USGS information products, including maps, imagery, and publications, visit <http://www.usgs.gov/pubprod>

To order this and other USGS information products, visit <http://store.usgs.gov>

Any use of trade, product, or firm names is for descriptive purposes only and does not imply endorsement by the U.S. Government.

Although this report is in the public domain, permission must be secured from the individual copyright owners to reproduce any copyrighted materials contained within this report.

Suggested citation:

Shanks III, W.C. Pat, 2012, Hydrothermal alteration in volcanogenic massive sulfide occurrence model: U.S. Geological Survey Scientific Investigations Report 2010-5070 -C, chap. 11, 12 p.

Contents

| | |
|--|-----|
| Relations among Alteration, Gangue, and Ore | 169 |
| Mineralogy, Textures, and Rock Matrix Alteration..... | 170 |
| Mineral Assemblages and Zoning Patterns..... | 170 |
| Alteration in Modern Seafloor Volcanogenic Massive Sulfide Systems | 170 |
| Alteration Zoning in Ancient Volcanogenic Massive Sulfide Deposits | 173 |
| Lateral and Vertical Dimensions | 175 |
| Alteration Intensity | 175 |
| References Cited..... | 178 |

Figures

| | |
|---|-----|
| 11-1. Representative cross sections of alteration related to hydrothermal activity or fossil hydrothermal activity on the modern seafloor | 172 |
| 11-2. Representative examples of alteration zoning in volcanogenic massive sulfide deposits | 174 |
| 11-3. Fluid flow modeling showing water/rock ratios during hydrothermal circulation at <i>A</i> , the Panorama volcanogenic massive sulfide district and <i>B</i> , beneath the seafloor at the Lau Basin hydrothermal system | 176 |
| 11-4. Graphs showing geochemical techniques for quantifying hydrothermal alteration effects using (<i>A</i>) the Gresens mass balance approach and (<i>B</i>) the alteration box plot approach..... | 177 |

Table

| | |
|--|-----|
| 11-1. Diagnostic minerals in hydrothermally altered volcanogenic massive sulfide deposits at different metamorphic grades | 171 |
|--|-----|

11. Hydrothermal Alteration

By W.C. Pat Shanks III

The geochemical reactions that produce hydrothermal alteration in host rocks of VMS deposits are critically important for a number of reasons. First, three-dimensional distributions of hydrothermal alteration zones are produced by circulating hydrothermal fluids and thus provide evidence for pathways of fluid travel and geochemical evidence for the physical and chemical conditions of alteration. The chemical and mineralogical distributions of hydrothermal alteration zones are generally the only direct evidence of fluid circulation patterns related to VMS ore formation. Second, systematic arrangement of hydrothermal alteration zones, and recognition of this arrangement, may provide information useful in mineral exploration and may in some cases provide vectors to undiscovered deposits. Third, hydrothermal alteration can provide key information on the origin of metallic elements in VMS deposits. For example, depletion of key elements in altered rocks, combined with measured or inferred estimates of the volume of altered rock, can constrain possible sources of ore metals. Finally, identification and recognition of hydrothermal alteration assemblages and their zonal relationships in the field may provide important evidence that a terrane under assessment is favorable for occurrence of VMS deposits.

Hydrothermal alteration varies widely from district to district and among individual deposits, and the literature on this topic is voluminous. A detailed review is beyond the scope of this report; the interested reader is referred to the following summary references and additional citations therein: Slack (1993), Ohmoto (1996), Carvalho and others (1999), Galley and Koski (1999), Large and others (2001a), Herrington and others (2003), Gifkins and others (2005), Peter and others (2007), Galley and others (2007), Gibson and Galley (2007), and Goodfellow (2007).

Fortunately, alteration zones related to VMS deposits do show characteristic zonal arrangements (proximal, distal, comformable) that may be related to fluid flow and water/rock interaction processes (upflow, recharge, burial metamorphism). In addition, fairly standard alteration assemblages, defined by alteration mineralogy, also occur in country rocks around many deposits, and even metamorphosed alteration zones produce predictable assemblages.

Relations among Alteration, Gangue, and Ore

Ore is traditionally defined as a valuable mineral or chemical commodity that can be extracted at a profit. In VMS deposits, ore generally consists of sulfide or sulfosalt minerals that contain Cu, Pb, Zn, Ag, and (or) Au. Gangue is defined as any noneconomic mineral deposited together with ore; in VMS deposits this means essentially all nonsulfide minerals (see “Hypogene Gangue Characteristics,” Chapter 9, this volume) and some hydrothermal sulfide minerals (typically pyrite or pyrrhotite) that lack economic value. Hydrothermal alteration is defined as any alteration of rocks or minerals by the reaction of hydrothermal fluid with preexisting solid phases. Hydrothermal alteration can be isochemical, like metamorphism, and dominated by mineralogical changes, or it can be metasomatic and result in significant addition or removal of elements. Where alteration is intense, it can result in significant volume changes such that mass balance approaches using immobile elements are required to fully understand the alteration process (Gresens, 1967).

Some authors include gangue and hydrothermal alteration together (Beane, 1994) but, in the context of VMS deposits, it seems useful to continue distinguishing gangue from alteration. Alteration is by definition an epigenetic process that modifies preexisting rocks (or sediments), whereas gangue is generally a syngenetic mineral deposited on or near the seafloor along with the ore minerals. However, distinctions between gangue and alteration become difficult in cases where VMS mineralization occurred by replacement and open space filling in porous and permeable rocks in shallow zones beneath the seafloor.

In some cases, the bulk of the massive sulfide ore may be deposited in shallow subseafloor environments. In this mode of mineralization, hydrothermal fluids flow into highly permeable, high-porosity rocks, where sulfide precipitation is triggered by mixing with cold ambient seawater in the pore space. The prime example of this style of mineralization is the giant Kidd Creek deposit, where most mineralization occurred below the seafloor in permeable, fragmental felsic volcanic

rocks by infill and replacement (Hannington and others, 1999). A similar origin is inferred for the Horne mine (Kerr and Gibson, 1993), the Ansil deposit where laminated felsic ash flows/turbidites were replaced by sulfides and silica (Galley and others, 1995), and for the Turner-Albright ophiolitic deposit where massive sulfide formed below the seafloor within basaltic hyaloclastite (Zierenberg and others, 1988). Hannington and others (1999) suggested that subseafloor mineralization also formed some of the Bathurst (New Brunswick) deposits.

Mineralogy, Textures, and Rock Matrix Alteration

Hydrothermal alteration of volcanic host rocks involves the replacement of primary igneous glass and minerals (plagioclase, orthoclase, quartz, biotite, muscovite, amphibole, pyroxene, titanomagnetite) with alteration minerals stable at the conditions of alteration, generally in the temperate range of 150–400 °C. Alteration minerals in unmetamorphosed lithologies may include quartz and other forms of silica (chalcedony, opal, amorphous silica), illite, sericite, smectite, chlorite, serpentine (lizardite, chrysotile), albite, epidote, pyrite, carbonates, talc, kaolinite, pyrophyllite, sulfates (anhydrite, barite, alunite, jarosite), and oxides (magnetite, hematite, goethite). These hydrothermal alteration minerals may be transformed during metamorphism into andalusite, corundum, topaz, sillimanite, kyanite, cordierite, garnet, phlogopite, and various orthopyroxenes and orthoamphiboles (Bonnet and Corriveau, 2007).

Alteration textures range from weak alteration of only some of the minerals or matrix in the host rocks, producing a punky or earthy aspect to the overall rock, or to partially-altered phenocrysts. Such alteration may be difficult to distinguish from weathering in the field. Glassy rock matrix or fine-grained mesostasis can be particularly susceptible to alteration and may be massively silicified or replaced by chlorite or sericite as alteration intensity increases. At high alteration intensity, rocks may be pervasively altered, in which virtually all primary phases in the rock are altered to new hydrothermal minerals. In the extreme case of stringer zones immediately underlying massive sulfide deposits, it is not unusual to find massively altered rock that consists of quartz, chlorite, and chalcopyrite veins, with or without lesser amounts of pyrite, sericite, and carbonates. Stringer zone rocks may be unrecognizable in terms of original lithology.

Occasionally rock alteration leads to misidentification of lithology as in studies of the Amulet rhyolite in the Noranda district. Lithochemical studies using immobile element patterns have shown that the Upper Amulet rhyolite is actually a hydrothermally altered andesite-dacite (Gibson and others, 1983; Barrett and MacLean, 1999). Similarly, in the intensely silicified zones at the Turner-Albright VMS deposit, basaltic hyaloclastite has been progressively replaced by quartz-sericite-chlorite, quartz-chlorite, and finally quartz-sulfide

(Zierenberg and others, 1988). The completely silicified rocks were originally mapped as “chert exhalite,” but careful mineralogical, geochemical, and isotopic studies showed the presence of relict igneous chromium spinel, proving massive hydrothermal replacement. Similar extreme alteration has been documented locally in the amphibolite-facies wall rocks to the Elizabeth VMS deposit, Vt., where assemblages such as quartz-white mica-calcite and quartz-white mica-albite-staurolite-garnet-corundum contain uniformly high Cr/Zr and Ti/Zr ratios, which reflect protoliths of tholeiitic basalt that were pervasively metasomatized during seafloor hydrothermal mineralization (Slack, 1999; Slack and others, 2001).

These studies underscore the importance of understanding the nature and effects of hydrothermal alteration in VMS systems, including overprinting by postore regional metamorphism.

Mineral Assemblages and Zoning Patterns

Early studies of alteration mineral assemblages emphasized zonal arrangements of mineralogy around sulfide veins at Butte, Mont. and at several porphyry copper deposits (Sales and Meyer, 1948; Titley and Hicks, 1966; Meyer and Hemley, 1967; Meyer and others, 1968). Studies of alteration assemblages in these continental hydrothermal settings led to a series of commonly recognized alteration zones: potassic, argillic, phyllic, and propylitic, with distinct mineralogy and decreasing intensity of alteration developed away from the vein or pluton, respectively. Bonnet and Corriveau (2007) retained some of these classification terms (table 11–1) and used some of the assemblage names for VMS deposits, but substituted sericitic for phyllic and, like other researchers, added chloritic as an important alteration zone in subseafloor settings. Advanced argillic is a special type of alteration that forms in highly acidic, high sulfidation-state conditions characteristic of near-seafloor (or near-surface) oxidation of SO₂ or H₂S to produce sulfuric acid.

Experimental and theoretical geochemical studies (Hemley and Jones, 1964; Beane, 1994; Reed and Palandri, 2006) have established a firm thermodynamic basis for the occurrence of these hydrothermal alteration assemblages. Studies of metamorphosed VMS deposits have clearly shown that the primary alteration minerals are transformed into predictable higher temperature and pressure mineral assemblages (table 11–1) (Bonnet and Corriveau, 2007).

Alteration in Modern Seafloor Volcanogenic Massive Sulfide Systems

Subseafloor VMS hydrothermal alteration zoning is less studied than equivalent systems on the continents because of the primitive level of exploration and relative paucity of drilling, but such zoning is important because the deposits have

Table 11–1. Diagnostic minerals in hydrothermally altered volcanogenic massive sulfide deposits at different metamorphic grades.

[Modified from Bonnet and Corriveau, 2007. Fe, iron; K, potassium; Mg, magnesium]

| Alteration type | Diagnostic minerals: unmetamorphosed deposits | Diagnostic minerals: greenschist facies | Diagnostic minerals: granulite facies |
|----------------------|---|---|---|
| Advanced argillic | Kaolinite, alunite, opal, smectite | Kaolinite, pyrophyllite, andalusite, corundum, topaz | Sillimanite, kyanite, quartz |
| Argillic | Sericite, illite, smectite, pyrophyllite, opal | Sericite, illite, pyrophyllite | Sillimanite, kyanite, quartz, biotite, cordierite, garnet |
| Sericitic | Sericite, illite, opal | Sericite, illite, quartz | Biotite, K-feldspar, sillimanite, kyanite, quartz, cordierite, garnet |
| Chloritic | Chlorite, opal, quartz, sericite | Chlorite, quartz, sericite | Cordierite, orthopyroxene, orthoamphibole, phlogopite, sillimanite, kyanite |
| Carbonate propylitic | Carbonate (Fe, Mg), epidote, chlorite, sericite, feldspar | Carbonate (Fe, Mg), epidote, chlorite, sericite, feldspar | Carbonate, garnet, epidote, hornblende, diopside, orthopyroxene |

not experienced significant deformation or metamorphism. Several areas on the seafloor have provided enough information to begin to understand alteration mineralogy and chemistry and the spatial arrangement of alteration types related to VMS systems: the Galapagos Rift stockwork zone, mafic systems at TAG, a siliciclastic mafic system at Middle Valley, and a bimodal felsic system in Manus Basin north of Papua New Guinea (fig. 11–1).

A remarkable stockwork alteration zone has been studied at the Galapagos Rift beneath a presently inactive sulfide mound where a host block provides outcrop exposure (fig. 11–1A) (Embley and others, 1988; Ridley and others, 1994). The inner zone of the stockwork in basaltic pillows, lava flows, and hyaloclastite contains sulfide veins and Fe-rich chlorite-smectite-kaolinite-quartz alteration of selvages and host rocks. Peripheral to the inner zone, alteration is weak and dominated by Mg-rich chlorite, clays, iron oxides, and silica.

Studies by ODP drilling of the TAG VMS mound on the Mid-Atlantic Ridge (fig. 14–1B) emphasize seafloor precipitation and remobilization of hydrothermal sulfide and sulfate minerals and provide a crude picture of alteration zoning in the host rocks beneath TAG. Basically, the stockwork zone immediately beneath the deposit is a silicified, pyritic wallrock breccia with minor paragonite (also referred to as sericite) that increases with depth in this zone. Beneath, and to some extent surrounding, the stockwork zone is a chloritized basalt breccia that consists primarily of chlorite-quartz-pyrite with minor hematite, and smectite and talc in the altered rock matrix (Honnorez and others, 1998). Drilling did not penetrate deeper into basement and the expected peripheral sericitic and propylitic alteration zones were not encountered.

Manus Basin, where dacite-dominated (andesite to rhyodacite) lava flows and hydrothermal vents occur on Paul

Ridge, was drilled during ODP Leg 193 to a maximum depth of 387 m (Binns and others, 2007). Three holes penetrated hydrothermally altered rocks (fig. 11–1C). Most of the alteration is represented by clays plus silica. Silica occurs as opal-A in near-surface rocks, with progressive transition to cristobalite and then quartz with depth. Clays are chlorite, illite, and mixed-layer phases including chlorite, smectite, illite, and vermiculite (Lackschewitz and others, 2004). Pyrophyllite occurs in patches and is believed to be related to acid-sulfate alteration. Beneath the Roman Ruins hydrothermal vent area, there are a well-developed pyrite-quartz-anhydrite stockwork and an unusual K-feldspar alteration zone. Zonation is not particularly systematic at this site, and is somewhat different than that at most ancient massive sulfides, but may well represent precursor alteration zones to those defined in lithified or metamorphosed rocks.

Alteration related to the Middle Valley hydrothermal system provides a good example of altered sediment and basalt in a siliciclastic-mafic system (fig. 11–1D). Goodfellow and Peter (1994) found well-defined alteration zones from ODP Leg 139 drilling in the sedimentary host rocks around the massive sulfide deposit at Bent Hill. Alteration facies range from a deep inner zone of quartz-chlorite-smectite-rutile, outward to albite-chlorite-muscovite-pyrite, anhydrite-pyrite-illite, and calcite-pyrite-illite. These zones may roughly correspond to an inner chloritic zone and an outer sericitic (illitic) zone, with the calcite-pyrite zone showing similarities to propylitic alteration (table 11–1). ODP Leg 169 (Zierenberg and others, 1998) deepened and widened drill coverage in and around the Bent Hill massive sulfide deposit (see fig. 3–2B, this volume). In particular, deepening of Hole 856H penetrated 107 m of a sulfide feeder zone within altered turbidites beneath the massive sulfide, 221 m of interbedded turbidites and pelagic

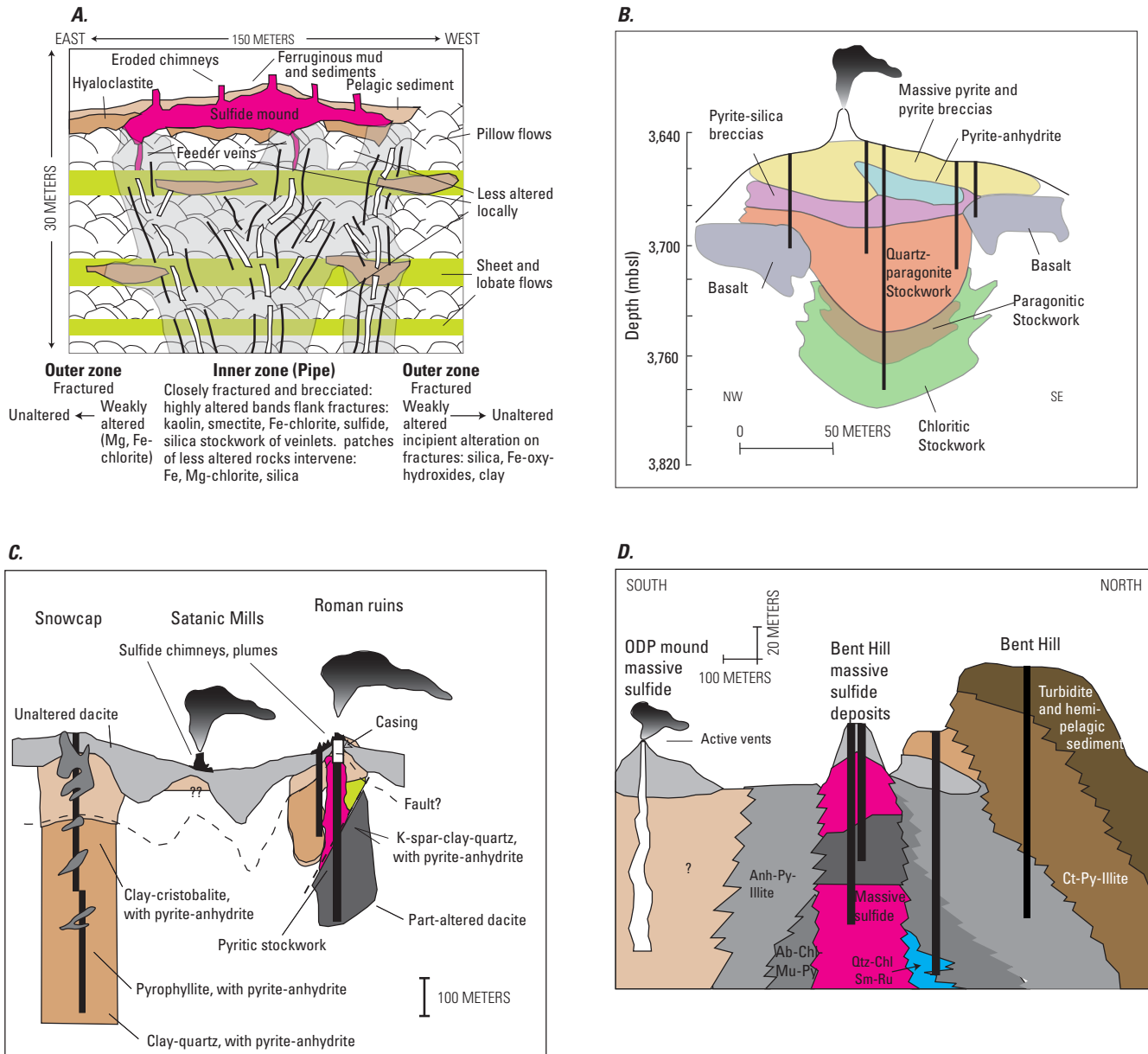


Figure 11–1. Representative cross sections of alteration related to hydrothermal activity or fossil hydrothermal activity on the modern seafloor. *A*, Alteration mineralogy of a stockwork zone exposed by faulting on the Galapagos Rift after Ridley and others (1994). *B*, Alteration mineralogy at the TAG deposit Honnorez and others (1998). *C*, Alteration zonation at Pacmanus, Ocean Drilling Program (ODP) Leg 193, Manus Basin, Papua New Guinea (PNG) after Binns and others (2007). *D*, Middle Valley alteration zonation after Goodfellow and Peter (1994). [Ca, calcium; Fe, iron; K, potassium; Mg, magnesium; Na, sodium; ab, albite; anh, anhydrite; chl, chlorite; ct, calcite; mu, muscovite; py, pyrite; qtz, quartz; ru, rutile; sm, smectite]

sediments, a 39-m interval of basaltic sills and sediment, and 29 m of basaltic flows. The entire sedimentary section beneath the deposit, including the feeder zone, is altered to chlorite and quartz (Lackschewitz and others, 2000), including layers of monomineralic chlorite. On the flanks of the deposit, less intense alteration produced dolomite, mixed-layer chlorite-smectite, corrensite, chlorite, and quartz. Teagle and Alt (2004) studied alteration in the deep basalt sills and flows and found quartz, chlorite, and titanite, with subsidiary epidote, Cu-Fe sulfides, and rare actinolite.

A broader, more distal picture of alteration in the oceanic crust emerges from studies of ODP Site 504, where repeated deepening of drill holes has now penetrated successively oxidized and weathered upper lavas, altered lower lavas, a transition zone that contains a sulfide stockwork, and more than 1 km of altered sheeted dikes (Alt and others, 1996). The lava section is 572 m thick with the upper half altered to iron oxides, carbonates, clays, and zeolites. The lower lava section is altered to chlorite and mixed-layer chlorite-illite, talc, zeolites, quartz, calcite, pyrite, and anhydrite. The transition zone and upper dikes were altered as upwelling hydrothermal fluids mixed with cooler seawater, producing heterogeneous alteration assemblages that include chlorite, actinolite, albite-oligoclase, and titanite and, in places, quartz-epidote-sulfide in discordant veins that record upflow zones. The lower dikes have an early, high-temperature (>400°C) alteration stage that produced hornblende and calcic plagioclase, consistent with reactions predicted from experimental studies (Seyfried and Shanks, 2004). Zones that contain these higher temperature alteration reactions are believed to represent the deep reaction zone for VMS producing systems, an interpretation confirmed by Cu, Zn, and S depletions in the altered rocks of the lower dikes (Alt and others, 1996).

Alteration Zoning in Ancient Volcanogenic Massive Sulfide Deposits

Australian VMS deposits (Large, 1992), which are mostly bimodal-felsic types, have stringer zones that are dominated by chlorite-quartz associated with sulfides. Strong chlorite-sericite-quartz-pyrite alteration occurs in envelopes surrounding stringer zone mineralization. Less intense alteration, further from the deposits, is sericite-quartz-pyrite.

Ancient unmetamorphosed to weakly metamorphosed deposits (Cyprus, Kuroko, Noranda, Turkey) show spatial differences in Fe/(Fe+Mg) ratios of chlorite and related Fe-Mg phyllosilicates with distance from the sulfide ores. High Fe/(Fe+Mg) chlorite typically occurs in cores of feeder zones (Millenbach, Mathiati) and low Fe/(Fe+Mg) chlorite occurs along the margins (Lydon, 1996). These effects apparently are due to sealing of the inner parts of the feeder zone from seawater influx and alteration by the undiluted endmember hydrothermal fluid flow in the core of the feeder zone. The opposite pattern has been observed in a few deposits where presumably seawater was entrained into the feeder zone core (see Large,

1992; Gifkins and others, 2005). In metamorphosed deposits, primary Fe/(Fe+Mg) ratios in tourmaline are preserved, such as at Kidd Creek, where tourmalines in the core of feeder zone are Fe-rich whereas those along the margins are Mg-rich (Slack and Coad, 1989). Additionally, stratabound and stratiform chlorite-rich layers and lenses, which in places are nearly monomineralic chloritites, occur in the immediate footwall or hanging wall. Chlorite-rich layers, lenses, and veins likely form via seawater entrainment into ascending hydrothermal fluids, with seawater providing Mg for metasomatic processes.

Representative examples of alteration zoning from several VMS deposit subtypes (fig. 11–2) include a siliciclastic-felsic type (Bathurst, New Brunswick), a mafic type (Turner-Albright, Josephine Ophiolite, Oreg.), and bimodal-mafic types at Chisel Lake, Manitoba, and bimodal-mafic deposits in the Noranda district, Quebec.

Alteration in the Bathurst district (fig. 11–2A) (Goodfellow, 2007) shows quartz and Fe-rich chlorite immediately underlying the massive sulfide and in the stockwork zone. Peripheral to that is a Mg-rich chlorite-sericite zone, which transitions outward to chlorite-phengite (silica-enriched sericite). Bathurst deposits also show phengite-chlorite alteration in the hanging wall above the massive sulfide horizon, which records ongoing hydrothermal activity after burial of the deposit.

Alteration in the mafic, ophiolitic Turner-Albright deposit (fig. 11–2B) (Zierenberg and others, 1988) shows an alteration pattern related to replacement mineralization in a porous and permeable hyaloclastite pile with general similarities to alteration at TAG and the Galapagos Rift (fig. 11–1A and B). Immediately beneath the massive sulfide deposit, quartz-sulfide alteration is prevalent as a result of massive replacement of basalt hyaloclastite. Beneath this are zones of quartz-sericite-smectite-chlorite and quartz-chlorite.

Deposits in metamorphosed terranes like the Chisel Lake deposit in the Snow Lake district, where alteration has undergone amphibolite-grade regional metamorphism (fig. 11–2C), show distinct assemblages related to premetamorphic alteration. In this deposit, the stringer zones are quartz- and amphibole-rich, and peripheral alteration consists of chlorite-stauroilite and biotite-garnet zones (Galley and others, 1993).

Semi-conformable alteration zones that occur in many VMS districts can be traced over many kilometers of strike length (fig. 11.–2D) (Galley, 1993; Hannington and others, 2003), and are clearly discordant to regional metamorphic isograds. Such conformable zones are probably related to premetamorphic, horizontal hydrothermal circulation driven by the heat of underlying sills or other intrusive bodies. One distinctive type of semi-conformable alteration comprises white mica+chloritoid±chlorite±carbonate assemblages in the stratigraphic footwall of deposits such as Mattabi in Ontario (Franklin and others, 1975) and those in the Delta district of northern Alaska (Dashevsky and others, 2003). This type of alteration reflects pervasive hydrothermal metasomatism of permeable felsic volcanic or volcanoclastic rocks involving alkali leaching, iron addition, and residual enrichment of

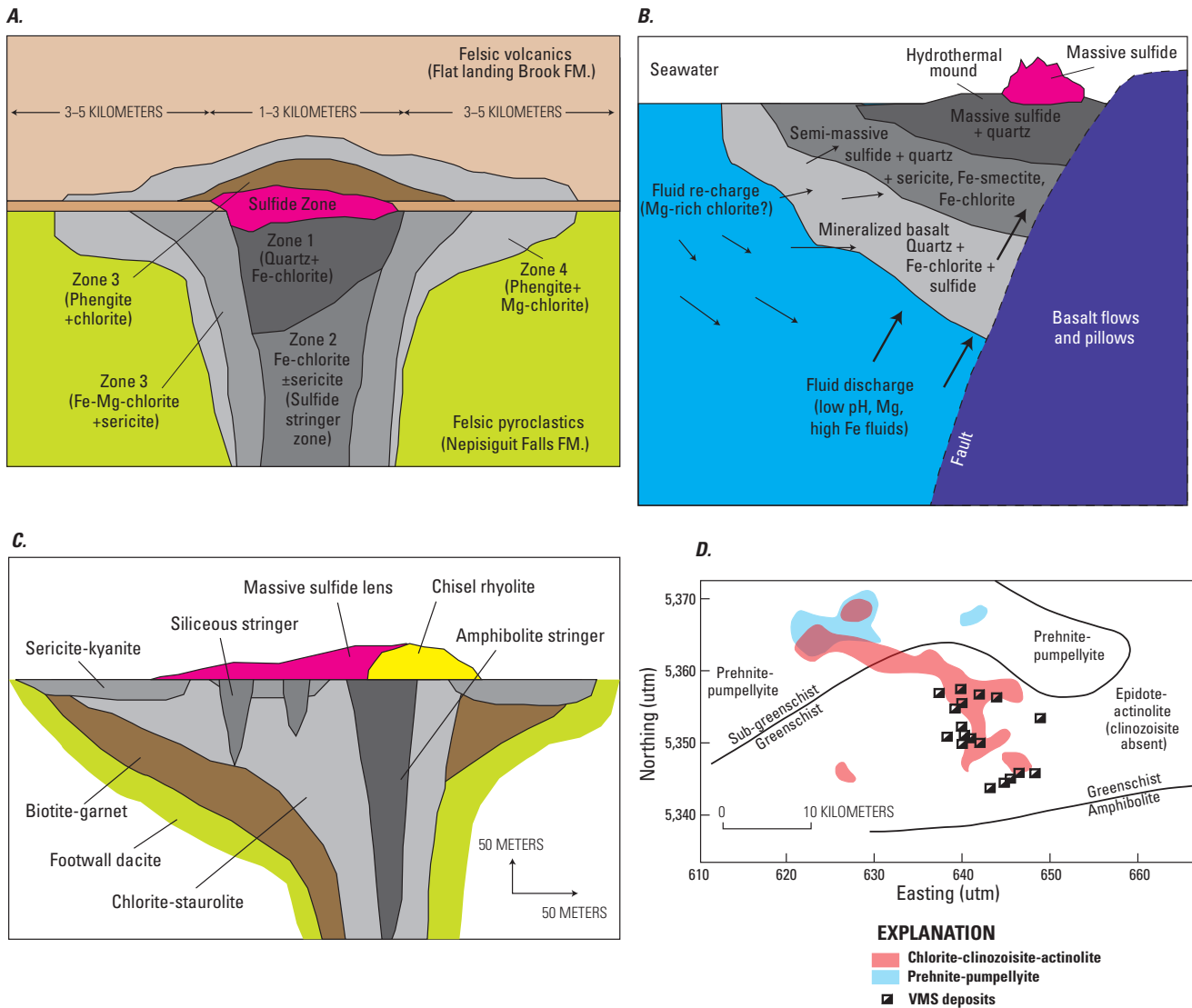


Figure 11-2. Representative examples of alteration zoning in volcanogenic massive sulfide deposits. *A*, Hydrothermal alteration in the Bathurst district after Goodfellow (2007). *B*, Alteration in the mafic, ophiolitic Turner-Albright, OR, deposit (Zierenberg and others, 1988) shows an alteration pattern related to replacement mineralization in a porous and permeable hyaloclastite pile with general similarities to alteration at TAG and the Galapagos Rift. *C*, Chisel Lake deposit in the Snow Lake district, Manitoba, where alteration has undergone amphibolite-grade regional metamorphism (Galley and others, 1993). *D*, Semi-conformable alteration zones (Hannington and others, 2003) that are clearly discordant to regional metamorphic isograds in the Blake River Group, Noranda volcanic complex, western Abitibi subprovince, Ontario. [Fe, iron; Mg, magnesium; Fm., formation]

alumina, followed by greenschist-grade regional metamorphism. At higher amphibolite metamorphic grade, mineral assemblages in these semi-conformable zones may contain abundant kyanite, sillimanite, or cordierite.

Lateral and Vertical Dimensions

Dimensions of alteration zones are often difficult to determine because of lack of exposure and lack of drilling beyond the vicinity of VMS deposits. Most proximal alteration zones can be traced for approximately 2–3 times the horizontal dimension of the massive sulfide deposit and may extend to depths roughly 10 times the thickness of the deposit (figs. 6–1, 11–1, 11–2). Many deposits overlie semi-conformable alteration zones that can have a strike length of 5–50 km and thicknesses of 1–3 km, especially in caldera settings (Galley and others, 2007).

Fluid flow modeling has been used extensively to help constrain seafloor processes in modern and ancient massive sulfide deposits (Parmentier and Spooner, 1978; Cathles, 1983; Lowell and Rona, 1985; Schardt and Large, 2009). These models are limited by lack of information on crustal architecture, structures, permeability, magmatic heat supply, and fluid properties in the sub- and super-critical regions. However, the most recent models include many of these variables. Schardt and Large (2009) have attempted modeling with realistic permeability structures (fig. 11–3). Results indicate intense alteration along faults with dimensions up to a few hundred meters. In some cases, semi-conformable alteration is produced with dimensions of 500–700 m vertically and up to 30 km horizontally, but these dimensions are probably strongly affected by the dimensions of the model and the permeability structure within the volcanic sequence. Nevertheless, this fluid flow modeling approach has great potential for future understanding of alteration processes.

Alteration Intensity

Alteration intensity is often described in the field using qualitative terminology such as weak-moderate-strong or incipient-patchy-pervasive, and these descriptions are critical to mapping and understanding alteration patterns. However, the recent literature abounds with quantitative tools for measuring and discriminating alteration intensity (Leitch and Lentz, 1994; Large and other, 2001b). These tools allow quantification of elemental gains and losses (and volume gain or loss) and characterization of specific types of alteration. The tools are increasingly important in exploration and, in ideal cases, may provide vectors to more intense alteration and mineralization. They also have great potential for use in mineral resource assessments; simple whole-rock geochemical data for altered rocks and representative fresh rocks are all that are needed for this type of analysis.

Gresens (1967) introduced mass balance approaches to metasomatic analyses, and Leitch and Lentz (1994) provided an update on effective application of the Gresens method, which essentially involves normalization relative to fresh unaltered rocks using immobile elements and calculation of volume changes during alteration using densities or compositional changes. Results of this approach for the Brunswick No. 12 deposit in the Bathurst district are shown in figure 11–4A. In this case, the percent change of major oxides clearly shows trends for silicification and for addition of hydrothermal sericite, Mg-chlorite, and Fe-chlorite. Changes in oxide content as large as 5,000 percent indicate that very intense metasomatism was involved in the alteration process. Numerous workers have applied these techniques to alteration studies in volcanogenic massive sulfide systems (Galley and others, 1993; Goodfellow and Peter, 1994; Barrett and MacLean, 1999; Gemmell and Fulton, 2001; Large and others, 2001a; Piercey, 2009).

Another approach is the alteration box plot of Large and others (2001b), which combines (1) the alteration index (AI) of Ishikawa defined as the ratio of $K_2O + MgO$ to the sum of all alkaline and alkaline earth oxides versus (2) a new chlorite-carbonate-pyrite (CCP) index defined as the ratio of $MgO + FeO$ to these oxides plus alkali oxides (fig. 11–4B). Combining these indices on a common plot yields clear identification of alteration processes that affect whole-rock composition (fig. 11–4B). This approach allows individual reactions to be identified and offers potential for discriminating burial diagenetic and hydrothermal processes, which may be essential in assessing mineral resource potential of a terrane.

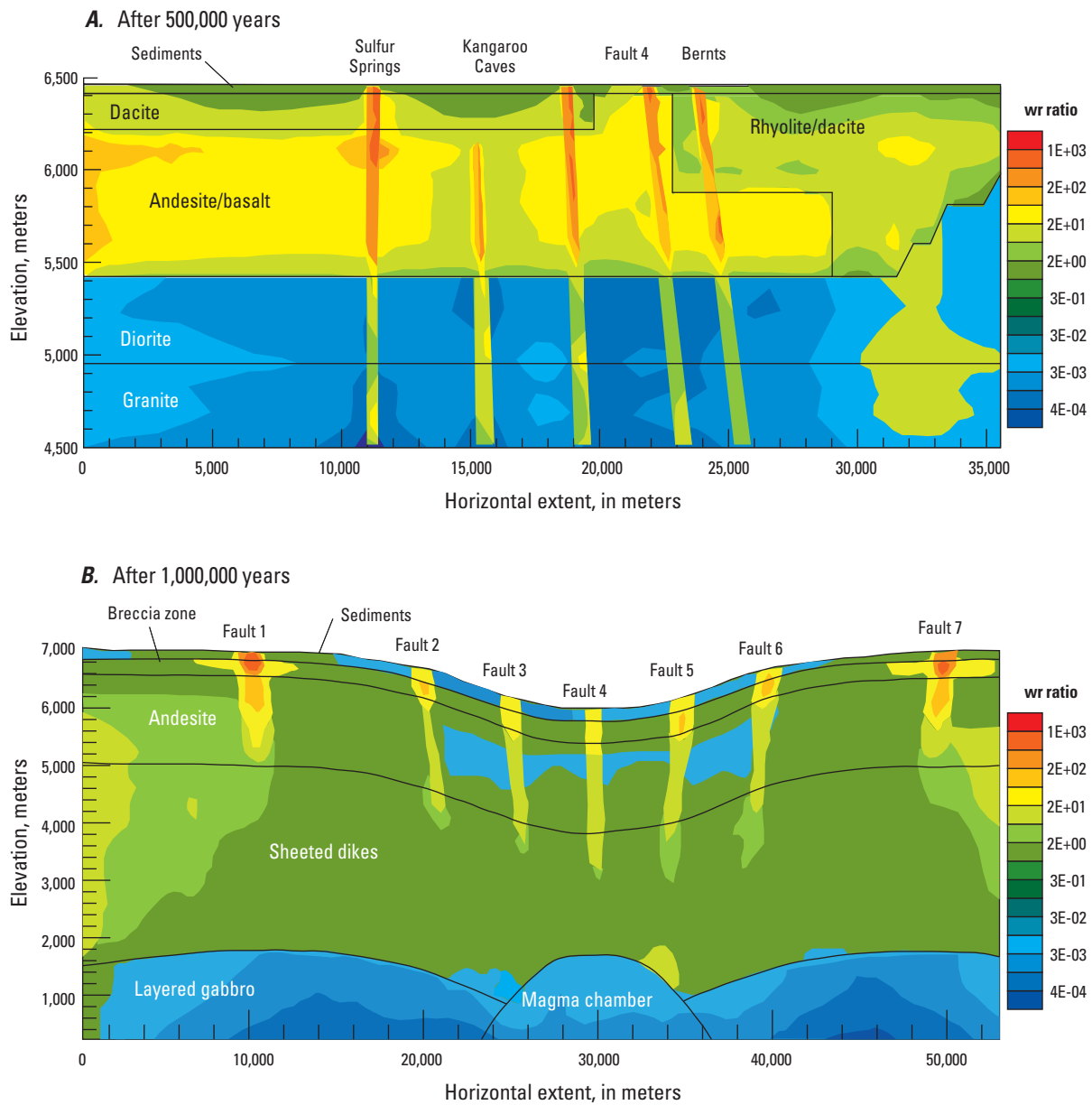


Figure 11-3. Fluid flow modeling showing water/rock ratios during hydrothermal circulation (*A*) at the Panorama volcanogenic massive sulfide district and (*B*) beneath the seafloor at the Lau Basin hydrothermal system. Areas of high water-rock ratio are inferred to be intensely altered due to the high flux of reactant fluid. From Schardt and Large (2009). [wr, water/rock]

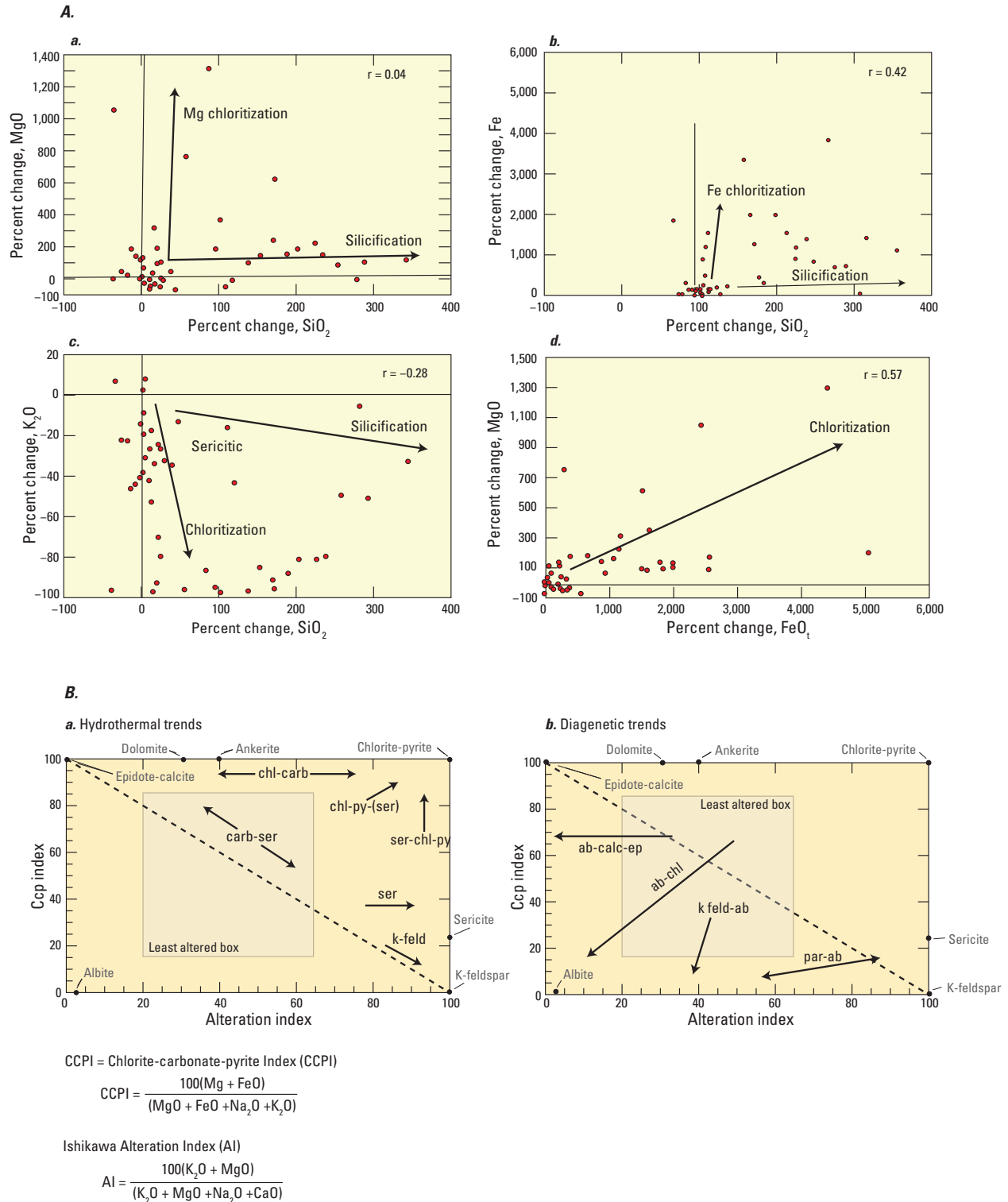


Figure 11-4. Geochemical techniques for quantifying hydrothermal alteration effects using (A) the Gresens mass balance approach and (B) the alteration box plot approach. Both approaches allow identification of alteration reactions and quantification of the amount of alteration. A, Percent change alteration plots for the Brunswick No. 12 deposit based on the Gresens approach and normalizing to Al_2O_3 after Leitch and Lentz (1994). B, Alteration box plots after Large and others (2001). [Mg, magnesium; ab, albite; calc, calcite; carb, carbonate; chl, chlorite; ep, epidote; k-feld, potassium feldspar; par, paragonite; py, pyrite; ser, sericite; CCP, chlorite-carbonate-pyrite]

References Cited

- Alt, J.C., Laverne, C., Vanko, D., Tartarotti, P., Teagle, D.A.H., Bach, W., Zuleger, E., Erzinger, J., Honnerez, J., Pezard, P.A., Becker, K., Salisbury, M.H., and Wilkens, R.H., 1996, Hydrothermal alteration of a section of upper oceanic crust in the eastern equatorial Pacific, *in* Alt, J.C., Kinoshita, H., Stokking, L.B., and Michael, P.J., eds., *Costa Rica Rift, sites 504 and 896: Proceedings of the Ocean Drilling Program, Scientific Results*, v. 148, p. 417–434.
- Barrett, T.J., and MacLean, W.H., 1999, Volcanic sequences, litho-geochemistry, and hydrothermal alteration in some bimodal volcanic-associated massive sulfide deposits, *in* Barrie, C.T., and Hannington, M.D., eds., *Volcanic-associated massive sulfide deposits—Processes and examples in modern and ancient settings: Reviews in Economic Geology*, v. 8, p. 101–131.
- Beane, R., 1994, A graphic view of hydrothermal mineral stabilities, *in* Lentz, D.R., ed., *Alteration and alteration processes associated with ore-forming systems: Geological Association of Canada, Short Course Notes*, v. 11, p. 1–30.
- Binns, R.A., Barriga, F.J.A.S., and Miller, D.J., 2007, Leg 193 synthesis—Anatomy of an active felsic-hosted hydrothermal system, eastern Manus Basin, Papua New Guinea, *in* Barriga, F.J.A.S., Binns, R.A., Miller, D.J., and Herzig, P.M., eds., *Anatomy of an active felsic-hosted hydrothermal system, Eastern Manus Basin, sites 1188–1191: Proceedings of the Ocean Drilling Program, Scientific Results*, v. 193, p. 1–71.
- Bonnet, A.-L., and Corriveau, L., 2007, Alteration vectors to metamorphosed hydrothermal systems in gneissic terranes, *in* Goodfellow, W.D., ed., *Mineral deposits of Canada—A synthesis of major deposit-types, district metallogeny, the evolution of geological provinces, and exploration methods: Geological Association of Canada, Mineral Deposits Division, Special Publication No. 5*, p. 1035–1049.
- Carvalho, D., Barriga, F.J.A.S., and Munha, J., 1999, Bimodal-siliciclastic systems—The case of the Iberian Pyrite Belt, *in* Barrie, C.T., and Hannington, M.D., eds., *Volcanic-associated massive sulfide deposits—Processes and examples in modern and ancient settings: Reviews in Economic Geology*, v. 8, p. 375–408.
- Cathles, L.M., 1983, An analysis of the hydrothermal system responsible for massive sulfide deposition in the Hokuroku Basin of Japan, *in* Ohmoto, H., and Skinner, B.J., eds., *The Kuroko and related volcanogenic massive sulfide deposits: Economic Geology Monograph 5*, p. 439–487.
- Dashevsky, S.S., Schaefer, C.F., and Hunter, E.N., 2003, Bedrock geologic map of the Delta mineral belt, Tok mining district, Alaska: Alaska Division of Geological and Geophysical Surveys Professional Report 122, 122 p., 2 plates, scale 1:63,360.
- Embley, R.W., Jonasson, I.R., Perfit, M.R., Franklin, J.M., Tivey, M.A., Malahoff, A., Smith, M.F., and Francis, T.J.G., 1988, Submersible investigation of an extinct hydrothermal system on the Galapagos Ridge—Sulfide mounds, stockwork zone, and differentiated lavas: *Canadian Mineralogist*, v. 26, p. 517–539.
- Franklin, J.M., Kasarda, J., and Poulsen, K.H., 1975, Petrology and chemistry of the alteration zone of the Mattabi massive sulfide deposit: *Economic Geology*, v. 70, p. 63–79.
- Galley, A.G., 1993, Characteristics of semi-conformable alteration zones associated with volcanogenic massive sulphide districts: *Journal of Geochemical Exploration*, v. 48, p. 175–200.
- Galley, A.G., Bailes, A.H., and Kitzler, G., 1993, Geological setting and hydrothermal evolution of the Chisel Lake and North Chisel Zn-Pb-Ag-Au massive sulphide deposit, Snow Lake, Manitoba: *Exploration and Mining Geology*, v. 2, p. 271–295.
- Galley, A.G., Hannington, M., and Jonasson, I., 2007, Volcanogenic massive sulphide deposits, *in* Goodfellow, W.D., ed., *Mineral deposits of Canada—A synthesis of major deposit-types, district metallogeny, the evolution of geological provinces, and exploration methods: Geological Association of Canada, Mineral Deposits Division, Special Publication 5*, p. 141–161.
- Galley, A.G., and Koski, R.A., 1999, Setting and characteristics of ophiolite-hosted volcanogenic massive sulfide deposits, *in* Barrie, C.T., and Hannington, M.D., eds., *Volcanic-associated massive sulfide deposits—Processes and examples in modern and ancient settings: Reviews in Economic Geology*, v. 8, p. 221–246.
- Galley, A.G., Watkinson, D.H., Jonasson, I.R., and Riverin, G., 1995, The seafloor formation of volcanic-hosted massive sulfide—Evidence from the Ansil deposit, Rouyn-Noranda, Canada: *Economic Geology*, v. 90, no. 7, p. 2006–2017.
- Gemmell, J.B., and Fulton, R., 2001, Geology, genesis, and exploration implications of the footwall and hanging-wall alteration associated with the Hellyer volcanic-hosted massive sulfide deposit, Tasmania, Australia: *Economic Geology*, v. 96, p. 1003–1035.
- Gibson, H.L., and Galley, A.G., 2007, Volcanogenic massive sulphide deposits of the Archean, Noranda district, Québec, *in* Goodfellow, W.D., ed., *Mineral deposits of Canada—A synthesis of major deposit-types, district metallogeny, the evolution of geological provinces, and exploration methods: Geological Association of Canada, Mineral Deposits Division, Special Publication 5*, p. 533–552.
- Gibson, H.L., Watkinson, D.H., and Comba, C.D.A., 1983, Silicification—Hydrothermal alteration in an Archean geothermal system within the Amulet Rhyolite formation: *Economic Geology*, v. 78, p. 954–971.

- Gifkins, C., Herrmann, W., and Large, R.R., 2005, Altered volcanic rocks—A guide to description and interpretation: Hobart, Tasmania, Centre for Ore Deposit Research, University of Tasmania, 275 p.
- Goodfellow, W.D., 2007, Metallogeny of the Bathurst mining camp, northern New Brunswick, *in* Goodfellow, W.D., ed., Mineral deposits of Canada—A synthesis of major deposit-types, district metallogeny, the evolution of geological provinces, and exploration methods: Geological Association of Canada, Mineral Deposits Division, Special Publication 5, p. 449–469.
- Goodfellow, W.D., and Peter, J.M., 1994, Geochemistry of hydrothermally altered sediment, Middle Valley, northern Juan de Fuca Ridge, *in* Mottl, M.J., Davis, E.E., Fisher, A.T., and Slack, J.F., eds., Middle Valley, Juan de Fuca Ridge, sites 855–858: Proceedings of the Ocean Drilling Program, Scientific Results, v. 139, p. 207–289.
- Gresens, R.L., 1967, Composition-volume relationships of metasomatism: *Chemical Geology*, v. 2, p. 47–65.
- Hannington, M.D., Barrie, C.T., and Bleeker, W., 1999, Preface and introduction, *in* Hannington, M.D., and Barrie, C.T., eds., The giant Kidd Creek volcanogenic massive sulfide deposit, western Abitibi Subprovince, Canada: *Economic Geology Monograph* 10, p. 1–30.
- Hannington, M.D., Santaguida, F., Kjarsgaard, I.M., and Cathles, L.M., 2003, Regional-scale hydrothermal alteration in the central Blake River Group, western Abitibi subprovince, Canada—Implications for VMS prospectivity: *Mineralium Deposita*, v. 38, p. 392–422.
- Hemley, J.J., and Jones, W.R., 1964, Chemical aspects of hydrothermal alteration with emphasis on hydrogen metasomatism: *Economic Geology*, v. 59, p. 538–569.
- Honnorez, J.J., Alt, J.C., Humphris, S.E., Herzig, P.M., Miller, D.J., Becker, K., Brown, D., Bruegmann, G.E., Chiba, H., Fouquet, Y., Gemmell, J.B., Guerin, G., Hannington, M.D., Holm, N.G., Iturrino, G.J., Knott, R., Ludwig, R.J., Nakamura, K.-i., Petersen, S., Reysenbach, A.-L., Rona, P.A., Smith, S.E., Sturz, A.A., Tivey, M.K., and Zhao, X., 1998, Vivisection and autopsy of active and fossil hydrothermal alterations of basalt beneath and within the TAG hydrothermal mound, *in* Herzig, P.M., Humphris, S.E., Miller, D.J., and Zierenberg, R.A., eds., TAG—Drilling an active hydrothermal system on a sediment-free slow-spreading ridge, site 957: Proceedings of the Ocean Drilling Program, Scientific Results, v. 158, p. 231–254.
- Kerr, D.J., and Gibson, H.L., 1993, A comparison of the Horne volcanogenic massive sulfide deposit and intracauldron deposits of the Mine Sequence, Noranda, Quebec: *Economic Geology*, v. 88, p. 1419–1442.
- Lackschewitz, K.S., Devey, C.W., Stoffers, P., Botz, R., Eisenhauer, A., Kummert, M., Schmidt, M., and Singer, A., 2004, Mineralogical, geochemical and isotopic characteristics of hydrothermal alteration processes in the active, submarine, felsic-hosted PACMANUS field, Manus Basin, Papua New Guinea: *Geochimica et Cosmochimica Acta*, v. 68, p. 4405–4427.
- Lackschewitz, K.S., Singer, A., Botz, R., Garbe-Schönberg, D., Stoffers, P., and Horz, K., 2000, Formation and transformation of clay minerals in the hydrothermal deposits of Middle Valley, Juan de Fuca Ridge, ODP Leg 169: *Economic Geology*, v. 95, p. 361–390.
- Large, R.R., 1992, Australian volcanic-hosted massive sulfide deposits—Features, styles, and genetic models: *Economic Geology*, v. 87, p. 471–510.
- Large, R.R., Allen, R.L., Blake, M.D., and Herrmann, W., 2001a, Hydrothermal alteration and volatile element halos for the Rosebery K Lens volcanic-hosted massive sulfide deposit, Western Tasmania: *Economic Geology*, v. 96, p. 1055–1072.
- Large, R.R., Gemmell, J.B., Paulick, H., and Huston, D.L., 2001b, The alteration box plot—A simple approach to understanding the relationship between alteration mineralogy and litho-geochemistry associated with volcanic-hosted massive sulfide deposits: *Economic Geology*, v. 96, p. 957–971.
- Leitch, C.H.B., and Lentz, D.R., 1994, The Gresens approach to mass balance constraints of alteration systems—Methods, pitfalls, examples, *in* Lentz, D.R., ed., Alteration and alteration processes associated with ore-forming systems: Geological Association of Canada Short Course Notes, v. 11, p. 161–192.
- Lowell, R.P., and Rona, P.A., 1985, Hydrothermal models for the generation of massive sulfide ore deposits: *Journal of Geophysical Research*, v. 90, p. 8769–8783.
- Lydon, J.W., 1996, Characteristics of volcanogenic massive sulfide deposits—Interpretations in terms of hydrothermal convection systems and magmatic hydrothermal systems: Instituto Tecnológico Geominero de España, Boletín Geológico y Minero, v. 107, no. 3–4, p. 15–64.
- Meyer, C., and Hemley, J.J., 1967, Wall rock alteration, *in* Barnes, H.L., ed., Geochemistry of hydrothermal ore deposits: New York, Holt, Rinehart, and Winston, Inc., p. 166–235.
- Meyer, C., Shea, E.P., Goddard, C.C., Jr., and staff, 1968, Ore deposits at Butte, Montana, *in* Ridge, J.D., ed., Ore deposits of the United States, 1933–1967 (Graton-Sales volume): New York, American Institute of Mining, Metallurgical, and Petroleum Engineers, p. 1373–1416.
- Ohmoto, H., 1996, Formation of volcanogenic massive sulfide deposits—The Kuroko perspective, *in* Vielreicher, R.M., Groves, D.I., Heinrich, C.A., and Walshe, J.L., eds., Ore geology reviews: Amsterdam, Elsevier, p. 135–177.

- Parmentier, E.M., and Spooner, E.T.C., 1978, A theoretical study of hydrothermal convection and the origin of the ophiolitic sulphide ore deposits of Cyprus: *Earth and Planetary Science Letters*, v. 40, p. 33–44.
- Peter, J.M., Layton-Matthews, D., Piercey, S., Bradshaw, G., Paradis, S., and Boulton, A., 2007, Volcanic-hosted massive sulphide deposits of the Finlayson Lake district, Yukon, *in* Goodfellow, W.D., ed., *Mineral deposits of Canada—A synthesis of major deposit-types, district metallogeny, the evolution of geological provinces, and exploration methods*: Geological Association of Canada Special Publication 5, p. 471–508.
- Piercey, S.J., 2009, Litho-geochemistry of volcanic rocks associated with volcanogenic massive sulphide deposits and applications to exploration, *in* Cousens, B., and Piercey, S.J., eds., *Submarine volcanism and mineralization—Modern through ancient*: Geological Association of Canada, Short Course Notes, v. 19, p. 15–40.
- Reed, M.H., and Palandri, J., 2006, Sulfide mineral precipitation from hydrothermal fluids, *in* Vaughan, D.J., ed., *Sulfide mineralogy and geochemistry*: Mineralogical Society of America, *Reviews in Mineralogy and Geochemistry* 61, p. 609–631.
- Ridley, W.I., Perfit, M.R., Jonasson, I.R., and Smith, M.F., 1994, Hydrothermal alteration in oceanic ridge volcanics—A detailed study at the Galapagos fossil hydrothermal field: *Geochimica et Cosmochimica Acta*, v. 58, p. 2477–2494.
- Sales, R.H., and Meyer, C., 1948, Wall rock alteration at Butte, Montana: *American Institute of Mining and Metallurgical Engineers Transactions*, v. 178, p. 9–35.
- Schardt, C., and Large, R.R., 2009, New insights into the genesis of volcanic-hosted massive sulfide deposits on the seafloor from numerical modeling studies: *Ore Geology Reviews*, v. 35, p. 333–351.
- Seyfried, W.E., Jr., and Shanks, W.C., III, 2004, Alteration and mass transport in mid-ocean ridge hydrothermal systems—Controls on the chemical and isotopic evolution of high-temperature crustal fluids, *in* Davis, E.E., and Elderfield, H., eds., *Hydrogeology of the oceanic lithosphere*: Cambridge, Cambridge University Press, p. 451–494.
- Slack, J.F., 1993, Descriptive and grade-tonnage models for Besshi-type massive sulphide deposits, *in* Kirkham, R.V., Sinclair, W.D., Thorpe, R.I., and Duke, J.M., eds., *Mineral deposit modeling*: Geological Association of Canada Special Paper 40, p. 343–371.
- Slack, J.F., 1999, Coarse garnet schists at the Elizabeth mine, VT—Products of seafloor-hydrothermal alteration not syn-metamorphic Acadian fluid flow [abs.]: *Geological Society of America Abstracts with Programs*, v. 31, p. A-69.
- Slack, J.F., and Coad, P.R., 1989, Multiple hydrothermal and metamorphic events in the Kidd Creek volcanogenic massive sulphide deposit, Timmins, Ontario—Evidence from tourmalines and chlorites: *Canadian Journal of Earth Sciences*, v. 26, p. 694–715.
- Slack, J.F., Offield, T.W., Woodruff, L.G., and Shanks, W.C., III, 2001, Geology and geochemistry of Besshi-type massive sulfide deposits of the Vermont copper belt, *in* Hammarstrom, J.M., and Seal, R.R., II, eds., *Environmental geochemistry and mining history of massive sulfide deposits in the Vermont copper belt*: Society of Economic Geologists Guidebook Series, v. 35, part II, p. 193–211.
- Teagle, D.A.H., and Alt, J.C., 2004, Hydrothermal alteration of basalts beneath the Bent Hill massive sulfide deposit, Middle Valley, Juan de Fuca Ridge: *Economic Geology*, v. 99, p. 561–584.
- Titley, S.R., and Hicks, C.L., eds., 1966, *Geology of the porphyry copper deposits—Southwestern North America*: Tucson, Ariz., University of Arizona Press, 287 p.
- Zierenberg, R.A., Fouquet, Y., Miller, D.J., Bahr, J.M., Baker, P.A., Bjerkgarden, T., Brunner, C.A., Duckworth, R.C., Gable, R., Gieskes, J.M., Goodfellow, W.D., Groeschel-Becker, H.M., Guerin, G., Ishibashi, J., Iturrino, G.J., James, R.H., Lackschewitz, K.S., Marquez, L.L., Nehlig, P., Peter, J.M., Rigsby, C.A., Schultheiss, P.J., Shanks, W.C., III, Simoneit, B.R.T., Summit, M., Teagle, D.A.H., Urbat, M., and Zuffa, G.G., 1998, The deep structure of a sea-floor hydrothermal deposit: *Nature*, v. 392, no. 6675, p. 485–488.
- Zierenberg, R.A., Shanks, W.C., III, Seyfried, W.E., Jr., Koski, R.A., and Strickler, M.D., 1988, Mineralization, alteration, and hydrothermal metamorphism of the ophiolite-hosted Turner-Albright sulfide deposit, southwestern Oregon: *Journal of Geophysical Research*, v. 93, p. 4657–4674.

12. Supergene Ore and Gangue Characteristics

By Randolph A. Koski

12 of 21

Volcanogenic Massive Sulfide Occurrence Model

Scientific Investigations Report 2010–5070–C

**U.S. Department of the Interior
U.S. Geological Survey**

U.S. Department of the Interior
KEN SALAZAR, Secretary

U.S. Geological Survey
Marcia K. McNutt, Director

U.S. Geological Survey, Reston, Virginia: 2012

For more information on the USGS—the Federal source for science about the Earth, its natural and living resources, natural hazards, and the environment, visit <http://www.usgs.gov> or call 1-888-ASK-USGS.

For an overview of USGS information products, including maps, imagery, and publications, visit <http://www.usgs.gov/pubprod>

To order this and other USGS information products, visit <http://store.usgs.gov>

Any use of trade, product, or firm names is for descriptive purposes only and does not imply endorsement by the U.S. Government.

Although this report is in the public domain, permission must be secured from the individual copyright owners to reproduce any copyrighted materials contained within this report.

Suggested citation:

Koski, R.A., 2012, Supergene ore and gangue characteristics in volcanogenic massive sulfide occurrence model: U.S. Geological Survey Scientific Investigations Report 2010-5070-C, chap. 12, 6 p.

Contents

| | |
|--|-----|
| Mineralogy and Mineral Assemblages | 185 |
| Paragenesis and Zoning Patterns..... | 185 |
| Textures, Structures, and Grain Size | 187 |
| References Cited..... | 189 |

Figure

| | |
|---|-----|
| 12-1. Sequence of supergene mineralization summarized from volcanogenic massive sulfide deposits in the Bathurst mining camp..... | 188 |
|---|-----|

Tables

| | |
|---|-----|
| 12-1. Mineral assemblages of supergene environments in selected volcanogenic massive sulfide deposits | 186 |
| 12-2. Mineralogy of supergene sulfide zones and gossans..... | 187 |

12. Supergene Ore and Gangue Characteristics

By Randolph A. Koski

Mineralogy and Mineral Assemblages

In the traditional view, supergene ore and gangue minerals are the products of reactions between hypogene sulfide minerals and descending, acidic meteoric waters; these processes take place at or near the ground surface in subaerial environments (Guilbert and Park, 1986). In VMS deposits, copper and other metals are mobilized from primary massive sulfide ore and reprecipitated at depth. This precipitation of Cu sulfides with high Cu/S ratios can produce an economically significant copper enrichment at the reactive redox boundary between massive sulfide protore and downward penetrating fluids. The supergene enrichment “blanket” is overlain by an intensely altered and leached Fe oxide-rich gossan (the remains of the original massive sulfide) that extends upward to the paleosurface.

Studies of hydrothermal sulfide mounds and chimneys on oceanic spreading axes reveal a second type of gossan formation: oxidation of sulfide minerals by interaction with oxygen-rich ambient seawater. This process, sometimes referred to as “seafloor weathering,” is accompanied by formation of secondary, low-temperature Cu sulfide minerals as well as the Cu chloride mineral atacamite at the TAG site, Mid-Atlantic Ridge (Hannington and others, 1988; Hannington, 1993). Based on observations at TAG, bedded ocher overlying massive sulfide at Skouriotissa, Cyprus, has been reinterpreted as a submarine gossan (Herzig and others, 1991). Submarine and subaerial weathering processes are described in greater detail in “Weathering Processes,” Chapter 13, this volume.

The mineral assemblages of supergene enrichment zones and their related gossans for a selected group of VMS deposits are presented in table 12–1; a list of secondary minerals and their chemical formulas are presented in table 12–2. The supergene sulfide mineral assemblages in ancient deposits are dominated by a small group of Cu-rich minerals: chalcocite, bornite, covellite, digenite, and enargite. In the supergene blanket, these sulfides may be intergrown with varying amounts of relict hypogene sulfides such as pyrite, chalcopyrite, and sphalerite. Studies of analogous seafloor massive sulfides reveal that in situ seafloor weathering has produced a comparable suite of secondary sulfide minerals (TAG deposit in table 12–1) (Hannington and others, 1988).

In deposits where the zone of weathering is well developed and preserved, the gossan may contain identifiable mineral subzones dominated by sulfates, carbonates, phosphates, or oxides (table 12–1) (Scott and others, 2001). The chemical compositions of oxidized minerals in gossans reflect, to some extent, the antecedent sulfide mineralogy (Boyle, 1996). For example, high Pb contents (Pb tends to be less mobile in these environments) and secondary Pb carbonate and sulfate minerals (cerussite, smithsonite, anglesite) occur in gossanous zones overlying VMS mineralization containing significant amounts of galena (Scott and others, 2001). In deposits of the Bathurst mining camp and the Iberian Pyrite Belt, complex sulfates or sulfate-arsenate minerals such as plumbojarosite and beudantite also act as significant sinks for Pb in the oxidization zone (Boyle, 2003; Nieto and others, 2003).

The residual concentration of precious metals in gossans, in the form of native gold, electrum, and a variety of silver minerals, can be economically important in VMS deposits (Boyle, 1996). At the Canatuan (Philippines) VMS deposit, for example, Sherlock and Barrett (2004) estimate a 45 percent increase in gold content, as electrum, in gossan weathered from pyritic massive sulfides. Likewise, the concentration of native gold in gossan overlying the Flambeau (Wisconsin) VMS deposit corresponds to a sixfold Au enrichment relative to massive sulfide protore (Ross, 1997). Boyle (1996) lists Au and Ag enrichments in gossans of four Canadian VMS deposits as follows: Murray Brook (2.5, 1.2), Caribou (4.0, 2.4), Heath Steele (3.5, 2.5), and Windy Craggy (8.5, 3.4). Studies of modern seafloor mineralization also reveal enrichment of gold in oxidized zones of massive sulfide deposits (for example, TAG: Hannington and others, 1988; Escanaba Trough: Törmänen and Koski, 2005).

Paragenesis and Zoning Patterns

The development of a supergene enrichment zone along with its overlying gossan in VMS deposits produces a distinctive paragenetic sequence. For illustrative purposes, a diagram compiled by Boyle (2003), based on supergene mineralization at numerous deposits in the Bathurst mining camp, captures some of the complexity of supergene mineral successions (fig. 12–1). During early stages of alteration, the less resistant minerals chalcopyrite, sphalerite, and tetrahedrite (if present)

Table 12–1. Mineral assemblages of supergene environments in selected volcanogenic massive sulfide (VMS) deposits. Minerals in italics are present in minor or trace amounts.

| New South Wales, Australia ¹ | Flambeau VMS deposit, Wisconsin ² | Bathurst deposits, Canada ³ | Bisha mine, Eritrea ⁴ | TAG site, Mid-Atlantic Ridge ⁵ |
|--|---|---|---|--|
| Gossan: goethite, hematite | Chert gossan: quartz (chert), hematite, goethite, jarosite, native <i>copper</i> , native <i>gold</i> | Massive sulfide gossan: goethite, amorphous silica, jarosite, plumbojarosite, argentojarosite, beudantite, scorodite, <i>bindheimite</i> | Hematite-goethite-quartz oxide zone (gossan): hematite, goethite, quartz, chalcedony, <i>native gold</i> , <i>pyrargyrite</i> | Oxidized sulfides: amorphous Fe oxyhydroxide, goethite, jarosite, amorphous silica, atacamite, <i>native copper</i> |
| Phosphate zone: pyromorphite | Argillic gossan: quartz, hematite, goethite, chlorite, montmorillonite, <i>alunite-jarosite</i> | | Kaolinite-quartz-sulfate zone: kaolinite, illite, gypsum, alunite, quartz, <i>beudantite</i> , <i>anglesite</i> , <i>cerrusite</i> , <i>siderite</i> , <i>chlorargyrite</i> , <i>native gold</i> | |
| Carbonate zone: cerussite, smithsonite | Ankerite gossan: ankerite, hematite, <i>native gold</i> | | | |
| Sulfate zone: anglesite, alunite, plumbojarosite, <i>malachite</i> , <i>azurite</i> , <i>barite</i> , <i>stolzite</i> , <i>scorodite</i> | Oxide zone: cuprite, goethite, malchite, <i>azurite</i> , <i>native silver</i> | | | |
| Supergene sulfide zone | | | | |
| chalcocite, enargite | chalcocite, bornite, chalcopyrite | covellite, chalcocite, digenite, <i>acanthite</i> , <i>anglesite</i> | chalcocite, digenite, covellite, bornite, <i>enargite</i> | digenite, covellite, borite, <i>native gold</i> , <i>native copper</i> |
| Primary massive sulfide | | | | |
| pyrite, sphalerite, galena, chalcopyrite, <i>arsenopyrite</i> , <i>tetrahedrite-tennantite</i> | pyrite, chalcopyrite, sphalerite, <i>galena</i> , <i>pyrrhotite</i> | pyrite, sphalerite, galena, chalcopyrite, <i>arsenopyrite</i> | pyrite, sphalerite, chalcopyrite, galena, <i>pyrrhotite</i> , <i>arsenopyrite</i> , <i>tetrahedrite</i> , <i>tennantite</i> | marcasite, pyrite, sphalerite, chalcopyrite, <i>bornite</i> |

¹ Scott and others (2001)² May and Dinkowitz (1996)³ Boyle (2003)⁴ Barrie and others (2007)⁵ Hannington and others (1988); Hannington (1993)

Table 12–2. Mineralogy of supergene sulfide zones and gossans.

[Sources: Hannington and others (1988); May and Dinkowitz (1996); Scott and others (2001); Boyle (2003); Sherlock and Barrett (2004); Barrie and others (2007). Mineral formulas are from Frye (1981)]

| Mineral | Formula |
|---------------------------|--|
| Supergene | |
| chalcocite | Cu ₂ S |
| bornite | Cu ₅ FeS ₄ |
| digenite | Cu ₉ S ₅ |
| covellite | CuS |
| enargite | Cu ₃ AsS ₄ |
| chalcopyrite | CuFeS ₂ |
| acanthite | Ag ₂ S |
| Gossan | |
| goethite | FeO(OH) |
| hematite | Fe ₂ O ₃ |
| amorphous Fe oxyhydroxide | |
| amorphous silica | SiO ₂ •nH ₂ O |
| quartz | SiO ₂ |
| kaolinite | Al ₂ Si ₂ O ₅ (OH) ₄ |
| chlorite | |
| montmorillonite | |
| gypsum | CaSO ₄ •2H ₂ O |
| jarosite | KFe ₃ (SO ₄) ₂ (OH) ₆ |
| plumbojarosite | PbFe ₆ (SO ₄) ₄ (OH) ₁₂ |
| argentojarosite | AgFe ₃ (SO ₄) ₂ (OH) ₆ |
| alunite | KAl ₃ (OH) ₆ (SO ₄) ₂ |
| beudantite | PbFe ₃ (AsO ₄)(SO ₄)(OH) ₆ |
| corkite | PbFe ₃ (PO ₄)(SO ₄)(OH) ₆ |
| hinsdalite | (Pb,Sr)Al ₃ (PO ₄)(SO ₄)(OH) ₆ |
| plumbogummite | PbAl ₃ (PO ₄)(PO ₃ OH)(OH) ₆ |
| anglesite | PbSO ₄ |
| barite | BaSO ₄ |
| pyromorphite | Pb ₅ Cl(PO ₄) |
| siderite | FeCO ₃ |
| cerussite | PbCO ₃ |
| smithsonite | ZnCO ₃ |
| ankerite | CaFeMg(CO ₃) ₂ |
| malachite | Cu ₂ CO ₃ (OH) ₂ |
| azurite | Cu ₃ (CO ₃) ₂ (OH) ₂ |
| scorodite | FeAsO ₄ •2H ₂ O |
| bindheimite | Pb ₂ Sb ₂ O ₆ (O,OH) |
| cinnabar | HgS |
| cuprite | Cu ₂ O |
| stolzite | PbWO ₄ |
| native silver | Ag |
| acanthite/argentite | Ag ₂ S |
| chlorargyrite | AgCl |
| iodargyrite | AgI |
| native gold | Au |
| electrum | (Au,Ag) |
| native copper | Cu |
| atacamite | Cu ₂ Cl(OH) ₃ |

are replaced by chalcocite, digenite, covellite, and other Cu-rich sulfides. Acanthite may form in the supergene zone as silver is released from tetrahedrite. As oxidizing conditions extend to greater depths, covellite and digenite are ultimately replaced by chalcocite (Boyle, 2003).

With encroachment of the oxidation front, supergene sulfides as well as pyrite and other remaining primary sulfides become unstable. The susceptibility of pyrrhotite to oxidation implies a rapid breakdown of pyrrhotite-rich ores. Dissolution of galena and arsenopyrite, if present, promotes the precipitation of a variety of Pb- and As-bearing metal sulfate and carbonate minerals (fig. 12–1; table 12–1). Gold mineralization resulting from dissolution of Au-bearing arsenopyrite and pyrite grains can also be included in the supergene paragenesis (fig. 12–1). Coincident with mineral changes in the supergene enrichment zone, primary carbonate minerals are dissolved and aluminosilicate minerals are replaced by clays and amorphous silica in the gossan. The mature stage of gossan development is represented by an assemblage of Fe oxides, quartz (or amorphous silica), clay minerals, sulfates, and carbonates overlying the supergene enrichment blanket.

Zonation of supergene minerals is most prominently developed in a vertical sense with respect to the weathered paleosurface. A basic weathering profile for VMS deposits contains four zones from the original ground surface downward: (1) a leached capping dominated by Fe oxides, clay minerals, and quartz, (2) an oxidized zone dominated by secondary sulfates, (3) the supergene enrichment zone with abundant chalcocite and other Cu-rich sulfides, and (4) the top of the underlying massive sulfide protore. More complex zonation patterns are evident in mature supergene profiles developed on VMS deposits, especially deposits rich in Zn, Pb, and As (table 12–1). The thicknesses of individual zones are highly variable and increase toward margins of massive sulfide bodies and along structural features crosscutting protore.

Textures, Structures, and Grain Size

A variety of textures related to replacement and dissolution reactions are prominent characteristics of the weathering and supergene mineralization zones. Overgrowths and replacement rims of bornite, covellite, or chalcocite on chalcopyrite are frequently observed indicators of incipient supergene alteration. Chalcocite typically occurs as soft sooty coatings on other minerals. More advanced alteration of primary sulfides results in partial to complete pseudomorphous replacement textures, first involving Cu sulfides, then various combinations of secondary sulfide, sulfate, and carbonate minerals, and ultimately Fe oxides and oxyhydroxides. Secondary pyrite and galena with colloform, botryoidal, skeletal, and framboidal textures have been identified in the partly leached gossans of several Uralian deposits (Belogub and others, 2008). A major textural change during supergene processes is the development of secondary porosity. Porous and spongy textures are typical

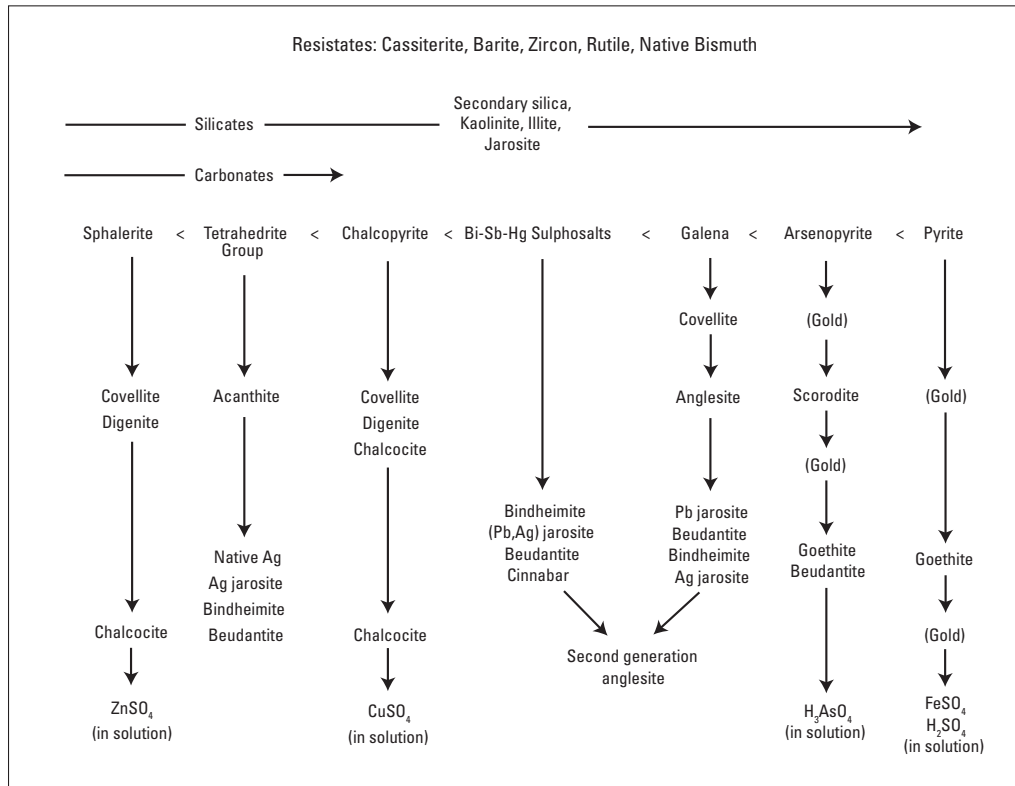


Figure 12–1. Sequence of supergene mineralization summarized from volcanogenic massive sulfide deposits in the Bathurst mining camp (after Boyle, 2003). The stabilities of sulfide minerals under oxidizing conditions increase from left to right. Thus, primary sulfides to the left (especially chalcopyrite) are readily altered and replaced by secondary copper sulfides in the enrichment zone. Oxidation of sulfosalt minerals and galena favors deposition of acanthite in the enrichment blanket and secondary lead minerals in the oxide zone. The precipitation of gold during oxidation of arsenopyrite and pyrite is also indicated. Following dissolution of sulfide and carbonate minerals, the leached gossan is represented by secondary silicates, iron oxides, and oxidation-resistant minerals such as cassiterite and barite. [Ag, silver; Bi, bismuth; Hg, mercury; Pb, lead; Sb, antimony]

of the supergene enrichment zone as well as in gossanous material, especially the cellular boxworks resulting from dissolution of pyrite. Iron oxyhydroxides and other secondary minerals typically appear as colloform and botryoidal infillings within void spaces or laminar overgrowths on resistate minerals such as quartz or cassiterite. The occurrences of beudantite in gossans of the Bathurst mining camp illustrate a variety of supergene textures: microcrystalline coatings, massive spongy interstitial material, vermiform layers lining voids, cubic crystal masses, and colloform masses (Boyle, 2003).

Fragmental zones are a common structural feature of VMS gossans. They appear to represent solution collapse breccias that form after extensive dissolution of primary sulfide and carbonate minerals (Sherlock and Barrett, 2004).

Poorly consolidated layers of quartz and pyrite sand in gossans overlying supergene enrichment zones are another distinctive feature of VMS deposits in Canada, the United States, and the southern Urals (Boyle, 1994; May and Dinkowitz, 1996; Belogub and others, 2008). These sands may result from leaching of sulfide-bearing gossan during advective flow of modern groundwaters (Boyle, 1994).

Pseudomorphic replacement and void infilling mineralization result in grain size variations that are equivalent to or of a finer grain than that of sulfide minerals in the protore. The following occurrences of beudantite in gossans of the Bathurst mining camp are representative of the fine-grained nature of secondary minerals: microcrystalline coatings, massive spongy interstitial material, vermiform layers lining voids, cubic crystal masses, and colloform masses (Boyle, 2003).

References Cited

- Barrie, C.T., Nielsen, F.W., and Aussant, C.H., 2007, The Bisha volcanic-associated massive sulfide deposit, western Nakfa terrane, Eritrea: *Economic Geology*, v. 102, p. 717–738.
- Belogub, E.V., Novoselov, K.A., Yakovleva, V.A., and Spiro, B., 2008, Supergene sulphides and related minerals in the supergene profiles of VHMS deposits from the South Urals: *Ore Geology Reviews*, v. 33, p. 239–254.
- Boyle, D.R., 1994, Oxidation of massive sulfide deposits in the Bathurst mining camp, New Brunswick, *in* Alpers, C.N., and Blowes, D.W., eds., *Environmental geochemistry of sulfide oxidation: American Chemical Society Symposium Series 550*, p. 535–550.
- Boyle, D.R., 1996, Supergene base metals and precious metals, *in* Eckstrand, O.R., Sinclair, W.D., and Thorpe, R.I., eds., *Geology of Canadian mineral deposit types: Geologic Survey of Canada, Geology of Canada no. 8; Geological Society of America, Decade of North American Geology v. P1*, p. 92–108.
- Boyle, D.R., 2003, Preglacial weathering of massive sulfide deposits in the Bathurst mining camp—Economic geology, geochemistry, and exploration applications, *in* Goodfellow, W.D., McCutcheon, S.R., and Peter, J.M., eds., *Massive sulfide deposits of the Bathurst mining camp, New Brunswick, and northern Maine: Economic Geology Monograph 11*, p. 689–721.
- Frye, K., ed., 1981, *The encyclopedia of mineralogy. Encyclopedia of earth sciences*, v. 4B: Stroudsburg, Penn., Hutchinson Ross, 794 p.
- Guilbert, J.M., and Park, C.F., 1986, *The geology of ore deposits*: New York, W.H. Freeman, 985 p.
- Hannington, M.D., 1993, The formation of atacamite during weathering of sulfides on the modern seafloor: *The Canadian Mineralogist*, v. 31, p. 945–956.
- Hannington, M.D., Thompson, G., Rona, P.A., and Scott, S.D., 1988, Gold and native copper in supergene sulphides from the Mid-Atlantic Ridge: *Nature*, v. 333, p. 64–66.
- Herzig, P.M., Hannington, M.D., Scott, S.D., Maliotis, G., Rona, P.A., and Thompson, G., 1991, Gold-rich sea-floor gossans in the Troodos ophiolite and on the Mid-Atlantic Ridge: *Economic Geology*, v. 86, p. 1747–1755.
- May, E.R., and Dinkowitz, S.R., 1996, An overview of the Flambeau supergene enriched massive sulfide deposit—Geology and mineralogy, Rusk County, Wisconsin, *in* Laberge, G.L., ed., *Volcanogenic massive sulfide deposits of northern Wisconsin—A commemorative volume*, v. 2 of *Institute on Lake Superior Geology, 42nd annual meeting*, Cable, Wisc., 15–19 May 1996, *Proceedings: St. Paul, Minn., The Institute*, p. 67–93.
- Nieto, J.M., Capitán, A., Sáez, R., and Almodóvar, G.R., 2003, Beudantite—A natural sink for As and Pb in sulfide oxidation processes: *Applied Earth Science*, v. 112, p. B293–B296.
- Ross, A.M., 1997, Supergene gold enrichment of the Precambrian aged Flambeau gossan, Flambeau mine, Rusk County, Wisconsin: Salt Lake City, University of Utah, M.S. thesis, 56 p.
- Scott, K.M., Ashley, P.M., and Lawie, D.C., 2001, The geochemistry, mineralogy and maturity of gossans derived from volcanogenic Zn-Pb-Cu deposits of the eastern Lachlan Fold Belt, NSW, Australia: *Journal of Geochemical Exploration*, v. 72, p. 169–191.
- Sherlock, R.L., and Barrett, T.J., 2004, Geology and volcanic stratigraphy of the Canatuan and Malusok volcanogenic massive sulfide deposits, southwestern Mindanao, Philippines: *Mineralium Deposita*, v. 39, p. 1–20.
- Törmänen, T.O., and Koski, R.A., 2005, Gold enrichment and the Bi-Au association in pyrrhotite-rich massive sulfide deposits, Escanaba Trough, southern Gorda Ridge: *Economic Geology*, v. 100, p. 1135–1150.

13. Weathering Processes

By W. Ian Ridley

13 of 21

Volcanogenic Massive Sulfide Occurrence Model

Scientific Investigations Report 2010–5070–C

U.S. Department of the Interior
U.S. Geological Survey

U.S. Department of the Interior
KEN SALAZAR, Secretary

U.S. Geological Survey
Marcia K. McNutt, Director

U.S. Geological Survey, Reston, Virginia: 2012

For more information on the USGS—the Federal source for science about the Earth, its natural and living resources, natural hazards, and the environment, visit <http://www.usgs.gov> or call 1-888-ASK-USGS.

For an overview of USGS information products, including maps, imagery, and publications, visit <http://www.usgs.gov/pubprod>

To order this and other USGS information products, visit <http://store.usgs.gov>

Any use of trade, product, or firm names is for descriptive purposes only and does not imply endorsement by the U.S. Government.

Although this report is in the public domain, permission must be secured from the individual copyright owners to reproduce any copyrighted materials contained within this report.

Suggested citation:

Ridley, W. Ian, 2012, Weathering processes in volcanogenic massive sulfide occurrence model: U.S. Geological Survey Scientific Investigations Report 2010-5070 -C, chap. 13, 8 p.

Contents

| | |
|--|-----|
| Mineralogic Reactions to Establish Process | 195 |
| Geochemical Processes..... | 196 |
| Factors Controlling Rates of Reaction..... | 198 |
| Effects of Microclimate and Macroclimate | 199 |
| Effects of Hydrologic Setting | 199 |
| References Cited..... | 200 |

13. Weathering Processes

By W. Ian Ridley

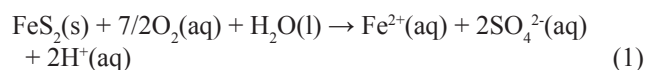
Seafloor massive sulfides (SMS), the presumed precursors of ancient VMS deposits, are unstable in the presence of even small concentrations of oxygen. They are potentially subjected to ambient temperature weathering and other processes that can cause substantial postdepositional changes in mineralogy and geochemistry (Koski and others, 2003). Submarine weathering (halmyrolysis) at the site of ore deposition results from a variety of reactions that are initially mediated by oxygenated seawater that circulates through the deposit. Oxidation begins at the deposit/seawater interface, and the oxidation front gradually moves into the deposit, resulting in mass wasting of the ore deposit at ambient temperatures of 1–2 °C.

In principle, the process of seafloor weathering can produce intermediate stages of supergene enrichments by complete or partial replacement of primary sulfides by secondary sulfides and enriched gossans (Hannington and others, 1988; Herzig and others, 1991), but the continued circulation of oxygenated seawater eventually results in the physical and chemical destruction of the deposit. Consequently, weathering of SMS deposits is an inevitable consequence of exposure to seawater unless the deposit is rapidly covered by sediment and(or) volcanic material that shields sulfides from seawater contact. Anoxic, circumneutral bottom waters also contain a small amount of oxygen so that, under anoxic conditions, the weathering of the deposit may be slowed but not halted.

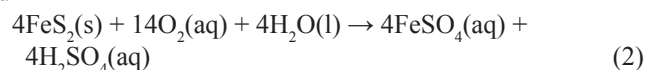
Microbial degradation of seafloor sulfides—for instance, pyrrhotite—also may be an important process of seafloor weathering (Toner and others, 2009). If a VMS deposit is preserved in the rock record, which must be a relatively rare event, it may be subject to subaerial degradation if exposed to abiotic reactions involving surface and near-surface oxygenated fluids, atmospheric oxygen, and biotic reactions involving bacterial activity. Halmyrolysis and subaerial degradation require similar oxidative chemical reactions, the differences being largely determined by the presence or absence of gaseous oxygen, dissolved oxygen and iron concentrations, and hydrologic setting. The deleterious environmental consequences of subaerial degradation of VMS ores and the resulting acid drainage production, has received particular attention from environmental geochemists over the past few decades (Evangelou, 1995; Plumlee, 1999).

Mineralogic Reactions to Establish Process

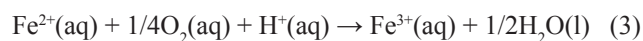
The physical and chemical degradation of a deposit is largely determined by the rates of oxidation of sulfides. There is a substantive amount of literature on the mechanisms and rates of pyrite oxidation (see Evangelou, 1995, for a review) but less information on other sulfides that are commonly found in VMS deposits. Pyrite can be directly oxidized by seawater oxygen depending upon the oxygen concentration, which is a function of the rate of fresh seawater renewal and the degree of bottom water anoxia:



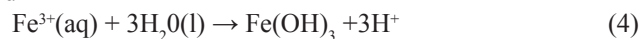
and



Both reactions produce significant acidity, but the extent to which the fluid acidity is maintained is determined by the degree to which these initial reactions occur in a closed system. Pyrite oxidation also can be accomplished through indirect exothermic reactions using oxygen and ferric iron. Solubility of Fe(III) is strongly pH dependent; however, even in circumneutral seawater the concentrations of Fe(III) are sufficient to dominate the oxidation of iron sulfides. In a system that is open to seawater circulation, the acidity and dissolved iron are removed into the large reservoir of ocean water. The presence of a carapace of seafloor gossan, composed principally of ferric oxides and oxy-hydroxides, reflects the low solubility of Fe(III) in solution and implies fluid pH values that are either neutral or slightly alkaline:



and



These reactions continue until the solid pyrite is exhausted or the sulfidic material is isolated from ambient seawater. The presence of a surface in situ gossan may

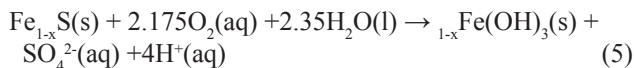
substantially slow down the rate at which the underlying sulfidic material is oxidized. Initially, gossans have a high porosity and permeability, so they do not form an efficient impermeable barrier to the circulation of seawater, but, upon compaction, gossans can form a highly effective impermeable barrier. The slowest step of reactions 1-4, and possibly other intermediate steps, initially determines the rate of pyrite oxidation. However, the rate of oxidation is also a function of available dissolved oxygen and the extent to which ferric-bearing minerals encapsulate, and hence shield, pyrite from reaction with oxygenated seawater.

The origin of gossans associated with VMS deposits is not clearly established. Some appear to have formed on the seafloor whilst others are related to subaerial oxidation. The chemistry of seafloor gossans (Mills and others, 2001) has been interpreted in terms of precipitation from low-temperature vent fluids and hydrogenous reactions involving ambient seawater. However, seafloor weathering of unstable sulfide minerals ultimately produces metal oxides and oxyhydroxides, so some gossans must be a product of halmyrolysis. It seems likely that seafloor gossans represent a spectrum of overlapping processes involving low-temperature vent fluids and ambient seawater.

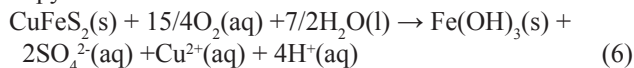
Modern SMS deposits are the sites of abundant micro- and macrofauna, and fossilized macrofauna have been encountered in ancient VMS deposits, such as those in the southern Urals (Little and others, 1997) and the Troodos (Little and others, 1999). Because the food chain for macro fauna begins at the bacterial level, it is reasonable to assume that ancient VMS deposits were also the sites of abundant microfauna. Thus, direct and indirect oxidation of sulfides also may be mediated by chemosynthetic bacteria, which is a common phenomenon in modern SMS deposits (Toner and others, 2009).

Of the major iron sulfides found in VMS deposits (pyrite, pyrrhotite, and marcasite), pyrrhotite is the most reactive and pyrite the least. This appears to be true for both abiotic and biotic oxidation. Other sulfides are also unstable in ambient, oxygenated seawater. The extent to which these sulfides are destroyed is a function of: (1) their iron content and, hence, the extent to which Fe(II) is available for redox reactions; (2) the stability of the crystal lattice, which is partly a function of the degree to which the lattice can accommodate minor and trace elements; and (3) the metal/sulfur ratio that determines the extent of sulfuric acid production (Lottermoser, 2003). Some reactions that involve iron-bearing sulfides and dissolved oxygen under abiotic conditions are shown below, in which ferric hydroxide $[\text{Fe}(\text{OH})_3]$ is used as a generalized formula for a potential complex series of secondary oxides and oxyhydroxides:

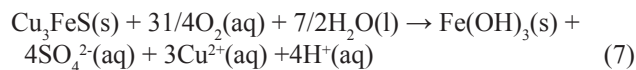
Pyrrhotite:



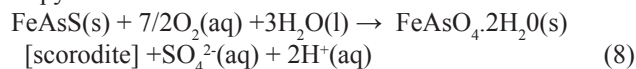
Chalcopyrite:



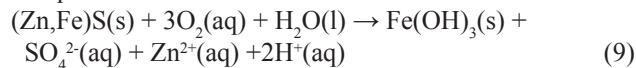
Bornite:



Arsenopyrite:

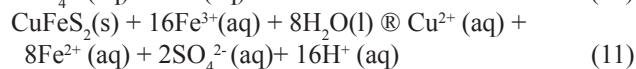
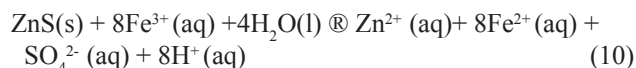


Fe-rich sphalerite:



In these cases, the reduced dissolved metal species are more soluble than dissolved Fe(III) and (or) their precipitation is kinetically inhibited, so that Fe(III)-bearing minerals tend to dominate the mineralogy of seafloor gossans associated with VMS deposits. Initially, however, the presence of cations other than iron in solution results in replacement of iron sulfides by secondary minerals, such as copper, zinc and lead sulfides, and possibly sulfates. The different solubilities of ferric iron and manganese can result in large variations in the Fe/Mn ratios of seafloor gossans (Mills and others, 2001). Common minerals formed during halmyrolysis include goethite, hematite, birnesite, todorike, Fe-smectite, and various silica polymorphs. Iron silicates, usually smectite, can also occur as a major component of several "postdepositional" hydrothermal deposits.

Koski and others (2008) determined a resistance to oxidation in the subaerial environment in the order pyrrhotite < sphalerite < chalcopyrite < pyrite, but it is unknown if this sequence also applies to the seafloor environment. The common presence of sphalerite in seafloor gossans suggests that sphalerite, or at least Fe-poor varieties, may be resistant to oxidation. Some nonferrous sulfides, such as galena, are highly resistant to oxidative weathering. Although pyrite may be the most resistant of the major sulfide components of VMS deposits, it is often the dominant sulfide phase, so frequently pyrite oxidation is the rate-determining step in mass oxidative wasting. Rimstidt and others (1994), Plumlee (1999), Koski and others (2008), and Corkhill and others (2008) consider that the reaction rates in the oxidation of sphalerite, chalcopyrite, arsenopyrite, and enargite are not primarily determined by oxygen but by redox reactions involving bacterially-produced ferric iron; for example:



Geochemical Processes

Halmyrolic degradation is the rule rather than the exception during the life cycle of a VMS deposit, the corollary being that exceptional circumstances are required to preserve a VMS deposit in the rock record. The most important consequence of seafloor weathering is initial high-grading of the deposit due to supergene replacement processes, but eventually there

is a substantive loss of metals into the water column and(or) a physical degradation of the deposit as it loses coherence (Koski and others, 2003). At an advanced stage of degradation, insoluble oxides and oxyhydroxides precipitate and have a high adsorptive capacity. These minerals scavenge elements, particularly transitional metals, from seawater and(or) from pore fluids after they have been released from sulfides and secondary minerals. The scavenging efficiencies are principally determined by the rate of accumulation of the oxides and oxyhydroxides. Probably ninety nine percent or more of metals are lost during seafloor weathering if gossans are formed.

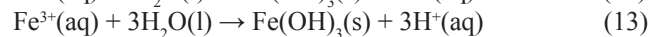
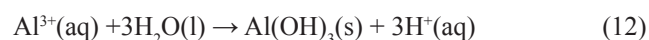
The extent to which the transfer of material to the water column during halmyrolysis contributes to the marine element budget has yet to be assessed, but it may be a significant effect. Precious metals may be high graded in secondary gossans, especially if the original sulfide ore contained Au and Ag primary minerals. For instance, the Letneye deposit in the southern Urals contains a variety of primary precious metal tellurides—such as sylvanite, volynskite, attaitite, and stutzite—that, upon oxidation either released native precious metals or produced secondary, high grade minerals such as hessite and acanthite.

Thus, the common late-stage products of seawater weathering include the formation of gossans that have many physical and chemical features in common with subaerial gossans. In the literature, they have received relatively little attention, except as indicators of subsurface mineralization. Exceptions include the Cretaceous-age ochres of Troodos (Constantinou and Govett, 1972; Robertson and Hudson, 1973; Robertson, 1976; Robertson and Fleet, 1976; Herzig and others 1991), various deposits in the southern Urals (Yaman-Kasy, Sibay, Uchaly, Letneye; Herrington and others, 2005), and the gossans associated with the TAG hydrothermal field (Hannington and others, 1988). Ochres associated with the sulfide deposits in Troodos are economic for precious metals (Constantinou and Govett, 1972).

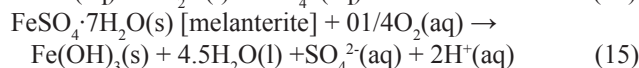
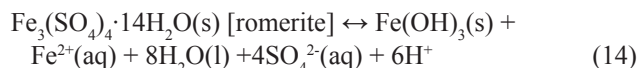
The formation of secondary oxides and oxyhydroxides also produces a substantial reduction in density relative to the original sulfide ore. This property can result in the transport through bottom currents of the secondary products away from the origin site of ore deposition, which in turn results in an increase in the aspect ratio (length:thickness) of the deposit (Herrington and others, 2005). However, the gossans may remain physically associated with sulfide ore if the degree of weathering is limited and the deposit is rapidly covered, for example, the ochres within the Skouriotissa VMS deposit in the Troodos Massif, Cyprus. Gossans also may be preserved if there is an absence of seawater movement in bottom currents. The gossans may be associated with other chemical sediments, such as the umbers of Troodos. The genetic relationships between ochres and umbers is unclear, although the latter appear to be a consequence of low-temperature hydrothermal venting, as observed at the TAG hydrothermal field (Mills and others, 2001), and have many features in common with metaliferous sediments at mid-ocean ridges (Bostrom and Peterson, 1969).

The various reactions highlighted above, which also may be extended to subaerial oxidation, provide a useful general picture of the geochemical changes that occur during seafloor halmyrolysis. Subaerial weathering of exposed VMS deposits and, if mined, their mill tailings and spoil heaps involves processes and products that have commonality with seafloor weathering. Notable differences involve the presence of gaseous oxygen, oxygen-rich meteoric water, variable climate, and hydrology, all of which affect the processes and products of sulfide oxidation. The effect of subaerial weathering is the development of drainage with a high acidity and metal content that may have deleterious environmental effects (Eppinger and others, 2007). The limitations on acidity are provided by the availability of sulfide minerals to suitable oxidation reactions and (or) acid buffering reactions. These latter reactions involve gangue minerals and country rock that consume hydrogen ions, such as silicates and carbonates.

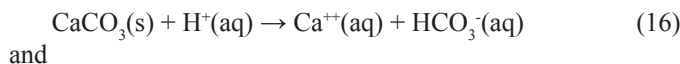
The manganese-rich nature of subaerial gossans contrasts with the manganese-poor gossans developed on the seafloor, where dissolved manganese may be transported away from the site of gossan development. In the subaerial environment, solutions may be more static, so their chemical evolution may result in dissolution of Mn-bearing minerals and precipitation of manganese oxides, hydroxides, and oxyhydroxides at the same site as precipitation of ferric minerals. High acidity develops if reactions take place under lower water/rock ratios, and the weathering process can be considered as a one-pass continuous flow reactor. The reactions described above for seawater weathering are generally applicable for subaerial weathering, but the increased acidity results in increased solubility of cations. In effect, subaerial oxidation of a VMS deposit is a significantly faster process than halmyrolysis. Increased solubility of cations, such as Fe(III) and Al(III), produce additional acidity by precipitation of hydroxides, such as ferric and aluminum hydroxides, and sulfates may precipitate upon fluid mixing and(or) evaporation:



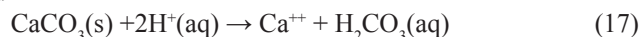
Such phases remain highly stable. These reactions produce a positive redox feedback loop (reduced species in sulfide minerals and oxidized species in solution) that continuously increases acidity in solution. During subaerial weathering, a wide variety of complex sulfates, hydroxysulfates, oxides, hydroxides, carbonates, silicates, and native metals may precipitate as secondary minerals, commonly as a result of evaporation. Over 100 minerals have been recognized, many of which are inherently unstable in an aqueous environment. As noted above, the precipitation of some hydroxides releases acidity, whereas the formation of sulfates and hydroxysulfates—such as jarosite, alunite, schwertmannite, and romerite—consumes protons. Many of these minerals are soluble, whereby acidity is again released; for instance:



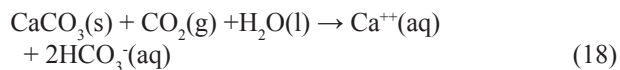
The presence of limestone country rock, or any carbonate-bearing assemblages, can mitigate the effects of acid drainage. Congruent reactions of acid drainage that involve carbonates (calcite, dolomite, siderite, ankerite, magnesite) result in partial or complete mineral dissolution and production of bicarbonate ions or carbonic acid, depending upon the pH of the acidic solution (Sherlock and others, 1995). Calcite is more easily dissolved than other carbonate minerals. In the absence of gaseous CO_2 in the phreatic zone, the dissolution of calcite occurs in a closed system and the reactions proceed as follows:



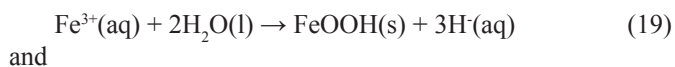
and



However, the presence of gaseous CO_2 in the vadose zone results in open system behavior limited only by the availability of one or more carbonate minerals. Increased calcite dissolution generates more bicarbonate ions and enhances consumption of acidity:



Some VMS deposits contain siderite, whose acid consumption capability is E_h dependent. Under reducing conditions, iron is released into solution as Fe(II) ions. In the presence of gaseous oxygen, released iron is present as Fe(III) and is subsequently hydrolyzed to ferric oxide or ferric oxyhydroxide (reactions 15,16), which produces acidity. In this case, the presence of siderite has no effect on the acidity of the solution.

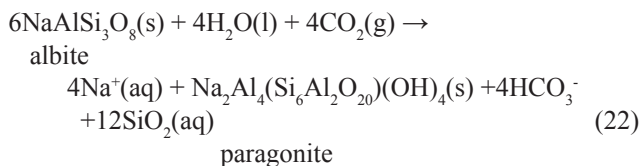
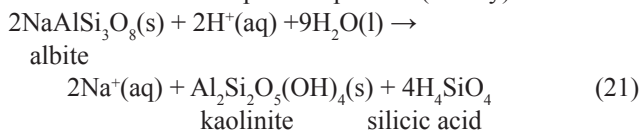


and



Silicate minerals are a ubiquitous part of VMS deposits. They occur as: (1) gangue minerals intimately associated with sulfides; (2) minerals within rocks that form a part of the VMS stratigraphic framework; and (3) secondary minerals developed during hydrothermal, supergene, and weathering processes. A very large variety of silicates are associated with VMS deposits, ranging from ferromagnesian minerals (olivine, pyroxene, amphibole, mica), to alkali-bearing aluminosilicates (feldspar, clay), to simple oxides (magnetite, hematite, quartz). The acid buffering capacity of these minerals and their host rocks vary widely in terms of potential chemical reactions and hydrologic considerations that determine the pathways of fluid movement. Highly siliceous rocks, such as rhyolites, quartzites, and siliceous argillites, have little buffering capacity. In

contrast, basic and ultrabasic igneous rocks and shales have a stronger buffering capacity. Generally, reactions with silicates are incongruent with the formation of secondary minerals (kaolinite, illite, montmorillonite), silicic acid, or bicarbonate ions and with the consumption of protons (acidity).



If dissolved silica in reaction 22 reaches saturation, then either chalcedony or opal may precipitate. The buffering capacity of the system is limited by further reactions that produce protons, such as precipitation of gibbsite.

Factors Controlling Rates of Reaction

There have been relatively high numbers of experimental studies of the kinetics of sulfide oxidation for those sulfides that are least resistant to oxidation (pyrite, marcasite, and pyrrhotite; Lawson, 1982; Wiersma and Rimstidt, 1984; McKibben and Barnes, 1986; Moses and others, 1987; Moses and Herman, 1991; Evangelou and Zhang, 1995; Janzen and others, 2000). However, there have been fewer studies for sulfides that are common in VMS deposits but are more resistant to weathering (molybdenite, cinnabar; Daskalakis and Helz, 1993; Jambor, 1994; Rimstidt and others, 1994; Weisener and others, 2003). The factors controlling the rates of sulfide oxidation are both chemical and physical. The physical factors include:

11. hydrologic considerations—such as grain and fracture porosity/permeability (Plumlee, 1999) and hydraulic head—that determine the velocity of fluid movement and the extent to which advection moves reactant products from reaction sites and prevents surface poisoning; and
12. the geometry of sulfide minerals—such as crystal form, grain sizes and shapes, surface roughness, fractures, cleavage planes, pits, and edges—that collectively determines the specific surface area of reactant minerals and the presence of high energy domains.

Chemical factors include:

1. the pH of the reactant fluid that determines the solubility of Fe(III);
2. the presence of dissolved oxygen, Fe(II) and Fe(III) ions, and their solution concentrations;

3. mineral phase chemistry;
4. species activation energies for reaction progress;
5. rate laws (equations) for specific oxidative reactions; and
6. the physicochemical prehistory of the solid reactants, particularly temperature.

Non-oxidative reactions are pH dependent. Pyrite and marcasite do not undergo such reactions. Pyrrhotite and some other sulfides, such as sphalerite, can undergo non-oxidative dissolution by acidic solutions in the absence of dissolved oxygen and ferric iron (Janzen and others, 2000). Such conditions are unlikely in nature but might occur in the saturated zone.

The solubility of ferric iron is strongly pH dependent, being inversely correlated. At high initial ferric iron concentrations in acidic systems, the rate of oxidation of iron sulfides (FeS_2 , Fe_{1-x}S) is efficient and obeys a zero order rate law, that is, the rate of oxidation is independent of concentration of reactants. At low ferric iron concentrations, as might be expected in circumneutral and alkaline systems, the oxidation of iron sulfide is dominated by reduction of ferric iron but the rate law is fractional. The rate constant, as measured by the rate of ferrous iron production, is approximated at 0.5, that is, the oxidation rate is proportional to the square root of ferric iron concentration.

Over a wide range of pH conditions and, hence, dissolved ferric iron concentrations, the rate laws are consistent with oxidation that involves complex sorption and desorption processes at the solid crystal surface. For instance, Moses and Herman (1991) demonstrate that ferrous iron adsorbed onto the surface of pyrite is a critical part of pyrite oxidation, as originally proposed by Singer and Stumm (1970). Reactions 1 and 3 indicate the importance of dissolved Fe(II) as an intermediary in electron transfer between pyrite and dissolved oxygen. The overall mechanism takes advantage of the preferential adsorption of Fe(II) onto pyrite surfaces and the preference of Fe(III) as the pyrite oxidant. The surface concentration of Fe(II) determines the reaction rate. Electrons are transferred from the pyrite surface to dissolved oxygen via adsorbed Fe(II) that is consequently oxidized to Fe(III). The latter is subsequently reduced to adsorbed Fe(II) by fast transfer of another electron from the pyrite surface and the cycle of oxidation and reduction is then repeated.

Effects of Microclimate and Macroclimate

Plumlee (1999) provides a useful summary of the weathering of sulfidic ores in varying climatic zones. A fundamental consideration in the oxidation of such ores in the subaerial environment and the formation and dispersal of acid drainage is the availability and flow of water. The latter is determined by the hydraulic conductivity of the overall system and also

by the hydrologic cycle, both being determined by climate to some degree. The hydraulic conductivity of rocks depends upon: (1) the intrinsic permeability (grain-to-grain, fracture, mine workings); and (2) the degree of fluid saturation, this being determined by the position of the water table, which is a function of climate and local topography. Microclimates are particularly important in areas of significant elevation changes, for example, the Rocky Mountains, where precipitation changes can be extreme and periods of freezing and thawing can produce changes in hydraulic conductivity and increased rock exposure caused by the absence of significant biological groundcover. Extremes of microclimate are also important in remediation efforts where accessibility and biologic activity may be seasonally limited.

The availability of water is determined by the regional and local cycles of precipitation/evapotranspiration and humidity, which are functions of climate. In arid and semiarid climates, the flow of surface water may be seasonal, limited by the duration of wet periods punctuated by periods when surface evaporation exceeds rainfall (Nordstrom, 2009). Under these conditions, acidic surface waters may either disappear to dryness, or be greatly reduced in volume, resulting in precipitation of minerals that carry substantial acidity, for example, melanterite ($\text{FeSO}_4 \cdot 7\text{H}_2\text{O}$) and chalcantite ($\text{CuSO}_4 \cdot 5\text{H}_2\text{O}$). Nordstrom and Alpers (1999) provide a classic description of the processes of evaporation and re-solution at the Iron Mountain, Calif., VMS deposit. Subsequent periods of rainfall may result in re-solution of these minerals and dispersal of acid waters into surface waters and groundwaters. In temperate and tropical climates, abundant rainfall may result in excessive weathering, particularly through the action of organic acids. Flooding may result in physical transport of materials, for instance, downstream movement and dispersal of mine tailings, with the consequent increase in water turbidity and aerial extension of plumes of acidic drainage.

Effects of Hydrologic Setting

A fundamental consideration in the oxidation of sulfidic ores in the subaerial environment and the formation and dispersal of acid drainage is the availability and flow of water. The latter is determined by the hydraulic conductivity of the overall system and also by the hydrologic cycle, both being determined by climate to some degree. The hydraulic conductivity of rocks depends upon: (1) the intrinsic permeability (grain-to-grain, fracture, mine workings); and (2) the degree of fluid saturation, this being determined by the position of the water table, which is a function of climate and local topography. In arid and semiarid climates, subaerial gossans developed atop VMS ores provide a porous cap that allows further access to the underlying fresh ore.

References Cited

- Boström, K., and Peterson, M.N.A., 1969, The origin of aluminum-poor ferromanganous sediments in areas of high heat flow on the East Pacific Rise: *Marine Geology*, v. 7, p. 427–447.
- Constantinou, G., and Govett, G.J.S., 1972, Genesis of sulfide deposits—Ochre and amber of Cyprus: *Transactions of Institute of Mining and Metallurgy*, v. 81, p. B34–B46.
- Corkhill, C.L., Wincott, P.L., Lloyd, J.R., and Vaughan, D.J., 2008, The oxidative dissolution of arsenopyrite (FeAsS) and enargite (Cu₃AsS₄) by *Leptosprillum ferrooxidans*: *Geochimica et Cosmochimica Acta*, v. 72, p. 5616–5633.
- Daskalakis, K.D., and Helz, G.R., 1993, The solubility of sphalerite (ZnS) in sulfidic solutions at 25°C and 1 atm pressure: *Geochimica et Cosmochimica Acta*, v. 57, p. 4923–4931.
- Eppinger, R.G., Briggs, P.H., Dusel-Bacon, C., Giles, S.A., Gough, L.P., Hammerstrom, J.M., and Hubbard, B.E., 2007, Environmental geochemistry at Red Mountain, an unmined volcanogenic massive sulfide deposit in the Bonfield district, Alaska Range, east-central Alaska: *Geochemistry—Exploration, Environment, Analysis*, v. 7, p. 207–223.
- Evangelou, V.P., 1995, Pyrite oxidation and its controls: Boca Raton, Fla., CRC Press, 293 p.
- Evangelou, V.P., and Zhang, Y.L., 1995, A review—Pyrite oxidation mechanisms and acid mine drainage prevention: *Critical Reviews in Environmental Science and Technology*, v. 25, p. 141–199.
- Hannington, M.D., Thompson, G., Rona, P.A., and Scott, S.D., 1988, Gold and native copper in supergene sulphides from the Mid-Atlantic Ridge: *Nature*, v. 333, p. 64–66.
- Herrington, R.J., Maslennikov, V., Zaykov, V., Seravkin, I., Kosarev, A., Buschmann, B., Orgeval, J.-J., Holland, N., Tesalina, S., Nimis, P., and Armstrong, R., 2005, Classification of VMS deposits—Lessons from the South Uralides: *Ore Geology Reviews*, v. 27, p. 203–237.
- Herzig, P.M., Hannington, M.D., Scott, S.D., Maliotis, G., Rona, P.A., and Thompson, G., 1991, Gold-rich sea-floor gossans in the Troodos ophiolite and on the Mid-Atlantic Ridge: *Economic Geology*, v. 86, p. 1747–1755.
- Jambor, J.L., 1994, Mineralogy of sulfide-rich tailings and their oxidation products, *in* Jambor, J.L., and Blowes, D.W., eds., *Environmental geochemistry of sulfide mine-wastes: Mineralogical Association of Canada Short Course Series*, v. 22, p. 59–102.
- Janzen, M.P., Nicholson, R.V., and Scharer, J.M., 2000, Pyrrhotite reaction kinetics—Reaction rates for oxidation by oxygen, ferric iron, and for nonoxidative dissolution: *Geochimica et Cosmochimica Acta*, v. 64, p. 1511–1522.
- Koski, R.A., German, C.R., and Hein, J.R., 2003, Fate of hydrothermal products from mid-ocean ridge hydrothermal systems—Near-field to global perspectives, *in* Halbach, P.E., Tunnicliffe, V., and Hein, J.R., eds., *Energy and mass transfer in marine hydrothermal systems*: Berlin, Dahlem University Press, p. 317–335.
- Koski, R.A., Munk, L., Foster, A.L., Shanks, W.C., III, and Stillings, L.L., 2008, Sulfide oxidation and distribution of metals near abandoned copper mines in coastal environments, Prince William Sound, Alaska, USA: *Applied Geochemistry*, v. 23, p. 227–254.
- Little, C.T.S., Herrington, R.J., Maslennikov, V.V., Morris, N.J., and Zaykov, V.V., 1997, Silurian hydrothermal-vent community from the southern Urals, Russia: *Nature*, v. 385, p. 146–148.
- Little, C.T.S., Cann, J.R., Herrington, R.J., and Morisseau, M., 1999, Late Cretaceous hydrothermal vent communities from the Troodos ophiolite, Cyprus: *Geology*, v. 27, p. 1027–1030.
- Lottermoser, B., 2003, *Mine wastes*: Berlin, Springer, 277 p.
- Lowson, R.T., 1982, Aqueous oxidation of pyrite by molecular oxygen: *Chemical Reviews*, v. 82, p. 461–497.
- McKibben, M.A., and Barnes, H.L., 1986, Oxidation of pyrite in low temperature acidic solutions—Rate laws and surface textures: *Geochimica et Cosmochimica Acta*, v. 50, p. 1509–1520.
- Mills, R.A., Wells, D.M., and Roberts, S., 2001, Genesis of ferromanganese crusts from the TAG hydrothermal field: *Chemical Geology*, v. 176, p. 283–293.
- Moses, C.O., and Herman, J.S., 1991, Pyrite oxidation at circumneutral pH: *Geochimica et Cosmochimica Acta*, v. 55, p. 471–482.
- Moses, C.O., Nordstrom, D.K., Herman, J.S., and Mills, A.L., 1987, Aqueous pyrite oxidation by dissolved oxygen and by ferric iron: *Geochimica et Cosmochimica Acta*, v. 51, p. 1561–1571.
- Nordstrom, D.K., 2009, Acid rock drainage and climate change: *Journal of Geochemical Exploration*, v. 100, p. 97–104.

- Nordstrom, D.K., and Alpers, C.N., 1999, Geochemistry of acid mine waters, *in* Plumlee, G.S., and Logsdon, M.J., eds., The environmental geochemistry of mineral deposits—Part A. Processes, techniques, and health issues: Reviews in Economic Geology, v. 6A, p. 161–182.
- Plumlee, G.S., 1999, The environmental geology of mineral deposits, *in* Plumlee, G.S., and Logsdon, M.J., eds., The environmental geochemistry of mineral deposits—Part A. Processes, techniques, and health issues: Reviews in Economic Geology, v. 6A, p. 71–116.
- Rimstidt, J.D., Chermak, J.A., and Gagen, P.M., 1994, Rates of reaction of galena, sphalerite, chalcopyrite, and arsenopyrite with Fe(III) in acidic solutions, *in* Alpers, C.N., and Blowes, D.W., eds., Environmental geochemistry of sulfide oxidation: American Chemical Society, v. 550, p. 2–13.
- Robertson, A.H.F., 1976, Origin of ochres and umbers—Evidence from Skouriotissa, Troodos Massif, Cyprus: Transactions of Institute of Mining and Metallurgy, v. 86, p. B245–B251.
- Robertson, A.H.F., and Fleet, A.J., 1976, Rare-earth element evidence for the genesis of the metalliferous sediments of Troodos, Cyprus: Earth and Planetary Science Letters, v. 28, p. 385–394.
- Robertson, A.H.F., and Hudson, J.D., 1973, Cyprus umbers—Chemical precipitates on a Tethyan ocean ridge: Earth and Planetary Science Letters, v. 18, p. 93–101.
- Sherlock, E.J., Lawrence, R.W., and Poulin, R., 1995, On the neutralization of acid rock drainage by carbonate and silicate minerals: Environmental Geology, v. 25, p. 43–54.
- Singer, P.C., and Stumm, W., 1970, Acidic mine drainage—The rate-determining step: Science, v. 167, p. 1121–1123.
- Toner, B.M., Santelli, C.M., Marcus, M.A., Wirth, R., Chan, C.S., McCollum, T., Bach, W., and Edwards, K.J., 2009, Biogenic iron oxyhydroxide formation at mid-ocean ridge hydrothermal vents—Juan de Fuca Ridge: *Geochimica et Cosmochimica Acta*, v. 73, p. 388–403.
- Wiersma, C.L., and Rimstidt, J.D., 1984, Rates of reaction of pyrite and marcasite with ferric iron at pH 2: *Geochimica et Cosmochimica Acta*, v. 48, p. 85–92.
- Weisener, C.G., Smart, R.St.C., and Gerson, A.R., 2003, Kinetics and mechanisms of the leaching of low Fe sphalerite: *Geochimica et Cosmochimica Acta*, v. 67, p. 823–830.

14. Geochemical Characteristics

By W. Ian Ridley

14 of 21

Volcanogenic Massive Sulfide Occurrence Model

Scientific Investigations Report 2010–5070–C

U.S. Department of the Interior
U.S. Geological Survey

U.S. Department of the Interior
KEN SALAZAR, Secretary

U.S. Geological Survey
Marcia K. McNutt, Director

U.S. Geological Survey, Reston, Virginia: 2012

For more information on the USGS—the Federal source for science about the Earth, its natural and living resources, natural hazards, and the environment, visit <http://www.usgs.gov> or call 1-888-ASK-USGS.

For an overview of USGS information products, including maps, imagery, and publications, visit <http://www.usgs.gov/pubprod>

To order this and other USGS information products, visit <http://store.usgs.gov>

Any use of trade, product, or firm names is for descriptive purposes only and does not imply endorsement by the U.S. Government.

Although this report is in the public domain, permission must be secured from the individual copyright owners to reproduce any copyrighted materials contained within this report.

Suggested citation:

Ridley, W. Ian, 2012, Geochemical characteristics in volcanogenic massive sulfide occurrence model: U.S. Geological Survey Scientific Investigations Report 2010-5070 -C, chap. 14, 18 p.

Contents

| | |
|---|-----|
| Trace Elements and Element Associations | 207 |
| Zoning Patterns | 207 |
| Fluid-Inclusion Thermometry and Geochemistry | 211 |
| Stable Isotope Geochemistry | 215 |
| $\delta^{18}\text{O}$ and δD | 215 |
| $\delta^{34}\text{S}$ | 216 |
| $\delta^{11}\text{B}$, $\delta^{64}\text{Cu}$, $\delta^{66}\text{Zn}$, $\delta^{57}\text{Fe}$, $\delta^{82}\text{Se}$ | 216 |
| Radiogenic Isotope Geochemistry..... | 220 |
| References Cited..... | 222 |

Figures

| | |
|--|-----|
| 14-1. Idealized cross sections through the two main stages of growth of a massive sulfide chimney | 209 |
| 14-2. Idealized cross section through the Trans-Atlantic Geothermal hydrothermal field based on Alvin dive observations and Ocean Drilling Program drilling during Leg 158 | 210 |

Tables

| | |
|--|-----|
| 14-1. Modern and ancient volcanogenic massive sulfide deposits with high sulfidation state minerals | 208 |
| 14-2. Fluid inclusion thermometry and chemical compositions for selected volcanogenic massive sulfide deposits | 212 |
| 14-3. Some transitional metal isotope ratios in volcanogenic massive sulfide deposits and related rocks..... | 218 |
| 14-4. Lead isotopic composition of selected volcanogenic massive sulfide deposits..... | 221 |

14. Geochemical Characteristics

By W. Ian Ridley

Trace Elements and Element Associations

Volcanogenic massive sulfide deposits are important resources of base and precious metals and a variety of rare elements. The precious and rare metals usually are present at trace concentrations, but natural refining of such metals can determine the economic viability of a deposit. The list of trace elements includes the following: Co, Ni, Ga, Ge, As, Se, Mo, Ag, Cd, In, Sn, Sb, W, Au, Hg, Tl, and Bi. The proportions of metals and their concentrations are largely a function of the overall rock associations and fluid chemistry. For instance, in Canadian VMS deposits, felsic-dominated deposits have high Pb and Ag, whereas the bimodal-felsic deposits contain the highest Au concentrations. In many cases, the trace-element associations are determined by the overall chemistry of the various lithologies that are encountered by fluid during hydrothermal circulation, and they may be determined by lithologies that are distal to the deposit. For instance, the Mount Read deposits in Tasmania carry anomalously high concentrations of Au that appear to have been sourced from distal high-Ti basalts (Stolz and Large, 1992). Volcanogenic massive sulfide deposits, associated primarily with mafic and ultramafic assemblages, tend to have high Co, Ni, and Se concentrations (Galley and others, 2007).

Trace elements may precipitate during mixing of reduced hydrothermal fluids with heated or ambient seawater as a function of the sulfidation state of the fluid. Modern and ancient VMS deposits cover a wide range of sulfidation states based on sulfide mineral assemblages and associated alteration assemblages (Sillitoe and others, 1996). In the presence of low to intermediate sulfidation minerals (pyrrhotite, pyrite, chalcopyrite, arsenopyrite, tennantite, high-Fe sphalerite, galena), trace metals may precipitate as native elements (Bi, Ag, Hg, Sb, Sn). These conditions appear to be mostly met in Cu-Zn deposits associated with mafic assemblages and minor felsic components. In the presence of intermediate to very high sulfidation minerals (pyrite, bornite, digenite, enargite, low-Fe sphalerite), trace elements tend to be fixed in sulfides and sulfosalts, such as famantinite (Cu_3SbS_4), cinnabar (HgS), berthierite (FeSb_2S_4), bismuthinite (Bi_2S_3), stibnite (Sb_2S_3), argentite (Ag_2S), and tennantite ($[\text{Cu,Fe}]_{12}\text{As}_4\text{S}_{13}$) but may also be associated with native Au. In active marine hydrothermal

systems, high sulfidation fluids are associated with island-arc settings, and in ancient VMS deposits they occur in siliciclastic-felsic and felsic lithologic associations (Sillitoe and others, 1996). A list of deposits with high sulfidation characteristics is shown in table 14–1. In many cases, the precipitation of exotic minerals that represent only trace constituents is paragenetically late and spatially associated with barite-rich lithologies, consistent with an increase in sulfidation state with decreasing temperature. The close spatial association with advanced argillic and alunitic alteration indicates that the hydrothermal fluids were highly acidic and corrosive, and the high sulfidation state of the fluids may indicate the involvement of magmatic fluids and gases. This also may be the source of some of the trace elements associated with the high sulfidation minerals.

Zoning Patterns

All VMS deposits show some degree of geochemical/mineralogical zoning that is a function of fluid composition, fluid mixing, temperature, and porosity/permeability. In ancient VMS deposits, the geochemical/mineralogical evolution of deposit growth is difficult to follow, as the later stages of sulfide precipitation tend to overprint earlier stages and there commonly have been several stages of ore mineralization. However, studies of modern black smoker chimneys, for example, those at 21°N and 9°50'N on the East Pacific Rise and at the TAG active hydrothermal field at the Mid-Atlantic Ridge, provide insights into the evolution of sulfide growth. To some degree, these patterns are microcosms of the larger scale zonation observed at the deposit scale because in both cases the mineralogical zonation is a function of fluid chemistry (mixing between hydrothermal fluid and seawater) and a steep temperature gradient (hydrothermal fluid at up to 400 °C and ambient seawater at 1–2 °C). In modern chimney growth, the critical initial stage is the precipitation of anhydrite [CaSO_4] ± caminite [$\text{Mg}_7(\text{SO}_4)_5(\text{OH})_4 \cdot \text{H}_2\text{O}$] from conductively heated seawater as a consequence of the reverse solubility of these minerals. It is the outward and upward precipitation of anhydrite at the seawater interface that stabilizes chimney growth and provides a matrix for precipitation of sulfide phases (Haymon, 1983). The chimney advances upward and outward by anhydrite growth. Hot hydrothermal fluid that circulates

Table 14-1. Modern and ancient volcanogenic massive sulfide deposits with high sulfidation state minerals (after Sillitoe and others, 1996).

[Ag, silver; As, arsenic; Au, gold; Bi, bismuth; Cu, copper; Zn, zinc; al, alunite; and, andalusite; aspy, arsenopyrite; ba, barite; bn, bornite; cass, cassiterite; cc, chalcocite; cinn, cinnabar; cor, corundum; cord, cordierite; cp, chalcopyrite; cv, covellite; dia, diaspore; dig, digenite; en, enargite; gal, galena; gyp, gypsum; id, idiate; kao, kaolinite; ky, kyanite; luz, luzonite; marc, marcasite; mont, montmorillonite; musc, muscovite; ns, native sulfur; po, pyrrhotite; py, pyrite; pyro, pyrophyllite; qz, quartz; rut, rutile; ser, sericite; sp, sphalerite; sulf, sulfosalts; tenn, tennantite; tetra, tetrahedrite; top, topaz; zir, zircon; Mt, million metric tons; g/t, gram per ton]

| Name | Grade, tonnage | Age | Host rocks | Minealization style | Hypogene alteration | Hypogene sulfides |
|----------------------|--|---------------------------------|-------------------------------|--|---|---|
| Hine Hina, Lau Basin | no data | Recent | Andesites | Seafloor massive sulfide | qz, kao,pyro, al, ns, ba | sp, py, marc, bn, cp, tenn, gal, sulf |
| Undu, Fiji | 1.5×105 t 6% Cu, 7% Zn | Pliocene | Dacitic pumice breccia | Massive sulfide pods in pipelike body | qz, kao, mont, gyp, ba | py, cp, sp, gal, en, tenn, cv, id |
| Tsuchihata, Japan | >4.5 Mt 1.2% Cu, Au + Ag | Miocene | Rhyolite dome | Stockwork | qz | py, cp, tetra, en, luz |
| Kizilkaya, Turkey | 10 Mt 1% Cu, 1.5% Zn | Cretaceous | Dacitic volcanics | Stockwork and massive sulfide remnants | qz, ser, kao, dia | py, sp, cp |
| Brewer, USA | 4.6 Mt 14 g/t Au | Late Proterozoic–Early Cambrian | Volcanics and volcanoclastics | Pipe breccia, massive sulfides | and, cord, pyro, al, top, ba, dia, rut, zir | py, en, cv, bn, tenn, cass, Bi, sp, gal, cinn |
| Boliden, Sweden | 8.3 Mt 1.4% Cu, 6.8% As, 15 g/t Au, 50 g/t Ag | Proterozoic | Dacite, qz porphyry, schist | Pipelike massive sulfide | qz, and, musc, dia, cor | py, cp, aspy, po, sp, gal, sulf |
| Bousquet, Canada | No. 1: 20.7 Mt 4.5 g/t Au; No. 2: 7.4 Mt 6.1g/t Au, 16 g/t Ag, 0.6% Cu | Archean | Qz-sericite schist | Stockwork and massive sulfide | qz, and, ky, musc | py, bn, cp, sp, cc, dig, tenn |

within the anhydrite matrix close to the seawater interface is rapidly cooled and precipitates fine-grained, metastable pyrrhotite (po) and Fe-rich sphalerite (sp). As the anhydrite-sulfide matrix grows outward, the inner wall pyrrhotite is replaced by stable pyrite (py) as a result of the admixture of hydrothermal fluid and seawater. Pyrite becomes the dominant mineral phase during chimney growth. Once the chimney structure is established by anhydrite growth, the hydrothermal fluid is isolated and high temperature phases precipitate. Pyrite + Cu-Fe sulfides (chalcopyrite (cp), cubanite (cb; CuFe_2S_3)) precipitate at the inner wall so that the chimney grows inward (fig. 14–1) and also outward, replacing the anhydrite matrix. The diameter of the inner fluid-filled channel is maintained at an equilibrium value as a function of the fluid flow rate, which determines the rate of sulfide precipitation and the rate of abrasion of precipitated material.

Haymon (1983) recognized four different pathways of further chimney evolution: one bornite (bn) sequence and three bornite-absent sequences (a chalcopyrite-dominant sequence, a chalcopyrite-intermediate solid solution (iss) sequence, and a cubanite sequence). These four sequences represent a gradual change in mineralogy (largely by replacement), $p\text{S}_2$, Eh, pH, fluid mixing, and temperature, from an early bornite mineralogy to a late cubanite mineralogy.

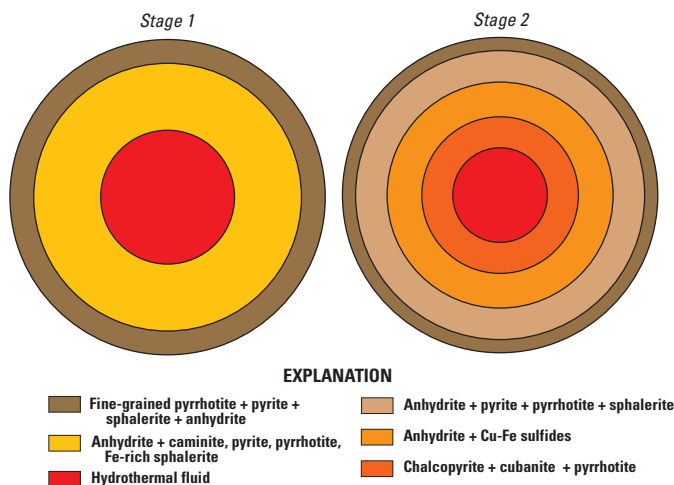


Figure 14–1. Idealized cross sections through the two main stages of growth of a massive sulfide chimney. Stage 1 involves initial deposition of anhydrite followed by precipitation of Fe sulfides and Fe-rich sphalerite in the porous network of anhydrite minerals. The chimney grows outward by addition of anhydrite to the outer chimney wall due to heating of ambient seawater by hot hydrothermal solutions diffusing outward from the central fluid core. Stage 2 growth involves deposition of high-temperature sulfides (chalcopyrite, isocubanite, pyrrhotite) from hydrothermal fluids that are essentially shielded from contact with cool seawater. Percolation of hydrothermal fluid across the chimney wall results in cooling and precipitation of lower temperature sulfides, such as sphalerite. Modified from Haymon (1983). [Cu, copper; Fe, iron]

The bornite sequence involves the precipitation of a sheath of cp around the central fluid channel, followed outward by a zone of bn(Cu_5FeS_4) + chalcocite (cc; Cu_2S) and a zone of covellite (cv; CuS) + digenite (dg; Cu_9S_5) + anhydrite, all of which are accompanied by precipitation of py + sp. This is a sequence of outwardly increasing Cu/Fe ratio, sulfidation, and oxidation state. The chalcopyrite-dominant sequence has a central sheath of cp with outward increase in Cu/Fe ratio and an outer sheath of randomly distributed cp + iss + cp-iss + cb + py + sp in an anhydrite matrix. In the cp-iss sequence, the inner sheath of cp with outward increase in Cu/Fe ratio is surrounded by a sheath of cp-iss + iss with an outward decrease in Cu/Fe ratio. The cb series has a central sheath of cb (no cp) and an outer sheath of randomly scattered grains of cb + py + sp in an anhydrite matrix. The latter sequence forms in mature chimneys where hot (350 °C or hotter) fluids are sufficiently reduced to stabilize cubanite and pyrrhotite, which are also the common sulfide minerals observed in black smoker effluent quenched from 360 °C by ambient seawater.

A field of black (and white) smoker chimneys is not, of itself, an economic resource. In addition, the simple accumulation of black smoker debris on the seafloor would not mimic the clear geochemical/mineralogical zonation commonly observed in ancient VMS deposits. It would instead represent a spatially random collection of sulfide minerals. In 1985, a critical unknown link to ancient VMS deposits was solved with the discovery of the TAG active mound at the Mid-Atlantic Ridge, a roughly circular structure with an estimated total massive sulfide resource of 2.7 Mt (2 percent Cu) and 1.2 Mt of mineralized stockwork breccia (1 percent Cu). The TAG mound was subsequently drilled during Leg 158 of the Ocean Drilling Project, thus providing a three-dimensional perspective of the development of a modern VMS deposit (fig. 14–2). Although the open ocean setting of the TAG deposit probably has no equivalent in ancient VMS deposits, it does have chemical, mineralogical, and volcanological similarities to Cyprus-type VMS deposits.

Probably the most important discovery at TAG was the recognition of intermittent periods of fluid flow within and beneath the sulfide mound, interspersed with periods of fluid discharge at the mound surface. The intermittent behavior was assumed to be in response to: (1) periods of enhanced porosity/permeability within the mound due to mineral dissolution and hydro-fracturing that allowed for dispersed fluid flow at low flow rates and limited entrainment of seawater, and (2) periods of porosity/permeability occlusion due to mineral precipitation (mainly anhydrite, due to the conductive heating of small volumes of seawater) that led to focused, high-rate fluid flow with enhanced entrainment of seawater. The movement of fluid from the base of the deposit (including the underlying stockwork zone) toward the deposit/seawater interface has produced a zone refining effect. The zone refining results from the interplay of variable temperature and fluid chemistry. The periodic movement of high temperature fluids preferentially incorporates phases precipitated earlier from lower temperature fluids. For instance, the preferential dissolution

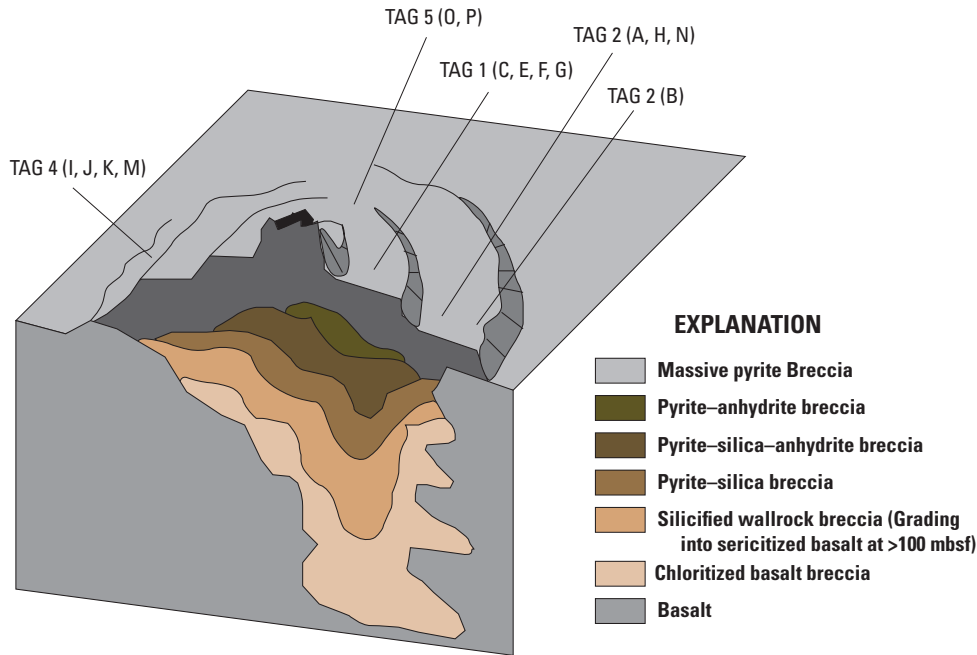


Figure 14-2. Idealized cross section through the Trans-Atlantic Geothermal (TAG) hydrothermal field based on Alvin dive observations and Ocean Drilling Program (ODP) drilling during Leg 158. The ODP holes are shown at TAG 1–5. The TAG field is a combination of inactive vents and active black smoker vents, a mound of sulfide breccia and a carapace of iron oxides (ochres) and weathered sulfide. Drilling has revealed a mineralogically and chemically zoned deposit lying above a silicified stockwork. The main sulfide body is composed of a complex assemblage of sulfide-anhydrite-quartz breccia, but containing very low base metal concentrations compared to surface samples. This is due to continuous zone-refining that causes dissolution of low-temperature minerals and redeposition at the seawater interface. Modified from Humphris and Tivey (2000) and Petersen and others (2000). [mbsf, meters below sea floor]

of Zn-S phases results in the zone purification of Cu-Fe-S ore. The periodic movement of fluids that are undersaturated with respect to some previously precipitated phases also results in dissolution and mass transfer along the fluid gradient. The overall effect is the preferential movement of major and trace elements along a thermal gradient that results in purification, but it also results in the concentration of trace elements into economic grades at the low temperature part of the zone refining pathway. For instance, at the TAG mound, dissolution and recrystallization has produced an almost pure Cu-Fe-S deposit leached of Zn, Cd, Ag, Sb, Pb, and Au that are now redeposited and concentrated within the upper 10 m of the deposit. In principle, the end result would be a barren pyritic ore and the loss and dispersal of other base and other metals into the water column through zone refining, secondary supergene enrichment, and seafloor weathering.

Zone refining provides a useful model for the zonal patterns observed in ancient VMS deposits (Galley and others, 2007). In back-arc mafic settings, the stockwork is frequently a subsurface breccia of chlorite + pyrite and quartz + pyrite

beneath a core of massive pyrite and pyrite + quartz breccia. The latter is sheathed with a marginal facies of sphalerite + chalcopyrite covered with a banded jasper-chert carapace. In the bimodal mafic-felsic setting, the stockwork frequently shows a complex zoned mineralogy that grades outward from pyrrhotite + pyrite + chalcopyrite through quartz + chlorite and chlorite + sulfide to sercite + chlorite. The main sulfide ores grade outward from massive pyrite + pyrrhotite + chalcopyrite to massive pyrite + sphalerite + chalcopyrite. In the bimodal felsic setting, the massive ore commonly grades outward from chalcopyrite + pyrrhotite + pyrite through pyrite + sphalerite + chalcopyrite, pyrite + sphalerite + galena to pyrite + sphalerite + galena + tetrahedrite + Ag + Au. In the felsic-siliciclastic setting, the stockwork zone is highly siliceous and associated with chlorite + pyrrhotite + pyrite + chalcopyrite and may also be Au-bearing, as observed at several of the Mount Read deposits. The massive ores are commonly pyrite + pyrrhotite + chalcopyrite with some Au mineralization grading outward to layered pyrite + sphalerite + galena + Au + Ag.

Thus, zone refining provides an efficient way for upgrading the base metal and precious metal grades of VMS deposits (Shwarz-Schampera and Herzig, 2002). In settings dominated by felsic volcanics, the base metal association of Fe-Zn-Pb-Cu dominates and these deposits frequently contain high-graded, economic amounts of Au, Ag, Sn, Sb, Bi, Co, and In, such as in deposits found at Kidd Creek. Such deposits commonly have a Cu-rich base and a Zn \pm Pb carapace. In addition, there exists a temperature-dependent element fractionation. First, a high-temperature suite forms involving the limited solubility of Cu, Co, Se, In \pm Ni. Second, a low-temperature suite forms, determined by a combination of solubility and volatility, involving Zn, Ag, Au, Pb, Hg, Cd, Bi, Sn, Sb, As, Ga, Hg, \pm Tl \pm W. These high-graded metals may be present as complex sulfides, such as roquesite (CuInS), amalgams, selenides, and sulfosalts.

Fluid-Inclusion Thermometry and Geochemistry

Unlike modern VMS systems where hydrothermal fluids can be sampled directly, no such luxury applies in ancient VMS systems where the chemistry of hydrothermal (and metamorphic) fluids can only be sampled in fluid inclusions. Minuscule volumes of trapped fluids occur in a variety of gangue and ore minerals, but in most cases, studies are limited to inclusions encased in either gangue quartz or low-Fe sphalerite ore. Fluid inclusions most frequently have been used to measure temperatures of entrapment and fluid salinity utilizing microthermometry and, in rare cases, attempts have been made to directly measure gas content (CO₂, CH₄, N₂, SO₂, H₂S), major cation concentrations (Na, K, Ca, Mg), trace cation concentrations (ore elements: Fe, Cu, Zn, Pb, Ba; gangue elements: B, Li, Sr, Rb), and major anions (Cl, S, Br). The several techniques that are used in the study of fluid inclusions have been discussed in detail by Shepherd and Rankin (1998) and Brown (1998).

Fluid inclusions provide an opportunity to understand various aspects of ore deposition processes, including variations in temperature and salinity as a function of ore deposition evolution, fluid mixing and phase separation, and sources of fluids (and hence sources of metals and anions). Table 14-2 illustrates the wide variety of hydrothermal fluid temperatures and salinities observed in gangue and ore minerals involved in the formation of VMS deposits. Most studies of fluid inclusions in VMS deposits have recognized salinities close to seawater values and enhanced salinities in fluids that are generally interpreted as modified seawater. In the latter case, salinity may be increased during hydration reactions with rock minerals along the hydrothermal fluid pathways. In some cases, very high salinities are encountered that may be interpreted as the result of fluid boiling to produce a brine and low-salinity vapor, phase separation at depth, a magmatic fluid, or fluid interactions with evaporates. The fluid salinity

is important because it largely determines fluid density, which in turn determines if the hydrothermal fluid acts as a buoyant liquid when mixed with seawater and cooled or lacks buoyancy and ponds at the seafloor/seawater interface. In the case of buoyant hydrothermal plumes (as observed in modern black and white smoker systems), probably >95 percent of the entrained metals are lost from the immediate site of venting. In the case of stagnant hydrothermal fluids, probably >95 percent of the metals are retained at the site of fluid venting.

A number of studies of the siliciclastic-felsic associated deposits of the Iberian Pyrite Belt deposits have been carried out. These include studies at Neves Corvo and Salgadinho in Portugal and Tharsis, Concepción, San Miguel, Aguas Teñidas, San Telmo, Rio Tinto, and Aznalcóllar in Spain. At Aznalcóllar, the fluids increase in temperature and salinity with depth and toward the central, highly altered stockwork across a range of 200–400 °C. In addition, a low temperature, low salinity fluid also has been trapped that can be interpreted as either cooling upon mixing with a meteoric fluid or the presence of a cooled condensed vapor phase subsequent to fluid boiling (Almodovar and others, 1998). At Rio Tinto, high temperature fluid inclusions have not been found; the majority lies within a narrow temperature range of 130–230 °C with salinities between 2 and 10 percent NaCl equivalent (Nehlig and others, 1998). Evidence for postmineralization redistribution of metals has been found in metamorphic fluids trapped in inclusions at the Tharsis deposits (Marignac and others, 2003) and the Salgadinho deposit (Inverno and others, 2000). The former study is particularly interesting in demonstrating that metamorphic fluids peaked in temperature at 430 °C at 300 MPa pressure and then dropped to 170 °C at 40 MPa, a difference that the authors attributed to a change from lithostatic to hydrostatic conditions.

A detailed fluid inclusion study was carried out by Hou and others (2001) on the Gacun bimodal-felsic deposit in Sichuan, China. They demonstrated an increase in temperature and salinity with depth within the stringer zone involving very high salinity fluids (17–21 percent NaCl equivalent) of unknown origin. Overall, the fluid salinities varied from 4 to 21 percent, the lower values associated with late-stage, low-temperature barites.

There have been surprisingly few fluid inclusion studies of the siliciclastic-felsic associated VMS deposits of Japan, the major contribution being Pisutha-Arnond and Ohmoto (1983). In the Hokuroku District, they demonstrated variations in temperature from 200 to 380 °C but very small variations in fluid salinity (3–6 percent NaCl equivalent). The greatest temperature range was observed in the black ore minerals (200–330 °C), whereas the yellow ore minerals had a limited range (330 \pm 50 °C).

At the siliciclastic-felsic Hellyer deposit, Tasmania, Zaw and others (1996) identified three phases of vein development associated with mineralization. Fluid inclusion from these three phases (2A, 2B, 2C) and a postmineralization vein system provided both temperature and salinity information. Phase 2A inclusions in quartz and sphalerite

Table 14–2. Fluid inclusion thermometry and chemical compositions for selected volcanogenic massive sulfide deposits.

[Ca, calcium; Cl, chlorine; Cu, copper; Fe, iron; K, potassium; Mg, magnesium; Mn, manganese; Na, sodium; Pb, lead; Zn, zinc; TH, temperature; °C, degree Celcius; mmol, millimols; ppm, parts per million; eq, equivalents; temp, temperature; ass., associated]

| Deposit | Mineral | TH °C | Salinity NaCl equivalent | Na mmol | K mmol | Ca mmol | Mg mmol | Mn mmol |
|---|--------------|----------|--------------------------------|--------------|---------------|-------------|------------|------------|
| Hokuroku District, Japan | | | | | | | | |
| Uwamuki 2 | Chalcopyrite | 200–400 | | 220–310 | 9–38 | | | |
| | Quartz | 200–500 | | 76 | 7 | | 6 | |
| Uchinotai West | Pyrite | 200–400 | | 280–470 | | | | |
| | Quartz | 300–500 | | | | | | |
| Fukazawa | Pyrite | 200–400 | | 63–720 | 48–130 | 47–100 | 1–14 | |
| | Sphalerite | 200–400 | | 260–380 | 56 | | 8 | |
| Furutobe | Sphalerite | 200–400 | | 410 | | | 5 | |
| Matsumine | Quartz | 200–500 | | 75–120 | 27–37 | 37–48 | 13 | |
| Shakanai | Pyrite | 200–400 | | 390 | 26 | | | |
| | Quartz | 200–500 | | 150–730 | 3–50 | 3–30 | 2 | |
| Gacun, China | | | | | | | | |
| | Barite | 99–125 | 2.1–13.2 | | | | | |
| | Sphalerite | 125–221 | 6.1–14.5 | | | | | |
| | Quartz | 150–310 | 4.2–10.4 | | | | | |
| | Barite | 196–217 | 6.4–9.3 | | | | | |
| | Sphalerite | 213–258 | 5.7–12.9 | | | | | |
| | Quartz | 150–350 | 6–20.5 | | | | | |
| | Sphalerite | 185–260 | 5.1–7.8 | | | | | |
| | Quartz | 299–319 | 17.1–21.3 | | | | | |
| | Barite | 208–357 | 5.9–16.8 | | | | | |
| Iberian Pyrite Belt, Spain and Portugal | | | | | | | | |
| Rio Tinto | Quartz | 109–330 | 2–10 | | | | | |
| Salgadinho | Quartz | 225–235 | 4.2–5.7 | | | | | |
| Aznalcollar | Quartz | 139–214 | 0.4–7.2 | | | | | |
| | Quartz | 203–299 | 1.2–8.3 | | | | | |
| | Quartz | 306–384 | 4.3–12.4 | | | | | |
| Neves Corvo | Quartz | 230–260 | 2–8 | 0.008–0.019* | | | | |
| | | 280–370 | ~30 | | | | | |
| Tharsis | Quartz | 170–430 | 5.2–9.5 | | | | | |
| Northern Iberian Pyrite Belt | ? | 130–280 | 6–14 | | | | | |
| | ? | 82–110 | 16–24 | | | | | |
| | Quartz | 120–270 | ~4 | | | | | |
| Matagami, Quebec | | | | | | | | |
| Bell Allard | Quartz | 212±34 | 15.8±4.7 | | | | | |
| Isle Dieu | Quartz | 191±18 | 17.7±4.9 | | | | | |
| Orchan West | Quartz | 178±10 | 18.2±2.7 | | | | | |
| Mattagami Lake | Quartz | 233±9 | 15.5±3 | | | | | |
| Bell River Complex | Quartz | 373±44 | 38.2±1.9 | | | | | |
| Eskay Creek, British Columbia | | | | | | | | |
| | Quartz | 109–210 | | 471–1,741** | 43–3,360** | | | |
| | Sphalerite | 96–200 | | 537–2,650** | 231–3,829** | | | |
| Hellyer, Tasmania | | | | | | | | |
| | Quartz | 170–220 | 6.6–14.8 | | 1,030–11,900# | 913–10,300# | | 92–1,320# |
| | Quartz | 165–322 | | | 2,910–43,900# | 992–8,700# | | 140–493# |
| | Quartz | 190–256 | | | | | | |
| | Quartz | | | | 1,280–1,220# | 473–1,920# | | 94–335# |

Table 14–2. Fluid inclusion thermometry and chemical compositions for selected volcanogenic massive sulfide deposits.—Continued

[Ca, calcium; Cl, chlorine; Cu, copper; Fe, iron; K, potassium; Mg, magnesium; Mn, manganese; Na, sodium; Pb, lead; Zn, zinc; TH, temperature; °C, degree Celsius; mmol, millimols; ppm, parts per million; eq, equivalents; temp, temperature; ass., associated]

| Deposit | Cl mmol | SO ₄ mmol | CO ₂ mmol | CH ₄ mmol | Cu ppm | Pb ppm | Zn ppm | Fe ppm |
|---|------------------|-------------------------|-------------------------|-------------------------|------------|-----------|-----------|------------|
| Hokuroku District, Japan | | | | | | | | |
| Uwamuki 2 | 130–430 73 | | 10–140 | | | | | |
| Uchinotai West | 5–480 | | 350 240 | | | | | |
| Fukazawa | 22–270 20–580 | 150 | 210 | | | | | |
| Furutobe | 460 | | | | | | | |
| Matsumine | 290 | 130 | 60–250 | | | | | |
| Shakanai | 88 92–750 | 40–210 | 310 | | 0–4.4 | 0–25 | 0–2.1 | 0–5.6 |
| Gacun, China | | | | | | | | |
| Iberian Pyrite Belt, Spain and Portugal | | | | | | | | |
| Rio Tinto Salgadinho Aznalcollar | | | | | | | | |
| Neves Corvo | 0.008–0.019* | | 20–96* | 3–80* | | | | |
| Tharsis Northern Iberian Pyrite Belt | | | 3–25* | 0.02–1 | | | | |
| Matagami, Quebec | | | | | | | | |
| Bell Allard Isle Dieu Orchan West Mattagami Lake Bell River Complex | | | | | | | | |
| Eskay Creek, British Columbia | | | | | | | | |
| | 565–1,839** | | 0.02–0.99* | 0.07–1.39* | | | | |
| | 700–1,780** | | 0.1–2.64* | 0.35–1.17* | | | | |
| Hellyer, Tasmania | | | | | | | | |
| | 9,070–99,800# | | | | 153–170 | | 105–889 | 235–13,300 |
| | 2,910–43,900# | | | | 237–12,800 | | 373–6,660 | 858–27,200 |
| | 2,670–63,300# | | | | 61 | | 99–286 | 50–591 |

Table 14–2. Fluid inclusion thermometry and chemical compositions for selected volcanogenic massive sulfide deposits.—Continued

[Ca, calcium; Cl, chlorine; Cu, copper; Fe, iron; K, potassium; Mg, magnesium; Mn, manganese; Na, sodium; Pb, lead; Zn, zinc; TH, temperature; °C, degree Celsius; mmol, millimols; ppm, parts per million; eq, equivalents; temp, temperature; ass., associated]

| Deposit | Total salts wt. % | K/Na | Ca/Na | Mg/Na | Na/Cl | Comments | Reference |
|--|-------------------|-----------|-----------|------------|----------|--|----------------------------------|
| Hokuroku District, Japan | | | | | | | |
| Uwamuki 2 | 1.3–2.1 | 0.04–0.12 | | | 0.72–1.7 | Black ore minerals TH = 200–300°C Yellow ore minerals TH = 330±50°C | Pisutha-Armond and Ohmoto (1983) |
| | | 0.08 | | 0.08 | 3.3 | Little change in salinity: 3.5–6 % NaCl eq | |
| Uchinotai West | 2.7 | | | | 1.0 | | |
| Fukazawa | 1.4–5.2 | 0.08–0.18 | 0.12–0.14 | 0.004–0.03 | 0.85–11 | | |
| | 1.5–2.6 | 0.15 | | 0.03 | 0.65–2.6 | | |
| Furutobe | 2.4 | | | 0.01 | 0.90 | | |
| Matsumine | 1.0 | 0.31 | 0.15–0.31 | 0.02 | 1.2 | | |
| Shakanai | 2.5 | 0.07 | | | 4.5 | | |
| | 0.9–4.6 | 0.02–0.07 | 0.02–0.06 | 0.01 | 1–1.6 | | |
| Gacun, China | | | | | | | |
| | | | | | | Upper massive ore | Hou and others (2001) |
| | | | | | | Upper massive ore | |
| | | | | | | Upper massive ore | |
| | | | | | | Middle stringer zone | |
| | | | | | | Middle stringer zone | |
| | | | | | | Middle stringer zone | |
| | | | | | | Lower stringer zone | |
| | | | | | | Lower stringer zone | |
| | | | | | | Mound | |
| Iberian Pyrite Belt, Spain and Portugal | | | | | | | |
| Rio Tinto | | | | | | 90% of inclusion have TH=130–230°C | Nehlig and others (1998) |
| Salgadinho | | | | | | | Inverno and others (2000) |
| Aznalcollar | | | | | | High-T inclusions associated with central stockwork | Almodovar and others (1998) |
| | | | | | | Temp and salinity increase with depth | |
| | | | | | | Temp and salinity increase toward stockwork | |
| Neves Corvo | | | | | | Low salinity, low T fluids are most common | Moura (2005) |
| Tharsis | | | | | | High T, high salinity fluids rare | |
| Northern Iberian Pyrite Belt | | | | | | Fluids are from metamorphic overprint | Marignac and others (2003) |
| | | | | | | Most inclusions in this range | Sanchez-Espana and others (2000) |
| | | | | | | Minor population due to local boiling and cooling | |
| | | | | | | Regional metamorphic fluids | |
| Matagami, Quebec | | | | | | | |
| Bell Allard | | | | | | Low T fluids at all deposits carried Zn but low Cu | Ioannou and others (2007) |
| Isle Dieu | | | | | | | |
| Orchan West | | | | | | | |
| Matagami Lake | | | | | | | |
| Bell River Complex | | | | | | Fluid in zone of hydrothermal cracking, original T = 650–670°C | |
| Eskay Creek, British Columbia | | | | | | | |
| | | | | | | Most inclusions <140°C | Sherlock and others (1999) |
| | | | | | | Most inclusions <150°C | |
| Hellyer, Tasmania | | | | | | | |
| | | | | | | Stage 2A quartz ass. with mineralization | Zaw and others (1996) |
| | | | | | | Stage 2B quartz ass. with mineralization | |
| | | | | | | Stage 2C quartz ass. with mineralization | |
| | | | | | | Stage 4 quartz, post-mineralization metamorphic veins | |

* mole %; ** mmol/L; # ppm

had homogenization temperatures of 170–220 °C, phase 2B inclusions were trapped at 165–320 °C, and phase 2C inclusions were trapped at 190–256 °C. The variations in salinity were relatively small (8–11 percent NaCl equivalent), and the temperature variations at each stage of vein formation were interpreted as reflecting the waxing and waning of a hydrothermal system.

In summary, fluid inclusions in gangue and ore minerals provide important information on the variability of fluid temperature and composition during periods of mineralization and on the involvement of meteoric waters and magmatic fluids. Often, the salinity data alone cannot be uniquely interpreted because involvement of magmatic fluids, boiling, mixing, and phase separation can all produce large variations in fluid salinity. More constrained interpretations are possible if fluid inclusion data are combined with other information, such as stable isotope composition of gangue minerals.

Stable Isotope Geochemistry

Recent reviews of traditional stable isotopes (δD , $\delta^{13}C$, $\delta^{18}O$, $\delta^{34}S$) are provided by Huston (1999) and Ohmoto (1986) for ancient VMS deposits and by Shanks (2001) for modern seafloor hydrothermal VMS systems. Reviews of nontraditional stable isotopes (B, Fe, Cu, Zn, Mo) are provided by Johnson and Bullen (2004), Beard and Johnson (2004), and Albarede (2004). In ore deposit studies, stable isotopes have been used to establish the sources of ore fluids (H, C, O, S), temperatures of ore deposition (S), and silicate alteration (O). In VMS deposits, stable isotopes also have been used to establish pathways of fluid movement (O), fluid origin (H, O, S), redox variations (C, S), and fluid phase separation (O, H). Nontraditional stable isotopes have been used to develop the overall isotopic variability in VMS deposits, to better understand the causes of isotopic fractionations, and to fingerprint sources of metals.

$\delta^{18}O$ and δD

In several studies of whole rock $\delta^{18}O$ in the footwall (stockwork) and some hanging-wall sections of VMS deposits, there is a systematic variation in $\delta^{18}O$ as a function of alteration intensity. The lowest $\delta^{18}O$ values are found where the silicate alteration is most intense, which usually corresponds to the central zone of sericitic alteration, for example, Fukazawa, Japan (Green and others, 1983), Hercules, Tasmania (Green and Taheri, 1992), and Feitais-Estacao, Portugal (Barriga and Kerrich, 1984). Where the deposits can be spatially associated with shallow, subvolcanic stocks, the region of low $\delta^{18}O$ values forms a carapace above the intrusion from which narrow zones of low- $\delta^{18}O$ alteration extend upward into stringer zones beneath individual deposits. In some cases, there is a progressive increase in $\delta^{18}O$ upwards through the subvolcanic sequence (Holk and others, 2008) that probably reflects

the upward decrease in temperature from the magmatic heat source toward the surface. The low- $\delta^{18}O$ zones correspond to regions of focused high-temperature fluid flow surrounded by zones of higher $\delta^{18}O$ alteration that correspond to lower grade alteration mineralogies, such as montmorillonite and zeolite zones.

The final alteration $\delta^{18}O$ value is determined by a number of variables. Taylor (1977) and Green and others (1983) provide similar equations for integrating these variables (water/rock ratio, temperature of reaction, alteration mineralogy, initial bulk rock $\delta^{18}O$ value, fluid $\delta^{18}O$) into a single function. For VMS deposits, some of these variables can be measured or approximated. For instance, fluid $\delta^{18}O$ values have been measured in active seafloor hydrothermal systems (mean 0.91 ± 0.37 per mil, 122 measurements; Shanks, 2001), in fluid inclusions in gangue quartz in ancient VMS deposits (-0.7 ± 1.75 per mil), and in mineral pairs in which temperature is assumed. The fractionation of $\delta^{18}O$ between fluid and rock ($\Delta^{18}O_{R-W}$) as a function of temperature is approximated for felsic systems by using either the measured value for oligoclase-water, and for mafic systems by the measured value for bytownite-water, or by thermodynamic reaction path calculations. Given these constraints, Huston (1999) calculated altered rock $\delta^{18}O$ values as a function of water/rock (W/R) ratio and temperature. They showed that substantive negative changes in $\delta^{18}O$ relative to original fresh rock values (in this case, 8 per mil) can only be achieved at high W/R ratios and at high temperatures, whereas relative positive changes in $\delta^{18}O$ can only be achieved at high W/R ratios and low temperatures. This conclusion is fully consistent with the distribution of $\delta^{18}O$ in altered gangue assemblages described above. That is, hot hydrothermal fluids moving through silicate assemblages with high fracture porosity/permeability causes focused flow to produce alteration assemblages with low $\delta^{18}O$ values, whereas distal fluid flow at lower temperatures produces alteration assemblages with higher $\delta^{18}O$ values.

An important, but contentious, question concerns the origin of fluids for VMS deposits and, consequently, the origin of metals in VMS deposits (see Beatty and others, 1988, for a review). The stable isotopes of oxygen and hydrogen provide important, although somewhat ambiguous, information in this regard because the competing fluid sources (seawater and late-stage magmatic fluid) have quite different $\delta^{18}O$ and δD values (approx. 0 per mil for seawater $\delta^{18}O$ and δD , 5 to 10 per mil $\delta^{18}O$ and -35 to -50 per mil δD for magmatic fluids). Huston and Taylor (1999) and Taylor and Huston (1999) provide useful appraisals as to the shifts away from either seawater or magmatic fluid compositions of $\delta^{18}O$ and δD compositions in ore fluids. Some processes, such as evaporation and fluid/rock interactions, cannot reasonably produce the observed ore fluid isotopic variations, whereas mixing of magmatic fluid and seawater and (or) isenthalpic boiling are both possible mechanisms.

$\delta^{34}\text{S}$

Useful reviews of sulfur isotope geochemistry in VMS deposits are given by Ohmoto (1986) and Huston (1999) and in modern seafloor massive sulfides by Shanks (2001). Given that sulfur is the major metalloid in VMS deposits, there are consequently many hundreds of sulfur isotope analyses available. The most comprehensive list is given by Huston (1999).

There is a significantly wider range of $\delta^{34}\text{S}$ in Phanerozoic sulfides compared to Archean and Proterozoic sulfides. Although the dichotomy is probably real, it also may reflect fewer determinations in Archean and Proterozoic deposits. Sangster (1968) was the first to recognize that the trend of $\delta^{34}\text{S}$ variation in Proterozoic and Phanerozoic VMS deposits closely paralleled the ancient seawater curve but was offset to lighter $\delta^{34}\text{S}$ values by about 18 per mil. Subsequent studies have confirmed the general notion that seawater sulfate provides a source of reduced sulfur for VMS deposits—a conclusion that is consistent with detailed studies of modern seafloor hydrothermal sulfide systems (Shanks, 2001; Rouxel and others, 2004a) in open ocean settings.

In modern island-arc and back-arc settings, $\delta^{34}\text{S}$ variability is more evident, with a greater proportion of vent fluids having light $\delta^{34}\text{S}$. The reasons for these shifts are not evident but may indicate a source of reduced sulfur in addition to seawater, such as a sulfur source from the disproportionation of magmatic sulfate ($\text{SO}_2 + 2\text{H}_2\text{O} \rightarrow \text{H}_2\text{S} + \text{SO}_4^{2-} + 2\text{H}^+$). In modern systems, the dominant role of seawater is also indicated by the $\delta^{34}\text{S}$ of anhydrite sulfate being almost identical to modern seawater sulfate. There are also other potential sources of reduced sulfur for Phanerozoic deposits, these being magmatic degassed H_2S (and possible SO_2) and sulfide leached from volcanic rock by circulating seawater. Because magmatic H_2S and sulfides in volcanics have overlapping values (0–5 per mil), it is not possible to directly differentiate between these two sources. Either source would act to offset seawater sulfide to lighter values. The reduction of seawater sulfate could occur through either abiotic or biotic processes. Abiotic processes involve redox reactions between sulfate and cations present in reduced form, (such as carbon, iron, and copper). Biotically-mediated reactions involve disproportionation reactions involving sulfate reducing bacteria (McCollom and Shock, 1997).

Most $\delta^{34}\text{S}$ studies involve either whole-rock determinations or analyses of mineral separates. However, the ability to now measure in situ relatively precise and accurate $\delta^{34}\text{S}$ values on single sulfide mineral grains demonstrates added complexity in interpreting sulfur isotope compositions of ancient VMS deposits. Slack and others (2008) analyzed pyrite, sphalerite, galena, chalcopyrite, and tetrahedrite from the Late Devonian–Early Mississippian Dry Creek deposit in east-central Alaska and demonstrated a range of $\delta^{34}\text{S}$ values from -48 to 23 per mil. They interpreted the isotopic data to reflect a two-stage mineralizing process. The first stage involved initial hydrothermal activity and mineralization in a local basin that was open to seawater sulfate. Sulfide $\delta^{34}\text{S}$ values reflected variable

mixing of light anoxic pore fluid H_2S with oxic seawater sulfate to produce sulfides with $\delta^{34}\text{S}$ values between -40 and -10 per mil. Later sulfides formed in a Red Sea-type brine pool, producing $\delta^{34}\text{S}$ values of -10 to 9 per mil. Second, subsequent precipitation of sulfides (15–23 per mil) from anoxic bottom waters (10–60 per mil) formed when the basin became closed to oxic seawater. This type of highly detailed study is possible because the $\delta^{34}\text{S}$ data could be correlated both with mineral paragenesis and host lithology.

Unlike Phanerozoic deposits, VMS deposits of Proterozoic and Archean age have a much more limited range of $\delta^{34}\text{S}$ values, with a mean of about 0 per mil. If these data are truly representative, then different environmental conditions are implied. Although the seawater $\delta^{34}\text{S}$ curve cannot be extended into the Proterozoic and earlier (largely because of the lack of sulfate minerals associated with VMS deposits), the consistency of VMS $\delta^{34}\text{S}$ values (about 0 per mil) over 3 billion years of Earth history could only be achieved if: (a) the seawater sulfate value was close to the modern seawater value (approx. 21 per mil), and (b) ancient VMS deposits formed in the same way as Phanerozoic deposits. Both of these requirements may be correct, but there is no way to evaluate either criterion. Alternately, the geochemistry of Proterozoic and Archean oceans may have been fundamentally different because of a more anoxic atmosphere that limited the development of seawater sulfate (a layered ocean with only upper level sulfate) and limited the ocean bottom solubility of reduced sulfur under anoxic, alkaline conditions.

 $\delta^{11}\text{B}$, $\delta^{64}\text{Cu}$, $\delta^{66}\text{Zn}$, $\delta^{57}\text{Fe}$, $\delta^{82}\text{Se}$

The first study of boron isotopes in modern VMS systems was by Spivack and Edmond (1987) for bare-ridge settings. They determined B concentrations and isotope values in vent fluids at 13°N and 21°N, concluding that boron was leached from basalts without resolvable fractionation and that such data can be used to fingerprint fluid/rock ratios and the global flux of B into the oceans. Other B isotope studies of vent fluids were carried out by James and others (1995) at Broken Spur and by Palmer (1996) at TAG and MARK (Mid-Atlantic Ridge at the Kane Fracture Zone) at the MAR and at the EPR. These studies demonstrated that the low-temperature removal of boron was a function of spreading rate.

Experimental studies by Spivack and others (1990) showed that B isotope systematics primarily reflected the proportions of B from seawater and crustal sources, and Seyfried and Shanks (2004) highlighted the usefulness of boron isotopes in constraining seafloor alteration and water/rock ratios.

The first B isotope study of ancient VMS deposits by Palmer and Slack (1989) reported data for tourmaline from 14 deposits of Archean to Ordovician age and showed a $\delta^{11}\text{B}$ value range from -15.7 to -1.5 per mil. They suggested six likely controls: (1) composition of the B source, (2) postore regional metamorphism (heavier, not lighter, isotope fractionates into the fluid phase, hence metamorphically recrystallized

tourmaline becomes isotopically lighter), (3) water/rock ratios, (4) seawater entrainment, (5) formational temperature, and (6) secular variations in seawater $\delta^{11}\text{B}$. The most important control was inferred to be the composition of the B source in footwall lithologies. Two topical studies have been reported for tourmaline associated with VMS deposits. Bandyopadhyay and others (1993) analyzed six tourmaline samples from small VMS deposits of Proterozoic age in India that showed a $\delta^{11}\text{B}$ range from -13.8 to -13.0 per mil, consistent with a B source dominantly from footwall pelitic schists and also possibly felsic volcanic rocks. Deb and others (1997) analyzed tourmaline from the large Deri VMS deposit in India (also Proterozoic) and reported $\delta^{11}\text{B}$ data for two tourmaline samples not from the ore zone of -16.4 and -15.5 per mil, which were interpreted to reflect leaching of felsic volcanic and argillaceous sedimentary rocks in the footwall sequence.

A detailed study by Taylor and Huston (1999) on 15 tourmalines in the feeder zone (mainly) and massive sulfide from the giant Kidd Creek deposit (Archean) reported $\delta^{11}\text{B}$ values from -13.6 to -7.8 per mil. Combined with data for O and H isotopes in the same tourmalines, they suggested that three fluids were involved in formation of the tourmalines (and by inference, the sulfides): (1) slightly modified seawater, (2) greatly modified seawater via previous seafloor boiling, and (3) high-T supercritical fluid; the B isotope data in part imply fluid reaction with rocks that were previously altered at low temperatures.

Maréchal and others (1999) and Zhu and others (2000) first demonstrated the utility of transition metal isotopes as geochemical tracers. Transition metal isotopes have been applied to a variety of deposit types, including porphyry copper deposits (Larson and others, 2003; Graham and others, 2008; Markl and others, 2006; Mathur and others, 2009) and MVT (Mississippi Valley-type) deposits (Wilkinson and others, 2005), and have been examined experimentally (Ehrlich and others, 2004; Mathur and others, 2005). The application of nontraditional stable isotopes to VMS deposits is a relatively new enterprise that holds the promise of a deeper understanding of the source of metals to VMS systems and the various metal fractionations that might occur during the movement of hydrothermal fluids and the precipitation of sulfide minerals. In the environs of VMS deposits, the fractionation of transition metal isotopes is likely to be narrow at elevated temperatures and broader in situations that involve abiotic redox reactions and biotic reactions. Iron isotope behavior has been reviewed by Beard and others (2003), Beard and Johnson (2004), Johnson and others (2004); copper and zinc isotope behavior by Albarede (2004); and selenium isotopes by Johnson and Bullen (2004). Specific Fe isotope studies are found in Rouxel and others (2004a; 2008). Specific Cu isotope studies are found in Rouxel and others (2004b) and Mason and others (2005). Zinc isotope studies are found in Mason and others (2005), Wilkinson and others (2005) (MVT study) and John and others (2008). Table 14-3 shows ranges in transition metal isotopes that have been measured for modern and ancient VMS deposits.

Rouxel and others (2004a) have demonstrated that in modern hydrothermal sulfide systems both Fe and Se display mass-dependent fractionation. Se and S have very similar geochemistry. The usefulness of Se isotopes is that the Se/S ratio of seawater (6.3×10^{-8}) is very different than the mantle (MORB) values (1.5×10^{-4}), so that a combination of trace element analysis and isotopic determinations has the potential for recognizing different sources in hydrothermal systems. The Se isotopic composition ($\delta^{82}\text{Se}$) of modern seafloor hydrothermal sulfides varies by about 7 per mil and could result from a combination of redox reactions (selenate and selenide in seawater), biological reactions, and water/rock reactions. Rouxel and others (2002) indirectly measured the composition of modern seawater $\delta^{82}\text{Se}$ by assuming that the value was reflected in the isotopic composition of Mn-nodules (approx. -1.5 per mil). This value is thus indistinguishable from the mantle value so that the large variation of $\delta^{82}\text{Se}$ in sulfides could not be ascribed to mixing of volcanic Se with seawater Se. In addition, the Se/S ratio and Se concentration in seawater are so low that even partial reduction of oxidized forms of Se would have little effect on the $\delta^{82}\text{Se}$ of seafloor sulfides if seawater and hydrothermal fluid were mixed directly. However, redox reactions are the only known mechanism for producing very light Se, and there may be an unseen reservoir of light Se resulting from seawater redox reactions in the subsurface.

Rouxel and others (2004a) were the first investigators to take a multi-isotope (S-Se-Fe) approach to seafloor hydrothermal sulfide. The important contribution was the recognition of venting of pristine hydrothermal fluids that precipitated sulfides with Fe and Se isotopic values close to magmatic (about 0 per mil) accompanied by $\delta^{34}\text{S}$ values (approx. 1.5 per mil) that showed minimal involvement of seawater S. They also demonstrated other sulfide systematics that were consistent with substantial mixing of hydrothermal fluid and heated seawater and the necessity for a deep (subsurface) reservoir of light isotopic Se.

The $\delta^{57}\text{Fe}$ values of modern sulfide minerals appears to be a function of the environment in which the minerals either grew and (or) post-precipitation reworking, according to Rouxel and others (2008). These authors demonstrated a strong kinetic effect in the precipitation of iron sulfide minerals (pyrite, marcasite) during growth of active sulfide chimneys so that the $\delta^{57}\text{Fe}$ values were demonstrably different from vent fluid values. However, in inactive chimneys, the $\delta^{56}\text{Fe}$ values were essentially identical to vent fluid values, a result of postdepositional annealing.

There are relatively few studies of Cu and Zn isotopes in VMS deposits in modern and ancient settings. As a general conclusion, the isotopic fractionation of Zn ($\delta^{66}\text{Zn}$) is relatively small compared to copper ($\delta^{65}\text{Cu}$), largely as a reflection of its monovalent behavior. Mason and others (2005) report little variation in the $\delta^{65}\text{Cu}$ values of primary sulfides in the stockwork and massive sulfide zones of the Alexandrinka VMS deposit, but they report measurable differences in $\delta^{66}\text{Zn}$ variations between primary chalcopyrite and primary sphalerite, the former being lighter by about 0.4 per mil. They

Table 14-3. Some transitional metal isotope ratios in volcanogenic massive sulfide deposits and related rocks.

[Cu, copper; Fe, iron; Se, selenium; Zn, zinc; EPR, East Pacific Rise; MAR, Mid-Atlantic Ridge; ODP, Ocean Drilling Program; TAG, Trans-Atlantic Geothermal; U.S. Geological Survey geochemical reference materials: BCR, Basalt, Columbia River; BHVO, Basalt, Hawaiian Volcanic Observatory; BIR, Icelandic Basalt]

| Deposit | Analysis type | $\delta^{64}\text{Cu}$ per mil | $\delta^{66}\text{Zn}$ per mil | $\delta^{57}\text{Fe}$ per mil | $\delta^{82}\text{Se}$ per mil | Comments | Reference |
|--------------------|---------------------------|-----------------------------------|-----------------------------------|-----------------------------------|-----------------------------------|---|------------------------------|
| BCR-1 Standard | Whole rock | | | 0.08 ± 0.1 | | | |
| BIR-1 Standard | Whole rock | | | 0.01 | | | |
| BHVO-1 Standard | Whole rock | | | 0.22 ± 0.13 | | | |
| ODP Site 801C | Altered basalt | | | 0.12 to 0.23 | | Fe isotope variations up to 4 per mil could be abiotic and (or) biotic | |
| | Deep-sea sediments | | | -0.07 to 0.23 | | | |
| | Chemical sediments | | | -2.5 to 1.0 | | | |
| | Chert | | | -2.5 | | | |
| | Fe-oxyhydroxide sediments | | | -0.52 to 0.39 | | | |
| | Celadonite | | | 1.86 | | | |
| Lucky Strike, MAR | Chalcopyrite | 1.7 to 4.6, avg. 3.4 | | -0.12 ± 0.48 | -3.22 ± 1.52 | Variation in Cu isotopic composition due to sulfide oxidation | Rouxel and others (2004a, b) |
| | Atacamite | 0.5 to 1.2, avg. 1.0 | | | | | |
| | Pyrite/marcasite | | | -2.37 ± 0.46 | -3.52 ± 1.15 | Se-poor chalcopyrite has ^{57}Fe -1 to -3 per mil. Se-rich chalcopyrite has ^{57}Fe \sim 0 per mil. Abiotic fractionation of Fe isotopes during sulfide precipitation | |
| Logachev, MAR | Chalcopyrite | -1.0 to 0.7, avg. 0.14 | | | | Variation in isotopic composition due to sulfide oxidation | Rouxel and others (2004a, b) |
| | Atacamite | 0.4 to 4.7, avg. 2.6 | | | | | |
| | Bornite/covellite | -0.7 to 2.7, avg. 2.1 | | | | Variation in isotopic composition due to sulfide oxidation | |

Table 14-3. Some transitional metal isotope ratios in volcanogenic massive sulfide deposits and related rocks.—Continued

[Cu, copper; Fe, iron; Se, selenium; Zn, zinc; EPR, East Pacific Rise; MAR, Mid-Atlantic Ridge; ODP, Ocean Drilling Program; TAG, Trans-Atlantic Geothermal; U.S. Geological Survey geochemical reference materials: BCR, Basalt, Columbia River; BHVO, Basalt, Hawaiian Volcanic Observatory; BIR, Icelandic Basalt]

| Deposit | Analysis type | $\delta^{64}\text{Cu}$ per mil | $\delta^{66}\text{Zn}$ per mil | $\delta^{57}\text{Fe}$ per mil | $\delta^{82}\text{Se}$ per mil | Comments | Reference |
|--------------------------|----------------------------------|-----------------------------------|-----------------------------------|-----------------------------------|-----------------------------------|-------------------------------------|------------------------------------|
| Rainbow, MAR | Chalcopyrite/ isocubanite | 0.11 | | | | | Rouxel and others (2004a, b) |
| | Bornite/ covellite | 3.3 | | | | | |
| EPR 21oN | Vent fluids | | 0.31 ± 0.19 | | | Fluid temperatures: 273–385oC | John and others (2008) |
| EPR 9oN | Vent fluids | | 0.56 ± 0.56 | -0.54 ± 0.58 | | Fluid temperatures: 203–383oC | Rouxel and others (2008) |
| | Chalcopyrite | | 0.16 ± 0.07 | -0.23 ± 0.09 | | | |
| | Pyrite/ sphalerite/ galena | | 0.92 ± 0.28 | -0.69 ± 0.02 | | | |
| | Pyrite/sphal- erite | | 0.40 ± 0.42 | -0.88 ± 0.34 | | | |
| TAG, MAR | Pyrite | | | -0.85 ± 0.50 | | | |
| | Vent fluids | | 0.25 ± 0.15 | | | Fluid temperatures: 290–360oC | |
| Alexandrin- ka, Urals | Stockwork | 0.12 to 0.30 | 0.45 to 0.05 | | | Chalcopyrite, sphalerite, galena | Mason and others (2005) |
| | Main ore | 0.28 to 0.32 | -0.02 to 0.21 | | | Sphalerite | |

interpret this difference in terms of an equilibrium fractionation between the two phases, although this conclusion is at odds with the measurements made by John and others (2008) at modern hydrothermal sulfide settings. The observable differences in $\delta^{65}\text{Cu}$ values were associated with epigenetic versus supergene Cu phases, the latter being up to 0.6 per mil lighter as a result of isotopic fractionation associated with the reduction of Cu(II) to Cu(I) during supergene enrichment. Rouxel and others (2004a, b) observed $\delta^{65}\text{Cu}$ variations of up to 3 per mil in modern hydrothermal sulfide systems that they associated with seafloor oxidation of copper-bearing minerals. However, the $\delta^{65}\text{Cu}$ values became heavier in sulfides that had been subjected to seafloor weathering, and the isotopically heavy Cu was subsequently remobilized during further periods of high-T fluid flow and either redeposited at the periphery of the deposit or lost into the hydrothermal fluid.

A new compilation of Pb isotope data that includes the previous compilation of Gulson (1986) for sulfides from a variety of VMS deposits is shown in table 14–4. Of particular note are the following: (1) the Pb isotope data for individual districts tend to be homogeneous, showing a maximum variation of about 2 percent; (2) the Pb isotope signature is the isotopic signature of the protolith, suggesting that either the individual protoliths are isotopically homogeneous or the hydrothermal systems are able to homogenize the Pb isotopic composition of heterogeneous protoliths; and (3) the Pb isotopic composition of ore galena has been used to define the lead crustal evolution (growth curves), so it follows that the calculated model ages should be close to the deposit ages.

Radiogenic Isotope Geochemistry

In base metal deposits, radiogenic isotopes are restricted to the study of lead isotopes in primarily galena and, more recently, rhenium-osmium (Re-Os) studies of a variety of sulfide phases. Reviews of Pb isotopes in a variety of ores, including a few VMS deposits, are provided by Gulson (1986) and Sangster and others (2000).

MVT and SEDEX deposits are the major global sources of Pb; there has been a proportionately large number of Pb isotope ratios measured for these two deposit types. VMS deposits do not constitute a major Pb source, and there is a limited literature dealing with their Pb isotopic signatures. However, Mortensen and others (2006) present an extensive compilation of lead isotopic compositions of sulfide samples from VMS deposits and occurrences in the northern North American Cordillera. Lead isotopes in galena, or other ore containing Pb and negligible U and Th, have the advantage that no age correction has to be made for the growth of radiogenic Pb. Consequently, the Pb isotopic composition reflects principally the age of the ore deposit (older deposits carry less radiogenic Pb) and secondarily the geochemistry (U/Th ratio) of the Pb source. Of the Pb isotope values for 151 deposits compiled by Sangster and others (2000), only 5 percent are for VMS deposits (Hellyer, Rosebery, Que River [Australia]; Verviers district [Belgium]; Bathurst district, Buchans, Buttle Lake [Canada]; Ambaji-Sendra belt [India]; Kuroko district [Japan]), of which only the Bathurst and Kuroko districts have been significant producers of Pb.

Table 14–4. Lead (Pb) isotopic composition of selected volcanogenic massive sulfide deposits.

[Ba, barium; Cu, copper; Zn, zinc]

| Deposit/district | Mineral | Age | $^{208}\text{Pb}/^{204}\text{Pb}$ | $^{207}\text{Pb}/^{204}\text{Pb}$ | $^{206}\text{Pb}/^{204}\text{Pb}$ | Data source | |
|---------------------|---------|----------|-----------------------------------|-----------------------------------|-----------------------------------|----------------------------|----------------------------|
| Tasmania, Australia | | | | | | | |
| Mount Read | | Cambrian | | | | | |
| Rosebery-Hercules | Galena | | 38.064 | 15.598 | 18.271 | Sangster and others (2000) | |
| | | | 38.083 | 15.609 | 18.273 | | |
| | | | 38.081 | 15.606 | 18.272 | | |
| | | | 38.041 | 15.594 | 18.266 | | |
| | | | 38.068 | 15.603 | 18.279 | | |
| | | | 38.041 | 15.594 | 18.273 | | |
| | | | 38.053 | 15.583 | 18.277 | | |
| | | | 38.053 | 15.595 | 18.272 | | |
| | | | 38.138 | 15.611 | 18.286 | | |
| | | | 38.093 | 15.608 | 18.276 | | |
| | | | 38.047 | 15.597 | 18.268 | | |
| Que River | Galena | | 38.191 | 15.618 | 18.348 | | Sangster and others (2000) |
| | | | 38.196 | 15.628 | 18.321 | | |
| | | | 38.187 | 15.622 | 18.332 | | |
| | | | 38.162 | 15.614 | 18.311 | | |
| | | | 38.174 | 15.619 | 18.318 | | |
| | | | 38.182 | 15.622 | 18.323 | | |
| | | | 38.231 | 15.629 | 18.369 | | |
| | | | 38.15 | 15.619 | 18.328 | | |
| | | | 38.114 | 15.602 | 18.317 | | |
| | | | 38.22 | 15.638 | 18.346 | | |
| | | | 38.128 | 15.614 | 18.328 | | |
| | | | 38.143 | 15.613 | 18.331 | | |
| | | | 38.166 | 15.621 | 18.328 | | |
| | | | 38.253 | 15.644 | 18.359 | | |
| | | | 38.233 | 15.637 | 18.355 | | |
| Hellyer | Galena | | 38.219 | 15.624 | 18.372 | Sangster and others (2000) | |

References Cited

- Albarede, F., 2004, The stable isotope geochemistry of copper and zinc, *in* Johnson, C.M., Beard, B.L., and Albarede, F., eds., *Geochemistry of non-traditional stable isotopes: Reviews in Mineralogy and Geochemistry*, v.55, p. 409–427.
- Almodovar, G.R., Saez, R., Pons, J.M., Maestre, A., Toscano, M., and Pascual, E., 1998, Geology and genesis of the Aznalcollar massive sulfide deposits, Iberian Pyrite Belt, Spain: *Mineralium Deposita*, v. 33, p.111–136.
- Bandyopadhyay, B.K., Slack, J.R., Palmer, M.R., and Roy, A., 1993, Tourmalinites associated with stratabound massive sulfide deposits in Proterozoic Sakoli Group, Nagpur District, Central India, *in* Maurice, Y.T., ed., Eighth quadrennial IAGOD symposium, Ottawa, Canada, 12–18 August 1990, *Proceedings: International Association on the Genesis of Ore Deposits*, Stuttgart, Germany, E. Schweizerbart'sche Verlag, p. 867–885.
- Barriga, F.J.A.S., and Kerrich, R., 1984, Extreme ^{18}O -enriched volcanics and ^{18}O -evolved marine water, Aljustrel, Iberian pyrite belt—Transition from high to low Rayleigh number convective regimes: *Geochimica et Cosmochimica Acta*, v. 48, p. 1021–1031.
- Beard, B.L., and Johnson, C.M., 2004, Fe isotope variations in the modern and ancient earth and other planetary bodies, *in* Johnson, C.M., Beard, B.L., and Albarede, F., eds., *Geochemistry of non-traditional stable isotopes: Reviews in Mineralogy and Geochemistry*, v. 55, p. 319–357.
- Beard, B.L., Johnson, C.M., Skulan, J.L., Neelson, K.H., Cox, L., and Sun, H., 2003, Application of Fe isotopes to tracing the geochemical and biological cycling of Fe: *Chemical Geology*, v. 195, p. 87–117.
- Beaty, D.W., Taylor, H.P., Jr., and Coads, P.R., 1988, An oxygen isotope study of the Kidd Creek, Ontario, massive sulfide deposit—Evidence for a ^{18}O ore fluid: *Economic Geology*, v. 83, p. 1–17.
- Booij, E., Bettison-Varga, L., Farthing, D., and Staudigel, H., 2000, Pb-isotope systematics of a fossil hydrothermal system from the Troodos ophiolite, Cyprus—Evidence for a polyphased alteration history: *Geochimica et Cosmochimica Acta*, v. 64, p. 3559–3569.
- Brown, P.E., 1998, Fluid inclusion modeling for hydrothermal systems, *in* Richards, J.P., and Larson, P.B., eds., *Techniques in hydrothermal ore deposit geology: Reviews in Economic Geology*, v. 10, p. 151–171.
- Deb, M., Tiwary, A., and Palmer, M.R., 1997, Tourmaline in Proterozoic massive sulfide deposits from Rajasthan, India: *Mineralium Deposita*, v. 32, p. 94–99.
- Ehrlich, S., Butler, I., Halicz, L., Rickard, D., Oldroyd, A., and Mathews, A., 2004, Experimental study of the copper isotope fractionation between aqueous Cu(II) and covellite, CuS: *Chemical Geology*, v. 209, p. 259–269.
- Fehn, U., Doe, B.R., and Delevaux, M.H., 1983, The distribution of lead isotopes and the origin of Kuroko ore deposits in the Hokuroku District, Japan, *in* Ohmoto, H., and Skinner, B.J., eds., *The Kuroko and related volcanogenic massive sulfide deposits: Economic Geology Monograph 5*, p. 488–506.
- Fouquet, Y., and Marcoux, E., 1995, Lead isotope systematics in Pacific hydrothermal sulfide deposits: *Journal of Geophysical Research*, v. 100, p. 6025–6040.
- Galley, A.G., Hannington, M.D., and Jonasson, I.R., 2007, Volcanogenic massive sulphide deposits, *in* Goodfellow, W.D., ed., *Mineral deposits of Canada—A synthesis of major deposit-types, district metallogeny, the evolution of geological provinces, and exploration methods: Geological Association of Canada, Mineral Deposits Division, Special Publication 5*, p. 141–161.
- Gokce, A., and Gulcan, B., 2004, Lead and sulfur isotope evidence for the origin of the Inler Yaylasi lead zinc deposit, northern Turkey: *Journal of Asian Earth Sciences*, v. 26, p. 91–97.
- Goodfellow, W.D., and McCutcheon, S.R., 2003, Geologic and genetic attributes of volcanic sediment-hosted massive sulfide deposits of the Bathurst mining camp, New Brunswick—A synthesis, *in* Goodfellow, W.D., McCutcheon, S.R., and Peter, J.M., eds., *Massive sulfide deposits of the Bathurst mining camp, New Brunswick, and northern Maine: Economic Geology Monograph 11*, p. 245–301.
- Goodwin, C.I., Robinson, M., and Juras, S.J., 1996, Galena lead isotopes, Buttle Lake mining camp, Vancouver Island, British Columbia, Canada: *Economic Geology*, v. 91, p. 549–562.
- Graham, I.J., Reyes, A.G., Wright, I.C., Peckett, K.M., Smith, I.E.M., and Arculus, R.J., 2008, Structure and petrology of newly discovered volcanic centers in the northern Kermadec-southern Tofa arc, South Pacific Ocean: *Journal of Geophysical Research*, v. 113, B08S02, 24 p., doi:10.1029/2007JB005453.

- Green, G.R., Ohmoto, H., Date, J., and Takahashi, T., 1983, Whole-rock oxygen isotope distribution in the Fukazawa-Kosaka area, Hokuroku district, Japan, and its potential application to mineral exploration, *in* Ohmoto, H., and Skinner, B.J., eds., *The Kuroko and related volcanogenic massive sulfide deposits: Economic Geology Monograph 5*, p. 395–411.
- Green, G.R., and Taheri, J., 1992, Stable isotopes and geochemistry as exploration indicators: *Geological Survey of Tasmania Bulletin 70*, p. 84–91.
- Gulson, B.L., 1986, *Lead isotopes in mineral exploration: Amsterdam, Elsevier*, 245 p.
- Halbach, P., Hansmann, W., Koppel, V., and Pracejus, B., 1997, Whole-rock and sulfide lead-isotope data from the hydrothermal JADE field in the Okinawa back-arc trough: *Mineralium Deposita*, v. 32, p. 70–78.
- Haymon, R.M., 1983, Growth history of hydrothermal black smoker chimneys: *Nature*, v. 301, p. 695–698.
- Holk, G.J., Taylor, B.E., and Galley, A.G., 2008, Oxygen isotope mapping of the Archean Sturgeon Lake caldera complex and VMS-related hydrothermal system, northwestern Ontario, Canada: *Mineralium Deposita*, v. 43, p. 623–640.
- Hou, Z., Zaw, K., Xiaoming, Q., Qingtong, Y., Jinjie, Y., Mingji, X., Deming, F., and Xiannke, Y., 2001, Origin of the Gacun volcanic-hosted massive sulfide deposit in Sichuan, China—Fluid inclusion and oxygen isotope evidence: *Economic Geology*, v. 96, p. 1491–1512.
- Humphris, S.E., and Tivey, M.K., 2000, A synthesis of geological and geochemical investigations of the TAG hydrothermal field—Insights into fluid flow and mixing processes in a hydrothermal system, *in* Dilek, Y., Moorse, E., Elthon, D., and Nicholas, A., eds., *Ophiolites and oceanic crust—New insights from field studies and the ocean drilling program: Geological Society of America Special Paper 349*, p. 213–236.
- Huston, D.L., 1999, Stable isotopes and their significance for understanding the genesis of volcanic-hosted massive sulfide deposits—A review, *in* Barrie, C.T., and Hannington, M.D., eds., *Volcanic-associated massive sulfide deposits—Processes and examples in modern and ancient settings: Reviews in Economic Geology*, v. 8, p. 157–179.
- Huston, D.L., and Taylor, B.E., 1999, Genetic significance of oxygen and hydrogen isotope variations at the Kidd Creek volcanic-hosted massive sulfide deposit, Ontario, Canada, *in* Hannington, M.D., and Barrie, C.T., eds., *The giant Kidd Creek volcanogenic massive sulfide deposit, western Abitibi subprovince, Canada: Economic Geology Monograph 10*, p. 335–350.
- Inverno, C.M.C., Lopes, C.J.C.D., d'Orey, F.L.C., and de Carvalho, D., 2000, The Cu-(Au) stockwork of Salgadinho, Cercal, Pyrite Belt, SW Portugal—Paragenetic sequence and fluid inclusion investigations, *in* Gemmill, J.B., and Pongratz, J., eds., *Volcanic environments and massive sulfide deposits: University of Tasmania, Australian Research Council, Center of Excellence in Ore Deposits (CODES) Special Publication 3*, p. 99–101.
- Ioannou, S.E., Spooner, E.T.C., and Barrie, C.T., 2007, Fluid temperature and salinity characteristics of the Matagami volcanogenic massive sulfide district, Quebec: *Economic Geology*, v. 102, p. 691–713.
- James, R.H., Elderfield, H., and Palmer, M.R., 1995, The chemistry of hydrothermal fluids from the Broken Spur site, 29°N Mid-Atlantic Ridge: *Geochimica et Cosmochimica Acta*, v. 59, p. 651–659.
- John, S.G., Rouxel, O.J., Craddock, P.R., Engwell, A.M., and Boyle, E.A., 2008, Zinc stable isotopes in seafloor hydrothermal vent fluids and chimneys: *Earth and Planetary Science Letters*, v. 269, p. 17–28.
- Johnson, C.M., Beard, B.L., Roden, E.E., Newman, D.K., and Nealon, K.H., 2004, Isotopic constraints on biogeochemical cycling of Fe, *in* Johnson, C.M., Beard, B.L., and Albarede, F., eds., *Geochemistry of non-traditional stable isotopes: Reviews in Mineralogy and Geochemistry*, v. 55, p. 359–408.
- Johnson, T.M., and Bullen, T.D., 2004, Mass-dependent fractionation of selenium and chromium isotopes in low-temperature environments, *in* Johnson, C.M., Beard, B.L., and Albarede, F., eds., *Geochemistry of non-traditional stable isotopes: Reviews in Mineralogy and Geochemistry*, v. 55, p. 289–317.
- Larson, P.B., Maher, K., Ramos, F.C., Chang, Z., Gaspar, M., and Meinert, L.D., 2003, Copper isotope ratios in magmatic and hydrothermal ore forming environments: *Chemical geology*, v. 201, p. 337–350.
- Marcoux, E., 1998, Lead isotope systematics of the giant massive sulfide deposits in the Iberian Pyrite Belt: *Mineralium Deposita*, v. 33, p. 45–58.
- Maréchal, C.D., Télouk, P., and Albarède, F., 1999, Precise analysis of copper and zinc isotopic compositions by plasma-source mass spectrometry: *Chemical Geology*, v. 156, p. 251–273.
- Marignac, C., Diagona, B., Cathelineau, M., Boiron, M.-C., Banks, D., Fourcade, S., and Vallance, J., 2003, Remobilization of base metals and gold by Variscan metamorphic fluids in the southern Iberian pyrite belt—Evidence from the Tharsis deposit: *Chemical Geology*, v. 194, p. 143–165.

- Markl, G., Lahaye, Y., and Schwinn, G., 2006, Copper isotopes as monitors of redox processes in hydrothermal mineralization: *Geochimica et Cosmochimica Acta*, v. 70, p. 4215–4228.
- Marumo, K., Urabe, T., Goto, A., Takano, Y., and Nakaseama, M., 2008, Mineralogy and isotope geochemistry of active hydrothermal field at Suiyo seamount, Izu-Bonin arc, west Pacific Ocean: *Resource Geology*, v. 58, p. 220–248.
- Mason, T.F.D., Weiss, D.J., Chapman, J.B., Wilkinson, J.J., Tessalina, S.G., Spiro, B., Horstwood, M.S.A., Spratt, J., and Coles, B.J., 2005, Zn and Cu isotopic variability in the Alexandrinka volcanic-hosted massive sulfide (VHMS) ore deposit, Urals, Russia: *Chemical Geology*, v. 221, p. 170–187.
- Mathur, R., Ruiz, J., Tittley, S., Liermann, L., Buss, H., and Brantley, S.L., 2005, Cu isotope fractionation in the supergene environment with and without bacteria: *Geochimica et Cosmochimica Acta*, v. 69, p. 5233–5246.
- Mathur, R., Tittley, S., Bara, F., Brantley, S., Wilson, M., Phillips, A., Munizaga, F., MaksaeV, V., Vervoort, J., and Hart, G., 2009, Exploration potential of Cu isotope fractionation in porphyry copper deposits: *Journal of Geochemical Exploration*, v. 102, p. 1–6.
- McCullom, T., and Shock, E.L., 1997, Geochemical constraints on chemolithoautotrophic metabolism by microorganisms in seafloor hydrothermal systems: *Geochimica et Cosmochimica Acta*, v. 61, p. 4375–4391.
- Mortensen, J.K., Dusel-Bacon, C., Hunt, J., and Gabites, J., 2006, Lead isotopic constraints on the metallogeny of middle and late Paleozoic syngenetic base metal occurrences in the Yukon-Tanana and Slide Mountain/Seventymile Terranes and adjacent portions of the North American miogeocline, *in* Colpron, M., and Nelson, J.L., eds., *Paleozoic evolution and metallogeny of pericratonic terranes at the ancient Pacific margin of North America, Canadian and Alaskan Cordillera*: Geological Association of Canada, Special Paper 45, p. 261–279.
- Mortensen, J.K., Hall, B.V., Bissig, T., Friedman, R.M., Danielson, T., Oliver, J., Rhys, D.A., Ross, K.V., and Gabites, J.E., 2008, Age and paleotectonic setting of volcanogenic massive sulfide deposits in the Guerrero Terrane of central Mexico—Constraints from U-Pb age and Pb isotope studies: *Economic Geology*, v. 103, p. 117–140.
- Moura, A., 2005, Fluids from the Neves Corvo massive sulfide ores, Iberian Pyrite Belt, Portugal: *Chemical Geology*, v. 223, p. 153–169.
- Nehlig, P., Cassard, D., and Marcoux, E., 1998, Geometry and genesis of feeder zones of massive sulfide deposits—Constraints from the Rio Tinto ore deposit (Spain): *Mineralium Deposita*, v. 33, p. 137–149.
- Ohmoto, H., 1986, Stable isotope geochemistry of ore deposits: *Reviews in Mineralogy*, v. 16, p. 491–559.
- Palmer, M., and Slack, J.F., 1989, Boron isotope composition of tourmaline from massive sulfide deposits and tourmalinites: *Contributions to Mineralogy and Petrology*, v. 103, p. 434–451.
- Palmer, M.R., 1996, Hydration and uplift of the oceanic crust on the Mid-Atlantic Ridge associated with hydrothermal activity—Evidence from boron isotopes: *Geophysical Research Letters*, v. 23, p. 3479–3482.
- Petersen, S., Herzig, P.M., and Hannington, M.D., 2000, Third dimension of a presently forming VMS deposit—TAG hydrothermal mound, Mid-Atlantic Ridge, 26°N: *Mineralium Deposita*, v. 35, p. 233–259.
- Pisutha-Arnond, V., and Ohmoto, H., 1983, Thermal history and chemical and isotopic compositions of the ore-forming fluids responsible for the Kuroko massive sulfide deposits in the Hokuroku District of Japan, *in* Ohmoto, H., and Skinner, B.J., eds., *The Kuroko and related volcanogenic massive sulfide deposits*: *Economic Geology Monograph 5*, p. 523–558.
- Rouxel, O., Fouquet, Y., and Ludden, J.N., 2004a, Subsurface processes at the Lucky Strike hydrothermal field, Mid-Atlantic Ridge—Evidence from sulfur, selenium, and iron isotopes: *Geochimica et Cosmochimica Acta*, v. 68, p. 2295–2311.
- Rouxel, O., Fouquet, Y., and Ludden, J.N., 2004b, Copper isotope systematics of the Lucky Strike, Rainbow, and Logachev sea-floor hydrothermal fields on the Mid-Atlantic Ridge: *Economic Geology*, v. 99, p. 585–600.
- Rouxel, O., Ludden, J., Carignon, J., Marin, L., and Fouquet, Y., 2002, Natural variations of Se isotopic composition determined by hydride generation multiple collector coupled mass spectrometry: *Geochimica et Cosmochimica Acta*, v. 66, p. 3191–3193.
- Rouxel, O., Shanks, W.C., Bach, W., and Edwards, K., 2008, Integrated Fe and S isotope study of seafloor hydrothermal vents at East Pacific Rise 9–10°N: *Geochimica et Cosmochimica Acta*, v. 72, p. 214–227.

- Sanchez-Espana, J., Velasco, F., and Yusta, I., 2000, Hydrothermal alteration of felsic volcanic rocks associated with massive sulfide deposition in the northern Iberian Pyrite Belt (SW Spain): *Applied Geochemistry*, v. 15, p. 1265–1290.
- Sangster, D.F., 1968, Relative sulphur isotope abundances of ancient seas and strata-bound sulfide deposits: *Proceedings of the Geological Association of Canada*, v. 19, p. 79–91.
- Sangster, D.F., Outridge, P.M., and Davis, W.J., 2000, Stable lead isotope characteristics of lead ore deposits of environmental significance: *Environmental Reviews*, v. 8, p. 115–147.
- Seyfried, W.E., Jr., and Shanks, W.C., III, 2004, Alteration and mass transport in mid-ocean ridge hydrothermal systems—Controls on the chemical and isotopic evolution of high-temperature crustal fluids, *in* Davis, E.E., and Elderfield, H., eds., *Hydrogeology of the oceanic lithosphere*: Cambridge, Cambridge University Press, p. 451–458.
- Shanks, W.C., III, 2001, Stable isotopes in seafloor hydrothermal systems—Vent fluids, hydrothermal deposits, hydrothermal alteration, and microbial processes, *in* Valley, J.W., and Cole, D.R., eds., *Stable isotope geochemistry: Reviews in Mineralogy and Geochemistry*, v. 43, p. 469–525.
- Shepherd, T.J., and Rankin, A.H., 1998, Fluid inclusion techniques of analysis, *in* Richards, J.P., and Larson, P.B., eds., *Techniques in hydrothermal ore deposit geology: Reviews in Economic Geology*, v. 10, p. 125–149.
- Sherlock, R.L., Roth, T., Spooner, E.T.C., and Bray, C.J., 1999, Origin of the Eskay Creek precious metal-rich volcanogenic massive sulfide deposit—Fluid inclusion and stable isotope evidence: *Economic Geology*, v. 94, p. 803–824.
- Shwarz-Schampera, U., and Herzig, P.M., 2002, *Indium geology, mineralogy and economics*: Berlin, Springer, 257 p.
- Sillitoe, R.H., Hannington, M.D., and Thompson, J.F.H., 1996, High sulfidation deposits in the volcanogenic massive sulfide environment: *Economic Geology*, v. 91, p. 204–212.
- Slack, J.F., Ridley, W.I., Dusel-Bacon, C., and Fayek, M., 2008, Extreme sulfur isotope variation in the Dry Creek volcanogenic massive sulfide deposit, east-central Alaska: *Geochimica et Cosmochimica Acta*, v. 72, p. A876.
- Spivack, A.J., Berndt, M.E., and Seyfried, W.E., 1990, Boron isotope fractionation during supercritical phase separation: *Geochimica et Cosmochimica Acta*, v. 54, p. 2337–2339.
- Spivack, A.J., and Edmond, J.M., 1987, Boron isotope exchange between seawater and the oceanic crust: *Geochimica et Cosmochimica Acta*, v. 51, p. 1033–1043.
- Stolz, J., and Large, R.R., 1992, Evaluation of the source-rock control on precious metal grades in volcanic-hosted massive sulfide deposits from western Tasmania: *Economic Geology*, v. 87, p. 720–738.
- Taylor, B.E., and Huston, D.L., 1999, Regional ^{18}O zoning and hydrogen isotope studies in the Kidd Creek volcanic complex, Timmins, Ontario, *in* Hannington, M.D., and Barrie, C.T., eds., *The giant Kidd Creek volcanogenic massive sulfide deposit, western Abitibi subprovince, Canada: Economic Geology Monograph 10*, p. 351–378.
- Taylor, H.P., 1977, Water/rock interactions and the origin of H_2O in granitic batholiths: *Journal of the Geological Society of London*, v. 133, p. 509–558.
- Wilkinson, J.J., Weiss, D.J., Mason, T.F.D., and Coles, B.J., 2005, Zinc isotope variation in hydrothermal systems—Preliminary evidence from the Irish Midlands ore field: *Economic Geology*, v. 100, p. 583–590.
- Zaw, K., Gemmell, J.B., Large, R.R., Mernagh, T.P., and Ryan, C.G., 1996, Evolution and source of ore fluids in the stringer system, Hellyer VHMS deposit, Tasmania, Australia—Evidence from fluid inclusion microthermometry and geochemistry: *Ore Geology Reviews*, v. 10, p. 251–278.
- Zhu, X.K., O’Nions, R.K., Guo, Y., Belshaw, N.S., and Rickard, D., 2000, Determination of the natural Cu-isotope variation by plasma-source mass spectrometry—Implications for use as geochemical tracers: *Chemical Geology*, v. 163, p. 139–149.

15. Petrology of Associated Igneous Rocks

By W. Ian Ridley

15 of 21

Volcanogenic Massive Sulfide Occurrence Model

Scientific Investigations Report 2010–5070–C

U.S. Department of the Interior
U.S. Geological Survey

U.S. Department of the Interior
KEN SALAZAR, Secretary

U.S. Geological Survey
Marcia K. McNutt, Director

U.S. Geological Survey, Reston, Virginia: 2012

For more information on the USGS—the Federal source for science about the Earth, its natural and living resources, natural hazards, and the environment, visit <http://www.usgs.gov> or call 1–888–ASK–USGS.

For an overview of USGS information products, including maps, imagery, and publications, visit <http://www.usgs.gov/pubprod>

To order this and other USGS information products, visit <http://store.usgs.gov>

Any use of trade, product, or firm names is for descriptive purposes only and does not imply endorsement by the U.S. Government.

Although this report is in the public domain, permission must be secured from the individual copyright owners to reproduce any copyrighted materials contained within this report.

Suggested citation:

Ridley, W. Ian, 2012, Petrology of associated igneous rocks in volcanogenic massive sulfide occurrence model: U.S. Geological Survey Scientific Investigations Report 2010–5070 –C, chap. 15, 32 p.

Contents

| | |
|--|-----|
| Importance of Igneous Rocks to Deposit Genesis | 231 |
| Rock Names | 231 |
| Rock Associations | 231 |
| Mafic-Ultramafic Association | 231 |
| Siliciclastic-Mafic Association | 232 |
| Bimodal-Mafic Association | 232 |
| Bimodal-Felsic Association..... | 233 |
| Siliciclastic-Felsic Association | 234 |
| Mineralogy | 234 |
| Textures and Structures | 234 |
| Petrochemistry | 235 |
| Major-Element Geochemistry | 235 |
| Trace-Element Geochemistry | 235 |
| Isotope Geochemistry | 242 |
| Radiogenic Isotopes..... | 242 |
| MORB, OIB, BABB, IAB, and Related Volcanics | 242 |
| Strontium, Neodymium, Lead..... | 242 |
| Traditional Stable Isotopes..... | 243 |
| Deuterium/Hydrogen | 243 |
| $^{18}\text{O}/^{16}\text{O}$ | 246 |
| $\delta^{34}\text{S}$ | 252 |
| Depth of Emplacement..... | 252 |
| References Cited..... | 256 |

Figures

| | |
|--|-----|
| 15-1. Schematic diagram showing the principal components and processes involved in the production of island-arc and back-arc volcanics that are major lithostratigraphic units associated with volcanogenic massive sulfide deposits | 233 |
| 15-2. Two classifications of common igneous rocks..... | 237 |
| 15-3. The use of trace-element abundances and trace-element ratios as proxies for the subduction input to the overlying mantle preserved in the mantle partial melts that form island-arc and back-arc volcanics | 241 |
| 15-4. Trace-element patterns for several types of volcanics from modern tectonic environments that are commonly associated with volcanogenic massive sulfide deposits | 242 |
| 15-5. Frequency distributions of copper in various modern volcanics. | 243 |
| 15-6. Relationships between strontium, neodymium, and lead isotopes in a variety of mid-ocean ridge basalts and oceanic island basalts | 244 |
| 15-7. Strontium, neodymium, and lead isotopic variability in island-arc basalt volcanics and back-arc basin basalt volcanics | 245 |

| | | |
|-------|--|-----|
| 15-8. | Hydrogen and oxygen isotopic composition of various types of terrestrial waters | 246 |
| 15-9. | Oxygen isotopic composition of various lithologic units relative to mid-ocean ridge basalt | 251 |

Tables

| | | |
|-------|---|-----|
| 15-1. | Major and trace element composition of major minerals observed in igneous rocks associated with modern seafloor massive sulfides in a variety of settings | 235 |
| 15-2. | Common textures observed in pristine igneous rocks associated with modern seafloor massive sulfides | 236 |
| 15-3. | Average major element composition of basaltic rocks associated with volcanogenic massive sulfide deposits | 238 |
| 15-4. | Major element compositions of various volcanic rock series associated with volcanogenic massive sulfide deposits | 239 |
| 15-5. | Hydrogen isotope compositions of ore and alteration fluids, whole rocks, and minerals for selected volcanogenic massive sulfide deposits | 247 |
| 15-6. | Selected oxygen isotope studies of volcanic rocks hosting volcanogenic massive sulfide deposits | 253 |
| 15-7. | Whole rock $\delta^{18}\text{O}$ values for lithostratigraphic units associated with volcanogenic massive sulfide deposits | 254 |

15. Petrology of Associated Igneous Rocks

By W. Ian Ridley

Importance of Igneous Rocks to Deposit Genesis

Volcanogenic massive sulfide deposits, by definition, are either hosted within or closely spatially associated with volcanic and subvolcanic intrusive rocks. Consequently, there is a well-documented genetic association between magmatism and development of VMS deposits (Lydon, 1988; Lowell and others, 1995, 2008; Franklin and others, 2005). Magmatism is a prerequisite in the following ways:

1. As a heat engine to drive deep hydrothermal flow systems (MacLennan, 2008), highlighted in modern systems by the association of melt-rich crustal regions of modern ridge systems and seafloor hydrothermal activity (Singh and others, 1999, 2006).
2. As a focus of hydrothermal circulation (Lowell and others, 2008). Subvolcanic intrusions act as “pinpoint” heat sources that focus descending fluids from recharge areas into narrow upflow and discharge zones. Models of heat and mass transport suggest that the hydrothermal flow system has an aspect ratio of approximately one. Focused flow is required to produce an ore deposit at the seafloor and subseafloor (Hannington and others, 2005) and is consistent with the alteration patterns observed in ancient VMS deposits (Large and others, 2001c).
3. As a source of chemical components to hydrothermal systems (Seyfried and others, 1999; Openholzer and others, 2003; Yang and Scott, 2006). Although it is generally accepted that metals are sourced from hydrothermal fluid/rock interactions along the fluid-flow path, metals may also be added from magmatic fluids and gases associated with the late stages of magmatic crystallization, as inferred in the current mineralizing system on Papua New Guinea (Gemell and others, 2004).

Rock Names

Rock names and rock associations that are commonly found with VMS deposits can be found in Le Maitre (2002) and the various figures therein.

Rock Associations

The lithochemistry of volcanic rock associations generally can be applied to specific tectonic settings. Here, the rock associations are classified as mafic, bimodal-mafic, siliciclastic-mafic, bimodal-felsic, and siliciclastic-felsic. The identification of specific tectonic settings for VMS deposits is referenced to the lithochemistry of volcanics in modern tectonic settings (Pearce and Cann, 1973; Pearce, 1995; Pearce and Peate, 1995; Piercey, 2009). It is common to observe more than one lithologic association in large VMS districts; for instance, the giant Bathurst district contains deposits that are associated with bimodal-mafic and siliciclastic-felsic associations (Goodfellow and others, 2003). Although these associations form a reasonable descriptive system, gradations between associations are common depending upon the scale of description (regional versus local). Mapping of VMS deposits often identifies felsic lava flows and subvolcanic felsic intrusions as the local-scale igneous associations (Large and others, 2001a, c; Monecke and others, 2006). The details of volcanic architecture and their volcanologic implications can be found in Chapter 5 (Morgan and Schulz, this volume); they have also been discussed in detail by Cas (1992). Rock associations are important features of VMS deposits because: (1) at the local scale, they identify sources of heat that drive hydrothermal circulation and local sources of magmatic metals and acidity; (2) at the more regional scale, they provide information on sources of metals that may give a VMS deposit its specific metal signature (Large, 1992; Stolz and Large, 1992); and (3) they provide a mechanism for the rapid burial of a massive sulfide deposit, for example, the geologically instantaneous emplacement of volcanoclastic turbidites.

Mafic-Ultramafic Association

The mafic-ultramafic association represents VMS deposits that are spatially connected with lithologies dominated by basaltic and (or) ultramafic rocks. The latter are rare occurrences in the rock record, for example, Greens Creek (Duke and others, in press), and their genetic relationship to ore is unclear. In Archean greenstone belts, VMS deposits may be associated with komatiite lavas. The VMS mafic-ultramafic associations dominated by basaltic rocks are found in the upper parts of obducted ophiolite complexes, for example,

Oman, Troodos, and Turner-Albright. In the modern oceans, the mafic association is found in two specific settings: mid-ocean ridges and mature back-arc basins. Hydrothermal activity spatially associated with ultramafic rocks, usually serpentinites, has been observed at several localities proximal to the Mid-Atlantic Ridge, for example, Lost City (Kelley and others, 2007), Logachev (Krasnov and others, 1995a), and the Gakkel Ridge (Edmonds and others, 2003). These hydrothermal systems are associated with oceanic core complexes formed during attenuation of the ocean crust at magma starved ridges. Although serpentinization is an exothermic process, which may be a significant source of heat in low-temperature (<100 °C) hydrothermal systems, it is likely the heat engine for high-temperature (350–450 °C) hydrothermal circulation is driven by subjacent gabbroic intrusives (Alt and Shanks, 2003; Allen and Seyfried, 2004; Alt and others, 2008). Further, Allen and Seyfried (2004) have argued that the geochemistry of the vent fluids at the Lost City low-temperature hydrothermal system indicates they are spent and cooled higher temperature fluids.

Olivine tholeiites are the common volcanic rock type found at mid-ocean ridges (MORs) and are collectively known as mid-ocean ridge basalts (MORBs). They are further divided into DMORB (depleted), NMORB (normal), TMORB (transitional), and EMORB (enriched) depending principally on their K/Ti ratios and incompatible element compositions. Many sites of active and extinct hydrothermal sulfide accumulation have been discovered along the mid-ocean ridge system, especially along the northern East Pacific Rise, but almost all have grades and tonnages that would be uneconomic if preserved in the rock record. An exception is the 3.9-Mt TAG deposit on the Mid-Atlantic Ridge (Hannington and others, 1998), but deposits with grades and tonnages equivalent to the larger VMS deposits have yet to be found at either mid-ocean ridge or back-arc basin sites.

It should also be noted that at some MOR sites that are regionally dominated by mafic lithologies, there exist more localized but still volumetrically substantial accumulations of basaltic andesite, andesite, dacite, and rhyolite. Examples include the overlapping spreading center at 9 °N on the East Pacific Rise (Wanless and others, 2010), the Galapagos spreading center (Embley and others, 1988; Perfit and others, 1999), and the southern Juan de Fuca Ridge (Cotsonika and others, 2005). In these environments, the more evolved igneous rock types are associated with hydrothermal activity and are the product of fractional crystallization of MORB and assimilation due to anatexis of shallow, hydrated basaltic crust. Consequently, in the absence of other information, the presence of more evolved rocks in an otherwise mafic association does not eliminate the possibility of an open-ocean setting.

The presence of the mafic-ultramafic association in back-arc basins is a function of proximity to the seaward island arc and is most clearly observed in mature back-arc basins that have well-organized spreading, for instance, east Scotia Sea, Lau Basin, and the Mariana Trough. The chemistry of basalts associated with island-arc systems is a complex function of

mantle chemistry and interactions between the mantle and fluids/melts ascending from the subducting slab (fig. 15–1).

In these settings, the hydrothermal systems are distinct from mid-ocean ridge systems in having much higher volatile contents that reflect the general, although not universal, volatile-rich nature of the associated volcanics and presumed subvolcanic intrusions (Gamo and others, 2006). The higher volatile contents also result in hydrothermal fluids that have pH values as low as 2, substantially less than found in mid-ocean ridge hydrothermal fluids and probably related to disproportionation of dissolved SO₂. A variety of basalts have been identified in back-arc basins, including MORBs that are chemically indistinguishable from those observed in open-ocean settings, and they range in composition from DMORB (central Lau Basin) to EMORB (north Fiji Basin). Importantly, a basalt type unique to the back-arc setting has been recognized and termed back-arc basin basalt (BABB). The latter has unique trace element signatures, particularly depletion in high field strength elements reflecting the subduction environment, and includes both depleted and enriched varieties (Pearce and Stern, 2006).

Siliciclastic-Mafic Association

This association is defined as subequal volumes of siliciclastic, sometimes pelitic, sediments and mafic, occasionally ultramafic, volcanic rocks. The mafic component is largely composed of volcanics with MORB-like affinities. The deposits of the Besshi district are the classic examples, but other examples include Windy Craggy and the small Hart River and Ice deposits in Canada and Greens Creek in the United States. Modern analogs include open-ocean spreading ridges with active hydrothermal systems that are sufficiently proximal to continents to receive significant volumes of sediment, such as observed at Escanaba Trough on the Gorda Ridge, Middle Valley on the northern Juan de Fuca Ridge, and Guaymas Basin in the Gulf of California. The relationship of the siliciclastic component to generation of VMS deposits is tenuous. Most VMS deposits form in relatively deep water (>1 km), which many workers propose inhibits exsolution of volatiles and formation of fragmental rocks, other than autobreccias, and results in a proximal volcanic stratigraphy that is dominated by lava flows. However, this interpretation of a nonfragmental requirement is controversial. Most silicic volcanoclastics appear to be redeposited lithologies (Monecke and others, 2006) sourced at shallow depths and emplaced in turbidity currents.

Bimodal-Mafic Association

This association is defined as VMS deposits that are principally correlated with mafic lithologies, but with up to 25 percent felsic rocks. Examples include the giant Kidd Creek, Flin Flon, Ruttan, and Bathurst deposits in Canada; the small Sumdum and Bald Mountain deposits in the United States

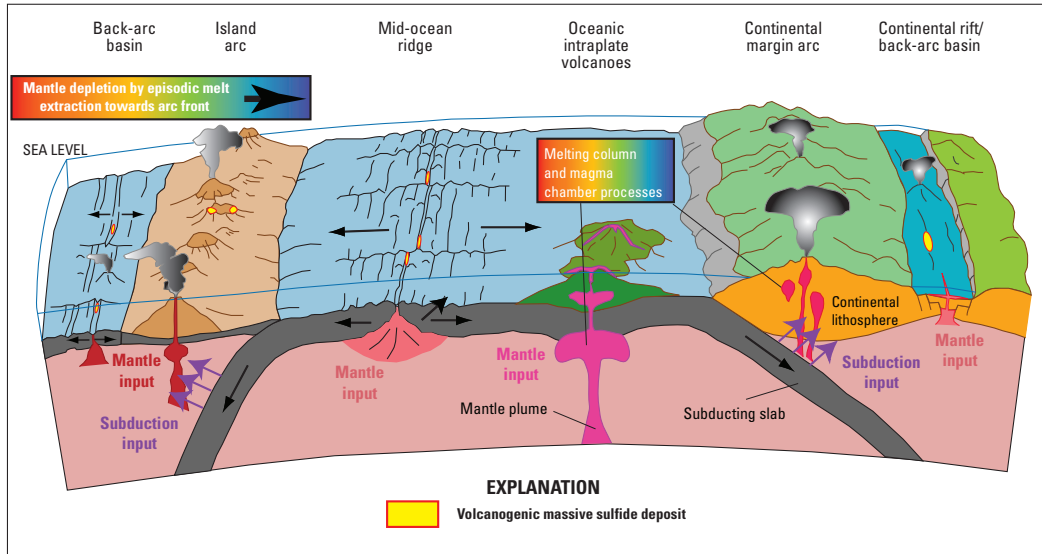


Figure 15-1. Schematic diagram showing the principal components and processes involved in the production of island-arc and back-arc volcanics that are major lithostratigraphic units associated with volcanogenic massive sulfide deposits. Subduction input includes (1) fluids released at shallow depths due to dehydration reactions, and (2) silicate melts released during partial melting at greater depths. These two processes metasomatize the overlying mantle, adding distinct trace-element assemblages. Movement of the asthenosphere is in response to the subduction process and may involve arc-parallel and arc-oblique movement. Two different mantle domains have been recognized in the western Pacific arcs—"Indian" and "Pacific"—based on isotopic systematics (Klein and others, 1988). Mantle melt extraction at shallow levels and subsequent mixing and fractionation produces a wide variety of volcanics at the surface, most of which are characterized by their hydrous nature. Island-arc volcanics are fundamentally different from back-arc volcanics because of the different inputs from the subducting oceanic crust. Modified from Pearce and Stern (2006).

(Schultz and Ayuso, 2003); and the Eulaminna deposit in Australia. The important criterion is that the felsic rocks commonly host the deposits (Barrie and Hannington, 1999; Galley and others, 2007). The mafic component may include MORB-type basalts, BABB-type basalts, and boninites that are associated with rhyolites. The tectonic setting is either:

- formed in a back-arc basin that is proximal to an island arc, for instance, the East Lau spreading center, north and south Mariana Trough, and the Kermadec Arc. The volcanics have a strong subduction component and (or) include felsic volcanics formed by partial melting of the root zones of a mature arc;
- formed in a fore-arc setting where the initiation of the volcanic front is dominated by basalts with minor components of more fractionated felsic volcanics (Jakes and White, 1971); or
- formed in an epicontinental arc setting in which the felsic components are sourced within the continental crust.

Bimodal-Felsic Association

This association is defined as VMS deposits that are principally correlated with felsic volcanics with a minor component of mafic volcanics. Examples include the deposits of the Kuroko and the Buchans districts. The minor mafic component may include MORB-like basalts, often with EMORB chemical signatures, and alkalic basalts that have ocean-island basalt (OIB) signatures and may also include shoshonites. This association is frequently associated with epicontinental arc environments. The felsic component may include andesites, dacites, and rhyolites but is often dominated by rhyolite that often has calc-alkaline affinities, for example, Mount Read deposits, Tasmania.

In modern arc settings, the bimodality is often developed at the mature stage of volcanism, such as with the Aleutian and Melanesian arcs, and the abundant rhyolites are considered to form by partial melting of the deeper, basaltic parts of the volcanic superstructure. The presence of highly alkalic magmas, particularly the eruption of shoshonites, is usually associated

with late-stage, low-volume volcanism, as observed in New Guinea. Bimodal felsic associations also may form during the incipient stages of back-arc basin development, where volcanics with arclike affinities are associated with alkalic magmas produced by lithospheric melting with a progression toward MORB-like magmas as the crust becomes attenuated.

Siliciclastic-Felsic Association

This association has a minor component of mafic volcanics, which may be as little as 20 percent, as observed in some of the Bathurst district deposits. The geochemistry of felsic volcanics, which include submarine pyroclastic and epiclastic flows (turbidites), crystal tuffs of dacitic, and rhyolitic composition, indicates a source by incorporation of variable amounts of continental crust with the heat sources being basaltic to gabbroic magmas that were ponded at a density barrier within the thick crust. This association also hosts major VMS deposits, such as the Iberian Pyrite Belt and parts of the Bathurst district. In the United States, VMS deposits at Crandon, Red Ledge, and Iron Mountain have this lithologic association.

Mineralogy

The primary mineralogy of volcanic rocks reflects crystallization during magmatic cooling over a temperature interval from approximately 1,300 to 900 °C. However, during interaction with hydrothermal fluids at much lower temperatures (450–350 °C and lower), the primary minerals and volcanic glass are destabilized. Consequently, rocks that compose the volcanic stratigraphy associated with VMS deposits, particularly in the footwall, are invariably, and pervasively, altered. In addition, secondary phases may be produced during postore metamorphic reactions. The primary magmatic minerals provide a feedstock and a sink of major, minor, and trace elements to circulating hydrothermal fluids. The major-element compositions of the principal primary minerals and the more common mineral-fluid ion exchanges involving major, minor, and trace elements are shown in table 15–1.

The pristine rocks also may contain glass, varying in amount from an interstitial component to a major constituent. The glass can be highly variable in composition, from ultra-mafic through basaltic to rhyolitic, with a wide suite of incompatible trace elements. Glass is highly unstable and is usually the first primary phase to be altered under hydrothermal conditions. In lithologies dominated by basaltic and andesitic rocks, glass is likely to be a minor component and contribute only a minor amount of trace elements to circulating fluids. However, more felsic rocks, such as dacites and rhyolites, may have a major glassy component.

Textures and Structures

The primary volcanic textures of igneous rocks associated with VMS deposits are usually overprinted during fluid/rock interactions. However, textures play an important role, along with fluid chemistry and temperature, in determining the rate at which the various primary phases are destabilized. Based on examination of volcanics associated with modern marine sulfide deposits, there exists a wide range of crystallinities from entirely crystalline (holocrystalline) through intermediate crystallinities (hypocrystalline or hypohyaline) to entirely glassy (holohyaline). Some common volcanic textures are described in table 15–2.

The structures of volcanic rocks associated with VMS deposits are highly variable and are a function of composition and submarine structural setting. Most volcanic successions are emplaced in rift settings that are dominated by island-arc or continental-margin-arc environments and may involve back-arc and intra-arc rifting. Siliciclastic-mafic-type deposits have a large component of clastic sediments mixed with basaltic dikes and sills and form on rifted open-ocean ridges proximal to a continental source of sediment. Modern settings include Middle Valley, Escanaba Trough, and Guaymas Basin. Particularly important is the relationship between composition, viscosity, and dissolved gas contents, which determine the explosive potential of magma. Apart from VMS deposits formed in shallow (<500 m) submarine settings, the volcanic architecture is dominated by flows and related autobreccias with spatially associated volcanoclastic rocks being derived from shallow, distal environments that may be either submarine or subaerial. In mafic-associated VMS deposits, the basalts are usually thin lava flows (pillows, sheet flows, and hummocky flows) with a large aspect ratio, excepting cases where ponding against neovolcanic faults produces thickened lava lakes. In VMS deposits associated principally with felsic volcanics, the latter are dominantly lava flows with flow domes, small aspect ratios, peperites, and autoclastic breccias. As described above, pumice-rich breccias, hyaloclastites, lapilli tuffs, crystal tuffs, vitric tuffs, ash fall deposits, and ash flows (ignimbrites) generally have distal, shallow sources. In stacked VMS deposits, intercalated volcanoclastics provide enhanced porosity and permeability resulting in diffuse fluid flow, whereas more focused flow may be related to fracture porosity provided by flows and flow domes. In some cases, subvolcanic intrusions may be exposed and are usually quartz-feldspar porphyries. The variations and types of structures that develop depend largely on the specific volcanic environment of deposition. Caldera settings have been proposed for some Kuroko deposits (Ohmoto and Takahashi, 1983), although these cannot be formed by explosive release of subvolcanic magma in the classic sense of central volcano collapse, and

Table 15-1. Major and trace element composition of major minerals observed in igneous rocks associated with modern seafloor massive sulfides in a variety of settings.

[PGE, platinum group elements; REE, rare earth elements; Ag, silver; Al, aluminum; As, arsenic; Au, gold; Ba, barium; Be, beryllium; Ca, calcium; Cl, chlorine; Co, cobalt; Cr, chromium; Cu, copper; Eu, europium; F, fluorine; Fe, iron; In, indium; K, potassium; Li, lithium; Mg, magnesium; Mn, manganese; Na, sodium; Ni, nickel; Pb, lead; Rb, rubidium; S, sulfur; Sc, scandium; Si, silicon; Sr, strontium; Ti, titanium; V, vanadium; Zn, zinc]

| Minerals | Major elements | Trace elements |
|---------------|---|---|
| Plagioclase | $\text{CaAl}_2\text{Si}_2\text{O}_8$ (anorthite) – $\text{NaAlSi}_3\text{O}_8$ (albite) solid solution | Na ⁺ , Al ⁺⁺⁺ , Ca ⁺⁺ , Sr ⁺⁺ , Ba ⁺⁺ , Eu ⁺⁺ |
| K-Feldspar | KAlSi_3O_8 (orthoclase, sanidine) | Li ⁺ , Al ⁺⁺⁺ , K ⁺ , Rb ⁺ , Ba ⁺⁺ , REE |
| Olivine | Mg_2SiO_4 (forsterite) – Fe_2SiO_4 (fayalite) solid solution | Mg ⁺⁺ , Fe ⁺⁺ , Co ⁺⁺ , Ni ⁺⁺ |
| Clinopyroxene | CaSiO_3 (wollastonite) – MgSiO_3 (enstatite) – FeSiO_4 (ferrosilite) solid solution | Mg ⁺⁺ , Al ⁺⁺⁺ , Ca ⁺⁺ , Sc ⁺⁺ , Ti ⁺⁺⁺⁺ , Cr ⁺⁺⁺ , Mn ⁺⁺ , Fe ⁺⁺ , REE |
| Orthopyroxene | MgSiO_4 (enstatite) – FeSiO_4 (ferrosilite) solid solution | Mg ⁺⁺ , Al ⁺⁺⁺ , Mn ⁺⁺ , Fe ⁺⁺ , Co ⁺⁺ , Zn ⁺⁺ |
| Amphibole | $(\text{Ca}, \text{Na})(\text{Ca}, \text{Fe}^{2+}, \text{Mg}, \text{Na})_2(\text{Al}, \text{Fe}^{2+}, \text{Fe}^{3+}, \text{Mg})_5(\text{Al}, \text{Si}, \text{Ti})_8\text{O}_{22}(\text{OH}, \text{F}, \text{Cl})_2$ (general formula) | F ⁻ , Cl ⁻ , Na ⁺ , Mg ⁺⁺ , Al ⁺⁺⁺ , Ca ⁺⁺ , Ti ⁺⁺⁺⁺ , V ⁺⁺⁺ , Cr ⁺⁺⁺ , Mn ⁺⁺ , Fe ⁺⁺ , Fe ⁺⁺⁺ , Co ⁺⁺ , Ni ⁺⁺ , Zn ⁺⁺ |
| Mica | $\text{K}(\text{Fe}^{2+})_3(\text{Al}, \text{Fe}^{3+})\text{Si}_3\text{O}_{10}(\text{OH}, \text{F}, \text{Cl})_2$ (biotite) – $\text{KMg}_3\text{AlSi}_3\text{O}_{10}(\text{OH}, \text{F}, \text{Cl})_2$ (phlogopite) solid solution | Be ⁺⁺ , F ⁻ , Mg ⁺⁺ , Al ⁺⁺⁺ , Cl ⁻ , K ⁺ , Fe ⁺⁺ , Fe ⁺⁺⁺ , V ⁺⁺⁺ , Zn ⁺⁺ |
| White mica | $\text{KAl}_2(\text{Si}_3\text{Al})\text{O}_{10}(\text{OH}, \text{F}, \text{Cl})_2$ (muscovite) | Li ⁺ , Be ⁺⁺ , F ⁻ , Al ⁺⁺⁺ , Cl ⁻ , K ⁺ |
| Spinel | $\text{Fe}^{2+}\text{Fe}^{3+}\text{O}_4$ (magnetite) – $\text{MgFe}_2^{3+}\text{O}_4$ (magnesioferrite) – $\text{Fe}^{2+}\text{Cr}_2\text{O}_4$ (chromite) – MgAl_2O_4 (spinel) solid solution | Mg ⁺⁺ , Al ⁺⁺⁺ , Ti ⁺⁺⁺⁺ , V ⁺⁺⁺ , Cr ⁺⁺⁺ , Mn ⁺⁺ , Mn ⁺⁺⁺ , Fe ⁺⁺ , Fe ⁺⁺⁺ , Co ⁺⁺ , Ni ⁺⁺ |
| Oxide | FeTiO_3 (ilmenite) – MgTiO_3 (geikielite) solid solution | Mg ⁺⁺ , Si ⁺⁺⁺⁺ , Ti ⁺⁺⁺⁺ , Mn ⁺⁺ , Fe ⁺⁺ |
| Sulfide | (Fe, Ni)S (monosulfide solid solution). (Fe, Ni, Cu)S (intermediate solid solution). FeS_2 (pyrite). Fe_{1-x}S (pyrrhotite) | S ⁻ , Fe ⁺⁺ , Co ⁺⁺ , Ni ⁺⁺ , Cu ⁺⁺ , Zn ⁺⁺ , As ⁻⁻⁻ , In ⁺⁺⁺ , Ag ⁺ , Au ⁺⁺⁺ , rare metals, PGE, Pb ⁺⁺ |
| Notes: | Silicates are also a major source of silica to solution. Metals may be carried as either chloride or bisulfide complexes. | |

well-defined caldera structures have not been mapped. More detailed descriptions of volcanic architecture can be found in Chapter 5.

Petrochemistry

Many different schemes for the classification of igneous rocks have been proposed (Philpotts, 1990). Two that are commonly used and quoted are shown in figure 15-2.

Major-Element Geochemistry

The major-element chemistry of volcanic rocks associated with VMS deposits is determined by a combination of source composition, temperature and pressure (mantle and crustal regimes), and subsequent fractional crystallization and (or) assimilation. Generally, the major basaltic series are divided into tholeiitic (MORB, BABB), calc-alkalic (island-arc basalt [IAB]), and alkalic (OIB), but island-arc settings also include the boninite and shoshonite series. The major-element compositions of different types of basaltic rocks associated with VMS deposits are found in table 15-3 and more evolved rocks in table 15-4.

The major-element composition of altered volcanics reflects the degree of alteration and alteration mineralogy and

is a useful guide to the proximity of ore. For instance, Offler and Whitford (1992) show that the alteration halo around the Que River deposit, Tasmania, can be mapped using major-element compositions and associated mineral chemistry. Large and others (2001b) developed the “alteration box plot” that employs two major element alteration indices: the Ishikawa alteration index:

$$100(\text{K}_2\text{O}+\text{MgO})/(\text{K}_2\text{O}+\text{MgO}+\text{Na}_2\text{O}+\text{CaO}),$$

and a chlorite-carbonate-pyrite index or CCPI:

$$100(\text{MgO}+\text{FeO})/(\text{MgO}+\text{FeO}+\text{Na}_2\text{O}+\text{K}_2\text{O}),$$

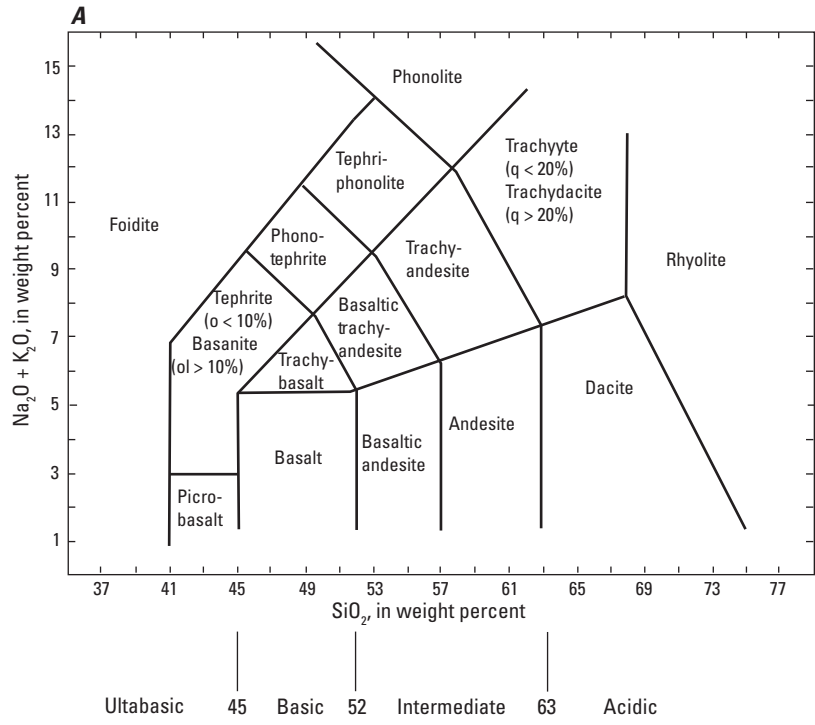
which they modify from Lentz (1999). This scheme: (1) can generally be used to distinguish alteration effects from subsequent metamorphic overprint; (2) cannot recognize quartz gangue mineralization; (3) is mainly useful for felsic versus mafic volcanics; and (4) cannot be used for altered clastic sedimentary rocks.

Trace-Element Geochemistry

An overview of the litho-geochemistry, including trace-element geochemistry, of volcanic rocks associated with VMS deposits can be found in Piercey (2009). Trace elements have played a fundamental role in the classification of igneous rocks from a wide variety of tectonic settings, and their geochemical behavior has been used extensively to identify and separate the geologic processes active in the production of the

Table 15-2. Common textures observed in pristine igneous rocks associated with modern seafloor massive sulfides.

| Name | Description |
|-----------------|---|
| Hyaline | A completely glassy rock that may contain minor quenched crystals (crystallites). Commonly observed in submarine volcanics as quenched surfaces in basalts, basaltic andesites and andesites. Glass may make up a large volume of submarine and terrestrial evolved volcanics (dacites, rhyolites) if the melts are relatively dry. These latter volcanics often display distinct banding due to differences in: (a) crystallite abundances and orientations; (b) degree of devitrification; (c) degree of spherulite formation. Glass may also be the main product of submarine and terrestrial fire fountaining and welded and unwelded rhyolite tuffs. In the case of rhyolitic tuffs the texture is unwelded if the glass fragments are not welded together and are commonly found in a matrix of very fine grained glass (ash). In the case of welded tuffs the rock often has a laminated appearance due to extreme compaction and welding of original pumice fragments. The regular alignment of flattened pumice produces a texture known as eutaxitic. |
| Hypocrystalline | A partly crystalline rock that shows distinct differences in granularity due to presence of both crystals and glass. These rocks are often called vitrophyres or pitchstones with the modifying terms of the main phenocryst phases, for example, plagioclase-augite vitrophyre. In some cases the glass may have severely devitrified if it contains substantial dissolved water |
| Holocrystalline | A completely crystalline rock that may be equigranular or porphyritic. Equigranular rocks may be cryptocrystalline (individual crystals are submicroscopic) or microcrystalline (individual crystals are microscopic) or phaneritic (individual crystals can be discerned by eye). Equigranular rocks may be: (a) intersertal (hyalophitic, subophitic, ophitic), in which plagioclase is partly or completely surrounded by pyroxene and (or) olivine; (b) intergranular, in which one mineral phase dominates and other phases fill in the spaces between this phase; (c) trachytic, in which small feldspar crystals are aligned in a distinct flow texture. A variety is trachytoidal in which the feldspar crystals are larger yet still aligned in a flow pattern. Despite the name, these flow textures can be observed in rocks from basaltic to rhyolitic. |
| Cavity textures | A variety of cavity textures may also exist that include vesicular textures due to presence of irregular holes (vesicles) due to exsolution of a gas phase during magmatic cooling, amygdaloidal textures in which former vesicles are filled by late-magmatic or post-magmatic minerals (commonly carbonates, zeolites, quartz). In some coarser rocks the irregular-shaped gas cavities may be filled with late-magmatic, euhedral crystals and the texture is termed miarolitic. |
| Note: | The various textures of igneous rocks are important in determining the extent to which individual minerals react with percolating hydrotherm fluids. In turn, this determines the interchange of metals and other elements between the rock and the fluid. |



| Further subdivisions for the following: | Trachybasalt | Basaltic trachyandesite | Trachyandesite |
|---|-----------------------|-------------------------|----------------|
| $\text{Na}_2\text{O} - 2.0 \geq \text{K}_2\text{O}$ | Hawaiite | Mugearite | Benmoreite |
| $\text{Na}_2\text{O} - 2.0 \leq \text{K}_2\text{O}$ | Potassic trachybasalt | Shoshonite | Latite |

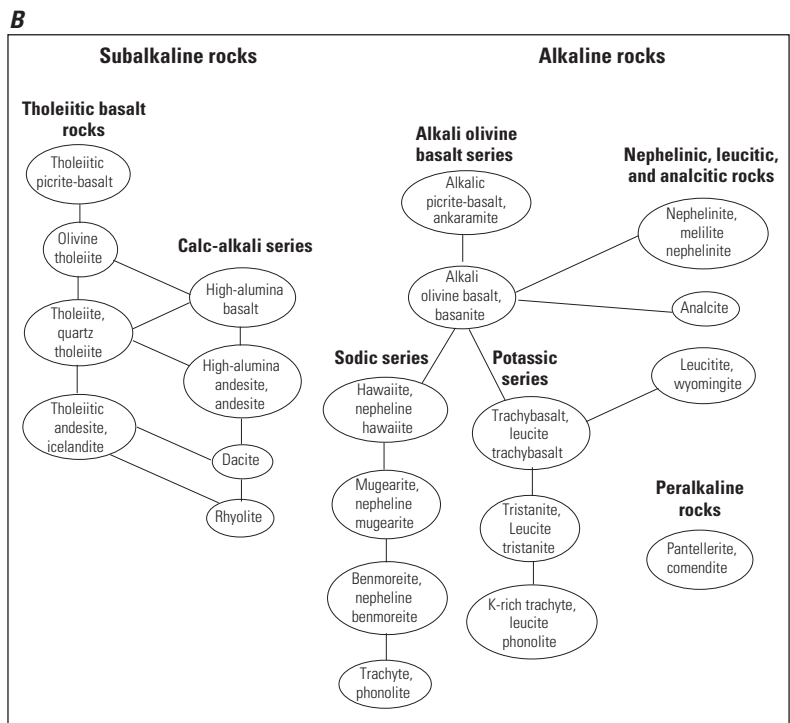


Figure 15-2. Two classifications of common igneous rocks. **A**, Total alkali ($\text{Na}_2\text{O} + \text{K}_2\text{O}$) versus silica (SiO_2), or TAS, classification system. After Le Maitre (2002). **B**, Classification based on general chemical characteristics, with lines connecting commonly associated rocks. After Irvine and Baragar (1971).

Table 15-3. Average major element composition of basaltic rocks associated with volcanogenic massive sulfide deposits.

[DMORB, depleted mid-ocean ridge basalt; NMORB, normal mid-ocean ridge basalt; TMORB, transitional mid-ocean ridge basalt; EMORB, enriched mid-ocean ridge basalt; BABB, back-arc basin basalt; IAB, island-arc basin basalt. $K/Ti = K_2O \cdot 100 / TiO_2$; $Mg\# = \text{molar } MgO / [MgO + FeO \text{ (Total)}]$. Data sources: IAB, Shoshonite from Jakes and White (1971); MORB data from northern East Pacific Rise; BABB data from Fiji and Lau Basins; Data from PetDB, Petrologic Database of the Ocean Floor (www.petdb.org)]

| | DMORB¹ | NMORB² | TMORB³ | EMORB⁴ | BABB⁵ | BABB⁶ | BABB⁷ | BABB⁸ | IAB | Shoshonite |
|--------------------------------|--------------------------|--------------------------|--------------------------|--------------------------|-------------------------|-------------------------|-------------------------|-------------------------|------------|-------------------|
| SiO ₂ | 50.32 | 50.17 | 50.34 | 50.56 | 49.09 | 49.15 | 49.04 | 50.40 | 50.59 | 53.74 |
| TiO ₂ | 1.17 | 1.19 | 1.22 | 1.24 | 1.29 | 1.16 | 0.99 | 0.99 | 1.05 | 1.05 |
| Al ₂ O ₃ | 15.47 | 15.79 | 16.02 | 15.40 | 16.83 | 16.30 | 16.55 | 16.52 | 16.29 | 15.84 |
| FeO (Total) | 9.09 | 8.28 | 8.69 | 8.45 | 9.59 | 9.32 | 8.14 | 8.78 | 8.37 | 7.77 |
| MnO | 0.18 | 0.16 | 0.15 | 0.16 | 0.11 | 0.14 | 0.15 | 0.17 | 0.17 | 0.11 |
| MgO | 9.14 | 8.33 | 8.12 | 8.58 | 8.91 | 8.85 | 8.70 | 8.42 | 8.96 | 6.36 |
| CaO | 11.54 | 12.07 | 11.99 | 11.83 | 12.46 | 12.37 | 12.88 | 11.08 | 9.50 | 7.90 |
| Na ₂ O | 2.43 | 2.45 | 2.44 | 2.41 | 2.61 | 2.37 | 2.36 | 2.94 | 2.89 | 2.38 |
| K ₂ O | 0.05 | 0.10 | 0.18 | 0.38 | 0.05 | 0.09 | 0.14 | 0.21 | 1.07 | 2.57 |
| P ₂ O ₅ | 0.12 | 0.11 | 0.13 | 0.16 | 0.16 | 0.14 | 0.08 | 0.13 | 0.21 | 0.54 |
| K/Ti | 3.7 | 8.1 | 15.0 | 29.7 | 4.0 | 7.4 | 14.1 | 21.1 | 20.0 | 51.4 |
| Mg# | 63.7 | 62.4 | 63.5 | 64.1 | 62.6 | 63.0 | 65.7 | 63.0 | 65.8 | 60.0 |

¹ DMORB: $K/Ti < 5$; $Mg\# > 60$

² NMORB: $K/Ti 5-11.5$; $Mg\# > 60$

³ TMORB: $K/Ti 11.5-20$; $Mg\# > 60$

⁴ EMORB: $K/Ti > 20$; $Mg\# > 60$

⁵ BABB with $K/Ti < 5$; $Mg\# > 60$

⁶ BABB with $K/Ti 5-11.5$; $Mg\# > 60$

⁷ BABB with $K/Ti 11.5-20$; $Mg\# > 60$

⁸ BABB with $K/Ti > 20$; $Mg\# > 60$

Table 15–4. Major element compositions of various volcanic rock series associated with volcanogenic massive sulfide deposits.

[MORB, Mid-ocean ridge basalt; NMORB, normal mid-ocean ridge basalt; n.d., no data; Al, aluminum]

| | Boninite series ¹ | | | | MORB series ² | | | Calc-alkaline series ³ | | | |
|--------------------------------|------------------------------|----------|--------|----------|--------------------------|----------|--------|-----------------------------------|----------|--------|----------|
| | Boninite | Andesite | Dacite | Rhyolite | NMORB | Andesite | Dacite | High-Al basalt | Andesite | Dacite | Rhyolite |
| SiO ₂ | 56.45 | 59.50 | 66.88 | 66.88 | 50.17 | 56.82 | 65.08 | 50.59 | 59.64 | 66.80 | 70.70 |
| TiO ₂ | 0.10 | 0.20 | 0.20 | 0.20 | 1.19 | 1.71 | 0.83 | 1.05 | 0.76 | 0.23 | 0.30 |
| Al ₂ O ₃ | 13.59 | 13.91 | 10.64 | 10.64 | 15.79 | 13.64 | 12.91 | 16.29 | 17.38 | 18.24 | 13.40 |
| FeO (total) | 7.82 | 7.72 | 4.54 | 4.54 | 8.28 | 10.13 | 6.81 | 8.37 | 5.00 | 2.14 | 3.50 |
| MnO | 0.10 | 0.11 | 0.07 | 0.07 | 0.16 | 0.19 | 0.12 | 0.17 | 0.09 | 0.06 | 0.30 |
| MgO | 5.40 | 3.04 | 0.43 | 0.43 | 8.33 | 3.09 | 0.8 | 8.96 | 3.95 | 1.50 | 0.05 |
| CaO | 9.19 | 7.63 | 3.04 | 3.04 | 12.07 | 6.55 | 3.16 | 9.50 | 5.93 | 3.17 | 2.80 |
| Na ₂ O | 2.09 | 2.57 | 3.39 | 3.39 | 2.45 | 4.12 | 4.81 | 2.89 | 4.40 | 4.97 | 4.90 |
| K ₂ O | 0.52 | 0.56 | 0.97 | 0.97 | 0.10 | 0.68 | 1.34 | 1.07 | 2.04 | 1.92 | 2.00 |
| P ₂ O ₅ | n.d. | n.d. | n.d. | n.d. | 0.11 | 0.23 | 0.19 | 0.21 | 0.28 | 0.09 | 0.01 |
| K/Ti | 544.44 | 273.40 | 483.75 | 506.25 | 8.11 | 39.72 | 161.45 | 101.90 | 268.42 | 834.78 | 666.67 |
| Mg# | 55.10 | 41.22 | 14.22 | 14.22 | 62.40 | 35.47 | 17.45 | 65.83 | 58.71 | 55.79 | 2.51 |

¹ Dobson and others (2006)² V.D. Wanless, Woods Hole Oceanographic Institution, unpublished data (2009)³ Jakes and White (1971); Baker (1982)⁴ Ridley (1970); Chester and others (1985)**Table 15–4.** Major element compositions of various volcanic rock series associated with volcanogenic massive sulfide deposits.—Continued

[MORB, Mid-ocean ridge basalt; NMORB, normal mid-ocean ridge basalt; n.d., no data; Al, aluminum]

| | Shoshonite series ³ | | | | Ocean island series ⁴ | | | |
|--------------------------------|--------------------------------|--------|----------|-----------------------|----------------------------------|-----------|-----------|-----------|
| | Shoshonite | Latite | Basanite | Alkali olivine basalt | Hawaiite | Mugearite | Benmorite | Phonolite |
| SiO ₂ | 53.74 | 59.27 | 44.22 | 48.04 | 47.21 | 56.36 | 60.95 | 62.08 |
| TiO ₂ | 1.05 | 0.56 | 12.74 | 1.47 | 1.62 | 1.71 | 1.44 | 0.98 |
| Al ₂ O ₃ | 15.84 | 15.90 | 2.93 | 15.35 | 16.50 | 15.37 | 17.62 | 16.32 |
| FeO (total) | 7.77 | 5.18 | 11.70 | 9.26 | 10.43 | 9.24 | 4.69 | 3.68 |
| MnO | 0.11 | 0.10 | 0.14 | 0.18 | 0.21 | 0.16 | 0.14 | 0.10 |
| MgO | 6.36 | 5.45 | 11.85 | 9.74 | 6.23 | 3.07 | 1.19 | 0.49 |
| CaO | 7.90 | 5.90 | 10.86 | 9.52 | 11.06 | 6.36 | 3.92 | 1.21 |
| Na ₂ O | 2.38 | 2.67 | 3.05 | 3.80 | 3.20 | 4.18 | 5.66 | 7.11 |
| K ₂ O | 2.57 | 2.68 | 1.01 | 0.65 | 1.76 | 2.11 | 2.77 | 5.45 |
| P ₂ O ₅ | 0.54 | 0.41 | 0.61 | 0.37 | 0.51 | 0.69 | 0.41 | 0.13 |
| K/Ti | 244.76 | 478.57 | 7.93 | 44.22 | 108.64 | 123.39 | 192.36 | 556.12 |
| Mg# | 59.57 | 65.44 | 64.58 | 65.44 | 51.81 | 37.42 | 31.35 | 19.33 |

various rock series that are associated with VMS deposits. One group of trace elements is particularly useful; the incompatible or lithophile trace elements that have a strong affinity for the melt phase during partial melting and fractional crystallization. Some of these elements also show chalcophilic (sulfur-seeking) behavior. The group includes the elements Li, Be, B, Sc, V, Cr, Rb, Sr, Cs, Ba, Nb, W, Pb, U, and Th. Some lithophile trace elements, such as Rb, Cs, and U, are mobile during post-emplacement weathering, diagenesis, metasomatism, and metamorphism. They may exhibit open system behavior and be selectively redistributed within the volcanic stratigraphy or lost completely.

It is common to separate out two subsets of incompatible elements: the high field strength elements (HFSE) and the rare earth elements (REE). The HFSE include Y, Zr, Hf, Nb, Ta, and the major element Ti. They are characterized by very similar geochemical behavior, are highly insoluble in aqueous fluids, and hence tend to be very immobile. The REE are the elemental series between La and Lu, and, except for Eu and in some cases Ce, behave as a coherent group of elements that is also substantially insoluble in aqueous fluids, excepting carbonate waters where they can form soluble and, hence, mobile carbonate species. The HFSE and REE are particularly useful because their immobility and fluid-insoluble nature results in: (1) a tendency to retain protolith geochemical characteristics that may prove useful to determine tectonic setting (fig. 15–2) (Dusel-Bacon and others, 2004; Piercey, 2009); and (2) a method to separate mantle processes from subduction slab processes. Many VMS studies use HFSE and REE to identify protolith provenance, for example, Whitford and Ashley (1992).

A useful graphical representation of trace-element abundances is the use of the so-called binary “spider diagram,” an extension of the familiar REE-normalized abundance diagram. Each individual pattern is called a “spidergram” and is constructed by plotting an array of trace elements on the X-axis in order of decreasing incompatibility against elemental abundances on the Y-axis. The latter can be adjusted to a variety of normalizing values, depending upon the problem at hand, for example, primordial mantle, chondrites, MORB, average upper crust, North American shale (fig. 15–4).

Piercey (2009) has extended the spidergram to include the compatible elements Al, V, and Sc that may also be relatively immobile during alteration. Pearce and Stern (2006) have shown that normalization to MORB abundances and then renormalizing, so that $YB_N = 1$, is particularly useful in describing volcanic rocks in the various tectonic settings that host VMS deposits, especially those settings that involve suprasubduction and back-arc settings (fig. 15–4). Pearce and Stern (2006) have used trace elements to show that back-arc basins actually contain not only BABB volcanics, but also basalts that closely resemble the spectrum of compositions found at ocean-ridge systems, that is, DMORB to EMORB. These basalts must have depleted mantle sources that are geochemically similar to mantle underlying mid-ocean ridge

magmatic systems. In contrast, spidergrams for BABB show much more element-to-element variability due to the influence of the subducting slab, for example, anomalous abundances of K, Ba, and Pb.

Spidergrams are useful in separating out the effects of mantle geochemistry, for instance, use of the Nb/Yb ratio (fig. 15–3). Discussions regarding trace-element behavior can be quite nuanced (Langmuir and others, 2006; Pearce and Stern, 2006), but some generalizations can be made. The geochemistry of back-arc basin basalts (BABB) is primarily determined by chemical interactions between mantle and fluids and (or) melts generated within the subducting slab. These interactions tend to decrease as a function of distance of the back-arc spreading system from the island-arc system. Secondly, the geochemistry is determined by fractional crystallization and by assimilation, the latter being also a function of distance from the arc or an extending continental margin.

Besides their usefulness in petrogenetic studies, trace elements in VMS protoliths are an important source of cations and anions to circulating hydrothermal fluid. In particular, metals are efficiently leached from volcanic rocks at temperatures in excess of 300 °C (Seyfried and others, 1999, see Chapter 13, this report).

Transition element (Cr, V, Ni, Co, Cu) abundances decrease as a function of increasing silica content in all magma series (alkalic, tholeiitic, and calc-alkaline), whereas Pb concentrations increase. Generally, the concentration of transition metals in IAB (average 105 ppm Cu, 74 ppm Zn) and MORB (average 71 ppm Cu, 84 ppm Zn) is substantial (fig. 15–5) (Stanton, 1994). The dilution as a function of silica content is a reflection of the compatible nature of transition metals all having a bulk K_D substantially greater than one (Perfit and others, 1999). The decrease in transition metal abundances during fractional crystallization is principally a function of the precipitation of olivine, Fe-Ti oxides, and immiscible sulfides. The crystallization of Fe-Ti oxides is largely governed by the melt redox state. In IAB melts, high pO_2 results in the early crystallization of Fe-Ti oxides and the transitional elements are depleted at an early stage of crystallization. In MORB melts, the low pO_2 results in build up of FeO and TiO_2 in the melt phase during fractional crystallization and the Fe-Ti oxides are a late phase to crystallize. Consequently, the transition metals are depleted at a slower rate in MORB relative to IAB melts.

In principal, the separation of an immiscible sulfide phase should have a dramatic effect on the melt concentrations of transition metals, particularly Ni and Cu. However, sulfur solubility systematics, which control the saturation of sulfides in silicate melts, are complicated by the dissolution of a gaseous sulfur phase. Nonetheless, the systematic behavior of Cu and Zn relative to S suggests that sulfide precipitation is an important process during fractional crystallization in moderating the concentrations of some transition metals. In basalts, the concentrations of S are as high as 1,500 ppm and increase to approx. 2,500 ppm at the andesite stage of crystallization,

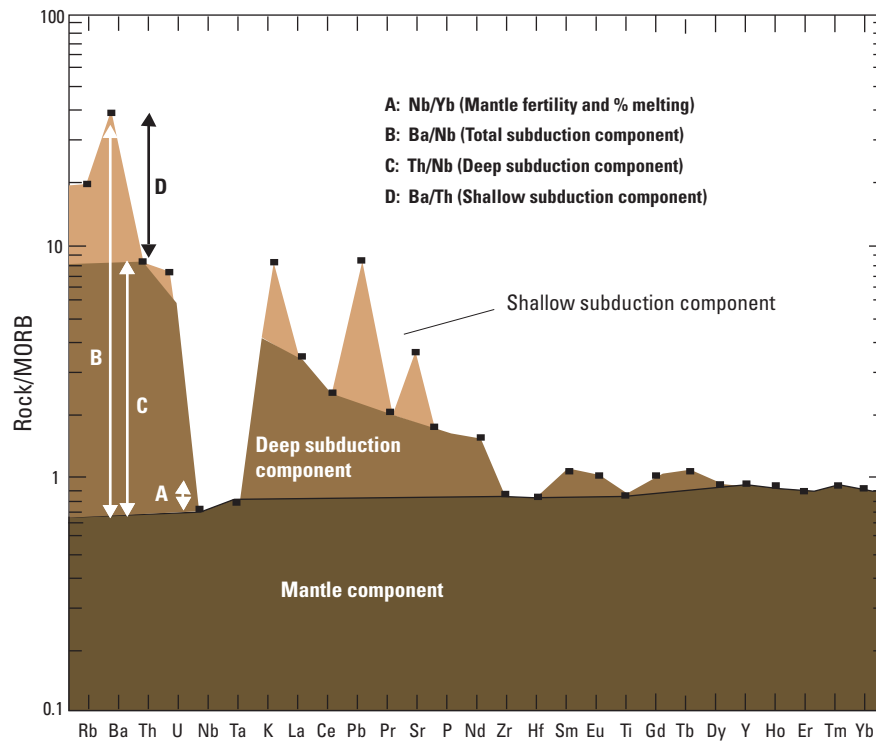


Figure 15-3. The use of trace-element abundances and trace-element ratios as proxies for the subduction input to the overlying mantle preserved in the mantle partial melts that form island-arc and back-arc volcanics. The pristine (depleted) mantle component is represented by mid-ocean ridge basalt (MORB) trace-element values. The deep subduction component is represented by trace-element signatures of partial melting of the subducting crust, that is, concentrations and element ratios that are a function of element incompatibility. The shallow subduction process is represented by trace-element concentrations and ratios that partly reflect sediment-derived fluids. Modified from Pearce and Stern (2006). [Ba, barium; Ce, cerium; Dy, dysprosium; Er, erbium; Eu, europium; Gd, gadolinium; Hf, hafnium; Ho, holmium; K, potassium; La, lanthanum; Nb, niobium; Nd, neodymium; P, phosphorus; Pb, lead; Pr, praseodymium; Rb, rubidium; Sr, strontium; Sm, samarium; Ta, tantalum; Tb, terbium; Th, thorium; Ti, titanium; Tm, thulium; U, uranium; Y, yttrium; Yb, ytterbium; Zr, zirconium]

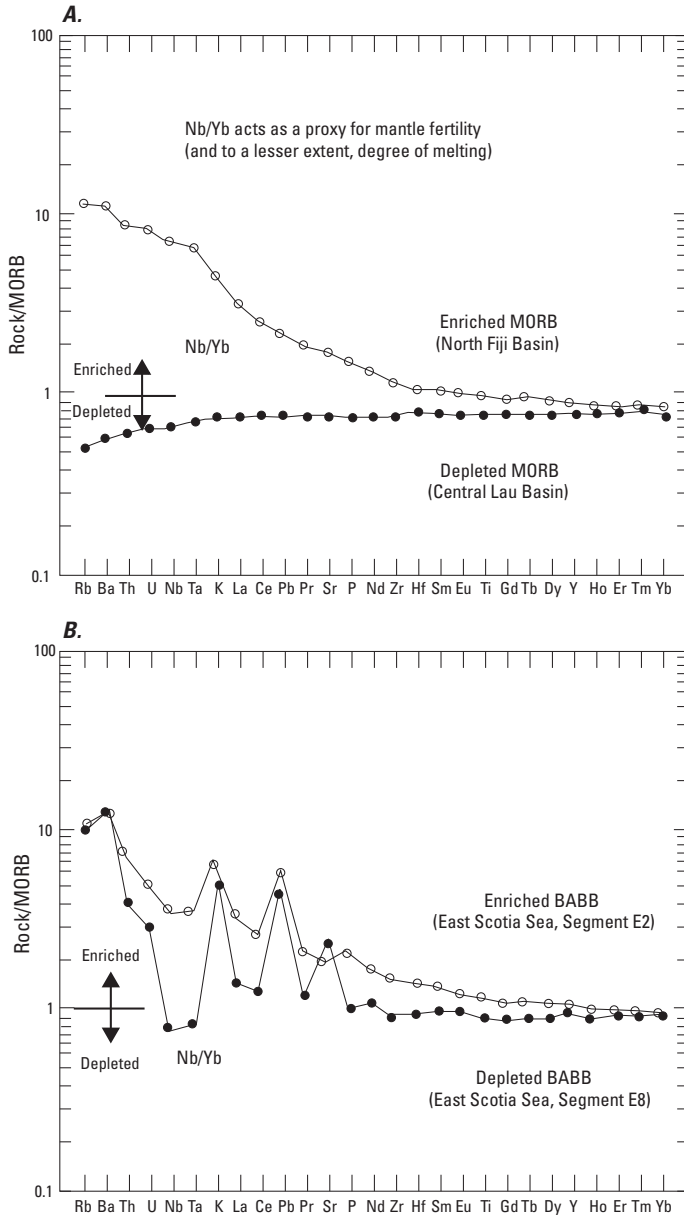


Figure 15-4. Trace-element patterns for several types of volcanics from modern tectonic environments that are commonly associated with volcanogenic massive sulfide (VMS) deposits. These patterns can be compared to those in Pearce (2009) from ancient VMS lithostratigraphic associations. The Nb/Yb ratio is a useful discriminant between enriched and depleted (A) mid-ocean ridge basalt (MORB) and (B) back-arc basin basalt (BABB). Note that the patterns for BABB are quite distinct from the MORB patterns. The latter reflect degrees of melting of depleted (and perhaps slightly enriched) mantle. The former reflect the additional complexities of subduction dehydration and melting. Modified from Pearce and Stern (2006). [Ba, barium; Ce, cerium; Dy, dysprosium; Er, erbium; Eu, europium; Gd, gadolinium; Hf, hafnium; Ho, holmium; K, potassium; La, lanthanum; Nb, niobium; Nd, neodymium; P, phosphorus; Pb, lead; Pr, praseodymium; Rb, rubidium; Sr, strontium; Sm, samarium; Ta, tantalum; Tb, terbium; Th, thorium; Ti, titanium; Tm, thulium; U, uranium; Y, yttrium; Yb, ytterbium; Zr, zirconium]

after which the abundances steadily decrease. Thus, it is evident that the protoliths to VMS deposits are a rich source of S for hydrothermal fluids.

Isotope Geochemistry

Isotope geochemistry of fresh volcanic rocks is divided into two principal discussions, the radiogenic isotopes (Sr, Nd, Pb) and the stable isotopes. The latter are further divided into the traditional stable isotopes (H, O, S) and the nontraditional isotopes (B, Fe, Cu, Zn). Rubidium and to a lesser degree Sr are alteration mobile elements and may exchange with percolating fluids during hydrothermal alteration (Ridley and others, 1994). Volcanic lithologies associated with VMS deposits may retain some of their isotopic signatures depending upon the degree of alteration, either during hydrothermal flow associated with the formation of VMS deposits or through later metamorphism. It is therefore useful to initially discuss the isotopic signatures of fresh volcanics.

In modern seafloor hydrothermal systems, stable isotopes may be used to examine fluid-flow pathways in exposed stockworks, and this approach also has been used to map paleohydrothermal systems in ancient VMS deposits (Holk and others, 2008).

Radiogenic Isotopes

MORB, OIB, BABB, IAB, and Related Volcanics

Strontium, Neodymium, Lead

Strontium, Nd and Pb isotopic composition of basalts erupted at mid-ocean ridges (Ito and others, 1987) shows a negative correlation between $^{87}\text{Sr}/^{86}\text{Sr}$ versus $^{143}\text{Nd}/^{144}\text{Nd}$ and a positive correlation between $^{87}\text{Sr}/^{86}\text{Sr}$ and Pb isotopes (fig. 15-6).

Probably the most extensively studied of the ocean-based island-arc systems is the Izu-Bonin-Marianas system (Stern and others, 2003). Strontium, Nd and Pb isotopic relationships between IAB volcanics and BABB volcanics are shown in figure 15-7. Back-arc basins include both MORB-type volcanics and back-arc basin volcanics (BABB, *ss*). Although BABB in back-arc basins covers a wide variety of trace-element compositions, the radiogenic and stable isotope compositions are much more restricted and similar to values in MORB from open-ocean settings. BABB volcanics have similar $^{87}\text{Sr}/^{86}\text{Sr}$ to MORB but have lower $^{143}\text{Nd}/^{144}\text{Nd}$ and higher values for ^{206}Pb , ^{207}Pb and $^{208}\text{Pb}/^{204}\text{Pb}$.

Island-arc volcanics carry more radiogenic Sr and Pb and less radiogenic Nd relative to MORB (fig. 15-7),

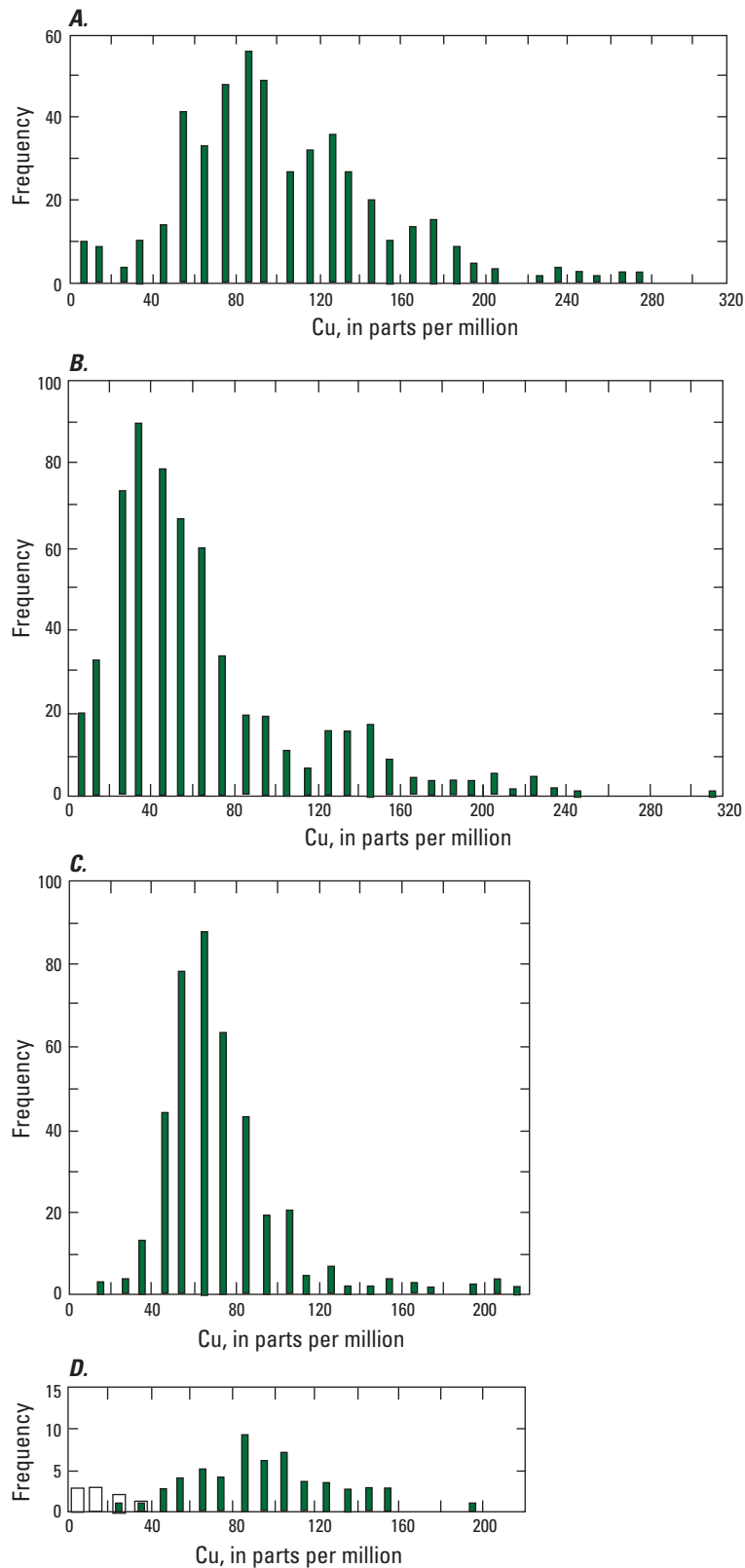


Figure 15-5. Frequency distributions of copper (Cu) in various modern volcanics. *A*, Arc basalts ($\text{SiO}_2 < 52\%$). *B*, Arc lavas ($\text{SiO}_2 > 52\%$). *C*, Mid-ocean ridge basalt. *D*, Oceanic island basalt (Iceland). Modified from Stanton (1994).

consistent with their higher Rb/Sr ratios and more fractionated REE patterns. These characteristics indicate that the IAB mantle sources are more enriched in lithophile trace elements than the MORB mantle, but also may reflect crustal assimilation and complex crustal mixing processes. This is also consistent with the addition of slab components to the IAB mantle. These components include fluids from dehydration of seawater-altered oceanic crust at shallow subduction levels and partial melts of oceanic crust at deeper levels. Volcanic rocks (andesites, dacites, rhyolites) associated with continental arcs are more radiogenic with regard to Sr, Nd, and Pb compared to island-arc volcanic rocks because of the involvement of highly radiogenic upper continental crust.

Commonly, volcanic rocks show some degree of exchange of Sr with seawater at shallow crustal levels during hydrothermal alteration because seawater contains significant concentrations of Sr (approx. 8 ppm). In modern systems, this is manifest by an overprint of more radiogenic Sr because of the isotopic composition of seawater (0.7091). In ancient VMS deposits, similar alteration processes are likely to occur, except the isotopic composition of seawater is variable in the geologic past (Veizer and others, 1999). In the rock record, if Rb is lost from the system during hydrothermal alteration and exchange with fluids is limited, then the isotopic composition of the original rock may be preserved. However, this is a rare occurrence and most volcanics show Sr exchange with a fluid, either seawater or altered seawater. The latter may have radiogenic Sr inherited from radiogenic continental crust (Whitford and others, 1992). Neodymium isotopes are more robust during hydrothermal alteration because Nd is immobile during alteration, and exchange with seawater is limited by the very low concentrations of Nd in the latter. Lead isotopes are also quite robust; Pb is relatively immobile compared to either U or Th, so the original Pb isotopic composition may be preserved.

Traditional Stable Isotopes

Deuterium/Hydrogen

Because of the large difference in mass between hydrogen and deuterium, D/H fractionations in nature can be very substantial. The hydrogen and oxygen compositions of a variety of waters are shown in figure 15-8.

The hydrogen isotope composition of ancient seawater, based on sediment values, does not appear to have changed much over the past 3 billion years (Sheppard, 1986), and modern ocean water has a canonical value of 0 per mil. Hydrothermal vent

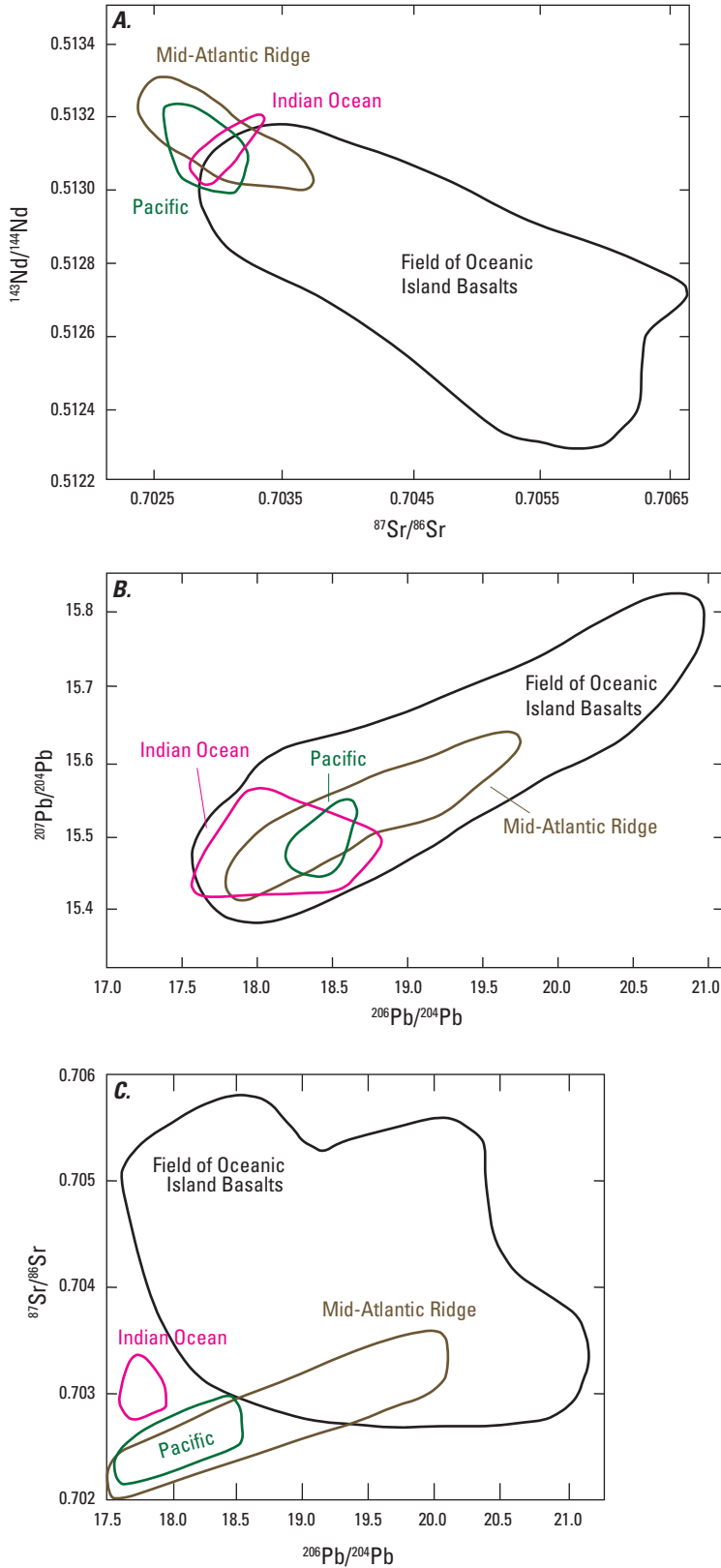


Figure 15-6. Relationships between strontium (Sr), neodymium (Nd), and lead (Pb) isotopes in a variety of mid-ocean ridge basalts (MORB) and oceanic island basalts (OIB). The MORB radiogenic isotopes reflect the nonradiogenic nature of depleted asthenosphere beneath mid-ocean ridges that has been depleted in the Proterozoic. The field of OIB extends to substantially more radiogenic compositions and reflects more radiogenic asthenospheric mantle sources that may have undergone periods of trace-element metasomatism and (or) that include radiogenic plume components. In some cases, the radiogenic OIB also involves a component of lithospheric mantle due to lithospheric thinning above an ascending plume head.

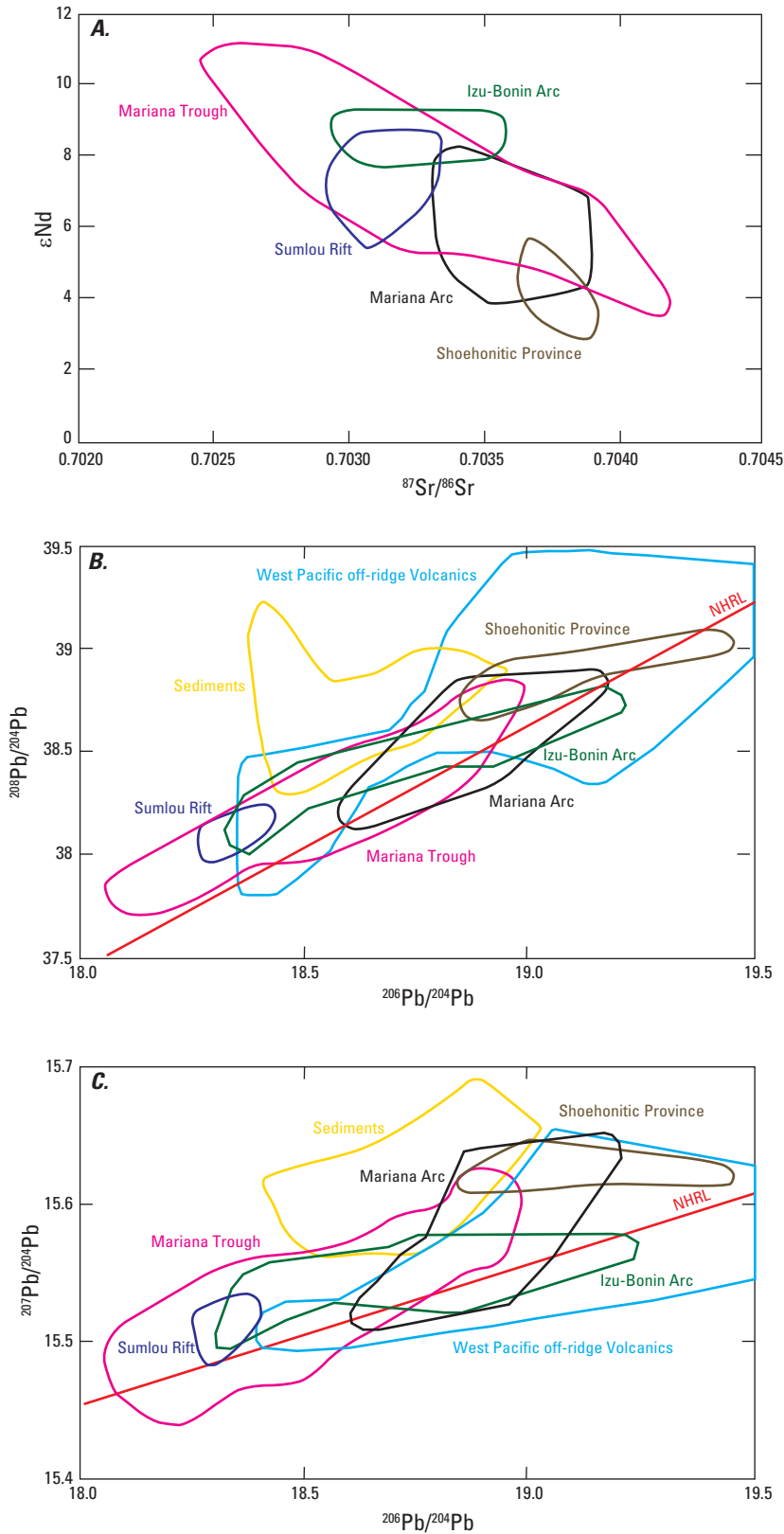


Figure 15-7. Strontium (Sr), neodymium (Nd), and lead (Pb) isotopic variability in island-arc basalt (IAB) volcanics (Izu-Bonin, Marianas arcs, shoshonite province) and back-arc basin basalt (BABB) volcanics (Mariana Trough). The majority of the BABB volcanics have Sr isotope values <0.7032 and ϵ_{Nd} values >9 and, thus, are distinct from most IAB volcanics, but similar to mid-ocean ridge basalt (MORB). The IAB volcanics are uniformly more radiogenic than MORB but overlap the field of OIBs. The field of shoshonite volcanics (late-stage IAB volcanism) has the most radiogenic Sr compositions. Although it is reasonable to assume that the radiogenic isotope composition of IAB volcanics reflects variable input of radiogenic isotopes from the subducting slab, the data alone cannot preclude the possibility that the IAB and OIB mantles are similar. [NHRL, Northern Hemisphere Reference Line]

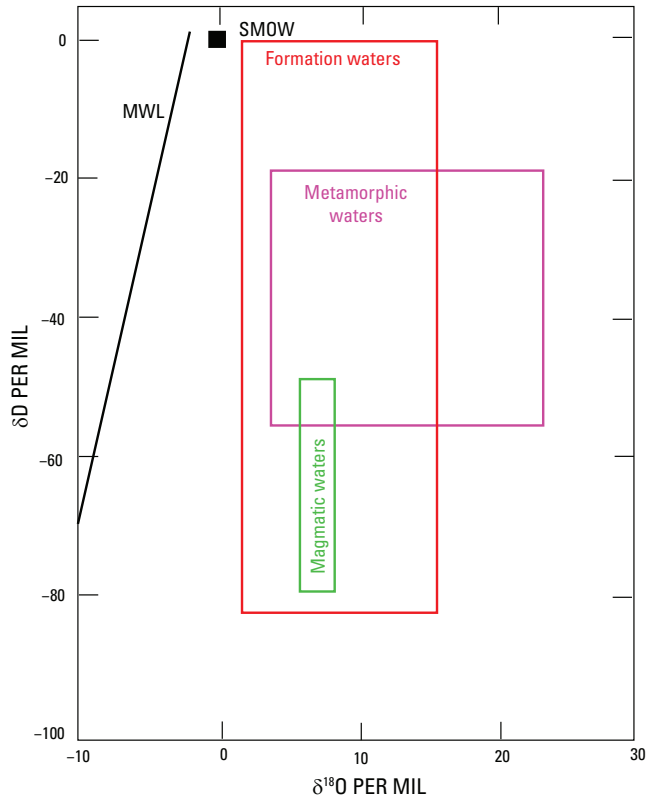


Figure 15-8. Hydrogen and oxygen isotopic composition of various types of terrestrial waters. Modified from Hoefs (2004). [SMOW, standard mean ocean water; MWL, meteoric water line]

fluids have δD values close to seawater (3 to -2 per mil) as a result of fluid/rock reactions under variable water/rock ratios, phase separation in some cases, and addition of small amounts of magmatic water (Shanks and others, 1995). Most magmatic waters have δD values between -50 and -85 per mil, within the range found in MORB and OIB volcanics. Magmatic waters associated with mafic magmas range from -60 to -80 per mil, whereas those associated with felsic magmas range from -85 to -18 per mil. Oceanic basalts (MORB and OIB) show a range in δD values from -20 to -100 per mil with an average value of -80 per mil (Bell and Ihinger, 2000, and references therein). A part of this variation may result from loss of hydrogen during eruption by outgassing of H_2O and, in limited cases, outgassing of CH_4 and H_2 , which all cause isotopic fractionation. Kyser and O'Neil (1984) and Poreda and others (1986) suggest that the primary δD values for MORB and OIB volcanics are indistinguishable at -80 ± 5 per mil, similar to values for continental lithosphere (-63 to -70 for phlogopites in kimberlites; Boettcher and O'Neil, 1980). This value is distinct from the values observed in hydrous mantle minerals (-20 to -140 per mil) and in nominally anhydrous mantle minerals (-90 to -120 per mil). These large ranges in δD values suggest either perturbation of the "mantle value" by interactions with

surface and near-surface fluids and (or) an upper mantle that is heterogeneous with regard to hydrogen isotopic composition.

Back-arc basin basalts have been measured from Lau Basin and Mariana Trough (Poreda, 1985) and from Okinawa Trough (Honma and others, 1991). The Lau samples and Okinawa Trough samples have δD values that are MORB-like (-63 to -70 per mil) and do not require a mantle source with a subduction-related component. This is consistent with other radiogenic isotope and trace element data that indicate MORB-type mantle beneath the Lau Basin. In contrast, BABB samples from the Mariana Trough and Okinawa Trough are isotopically heavier (Mariana: -32 to -46 per mil; Okinawa: -50 per mil), indicating a mantle component of water (about -25 per mil) from the subducting slab.

Crystal fractionation in magmatic systems extends the range of hydrogen isotope compositions to lighter values, and δD values of -140 have been measured in rhyolites that have magmatic $\delta^{18}O$ values and thus have not been contaminated by assimilation of meteoric water. Frequently, the hydrogen isotope composition is correlated with water content; δD decreases with decreasing wt% H_2O , suggesting that the range of isotopic compositions is related to magmatic degassing.

Deep drilling in the modern oceans provides a perspective on the changes in hydrogen isotopic composition of altered oceanic crust caused by deep hydrothermal circulation. The 2.5-km-deep core from ODP Hole 504B shows that the pillow basalts of Layer 2A have variable δD values (-60 to -110 per mil), whereas the sheeted dike section of Layer 2B has more uniform δD values (about -40 per mil) (Alt and others, 1996). The latter values are consistent with exchange of hydrogen between evolved seawater (1-2 per mil) and pristine volcanics at high temperatures (350 °C to >400 °C), whereas the variability of the former reflect fluid/rock reactions between altered seawater, pristine seawater, and volcanics at a range of lower temperatures (Shanks, 2001).

Huston (1999) provides a synopsis of D/H data for ore fluids associated with VMS deposits. Table 15-5 incorporates these data with temperature information from fluid/mineral $\delta^{18}O$ equilibria. Table 15-5 also provides information on δD values for whole rocks and minerals. A general consensus of this information, when combined with $\delta^{18}O$, is that the ore-forming fluids for VMS deposits and rock alteration fluids have seawater or altered seawater compositions and circulated at a wide variety of temperatures from <125 °C to >350 °C. In some deposits there is an increase in δD toward ore and increasing grade of alteration (West Shasta, Troodos, some Kuroko deposits) but at others (Ducktown, Kidd Creek) postmineralization/postalteration metamorphism has acted to homogenize δD (Huston, 1999).

$^{18}O/^{16}O$

A useful overview of the oxygen isotopic composition of volcanic rocks is provided by Eiler (2001). The oxygen isotope composition (expressed in $\delta^{18}O$ notation) of fresh MORB is almost invariant at 5-6 per mil (Eiler, 2001). This

Table 15-5. Hydrogen isotope compositions of ore and alteration fluids, whole rocks, and minerals for selected volcanogenic massive sulfide deposits. Modified from Huston (1999), with additions.

[D, deuterium; O, oxygen; T, temperature]

| District/ deposit | Association | Temperature (°C) | δD (mineral) | δD (rock) | δD (fluid) | δ ¹⁸ O (fluid) | Comment | Reference |
|-------------------------|--------------------------|------------------------|--------------------------|---|---------------|---|---|---|
| Modern seafloor | mafic | 200–410 °C | | –60 to –120 –20 to –60 | 1 ± 3 | 0.4 to 2.1 | Layer 2A lavas Layer 2B dikes | Shanks (2001) |
| Kuroko-type | siliciclastic- felsic | | | | | | | |
| Hokuroku, Japan | | 230–270 | | | –10 to –30 | –2.3 to 0.9 | Fluid inclusion analysis | Ohmoto and Rye (1974); Hattori and Sakai (1979) |
| Kosaka, Japan | | 220–230 | | | 15 to –30 | –1.0 to 3.0 | Fluid inclusion analysis | Hattori and Muehlenbachs (1980); Pisutha-Armond and Ohmoto (1983) |
| Iwami, Japan | | 230–270 | | | –35 to –55 | –3.4 to –1.6 | Fluid inclusion analysis | Hattori and Sakai (1979) |
| Inarizami, Japan | | | | –24 to –32 | | | Kaolin minerals | Marumo (1989) |
| Minamishiraoi, Japan | | | | | | Kaolin minerals | Marumo (1989) | |
| Troodos, Cyprus | mafic | ~ 350 | | –43 to –78 (least altered); –33 to –41 (altered) | 5 to –5 | –0.5 to 1.5 | Assumed temperature | Heaton and Sheppard (1977) |
| Josephine, USA | mafic | 150–250 | | –38 to –54 | 0 to –7 | | δ ¹⁸ O mineral-fluid equilibria for T | Harper and others (1988) |
| | | 250–450 | | –37 to –50 | 0 to –7 | | δ ¹⁸ O mineral-fluid equilibria for T | |
| | | 450–600 | | –45 to –59 | 0 to –7 | | δ ¹⁸ O mineral-fluid equilibria for T | |
| | | >600 | | –35 | 0 to –7 | | δ ¹⁸ O mineral-fluid equilibria for T | |
| Buchans, Canada | | 240–370 | | | –6 to –10 | –1.5 to 4.5 | δ ¹⁸ O mineral-fluid equilibria for T | Kowalik and others (1981) |
| Iberian Pyrite Belt | siliciclastic- felsic | | | | | | | |
| Aljustrel | | 200–270 (stockwork) | –32 to –40 (chlorite) | | 0 to 15 | 1.3 to 5.1 | δ ¹⁸ O mineral-fluid equilibria for T | Munha and others (1986) |
| | | 160–175 (ore zone) | | | 0 to 15 | | δ ¹⁸ O mineral-fluid equilibria for T | |
| | 120 (hanging wall) | | | 0 to 15 | | δ ¹⁸ O mineral-fluid equilibria for T | | |

Table 15–5. Hydrogen isotope compositions of ore and alteration fluids, whole rocks, and minerals for selected volcanogenic massive sulfide deposits. Modified from Huston (1999), with additions.—Continued

[D, deuterium; O, oxygen; T, temperature]

| District/ deposit | Association | Temperature (°C) | δD (mineral) | δD (rock) | δD (fluid) | $\delta^{18}O$ (fluid) | Comment | Reference |
|--------------------------|--------------------------|------------------------|-----------------------------|---|----------------------------|---------------------------|--|--|
| Feitas- Estação | | 200–270 (stockwork) | –32 to –40 (chlorite) | | 0 to 15 | | $\delta^{18}O$ mineral-fluid equilibria for T | Munha and others (1986) |
| | | 160–175 (ore zone) | | | 0 to 15 | | $\delta^{18}O$ mineral-fluid equilibria for T | |
| | | 120 (hanging wall) | | | 0 to 15 | | $\delta^{18}O$ mineral-fluid equilibria for T | |
| Rio Tinto | | 210–230 | –40 to –45 (chlorite) | | –5 to +8 | 0 to 1.4 | $\delta^{18}O$ mineral-fluid equilibria for T | Munha and others (1986) |
| Chanca | | 220 | –40 to –45 (chlorite) | | –10 to 0 | 0.9 | $\delta^{18}O$ mineral-fluid equilibria for T | Munha and others (1986) |
| Salgadinho | | 230 | –30 (muscovite) | | –10 to 0 | 4.0 | $\delta^{18}O$ mineral-fluid equilibria for T | Munha and others (1986) |
| Crandon, USA | siliciclastic- felsic | 210–290 | | –50 to –52 (distal footwall) –55 (footwall) –50 to –52 (hanging wall) | –2 to –12 | –1.7 to –0.1 | | Munha and others (1986) |
| West Shasta, USA | siliciclastic- felsic | 200–300 | | –45 to –73 (basalt to dacite) –50 to –65 (trond- hjemite) | 0 (assumed) | | Assumed temperature | Casey and Taylor (1982); Taylor and South (1985) |
| Blue Hill, USA | bimodal- mafic | 240–350 | –54 to –65(mus- covite), | | | | | |
| –60 to –68 (chlorite) | | –20 to –38 | 5.0 to 7.0 | $\delta^{18}O$ mineral-fluid equilibria for T | Munha and others (1986) | | | |

Table 15-5. Hydrogen isotope compositions of ore and alteration fluids, whole rocks, and minerals for selected volcanogenic massive sulfide deposits. Modified from Huston (1999), with additions.—Continued

[D, deuterium; O, oxygen; T, temperature]

| District/ deposit | Association | Temperature (°C) | δD (mineral) | δD (rock) | δD (fluid) | $\delta^{18}O$ (fluid) | Comment | Reference |
|-----------------------------|--------------------------|---------------------|---|----------------------|---|---------------------------|--|--|
| Ducktown, USA | siliciclastic- felsic | 450–580 | –69 to –76 (country rock biotite); –59 to –50 (country rock muscovite); –68 to –77 (ore zone biotite); –51 to –54 (ore zone muscovite); –62 to –69 (ore zone chlorite) | | –33 to –36 (local alteration), –31 to –32 (re- gional) | 5.4 to 7.0 | $\delta^{18}O$ mineral-fluid equilibria for T | Addy and Ypma (1977) |
| Bruce, USA | siliciclastic- felsic | 250–300 | | | | 1.1 to 2.1 | Assumed temperature | Larson (1984) |
| Mattgami Lake, Canada | bimodalmafic | 240–350 | | | 0.5 to 2.0 | | Fluid inclusions; mineral equilibria | Costa and others (1983) |
| Noranda Horne | bimodal-mafic | 250–350 | | | –30 to –40 | 1.5 to 4.5 | $\delta^{18}O$ mineral-fluid equilibria for T | MacLean and Hoy (1991); Hoy (1993) |
| Mobrun | bimodal-mafic | 150–250 | | | | 0 to 4.0 | $\delta^{18}O$ mineral-fluid equilibria for T | Hoy (1993) |
| Norbec | bimodal-mafic | 200–300 | | | | –1.0 to 3.0 | $\delta^{18}O$ mineral-fluid equilibria for T | Hoy (1993) |
| Amulet | bimodal-mafic | 250–350 | | | | –0.5 to 2.0 | $\delta^{18}O$ mineral-fluid equilibria for T | Hoy (1993) |
| Ansil | bimodal-mafic | 200–350 | | | | –2.0 to 1.0 | $\delta^{18}O$ mineral-fluid equilibria for T | Hoy (1993) |
| Corbet | bimodal-mafic | 250–300 | | | | –4.0 to 0 | | Hoy (1993) |

Table 15-5. Hydrogen isotope compositions of ore and alteration fluids, whole rocks, and minerals for selected volcanogenic massive sulfide deposits. Modified from Huston (1999), with additions.—Continued

[D, deuterium; O, oxygen; T, temperature]

| District/ deposit | Association | Temperature (°C) | δD (mineral) | δD (rock) | δD (fluid) | $\delta^{18}O$ (fluid) | Comment | Reference | |
|-----------------------|----------------|---------------------|-------------------------|-----------------------------------|-----------------------|---------------------------|--|-----------------------------|-----------------------------|
| Kidd Creek, Canada | bimodal-mafic | 300–350 | | Local | | | | Huston and Taylor (1999) | |
| | | | | –25 to –50 (qz por- phyry) | –13 to –3 | 3.3 to 4.3 | $\delta^{18}O$ mineral-fluid equilibria for T | | |
| | | | | –25 to –70 (ore host rhyolite) | | | | | |
| | | | | –25 to –70 (footwall rhyolite) | | | | | |
| | | | | Regional | | | | | Taylor and Huston (1999) |
| | | | | –25 to –60 (mafics) | +20 | 4 | $\delta^{18}O$ mineral-fluid equilibria for T | | |
| South Bay, Canada | bimodal-felsic | 300 | | –25 to –65 (ultramafics) | | | | | |
| | | | | –15 to –45 (felsics) | | 2.1 to 4.5 | $\delta^{18}O$ mineral-fluid equilibria for T | Urabe and Scott (1983) | |

is also the value for fresh mantle peridotites, so is assumed to be the mantle value. Ito and others (1987) could not find isotopic variations related to geographic setting or MORB type (DMORB to EMORB). However, high precision oxygen isotope data (Eiler and others, 2000) reveal subtle variations that systematically relate to incompatible element concentrations and ratios and are interpreted in terms of fractional crystallization and subtle variations in the isotopic composition of mantle sources. Ocean-island basalt shows a slightly extended range of oxygen isotope values (4.6–6.1 per mil) compared to MORB samples, which reflect the more complex mantle source reservoirs of OIB. Lower isotopic values may reflect the involvement of ancient lower oceanic crust whereas higher values may reflect a component of pelagic sediment (fig. 15–8).

Back-arc basin basalt shows a relatively restricted range of oxygen isotope compositions. Sixteen basalts from the Lau Basin vary between 5.6 and 6.4 per mil, and seven basalts from the Mariana Trough vary from 5.5 to 5.7 per mil. Island-arc basalts and related volcanics show a wider range of oxygen isotope compositions compared to MORB, OIB, or BABB volcanics. In IAB mafic volcanics, the range is small (4.8–5.8 per mil) but is larger if more evolved felsic volcanics are included, as high as 14 per mil. Only part of this variation can be related to crystal fractionation, which is expected to increase the isotopic composition by only about 1–2 per mil. The $\delta^{18}\text{O}$ values of IAB magmas and their derivatives are complicated by the potential for mixing and assimilation if magma erupts through thick sequences of sediment and (or) continental crust. The higher $\delta^{18}\text{O}$ values for IABs, relative to MORB, almost certainly reflect some type of contamination, probably from pelagic sediment. Recent measurements (Eiler, 2001) suggest that the range of uncontaminated volcanics is 5 ± 1 per mil, identical to the MORB values, but that there may be subtle indications of the effects of material added to the mantle from the subducted slab.

In modern seafloor hydrothermal systems, perturbation of the pristine oxygen isotope compositions of volcanics occurs by alteration of the oceanic crust by seawater ($\delta^{18}\text{O} = 0$ per mil) or evolved seawater, that is, vent fluids ($\delta^{18}\text{O} = 0.5$ – 2 per mil), a process that is a function of depth (a proxy for temperature) and spreading rate. The oxygen isotopic composition of seawater is perturbed because of water/rock reactions that cause isotopic exchange between circulating fluids and primary minerals, resulting in isotopic equilibria between fluid and secondary minerals (Shanks, 2001).

At intermediate- and slow-spreading ridges, the tectonic disruption of the oceanic crust results in increased permeability and fracture porosity, allowing for deep penetration of seawater, cooling of the crust and alteration assemblages formed at low temperatures. Under these circumstances, the overall fluid pathway is increased in length, allowing for greater extents of fluid/rock interaction (Bach and Humphris, 1999). At fast-spreading ridges, the crustal structure is less tectonically disturbed, and lower porosity and permeability allow circulating fluids to maintain higher temperatures (Alt

and Teagle, 2003). At slow-spreading ridges such as the Costa Rica rift (spreading rate 5 cm/yr), the hydrothermal circulation extends to the base of Layer 2B (sheeted dike complex) where depleted oxygen isotope compositions, as low as 4 per mil (Alt and others, 1996; Shanks, 2001), are observed. Hydrothermal fluids that penetrate into the upper homogeneous gabbros of Layer 3 also show a range of $\delta^{18}\text{O}$ values from 2 to 7.5 per mil (Shanks, 2001). In the upper parts of Layer 2B, enriched oxygen isotope compositions are observed, 8 per mil or higher, and elevated values are found in Layer 2A (fig. 15–9).

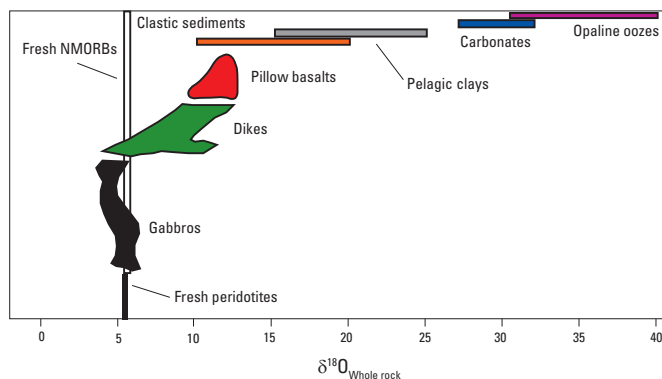


Figure 15–9. Oxygen isotopic composition of various lithologic units relative to mid-ocean ridge basalt (MORB). The sequence of peridotite–gabbro–dikes–pillow basalts represents a sequence through oceanic crust typically observed in ophiolites. The isotopic variability in this sequence reflects hydrothermal exchange with hydrothermal fluids and seawater. Modified from Eiler (2001).

Taylor (1974) demonstrated the utility of oxygen isotopes in ore deposit studies and Heaton and Sheppard (1977) first demonstrated, at Troodos, systematic variations in $\delta^{18}\text{O}$ of volcanic rocks hosting VMS deposits. Taylor (1990) recognized three types of fossil hydrothermal systems, based on temporal factors, temperatures, and water/rock ratios. Although applicable to a wide range of ore deposits, from epithermal to mesothermal, the classification does have relevance to VMS deposits. The three types, which are not mutually exclusive in space and time, are (Hoefs, 2004):

- Type I—Epizonal systems with a variety of $\delta^{18}\text{O}$ values and extreme isotopic disequilibria between coexisting mineral phases. These systems have temperatures between 200 and 600 °C and lifetimes of $<10^6$ years. Type I systems are most applicable to VMS systems that form at <3 – 4 km depth and involve the totality of hydrothermal flow from surface to the proximal parts of subsurface intrusions.
- Type II—Deeper-seated and (or) longer lived systems, also with a range of whole-rock $\delta^{18}\text{O}$ values but with equilibrium between coexisting mineral phases. These systems have temperatures between 400 and 700 °C

and life times of $>10^6$ years. Some of the deeper parts of large VMS systems may be included in this category.

- Type III—Equilibrated systems with uniform $\delta^{18}\text{O}$ in all lithologies. These systems require large water/rock ratios and high temperatures (500–800 °C) and long life times (about 5×10^6 years).

Subsequent to these studies, there have been many studies that deal with various aspects of oxygen isotope variability in volcanic rocks that host VMS deposits (table 15–6). Volcanics associated with VMS deposits invariably show some degree of exchange of oxygen during hydrothermal alteration. Wherever detailed studies have been performed, the isotopic composition of altered volcanics can be correlated with specific zones of alteration that may be conformable or crosscut local and regional lithologies. These correlations are a function of alteration temperatures and fluid/rock ratios that produce alteration zones from zeolite facies through upper greenschist facies. In some cases, these alteration zones may be overprinted by later amphibolite facies assemblages. In many cases, these fluid systems are of regional extent, extending laterally for several kilometers outside of the immediate domains of ore deposits. They also may extend vertically for hundreds of meters into the footwall lithologies and into hanging wall lithologies. Table 15–7 provides a synopsis of the range of $\delta^{18}\text{O}$ values observed in volcanic rocks associated with VMS deposits.

$\delta^{34}\text{S}$

The mantle value for $\delta^{34}\text{S}$ varies from -7 to 7 per mil. High-S peridotites have values from about 0 to -5 per mil, whereas low-S peridotites have values from about 0 to +5 per mil (Ionov and others, 1992). Most fresh MORB samples have $\delta^{34}\text{S}$ values of 0 ± 2 per mil (Sakai and others, 1984). However, hydrothermally altered MORB has significantly heavier $\delta^{34}\text{S}$ values that generally correlate with $^{87}\text{Sr}/^{86}\text{Sr}$ because of interaction with modern seawater ($\delta^{34}\text{S}$ approx. 21 per mil). The principal sulfur gas in equilibrium with mafic melts at low pressure and high temperature is SO_2 . With decreasing temperature and (or) increasing $f/\text{H}_2\text{O}$, H_2S becomes more stable.

Modern volcanic gases associated with basaltic volcanism have $\delta^{34}\text{S}$ of about 1 ± 1.5 per mil (Sakai and others, 1982; Allard, 1983), whereas gases associated with felsic volcanism have heavier $\delta^{34}\text{S}$ values (up to 5 per mil; Poorter and others, 1991).

Alteration of volcanics associated with VMS deposits results in changes in bulk $\delta^{34}\text{S}$ due to precipitation of sulfide and (or) sulfate minerals.

Depth of Emplacement

The location of heat that drives hydrothermal circulation is uncertain in most modern VMS settings. In ancient VMS settings, a systematic relationship between hydrothermal alteration and the location of a specific intrusive body may also provide depth information, but the common dismemberment of VMS deposits makes this criterion difficult to apply. In modern MOR settings, small melt lenses have been seismically imaged beneath several segments of the East Pacific Rise, along the Juan de Fuca Ridge, and at the Mid-Atlantic Ridge. The melt lenses frequently are associated with surface hydrothermal venting. They are assumed to be the heat source that drives the hydrothermal circulation and lie close to the base of Layer 2B that is at approximately 2 km beneath the ocean floor at fast spreading ridges (Singh and others, 1999) and up to 3 km at slow spreading ridges (Sinha and others, 1998). These depths are expected to be appropriate for VMS deposits with mafic-ultramafic volcanic associations. However, at MOR and back-arc settings, the high-level melt lenses are underlain with a substantial (several kilometers) crystal-melt mush that also must contribute to the thermal energy required to drive hydrothermal circulation. The common association of VMS deposits with felsic volcanics, even in mafic-dominated environments, suggests that felsic plutons provided the required heat. The presence of felsic volcanics at the surface presumably implies the presence of felsic intrusions at depth, although little is known as to the exact depth. Generally, in modern environments, individual high-level intrusions are ephemeral in their ability to supply heat to drive hydrothermal circulation.

Table 15–6. Selected oxygen isotope studies of volcanic rocks hosting volcanogenic massive sulfide (VMS) deposits.

| Deposit | Age | Application | Reference |
|---|---------------|--|---|
| General | | Taylor: Seminal study of $\delta^{18}\text{O}$ variations in lithostratigraphic successions associated with a wide variety of ore deposits, including VMS deposits of western Cascades. Huston: An in-depth review of stable isotope geochemistry applied to VMS deposits | Taylor (1974); Huston (1999) |
| Kidd Creek, Ontario | Archean | Isotope composition of hanging wall and footwall rhyolites and mafic volcanics (bimodal mafic association). Regional isotope mapping recognizes isotopic shifts due to hydrothermal alteration and regional greenschist facies metamorphism. | Beaty and others (1988); Huston and others (1995); Huston and Taylor (1999) |
| Sturgeon Lake, Ontario | Archean | Local and regional scale isotope studies of caldera complex (bimodal felsic association). Identified syn- and post-mineralization fluids of hydrothermal (modified seawater) and seawater origin and fluid temperatures. | King and others (2000); Holk and others (2008) |
| Noranda, Quebec | Archean | Local and regional scale isotope mapping of volcanic sequences (bimodal mafic association) to understand fluid flow and nature of hydrothermal fluids. | Beaty and Taylor (1982); Cathles (1993); Hoy (1993); Paradis and others (1993) |
| Mattagami Lake, Quebec | Archean | Origin of hydrothermal fluids in shallow brine pool | Costa and others (1983) |
| Hercules, Tasmania | Cambrian | Use of stable isotopes for regional exploration | Green and Taheri (1992) |
| Samail, Oman | Cretaceous | Regional isotope study of classical "Penrose" ophiolite (mafic association). Pillow lavas and sheeted dikes are isotopically enriched, gabbros and peridotites are depleted due to interactions with seawater at shallow levels and altered seawater at deeper levels. Hydrothermal fluids penetrated to Moho in off-axis sections | Gregory and Taylor (1981); Stakes and Taylor (1992) |
| Josephine, United States | Jurassic | Regional study of ophiolite complex, mainly extrusive sequence and sheeted dikes (mafic association). Isotopic compositions allow recognition of discharge and recharge zones | Harper and others (1988) |
| West Shasta, United States | Devonian | Regional scale study of mining district (siliciclastic felsic association) to identify fluid sources and temperatures of alteration. | Casey and Taylor (1982); Taylor and South (1985) |
| Iberian Pyrite Belt, Spain and Portugal | Carboniferous | Regional isotopic study (siliciclastic-felsic association) to understand nature of ore fluids, some being basinal brines. | Munha and Kerrich (1980); Munha and others (1986); Tornos and others (2008) |
| Crandon, United States | Proterozoic | Local and regional isotope study to evaluate fluid compositions and temperatures. | Munha and others (1986) |
| Kuroko, Japan | Miocene | Regional (district-wide) and local (mine scale) studies of lithostratigraphic units (siliciclastic-felsic association) to identify isotopic variations as function of alteration grade and establish exploration strategies. | Ohmoto and Rye (1974); Green and others (1983); Pisutha-Arnond and Rye (1983); Watanabe and Sakai (1983); Marumo (1989) |

Table 15–7. Whole rock $\delta^{18}\text{O}$ values for lithostratigraphic units associated with volcanogenic massive sulfide deposits (selected studies). Modified from Huston (1999), with additions.

[O, oxygen; alb, albite; amph, amphibole; carb, carbonate; chl, chlorite; epi, epidote; fuch, fuchsite; kaol, kaolinite; mont, montmarillonite; qz, quartz; ser, sericite; sil, sillimanite; zeol, zeolite]

| Deposit | Association | Age | $\delta^{18}\text{O}$ (least altered lithologies) | $\delta^{18}\text{O}$ (most altered lithologies) | Alteration zones/ lithology | References |
|------------------------------|-----------------------|---------------|--|---|--------------------------------|--|
| Fukazawa, Japan | Siliciclastic-felsic | Miocene | 11.6–22.4 | | zeol | Green and others (1983) |
| | | | 6.5–16.8 | | mont | |
| Uwamuki, Japan | Siliciclastic-felsic | Miocene | 8.8–10.4 | 4.6–10.5 | ser-chl | Urabe and others (1983) Hattori and Muehlenbachs (1980) |
| | | | 7.3–10.9 | | kaol-qz-ser±chl±alb | |
| | | | | | alb-ser-chl-qz | |
| | | | | 8.2–9.6 | clay-ser-chl-qz (1980) | |
| | | | | 7.0–9.2 | ser-chl-qz | |
| | | | | 6.7–8.6 | qz-ser | |
| Troodos, Cyprus | Mafic | Cretaceous | 11.8–16.0 | | 8.1–8.3 | Upper pillow lavas |
| | | | | | | |
| Samail, Oman | Mafic | Cretaceous | | 1.4–4.1 | Stockwork | Stakes and Taylor (1992) |
| | | | | 2.0–7.0 | Gabbro | |
| | | | | 5.0–9.0 | epi-chl sheeted dikes | |
| Seneca, Canada | | Jurassic | 10.7–11.6 | | epi-chl pillow lavas | Urabe and others (1983) |
| | | | | | Felsic breccia | |
| Freitas-Estação, Portugal | Siliciclastic-felsic | Carboniferous | 15.7–18.1 | 6.9–8.7 | Sil felsic breccia | Barriga and Kerrich (1984) |
| | | | | | Volcanoclastic rhyolites | |
| | | | | 13.9–14.4 | Stockwork-peripheral | |
| Hercules, Tasmania | Siliciclastic-felsic | Cambrian | 11.2–15.5 | 11.6–12.5 | Stockwork | Green and Taheri (1992) |
| | | | | | Rhyolitic flows | |
| Hellyer, Tasmania | Siliciclastic-felsic | Cambrian | 10.4–12.2 | 6.8–10.0 | qz-chl-ser | Green and Teheri (1992) |
| | | | | | Footwall andesite | |
| | | | | 8.0–11.6 | ser-qz stringer (distal) | |
| | | | | 7.0–9.6 | chl-ser stringer (proximal) | |
| Ducktown, United States | Siliciclastic-felsic? | Proterozoic | 9.6–14.0 | | Hanging wall basalt | Addy and Ypma (1977) |
| | | | | 9.4–11.8 | fuch-carb hanging wall basalt | |
| | | | 8.6–10.8 | | Country rock | |
| | | | 10.2–11.5 | | qz (country rock) | |
| | | | | 8.3–9.7 | qz (altered rock) | |
| | | 8.1–10.3 | | qz (ore zone) | | |

Table 15–7. Whole rock $\delta^{18}\text{O}$ values for lithostratigraphic units associated with volcanogenic massive sulfide deposits (selected studies). Modified from Huston (1999), with additions.—Continued

[O, oxygen; alb, albite; amph, amphibole; carb, carbonate; chl, chlorite; epi, epidote; fuch, fuchsite; kaol, kaolinite; mont, montmarillonite; qz, quartz; ser, sericite; sil, sillimanite; zeol, zeolite]

| Deposit | Association | Age | $\delta^{18}\text{O}$ (least altered lithologies) | $\delta^{18}\text{O}$ (most altered lithologies) | Alteration zones/ lithology | References |
|------------------------|----------------------|-------------|---|--|-----------------------------------|---|
| Bruce, United States | Siliciclastic-felsic | Proterozoic | 6.0–7.6 | | andesite | |
| | | | | 2.4–5.6 | chl | |
| Mattagami Lake, Canada | Bimodal-mafic | Archean | 8.5–9.2 | | rhyolite | Costa and others (1983) |
| | | | | 2.0–7.6 | rhyolite | |
| | | | | 1.8–4.9 | chl altered footwall | |
| Horne, Canada | Bimodal-mafic | Archean | 7.0–9.0 | | rhyolite | Hoy (1993) |
| | | | | 6.6–11.6 | qz-ser-chl rhyolite | |
| | | | | 3.9–4.4 | chl-rich rhyolite | |
| Mobrun, Canada | Bimodal-mafic | Archean | 6.0–14.0 | | qz-ser rhyolite | Hoy (1993) |
| Norbec, Canada | Bimodal-mafic | Archean | | 3.0–7.0 | dalm below ore | Hoy (1993) |
| | | | | | qz-ser rhyolite | |
| Amulet, Canada | Bimodal-mafic | Archean | 6.3–6.4 | | andesite | Beaty and Taylor (1982) |
| | | | | 4.0–4.8 | grid fractured zone (stock-work?) | |
| | | | | 3.6–3.8 | dalm | |
| Ansil, Canada | Bimodal-mafic | Archean | 4.0–6.0 | | rhyolite, andesite | Hoy (1993) |
| | | | | 2.0–4.0 | qz-ser altered rhyolite, andesite | |
| Corbet, Canada | Bimodal-mafic | Archean | 6.0–9.8 | | andesite | Urabe and others (1983) |
| | | | | 2.3–4.2 | ore zone | |
| Kidd Creek, Canada | Bimodal-mafic | Archean | 12.0–15.8 | | rhyolite | Beaty and others (1988) |
| | | | 9.7–14.9 | | rhyolite (ore host) | Huston and Taylor (1999); Beaty and others (1988) |
| | | | 9.1–13.6 | | hanging wall porphyry | Huston and Taylor (1999) |
| | | | | 9.0–12.3 | cherty breccia | |
| | | | | 4.3–7.8 | chloritite | |

Table 15–7. Whole rock $\delta^{18}\text{O}$ values for lithostratigraphic units associated with volcanogenic massive sulfide deposits (selected studies). Modified from Huston (1999), with additions.—Continued

[O, oxygen; alb, albite; amph, amphibole; carb, carbonate; chl, chlorite; epi, epidote; fuch, fuchsite; kaol, kaolinite; mont, montmarillonite; qz, quartz; ser, sericite; sil, sillimanite; zeol, zeolite]

| Deposit | Association | Age | $\delta^{18}\text{O}$ (least altered lithologies) | $\delta^{18}\text{O}$ (most altered lithologies) | Alteration zones/ lithology | References |
|--------------------------|--------------------|---------|---|--|--------------------------------|----------------------------|
| Sturgeon Lake, Canada | Bimodal- felsic | Archean | 7.2–7.9 | | gabbro, tonalite | King and others (2000); |
| | | | | 7.0–7.4 | chl-epi-amph (intrusives) | Holk and others (2008) |
| | | | | 12.3–14.3 | epi-chl-ser | |
| | | | | 9.00–15.0 | sil | |
| | | | | 8.34–13.3 | rhyolite (ore host) | |
| | | | | 11.05–14.3 | andesite | |

References Cited

- Addy, S.K., and Ypma, P.J.M., 1977, Origin of massive sulfide deposits at Ducktown, Tennessee—An oxygen, carbon, and hydrogen isotope study: *Economic Geology*, v. 72, p. 1245–1268.
- Allard, P., 1983, The origin of hydrogen, carbon, sulphur, nitrogen, and rare gases in volcanic exhalatives—Evidence from isotope geochemistry, *in* Tazieff, H., and Sabroux, J.C., eds., *Forecasting volcanic events*: Amsterdam, Elsevier, p. 233–246.
- Allen, D.E., and Seyfried, W.E., Jr., 2004, Serpentinization and heat generation—Constraints from Lost City and Rainbow hydrothermal systems: *Geochimica et Cosmochimica Acta*, v. 68, no. 6, p. 1347–1354.
- Alt, J.C., Laverne, C., Vanko, D., Tartarotti, P., Teagle, D.A.H., Bach, W., Zuleger, E., Erzinger, J., Honnorez, J., Pezard, P.A., Becker, K., Salisbury, M.H., and Wilkens, R.H., 1996, Hydrothermal alteration of a section of upper oceanic crust in the eastern equatorial Pacific, *in* Alt, J.C., Kinoshita, H., Stokking, L.B., and Michael, P.J., eds., *Costa Rica Rift, sites 504 and 896: Proceedings of the Ocean Drilling Program, Scientific Results*, v. 148, p. 417–434.
- Alt, J.C., and Shanks, W.C., III, 2003, Serpentinization of abyssal peridotites from the MARK area, Mid-Atlantic Ridge—Sulfur geochemistry and reaction modeling: *Geochimica et Cosmochimica Acta*, v. 67, no. 4, p. 641–653.
- Alt, J.C., Shanks, W.C., III, Bach, W., Paulick, H., Garrido, C.J., and Beaudoin, G., 2008, Hydrothermal alteration and microbial sulfate reduction in peridotite and gabbro exposed by detachment faulting at the Mid-Atlantic Ridge, 15°20'N (ODP Leg 209)—A sulfur and oxygen isotope study: *Geochemistry, Geophysics, Geosystems*, v. 8, no. 8, 22 p., doi:10.1029/2007GC001617.
- Alt, J.C., and Teagle, D.A.H., 2003, Hydrothermal alteration of upper oceanic crust formed at a fast-spreading ridge—Mineral, chemical, and isotopic evidence from ODP Site 801: *Chemical Geology*, v. 201, p. 191–211.
- Bach, W., and Humphris, S.E., 1999, Relationship between the Sr and O isotope composition of hydrothermal fluids and the spreading and magma-supply rates at oceanic spreading centers: *Geology*, v. 27, p. 1067–1070.
- Baker, P.E., 1982, Evolution and classification of orogenic volcanic rocks, *in* Thorpe, R.S., ed., *Andesites—Orogenic andesites and related rocks*: New York, John Wiley and Sons, p. 11–23.
- Barrie, C.T., and Hannington, M.D., 1999, Classification of volcanic-associated massive sulfide deposits based on host-rock composition, *in* Barrie, C.T., and Hannington, M.D., eds., *Volcanic-associated massive sulfide deposits—Processes and examples in modern and ancient settings: Reviews in Economic Geology*, v. 8, p. 1–11.

- Barriga, F.J.A.S., and Kerrich, R., 1984, Extreme ^{18}O -enriched volcanics and ^{18}O -evolved marine water, Aljustrel, Iberian pyrite belt—Transition from high to low Rayleigh number convective regimes: *Geochimica et Cosmochimica Acta*, v. 48, p. 1021–1031.
- Beaty, D.W., and Taylor, H.P., 1982, Some petrologic and oxygen isotopic relationships in the Amulet Mine, Noranda, Quebec, and their bearing on the origin of Archean massive sulfide deposits: *Economic Geology*, v. 77, p. 95–108.
- Beaty, D.W., Taylor, H.P., Jr., and Coads, P.R., 1988, An oxygen isotope study of the Kidd Creek, Ontario, massive sulfide deposit—Evidence for a ^{18}O ore fluid: *Economic Geology*, v. 83, p. 1–17.
- Boettcher, A.L., and O'Neal, J.R., 1980, Stable isotope, chemical and petrographic studies of high pressure amphiboles and micas—Evidence for metasomatism in the mantle source regions of alkali basalts and kimberlites: *American Journal of Science*, v. 280-A, p. 594–621.
- Cas, R.A.F., 1992, Submarine volcanism—Eruption styles, products, and relevance to understanding the host-rock successions to volcanic-hosted massive sulfide deposits: *Economic Geology*, v. 87, p. 511–541.
- Casey, W.H., and Taylor, B.E., 1982, Oxygen, hydrogen, and sulfur isotope geochemistry of a portion of the West Shasta Cu-Zn District, California: *Economic Geology*, v. 77, p. 38–49.
- Cathles, L.M., 1993, Oxygen alteration in the Noranda Mining District, Abitibi Greenstone Belt, Quebec: *Economic Geology*, v. 88, p. 1483–1511.
- Chester, D.K., Duncan, A.M., Guest, J.E., and Kilburn, C.R.J., 1985, Mount Etna—The anatomy of a volcano: Stanford, Stanford University Press, 404 p.
- Costa, U.R., Barnett, R.L., and Kerrich, R., 1983, The Matagami Lake Mine Archean Zn-Cu sulfide deposit, Quebec—Hydrothermal precipitation of talc and sulfides in a sea-floor brine pool—Evidence from geochemistry, $^{18}\text{O}/^{16}\text{O}$, and sulfide chemistry: *Economic Geology*, v. 78, p. 1144–1203.
- Cotsonika, L.A., Perfit, M.R., Stakes, D., and Ridley, W.I., 2005, The occurrence and origin of andesites and dacites from the southern Juan de Fuca Ridge [abs.]: EOS, Transactions, American Geophysical Union, v. 86, no. 52, Fall meeting supplement, abstract V13B-0551.
- Dobson, P.F., Blank, J.G., Maruyama, S., and Liou, J.G., 2006, Petrology and geochemistry of boninite series volcanic rocks, Chichi-jima, Bonin Islands, Japan: *International Geology Review*, v. 48, p. 669–701.
- Duke, N.A., Lindberg, P.A., and West, W.A., in press, Geology of the Greens Creek mining district, in Taylor, C.D., and Johnson, C.A., eds., *Geology, geochemistry, and genesis of the Greens Creek massive sulfide deposit, Admiralty Island, southeastern Alaska*: U.S. Geological Survey Professional Paper 1763.
- Dusel-Bacon, C., Wooden, J.L., and Hopkins, M.J., 2004, U-Pb zircon and geochemical evidence for bimodal mid-Paleozoic magmatism and syngenetic base-metal mineralization in the Yukon-Tanana terrane, Alaska: *Geological Society of America Bulletin*, v. 116, p. 989–1015.
- Edmonds, H.N., Michael, P.J., Baker, E.T., Connelly, D.P., Snow, J.E., Langmuir, C.H., Dick, H.J.B., Mühe, R., and German, C.R., 2003, Discovery of abundant hydrothermal venting on the ultraslow-spreading Gakkel ridge in the Arctic Ocean: *Nature*, v. 421, p. 252–256.
- Eiler, J.M., 2001, Oxygen isotope variations of basaltic lavas and upper mantle rocks, in Valley, J.W., and Cole, D.R., eds., *Stable isotope geochemistry: Reviews in Mineralogy and Geochemistry*, v. 43, p. 319–364.
- Eiler, J.M., Schiano, P., Kitchen, N., and Stolper, E.M., 2000, Oxygen isotope evidence for recycled crust in the sources of mid-ocean ridge basalts: *Nature*, v. 403, p. 530–534.
- Embley, R.W., Jonasson, I.R., Perfit, M.R., Franklin, J.M., Tivey, M.A., Malahoff, A., Smith, M.F., and Francis, T.J.G., 1988, Submersible investigation of an extinct hydrothermal system on the Galapagos Ridge—Sulfide mounds, stock-work zone, and differentiated lavas: *Canadian Mineralogist*, v. 26, p. 517–539.
- Franklin, J.M., Gibson, H.L., Jonasson, I.R., and Galley, A.G., 2005, Volcanogenic massive sulfide deposits, in Hedenquist, J.W., Thompson, J.F.H., Goldfarb, R.J., and Richards, J.P., eds., *Economic Geology 100th anniversary volume, 1905–2005*: Littleton, Colo., Society of Economic Geologists, p. 523–560.

- Galley, A.G., Hannington, M., and Jonasson, I., 2007, Volcanogenic massive sulphide deposits, *in* Goodfellow, W.D., ed., Mineral deposits of Canada—A synthesis of major deposit-types, district metallogeny, the evolution of geological provinces, and exploration methods: Geological Association of Canada, Mineral Deposits Division, Special Publication 5, p. 141–161.
- Gamo, T., Ishibashi, J., Tsunogai, U., Okamura, K., and Chiba, H., 2006, Unique geochemistry of submarine hydrothermal fluids from arc-back-arc settings of the western Pacific, *in* Christie, D.M., Fisher, C.R., Lee, S.-M., and Givens, S., eds., Back-arc spreading systems, geological, biological, chemical, and physical interactions: American Geophysical Union, Geophysical Monograph 166, p. 147–161.
- Goodfellow, W.D., McCutcheon, S.R., and Peter, J.M., 2003, Introduction and summary of findings, *in* Goodfellow, W.D., McCutcheon, S.R., and Peter, J.M., eds., Massive sulfide deposits of the Bathurst mining camp, New Brunswick, and northern Maine: Economic Geology Monograph 11, p. 1–16.
- Green, G.R., Ohmoto, H., Date, J., and Takahashi, T., 1983, Whole-rock oxygen isotope distribution in the Fukazawa-Kosaka area, Hokuroku district, Japan, and its potential application to mineral exploration, *in* Ohmoto, H., and Skinner, B.J., eds., The Kuroko and related volcanogenic massive sulfide deposits: Economic Geology Monograph 5, p. 395–411.
- Green, G.R., and Taheri, J., 1992, Stable isotopes and geochemistry as exploration indicators: Geological Survey of Tasmania Bulletin 70, p. 84–91.
- Gregory, R.T., and Taylor, H.P., 1981, An oxygen isotope profile in a section of Cretaceous oceanic crust, Samail ophiolite, Oman—Evidence for $\delta^{18}\text{O}$ buffering of the oceans by deep (>5 km) seawater-hydrothermal circulation at mid-ocean ridges: *Journal of Geophysical Research*, v. 86, p. 2737–2755.
- Hannington, M.D., Galley, A.G., Herzig, P.M., and Petersen, S., 1998, Comparison of the TAG mound and stockwork complex with Cyprus-type massive sulfide deposits, *in* Herzig, P.M., Humphris, S.E., Miller, D.J., and Zierenberg, R.A., eds., TAG—Drilling an active hydrothermal system on a sediment-free slow-spreading ridge, site 957: Proceedings of the Ocean Drilling Program, Scientific Results, v. 158, p. 389–415.
- Harper, G.D., Bowman, J.R., and Kuhns, R., 1988, A field, chemical, and stable isotope study of subseafloor metamorphism of the Josephine ophiolite, California-Oregon: *Journal of Geophysical Research*, v. 93, p. 4625–4656.
- Hattori, K., and Meuhlenbachs, K., 1980, Marine hydrothermal alteration at the Kuroko ore deposit, Kosaka, Japan: *Contributions to Mineralogy and Petrology*, v. 74, p. 285–292.
- Hattori, K., and Sakai, H., 1979, D/H ratios, origins, and evolution of the ore-forming fluids for the Neogene veins and Kuroko deposits of Japan: *Economic Geology*, v. 74, p. 535–555.
- Heaton, T.H.E., and Sheppard, S.M.F., 1977, Hydrogen and oxygen isotope evidence for sea-water-hydrothermal alteration and ore deposition, Troodos complex, Cyprus, *in* Volcanic processes in ore genesis: Institute of Mining and Metallurgy, p. 42–57.
- Hoefs, J., 2004, *Stable isotope geochemistry*: New York, Springer, 244 p.
- Holk, G.J., Taylor, B.E., and Galley, A.G., 2008, Oxygen isotope mapping of the Archean Sturgeon Lake caldera complex and VMS-related hydrothermal system, northwestern Ontario, Canada: *Mineralium Deposita*, v. 43, p. 623–640.
- Honma, H., Kusakabe, M., Kagami, H., Iizumi, S., Sakai, H., Kodama, Y., and Kimura, M., 1991, Major and trace element chemistry and D/H, $^{18}\text{O}/^{16}\text{O}$, $^{87}\text{Sr}/^{86}\text{Sr}$ and $^{143}\text{Nd}/^{144}\text{Nd}$ ratios of rocks from the spreading center of the Okinawa Trough, a marginal back-arc basin: *Geochemical Journal*, v. 25, p. 121–136.
- Hoy, L.D., 1993, Regional evolution of hydrothermal fluids in the Noranda District, Quebec—Evidence from $\delta^{18}\text{O}$ values from volcanogenic massive sulfide deposits: *Economic Geology*, v. 88, p. 1526–1541.
- Huston, D.L., 1999, Stable isotopes and their significance for understanding the genesis of volcanic-hosted massive sulfide deposits—A review, *in* Barrie, C.T., and Hannington, M.D., eds., Volcanic-associated massive sulfide deposits—Processes and examples in modern and ancient settings: *Reviews in Economic Geology*, v. 8, p. 157–179.
- Huston, D.L., and Taylor, B.E., 1999, Genetic significance of oxygen and hydrogen isotope variations at the Kidd Creek volcanic-hosted massive sulfide deposit, Ontario, Canada, *in* Hannington, M.D., and Barrie, C.T., eds., The giant Kidd Creek volcanogenic massive sulfide deposit, western Abitibi subprovince, Canada: *Economic Geology Monograph* 10, p. 335–350.
- Huston, D.L., Taylor, B.E., Bleeker, W., Stewart, B., Cook, R., and Koopman, E.R., 1995, Isotope mapping around the Kidd Creek deposit, Ontario—Application to exploration and comparison with other geochemical indicators: *Exploration and Mining Geology*, v. 4, p. 175–185.

- Ionov, D.A., Hoefs, J., Wedepohl, K.H., and Wiechert, U., 1992, Content and isotopic composition of sulfur in ultramafic xenoliths from central Asia: *Earth and Planetary Science Letters*, v. 111, p. 269–286.
- Ito, E., White, E.M., and Gopel, C., 1987, The O, Sr, Nd and Pb isotope geochemistry of MORB: *Chemical Geology*, v. 62, p. 157–176.
- Jakes, P., and White, A.J.R., 1971, Composition of island arcs and continental growth: *Earth and Planetary Science Letters*, v. 12, p. 224–230.
- Kelley, D.S., Fruh-Green, J.A., Karson, J.A., and Ludwig, K.A., 2007, The Lost City hydrothermal field revisited: *Oceanography*, v. 20, p. 90–99.
- King, E.M., Valley, J.W., and Davis, D.W., 2000, Oxygen isotope evolution of volcanic rocks at the Sturgeon Lake volcanic complex, Ontario: *Canadian Journal of Earth Sciences*, v. 37, p. 39–50.
- Kowalik, J., Rye, R.O., and Sawkins, F.J., 1981, Stable-isotope study of the Buchans, Newfoundland, polymetallic sulfide deposit: *Geological Association of Canada Special Paper 22*, p. 229–254.
- Krasnov, S.G., Cherkashov, G.A., Stepanova, T.V., Batuyev, B.N., Krotov, A.G., Malin, B.V., Maslov, V.F., Poroshina, I.M., Samovarov, M.S., Ashadze, A.M., Lazareva, L.I., and Ermolayev, I.K., 1995a, Detailed geological studies of hydrothermal fields in the North Atlantic, *in* Parsons, L.M., Walker, C.L., and Dixon, D.R., eds., *Hydrothermal vents and processes: Geological Society of London Special Publication 87*, p. 43–64.
- Krasnov, S.G., Proroshina, I.M., and Cherkashev, G.A., 1995b, Geological setting of high-temperature hydrothermal activity and massive sulfide formation on fast and slow-spreading ridges, *in* Parson, L.M., Walker, C.L., and Dixon, D.R., eds., *Hydrothermal vents and processes: Geological Society of London Special Publication 87*, p. 17–32.
- Kyser, T.K., and O'Neal, J.R., 1984, Hydrogen isotope systematics of submarine basalts: *Geochimica et Cosmochimica Acta*, v. 48, p. 2123–2133.
- Langmuir, C.H., Bezos, A., Escrig, S., and Parman, S.W., 2006, Chemical systematics and hydrous melting of the mantle in back-arc basins, *in* Back-arc spreading systems, geological, biological, chemical, and physical interactions: American Geophysical Union, *Geophysical Monograph Series 166*, p. 87–146.
- Large, R.R., 1992, Australian volcanic-hosted massive sulfide deposits—Features, styles, and genetic models: *Economic Geology*, v. 87, p. 471–510.
- Large, R.R., Allen, R.L., Blake, M.D., and Herrmann, W., 2001a, Hydrothermal alteration and volatile element halos for the Rosebery K Lens volcanic-hosted massive sulfide deposit, Western Tasmania: *Economic Geology*, v. 96, p. 1055–1072.
- Large, R.R., Gemmell, J.B., Paulick, H., and Huston, D.L., 2001b, The alteration box plot—A simple approach to understanding the relationship between alteration mineralogy and lithochemistry associated with volcanic-hosted massive sulfide deposits: *Economic Geology*, v. 96, p. 957–971.
- Large, R.R., McPhie, J., Gemmell, J.B., Herrmann, W., and Davidson, G.J., 2001c, The spectrum of ore deposit types, volcanic environments, alteration halos, and related exploration vectors in submarine volcanic successions—Some examples from Australia: *Economic Geology*, v. 96, p. 913–938.
- Larson, P.B., 1984, Geochemistry of the alteration pipe at the Bruce Cu-Zn volcanogenic massive sulfide deposit, Arizona: *Economic Geology*, v. 79, p. 1880–1896.
- Le Maitre, R.W., 2002, *Igneous rocks—A classification and glossary of terms*: Cambridge, Cambridge University Press, 240 p.
- Lentz, D.R., 1999, Petrology, geochemistry, and oxygen isotope interpretation of felsic volcanic and related rocks hosting the Brunswick 6 and 12 massive sulfide deposits (Brunswick belt), Bathurst mining camp, New Brunswick, Canada: *Economic Geology*, v. 84-1A, p. 611–616.
- Lowell, R.P., Crowell, B.W., Lewis, K.C., and Liu, L., 2008, Modeling multiphase, multicomponent processes at oceanic spreading centers, *in* Lowell, R.P., Seewald, J.S., Matexas, A., and Perfit, M.R., eds., *Magma to microbe—Modeling hydrothermal processes at ocean spreading centers: American Geophysical Union, Geophysical Monograph Series 178*, p. 15–44.
- Lowell, R.P., Rona, P.A., and Von Herzen, R.P., 1995, Seafloor hydrothermal systems: *Journal of Geophysical Research*, v. 100, p. 327–352.
- Lydon, J.W., 1988, Volcanogenic massive sulfide deposits—Part 2. Genetic models: *Geoscience Canada*, v. 15, p. 43–65.
- MacLean, W.H., and Hoy, L.D., 1991, Geochemistry of hydrothermally altered rocks at the Horne Mine, Noranda, Quebec: *Economic Geology*, v. 86, p. 506–528.
- MacLennan, J., 2008, The supply of heat to mid-ocean ridges by crystallization and cooling of mantle melts, *in* Lowell, R.P., Seewald, J.S., Matexas, A., and Perfit, M.R., eds., *Magma to microbe—Modeling hydrothermal processes at ocean spreading centers: American Geophysical Union, Geophysical Monograph Series 178*, p. 45–73.

- Marumo, K., 1989, Genesis of Kaolin minerals and pyrophyllite in Kuroko deposits of Japan—Implications for the origins of the hydrothermal fluids from mineralogical and stable isotope data: *Geochimica et Cosmochimica Acta*, v. 53, p. 2915–2924.
- Monecke, T., Gemmell, J.B., and Herzig, P.M., 2006, Geology and volcanic facies architecture of the Lower Ordovician Waterloo massive sulfide deposit, Australia: *Economic Geology*, v. 101, p. 179–197.
- Munha, J., Barriga, F.J.A.S., and Kerrich, R., 1986, High ^{18}O ore-forming fluids in volcanic-hosted base metal massive sulfide deposits—Geologic, $^{18}\text{O}/^{16}\text{O}$, and D/H evidence from the Iberian Pyrite Belt; Crandon, Wisconsin; and Blue Hill, Maine: *Economic Geology*, v. 81, p. 530–532.
- Munha, J., and Kerrich, R., 1980, Sea water basalt interactions in spilites from the Iberian Pyrite Belt: *Contributions to Mineralogy and Petrology*, v. 73, p. 191–200.
- Offler, R., and Whitford, D.J., 1992, Wall-rock alteration and metamorphism of a volcanic-hosted massive sulfide deposit at Que River, Tasmania—*Petrology and mineralogy: Economic Geology*, v. 87, 686–705.
- Ohmoto, H., and Rye, R.O., 1974, Hydrogen and oxygen isotopic composition of fluid inclusions in the Kuroko deposits, Japan: *Economic Geology*, v. 69, p. 947–953.
- Openholzner, J.H., Schroettner, H., Golob, P., and Delgado, H., 2003, Particles from the plume of Popocatepetl volcano, Mexico—The FESEM/EDS approach, *in* Oppenheimer, C., Pyle, D.M., and Barclay, J., eds., *Volcanic degassing: Geological Society Special Publication 213*, p. 124–148.
- Paradis, S., Taylor, B.E., Watkinson, D.H., and Jonasson, I.J., 1993, Oxygen isotope zonation and alteration in the Noranda mining district, Abitibi greenstone belt, Quebec: *Economic Geology*, v. 88, p. 1512–1525.
- Pearce, J.A., 1995, A user's guide to basalt discrimination diagrams, *in* Wyman, D.A., ed., *Trace element geochemistry of volcanic rocks—Applications to massive-sulfide exploration: Geological Association of Canada Short Course Notes*, v. 12, p. 79–114.
- Pearce, J.A., and Cann, J.R., 1973, Tectonic setting of basic volcanic rocks determined using trace element analysis: *Earth Planetary Science Letters*, v. 19, p. 290–300.
- Pearce, J.A., and Peate, D.W., 1995, Tectonic implications of the composition of volcanic arc magmas: *Annual Reviews of Earth and Planetary Sciences*, v. 23, p. 251–285.
- Pearce, J.A., and Stern, R.J., 2006, Origin of back-arc basin magmas—Trace element and isotopic perspectives, *in* Christie, D.M., Fisher, C.R., Lee, S.-M., and Givens, S., eds., *Back-arc spreading systems, geological, biological, chemical, and physical interactions: American Geophysical Union, Geophysical Monograph Series 166*, p. 63–86.
- Perfit, M.R., Ridley, W.I., and Jonasson, I.R., 1999, Geologic, petrologic, and geochemical relationships between magmatism and massive sulfide mineralization at the Eastern Galapagos Spreading Center, *in* Barrie, C.T., and Hannington, M.D., eds., *Volcanic-associated massive sulfide deposits—Processes and examples in modern and ancient settings: Reviews in Economic Geology*, v. 8, p. 75–100.
- Philpotts, A.R., 1990, *Principles of igneous and metamorphic petrology*: New Jersey, Prentice Hall, 498 p.
- Piercey, S.J., 2009, Litho-geochemistry of volcanic rocks associated with volcanogenic massive sulphide deposits and applications to exploration, *in* Cousens, B., and Piercey, S.J., eds., *Submarine volcanism and mineralization—Modern through ancient: Geological Association of Canada, Short Course Notes*, v. 19, p. 15–40.
- Pisutha-Arnond, V., and Ohmoto, H., 1983, Thermal history and chemical and isotopic compositions of the ore-forming fluids responsible for the Kuroko massive sulfide deposits in the Hokuroku District of Japan, *in* Ohmoto, H., and Skinner, B.J., eds., *The Kuroko and related volcanogenic massive sulfide deposits: Economic Geology Monograph 5*, p. 523–558.
- Poorter, R.P.E., Varekamp, J.C., Poreda, R.J., Van Bergen, M.J., and Kreulen, R., 1991, Chemical and isotopic composition of volcanic gases from Sunda and Banda arcs, Indonesia: *Geochimica et Cosmochimica Acta*, v. 55, p. 3795–3807.
- Poreda, R., 1985, Helium-3 and deuterium in back arc basalts—Lau Basin and the Mariana Trough: *Earth and Planetary Science Letters*, v. 73, p. 244–254.
- Poreda, R. J., Schilling, J.-G., and Craig, H., 1986, Helium and hydrogen isotopes in ocean-ridge basalts north and south of Iceland: *Earth and Planetary Science Letters*, v. 78, p. 1–17.
- Ridley, W.I., 1970, The petrology of the Las Canadas volcanoes, Tenerife, Canary Islands: *Contributions to Mineralogy and Petrology*, v. 26, p. 124–160.
- Ridley, W.I., Perfit, M.R., Jonasson, I.R., and Smith, M.F., 1994, Hydrothermal alteration in oceanic ridge volcanic—A detailed study at the Galapagos Fossil Hydrothermal Field: *Geochimica et Cosmochimica Acta*, v. 58, p. 2477–2494.

- Sakai, H., Casadevall, T.J., and Moore, J.G., 1982, Chemistry and isotopic ratios of sulfur in basalts and volcanic gases at Kilauea volcano: *Geochimica et Cosmochimica Acta*, v. 46, p. 729–738.
- Sakai, H., DesMarais, D.J., Ueda, A., and Moore, J.G., 1984, Concentrations and isotope ratios of carbon, nitrogen and sulfur in ocean-floor basalts: *Geochimica et Cosmochimica Acta*, v. 48, p. 2433–2441.
- Schultz, K.J., and Ayuso, R.A., 2003, Litho-geochemistry and paleotectonic setting of the Bald Mountain massive sulfide deposit, northern Maine, *in* Goodfellow, W.D., McCutcheon, S.R., and Peter, J.M., eds., *Massive sulfide deposits of the Bathurst mining camp, New Brunswick, and northern Maine: Economic Geology Monograph 11*, p. 79–109.
- Seyfried, W.E., Jr., Ding, K., Berndt, M.E., and Chen, X., 1999, Experimental and theoretical controls on the composition of mid-ocean ridge hydrothermal fluids, *in* Barrie, C.T., and Hannington, M.D., eds., *Volcanic-associated massive sulfide deposits—Processes and examples in modern and ancient settings: Reviews in Economic Geology*, v. 8, p. 181–200.
- Shanks, W.C., III, 2001, Stable isotopes in seafloor hydrothermal systems—Vent fluids, hydrothermal deposits, hydrothermal alteration, and microbial processes, *in* Valley, J.W., and Cole, D.R., eds., *Stable isotope geochemistry: Reviews in Mineralogy and Geochemistry*, v. 43, p. 469–525.
- Shanks, W.C., III, Böhlke, J.K., and Seal, R.R., 1995, Stable isotopes in mid-ocean ridge hydrothermal systems—Interactions between fluids, minerals and organisms, *in* Humphris, S.E., Zierenberg, R.A., Mullineaux, L.S., and Thompson, R.E., eds., *Seafloor hydrothermal systems—Physical, chemical, biological, and geological interactions: American Geophysical Union, Geophysical Monograph 91*, p. 194–221.
- Sheppard, S.M.F., 1986, Characterization and isotopic variations in natural waters, *in* Valley, J.W., Taylor, H.P., Jr., and O'Neal, J.R., eds., *Stable isotopes: Reviews in Mineralogy*, v. 16, p. 165–183.
- Singh, S.C., Collier, J.S., Harding, A.J., Kent, G.M., and Orcutt, J.A., 1999, Seismic evidence for a hydrothermal layer above the solid roof of the axial magma chamber at the southern East Pacific Rise: *Geology*, v. 27, p. 219–222.
- Singh, S.C., Crawford, W.C., Carton, H., Seher, T., Combier, V., Cannat, M., Canales, J.P., Düsünür, D., Escartin, J., and Miranda, J.M., 2006, Discovery of a magma chamber and faults beneath a Mid-Atlantic Ridge hydrothermal field: *Nature*, v. 442, p. 1029–1032.
- Sinha, M.C., Contable, S.C., Peirce, C., White, A., Heinson, G., Macgregor, L.M., and Navin, D.A., 1998, Magmatic processes at slow spreading ridges—Implications of the RAMESSES experiment at 57° 45'N on the Mid-Atlantic Ridge: *Geophysical Journal International*, v. 135, p. 731–745.
- Stakes, D.S., and Taylor, H.P., 1992, The northern Samail ophiolite—An oxygen isotope, microprobe, and field study: *Journal of Geophysical Research*, v. 97, p. 7043–7080.
- Stanton, R.L., 1994, *Ore elements in arc lavas: Oxford*, Oxford Science Publications, 391 p.
- Stern, R.J., Fouch, M.J., and Klemperer, S.L., 2003, An overview of the Izu-Bonin-Marianas subduction factory, *in* Eiler, J., ed., *Inside the subduction factory: American Geophysical Union, Geophysical Monograph Series 138*, p. 175–222.
- Stolz, J., and Large, R.R., 1992, Evaluation of the source-rock control on precious metal grades in volcanic-hosted massive sulfide deposits from western Tasmania: *Economic Geology*, v. 87, p. 720–738.
- Taylor, B.E., and Huston, D.L., 1999, Regional ¹⁸O zoning and hydrogen isotope studies in the Kidd Creek volcanic complex, Timmins, Ontario, *in* Hannington, M.D., and Barrie, C.T., eds., *The giant Kidd Creek volcanogenic massive sulfide deposit, western Abitibi subprovince, Canada: Economic Geology Monograph 10*, p. 351–378.
- Taylor, B.E., and South, B.C., 1985, Regional stable isotope systematics of hydrothermal alteration and massive sulfide deposition in the West Shasta district, California: *Economic Geology*, v. 80, p. 2149–2163.
- Taylor, H.P., 1974, The application of oxygen and hydrogen isotope studies to problems of hydrothermal alteration and ore deposition: *Economic Geology*, v. 69, p. 843–883.
- Taylor, H.P., 1990, Oxygen and hydrogen isotope constraints on the deep circulation of surface waters into zones of hydrothermal metamorphism and melting, *in* *The role of fluids in crustal processes: The National Academies Press; Commission on Geosciences, Environment, and Resources; Geophysics Study Committee*, p. 72–95.
- Tornos, F., Solomon, M., Conde, C., and Spiro, B.F., 2008, Formation of the Tharsis massive sulfide deposit, Iberian pyrite belt—Geological, litho-geochemical, and stable isotope evidence for deposition in a brine pool: *Economic Geology*, v. 103, p. 185–214.
- Urabe, T., and Scott, S.D., 1983, Geology and footwall alteration of the South Bay massive sulfide deposit, northwestern Ontario, Canada: *Canadian Journal of Earth Sciences*, v. 20, p. 1862–1879.

- Urabe, T., Scott, S.D., and Hattori, K., 1983, A comparison of footwall-rock alteration and geothermal systems beneath some Japanese and Canadian volcanogenic massive sulfide deposits, *in* Ohmoto, H., and Skinner, B.J., eds., *The Kuroko and related volcanogenic massive sulfide deposits: Economic Geology Monograph 5*, p. 345–364.
- Veizer, J., Ala, D., Azmy, K., Bruckschen, P., Buhl, D., Bruhn, F., Carden, G.A.F., Diener, A., Ebner, S., Godderis, Y., Jasper, T., Korte, C., Pawellek, F., Podlaha, O.G., and Strauss, H., 1999, $^{87}\text{Sr}/^{86}\text{Sr}$, ^{13}C , ^{18}O evolution of Phanerozoic seawater: *Chemical Geology*, v. 161, p. 58–88.
- Wanless, V.D., Perfit, M.R., Ridley, W.I., and Klein, E., 2010, Dacite petrogenesis on mid-ocean ridges—Evidence for oceanic crustal melting and assimilation: *Journal of Petrology*, v. 51, p. 2377–2410.
- Watanabe, M., and Sakai, H., 1983, Stable isotope geochemistry of sulfates from the Neogene ore deposits of the Green Tuff region, Japan, *in* Ohmoto, H., and Skinner, B.J., eds., *The Kuroko and related volcanogenic massive sulfide deposits: Economic Geology Monograph 5*, p. 282–291.
- Whitford, D.J., Korsch, M.J., and Solomon, M., 1992, Strontium isotope studies of barites—Implications for the origin of base metal mineralization in Tasmania: *Economic Geology*, v. 87, p. 953–959.
- Yang, K., and Scott, S.D., 2006, Magmatic fluids as a source of metals in seafloor hydrothermal systems, *in* Christie, D.M., ed., *Back-arc spreading systems—Geological, biological, chemical, and physical interactions: American Geophysical Union, Geophysical Monograph Series 166*, p. 163–184.

16. Petrology of Sedimentary Rocks Associated with Volcanogenic Massive Sulfide Deposits

By Cynthia Dusel-Bacon

16 of 21

Volcanogenic Massive Sulfide Occurrence Model

Scientific Investigations Report 2010–5070–C

**U.S. Department of the Interior
U.S. Geological Survey**

U.S. Department of the Interior
KEN SALAZAR, Secretary

U.S. Geological Survey
Marcia K. McNutt, Director

U.S. Geological Survey, Reston, Virginia: 2012

For more information on the USGS—the Federal source for science about the Earth, its natural and living resources, natural hazards, and the environment, visit <http://www.usgs.gov> or call 1-888-ASK-USGS.

For an overview of USGS information products, including maps, imagery, and publications, visit <http://www.usgs.gov/pubprod>

To order this and other USGS information products, visit <http://store.usgs.gov>

Any use of trade, product, or firm names is for descriptive purposes only and does not imply endorsement by the U.S. Government.

Although this report is in the public domain, permission must be secured from the individual copyright owners to reproduce any copyrighted materials contained within this report.

Suggested citation:

Dusel-Bacon, Cynthia, 2012, Petrology of sedimentary rocks associated with volcanogenic massive sulfide deposits in volcanogenic massive sulfide occurrence model: U.S. Geological Survey Scientific Investigations Report 2010-5070 -C, chap. 16, 8 p.

Contents

| | |
|---|-----|
| Importance of Sedimentary Rocks to Deposit Genesis..... | 267 |
| Rock Names..... | 268 |
| Mineralogy..... | 269 |
| Textures..... | 269 |
| Grain Size..... | 269 |
| Environment of Deposition..... | 269 |
| References Cited..... | 271 |

16. Petrology of Sedimentary Rocks Associated with Volcanogenic Massive Sulfide Deposits

By Cynthia Dusel-Bacon

Importance of Sedimentary Rocks to Deposit Genesis

The importance and percentage of sedimentary rocks associated with VMS deposits differ among the various deposit types, defined by their lithologic settings. Sedimentary rocks are a negligible component in bimodal-mafic type deposits, make up a minor component in mafic-ultramafic type deposits, but are an important component in siliciclastic-mafic, bimodal-felsic, and siliciclastic-felsic type deposits (Franklin and others, 2005). In spite of the differing relative proportions of sedimentary rocks to mafic and felsic volcanic rocks, associated sedimentary lithofacies in the majority of the above VMS settings are all dominated by terrigenous clastic sedimentary rocks, primarily wacke, sandstone, siltstone, mudstone, and carbonaceous mudstone, with lesser amounts of chert, carbonate, marl, and iron-formation (Franklin and others, 2005). The absence of certain sedimentary facies also can provide important paleogeographic constraints. For example, the lack of unconformities or thick epiclastic sedimentary successions between or within the Archean volcanic formations of the Blake River Group that hosts the bimodal-mafic-type VMS deposits of the Noranda district suggests that volcanism was distal from subaerial or above storm-wave-base landmasses (Gibson and Galley, 2007).

The major- and trace-element compositions of sedimentary rocks associated with VMS deposits can reflect the distinct provenance types and tectonic settings of the associated sedimentary basins (Bhatia, 1983; Bhatia and Crook, 1986). Most of the sedimentary rocks were deposited in extensional basins. However, the VMS deposits themselves generally formed within volcanic centers that were located in smaller graben structures within a larger sediment-filled extensional basin (for example, Bathurst; Goodfellow and McCutcheon, 2003; Franklin and others, 2005). Trace-element data for VMS-associated volcanic rocks indicate that most VMS deposits formed during various stages of rifting associated with intra-arc and back-arc development (for example, Lentz, 1998; Piercey and others, 2001; Piercey, 2009). The distribution and thickening of sedimentary strata associated

with volcanic and volcanoclastic rocks can reveal the presence of synvolcanic growth faults that formed during rifting. These faults are a key tectonic element in the formation of hydrothermal convection systems that discharged metal-bearing fluids onto the seafloor or into permeable strata immediately below the seafloor to form the VMS deposits (for example, Franklin and others, 2005).

Clastic sedimentary strata, typically carbonaceous argillite, immature epiclastic volcanic wacke, and carbonate units, most commonly occur within the hanging wall succession of VMS deposits (for example, Bergslagen district, Sweden; Allen and others, 1997). Volcanoclastic deposits, defined by Fisher and Schmincke (1984, p. 89) to include “all clastic volcanic materials formed by any process of fragmentation, dispersed by any transporting agent, deposited in any environment or mixed in any significant portion with non-volcanic fragments,” are an important component in most VMS deposits and include both pyroclastic deposits and reworked and redeposited volcanic material that may be intercalated with terrigenous sediment (Franklin and others, 2005). Differentiating between primary volcanic textures and reworked epiclastic textures in such rocks can be difficult.

Sedimentary rocks, including redeposited felsic volcanoclastic strata associated with the felsic volcanic host rocks, can help elucidate the mode of deposition of the felsic volcanic rocks (subaerial or submarine), water depth at the time of the submarine volcanic eruptions and VMS formation, and the stages of extension and subsidence in a continental-margin incipient rift. For example, sedimentary facies associations at the strongly deformed Zn-Cu massive sulfide deposits at Benambra, Australia, indicate that mineralization occurred in the center of an ensialic back-arc or intra-arc basin following fault-controlled subsidence in a mixed subaerial and subaqueous environment with active rhyolitic volcanism, through a marine shelf environment with limestone-volcanoclastic sedimentation, to a moderate- to deep-water environment with mudstone and turbidite sedimentation and rhyolite to basaltic volcanism (Allen, 1992). The massive sulfides formed in siltstone within a proximal (near-vent) facies association of a mainly nonexplosive, moderate- to deep-water submarine volcano composed of turbiditic sediments interleaved with

rhyolitic to basaltic sills, lavas, and associated hyaloclastites during the advanced stage of extension and subsidence (Allen, 1992).

Interpreting the mode of emplacement of deep-marine silicic volcanic rocks, especially those that have undergone significant alteration, metamorphism, and deformation, is controversial, however, and debates regarding the possibility of deep-marine, explosive silicic volcanism have continued for decades. Some studies proposed that ignimbrites in subaqueous environments are confined to shallow-water, near-shore environments at water depths of tens of meters or less because higher confining pressures under deeper water conditions would impede vesiculation and hence explosive eruption (for example, Cas and Wright, 1987; Allen, 1988). Others concluded, however, that considerable volumes of pumiceous tephra were deposited directly into the marine environment at significant depths (>1.4 km) (for example, Fiske and Matsuda, 1964; Busby-Spera, 1984; Cashman and Fiske, 1991; Fiske and others, 2001; Busby and others, 2003). Depositional features of sedimentary rocks, especially volcanoclastic rocks, will play an important role in resolving this controversy for ancient VMS deposits.

Footwall sedimentary, as well as volcanic, strata can be important source rocks for VMS mineralization. For example, in the siliciclastic-felsic setting of the Bathurst district, the hydrothermal convective system that was responsible for forming the deposits extended into the prevolcanic, rift-related terrigenous sedimentary strata that disconformably underlie the volcanic sequence and VMS deposits (van Staal and others, 2003). The primary permeability and porosity of footwall lithofacies affect the movement of hydrothermal fluids and, thus, the distribution and development of semiconformable alteration zones. Regional semiconformable alteration assemblages are pervasive and widespread in permeable volcanoclastic and siliciclastic sedimentary facies of VMS deposits (Gifkins and Allen, 2001).

Differences in the primary permeability and porosity of volcanic and sedimentary lithofacies of VMS host rocks affect the morphology of their footwall alteration zones (Morton and Franklin, 1987; Gibson and others, 1999; Franklin and others, 2005). In VMS settings in which synvolcanic faults cut strata composed of unconsolidated volcanoclastic or siliciclastic rocks with high permeability and porosity, ascending hydrothermal fluids may defuse laterally away from the fault and discharge over a large area. If an aquaclude (such as subsurface, precipitated silica, clay, and minor sulfide minerals; fine-grained argillite; carbonaceous argillite; chert; and flows, sills, and cryptodomes within the volcanoclastic succession) develops within the footwall sequence, the initially poorly-focused discharge may become localized along structural conduits or may form discordant, broad, and locally stratiform footwall alteration zones (Franklin and others, 2005).

Porosity and grain size of sediments play an important role in the prevention of metal-bearing fluids dissipating onto the seafloor. Subseafloor accumulation and replacement provide an efficient mechanism to trap metals and may be

responsible for forming large, tabular VMS deposits. Some components of the circulating hydrothermal fluid become trapped in hanging-wall sediments and seafloor precipitates, and elements such as Si (as chert) and conserved elements (Mn, Eu, P, Tl, and base and precious metals) accumulate in these sediments, forming useful vectors to potential ore (Franklin and others, 2005). The subseafloor VMS deposits form as sulfide minerals are precipitated within the preexisting pore spaces and fractures of volcanic or sedimentary rocks or as a result of the replacement of volcanic or sedimentary constituents in a chemically reactive host, such as carbonate (Doyle and Allen, 2003, and references therein). The most favorable sedimentary rocks for such subseafloor deposits are deep-marine, terrigenous clastic rocks such as sandstone and wacke; subseafloor deposition within mudstone lithofacies is uncommon. Therefore, VMS deposits hosted by volcanic successions that are dominated by volcanoclastic and (or) siliciclastic lithofacies are preferred targets (Franklin and others, 2005).

Rock Names

Bimodal-mafic-type VMS deposits (for example, Noranda, Canada; Gibson and Kerr, 1993) are associated with terrigenous sedimentary rocks that are dominated by immature wacke, sandstone, and argillite, with local debris flows; hydrothermal chert is also common in the immediate hanging wall to some deposits. Mafic-ultramafic type VMS deposits (for example, Troodos, Cyprus; Constantinou and Govett, 1973) generally contain <10 percent sedimentary rocks consisting primarily of sulfidic, reduced, or hematitic-oxidized argillite, chert, and (or) tuff (Franklin and others, 2005).

Siliciclastic-mafic-type VMS deposits occur in mature, oceanic, back-arc successions in which thick marine sequences of clastic sedimentary rocks and intercalated basalt are present in subequal or pelite-dominated proportions (Slack, 1993). Examples are in the Besshi and Shimoakawa districts of Japan (Banno and others, 1970; Mariko, 1988) and the Windy Craggy deposit of British Columbia, Canada (Peter and Scott, 1999). Sedimentary rocks characteristic of a pelitic lithofacies include argillite, carbonaceous argillite, subordinate siltstone, marl, and carbonate (bioclastic and chemical) (Franklin and others, 2005). Other associated clastic rocks may include arenite, arenite conglomerate, and turbiditic slate and sandstone. Metachert, magnetite iron-formation, coticule (fine-grained quartz-spessartine rock), and tourmalinite occur in or near many metamorphosed Besshi-type deposits and may have originated as a result of premetamorphic hydrothermal alteration or chemical precipitation synchronous with massive sulfide deposition (Slack, 1993).

Bimodal-felsic type deposits, such as those in the Paleoproterozoic Skellefte district, Sweden (Allen and others, 1997) and the mid-Paleozoic Finlayson Lake district, Canada (Murphy and others, 2006; Peter and others, 2007), formed within incipiently-rifted, continental-margin arcs and related back

arcs and contain only about 10 percent terrigenous sedimentary strata (Franklin and others, 2005). Felsic volcanic rocks constitute the dominant lithology (35–70 percent of volcanic strata) with basalt making up 20–50 percent (Franklin and others, 2005). Submarine felsic volcanoclastic rocks are common in these districts and many of the felsic volcanic deposits were reworked by sedimentary processes. Common sedimentary rock types (or in many cases, the inferred sedimentary protoliths of metasedimentary rocks) intercalated with the volcanic rocks include rhyolitic tuffaceous siltstone and sandstone, carbonaceous siltstone and mudstone, feldspathic and quartzofeldspathic turbidite, sandstone, volcanic breccia-conglomerate, and volcanoclastic rocks with a lime matrix; limestone is rare by comparison.

Siliciclastic strata constitute up to 80 percent of the rocks associated with siliciclastic-felsic-type deposits, which form in a mature epicontinental back-arc setting, examples being the Iberian Pyrite Belt, Spain and Portugal (Carvalho and others, 1999; Tornos, 2006), and Bathurst, Canada (Goodfellow and others, 2003). Franklin and others (2005) define a siliciclastic sedimentary lithofacies as one consisting predominantly of wacke, sandstone, argillite, siltstone, and locally iron-formation or Fe-Mn-rich argillite. Associated lithologies include felsic volcanoclastic rocks and minor flows, domes, and their intrusive equivalents (about 25 percent) and mafic flows, sills, and minor volcanoclastic rocks (about 10 percent). Argillaceous and carbonaceous sedimentary rocks and their phyllitic or schistose equivalents, as well as Fe-, Mn-, Ca-, and Ba-rich chemical sedimentary rocks, are common in the hanging wall of this deposit type (Franklin and others, 2005). Typical sedimentary rock types in the Iberian Pyrite Belt are shale (black, dark gray, green, and purple) graywacke, quartzwacke, impure quartzite, siliceous chemical sedimentary rocks (jasper or chert), and radiolarite; minor limestone occurs as lenses and nodules (Carvalho and others, 1999).

Mineralogy

Given that the vast majority of VMS deposits and their host rocks have been metamorphosed, the mineralogy of (meta)sedimentary rocks associated with the various deposit types rarely preserves the primary clay-SiO₂-feldspar ± hornblende ± pyroxene mineralogy of the sediments and will vary according to metamorphic grade, as discussed in Chapter 17 of this report. Common detrital or matrix minerals present in the sedimentary rocks include quartz, phyllosilicates (for example, illite, kaolinite, chlorite, sericite, biotite, and muscovite, sequentially developed with increasing metamorphic grade), plagioclase, K-feldspar, carbonate minerals, detrital olivine, pyroxene and amphibole, and the metamorphic minerals that replace them (for example, epidote, titanite, ilmenite), and pyrite and (or) organic material/graphite. Magnetite, cotchule, and tourmaline are characteristic minerals in chemically-precipitated sedimentary rocks in siliciclastic-mafic-type deposits.

Textures

Textures in sedimentary rocks associated with VMS deposits, where not subsequently modified by dynamothermal metamorphism, include soft-sediment deformation structures, rhythmic turbidite layering, graded beds, crossbedding, thinning or thickening of beds associated with synvolcanic faulting, rhythmic fine-scale banding of carbonaceous and volcanic laminae, bimodal size distribution of reworked volcanoclastic rocks (particularly those containing quartz phenocrysts), and poorly-sorted sedimentary breccias and conglomerates. Clastic textures are also present in the massive sulfide deposits. For example, in the Iberian Pyrite Belt, sedimentary structures such as graded bedding, crossbedding, sedimentary breccias, and slump structures are common in massive, laminated ores (Carvalho and others, 1999).

Grain Size

Grain sizes of the sedimentary rocks intercalated with VMS deposits or those present in the nearby submarine depositional environment range from submillimeter particles in fine-grained mudstones to clasts tens of centimeters in diameter in volcanic and sedimentary breccias/conglomerates within rift basins. Bimodal grain size distributions, particularly of quartz and feldspar, are common in epiclastic rocks derived from the remobilization of crystal tuffs or subvolcanic porphyry intrusions. Metamorphic recrystallization generally results in an increase in grain size, but this increase can be countered by comminution of grains during penetrative deformation and shearing. High-grade, postore regional or contact metamorphism can produce coarse-grained garnet, andalusite, cordierite, hornblende, or other minerals in originally fine-grained sedimentary rocks. Clastic sulfides eroded from chimneys and mounds generally consist of sand- to silt-sized grains in bedded deposits, and cobble- to boulder-sized clasts of massive sulfides occur rarely in debris-flow channel deposits, as discussed in Chapter 4 of this report.

Environment of Deposition

Sedimentary rocks associated with bimodal-mafic type VMS deposits were deposited within an incipiently rifted bimodal volcanic arc above an intraoceanic subduction zone. Sedimentary rocks in mafic-ultramafic type VMS deposits accumulated in a mature, intraoceanic, back-arc and related transform-fault setting or, less commonly, in an oceanic island or late-stage continental back-arc seamount environment (Franklin and others, 2005).

The geologic features of siliciclastic-mafic type deposits suggest that the best modern analogues are pyrrhotite-rich sulfide accumulations on and within thick sedimentary sequences overlying oceanic spreading ridges in the northeast Pacific, such as Guaymas Basin, Escanaba Trough, and Middle Valley

(Koski, 1990). In all of these modern-day analogues, eroded material from nearby continental landmasses provides a major component of the clastic sediment. Sedimentary fill in these modern analogues consists of turbidite muds, which may be intercalated with diatomaceous ooze, silt, arkosic sand, and local carbonaceous sediment (Slack, 1993, and references therein). Oceanic basalt and related mafic dikes and sills of MORB composition occur along the spreading ridges and are an important heat source for the hydrothermal circulation. Several tectonic settings contain the above elements: intracontinental rifts, rifted continental margins, oceanic spreading ridges near continental landmasses, back-arc basins, and a spreading ridge that is being consumed by a subduction zone (Koski, 1990; Slack, 1993). Sheet-like metalliferous sediments in the Red Sea also have been suggested as possible modern analogues of the siliciclastic-mafic type deposits (for example, Degens and Ross, 1969; Shanks and Bischoff, 1980; Pottorf and Barnes, 1983). There, hot metal-rich brines and the metalliferous sediments overlie tholeiitic basalt and evaporites and shales; current sedimentation consists mainly of calcareous mud (Shanks and Bischoff, 1980).

Sedimentary rocks associated with bimodal-felsic type deposits accumulated in incipiently-rifted continental margin arc and back-arc settings. The Paleoproterozoic Skellefte district, Sweden, exemplifies the complex and variable paleogeography in which magmatism, base-metal mineralization, and sedimentation have been documented for this deposit type (Allen and others, 1997). Changes in the intensity and location of marine volcanism resulted in subregional disconformities and differential uplift and subsidence that resulted in a complex system of horsts and grabens. Sedimentation in this horst and graben system varied in time and space and included prograding fluvial-deltaic sediments and mudstone and sandstone turbidites. Consequently, the massive sulfides in the Skellefte district are thought to have spanned a range in ore deposit styles from deep-water seafloor precipitation to subseafloor replacements, to shallow water and possibly subaerial synvolcanic replacements (Allen and others, 1997).

Siliciclastic-felsic type VMS deposits formed in a mature continental or epicontinental back-arc setting. Sedimentary rocks associated with this deposit type accumulated in an extending, submarine, fault-controlled basin with restricted circulation and reduced oxidation. Pre- or synvolcanic faults and their intersection with other regional structures played important roles in determining sites of volcanic centers and associated hydrothermal activity within the basins.

Cashman and Fiske (1991) conducted experiments on water-saturated pumice and rock fragments (lithics) and showed that particles settling to the seafloor at terminal velocities will display conspicuous bimodality of particle diameters: pieces of pumice can be five to ten times as large as co-deposited lithic fragments. They also showed that similar material that is erupted into the air and deposited on land has much less well-developed size bimodality, with pumice diameters being generally only two to three times as large as the associated lithics. As pointed out by Cashman and Fiske (1991), these

textural differences may be used to infer a subaqueous origin for some of the great thicknesses of non-fossiliferous volcanic deposits in ancient volcanic terranes whose environment of deposition has been uncertain.

Constraints on the water depths of sedimentation associated with VMS deposits can be provided by sedimentologic features of stratigraphic sections above and below the deposits, by fossil assemblages, and by studies of fluid inclusions in the associated massive sulfide minerals. At the bimodal-mafic Bald Mountain deposit in northern Maine, for example, deep-water depositional conditions are suggested by a sedimentary sequence that lacks any wave-generated sedimentary structures; any in situ shallow-marine fauna and even any resedimented shallow-marine fauna; and any evidence for subaerial exposure, erosion, or fluvial sedimentation (Busby and others, 2003). Additional evidence cited by Busby and others for a deep-water environment at Bald Mountain is the presence of carbonaceous mudstones that occur throughout the section, which, typically, although not exclusively, form in deep-water environments >200 m deep (Pickering and others, 1989). These deep-water sedimentologic features are confirmed by fluid inclusion analyses of primary hydrothermal quartz in the Bald Mountain deposit that indicate a hydrostatic pressure corresponding to a paleowater depth of >1.45 km (Foley, 2003).

In contrast, stratigraphic evidence from the Mount Chalmers siliciclastic-felsic type VMS deposit—a massive sulfide plus footwall stockwork Cu-Au orebody in Queensland, Australia—indicates a shallow-water depositional setting at the time of mineralization (Sainty, 1992). Fossils identified from the Permian Chalmers sedimentary section consist of brachiopods, gastropods, bivalves, and bryozoans that show limited reworking and trace fossils typical of the Cruziana ichnofacies. These fossil assemblages indicate deposition below the effective wave base and suggest seawater depths of 200–300 m during deposition of the massive sulfides (Sainty, 1992). This shallow depth determination has important implications for the interplay between water depth, boiling of hydrothermal fluids, and the formation of VMS deposits. Ohmoto and Takahashi (1983) proposed that a marine environment with a minimum depth of 1,000 m was necessary to prevent the boiling of ascending hydrothermal fluids that would induce sulfide precipitation and the production of disseminated or vein-type deposits rather than the formation of massive stratiform ores. However, Sainty (1992) suggested that the sedimentologic evidence for a shallow-water depth allows for the possibility that ore-forming fluids may have boiled prior to reaching the seafloor, especially if there had existed constrictions or self-sealing of the fluid channelways, and that boiling may have resulted in the Cu-rich footwall stringer zone and the elevated salinities in fluid inclusions at Mount Chalmers (Large and Both, 1980). Sainty (1992) pointed out that, in spite of likely boiling of hydrothermal fluids at the Chalmers deposit, two massive sulfide lenses were formed, and that this interpretation is consistent with examples from modern massive sulfide systems in which boiling at greater seawater depths, such as at the Explorer Ridge

(1,850 m) and Axial seamount (1,540 m), is accompanied by the deposition of massive sulfides (Kappel and Franklin, 1989; Jonasson and others, 1990).

Carbonaceous shale is a common constituent of most VMS deposits, for example, in the Archean Kidd Creek deposit (Hannington and others, 1999), in the early Paleozoic Bathurst camp (Goodfellow and McCutcheon, 2003), and in the mid-Paleozoic Finlayson Lake district (Peter and others, 2007), the Bonnifield district (Dusel-Bacon and others, 2004), and the Iberian Pyrite Belt (Tornos, 2006). The presence of carbonaceous sediments is important in indicating—in most cases—anoxic, generally deep water conditions. The large tonnage, shale-hosted orebodies of the southern part of the Iberian Pyrite Belt are interpreted to have formed in suboxic to anoxic third-order basins in which upwelling, sulfur-depleted fluids mixed with modified seawater that was rich in biogenically reduced sulfur, leading to the precipitation of massive sulfides on the seafloor (Tornos, 2006). Evidence for this exhalative origin includes a stratiform morphology, an absence of major metal refining, an abundance of sedimentary structures, a lack of sulfates, and a common presence of siderite-rich facies (Tornos, 2006). Carbonaceous units within volcanic piles represent a hiatus in volcanism that is typically characterized by low-temperature hydrothermal activity that was favorable for the generation of massive sulfides. For example, in the Archean bimodal-mafic-type Kidd Creek deposit, carbonaceous sediments occur as interflow deposits throughout the Kidd Creek volcanic complex; carbon isotope data indicate that hydrothermal activity most likely occurred concurrently in several isolated subbasins within a much larger, graben-like setting (Wellmer and others, 1999). Studies of hydrothermal activity at Guaymas Basin, a modern analogue of a siliciclastic-mafic deposit, showed that the presence of abundant sedimentary organic matter (2–4 wt%) in basin sediments strongly influenced mineralogical alteration and the extent of chemical exchange within the oceanic crust, and that abundant C and S species in hydrothermal fluids and mineral deposits at sediment-covered spreading centers also strongly influenced pH, redox, and complexing reactions, which in turn directly constrained metal transport and depositional processes (Seewald and others, 1994, and references therein).

References Cited

- Allen, R.A., 1988, False pyroclastic textures in altered silicic lavas, with implications for volcanic-associated mineralization: *Economic Geology*, v. 83, p. 1424–1446.
- Allen, R.A., 1992, Reconstruction of the tectonic, volcanic, and sedimentary setting of strongly deformed Zn-Cu massive sulfide deposits at Benambra, Victoria: *Economic Geology*, v. 87, p. 825–854.
- Allen, R.A., Weihed, P., and Svenson, S.A., 1997, Setting of Zn-Cu-Au-Ag massive sulfide deposits in the evolution and facies architecture of a 1.9 Ga marine volcanic arc, Skellefte district, Sweden: *Economic Geology*, v. 91, p. 1022–1053.
- Banno, S., Takeda, H., and Sato, H., 1970, Geology and ore deposits in the Besshi mining district—Field trip guidebook 9, excursion 5, in IMA-IAGOD, 7th general meeting, Tokyo and Kyoto, Japan, 1970, Proceedings: International Mineralogical Association—International Association on the Genesis of Ore Deposits, 31 p.
- Bhatia, M.R., 1983, Plate tectonics and geochemical composition of sandstones: *Journal of Geology*, v. 91, p. 611–627.
- Bhatia, M.R., and Crook, K.A.W., 1986, Trace element characteristics of graywackes and tectonic setting discrimination of sedimentary basins: *Contributions to Mineralogy and Petrology*, v. 92, p. 181–193.
- Busby, C.J., Kessel, L., Schulz, K.J., Foose, M.P., and Slack, J.F., 2003, Volcanic setting of the Ordovician Bald Mountain massive sulfide deposit, northern Maine, in Goodfellow, W.D., McCutcheon, S.R., and Peter, J.M., eds., Massive sulfide deposits of the Bathurst mining camp, New Brunswick, and northern Maine: *Economic Geology Monograph* 11, p. 219–244.
- Busby-Spera, C.J., 1984, Large-volume rhyolitic ash flow eruptions and submarine caldera collapse in the lower Mesozoic Sierra Nevada, California: *Journal of Geophysical Research*, v. 89, p. 8417–8427.
- Carvalho, D., Barriga, F.J.A.S., and Munha, J., 1999, Bimodal-siliciclastic systems—The case of the Iberian Pyrite Belt, in Barrie, C.T., and Hannington, M.D., eds., Volcanic-associated massive sulfide deposits—Processes and examples in modern and ancient settings: *Reviews in Economic Geology*, v. 8, p. 375–408.
- Cas, R.A.F., and Wright, J.V., 1987, Volcanic successions—Modern and ancient: London, Allen and Unwin, 528 p.
- Cashman, K.V., and Fiske, R.S., 1991, Fallout of pyroclastic debris from submarine volcanic eruptions: *Science*, v. 253, p. 275–280.
- Constantinou, G., and Govett, G.J.S., 1973, Geology, geochemistry and genesis of Cyprus sulfide deposits: *Economic Geology*, v. 68, p. 843–858.
- Degens, E.T., and Ross, D.A., eds., 1969, Hot brines and recent heavy metal deposits in the Red Sea: Springer-Verlag, New York, NY, 600 p.
- Doyle, M.G., and Allen, R.L., 2003, Subsea-floor replacement in volcanic-hosted massive sulfide deposits: *Ore Geology Reviews*, v. 23, p. 183–222.

- Dusel-Bacon, C., Wooden, J.L., and Hopkins, M.J., 2004, U-Pb zircon and geochemical evidence for bimodal mid-Paleozoic magmatism and syngenetic base-metal mineralization in the Yukon-Tanana terrane, Alaska: *Geological Society of America Bulletin*, v. 116, no.7/8, p. 989–1015.
- Fisher, R.V., and Schmincke, H.-U., 1984, *Pyroclastic rocks*: Berlin, Springer-Verlag, 472 p.
- Fiske, R.S., and Matsuda, T., 1964, Submarine equivalents of ash flows in the Tokiwa Formation, Japan: *American Journal of Science*, v. 262, p. 76–106.
- Fiske, R.S., Naka, J., Iizasa, K., Yuasa, M., and Klaus, A., 2001, Submarine silicic caldera at the front of the Izu-Bonin arc, Japan—Voluminous seafloor eruptions of rhyolite pumice: *Geological Society of America Bulletin*, v. 113, p. 813–824.
- Foley, N.K., 2003, Thermal and chemical evolution of ore fluids and massive sulfide mineralization at Bald Mountain, Maine, in Goodfellow, W.D., McCutcheon, S.R., and Peter, J.M., eds., *Massive sulfide deposits of the Bathurst mining camp, New Brunswick, and northern Maine*: *Economic Geology Monograph* 11, p. 549–565.
- Franklin, J.M., Gibson, H.L., Jonasson, I.R., and Galley, A.G., 2005, Volcanogenic massive sulfide deposits, in Hedenquist, J.W., Thompson, J.F.H., Goldfarb, R.J., and Richards, J.P., eds., *Economic Geology 100th Anniversary Volume, 1905–2005*: Littleton, Colo., Society of Economic Geologists, p. 523–560.
- Gibson, H.L., and Galley, A.G., 2007, Volcanogenic massive sulphide deposits of the Archean, Noranda district, Québec, in Goodfellow, W.D., ed., *Mineral deposits of Canada—A synthesis of major deposit-types, district metallogeny, the evolution of geological provinces, and exploration methods*: Geological Association of Canada, Mineral Deposits Division, Special Publication 5, p.533–552.
- Gibson, H.L., and Kerr, D.J., 1993, Giant volcanic-associated massive sulphide deposits, with emphasis on Archean examples: *Society of Economic Geologists Special Publication* 2, p. 319–348.
- Gibson, H.L., Morton, R.L., and Hudak, G.J., 1999, Submarine volcanic processes, deposits and environments favorable for the location of volcanic-associated massive sulfide deposits: *Reviews in Economic Geology*, v. 8, p.13–51.
- Gifkins, C.C., and Allen, R.L., 2001, Textural and chemical characteristics of diagenetic and hydrothermal alteration in glassy volcanic rocks—Examples from the Mount Read volcanics: *Economic Geology*, v. 96, p. 13–51.
- Goodfellow, W.D., and McCutcheon, S.R., 2003, Geologic and genetic attributes of volcanic sediment-hosted massive sulfide deposits of the Bathurst Mining Camp, New Brunswick—A synthesis, in Goodfellow, W.D., McCutcheon, S.R., and Peter, J.M., eds., *Massive sulfide deposits of the Bathurst mining camp, New Brunswick, and northern Maine*: *Economic Geology Monograph* 11, p. 245–301.
- Goodfellow, W.D., McCutcheon, S.R., and Peter, J.M., 2003, Introduction and summary of findings, in Goodfellow, W.D., McCutcheon, S.R., and Peter, J.M., eds., *Massive sulfide deposits of the Bathurst mining camp, New Brunswick, and northern Maine*: *Economic Geology Monograph* 11, p. 1–16.
- Hannington, M.D., Bleeker, W., and Kjarsgaard, I., 1999, Sulfide mineralogy, geochemistry, and ore genesis of the Kidd Creek deposit—Part I. North, central, and south orebodies, in Hannington, M.D., and Barrie, C.T., eds., *The giant Kidd Creek volcanogenic massive sulfide deposit, western Abitibi subprovince, Canada*: *Economic Geology Monograph* 10, p. 163–224.
- Jonasson, I.R., Franklin, J.M., and Hannington, M.D., 1990, Massive sulphide deposits of Axial Seamount, Juan de Fuca Ridge [abs.], in IAGOD symposium, 8th, Ottawa, Canada, 12–18 August 1990, Program with abstracts: Ottawa, International Association on the Genesis of Ore Deposits and Geological Survey of Canada, p. A62.
- Kappel, E.S., and Franklin, J.M., 1989, Relationships between geologic development of ridge crests and sulfide deposits in the northeast Pacific Ocean: *Economic Geology*, v. 84, p. 485–505.
- Koski, R.A., 1990, A comparison of sulfide deposits from modern sediment-covered spreading axes with Besshi-type deposits of Japan, in McMurray, G.R., ed., *Gorda Ridge—A seafloor spreading center in the United States Exclusive Economic Zone*: New York, Springer-Verlag, p.117–130.
- Large, R.R., and Both, R.A., 1980, The volcanogenic sulfide ores at Mount Chalmers, eastern Queensland: *Economic Geology*, v. 75, p. 992–1009.
- Lentz, D.R., 1998, Petrogenetic evolution of felsic volcanic sequences associated with Phanerozoic volcanic-hosted massive sulfide systems—The role of extensional geodynamics: *Ore Geology Reviews*, v. 12, p. 289–327.
- Mariko, T., 1988, Volcanogenic massive sulphide deposits of Besshi type at the Shimokawa mine, Hokkaido, northern Japan, in Zachrisson, E., ed., *Seventh quadrennial IAGOD symposium, Lulea, Sweden, 18–22 August 1986, Proceedings: International Association on the Genesis of Ore Deposits, Stuttgart, Germany, E. Schweizerbart'sche Verlagsbuchhandlung*, p. 501–512.

- Morton, R.L., and Franklin, J.M., 1987, Two-fold classification of Archean volcanic-associated massive sulfide deposits: *Economic Geology*, v. 82, p. 1057–1063.
- Murphy, D.C., Mortensen, J.K., Piercey, S.J., Orchard, M.J., and Gehrels, G.E., 2006, Mid-Paleozoic to early Mesozoic tectonostratigraphic evolution of Yukon-Tanana and Slide Mountain terranes and affiliated overlap assemblages, Finlayson Lake massive sulphide district, southeastern Yukon, in Colpron, M. and Nelson, J.L., eds., *Paleozoic evolution and metallogeny of pericratonic terranes at the ancient Pacific margin of North America, Canadian and Alaskan Cordillera*: Geological Association of Canada, Special Paper 45, p. 75–105.
- Ohmoto, H., and Takahashi, T., 1983, Geological setting of the Kuroko deposits, Japan—Part III. Submarine calderas and Kuroko genesis, in Ohmoto, H., and Skinner, B.J., eds., *The Kuroko and related volcanogenic massive sulfide deposits*: *Economic Geology Monograph* 5, p. 39–54.
- Peter, J.M., and Scott, S.D., 1999, Windy Craggy, northwestern British Columbia—The world's largest Besshi-type deposit, in Barrie, C.T., and Hannington, M.D., eds., *Volcanic-associated massive sulfide deposits—Processes and examples in modern and ancient settings*: *Reviews in Economic Geology*, v. 8, p. 261–295.
- Peter, J.M., Layton-Matthews, D., Piercey, S., Bradshaw, G., Paradis, S., and Boulton, A., 2007, Volcanic-hosted massive sulphide deposits of the Finlayson Lake district, Yukon, in Goodfellow, W.D., ed., *Mineral deposits of Canada—A synthesis of major deposit types, district metallogeny, the evolution of geological provinces, and exploration methods*: Geological Association of Canada Special Publication 5, p. 471–508.
- Pickering, K.T., Hiscott, R.N., and Hein, F.J., 1989, *Deep marine environments*: London, Unwin, Hyman, 416 p.
- Piercey, S.J., 2009, Lithogeochemistry of volcanic rocks associated with volcanogenic massive sulphide deposits and applications to exploration, in Cousens, B., and Piercey, S.J., eds., *Submarine volcanism and mineralization—Modern through ancient*: Geological Association of Canada, Short Course Notes, v. 19, p. 15–40.
- Piercey, S.J., Paradis, S., Murphy, D.C., and Mortensen, J.K., 2001, Geochemistry and paleotectonic setting of felsic volcanic rocks in the Finlayson Lake volcanic-hosted massive sulfide district, Yukon, Canada: *Economic Geology*, v. 96, p. 1877–1905.
- Pottorf, R.J., and Barnes, H.L., 1983, Mineralogy, geochemistry, and ore genesis of hydrothermal sediments from the Atlantis II Deep, Red Sea, in Ohmoto, H., and Skinner, B.J., eds., *The Kuroko and related volcanogenic massive sulfide deposits*: *Economic Geology Monograph* 5, p. 198–223.
- Sainty, R.A., 1992, Shallow-water stratigraphy at the Mount Chalmers volcanic-hosted massive sulfide deposit, Queensland, Australia: *Economic Geology*, v. 87, p. 812–824.
- Seewald, J.S., Seyfried, W.E., Jr., and Shanks, W.C., III, 1994, Variations in the chemical and stable isotope composition of carbon and sulfur species during organic-rich sediment alteration—An experimental and theoretical study of hydrothermal activity at Guaymas Basin, Gulf of California: *Geochimica et Cosmochimica Acta*, v. 58, p. 5065–5082.
- Shanks, W.C., III, and Bischoff, J.L., 1980, Geochemistry, sulfur isotope composition, and accumulation rates of Red Sea geothermal deposits: *Economic Geology*, v. 75, p. 445–459.
- Slack, J.F., 1993, Descriptive and grade-tonnage models for Besshi-type massive sulphide deposits, in Kirkham, R.V., Sinclair, W.D., Thorpe, R.I., and Duke, J.M., eds., *Mineral deposit modeling*: Geological Association of Canada Special Paper 40, p. 343–371.
- Tornos, F., 2006, Environment of formation and styles of volcanogenic massive sulfides—The Iberian Pyrite Belt: *Ore Geology Reviews*, v. 28, p. 259–307.
- van Staal, C.R., Wilson, R.A., Rogers, N., Fyffe, L.R., Langton, J.P., McCutcheon, S.R., McNicoll, V., and Ravenhurst, C.E., 2003, Geology and tectonic history of the Bathurst Supergroup, Bathurst mining camp, and its relationships to coeval rocks in southwestern New Brunswick and adjacent Maine—A synthesis, in Goodfellow, W.D., McCutcheon, S.R., and Peter, J.M., eds., *Massive sulfide deposits of the Bathurst mining camp, New Brunswick, and northern Maine*: *Economic Geology Monograph* 11, p. 37–60.
- Wellmer, F.-W., Berner, U., Hufnagel, H., and Wehner, H., 1999, Carbon isotope geochemistry of Archean carbonate horizons in the Timmins area, in Hannington, M.D., and Barrie, C.T., eds., *The giant Kidd Creek volcanogenic massive sulfide deposit, western Abitibi subprovince, Canada*: *Economic Geology Monograph* 10, p. 441–456.

17. Petrology of Metamorphic Rocks Associated with Volcanogenic Massive Sulfide Deposits

By Cynthia Dusel-Bacon

17 of 21

Volcanogenic Massive Sulfide Occurrence Model

Scientific Investigations Report 2010–5070–C

**U.S. Department of the Interior
U.S. Geological Survey**

U.S. Department of the Interior
KEN SALAZAR, Secretary

U.S. Geological Survey
Marcia K. McNutt, Director

U.S. Geological Survey, Reston, Virginia: 2012

For more information on the USGS—the Federal source for science about the Earth, its natural and living resources, natural hazards, and the environment, visit <http://www.usgs.gov> or call 1-888-ASK-USGS.

For an overview of USGS information products, including maps, imagery, and publications, visit <http://www.usgs.gov/pubprod>

To order this and other USGS information products, visit <http://store.usgs.gov>

Any use of trade, product, or firm names is for descriptive purposes only and does not imply endorsement by the U.S. Government.

Although this report is in the public domain, permission must be secured from the individual copyright owners to reproduce any copyrighted materials contained within this report.

Suggested citation:

Dusel-Bacon, Cynthia, 2012, Petrology of metamorphic rocks associated with volcanogenic massive sulfide deposits in volcanogenic massive sulfide occurrence model: U.S. Geological Survey Scientific Investigations Report 2010-5070 -C, chap. 17, 10 p.

Contents

| | |
|---|-----|
| Importance of Metamorphic Rocks to Deposit Genesis | 279 |
| Rock Names..... | 281 |
| Mineralogy and Mineral Assemblages | 281 |
| Deformation and Textures | 284 |
| Grain Size | 284 |
| Examples of Information Gained from Study of Metamorphic Rocks Associated with Volcanogenic Massive Sulfide Deposits | 285 |
| References Cited..... | 285 |

Figure

- 17-1. Pressure/temperature diagram showing the principal eight metamorphic facies; the Al_2SiO_5 polymorphs kyanite, andalusite, and sillimanite and the three major types of pressure/temperature facies series.....281

Tables

- 17-1. Characteristic minerals for principal rock composition types in the various metamorphic facies.....280
- 17-2. Diagnostic mineralogy and major-element geochemistry of greenschist- and granulite-grade metamorphosed alteration products associated with volcanogenic massive sulfide deposits
- 282

17. Petrology of Metamorphic Rocks Associated with Volcanogenic Massive Sulfide Deposits

By Cynthia Dusel-Bacon

Importance of Metamorphic Rocks to Deposit Genesis

Metamorphic rocks associated with VMS deposits are described in terms of their metamorphic rock names, metamorphic mineral assemblages, and metamorphic facies. A succinct definition of a metamorphic facies, provided by Turner (1981, p. 54), states it to be “a set of metamorphic mineral assemblages, repeatedly associated in space and time, such that there is a constant and therefore predictable relation between mineral composition and bulk rock chemical composition.” Table 17–1 shows relationships among the various metamorphic facies and characteristic metamorphic mineral assemblages that develop in four principal bulk compositions during conditions of a given metamorphic facies. Locations of the most common metamorphic facies in pressure (P) and temperature (T) space are shown in figure 17–1.

The majority of ancient VMS deposits have been affected by regional metamorphism and deformation. Analysis of metamorphic grades reported by Mosier and others (2009) for 1,090 VMS deposits from throughout the world indicates that of the 819 deposits for which data were available, only 3 percent were reported as being unmetamorphosed. The rest were metamorphosed under the conditions of the following metamorphic facies (in decreasing frequency of occurrence): 62 percent greenschist facies; 13 percent contact metamorphism; 11 percent amphibolite facies; 7 percent sub-greenschist, prehnite-pumpellyite, or pumpellyite-actinolite facies; 2 percent blueschist- or eclogite-facies; 1.5 percent zeolite facies; and 0.5 percent granulite facies.

Coarse-grained suites of distinctive, upper greenschist- to amphibolite-facies minerals, including chloritoid, garnet, staurolite, kyanite, andalusite, phlogopite, and gahnite (zincian spinel), and upper amphibolite- to granulite-facies minerals such as sillimanite, cordierite, orthopyroxene, and orthoamphibole can define VMS hydrothermal alteration zones (for example, Morton and Franklin, 1987; Bonnet and Corriveau, 2007, and references therein). Aluminous minerals (garnet, chloritoid, staurolite, or the Al_2SiO_5 polymorphs kyanite, andalusite, and sillimanite) commonly occur close to high-temperature alteration pipes (Carpenter and Allard, 1982;

Sillitoe and others, 1996; Galley and others, 2007), reflecting residual enrichment of alumina during premetamorphic hydrothermal leaching of alkalis under high fluid/rock conditions. Using visual identification of distinctive metamorphic minerals and their modal abundances, and determining the unaltered composition of the precursor rock, alteration vectors can be constructed on major-element ternary diagrams that identify the configuration of the fossil hydrothermal alteration zones in VMS systems (Bonnet and Corriveau, 2007). Immobile major and trace-element whole-rock data can indicate whether the aluminous metamorphic minerals resulted from premetamorphic seafloor alteration/metasomatism of the protolith or from primary protolith composition (for example, Barrett and MacLean, 1999). The mineral chemistry of some alteration-associated metamorphic minerals, such as the Fe/Zn ratio of staurolite, also can serve as a vector to ore (Spry and Scott, 1986a). Because many of these metamorphic minerals are refractory during sedimentation, they have the potential to occur in heavy mineral separates collected in till-covered areas and, consequently, are valuable exploration aids for VMS districts (for example, Averill, 2001).

Estimation of pressure and temperature (P/T) conditions calculated from silicate, carbonate, and sulfide mineral assemblages in a given deposit can help determine the relationship between base-metal mineralization and metamorphism, specifically whether metamorphism pre- or postdated ore genesis. The pyrrhotite (sphalerite-pyrite) thermometer of Froese and Berman (1994) has been used by some workers to estimate peak metamorphic temperatures of sulfide assemblages, but Currie and others (2003) found that their results using this thermometer were unsatisfactory and speculated that partial inversion of pyrrhotite from hexagonal to monoclinic form had disturbed the distribution of FeS. The sphalerite geothermometer, based on the FeS content of sphalerite coexisting with pyrite and pyrrhotite, was used in the 1950s through the 1970s, but it is not reliable. However, the FeS content of sphalerite in pyrrhotite-sphalerite-pyrite assemblages can be useful for constraining pressure during metamorphism, with the caveat that care must be taken in order to characterize sphalerite paragenesis and identify sphalerite compositions that record peak metamorphic conditions and not later retrograde effects (Toulmin and others, 1991).

Table 17–1. Characteristic minerals for principal rock composition types in the various metamorphic facies. Modified from Blatt and others (2006).

[Al, aluminum; Ca, calcium; Mg, magnesium]

| Facies | Mafic rocks | Ultramafic rocks | Pelitic rocks | Calcareous rocks |
|----------------------|---|--|---|---|
| Zeolite | Analcime, Ca-zeolites, zoisite, albite | Serpentine, brucite, chlorite, dolomite, magnesite | Quartz, clays, illite, albite, chlorite | Calcite, dolomite, quartz, talc, clays |
| Prehnite-pumpellyite | Chlorite, prehnite, albite, pumpellyite, epidote | Serpentine, talc, forsterite, tremolite, chlorite | Quartz, illite, muscovite, albite, chlorite, stilp-nomelane | Calcite, dolomite, quartz, clays, talc, muscovite |
| Greenschist | Chlorite, actinolite, epidote or zoisite, albite | Serpentine, talc, tremolite, brucite, diopside, chlorite, magnetite | Quartz, plagioclase, chlorite, muscovite, biotite, garnet, pyrophyllite, graphite | Calcite, dolomite, quartz, muscovite, biotite |
| Epidote-amphibolite | Hornblende, actinolite, epidote or zoisite, plagioclase, sphene | Forsterite, tremolite, talc, serpentine, chlorite, magnetite | Quartz, plagioclase, chlorite, muscovite, biotite, graphite | Calcite, dolomite, quartz, muscovite, biotite, tremolite |
| Amphibolite | Hornblende, plagioclase, sphene, ilmenite | Forsterite, tremolite, talc, anthophyllite, chlorite, orthopyroxene, magnetite | Quartz, plagioclase, chlorite, muscovite, biotite, garnet, staurolite, kyanite, sillimanite, andalusite, graphite, ilmenite | Calcite, dolomite, quartz, biotite, tremolite, forsterite, diopside, plagioclase |
| Granulite | Hornblende, augite, orthopyroxene, plagioclase, ilmenite | Forsterite, orthopyroxene, augite, hornblende, garnet, Al-spinel | Quartz, plagioclase, orthoclase, biotite, garnet, cordierite, sillimanite, orthopyroxene | Calcite, quartz, forsterite, diopside, wollastonite, humite-chondrodite, Ca-garnet, plagioclase |
| Blueschist | Glaucophane, lawsonite, albite, aragonite, chlorite, zoisite | Forsterite, serpentine, diopside | Quartz, plagioclase, muscovite, carpholite, talc, kyanite, chloritoid | Calcite, aragonite, quartz, forsterite, diopside, tremolite |
| Eclogite | Mg-rich garnet, omphacite, kyanite, rutile | Forsterite, orthopyroxene, augite, garnet | Quartz, albite, phengite, talc, kyanite, garnet | Calcite, aragonite, quartz, forsterite, diopside |
| Albite-epidote | Albite, quartz, tremolite, actinolite, chlorite | Serpentine, talc, epidote or zoisite, chlorite | Quartz, plagioclase, tremolite, cordierite | Calcite, dolomite, epidote, muscovite, chlorite, talc, forsterite |
| Hornblende hornfels | Hornblende, plagioclase, orthopyroxene, garnet | Forsterite, orthopyroxene, hornblende, chlorite, Al spinel, magnetite | Quartz, plagioclase, muscovite, biotite, cordierite, andalusite | Calcite, dolomite, quartz, tremolite, diopside, forsterite |
| Pyroxene hornfels | Orthopyroxene, augite, plagioclase, garnet | Forsterite, orthopyroxene, augite, plagioclase, Al-spinel | Quartz, plagioclase, orthoclase, andalusite, sillimanite, cordierite, orthopyroxene | Calcite, quartz, diopside, forsterite, wollastonite |
| Sanidinite | Orthopyroxene, augite, plagioclase, garnet | Forsterite, orthopyroxene, augite, plagioclase | Quartz, plagioclase, sillimanite, cordierite, orthopyroxene, sapphirine, Al-spinel | Calcite, quartz, diopside, forsterite, wollastonite, monticellite, akermanite |

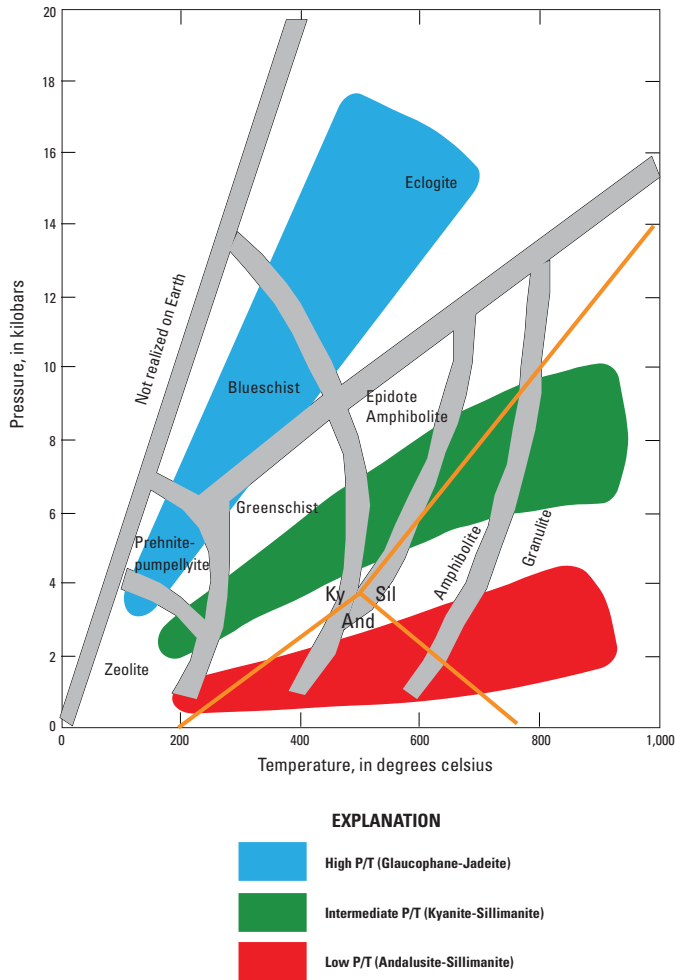


Figure 17-1. Pressure/temperature diagram showing the principal eight metamorphic facies; the Al_2SiO_5 polymorphs kyanite (Ky), andalusite (And), and sillimanite (Sil) (after Holdaway, 1971); and the three major types of pressure/temperature facies series (after Spear, 1993).

Another important piece of information that can be gleaned from the study of metamorphic rocks associated with VMS deposits is the identification of metamorphic protoliths (parent rock types). In many instances, it is difficult to see through the metamorphic overprint of the deposits and host rocks, but knowledge of the protolith assemblages is essential to reconstruction of the lithologic association at the time of mineralization and, in turn, the tectonic setting of the deposit. Trace elements and rare earth elements (REE) known to be immobile during low- to moderate-grade metamorphism (below upper amphibolite- to granulite-facies conditions) include Nb, Ta, Zr, Ti, Cr, and Y. These immobile elements are especially useful for identifying the magmatic compositions of metamorphosed igneous rocks associated with VMS deposits and for providing important information on the heat flow and tectonic environment of VMS formation (see Lentz, 1998;

Barrett and MacLean, 1999; Piercey and others, 2001; Piercey, 2009).

Finally, exploration of VMS ores within regionally metamorphosed and deformed sequences can be financially advantageous for the following reasons: (1) metamorphic recrystallization and concomitant increase in grain size and purity of the sulfide minerals (and in some cases nonmetallic minerals, such as kyanite within alteration zones) make their liberation and concentration easier and less costly; (2) ores typically are thicker in the hinge zones of folds, thus facilitating mining methods; and (3) selective mobilization during metamorphism can result in local enrichment of metal grades (Vokes, 1969, 2000; Marshall and others, 2000; Gauthier and Chartrand, 2005).

Rock Names

Depending on metamorphic grade, common rock types associated with VMS deposits that were derived by the metamorphism of mafic rocks are greenschist (chlorite-rich schist), greenstone, metagabbro, metadiabase, and amphibolite. Rocks derived by the metamorphism of sedimentary rocks include argillite, slate, phyllite, quartz-mica schist, metagraywacke, metaconglomerate, quartzite, limestone, marble, and calc-silicate. Quartzofeldspathic or mafic gneiss can be derived from either sedimentary or igneous protoliths.

Wall rocks (host rocks) typically associated with siliciclastic-mafic-type VMS deposits contain the most distinctive lithologies, which may include metachert, magnetite iron-formation, sericite- and chlorite-rich schist, cotecule (fine-grained quartz-spessartine rock), tourmalinite, albitite, and rarely marble. Chlorite- and muscovite-rich rocks, albitite, and magnetite iron-formation commonly form stratabound lenses or envelopes around the massive sulfide ores and can extend to as much as 10 m into the adjacent country rock. Thin, stratiform layers of cotecule, tourmalinite, and metachert can extend for some distance into the stratigraphic hanging wall or laterally for hundreds of meters beyond the massive sulfide deposits (Slack, 1993). Characteristic country rock associated with, but spatially more distal to, the siliciclastic-mafic type massive sulfide deposits and their adjacent wall rocks typically include pelitic schist, metagraywacke, and greenstone or amphibolite, depending on the degree of postore metamorphism.

Mineralogy and Mineral Assemblages

Many of the mineral assemblages that developed during seafloor hydrothermal alteration associated with the formation of VMS deposits are similar to those that may form during postore, regional, low-grade (zeolite, prehnite-pumpellyite, and greenschist facies) metamorphism (Franklin and others, 2005). Syngenetic alteration zones are generally semiconformable to the deposits and can extend up to tens of kilometers along strike and below the paleoseafloor to the depths of

subvolcanic intrusions. Semiconformable alteration has been documented in bimodal-mafic successions (for example, Noranda: Gibson and others, 1983), mafic-ultramafic dominated successions (for example, Oman: Koski and others, 2003), and bimodal-felsic successions (for example, Kuroko: Ohmoto and others, 1983) but is poorly documented in felsic-siliciclastic- and siliciclastic-mafic successions (Franklin and others, 2005). Metamorphic minerals developed at low metamorphic grades include chlorite, quartz, epidote, zoisite, clinozoisite, sericite, albite, titanite, and carbonate, depending on protolith composition. In addition to these common, low-temperature minerals, zeolite minerals (for example, analcime, laumontite, celadonite, and heulandite) typically form in the cavities or vesicles of volcanic rocks at zeolite-facies metamorphic grade, generally at temperatures less than about 250 °C. Prehnite-pumpellyite facies conditions are transitional between those of the lower grade zeolite facies and the higher grade greenschist facies and generally occur in temperature and pressure ranges of about 250–350 °C and 2–7 kbar, respectively. Characteristic mineral assemblages of the prehnite-pumpellyite facies that developed in mafic and ultramafic igneous rocks and in pelitic (mud-rich) and calcareous sedimentary rocks are shown in table 17–1.

The distribution of the mineralogical and geochemical characteristics of the low-grade assemblages can be used to identify large-scale, zoned hydrothermal alteration systems around VMS deposits and to differentiate them from superimposed, low-grade, postore regional metamorphic assemblages. Typically, broad zones of semiconformable alteration will show increases in Ca-Si (epidotization-silicification), Ca-Si-Fe (actinolite-clinozoisite-magnetite), Na (spilitization), or K-Mg (mixed chlorite-sericite ± K-feldspar) (Galley and others, 2007). In a simple system, alteration assemblages

are distributed with depth from near-surface diagenetic and zeolite assemblages to a spilitic greenschist-facies assemblage, and eventually to an epidote-quartz assemblage. However, in a long-lived, convective hydrothermal system, overprinting of alteration assemblages during progressive alteration and burial occurs (Franklin and others, 2005), complicating the interpretation of alteration or metamorphic textures. Regardless of these complexities, the distribution and relationship of chlorite-rich schists and sericite-rich schists in the wall rocks to VMS deposits can indicate the presence of primary alteration zones that developed during submarine mineralization. For example, Slater and others (1985) suggested that chlorite schists in the Ducktown VMS deposits were metamorphosed chloritic feeder pipes in the footwall to the deposits, and that the sericite-rich schists formed by the metamorphism of alteration zones analogous to those that are common in the hanging wall of Kuroko deposits. Identification of alteration zoning patterns can be difficult, however, given that the alteration pipes may extend beyond the ore deposit and merge laterally and (or) vertically with semiconformable alteration zones, and that the metamorphosed feeder pipes and semiconformable alteration zones can include similar metamorphic mineral assemblages (Franklin, 1984; Morton and Franklin, 1987.) Chloritoid- and staurolite-bearing assemblages can result from greenschist- to amphibolite-facies metamorphism of Al-Fe-Mg-rich alteration pipes or semiconformable alteration zones (Morton and Franklin, 1987; Spear, 1993).

Fossil hydrothermal zones are also recognizable by diagnostic mineral assemblages developed in VMS districts that have been metamorphosed under upper amphibolite- and granulite-facies conditions (Morton and Franklin, 1987; Bonnet and Corriveau, 2007). Diagnostic greenschist- and granulite-facies mineral assemblages developed in different

Table 17–2. Diagnostic mineralogy and major-element geochemistry of greenschist- and granulite-grade metamorphosed alteration products associated with volcanogenic massive sulfide deposits. From Bonnet and Corriveau (2007).

| Alteration type | Diagnostic minerals: greenschist facies | Diagnostic minerals: granulite facies | Diagnostic composition | Similar rocks (at granulite facies) |
|----------------------|---|---|---|--|
| Advanced argillic | Kaolinite, pyrophyllite, andalusite, corundum, topaz | Sillimanite, kyanite, quartz | Al ₂ O ₃ , SiO ₂ | Laterite |
| Argillic | Sericite, illite, pyrophyllite | Sillimanite, kyanite, quartz, biotite, cordierite, garnet | Al ₂ O ₃ , SiO ₂ , K ₂ O, Fe ₂ O ₃ , MgO | Pelite |
| Sericitic | Sericite, illite, quartz | Biotite, K-feldspar, sillimanite, kyanite, quartz, cordierite, garnet | K ₂ O, Al ₂ O ₃ , Fe ₂ O ₃ , ± MgO, ± SiO ₂ | Pelite |
| Chloritic | Chlorite, quartz, sericite | Cordierite, orthopyroxene, orthoamphibole, phlogopite, sillimanite, kyanite | Fe ₂ O ₃ , MgO, ± Al ₂ O ₃ , ± SiO ₂ | Pelite |
| Carbonate propylitic | Carbonate (Fe, Mg), epidote, chlorite, sericite, feldspar | Carbonate, grossular, epidote, hornblende, diopside, orthopyroxene | Fe ₂ O ₃ , CaO | Calc-silicate rock of sedimentary origin, marble or mafic rock |

[Fe, iron; Mg, magnesium]

hydrothermal alteration types, as well as in unaltered protoliths, are given in table 17–2. Bonnet and Corriveau (2007) caution that recognition of sericitic, argillic, and advanced argillic hydrothermal alteration zones in granulite-facies gneissic terranes is severely hampered by the resemblance of their metamorphic mineral assemblages to those developed in unmineralized sedimentary rocks and paleosoils that were metamorphosed under granulite-facies conditions (table 17–2); they accordingly recommend that identification of VMS-type hydrothermal alteration be based not only on distinctive metamorphic mineral assemblages, but also on field observations of relict primary volcanic structures and textures and field indicators of hydrothermal activity, such as the presence of meta-exhalites, stockworks, or sulfide mineralization. Recognition of metamorphosed chlorite in footwall alteration pipes is more straightforward and it is commonly expressed as cordierite, orthopyroxene, and orthoamphibole (anthophyllite or gedrite) in the inner alteration zone, where the chlorite may be more Mg-rich, and by talc, phlogopite, or one of the Al_2SiO_5 polymorphs, in the outer, locally Fe-rich chlorite alteration zone (Morton and Franklin, 1987; Bonnet and Corriveau, 2007).

Most of the upper amphibolite- and granulite-facies, polydeformed alteration systems have been identified in Proterozoic and Archean gneissic terranes (Morton and Franklin, 1987; Roberts and others, 2003; Bonnet and Corriveau, 2007). The Archean Geco deposit, a bimodal-mafic-type VMS deposit in the Superior province in Canada, is an example of a polydeformed, upper amphibolite-facies deposit in which syngenetic hydrothermal alteration is indicated by zones of abundant sillimanite, anthophyllite, garnet, and cordierite. All of the volcanic rocks in the Geco deposit are metamorphosed to schist and gneiss, and felsic metavolcanic rocks that host the ore consist predominantly of muscovite + quartz \pm sillimanite schist, interpreted as metamorphosed sericitic alteration zones (Friesen and others, 1982; Zaleski and Peterson, 1995). In addition to the development of Al-, Fe-, and Mg-rich assemblages during the metamorphism of alteration zones, plagioclase-rich rocks associated with some of the orebodies in the siliciclastic-mafic-type Ducktown and Gossan Lead VMS districts have been interpreted as metamorphosed sodic alteration zones (Nesbitt, 1979; Gair and Slack, 1984). Mapping of the intensity and distribution of anthophyllite, cordierite, sillimanite, garnet, quartz, muscovite, and staurolite also led to identification of footwall alteration zones and the discovery of the bimodal-mafic Archean Winston Lake deposit, Ontario (Severin and others, 1984; Morton and Franklin, 1987; Thomas, 1991; Bonnet and Corriveau, 2007).

Metamorphic mineral assemblages indicate not only relict VMS-type hydrothermal systems and T and P conditions during metamorphism, but also the thermal gradient and, hence, the crustal environment in which metamorphism occurred (fig. 17–1). A low geothermal gradient characterizes metamorphism in subduction zones with high-pressure, blueschist-facies metamorphism (glaucophane + lawsonite or epidote + albite \pm chlorite) at low temperatures, and eclogite-facies

metamorphism (garnet + omphacitic pyroxene) at high temperatures. Glaucophane-bearing, blueschist-facies assemblages have overprinted the Devonian-Mississippian Arctic deposit in northern Alaska (Hitzman and others, 1986) and the Jurassic–Lower Cretaceous VMS deposits in Cuba (Russell and others, 2000). An example of the high-temperature end of this high-pressure facies series is the amphibolite- to eclogite-facies metamorphism that overprinted the Paleoproterozoic rocks of the Sylarna deposit in Sweden (Grenne and others, 1999).

An intermediate geothermal gradient characterizes metamorphism in continental collisions and orogenic belts (fig. 17–1). Barrovian metamorphic zones, formed under these conditions, are defined by the sequential appearance in pelitic rocks, with increasing metamorphic grade, of chlorite, biotite, garnet, staurolite, kyanite, sillimanite, and sillimanite + K-feldspar. The Ducktown mining district, Tennessee, a siliciclastic-mafic-type VMS deposit in the Blue Ridge metamorphic province, was metamorphosed under greenschist- to amphibolite-facies conditions in a Barrovian metamorphic series. The known sulfide deposits of this district are restricted to the staurolite-kyanite zones (Nesbitt and Essene, 1982; Slater and others, 1985). Metamorphism occurred during the Taconic (450–480 Ma) orogeny and conditions ranged from chlorite grade in the west to staurolite (-kyanite) grade in the east (Slater and others, 1985). Pyrrhotite, the dominant sulfide, is present as stringers parallel to metamorphic cleavages and appears to have formed from pyrite during regional metamorphism; coarse euhedral pyrite porphyroblasts as much as 30 cm in diameter within the pyrrhotitic ore reflect prolonged growth during metamorphism (Brooker and others, 1987). Textural features and variations of sulfides present in the country rocks with increasing metamorphic grade have been interpreted to record significant remobilization of the sulfide constituents during regional metamorphism (Runyon and Misra, 1981; Slater and others, 1985). The bimodal-mafic, Archaean Izok Lake deposit in Northwest Territories, Canada, is an example of a deposit metamorphosed under granulite-facies conditions—the high-temperature end of an intermediate thermal gradient (Franklin and others, 2005).

A steep geothermal gradient characterizes metamorphism in island arcs, ocean ridges, and contact aureoles (fig. 17–1). Characteristic minerals formed in pelitic rocks in this low P/T setting define Buchan metamorphic zones in which biotite \rightarrow cordierite \rightarrow andalusite \rightarrow sillimanite. Synmetamorphic intrusions, including those in extensional settings, are commonly heat sources for Buchan-type metamorphism. More localized metamorphism in the vicinity of an igneous intrusion can result in a contact aureole of mineral zones around the heat source; minerals developed during contact metamorphism (hornfels) may include the same minerals that formed during regional Buchan metamorphism but, depending on the degree of synplutonic deformation, contact metamorphic minerals may be texturally distinct in lacking a preferred orientation. However, the division between Buchan and contact metamorphism is artificial in some settings, such as in Maine, where

metamorphic isograds are subparallel to the margins of plutons and metamorphism is best described as regional contact metamorphism (for example, Guidotti, 1989). Mosier and others (2009) list numerous deposits in Kazakhstan (for example, Kusmurun), Uzbekistan (for example, Kuldara), and China (for example, Bieluwutu) that experienced postore recrystallization during contact metamorphism.

In addition to deciphering thermal conditions from metamorphic minerals in host rocks, certain sulfide minerals preferentially recrystallize with increasing metamorphic grade. For example, zincian spinel ($(\text{Zn,Fe,Mg})\text{Al}_2\text{O}_4$) can form from either metamorphism of Zn-oxide phases, desulfidation of sphalerite, or the breakdown of Zn-bearing silicates such as staurolite (Heimann and others, 2005, and references therein); pyrrhotite (Fe_{1-x}S) can form from higher temperature recrystallization of pyrite (FeS_2). The composition of zincian spinel has been shown to be an effective exploration guide to metamorphosed massive sulfide deposits (Spry and Scott, 1986b; Heimann and others, 2005). However, Heimann and others (2005) demonstrated that the composition of the host rocks and the alteration types present in a given deposit should be considered when choosing the spinel compositions to be used as an exploration guide, especially where the rocks are magnesian.

Deformation and Textures

Basaltic rocks affected by low-grade, seafloor metamorphism generally preserve relict igneous textures, whereas those recrystallized during subsequent regional dynamothermal metamorphism show variable degrees of mineral alignment into planar fabrics. In sedimentary rocks, it may be difficult to differentiate between primary soft sediment deformation on the seafloor and postore regional deformation and folding. The presence of brittle deformational features in a deposit is one indication of postore chilling of the hydrothermal system prior to deformation and, consequently, would argue against deformation being synchronous with deposition of the VMS deposit. Textures, such as aluminous nodules in high-grade quartzofeldspathic gneiss and lapilli or larger block fragments in associated aluminous gneiss adjacent to clearly recognizable metamorphosed lapillistone units with similar sized fragments, are fairly reliable evidence of prior VMS-type hydrothermal alteration (Bonnet and Corriveau, 2007). Detailed thermochronology of the igneous crystallization ages of metaigneous host rocks associated with VMS deposits is required in order to differentiate between host rocks to VMS submarine mineralization and tectonically-juxtaposed lithologies that originated distant from the site of mineralization. Determination of metamorphic cooling ages for various host rock minerals that have a range of blocking temperatures also plays a crucial role in constraining the postore thermal and deformational history of VMS deposits.

Most VMS districts have been affected by fold-and-thrust-belt style deformation because the mineral belts formed in short-lived extensional basins near plate margins, which became inverted and deformed during subsequent basin closure (Allen and others, 2002; Tornos and others, 2002). Examples of folded, faulted, and sheared VMS deposits are given in the section of this report covering physical descriptions of the deposits. As mentioned above, one result of folding, which has the potential to be of great significance for mining operations, is that an originally relatively thin layer of ore can be thickened to economically viable dimensions. The most common explanation for thickening of the sulfide mass is flow of sulfides into fold hinges during deformation. However, some workers have pointed out the controlling effect that could be exerted on fold localization by a mass of sulfides already present in the rocks being deformed (Vokes, 2000).

A discussion of the deformational and metamorphic fabrics and textures developed in sulfide assemblages present in VMS deposits is beyond the scope and focus of this chapter, but excellent overviews are given in numerous publications (for example, Stanton, 1960; Craig and Vokes, 1993; Vokes, 1969, 2000; Marshall and Gilligan, 1993; Marshall and others, 2000).

Grain Size

The grain size of metamorphic rocks associated with VMS deposits generally increases with metamorphic grade and also is dependent on the metamorphic protolith. Likewise, the grain size of associated sulfides in a deposit varies as a function of the primary mineralogy and the extent of metamorphic recrystallization. Primary sulfide minerals of most Zn-Pb-Cu deposits are fine grained and intergrown, whereas those of the majority of Cu-Zn deposits are generally coarser grained (Franklin, 1993). The form and grain size that sulfide minerals take during metamorphic recrystallization depends on the pressure and temperature conditions during metamorphism, the nature of the fluid phase, and the deformational properties of the minerals (for example, Stanton, 1960; Craig and Vokes, 1993). In general, progressive regional metamorphism appears to cause an increase in the grain size of sulfide ores, provided deformation has not been too intense (Vokes, 1969). Very coarse (3–7 cm diameter) garnets are present in a distinctive schist unit at the Elizabeth mine, Vermont. Although the garnets formed as a result of heat supplied during the postore, regional Acadian (Early Devonian) metamorphism, the bulk composition required to produce them came about as a result of pre-Acadian seafloor metasomatism (Slack, 1999; Slack and others, 2001). Large hornblende crystals, as much as 10 cm long, also are present at the Elizabeth mine (Slack and others, 2001).

Examples of Information Gained from Study of Metamorphic Rocks Associated with Volcanogenic Massive Sulfide Deposits

In their study of the siliciclastic-mafic type massive sulfide deposits of the Vermont Copper Belt, Slack and others (2001) obtained major, minor, and trace-element geochemical data for mineralogically unusual amphibolite-facies wall rocks located within 80 m of the Elizabeth mine orebodies and compared those data to compositions of unaltered metasedimentary and metabasaltic (amphibolite) wall rocks in the district. Bulk-rock contents of immobile elements indicated an exhalative origin for cotecite, metachert, and iron-formation. Geochemical data for the other unusual lithologies in the district—quartz-muscovite-carbonate-staurolite-corundum schist and quartz-tourmaline-albite rock—suggested that these rocks are tholeiitic basalts that underwent extensive seafloor alteration and metasomatism prior to Acadian metamorphism (Slack, 1999). Evidence for their basaltic origin consists of high Cr contents and chondrite-normalized REE patterns that are broadly similar to those of unaltered metabasalt from the wall rocks. In addition to high Cr, some rocks are highly enriched in alumina, which Slack and others (2001) attributed to mass loss of other components during extreme premetamorphic hydrothermal alteration. Because the massive sulfides in the Vermont Copper Belt also have very low contents of relatively immobile elements such as Cr, Zr, and REE, Slack and others (2001) concluded that the sulfide bodies lack significant sedimentary or basaltic components and therefore did not form by subseafloor replacement of clastic sediments or mafic volcanics. Instead, they concluded that the massive sulfides originally precipitated by syngenetic-exhalative processes on the seafloor during Silurian and Early Devonian times.

Immobile trace-element and REE whole-rock data have successfully identified the metamorphic protoliths of rocks associated with several other siliciclastic-mafic type VMS deposits. Precursors of chlorite schists and granoblastic albitites from the Gossan Lead deposits, Virginia, were shown to be similar to those of the adjacent unaltered metasedimentary schists, suggesting that the chlorite schists and albitites were derived by hydrothermal metasomatism of clastic marine sediments and not from syngenetic precipitation of chemical exhalites (Gair and Slack, 1984). A clastic marine sedimentary origin was also indicated by trace element and REE ratios for chlorite schists, biotite schists, muscovite schists, and albitites adjacent to sulfide ores of the Ducktown deposits, Tennessee (Gair, 1988; Robinson and Gair, 1992). Geochemical data for chlorite- and biotite-rich schist from wall rocks to the Matchless deposit, Namibia, suggested that these rocks originated as tholeiitic basalt that was subsequently metasomatized (Klemd and others, 1989). Although the majority of the metabasaltic rocks associated with siliciclastic-mafic-type VMS deposits have chemical compositions of oceanic tholeiites, some

greenstones and amphibolites associated with these deposits, including those in the Sambagawa belt of Japan and Windy Craggy, Canada, have trace-element signatures indicative of alkalic, within-plate basalt (Slack, 1993, and references therein).

Thermobarometry of host rocks and sulfides, together with structural studies, have yielded important information regarding the timing of metamorphism, deformation, and formation of sulfide deposits. In a detailed study of the conditions of metamorphism of sulfide deposits and associated host rocks in the Bathurst mining camp, New Brunswick, Currie and others (2003) documented that greenschist-facies metamorphic conditions for the silicate assemblages occurring within, and in the host rocks of, the deposit were identical to those of the sulfide assemblages. This congruence of P/T conditions shows that the deposits formed prior to peak metamorphism during the first metamorphic episode, consistent with a syngenetic origin for the Bathurst deposits. Sphalerite barometry, applied to the appropriate sphalerite-pyrite-hexagonal pyrrhotite assemblages, gave consistent pressures between various structural nappes. Peak metamorphic temperatures, provided by arsenopyrite and chlorite-phengite thermometry, also were consistent between the Bathurst deposits and the structural nappes in which they occur. The narrow range of P/T conditions determined for the Bathurst deposits supports independent structural observations and suggests that the nappes were assembled and internally deformed prior to the first metamorphic episode (Currie and others, 2003, and references therein).

References Cited

- Allen, R.L., Weihed, P., and the global VMS research project team, 2002, Global comparisons of volcanic-associated massive sulphide districts, *in* Blundell, D.J., Neubauer, F., and von Quadt, A., eds., *The timing and location of major ore deposits in an evolving orogen*: Geological Society of London Special Publication 204, p. 13–37.
- Averill, S.A., 2001, The application of heavy indicator mineralogy in mineral exploration with emphasis on base metal indicators in glaciated metamorphic and plutonic terrains, *in* McClenaghan, M.B., Bobrowsky, P.T., Hall, G.E.M., and Cook, S.J., eds., *Drift exploration in glaciated terrain*: Geological Society of London Special Publication 185, p. 69–81.
- Barrett, T.J., and MacLean, W.H., 1999, Volcanic sequences, litho-geochemistry, and hydrothermal alteration in some bimodal volcanic-associated massive sulfide deposits, *in* Barrie, C.T., and Hannington, M.D., eds., *Volcanic-associated massive sulfide deposits—Processes and examples in modern and ancient settings*: *Reviews in Economic Geology*, v. 8, p. 101–131.

- Blatt, H., Tracy, R.J., and Owens, B.E., 2006, Petrology—Igneous, sedimentary, and metamorphic: New York, W.H. Freeman and Company, 530 p.
- Bonnet, A.-L., and Corriveau, L., 2007, Alteration vectors to metamorphosed hydrothermal systems in gneissic terranes, *in* Goodfellow, W.D., ed., Mineral Deposits of Canada—A synthesis of major deposit-types, district metallogeny, the evolution of geological provinces, and exploration methods: Geological Association of Canada, Mineral Deposits Division, Special Publication No. 5, p. 1035–1049.
- Brooker, D.D., Craig, J.R., and Rimstidt, J.D., 1987, Ore metamorphism and pyrite porphyroblast development at the Cherokee mine, Ducktown, Tennessee: *Economic Geology*, v. 82, p. 72–86.
- Carpenter, R.H., and Allard, G.O., 1982, Aluminosilicate assemblages—An exploration tool for metavolcanic terranes of the southeast, *in* Allard, G.O., and Carpenter, R.H., eds., Exploration for metallic resources in the southeast: Athens, Ga., University of Georgia, p. 19–22.
- Craig, J.R., and Vokes, F.M., 1993, The metamorphism of pyrite and pyritic ores—An overview: *Mineralogical Magazine*, v. 57, p. 3–18.
- Currie, K.L., van Staal, C.R., Peter, J.M., and Rogers, N., 2003, Conditions of metamorphism of the main massive sulfide deposits and surrounding rocks in the Bathurst mining camp, *in* Goodfellow, W.D., McCutcheon, S.R., and Peter, J.M., eds., Massive sulfide deposits of the Bathurst mining camp, New Brunswick, and northern Maine: *Economic Geology Monograph* 11, p. 65–78.
- Franklin, J.M., 1984, Characteristics of alteration associated with Precambrian massive sulfide deposits, *in* Morton, R.L., and Groves, D.A., eds., Volcanic rocks, hydrothermal alteration and associated massive sulfide and gold deposits: Duluth, University of Minnesota–Duluth, Short Course Notes, p. 92–105.
- Franklin, J.M., 1993, Volcanic-associated massive sulphide deposits, *in* Kirkham, R.V., Sinclair, W.D., Thorpe, R.I., and Duke, J.M., eds., Mineral deposit modeling: Geological Association of Canada Special Paper 40, p. 315–334.
- Franklin, J.M., Gibson, H.L., Jonasson, I.R., and Galley, A.G., 2005, Volcanogenic massive sulfide deposits, *in* Hedenquist, J.W., Thompson, J.F.H., Goldfarb, R.J., and Richards, J.P., eds., Economic Geology 100th anniversary volume, 1905–2005: Littleton, Colo., Society of Economic Geologists, p. 523–560.
- Friesen, R.G., Pierce, G.A., and Weeks, R.M., 1982, Geology of the Geco base metal deposit, *in* Hutchinson, R.W., Spence, C.D., and Franklin, J.M., eds., Precambrian sulphide deposits: Geological Association of Canada Special Paper 25, p. 343–363.
- Froese, E., and Berman, R.G., 1994, Oxidation and sulfidation reactions: Geological Association of Canada Short Course Notes, v. 11, p. 101–113.
- Gair, J.E., 1988, Origin of unusual lithologies at Ducktown, Tennessee, as indicated by rare-earth-element geochemistry [abs.]: Geological Association of Canada, Mineralogical Association of Canada, Program with Abstracts, v.13, p. A42.
- Gair, J.E., and Slack, J.F., 1984, Deformation, geochemistry, and origin of massive sulfide deposits, Gossan Lead district, Virginia: *Economic Geology*, v. 79, p. 1442–1478.
- Galley, A.G., Hannington, M.D., and Jonasson, I.R., 2007, Volcanogenic massive sulphide deposits, *in* Goodfellow, W.D., ed., Mineral deposits of Canada—A synthesis of major deposit-types, district metallogeny, the evolution of geological provinces, and exploration methods: Geological Association of Canada, Mineral Deposits Division, Special Publication 5, p. 141–161.
- Gauthier, M., and Chartrand, F., 2005, Metallogeny of the Grenville Province revisited: *Canadian Journal of Earth Sciences*, v. 42, p. 1719–1734.
- Gibson, H.L., Watkinson, D.H., and Comba, C.D.A., 1983, Silicification—Hydrothermal alteration in an Archean geothermal system within the Amulet rhyolite formation: *Economic Geology*, v. 78, p. 954–971.
- Grenne, T., Ihlen, P.M., and Vokes, F.M., 1999, Scandinavian Caledonide metallogeny in a plate tectonic perspective: *Mineralium Deposita*, v. 34, p. 422–471.
- Guidotti, C.V., 1989, Metamorphism in Maine—An overview, *in* Tucker, R.D., and Marvinney, R.G., eds., Igneous and metamorphic geology. Studies in Maine geology, v. 3: Maine Geological Survey, p. 1–17.
- Heimann, A., Spry, P.G., and Teale, G.S., 2005, Zincian spinel associated with metamorphosed Proterozoic base-metal sulfide occurrences, Colorado—A reevaluation of gahnite composition as a guide in exploration: *Canadian Mineralogist*, v. 43, p. 601–622.
- Hitzman, M.W., Proffett, J.M., Jr., Schmidt, J.M., and Smith, T.E., 1986, Geology and mineralization of the Ambler District, northwestern Alaska: *Economic Geology*, v. 81, no. 7, p. 1592–1618.

- Holdaway, M.J., 1971, Stability of andalusite and the aluminum silicate phase diagram: *American Journal of Science*, v. 271, p. 97–131.
- Klemd, R., Maiden, K.J., Okrusch, M., and Richter, P., 1989, Geochemistry of the Matchless metamorphosed massive sulfide deposit, South West Africa/Namibia—Wall rock alteration during submarine ore-forming processes: *Economic Geology*, v. 84, p. 603–617.
- Koski, R.A., Galley, A.G., and Hannington, M.D., 2003, Ophiolite-hosted volcanogenic massive sulfide deposits—A view in 2003 [abs.]: *Geological Society of America Abstracts with Programs*, v. 35, p. 12.
- Lentz, D.R., 1998, Petrogenetic evolution of felsic volcanic sequences associated with Phanerozoic volcanic-hosted massive sulfide systems—The role of extensional geodynamics: *Ore Geology Reviews*, v. 12, p. 289–327.
- Marshall, B., and Gilligan, L.B., 1993, Remobilization, syn-tectonic processes and massive sulphide deposits: *Ore Geology Reviews*, v. 8, p. 39–64.
- Marshall, B., Vokes, F.M., and Laroque, A.C.L., 2000, Regional metamorphic remobilization—Upgrading and formation of ore deposits, *in* Spry, P.G., Marshall, B., and Vokes, F.M., eds., *Metamorphic and metamorphogenic ore deposits: Reviews in Economic Geology*, v. 11, p. 19–38.
- Morton, R.L., and Franklin, J.M., 1987, Two-fold classification of Archean volcanic-associated massive sulfide deposits: *Economic Geology*, v. 82, p. 1057–1063.
- Mosier, D.L., Berger, V.I., and Singer, D.A., 2009, Volcanogenic massive sulfide deposits of the world—Database and grade and tonnage models: U.S. Geological Survey Open-File Report 2009–1034, 46 p.
- Nesbitt, B.E., 1979, Regional metamorphism of the Ducktown, Tennessee massive sulfide and adjoining portions of the Blue Ridge Province: Ann Arbor, Mich., University of Michigan, Ph.D. dissertation, 216 p.
- Nesbitt, B.E., and Essene, E.J., 1982, Metamorphic thermometry and barometry of a portion of the southern Blue Ridge Province: *American Journal of Science*, v. 282, p. 701–729.
- Ohmoto, H., Tanimura, S., Date, J., and Takahashi, T., 1983, Geologic setting of the Kuroko deposits, Japan—Part I. Geologic history of the Green tuff region. Part II. Stratigraphy and structure of the Hokuroku district. Part III. Submarine calderas and Kuroko genesis, *in* Ohmoto, H., and Skinner, B.J., eds., *The Kuroko and related volcanogenic massive sulfide deposits: Economic Geology Monograph 5*, p. 9–54.
- Piercey, S.J., 2009, Litho-geochemistry of volcanic rocks associated with volcanogenic massive sulphide deposits and applications to exploration, 2009, *in* Cousens, B., and Piercey, S.J., eds., *Submarine volcanism and mineralization—Modern through ancient: Geological Association of Canada, Short Course Notes*, v. 19, p. 15–40.
- Piercey, S.J., Paradis, S., Murphy, D.C. and Mortensen, J.K., 2001, Geochemistry and paleotectonic setting of felsic volcanic rocks in the Finlayson Lake volcanic-hosted massive sulfide district, Yukon, Canada: *Economic Geology*, v. 96, p. 1877–1905.
- Roberts, M.D., Oliver, N.H.S., Fairclough, M.C., Hölttä, P.S., and Lahtinen, R., 2003, Geochemical and oxygen isotope signature of sea-floor alteration associated with a polydeformed and highly metamorphosed massive sulfide deposit, Ruostesuo, central Finland: *Economic Geology*, v. 98, p. 535–556.
- Robinson, G.R., Jr., and Gair, J.E., 1992, Chemical alteration of clastic sediments during the formation of massive sulfide ore at Ducktown, Tennessee [abs.]: *Geological Society of America Abstracts with Programs*, v. 24, p. 61.
- Runyon, G.A., and Misra, K.C., 1981, Metamorphic mobilization of sulfide constituents in metasediments of the Great Smoky Group, Ducktown area, Tennessee [abs.]: *Geological Society of America Abstracts with Programs*, v. 13, p. 33.
- Russell, N., Moreira, J., and Sanchez, R., 2000, Volcanogenic massive sulphide deposits of Cuba, *in* Sherlock, R.L., and Logan, M.A., eds., *Volcanogenic massive sulphide deposits of Latin America: Geological Association of Canada Special Publication No. 2*, p. 241–258.
- Severin, P.W.A., Morton, R.L., and Balint, F., 1984, Volcanic stratigraphy and hydrothermal alteration in the vicinity of the Winston Lake massive sulfide deposit, *in* Morton, R.L., and Groves, D.A., eds., *Volcanic rocks, hydrothermal alteration and associated massive sulfide and gold deposits: Duluth, University of Minnesota—Duluth, Short Course Notes*, p. 168–190.
- Sillitoe, R.H., Hannington, M.D., and Thompson, J.F.H., 1996, High sulfidation deposits in the volcanogenic massive sulfide environment: *Economic Geology*, v. 91, p. 204–212.
- Slack, J.F., 1993, Descriptive and grade-tonnage models for Besshi-type massive sulphide deposits, *in* Kirkham, R.V., Sinclair, W.D., Thorpe, R.I., and Duke, J.M., eds., *Mineral deposit modeling: Geological Association of Canada Special Paper 40*, p. 343–371.

- Slack, J.F., 1999, Coarse garnet schists at the Elizabeth mine, VT—Products of seafloor-hydrothermal alteration not syn-metamorphic Acadian fluid flow [abs.]: Geological Society of America Abstracts with Programs, v. 31, no. 2, p. A-69.
- Slack, J.F., Offield, T.W., Woodruff, L.G., and Shanks, W.C., III, 2001, Geology and geochemistry of Besshi-type massive sulfide deposits of the Vermont copper belt, *in* Hammarstrom, J.M., and Seal, R.R., II, eds., Environmental geochemistry and mining history of massive sulfide deposits in the Vermont copper belt: Society of Economic Geologists Guidebook Series, v. 35, part II., p. 193–211.
- Slater, W.R., Misra, K.C., and Acker, C.P., II, 1985, Field Trip no. 5—Massive sulfide deposits of the Ducktown District, Tennessee, *in*, Woodward, N.B., ed., Field trips in the southern Appalachians—Southeastern Section, Geological Society of America 1985, Field trips 1–5,7: Knoxville, University of Tennessee, Department of Geological Sciences, Studies in Geology 9, p. 171–190.
- Spear, F.S., 1993, Metamorphic phase equilibria and pressure-temperature-time paths: Washington, D.C., Mineralogical Society of America, 799 p.
- Spry, P.G., and Scott, S.D., 1986a, The stability of zincian spinels in sulfide systems and their potential as exploration guides for metamorphosed massive sulfide deposits: Economic Geology, v. 81, p. 1446–1463.
- Spry, P.G., and Scott, S.D., 1986b, Zincian spinel and staurolite as guides to ore in the Appalachians and Scandinavian Caledonides: Canadian Mineralogist, v. 24, p. 147–163.
- Stanton, R.L., 1960, General features of the conformable “pyritic” orebodies—Part 2. Mineralogy: Canadian Mining and Metallurgical Bulletin, v. 53, p. 24–29.
- Thomas, D., 1991, Geology, mineralogy and hydrothermal alteration at the Winston Lake massive sulphide deposit, Marathon, Ontario: Kingston, Ontario, Queen’s University, M.S. thesis, 231 p.
- Tornos, F., César, C., Jorge, M.R.S., Relvas, J.M.R.S., Barriga, F.J.A.S., and Reinaldo Sáez, R., 2002, The relationship between ore deposits and oblique tectonics—The southwestern Iberian Variscan Belt, *in* Blundell, D.J., Neubauer, F., and von Quadt, A., eds., The timing and location of major ore deposits in an evolving orogen: Geological Society of London Special Publication 204, p. 179–195.
- Toulmin, P., III, Barton, P.B., Jr., and Wiggins, L.B., 1991, Commentary on the sphalerite geobarometer: American Mineralogist, v. 76, p. 1038–1051.
- Turner, F.J., 1981, Metamorphic petrology: New York, McGraw-Hill, p. 524.
- Vokes, F.M., 1969, A review of the metamorphism of sulphide deposits: Earth Science Reviews, v. 5, p. 99–143.
- Vokes, F.M., 2000, Ores and metamorphism—Chapter 1. Introduction and historical perspectives: Reviews in Economic Geology, v. 11, p. 1–18.
- Zaleski, E., and Peterson, V.L., 1995, Depositional setting and deformation of massive sulfide deposits, iron-formation, and associated alteration in the Manitouwadge greenstone belt, Superior Province, Ontario: Economic Geology, v. 90, p. 2244–2261.

18. Theory of Deposit Formation

By W.C. Pat Shanks III

18 of 21

Volcanogenic Massive Sulfide Occurrence Model

Scientific Investigations Report 2010–5070–C

U.S. Department of the Interior
U.S. Geological Survey

U.S. Department of the Interior
KEN SALAZAR, Secretary

U.S. Geological Survey
Marcia K. McNutt, Director

U.S. Geological Survey, Reston, Virginia: 2012

For more information on the USGS—the Federal source for science about the Earth, its natural and living resources, natural hazards, and the environment, visit <http://www.usgs.gov> or call 1-888-ASK-USGS.

For an overview of USGS information products, including maps, imagery, and publications, visit <http://www.usgs.gov/pubprod>

To order this and other USGS information products, visit <http://store.usgs.gov>

Any use of trade, product, or firm names is for descriptive purposes only and does not imply endorsement by the U.S. Government.

Although this report is in the public domain, permission must be secured from the individual copyright owners to reproduce any copyrighted materials contained within this report.

Suggested citation:

Shanks III, W.C. Pat, 2012, Theory of deposit formation in volcanogenic massive sulfide occurrence model: U.S. Geological Survey Scientific Investigations Report 2010-5070 -C, chap. 18, 12 p.

Contents

| | |
|--|-----|
| Ore Deposit Types..... | 293 |
| Sources of Metals and Other Ore Components..... | 293 |
| Sources of Ligands Involved in Ore Component Transport | 294 |
| Sources of Fluids Involved in Ore Component Transport..... | 295 |
| Chemical Transport and Transfer Processes..... | 295 |
| Fluid Drive Including Thermal, Pressure, and Geodynamic Mechanisms | 296 |
| Character of Conduits/Pathways that Focus Ore-Forming Fluids | 298 |
| Nature of Traps and Wallrock Interaction that Trigger Ore Precipitation..... | 298 |
| Structure and Composition of Residual Fluid Outflow Zones..... | 298 |
| References Cited..... | 298 |

Figures

| | |
|--|-----|
| 18-1. Reaction progress diagram showing mineral stabilities and amounts formed as 350 °C East Pacific Rise hot spring water mixes progressively with cold (2 °C) bottom seawater | 296 |
| 18-2. Schematic cross section of typical mid-ocean ridge crustal architecture | 297 |

18. Theory of Deposit Formation

By W.C. Pat Shanks III

Ore Deposit Types

The unifying characteristics of the volcanogenic massive sulfide deposit type are (1) association with volcanics, and (2) mineralization by hydrothermal solutions at or near the seafloor. Early papers referred to these deposits as stratiform and stratabound deposits, or exhalative deposits. Deposits in volcanic, clastic sedimentary, marine carbonate, and metamorphic terranes were lumped together. This meant that all massive sulfide deposits, including those strictly in volcanic terranes (VMS), those in shale basins (SEDEX), and those in carbonate strata (MVT), were grouped based on some gross similarities (base-metal deposits, massive sulfide ores, low-to-moderate temperature hydrothermal processes).

These early attempts at classification indicate that there is a more or less continuous spectrum of massive sulfide deposit types, and that classifications are sometimes difficult to apply even today because of the gradational nature of the deposit characteristics. The key distinction among VMS deposits is that they formed as seafloor massive sulfides from hydrothermal fluids that are driven by magmatic heat. This mineralizing process may involve convecting seawater that evolves by water/rock interaction into a slightly acidic metalliferous fluid, which may contain a significant component of magmatic volatiles. In some settings, volcanic or intrusive rocks are only present in the footwall sequence or are peripheral to the actual sulfide deposit, and in these cases a genetic link must be established using geology and geochemistry.

Volcanogenic massive sulfide deposits have clear system affinities to, and are transitional to, sedimentary-exhalative (SEDEX) deposits. Most SEDEX deposits occur in shale basins with little or no exposure of igneous rocks. In contrast to most (but not all) VMS deposits, they tend to be Zn-rich, commonly display fluid-inclusion evidence for formation from concentrated (basinal) brines, form at low to moderate temperatures (50–200 °C), and typically show evidence of sulfide derivation from local sources at the site of deposition (bacterial sulfide in pore-waters or dissolved H₂S in an anoxic water column).

However, there is accumulating fluid inclusion evidence that some VMS deposits, especially those in felsic-siliciclastic settings like the Tasmanian deposits in the Mt. Reed volcanics, the Bathurst deposits (New Brunswick), and the Iberian Pyrite Belt deposits in Spain and Portugal (Solomon and others,

2004; Solomon, 2008; Tornos and others, 2008), formed from saline fluids in brine pools on the seafloor. These deposits consist of sheet-like massive sulfide bodies due to deposition in areally extensive brine pools, similar to those of the modern Red Sea deposits (6×14 km, 20 m thick; fig. 3–2). Mafic-siliciclastic deposits like the Besshi deposits probably also formed from dense brine pools, but fluid inclusion evidence is not attainable from most Besshi deposits because of significant postore deformation. The Windy Craggy deposit, British Columbia, has well-preserved fluid inclusions that indicate formation from moderately saline fluids (9–17 wt% NaCl equivalent; Peter and Scott, 1999) that could have formed negatively buoyant brine-pools on the seafloor.

Finally, VMS deposits have some system affinities with high-sulfidation epithermal precious-metal deposits in marine volcanic rocks, volcanogenic manganese deposits, and Algoma-type iron-formations.

Sources of Metals and Other Ore Components

Despite thousands of published papers on VMS deposits resulting from intensive study over the past 50 years, and despite the incredible opportunities to observe and sample actively-forming deposits on the seafloor, there is continued debate about the fluids that form economic VMS ore deposits. In fact, the argument has not evolved much. For example, the debate in the 1850s about what we now know to be VMS deposits (Stanton, 1984, p. 1432–1433) can be distilled as follows:

...the Norwegians considered the replacing ore materials to have come from intrusive granitoid masses, whereas the Americans saw them as derived from the surrounding country, and segregated into the favorable beds by lateral secretion.

This debate was renewed in the 1960s with the discovery of widespread metalliferous sediment deposits on the seafloor (Bostrom and others, 1969) spatially associated (fig. 3–1) with the mid-ocean ridges (MORs). Corliss (1971) focused attention on the possibility of leaching incompatible elements from basaltic pillow interiors as seawater penetrates through cracks in the lavas. The discovery that heat flow on the flanks of

divergent plate boundaries is not nearly as high as expected for conductive heat loss (Anderson and others, 1977) implicated convective heat loss due to seawater circulation. Muehlenbachs and Clayton (1971, 1972, 1976) used $\delta^{18}\text{O}$ studies of greenstones and other metamorphosed volcanic rocks dredged from the seafloor to demonstrate that subseafloor metamorphism was due to high-temperature reactions of seawater with oceanic crust, which suggested convective seawater circulation could be a common process that significantly alters the oceanic crust. Hydrothermal experiments between seawater and basalt at 200–500 °C (Bischoff and Dickson, 1975; Seyfried and Bischoff, 1977; Mottl and Holland, 1978) showed strong Mg-removal due to the formation of secondary sheet silicates, producing acidic solutions capable of transporting ore-forming metals (Fe, Cu, Zn, Pb). Thus, the “lateral secretion” model of the past has become the water/rock interaction model of the present.

Research on ore genesis in VMS deposits and modern seafloor analogs over the last 30 years has focused mostly on water/rock interaction models, with direct magmatic contributions usually relegated to a minor or insignificant role (Bischoff and Dickson, 1975; Large, 1977; Ohmoto and others, 1983; Shanks, 2001; Seyfried and Shanks, 2004). Experimental studies of basalt/seawater interaction at temperatures up to 425 °C have shown that water/rock interaction, without the presence of magmatic volatiles, can account for the complete spectrum of observed metal contents of hydrothermal vent fluids that have been analyzed from the mid-ocean ridges (Seyfried and others, 2002, 2004; Seyfried and Shanks, 2004).

However, it is well established that magmatic degassing adds He (helium), CO_2 , CH_4 , and H_2S or SO_2 to convective hydrothermal systems (Lilley and others, 1982; Kadko and others, 1995; Glasby and others, 2008). A few researchers have consistently advocated for an important, perhaps pivotal, role for metal supply by magmatic fluids (Sawkins and Kowalik, 1981; Urabe and Marumo, 1991; de Ronde, 1995; Lydon, 1996; Yang and Scott, 1996, 2002, 2003, 2006). In particular, Yang and Scott (2002) have shown that in Manus Basin the compositions of metallic precipitates found in vesicles of melt inclusions and matrix glass progressively change from Ni + Cu + Zn + Fe in basalt and basaltic andesite, to Cu + Zn + Fe in andesite, to Cu + Fe in dacite, to Fe in rhyodacite, and to Fe + Zn (+ Pb?) in rhyolite. Williams-Jones and Heinrich (2005) provided further evidence from experimental studies and laser ICP-MS analyses of individual vapor-rich fluid inclusions that Cu and Au, together with As and Sb, are preferentially concentrated in magmatic vapor at concentrations that are much higher than those in Cl-rich brines. These observations, combined with studies that show the Cu, Au, As, and Sb enrichments in the seafloor massive sulfide deposits from rhyolitic and rhyodacitic settings in the eastern Manus Basin, suggest that pulses of magmatic fluids injected into seawater convective systems may be important metal contributors in

felsic environments, and that water/rock interaction may dominate metal supply in mafic settings. An alternative view is that magmatic volatile-rich fluids add acid to convective hydrothermal systems and the resulting very acidic fluids (pH < 1) are able to leach additional metals (Craddock and others, 2007).

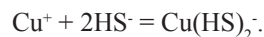
Sources of Ligands Involved in Ore Component Transport

The principal anion in seawater is Cl, with a remarkably constant concentration of 543 millimoles per liter (mM/L) or 19,277 milligrams per liter (mg/L). The next most important anion is SO_4 at 2,600 mg/L or 27 mM/L, followed by HCO_3 (140 mg/L), Br (65 mg/L), and H_3BO_4 (24 mg/L). Knowledge of the Cl content of fluids involved in the formation of VMS deposits comes from studies of fluid inclusions and from direct sampling of active hydrothermal systems on the modern seafloor. Fluid inclusion compositional variations are summarized in Chapter 14 of this report; fluid inclusions from most ancient VMS deposits have Cl concentrations close to that of seawater (3–6 wt% NaCl), but many have much higher Cl contents. Studies of active systems (Von Damm, 1995; Von Damm and others, 1995, 1997, 2003) have shown that the principal cause of salinity variation at mid-oceanic ridges is phase separation into low- and high-chloride fluid phases. Chlorine values in sampled vent fluids display a smaller range than in VMS fluid inclusions, ranging from 10 to 200 percent of seawater values (0.3–7 wt% NaCl). The Red Sea brine pools represent a unique modern case where convective seawater has reacted with subsurface evaporate minerals to achieve Cl contents about 8 times that of seawater (25 wt% NaCl), close to NaCl saturation (Zierenberg and Shanks, 1986).

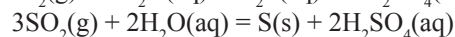
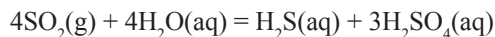
Hydrogen sulfide is the other anion that can be an important metal complexing agent, participating in reactions such as:



or



Hydrogen sulfide can be supplied to circulating hydrothermal fluids by (1) hydrothermal or bacterial reduction of seawater sulfate, (2) hydrolysis reactions with volcanic glass or sulfide phases in host rocks, or (3) direct injection of magmatic volatiles. Sulfur dioxide is unstable in aqueous environments and disproportionates to SO_4 and H_2S , or to SO_4 and native S (Holland, 1965; Symonds and others, 2001) by the following reactions:



Thus, SO_2 disproportionation reactions also strongly contribute to the acidity of hydrothermal fluids.

Sources of Fluids Involved in Ore Component Transport

The vast majority of chemical and isotopic studies of fluid compositions in modern and ancient VMS deposits indicate that seawater or evolved seawater is the dominant mineralizing fluid (see Chapter 14, this report). Seawater circulation in VMS deposits is driven by magmatic heat. The resulting convection system produces compositionally evolved seawater following reactions with host rocks along the flow path and fluid temperatures up to about 400 °C in the upflow zone and the hydrothermal vent site on the seafloor.

Other potentially important contributors to the ore-transport process are magmatic water and related volatiles. Typically, magmatic gases are about 90 mol percent H₂O, with 5–10 mol percent CO₂, 1–2 mol percent sulfur species such as SO₂ and (or) H₂S, and lesser amounts of H₂, HCl, and HF. HCl is an especially important magmatic volatile in island-arc and back-arc settings (Taran and others, 1995). All of these gas species can be directly absorbed into convecting seawater hydrothermal systems, and a substantial addition of the magmatic component would result in dilution of Cl by addition of H₂O, CO₂, S, and F (fluorine) and a decrease in pH.

The magmatic fluid may contribute significant amounts of carbon and sulfur components, and potentially appreciable metallic components. Some fluid-inclusion and experimental evidence indicates that magmatic vapors can carry exceptionally high metal contents (Williams-Jones and Heinrich, 2005), thus raising the possibility that a short-term, limited-volume, magmatic flux could be very important in providing metals to the system.

Magmatic water from a variety of igneous environments has δD of -40 to -80 per mil and $\delta^{18}O$ of 6 to 8 per mil (Rye, 1993), and these values can be applied to MOR systems. Arc and back-arc systems are somewhat different because of water contributed by dehydration of the descending slab; arc-related magmatic waters are estimated to have δD values of about -25 per mil (Giggenbach, 1992; Shaw and others, 2008). Thus, even small contributions of magmatic water should be distinguishable by negative δD values in hydrothermal fluids.

Shanks and others (1995) discovered vent fluids from the 1991 MOR volcanic eruption area at 9°45-52'N EPR with δD values as low as -2 per mil. These values, which are the only negative δD values found for vent fluids from MOR sites, could result from either a small component of magmatic water or an open system, isobaric phase-separation process (Berndt and others, 1996). Seawater convection is the process that cools axial magma chambers and mines heat from the oceanic crust. Seawater cannot quench magma without experiencing phase separation. Magmatic water mixing, together with fluid-basalt reactions that shift $\delta^{18}O_{H_2O}$ to higher values, could explain the isotope systematics of the D-depleted vents at 9–10°N. However, mid-ocean ridge basalts (MORBs) tend to be quite “dry,” with only about 0.2 wt% water (Dixon and others, 1988); studies of Hawaiian glasses have shown that

they never reach saturation with respect to water at eruption depths of more than a few hundred meters (Dixon and others, 1991). That is, seafloor basaltic lavas do not exsolve water at depths greater than a few hundred meters simply by freezing to form glass. However, complete crystallization of a MOR basalt dike containing only anhydrous phases could release magmatic water. In summary, the negative δD values from the 9–10°N EPR site do not provide conclusive proof of magmatic water in the convectively venting system there. Similarly, stable isotope and fluid inclusion evidence from VMS deposits for a magmatic water component is generally equivocal (Huston, 1999).

In a back-arc tectonic setting, vent fluids with negative δD values (-8.1 per mil) have been analyzed from the DESMOS vent field in Manus Basin (Gamo and others, 1997). This hydrothermal field is hosted by andesitic to rhyodacitic rocks, and the magmas that produce them are significantly more water-rich than MORB. Recent work (Craddock and others, 2007; Bach and others, 2007; Reeves and others, 2011) indicates that vent fluids from the eastern Manus Basin sites have fluid chemistries consistent with a mixture of two-thirds seawater and one-third magmatic water-rich volatiles.

Hydrogen sulfide also may be added to hydrothermal systems by magmatic degassing, but evidence of this process is ambiguous for MOR systems because H₂S is produced in abundance by leaching of igneous sulfides from basaltic rocks during water/rock interactions (Seyfried and Bischoff, 1981). Studies of $\delta^{34}S_{H_2S}$ in MOR black smoker vent fluids has indicated consistently that some seawater-derived sulfate is incorporated via sulfate-reduction reactions (Shanks, 2001; Ono and others, 2007), which produces the slightly positive $\delta^{34}S$ values observed in samples of vent fluid H₂S and massive sulfide.

Felsic magmas tend to be more oxidizing, relative to mafic magmas, so SO₂ is expected to be the dominant magmatic sulfur gas. Various investigators have invoked SO₂ disproportionation reactions (to H₂S and SO₄) to explain negative $\delta^{34}S$ values (-3 to -18 per mil) of H₂S and sulfide minerals and lower-than-seawater $\delta^{34}S_{SO_4}$ values (10–17 per mil) in associated SO₄ or sulfate minerals (McMurtry and others, 1993; Gamo and others, 1997; Alt and others, 1998; Herzig and others, 1998; Resing and others, 2007). The chemical and sulfur isotopic data provide an explanation for the negative $\delta^{34}S$ values of sulfides related to arc and back-arc volcanic-hosted VMS systems and strongly suggest derivation of the sulfur species from magmatic SO₂ vapor.

Chemical Transport and Transfer Processes

The ligands of most importance in ore-forming metallic element transport are Cl and HS, based on the current state of knowledge of aqueous complexes in hydrothermal solutions as summarized in databases like SUPCRT (Johnson and others,

1992) and SOLTHERM (Reed and Palandri, 2006). It has been known for many years, thanks to the seminal work of Harold Helgeson, that Cl is an important complexing agent that significantly increases the solubility of base metals (Fe, Cu, Pb, Zn) in hydrothermal solutions (Helgeson, 1969). Recent studies have suggested that sulfide complexing (MeHS) is important in increasing solubility of some metals (Me), especially Cu and Au (Mountain and Seward, 2003; Stefansson and Seward, 2004).

Geochemical reaction calculations that consider all possible aqueous species and their affect on mineral solubilities (Shanks and Bischoff, 1977; Reed, 1982; Janecky and Seyfried, 1984; Bowers and Taylor, 1985; Janecky and Shanks, 1988; Reed and Palandri, 2006) have clearly shown that fluids having seawater or higher salinity are capable of transporting metals and sulfide at temperatures above 200°C, and that deposition from VMS ore fluids is mainly due to temperature change as the hydrothermal fluids mix with cold, ambient bottom waters. Janecky and Seyfried (1984) predicted the sequence of sulfide, sulfate, and silicate minerals (fig. 18–1) that form as a result of mixing of 350°C fluid from 21°N EPR with cold, ambient, bottom seawater and showed that cooling is the most important factor.

Fluid Drive Including Thermal, Pressure, and Geodynamic Mechanisms

Fluid circulation in subseafloor hydrothermal systems is driven by buoyancy forces related to the heat of subvolcanic

intrusives (see Lowell and others, 2008). Inferred convective hydrothermal flow paths are shown in figures 4–2, 4–6, and 4–7 for fast and slow spreading ridges and submarine caldera settings, respectively. However, these relatively simple inferred pathways for hydrothermal circulation are difficult to constrain with any degree of certainty. Active seafloor systems provide only limited exposure, and technical difficulties have limited the amount of drilling into the roots of modern hydrothermal systems. For deposits exposed on the continents, there is generally better exposure of faults and alteration zones (see Chapters 4 and 11) that allow reconstruction of the hydrothermal systems, but unraveling long, complicated histories is difficult because of limited exposure and later tectonic and metamorphic events.

Fluid flow models have been used since the earliest studies of VMS deposits and MOR hydrothermal systems (Spooner, 1977; Turner and Gustafson, 1978; Fehn and Cathles, 1979; Lowell and Rona, 1985) and are very helpful in placing constraints on the overall nature of hydrothermal systems. In general, fluid flow models are limited by insufficient knowledge of lithologies and associated porosity/permeability, faulting and fracturing, and depth and nature of the heat source. In addition, flow models with capability for incorporating multi-phase fluid flow, phase-separation, magmatic volatile degassing, and permeability change due to mineral precipitation/dissolution are still being developed and improved.

The current state of VMS fluid flow models is summarized nicely by Lowell and others (2008) and Schardt and Large (2009). In principle, the nature of fluid and mass transport in subseafloor hydrothermal systems (Kelley and others, 2002) can be conceptualized as a simple problem (fig. 18–2). Convection is driven by magmatic heat, so there is

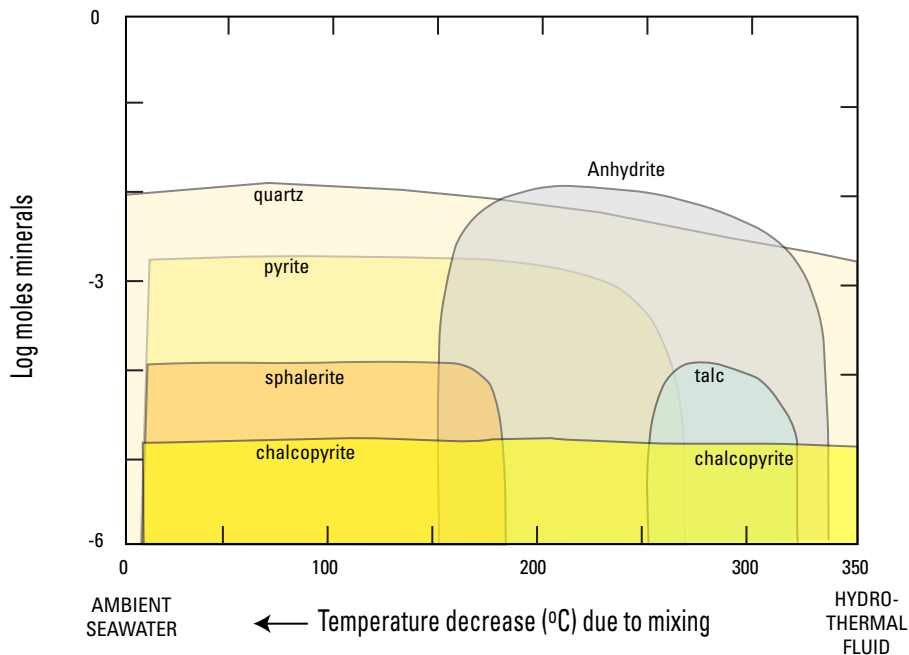


Figure 18–1. Reaction progress diagram showing mineral stabilities and amounts formed as 350°C East Pacific Rise hot spring water (right side) mixes progressively with cold (2°C) bottom seawater (toward the left side of the diagram). Abundant mineral precipitation occurs despite the dilution of the hydrothermal fluid, and cooling is the cause of pyrite, chalcopyrite, sphalerite, and quartz precipitation. Anhydrite, talc, and barite precipitate because of mixing and addition of sulfate and magnesium from seawater. The predicted sequence of minerals, especially chalcopyrite→anhydrite→pyrite-sphalerite agrees well with the sequence in some massive sulfide deposits and seafloor chimneys. Modified from Janecky and Seyfried (1984).

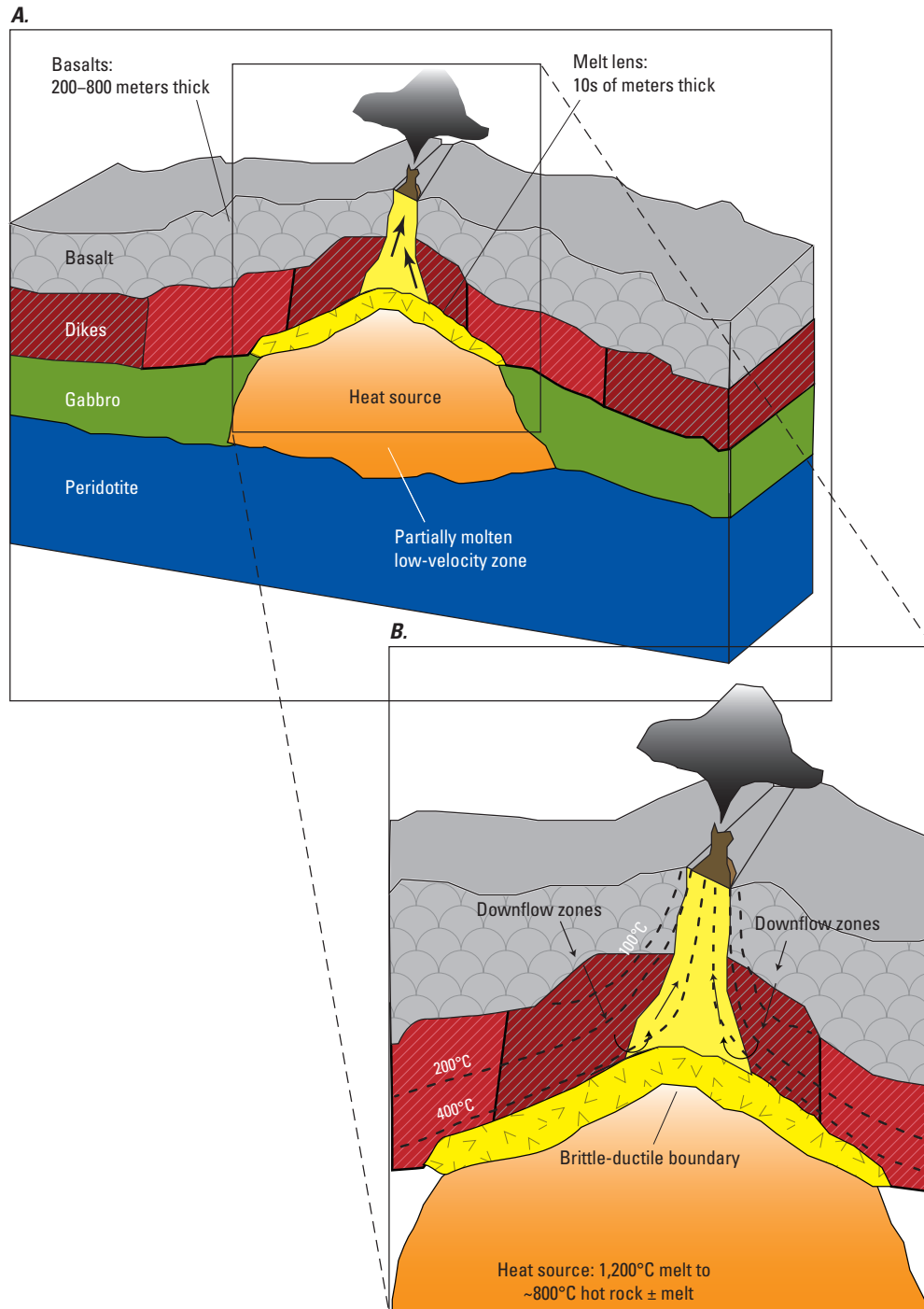


Figure 18–2. Schematic cross section of typical mid-ocean ridge crustal architecture. *A*, Cross section showing pillow lavas and pillow ridges, sheeted dikes, gabbros (including a convecting axial magma chamber), and ultramafic rocks. *B*, Closer view showing the magmatic heat source, brittle-ductile transition zone, and inferred hydrothermal fluid circulation patterns, including multiple downflow zones and a focused upflow zone beneath the ridge axis and black smoker vents on the seafloor within the axial rift zone. Modified from Kelley and others (2002).

a symmetrical down-flow zone where cold seawater recharges the system and a more focused upflow zone where heated fluid ascends buoyantly and rapidly to the seafloor. The systems of interest are typically dominated by one or two rock types and a single fluid, seawater. In practice, though, the process is very complicated. Lowell and others (2008) described recent modeling advances that consider dynamics related to dike injection, heat transfer from the magma chamber to the hydrothermal system, and convection and magma replenishment within the chamber. Lowell and others (2008) also presented new modeling approaches that allow realistic approximation of two-phase flow in the NaCl–H₂O system. This modeling allows simulation of different chemical and physical and transport processes in low-salinity vapor and high-salinity brine phases. These models are leading to a better understanding of the temporal evolution of seafloor hydrothermal systems and of the fate of brines produced in the subsurface by phase separation.

Schardt and Large (2009) summarized many fluid flow modeling studies of ancient and modern VMS systems and used coupled reactive transport models and fracture permeability models to gain understanding of the conditions necessary to form a large VMS deposit. They concluded that average-size VMS deposits (approx. 1.2 Mt total Zn and Cu) require 5,000 yrs to form and that supergiant deposits (>12 Mt Zn or 24 Mt Cu total metal; Singer, 1995) either require much longer (>35,000 yrs) or much higher metal contents in the fluid (>100 ppm).

Character of Conduits/Pathways that Focus Ore-Forming Fluids

Numerous studies of active hydrothermal vents on the seafloor show that focused, high-velocity flow (1–2 m/s) typically occurs in the highest temperature black smoker fluids. These flow rates require open fluid conduits, but there is little direct information on these in modern systems. However, stringer or feeder zones are observed in a number of cases on the modern seafloor or in drilling beneath seafloor massive sulfide deposits (Ridley and others, 1994; Humphris and others, 1995; Zierenberg and others, 1998). By analogy, stockwork zones, which are common in ancient VMS deposits, represent feeder zones below massive sulfide bodies.

Deeper portions of the upflow systems are even less well known. One area of proposed deep vigorous upflow is in the Solea graben, Cyprus, where massive epidote-quartz alteration developed in Cretaceous lavas reflects high water/rock reactions caused by high-temperature hydrothermal fluids (Bettison-Varga and others, 1992). Similar fossil upflow zones have been observed above subvolcanic intrusions in other ophiolitic VMS systems (Galley and Koski, 1999).

Recharge zones are more difficult to characterize because these flow systems are more diffuse and the resulting alteration

is less intense. Footwall alteration is extensive and in some cases semiconformable, suggesting low to moderate temperatures over a broad recharge zone. However, promising studies are underway on the seafloor, using microearthquakes to track near-surface fluid flow. These studies have shown predominantly along-axis fluid flow at 9°50'N on the EPR (Tolstoy and others, 2008), but much more work needs to be done in order to understand such recharge systems.

Nature of Traps and Wallrock Interaction that Trigger Ore Precipitation

In VMS systems, cooling at the seafloor is regarded as the principal cause of sulfide precipitation, and wall rock alteration is largely considered less significant to ore precipitation. However, observations of rapid oxidation of sulfides on the seafloor have led to suggestions of various mechanisms that preserved ancient deposits. These include anoxic (including sulfidic) bottom waters, capping lava flows, or chemical precipitates of silica or sulfate minerals that cap and isolate the system from oxidizing bottom waters (Barriga and Fyfe, 1988; Hannington and others, 2005; Schardt and Large, 2009).

Structure and Composition of Residual Fluid Outflow Zones

Hanging wall alteration is common in VMS deposits (Galley and others, 2007) and provides the best evidence of residual fluid outflow, probably because of continued fluid convection due to continued cooling of underlying plutons following the ore forming period.

References Cited

- Alt, J.C., Teagle, D.A.H., Brewer, T.S., Shanks, W.C., III, and Halliday, A.N., 1998, Alteration and mineralization of an oceanic forearc and the ophiolite-ocean crust analogy: *Journal of Geophysical Research—Solid Earth*, v. 103, no. B6, p. 12365–12380.
- Anderson, R.N., Langseth, M.G., and Sclater, J.G., 1977, Mechanisms of heat transfer through the floor of the Indian Ocean: *Journal of Geophysical Research*, v. 82, p. 3391–3409.
- Bach, W., Seewald, J.S., Tivey, M.A., Tivey, M.K., Yoerger, D., and Craddock, P.R., 2007, Hydrothermal systems in the eastern Manus Basin—Effects of phase separation and fluid mixing: *Geochimica et Cosmochimica Acta*, v. 71, p. A48.

- Barriga, F.J.A.S., and Fyfe, W.S., 1988, Giant pyritic base-metal deposits—The example of Feitais (Aljustrel, Portugal): *Chemical Geology*, v. 69, p. 331–343.
- Berndt, M.E., Seal, R.R., II, Shanks, W.C., III, and Seyfried, W.E., Jr., 1996, Hydrogen isotope systematics of phase separation in submarine hydrothermal systems—Experimental calibration and theoretical models: *Geochimica et Cosmochimica Acta*, v. 60, p. 1595–1604.
- Bettison-Varga, L., Varga, R.J., and Schiffman, P., 1992, Relation between ore-forming hydrothermal systems and extensional deformation in the Solea Graben spreading center, Troodos Ophiolite, Cyprus: *Geology*, v. 20, no. 11, p. 987–990.
- Bischoff, J.L., and Dickson, F.W., 1975, Sea water-basalt interaction at 200°C and 500 bars—Implications for origin of sea-floor heavy-metal deposits and regulation of sea water chemistry: *Earth and Planetary Science Letters*, v. 25, no. 3, p. 385–397.
- Boström, K., Peterson, M.N.A., Joensuu, O., and Fisher, D.E., 1969, Aluminum-poor ferromanganous sediments on active ocean ridges: *Journal of Geophysical Research*, v. 74, p. 3261–3270.
- Bowers, T.S., and Taylor, H.P., Jr., 1985, An integrated chemical and stable-isotope model of the origin of midocean ridge hot spring systems: *Journal of Geophysical Research*, v. 90, p. 12583–12606.
- Corliss, J.B., 1971, The origin of metal-bearing submarine hydrothermal solutions: *Journal of Geophysical Research*, v. 76, p. 8128–8138.
- Craddock, P.R., Tivey, M.K., Seewald, J.S., Rouxel, O., and Bach, W., 2007, The role of magmatic volatile input, near-surface seawater entrainment and sulfide deposition in regulating metal concentrations within Manus Basin hydrothermal systems [abs.]: EOS, Transactions, American Geophysical Union, v. 88, no. 52, Fall meeting supplement, abstract V34B-05.
- de Ronde, C.E.J., 1995, Fluid chemistry and isotopic characteristics of seafloor hydrothermal systems and associated VMS deposits—Potential for magmatic contributions, in Thompson, J.F.H., ed., *Magmas, fluids and ore deposits*: Ottawa, Ontario, Mineralogical Association of Canada Short Course Series, v. 23, p. 479–510.
- Dixon, J.E., Clague, D.A., and Stolper, E.M., 1991, Degasing history of water, sulfur, and carbon in submarine lavas from Kilauea Volcano, Hawaii: *Journal of Geology*, v. 99, p. 371–394.
- Dixon, J.E., Stolper, E., and Delaney, J.R., 1988, Infrared spectroscopic measurements of CO₂ and H₂O in Juan de Fuca Ridge basaltic glasses: *Earth and Planetary Science Letters*, v. 90, p. 87–104.
- Fehn, U., and Cathles, L.M., 1979, Hydrothermal convection at slow-spreading mid-ocean ridges, in Francheteau, J., ed., *Tectonophysics*: Amsterdam, Elsevier, p. 239–260.
- Galley, A.G., Hannington, M.D., and Jonasson, I.R., 2007, Volcanogenic massive sulphide deposits, in Goodfellow, W.D., ed., *Mineral deposits of Canada—A synthesis of major deposit-types, district metallogeny, the evolution of geological provinces, and exploration methods*: Geological Association of Canada, Mineral Deposits Division, Special Publication 5, p. 141–161.
- Galley, A.G., and Koski, R.A., 1999, Setting and characteristics of ophiolite-hosted volcanogenic massive sulfide deposits, in Barrie, C.T., and Hannington, M.D., *Volcanic-associated massive sulfide deposits—Processes and examples in modern and ancient settings*: Reviews in Economic Geology, v. 8, p. 221–246.
- Gamo, T., Okamura, K., Charlou, J.-L., Urabe, T., Auzende, J.-M., Ishibashi, J., Shitashima, K., and Chiba, H., 1997, Acidic and sulfate-rich hydrothermal fluids from the Manus back-arc basin, Papua New Guinea: *Geology*, v. 25, no. 2, p. 139–142.
- Giggenbach, W.F., 1992, Isotopic shifts in waters from geothermal and volcanic systems along convergent plate boundaries and their origin: *Earth and Planetary Science Letters*, v. 113, p. 495–510.
- Glasby, G.P., Iizasa, K., Hannington, M., Kubota, H., and Notsu, K., 2008, Mineralogy and composition of Kuroko deposits from northeastern Honshu and their possible modern analogues from the Izu-Ogasawara (Bonin) Arc south of Japan—Implications for mode of formation: *Ore Geology Reviews*, v. 34, no. 4, p. 547–560.
- Hannington, M.D., de Ronde, C.E.J., and Petersen, S., 2005, Sea-floor tectonics and submarine hydrothermal systems, in Hedenquist, J.W., Thompson, J.F.H., Goldfarb, R.J., and Richards, J.P., eds., *Economic Geology 100th anniversary volume 1905–2005*: Littleton, Colo., Society of Economic Geologists, p. 111–141.
- Helgeson, H.C., 1969, Thermodynamics of hydrothermal systems at elevated temperatures and pressures: *American Journal of Science*, v. 267, p. 729–804.

- Herzig, P.M., Hannington, M.D., and Arribas, A., Jr, 1998, Sulfur isotopic composition of hydrothermal precipitates from the Lau back-arc—Implications for magmatic contributions to seafloor hydrothermal systems: *Mineralium Deposita*, v. 33, p. 226–237.
- Holland, H.D., 1965, Some applications of thermochemical data to problems of ore deposits—Part 2. Mineral assemblages and the composition of ore forming fluids: *Economic Geology*, v. 60, p. 1101–1166.
- Humphris, S.E., Herzig, P.M., Miller, D.J., Alt, J.C., Becker, K., Brown, D., Brugmann, G., Chiba, H., Fouquet, Y., Gemmell, J.B., Guerin, G., Hannington, M.D., Holm, N.G., Honnorez, J.J., Iturrino, G.J., Knott, R., Ludwig, R., Nakamura, K., Petersen, S., Reysenbach, A.L., Rona, P.A., Smith, S., Sturz, A.A., Tivey, M.K., and Zhao, X., 1995, The internal structure of an active sea-floor massive sulphide deposit: *Nature*, v. 377, no. 6551, p. 713–716.
- Huston, D.L., 1999, Stable isotopes and their significance for understanding the genesis of volcanic-hosted massive sulfide deposits—A review, in Barrie, C.T., and Hannington, M.D., eds., *Volcanic-associated massive sulfide deposits—Processes and examples in modern and ancient settings: Reviews in Economic Geology*, v. 8, p. 157–179.
- Janecky, D.R., and Seyfried, W.E., Jr., 1984, Formation of massive sulfide deposits on oceanic ridge crests—Incremental reaction models for mixing between hydrothermal solutions and seawater: *Geochimica et Cosmochimica Acta*, v. 48, p. 2723–2738.
- Janecky, D.R., and Shanks, W.C., III, 1988, Computational modeling of chemical and sulfur isotopic reaction processes in seafloor hydrothermal systems—Chimneys, mounds, and subjacent alteration zones: *Canadian Mineralogist*, v. 26, p. 805–825.
- Johnson, J.W., Oelkers, E.H., and Helgeson, H.C., 1992, SUPCRT92—A software package for calculating the standard molal thermodynamic properties of minerals, gases, aqueous species, and reactions from 1-bar to 5000-bar and 0°C to 1000°C: *Computers and Geosciences*, v. 18, no. 7, p. 899–947.
- Kadko, D., Baross, J., and Alt, J.C., 1995, The magnitude and global implications of hydrothermal flux, in Humphris, S.E., Zierenberg, R.A., Mullineaux, L.S., and Thomson, R.E., eds., *Seafloor hydrothermal systems—Physical, chemical, biological, and geological interactions: Washington, D.C., American Geophysical Union*, p. 446–466.
- Kelley, D.S., Baross, J.A., and Delaney, J.R., 2002, Volcanoes, fluids, and life at mid-ocean ridge spreading centers: *Annual Review of Earth and Planetary Sciences*, v. 30, p. 385–491.
- Large, R.R., 1977, Chemical evolution and zonation of massive sulfide deposits in volcanic terrains: *Economic Geology*, v. 72, p. 549–572.
- Lilley, M.D., De Angelis, M.A., and Gordon, L.I., 1982, CH₄, H₂, CO and N₂O in submarine hydrothermal vent waters: *Nature*, v. 300, p. 48–50.
- Lowell, R.P., Crowell, B.W., Lewis, K.C., and Liu, L., 2008, Modeling multiphase, multicomponent processes at oceanic spreading centers, in Lowell, R.P., Seewald, J.S., Matexas, A., and Perfit, M.R., eds., *Magma to microbe—Modeling hydrothermal processes at ocean spreading centers: American Geophysical Union, Geophysical Monograph Series 178*, p. 15–44.
- Lowell, R.P., and Rona, P.A., 1985, Hydrothermal models for the generation of massive sulfide ore deposits: *Journal of Geophysical Research*, v. 90, p. 8769–8783.
- Lydon, J.W., 1996, Characteristics of volcanogenic massive sulfide deposits—Interpretations in terms of hydrothermal convection systems and magmatic hydrothermal systems: *Instituto Tecnológico Geominero de España, Boletín Geológico y Minero*, v. 107, no. 3–4, p. 15–64.
- Mottl, M., and Holland, H.D., 1978, Chemical exchange during hydrothermal alteration of basalt by seawater—Part I. Experimental results for major and minor components of seawater: *Geochimica et Cosmochimica Acta*, v. 42, p. 1103–1115.
- Mountain, B.W., and Seward, T.M., 2003, Hydrosulfide/sulfide complexes of copper(I)—Experimental confirmation of the stoichiometry and stability of Cu(HS)₂ to elevated temperatures: *Geochimica et Cosmochimica Acta*, v. 67, p. 3005–3014.
- Muehlenbachs, K., and Clayton, R.N., 1971, Oxygen isotope ratios of submarine diorites and their constituent minerals: *Canadian Journal of Earth Sciences*, v. 8, no. 12, p. 1591–1595.
- Muehlenbachs, K., and Clayton, R.N., 1972, Oxygen isotope geochemistry of submarine greenstones: *Canadian Journal of Earth Sciences*, v. 9, no. 5, p. 471–478.
- Muehlenbachs, K., and Clayton, R.N., 1976, Oxygen isotope composition of the oceanic crust and its bearing on seawater: *Journal of Geophysical Research*, v. 81, p. 4365–4369.
- Ohmoto, H., Mizukami, M., Drummond, E., Eldridge, C.S., Pisutha-Arnonda, V., and Lenagh, T.C., 1983, Chemical processes of Kuroko formation, in Ohmoto, H., and Skinner, B., eds., *The Kuroko and related volcanogenic massive sulfide deposits: Economic Geology Monograph 5*, p. 570–604.

- Ono, S., Shanks, W.C., III, Rouxel, O.J., and Rumble, D., 2007, S-33 constraints on the seawater sulfate contribution in modern seafloor hydrothermal vent sulfides: *Geochimica et Cosmochimica Acta*, v. 71, p. 1170–1182.
- Peter, J.M., and Scott, S.D., 1999, Windy Craggy, northwestern British Columbia—The world's largest Besshi-type deposit, in Barrie, C.T., and Hannington, M.D., eds., *Volcanic-associated massive sulfide deposits—Processes and examples in modern and ancient settings: Reviews in Economic Geology*, v. 8, p. 261–295.
- Reed, M.H., 1982, Calculation of multicomponent chemical equilibria and reaction processes involving minerals, gases and an aqueous phase: *Geochimica et Cosmochimica Acta*, v. 46, p. 513–528.
- Reed, M.H., and Palandri, J., 2006, Sulfide mineral precipitation from hydrothermal fluids, in Vaughan, D.J., ed., *Sulfide mineralogy and geochemistry: Mineralogical Society of America, Reviews in Mineralogy and Geochemistry* 61, p. 609–631.
- Reeves, E.P., Seewald, J.S., Saccocia, P., Bach, W., Craddock, P.R., Shanks, W.C., Sylva, S.P., Walsh, E., Pichler, T., and Rosner, M., 2011, Geochemistry of hydrothermal fluids from the PACMANUS, Northeast Pual and Vienna Woods hydrothermal fields, Manus Basin, Papua New Guinea: *Geochimica et Cosmochimica Acta*, v. 75, p. 1088–1123.
- Resing, J.A., Lebon, G., Baker, E.T., Lupton, J.E., Embley, R.W., Massoth, G.J., Chadwick, W.W., Jr., and de Ronde, C.E.J., 2007, Venting of acid-sulfate fluids in a high-sulfidation setting at NW Rota-1 submarine volcano on the Mariana Arc: *Economic Geology*, v. 102, no. 6, p. 1047–1061.
- Ridley, W.I., Perfit, M.R., Jonasson, I.R., and Smith, M.F., 1994, Hydrothermal alteration in oceanic ridge volcanics—A detailed study at the Galapagos fossil hydrothermal field: *Geochimica et Cosmochimica Acta*, v. 58, p. 2477–2494.
- Rye, R.O., 1993, The evolution of magmatic fluids in the epithermal environment—The stable isotope perspective: *Economic Geology*, v. 88, p. 733–753.
- Sawkins, F.J., and Kowalik, J., 1981, The source of ore metals at Buchans—Magmatic versus leaching models, in Swanson, E.A., Strong, D.F., and Thurlow, J.G., eds., *The Buchans Orebodies—Fifty years of geology and mining: Geological Association of Canada, Special Paper* 22, p. 255–267.
- Schardt, C., and Large, R.R., 2009, New insights into the genesis of volcanic-hosted massive sulfide deposits on the seafloor from numerical modeling studies: *Ore Geology Reviews*, v. 35, p. 333–351.
- Seyfried, W.E., Jr., and Bischoff, J.L., 1977, Hydrothermal transport of heavy metals by seawater—The role of seawater/basalt ratio: *Earth and Planetary Science Letters*, v. 34, no. 1, p. 71–77.
- Seyfried, W.E., Jr., and Bischoff, J.L., 1981, Experimental seawater-basalt interaction at 300°C, 500 bars, chemical exchange, secondary mineral formation and implications for the transport of heavy metals: *Geochimica et Cosmochimica Acta*, v. 45, p. 135–149.
- Seyfried, W.E., Jr., Ding, K., and Rao, B., 2002, Experimental calibration of metastable plagioclase-epidote-fluid equilibria at elevated temperatures and pressures—Applications to the chemistry of hydrothermal fluids at mid-ocean ridges, in Hellman, R., and Wood, S.A., eds., *Water-rock interactions, ore deposits and environmental geochemistry—A tribute to David A. Crerar: San Antonio, Tex., The Geochemical Society Special Publication* no. 7, p. 258–278.
- Seyfried, W.E., Jr., Foustoukos, D.I., and Allen, D.E., 2004, Ultramafic-hosted hydrothermal systems at mid-ocean ridges—Chemical and physical controls on pH, redox carbon reduction reactions: *American Geophysical Union, Geophysical Monograph* 148, p. 267–284.
- Seyfried, W.E., Jr., and Shanks, W.C., III, 2004, Alteration and mass transport in mid-ocean ridge hydrothermal systems—Controls on the chemical and isotopic evolution of high-temperature crustal fluids, in Davis, E.E., and Elderfield, H., eds., *Hydrogeology of the oceanic lithosphere: Cambridge, Cambridge University Press*, p. 451–494.
- Shanks, W.C., III, 2001, Stable isotopes in seafloor hydrothermal systems—Vent fluids, hydrothermal deposits, hydrothermal alteration, and microbial processes, in Valley, J.W., and Cole, D.R., eds., *Stable isotope geochemistry: Reviews in Mineralogy and Geochemistry*, v. 43, p. 469–525.
- Shanks, W.C., III, and Bischoff, J.L., 1980, Geochemistry, sulfur isotope composition, and accumulation rates of Red Sea geothermal deposits: *Economic Geology*, v. 75, p. 445–459.
- Shanks, W.C., III, Böhlke, J.K., and Seal, R.R., 1995, Stable isotopes in mid-ocean ridge hydrothermal systems—Interactions between fluids, minerals and organisms, in Humphris, S.E., Zierenberg, R.A., Mullineaux, L.S., and Thompson, R.E., eds., *Seafloor hydrothermal systems—Physical, chemical, biological, and geological interactions: American Geophysical Union, Geophysical Monograph* 91, p. 194–221.
- Shaw, A.M., Hauri, E.H., Fischer, T.P., Hilton, D.R., and Kelley, K.A., 2008, Hydrogen isotopes in Mariana arc melt inclusions—Implications for subduction dehydration and the deep-Earth water cycle: *Earth and Planetary Science Letters*, v. 275, p. 138–145.

- Singer, D.A., 1995, World-class base and precious metal deposits—A quantitative analysis: *Economic Geology*, v. 90, p. 88–104.
- Solomon, M., 2008, Brine pool deposition for the Zn-Pb-Cu massive sulphide deposits of the Bathurst mining camp, New Brunswick, Canada—Part I. Comparisons with the Iberian pyrite belt: *Ore Geology Reviews*, v. 33, p. 329–351.
- Solomon, M., Gemmel, J.B., and Zaw, K., 2004, Nature and origin of the fluids responsible for forming the Hellyer Zn-Pb-Cu, volcanic-hosted massive sulfide deposit, Tasmania, using fluid inclusions, and stable and radiogenic isotopes: *Ore Geology Reviews*, v. 25, p. 89–124.
- Spooner, E.T.C., 1977, Hydrodynamic model for the origin of the ophiolite cupriferous pyrite ore deposits of Cyprus, in *Volcanic Processes in Ore Genesis*, London, 21–22 January 1976, Proceedings: Geological Society of London–Volcanic Studies Group, Institution of Mining and Metallurgy, Geological Society of London Special Publication, p. 58–71.
- Stanton, R.L., 1984, Investigations of the Appalachian-Caledonide ore province and their influence on the development of stratiform ore genesis theory—A short historical review: *Economic Geology*, v. 79, p. 1428–1441.
- Stefansson, A., and Seward, T.M., 2004, Gold(I) complexing in aqueous sulphide solutions to 500°C at 500 bar: *Geochimica et Cosmochimica Acta*, v. 68, p. 4121–4143.
- Symonds, R., Gerlach, T., and Reed, M., 2001, Magmatic gas scrubbing—Implications for volcano monitoring: *Journal of Volcanology and Geothermal Research*, v. 108, p. 303–341.
- Taran, Y.A., Hedenquist, J.W., Korzhinsky, M.A., Tkachenko, S.I., and Shmulovich, K.I., 1995, Geochemistry of magmatic gases from Kudryavy volcano, Iturup, Kuril Islands: *Geochimica et Cosmochimica Acta*, v. 59, p. 1749–1761.
- Tolstoy, M., Waldhauser, F., Bohnenstiehl, D.R., Weekly, R.T., and Kim, W.-Y., 2008, Seismic identification of along-axis hydrothermal flow on the East Pacific Rise: *Nature*, v. 451, p. 181–185.
- Tornos, F., Solomon, M., Conde, C., and Spiro, B.F., 2008, Formation of the Tharsis massive sulfide deposit, Iberian Pyrite Belt—Geological, lithogeochemical, and stable isotope evidence for deposition in a brine pool: *Economic Geology*, v. 103, p. 185–214.
- Turner, J.S., and Gustafson, L.B., 1978, The flow of hot saline solutions from vents in the seafloor—Some implications for exhalative massive sulfide and other ore deposits: *Economic Geology*, v. 73, p. 1082–1100.
- Urabe, T., and Marumo, K., 1991, A new model for Kuroko-type deposits of Japan: *Episodes*, v. 14, p. 246–268.
- Von Damm, K.L., 1995, Temporal and compositional diversity in seafloor hydrothermal fluids: *Reviews of Geophysics*, v. 33, Supplement Part 2, p. 1297–1305.
- Von Damm, K.L., Buttermore, L.G., Oosting, S.E., Bray, A.M., Fornari, D.J., Lilley, M.D., and Shanks, W.C., III, 1997, Direct observation of the evolution of a seafloor “black smoker” from vapor to brine: *Earth and Planetary Science Letters*, v. 149, no. 1–4, p. 101–111.
- Von Damm, K.L., Lilley, M.D., Shanks, W.C., III, Brockington, M., Bray, A.M., O’Grady, K.M., Olson, E., Graham, A., Proskurowski, G., Collier, R., Cowen, J., Haymon, R., Tivey, M.K., Fornari, D., Nakamura, K., McLaughlin-West, E., Shank, T., Kaye, J., Hobson, J., Sarrazin, J., Sparrow, M., Hubbard, D., McGee, D., Brinson, S., and Cushman, B., 2003, Extraordinary phase separation and segregation in vent fluids from the southern East Pacific Rise: *Earth and Planetary Science Letters*, v. 206, no. 3–4, p. 365–378.
- Von Damm, K.L., Oosting, S.E., Kozłowski, R., Buttermore, L.G., Colodner, D.C., Edmonds, H.N., Edmond, J.M., and Grebmeier, J.M., 1995, Evolution of east pacific rise hydrothermal vent fluids following a volcanic eruption: *Nature*, v. 375, no. 6526, p. 47–50.
- Williams-Jones, A.E., and Heinrich, C.A., 2005, Vapor transport of metals and the formation of magmatic-hydrothermal ore deposits: *Economic Geology*, v. 100, p. 1287–1312.
- Yang, K., and Scott, S.D., 1996, Possible contribution of a metal-rich magmatic fluid to a seafloor hydrothermal system: *Nature*, v. 383, p. 420–423.
- Yang, K., and Scott, S.D., 2002, Magmatic degassing of volatiles and ore metals into a hydrothermal system on the modern sea floor of the Eastern Manus Back-Arc Basin, Western Pacific: *Economic Geology*, v. 97, p. 1079–1100.
- Yang, K., and Scott, S.D., 2003, Geochemical relationships of felsic magmas to ore metals in massive sulfide deposits of the Bathurst mining camp, Iberian Pyrite Belt, Hokuroko district and the Abitibi Belt, in Goodfellow, W.D., McCutcheon, S.R., and Peter, J.M., eds., *Massive sulfide deposits of the Bathurst mining camp, New Brunswick, and northern Maine*: *Economic Geology Monograph 11*, p. 457–478.
- Yang, K., and Scott, S.D., 2006, Magmatic fluids as a source of metals in seafloor hydrothermal systems, in Christie, D.M., ed., *Back-arc spreading systems—Geological, biological, chemical, and physical interactions*: *American Geophysical Union, Geophysical Monograph Series 166*, p. 163–184.

- Zierenberg, R.A., Fouquet, Y., Miller, D.J., Bahr, J.M., Baker, P.A., Bjerksgarden, T., Brunner, C.A., Duckworth, R.C., Gable, R., Gieskes, J.M., Goodfellow, W.D., Groeschel-Becker, H.M., Guerin, G., Ishibashi, J., Iturrino, G.J., James, R.H., Lackschewitz, K.S., Marquez, L.L., Nehlig, P., Peter, J.M., Rigsby, C.A., Schultheiss, P.J., Shanks, W.C., III, Simoneit, B.R.T., Summit, M., Teagle, D.A.H., Urbat, M., and Zuffa, G.G., 1998, The deep structure of a sea-floor hydrothermal deposit: *Nature*, v. 392, no. 6675, p. 485–488.
- Zierenberg, R.A., and Shanks, W.C., III, 1986, Isotopic constraints on the origin of the Atlantis II, Suakin and Valdivia brines, Red Sea: *Geochimica et Cosmochimica Acta*, v. 50, p. 2205–2214.

19. Exploration-Resource Assessment Guides

By John F. Slack

19 of 21

Volcanogenic Massive Sulfide Occurrence Model

Scientific Investigations Report 2010–5070–C

U.S. Department of the Interior
U.S. Geological Survey

U.S. Department of the Interior
KEN SALAZAR, Secretary

U.S. Geological Survey
Marcia K. McNutt, Director

U.S. Geological Survey, Reston, Virginia: 2012

For more information on the USGS—the Federal source for science about the Earth, its natural and living resources, natural hazards, and the environment, visit <http://www.usgs.gov> or call 1-888-ASK-USGS.

For an overview of USGS information products, including maps, imagery, and publications, visit <http://www.usgs.gov/pubprod>

To order this and other USGS information products, visit <http://store.usgs.gov>

Any use of trade, product, or firm names is for descriptive purposes only and does not imply endorsement by the U.S. Government.

Although this report is in the public domain, permission must be secured from the individual copyright owners to reproduce any copyrighted materials contained within this report.

Suggested citation:

Slack, J.F., 2012, Exploration-resource assessment guides in volcanogenic massive sulfide occurrence model: U.S. Geological Survey Scientific Investigations Report 2010-5070-C, chap. 19, 10 p.

Contents

| | |
|---|-----|
| Geological | 309 |
| Geochemical..... | 309 |
| Isotopic | 311 |
| Geophysical | 311 |
| Attributes Required for Inclusion in Permissive Tracts at Various Scales | 312 |
| Factors Influencing Undiscovered Deposit Estimates (Deposit Size and Density) | 312 |
| References Cited..... | 313 |

19. Exploration-Resource Assessment Guides

By John F. Slack

Geological

A variety of geological guides may be used in mineral exploration and resource assessments for VMS deposits. Detailed geological maps clearly provide the critical framework. For regions lacking known deposits, a first-order guide is the age of the volcanosedimentary sequence relative to the ages of sequences elsewhere in the world that contain significant VMS mineralization. The database of Franklin and others (2005) shows time periods in the geologic record during which appreciable tonnages of VMS deposits formed (fig. 4–4). Using these age-based data, globally in the Precambrian major VMS mineralization took place 2.75–2.65 Ga, 2.05–1.85 Ga, and 1.00–0.65 Ga (see also Huston and others, 2010). Volcanosedimentary terranes with ages outside of these time periods, including >3.25 Ga, 2.65–2.00 Ga, and 1.85–1.00 Ga, are less likely to contain large (>30 Mt) deposits. Such gaps in the secular distribution of Precambrian VMS deposits, if not artifacts of erosion or inadequate age control, reflect the evolution of fundamental crustal processes on Earth, especially plate tectonics and related assembly of major continental land masses (see Groves and others, 2005; Condie and others, 2009; Huston and others, 2010). During the Phanerozoic, the greatest tonnages of VMS deposits formed mainly 500–300 Ma (Late Cambrian–Late Carboniferous); no lengthy periods (>50 m.y.) are known that lack significant VMS deposits. Few deposits less than 15 Ma (Middle Miocene) occur on land (Franklin and others, 2005; Mosier and others, 2009), a result of limited obduction of younger marine volcanosedimentary sequences onto the continents.

Within sequences that contain known deposits, key guides are (1) favorable marine volcanosedimentary units including felsic or mafic lavas or tuffs, coarse breccias, and rhyolite domes that host mineralization within the same belt (Lydon, 1996); (2) VMS-type prospects or occurrences including stratabound sulfides and discordant veins; (3) exhalites, especially those containing barite and (or) high concentrations of Cu, Zn, or Pb (Spry and others, 2000); (4) synvolcanic structures such as growth faults, calderas, and fault intersections, which may have focused fluid flow and localized sulfide mineralization; (5) local fine-grained, highly carbonaceous or graphitic sedimentary rocks that record breaks in volcanism and in most cases indicate coeval anoxic or sulfidic bottom

waters that prevented seafloor weathering and oxidation of sulfides (Goodfellow and others, 2003); (6) large synvolcanic sills and (or) dikes, which typically occur in the stratigraphic footwall of the deposits, having served as sources of heat to drive the hydrothermal systems (Galley, 1993); (7) abundant chlorite or white mica and their metamorphosed equivalents (including Al-rich minerals), as evidence of VMS-type alteration (for example, Galley and others, 2007); and (8) abundant tourmaline and (or) gahnite (Slack, 1982; Spry and Scott, 1986; Huston and Patterson, 1995). Bonnet and Corriveau (2007) described the diagnostic mineralogy of metamorphosed alteration zones of VMS deposits, highlighting differences in greenschist-facies versus granulite-facies terranes. In the latter settings, which are dominated by gneisses, diagnostic minerals—where not affected by retrograde metamorphism—may include cordierite, diopside, orthopyroxene, garnet, K-feldspar, biotite, and Al-silicates especially kyanite and sillimanite.

Geochemical

Geochemically-based guides for VMS exploration and assessment can be divided into categories that focus on the following sample media: (1) rocks, (2) minerals, (3) stream sediments and heavy mineral concentrates, (4) glacial till, (5) lake sediments, (6) waters, and (7) soils and soil gases. The greatest effort probably has been directed towards rock geochemistry, involving searches for elevated contents of base and precious metals and for favorable indicators of VMS-type hydrothermal alteration. Igneous rocks within prospective belts typically have geochemical signatures that reflect formation in diverse geodynamic settings, including oceanic spreading ridges, rifted arcs and back-arcs, and rifted continental margins. Dominant is tholeiitic to transitional bimodal magmatism; alkaline and peralkaline volcanic rocks are rare by comparison (for example, Piercey, 2007). Within Precambrian terranes, favorable settings for VMS deposits include, but are not limited to, high-temperature rhyolites that have diagnostic compositions including high Zr (>300 ppm), Y/Zr ratios <7, negative Eu anomalies (chondrite-normalized basis [CN]), (La/Yb)_{CN} ratios <7, and (Gd/Yb)_{CN} ratios <2 (Galley and others, 2007, and references therein). In Phanerozoic terranes, compositions of

felsic (and mafic) igneous rocks associated with VMS deposits vary greatly, depending on whether the setting is petrologically primitive or evolved, and relative to Precambrian terranes are not as definitive (see Piercey, 2009).

Many studies have focused on compositional variations of the sulfide deposits, altered wall rocks, and associated exhalites as possible exploration guides to ore. The metal ratio $100 \text{ Zn}/(\text{Zn} + \text{Pb})$ was used by Huston and Large (1987) in the Mount Read volcanics of Tasmania to distinguish VMS deposits and occurrences from sulfide concentrations produced by other types of mineralization. Geochemical vectors proposed for wall rocks surrounding deposits include the “alteration box plot” of Large and others (2001a), which combines the Ishikawa alteration index, $100 (\text{K}_2\text{O} + \text{MgO})/(\text{K}_2\text{O} + \text{MgO} + \text{Na}_2\text{O} + \text{CaO})$, with the chlorite-carbonate-pyrite index, $100 (\text{MgO} + \text{FeO})/(\text{MgO} + \text{FeO} + \text{K}_2\text{O})$; increasing values of both parameters reflect the intensity of alteration in which sericite, chlorite, carbonate, and pyrite replace sodic feldspar and glass in volcanic rocks. This scheme may have advantages over previous approaches, such as those based on chemical gains and losses during alteration (for example, Barrett and MacLean, 1994; Leitch and Lentz, 1994), and is best applied to felsic volcanic rocks in concert with mineralogical and textural data on the analyzed samples. More recently, Piché and Jébrak (2004) devised a normative mineral alteration index that is less-sensitive to lithological variations among samples and better identifies ore-related hydrothermal mineral assemblages.

On a regional scale, hydrothermal fluid flow related to VMS mineralization may form distinctive mineral assemblages and mineral compositions that differ from those produced by greenschist-facies metamorphism, in which hydrothermally altered volcanic rocks preferentially contain abundant Fe-rich chlorite, ferroactinolite, and coarse-grained clinozoisite (Hannington and others, 2003). The loss of Na_2O during VMS alteration is a hallmark of this deposit type, occurring mainly in footwall zones, and by itself may be an effective guide to ore (for example, Hashiguchi and others, 1983; Lydon, 1996; Piercey, 2009). Other proposed vectors for altered wall rocks include increases of Tl, Sb, Ba/Sr, $\delta^{34}\text{S}$ values of sulfides, and Mn contents of carbonate towards ore (Large and others, 2001b, and references therein). Lentz (2005) summarized the use of Hg as an exploration guide. Another possible vector is variations in mineralogy and mineral chemistry in wall rocks caused by sulfide-oxide-silicate equilibria produced during metamorphism of the deposits. This process and its exploration applications were first described in detail by Nesbitt and Kelley (1980) and later amplified by Spry (2000), who highlighted the haloes and proportions of Mg- and (or) Zn-rich silicates and Zn-rich oxides that typically increase in intensity with proximity to ore. Compositions of minerals that formed during VMS and later superimposed metamorphic processes have been the focus of many topical studies, including tourmaline (Taylor and Slack, 1984; Griffin and others, 1996), Zn-rich staurolite (Heimann and others, 2005, and references therein), rutile (Clark and Williams-Jones, 2004), and magnetite (Beaudoin and others,

2007;). The presence of high gold concentrations in some deposits was studied by Hannington and Scott (1989) and Hannington and others (1999), resulting in the recognition of low-Fe sphalerite and certain sulfidation equilibria as guides to Au-rich systems. Some terranes, particularly those dominated by mafic volcanic rocks, may provide an enriched source rock control on the formation of Au-rich VMS deposits (Stolz and Large, 1992).

In some terranes the bulk geochemistry of VMS-related exhalites can be used as vectors to massive sulfide deposits. This approach is best used for exhalites that are exposed in outcrops and (or) drill cores, such that a stratigraphic continuity can be inferred and applied to sampling programs and interpretations of data. In most cases, however, exhalites cannot be traced along strike with confidence, thus limiting their usefulness as direct vectors to VMS deposits. In the Bathurst district of New Brunswick, Canada, exhalites are well exposed at two main stratigraphic levels, both of which have been intersected in numerous drill cores. These exhalites, consisting of different facies of iron formation (sulfide, carbonate, silicate, oxide), served as the focus of detailed mineralogical and geochemical studies of both the Brunswick and Heath Steele belts (Peter and Goodfellow, 1996, 2003; Peter and others, 2003a, b). These studies have produced the most complete databases known for laterally extensive exhalites related to ancient VMS mineralization, and they provide the best framework for evaluating the use of exhalite geochemistry in targeting high-temperature hydrothermal centers and, by inference, massive sulfide orebodies. Based on data for the Heath Steele exhalites, Peter and Goodfellow (2003) constructed a composite diagram showing idealized mineralogical and compositional zonations for proximal to distal settings relative to a single VMS source deposit. Among many identified parameters, some proposed as diagnostic of proximal exhalites (<500 m from massive sulfide) are the presence of chalcopyrite, sphalerite, and (or) galena; high concentrations of Cu, Pb, Zn, Ag, As, Au, Bi, Cd, Hg, In, Sb, Sn, and Tl; and high Fe/Ti, Ba/Ti, and Eu/Eu* ratios where Eu/Eu* is the magnitude of the Eu anomaly. Peter and Goodfellow (2003) used these compositional parameters, together with others (for example, P/Ti), to define a hydrothermal sediment index, which shows the consistently highest values at and near the three largest VMS deposits in the Heath Steele belt. Exhalative jasper related to VMS mineralization in the Løkken district of Norway, which can be traced along strike for 4–6 km, show a pattern in which As/Fe and Sb/Fe ratios increase towards the massive sulfide deposit (Grenne and Slack, 2005). In other terranes where exhalites may not be laterally extensive, favorable indicators of proximity to VMS deposits include the presence of base-metal sulfides (chalcopyrite, sphalerite, galena), elevated contents of trace metals such as Cu, Zn, Pb, and Tl, and positive Eu anomalies (Gale and others, 1997; Peter, 2003). Miller and others (2001) reported on the discovery of the West 45 deposit in Queensland, Australia, which was found in part by identifying a large positive Eu anomaly in a sample of exhalative jasper.

Other sample media have been used with varying success in VMS exploration. Stream sediments constitute parts of many regional-scale exploration and assessment programs, based on the delineation of geochemical anomalies that reflect erosion of sulfide-bearing rock from known deposits (for example, Slack and others, 1990; Telmer and others, 2002; Leybourne and others, 2003). Heavy mineral concentrates have been used less frequently, in part because of the much longer time required to obtain a sample (by panning), and because some sulfides like sphalerite are not mechanically strong and thus rarely survive as large grains for recovery in panned concentrate surveys. Heavy indicator minerals nevertheless may be useful in programs that focus on glacial dispersion trains (Averill, 2001) or on gahnite, spessartine garnet, or other resistant minerals that are common recorders of VMS-type mineralization (Spry and others, 2000). Bulk till geochemistry has been used in exploration programs for over 50 years, being most effective when integrated with surficial geology, especially till stratigraphy and ice flow patterns (for example, McMartin and McClenaghan, 2001); interpretations are constrained by the typically great dilution of deposit-related geochemical signatures by glacial materials and by occurrences of multiple till sheets. Lake sediments have been used in some regional geochemical surveys (McClenaghan and others, 1997); aqueous geochemical methods and applications are summarized by Leybourne (2007). Soil geochemical surveys (for example, Cameron and others, 2004) are generally limited in scope to localized targets that already are delineated by favorable geological features or geophysical anomalies. Comparative studies of conventional bulk versus selective leach methods suggest that the former technique is superior (Hall and others, 2003). Reconnaissance soil surveys have not been as widely used, although some large, unexposed VMS deposits have been found by this approach, such as Bald Mountain in northern Maine (Cummings, 1988). Soil gases have also proven useful because of their mobility in the vadose zone and glacial overburden (McCarthy and others, 1986; Kelley and others, 2006).

Isotopic

Among numerous stable and radiogenic isotopic systems, oxygen isotopes hold the greatest promise for direct application to mineral exploration and resource assessments for VMS deposits (for example, Miller and others, 2001). Oxygen isotope haloes have been delineated around many deposits. In one of the earliest studies, Green and others (1983) documented systematic oxygen isotope variations in part of the Hokuroku district of Japan, finding an overall pattern in which whole-rock $\delta^{18}\text{O}$ values correlate with alteration assemblage, irrespective of precursor lithology; in the footwall of the Fukazawa deposit, the values show a progressive increase of approximately 8 per mil from the outer zeolite zone to the inner chlorite-sericite zone. A similar regionally-based zonation was identified in the West Shasta VMS district of

California by Taylor and South (1985), including the vicinity of a synvolcanic pluton that likely was the heat source that drove the seafloor-hydrothermal system. Comparable results were obtained in regional oxygen isotope studies of the Noranda district in Quebec (Paradis and others, 1993), the Panorama district in Western Australia (Brauhart and others, 2000), the Iberian Pyrite Belt of Spain (Lerouge and others, 2001), and the Sturgeon Lake region of Ontario (Holk and others, 2008). An exception is the Palmeiropolis deposit in Brazil, which lacks an oxygen isotope contrast between hydrothermally altered wall rocks and unaltered host rocks, possibly due to isotopic homogenization during pervasive metamorphic fluid flow (Araujo and others, 1996). Detailed studies of individual feeder zones have confirmed the characteristic patterns described above, such as at the Bruce deposit in Arizona (Larson, 1984) and the Kidd Creek and Geco deposits in Ontario (Huston and others, 1995; Araujo and others, 1996). From exploration and assessment perspectives, detailed whole-rock oxygen isotope studies can define zones of hydrothermal downflow and upflow within a volcanic pile and use the latter upflow zones as a guide to undiscovered deposits in the region (Holk and others, 2008).

Geophysical

A diverse suite of geophysical methods has been used in VMS exploration both on regional and local scales. Ford and others (2007) highlighted the most effective methods, which are electromagnetic, magnetic, electrical, and gravimetric. In regional programs and in areas lacking detailed geologic maps, airborne surveys that combine electromagnetic and magnetic measurements can yield valuable information on geological features that are permissive for the occurrence of VMS deposits, including structures, intrusive bodies, and alteration zones (for example, Keating and others, 2003). Major contrasts in density, magnetism, and electrical conductivity of VMS deposits, relative to their volcanosedimentary host rocks, provide the foundation for these surveys. Many deposits have been discovered during airborne or ground electromagnetic surveys, some of the most notable being the giant Kidd Creek orebody in Ontario (Bleeker and Hester, 1999), the large Heath Steele and Brunswick No. 6 orebodies in New Brunswick (Keating and others, 2003), and the large Crandon deposit in Wisconsin (May and Schmidt, 1982). However, the electromagnetic (EM) method has two major drawbacks: First, that distinct anomalies may also be produced by unmineralized features including sulfide-free carbonaceous or graphitic sedimentary rocks and water-saturated overburden. A second limitation is the difficulty of delineating electromagnetically a Zn-rich deposit because of the poor conductivity of sphalerite relative to other sulfide minerals (Bishop and Emerson, 1999). If not deeply buried, deposits that contain appreciable magnetite or pyrrhotite generate distinctive magnetic anomalies, both from airborne and ground surveys. Magnetic data also can be useful for delineating large subvolcanic intrusions and, by

inference, the locations of undiscovered VMS deposits, based on the premise that such intrusions provide the heat sources that drive stratigraphically higher hydrothermal systems (Galley, 2003; Galley and others, 2007).

Disseminated sulfides such as those in footwall feeder zones can be delineated by induced polarization, which targets sulfide grains that are not electrically connected (Ford and others, 2007). Gravity surveys are especially useful for identifying high-density units such as barite-rich exhalites or Zn-rich massive sulfide that otherwise are poor geophysical targets. Radiometric surveys, typically employed in airborne surveys together with magnetic and EM measurements, involve gamma-ray spectroscopy for K, U, and Th that can improve knowledge of basic geology and delineate K-rich alteration zones that surround many deposits (Chung and Keating, 2002). Geophysical techniques that are less widely used in VMS exploration include electrochemical (Cameron and others, 2004), seismic and high-resolution seismic (Milkereit and others, 1996; Adam and others, 2000), oxidation-reduction and spontaneous potential (Hamilton and others, 2004), and various remote sensing methods (for example, Herrmann and others, 2001).

Attributes Required for Inclusion in Permissive Tracts at Various Scales

A permissive tract in mineral resource assessments is defined as an area where geologic features permit the occurrence of one or more deposit types (for example, Singer, 1993). Favorable geology is the most important attribute for identifying a permissive tract. In assessments for VMS deposits, key geologic criteria include:

- presence of a submarine volcanosedimentary sequence having an age that falls within a time period containing numerous VMS deposits with large aggregate tonnages and base metal contents (fig. 4–4);
- evidence of an extensional geodynamic setting and synvolcanic faulting as reflected in distinctive compositions of volcanic and synvolcanic intrusive rocks;
- presence of coarse volcanic breccias or felsic domes indicating proximity to a volcanic center;
- occurrence of exhalites, especially those containing base-metal sulfides or large positive Eu anomalies;
- evidence of VMS-type alteration zones represented by abundant chlorite or white mica, or their metamorphosed equivalents; and
- occurrence of large subvolcanic sills as heat sources for the hydrothermal systems.

Also critical in tract delineation are locations of known deposits and prospects, if clearly of VMS affinity. Other positive

criteria are anomalously high contents of base metals in stream sediments, presence of abundant indicator minerals such as gahnite or spessartine garnet in panned concentrates, and geophysical data that suggest the occurrence of hydrothermal alteration zones or continuity of favorable units under cover. Previous mineral-resource assessments that use the concept of permissive tracts include those by the U.S. Geological Survey (for example, Cox, 1993; Raines and Mihalasky, 2002) and the British Columbia Geological Survey (Grunsky and others, 1994). Integration of geologic, mineral-occurrence, geochemical, and geophysical data using geographic information systems (GIS) and similar spatial analysis methods provides a robust foundation for assessments (Bonham-Carter and others, 1993; Chung, 2003; Fallara and others, 2006; Nykänen and Ojala, 2007). The importance of mineral prospectivity mapping is discussed by Carranza and Sadeghi (2010), by which the spatial distribution of known VMS deposits in the Skellefte district of Sweden was compared to spatially related geological features, in order to outline recognition criteria for regional-scale VMS prospectivity.

Different map scales can have major influences on the shape and size of permissive tracts. Singer (1993) highlighted the problem of using large-scale geologic maps, which can result in generalization of a given tract, or of arbitrarily enlarging a tract in order to include deposit types that occur in restricted settings. A more detailed analysis of the problem was done by Singer and Menzie (2008), who found that use of more generalized maps tends to favor inclusion of geologic settings that are not permissive for a given deposit type, or of unreported cover sequences with permissive tracts thus producing a misleading appearance of clustered deposits. Singer and Menzie (2008) quantified this problem of map scale by Poisson distribution analysis, showing that, by comparison, a geologic map having twice the detail of a more generalized map will decrease the area of a permissive VMS tract by 50 percent.

Factors Influencing Undiscovered Deposit Estimates (Deposit Size and Density)

Estimates of the size and density of undiscovered mineral deposits are affected by several factors. In one of the earliest studies, Sangster (1980) noted that VMS deposits are characteristically found in clusters, and that for Canadian districts 47 percent of deposits occur in only six clusters (districts). Possible explanations for these clusters of VMS deposits, covering areas averaging 32 km in diameter, include the presence of abundant felsic volcanic rocks and related volcanic centers, and preferential occurrences within inferred submarine calderas (Sangster, 1980). This clustering of deposits was also highlighted by Galley and others (2007), who proposed that the diameter of each group of clustered deposits reflects the extent of regional-scale hydrothermal alteration systems; the

distribution of deposits within each cluster relates to synvolcanic fault distribution above subvolcanic intrusions. In the case of the Noranda district, the areal distribution of VMS deposits corresponds closely to the outlines of hydrothermally altered rocks and the Noranda cauldron (Gibson and Galley, 2007). Caution must be used in applying this caldera-based approach to highly deformed terranes, however, because of deformational effects on original geometry (Hollister, 1980) and, hence, on the related density of undiscovered deposits.

In modern settings, average densities of hydrothermal vent fields range from 1.9 to 6.6 sites per 100-km length (Masoth and others, 2007). This range of densities includes data for the back-arc Valu Fa Ridge, the Tonga and Kermadec arcs, and mid-ocean ridges in the eastern Pacific Ocean. The largest deposits on mid-ocean ridges tend to occur where the spreading rate is slow to intermediate and on the shallowest parts of the ridges; calculations based on heat flux suggest the presence, theoretically, of at least one black smoker vent for every 1 km of ridge length, but their distribution is not uniform and large clusters of black smoker vents occur at much greater spacings of about 50–100 km (Hannington and others, 2005). In ancient settings, deposit spacings are related to a variety of processes, yielding an estimated 5-km diameter for the scale of proximal hydrothermal alteration around each deposit (Galley and others, 2007).

A detailed statistical analysis by Mosier and others (2007) provides the most robust foundation for evaluating the density of undiscovered VMS deposits for a mineral-resource assessment. Their study used frequency distributions of deposit densities for 38 well-explored control areas worldwide. Mosier and others (2007) determined that 90 percent of the control areas have more than 100 VMS deposits per 100,000 km² and that both map scales and sizes of the control areas are predictors of deposit density. Map scales used to delineate permissive tracts also must be considered because they directly affect the spatial and frequency distribution of deposits and thus deposit densities (Singer, 2008; Singer and Menzie, 2008). For mineral-resource assessments, the most detailed geologic maps therefore should be used in order to maximize the knowledge base for VMS experts when estimating the numbers of undiscovered deposits in a given tract.

Estimates of the sizes of undiscovered mineral deposits rely mainly on statistical data for grades and tonnages for a given deposit type (for example, Cox and Singer, 1986). The largest resources of metals typically are contained in a few giant orebodies, hence very small or low-grade deposits do not greatly affect grade-tonnage distributions. Differences in cut-off grades and other economic factors are not significant, having minimal or at most minor influences on these parameters (Singer, 1993). Detailed statistical studies have documented several key relationships among major types of mineral deposits, including VMS: (1) the distribution of tonnages is approximately lognormal, (2) deposit size is inversely correlated with deposit density, (3) the size of the permissive tract and the size of contained deposits is correlated, and (4) the total amount of mineralized rock is proportional to the size of the median

deposit (Singer, 1993, 2008). Relationships derived from statistical studies, including those between sizes of permissive areas and deposit density, can thus be used together with grade-tonnage models as predictors of the number of undiscovered deposits and the total amount of undiscovered metal (Singer, 2008). Also important are craton- and terrane-scale features that likely determine metal endowment, including the occurrence and location of giant and super-giant deposits (Jaireth and Huston, 2010).

References Cited

- Adam, E., Perron, G., Milkereit, B., Wu, J., Calvert, A.J., Salisbury, M., Verpaelst, P., and Dion, D.-J., 2000, A review of high-resolution seismic profiling across the Sudbury, Selbaie, Noranda, and Matagami mining camps: *Canadian Journal of Earth Sciences*, v. 37, p. 503–516.
- Araujo, S.M., Scott, S.D., and Longstaffe, F.J., 1996, Oxygen isotope composition of alteration zones of highly metamorphosed volcanogenic massive sulfide deposits—Geco, Canada, and Palmeirópolis, Brazil: *Economic Geology*, v. 91, p. 697–712.
- Averill, S.A., 2001, The application of heavy indicator mineralogy in mineral exploration with emphasis on base metal indicators in glaciated metamorphic and plutonic terrains, in McClenaghan, M.B., Bobrowsky, P.T., Hall, G.E.M., and Cook, S.J., eds., *Drift exploration in glaciated terrain: Geological Society of London Special Publication 185*, p. 69–81.
- Barrett, T.J., and MacLean, W.H., 1994, Chemostratigraphy and hydrothermal alteration in exploration for VHMS deposits in greenstones and younger volcanic rocks, in Lentz, D.R., ed., *Alteration and alteration processes associated with ore-forming systems: Geological Association of Canada Short Course Notes*, v. 11, p. 433–467.
- Beaudoin, G., Dupuis, C., Gosselin, P., and Jébrak, M., 2007, Mineral chemistry of iron oxides—Application to mineral exploration, in Andrew, C.J., and others, eds., *Digging deeper (v. 1)—Ninth Biennial Meeting of the Society for Geology Applied to Mineral Deposits, Dublin, Ireland, 20–23 August 2007, Proceedings: Dublin, Ireland, Irish Association for Economic Geology*, p. 497–500.
- Bishop, J.R., and Emerson, D.W., 1999, Geophysical properties of zinc-bearing minerals: *Australian Journal of Earth Sciences*, v. 46, p. 311–328.
- Bleeker, W., and Hester, B.W., 1999, Discovery of the Kidd Creek massive sulfide orebody—A historical perspective, in Hannington, M.D., and Barrie, C.T., eds., *The giant Kidd Creek volcanogenic massive sulfide deposit, western Abitibi subprovince, Canada: Economic Geology Monograph 10*, p. 31–42.

- Bonham-Carter, G.F., Reddy, R.K.T., and Galley, A.G., 1993, Knowledge-driven modeling of volcanogenic massive sulphide potential with a geographic information system, *in* Kirkham, R.V., Sinclair, W.D., Thorpe, R.I., and Duke, J.M., eds., *Mineral deposit modeling: Geological Association of Canada, Special Paper 40*, p. 735–749.
- Bonnet, A.-L., and Corriveau, L., 2007, Alteration vectors to metamorphosed hydrothermal systems in gneissic terranes, *in* Goodfellow, W.D., ed., *Mineral deposits of Canada—A synthesis of major deposit-types, district metallogeny, the evolution of geological provinces, and exploration methods: Geological Association of Canada, Mineral Deposits Division, Special Publication No. 5*, p. 1035–1049.
- Brauhart, C.W., Huston, D.L., and Andrew, A.S., 2000, Oxygen isotope mapping in the Panorama VMS district, Pilbara craton, Western Australia—Applications to estimating temperatures of alteration and to exploration: *Mineralium Deposita*, v. 35, p. 727–740.
- Cameron, E.M., Hamilton, S.M., Leybourne, M.I., Hall, G.E.M., and McClenaghan, M.B., 2004, Finding deeply buried deposits using geochemistry: *Geochemistry—Exploration, Environment, Analysis*, v. 4, p. 7–32.
- Carranza, E.J.M., and Sadeghi, M., 2010, Predictive mapping of prospectivity and quantitative estimation of undiscovered VMS deposits in Skellefte district (Sweden): *Ore Geology Reviews*, v. 38, p. 219–241.
- Chung, C.-J., and Keating, P.B., 2002, Mineral potential evaluation based on airborne geophysical data: *Exploration Geophysics*, v. 33, p. 28–34.
- Chung, C.-J.F., 2003, Use of airborne geophysical surveys for constructing mineral potential maps, *in* Goodfellow, W.D., McCutcheon, S.R., and Peter, J.M., eds., *Volcanogenic massive sulfide deposits of the Bathurst mining camp, New Brunswick, and northern Maine: Economic Geology Monograph 11*, p. 879–891.
- Clark, J.R., and Williams-Jones, A.E., 2004, Rutile as a potential indicator mineral for metamorphosed metallic ore deposits: Montreal, Diversification de L'Exploration Minérale au Québec, Sous-projet SC2 final report, 17 p., accessed October 5, 2010, at <http://www.divex.ca/projets/doc/SC2-Williams-Jones-2004.pdf>.
- Condie, K.C., O'Neill, C., and Aster, R.C., 2009, Evidence and implications for a widespread magmatic shutdown for 250 My on Earth: *Earth and Planetary Science Letters*, v. 282, p. 294–298.
- Cox, D.P., 1993, Estimation of undiscovered deposits in quantitative mineral resource assessments—Examples from Venezuela and Puerto Rico: *Natural Resources Research*, v. 2, p. 82–91.
- Cox, D.P., and Singer, D.A., 1986, eds., *Mineral deposit models: U.S. Geological Survey Bulletin 1693*, 379 p.
- Cummings, J.S., 1988, *Geochemical detection of volcanogenic massive sulphides in humid-temperate terrain: Bangor, Maine*, J.S. Cummings, Inc., 298 p.
- Dupuis, C., and Beaudoin, G., 2011, Discriminant diagrams for iron oxide trace element fingerprinting of mineral deposit types: *Mineralium Deposita*, v. 46, p. 319–335.
- Fallara, F., Legault, M., and Rabeau, O., 2006, 3-D integrated geological modeling in the Abitibi subprovince (Québec, Canada)—Techniques and applications: *Exploration and Mining Geology*, v. 15, p. 27–41.
- Ford, K., Keating, P., and Thomas, M.D., 2007, Overview of geophysical signatures associated with Canadian ore deposits, *in* Goodfellow, W.D., ed., *Mineral deposits of Canada—A synthesis of major deposit-types, district metallogeny, the evolution of geological provinces, and exploration methods: Geological Association of Canada, Mineral Deposits Division, Special Publication 5*, p. 939–970.
- Franklin, J.M., Gibson, H.L., Jonasson, I.R., and Galley, A.G., 2005, Volcanogenic massive sulfide deposits, *in* Hedenquist, J.W., Thompson, J.F.H., Goldfarb, R.J., and Richards, J.P., eds., *Economic Geology 100th anniversary volume, 1905–2005: Littleton, Colo., Society of Economic Geologists*, p. 523–560.
- Gale, G.H., Dabek, L.B., and Fedikow, M.A.F., 1997, The application of rare earth element analyses in the exploration for volcanogenic massive sulfide type deposits: *Exploration and Mining Geology*, v. 6, p. 233–252.
- Galley, A.G., 1993, Characteristics of semi-conformable alteration zones associated with volcanogenic massive sulphide districts: *Journal of Geochemical Exploration*, v. 48, p. 175–200.
- Galley, A.G., 2003, Composite synvolcanic intrusions associated with Precambrian VMS-related hydrothermal systems: *Mineralium Deposita*, v. 38, p. 443–473.
- Galley, A.G., Hannington, M., and Jonasson, I., 2007, Volcanogenic massive sulphide deposits, *in* Goodfellow, W.D., ed., *Mineral deposits of Canada—A synthesis of major deposit-types, district metallogeny, the evolution of geological provinces, and exploration methods: Geological Association of Canada, Mineral Deposits Division, Special Publication 5*, p. 141–161.

- Gibson, H.L., and Galley, A.G., 2007, Volcanogenic massive sulphide deposits of the Archean, Noranda district, Québec, *in* Goodfellow, W.D., ed., *Mineral deposits of Canada—A synthesis of major deposit-types, district metallogeny, the evolution of geological provinces, and exploration methods*: Geological Association of Canada, Mineral Deposits Division, Special Publication 5, p. 533–552.
- Goodfellow, W.D., Peter, J.M., Winchester, J.A., and van Staal, C.R., 2003, Ambient marine environment and sediment provenance during formation of massive sulfide deposits in the Bathurst mining camp—Importance of reduced bottom waters to sulfide precipitation and preservation, *in* Goodfellow, W.D., McCutcheon, S.R., and Peter, J.M., eds., *Volcanogenic massive sulfide deposits of the Bathurst mining camp, New Brunswick, and northern Maine*: Economic Geology Monograph 11, p. 129–156.
- Green, G.R., Ohmoto, H., Date, J., and Takahashi, T., 1983, Whole-rock oxygen isotope distribution in the Fukazawa-Kosaka area, Hokuroku district, Japan, and its potential application to mineral exploration, *in* Ohmoto, H., and Skinner, B.J., eds., *The Kuroko and related volcanogenic massive sulfide deposits*: Economic Geology Monograph 5, p. 395–411.
- Grenne, T., and Slack, J.F., 2005, Geochemistry of jasper beds from the Ordovician Løkken ophiolite, Norway—Origin of proximal and distal siliceous exhalites: *Economic Geology*, v. 100, p. 1511–1527.
- Griffin, W.L., Slack, J.F., Ramsden, A.R., Win, T.T., and Ryan, C.G., 1996, Trace elements in tourmalines from massive sulfide deposits and tourmalinites—Geochemical controls and exploration applications: *Economic Geology*, v. 91, p. 657–675.
- Groves, D.I., Vielreicher, R.M., Goldfarb, R.J., and Condie, K.C., 2005, Controls on the heterogeneous distribution of mineral deposits through time, *in* MacDonald, I., Boyce, A.J., Butler, I.B., Herrington, R.J., and Polya, D., eds., *Mineral deposits and earth evolution*: Geological Society of London Special Publication 248, p. 71–101.
- Grunsky, E.C., Kilby, W.E., and Massey, N.W.D., 1994, Mineral resource assessment in British Columbia: *Natural Resources Research*, v. 3, p. 271–283.
- Hall, G.E.M., Parkhill, M.A., and Bonham-Carter, G.F., 2003, Conventional and selective leach geochemical exploration methods applied to humus and B horizon soil overlying the Restigouche VMS deposit, Bathurst mining camp, New Brunswick, *in* Goodfellow, W.D., McCutcheon, S.R., and Peter, J.M., eds., *Massive sulfide deposits of the Bathurst mining camp, New Brunswick, and northern Maine*: Economic Geology Monograph 11, p. 763–782.
- Hamilton, S.M., Cameron, E.M., McClenaghan, M.B., and Hall, G.E.M., 2004, Redox, pH and SP variation over mineralization in thick glacial overburden—Part II. Field investigation at Cross Lake VMS property: *Geochemistry—Exploration, Environment, Analysis*, v. 4, p. 45–58.
- Hannington, M.D., de Ronde, C.E.J., and Petersen, S., 2005, Sea-floor tectonics and submarine hydrothermal systems, *in* Hedenquist, J.W., Thompson, J.F.H., Goldfarb, R.J., and Richards, J.P., eds., *Economic geology 100th anniversary volume 1905–2005*: Littleton, Colo., Society of Economic Geologists, p. 111–141.
- Hannington, M.D., Poulsen, K.H., Thompson, J.F.H., and Sil-litoe, R.H., 1999, Volcanogenic gold in the massive sulfide environment, *in* Barrie, C.T., and Hannington, M.D., eds., *Volcanic-associated massive sulfide deposits—Processes and examples in modern and ancient settings*: *Reviews in Economic Geology*, v. 8, p. 325–356.
- Hannington, M.D., Santaguida, F., Kjarsgaard, I.M., and Cath-les, L.M., 2003, Regional-scale hydrothermal alteration in the central Blake River Group, western Abitibi subprovince, Canada—Implications for VMS prospectivity: *Mineralium Deposita*, v. 38, p. 392–422.
- Hannington, M.D., and Scott, S.D., 1989, Sulfidation equilibria as guides to gold mineralization in volcanogenic massive sulfides—Evidence from sulfide mineralogy and the composition of sphalerite: *Economic Geology*, v. 84, p. 1978–1995.
- Hashiguchi, H., Yamada, R., and Inoue, T., 1983, Practical application of low Na₂O anomalies in footwall acid lava for delimiting promising areas around the Kosaka and Fukazawa Kuroko deposits, Akita Prefecture, Japan, *in* Ohmoto, H., and Skinner, B.J., eds., *The Kuroko and related volcanogenic massive sulfide deposits*: Economic Geology Monograph 5, p. 387–394.
- Heimann, A., Spry, P.G., and Teale, G.S., 2005, Zincian spinel associated with metamorphosed Proterozoic base-metal sulfide occurrences, Colorado—A re-evaluation of gahnite composition as a guide in exploration: *Canadian Mineralogist*, v. 43, p. 601–622.
- Herrmann, W., Blake, M., Doyle, M., Huston, D., Kamprad, J., Merry, N., and Pontual, S., 2001, Short wavelength infrared (SWIR) spectral analysis of hydrothermal alteration zones associated with base metal sulfide deposits at Rosebery and Western Tharsis, Tasmania, and Highway-Reward, Queensland: *Economic Geology*, v. 96, p. 939–955.
- Holk, G.J., Taylor, B.E., and Galley, A.G., 2008, Oxygen isotope mapping of the Archean Sturgeon Lake caldera complex and VMS-related hydrothermal system, northwestern Ontario, Canada: *Mineralium Deposita*, v. 43, p. 623–640.

- Hollister, V.F., 1980, A mineralized Ordovician resurgent caldera complex in the Bathurst-Newcastle mining district, New Brunswick, Canada—A discussion: *Economic Geology*, v. 75, p. 618.
- Huston, D.L., and Large, R.R., 1987, Genetic and exploration significance of the zinc ratio ($100 \text{ Zn}/(\text{Zn} + \text{Pb})$) in massive sulfide systems: *Economic Geology*, v. 82, p. 1521–1539.
- Huston, D.L., and Patterson, D.J., 1995, Zincian staurolite in the Dry River South volcanic-hosted massive sulfide deposit, northern Queensland, Australia—An assessment of its usefulness in exploration: *Applied Geochemistry*, v. 10, p. 329–336.
- Huston, D.L., Pehrsson, S., Eglington, B.M., and Zaw, K., 2010, The geology and metallogeny of volcanic-hosted massive sulfide deposits—Variations through geologic time and with tectonic setting: *Economic Geology*, v. 105, p. 571–591.
- Huston, D.L., Taylor, B.E., Bleeker, W., Stewart, B., Cook, R., and Koopman, E.R., 1995, Isotope mapping around the Kidd Creek deposit, Ontario—Application to exploration and comparison with other geochemical indicators: *Exploration and Mining Geology*, v. 4, p. 175–185.
- Jaireth, S., and Huston, D., 2010, Metal endowment of cratons, terranes and districts—Insights from a quantitative analysis of regions with giant and super-giant deposits: *Ore Geology Reviews*, v. 38, p. 288–303.
- Keating, P., Thomas, M.D., and Kiss, F., 2003, Significance of a high-resolution magnetic and electromagnetic survey for exploration and geologic investigations, Bathurst mining camp, *in* Goodfellow, W.D., McCutcheon, S.R., and Peter, J.M., eds., *Massive sulfide deposits of the Bathurst mining camp, New Brunswick, and northern Maine: Economic Geology Monograph 11*, p. 783–798.
- Kelley, D.L., Kelley, K.D., Coker, W.B., Caughlin, B., and Doherty, M.E., 2006, Beyond the obvious limits of ore deposits—The use of mineralogical, geochemical, and biological features for the remote detection of mineralization: *Economic Geology*, v. 101, p. 729–752.
- Large, R.R., Gemmill, J.B., Paulick, H., and Huston, D.L., 2001a, The alteration box plot—A simple approach to understanding the relationship between alteration mineralogy and lithochemistry associated with volcanic-hosted massive sulfide deposits: *Economic Geology*, v. 96, p. 957–971.
- Large, R.R., McPhie, J., Gemmill, J.B., Herrmann, W., and Davidson, G.J., 2001b, The spectrum of ore deposit types, volcanic environments, alteration halos, and related exploration vectors in submarine volcanic successions—Some examples from Australia: *Economic Geology*, v. 96, p. 913–938.
- Larson, P.B., 1984, Geochemistry of the alteration pipe at the Bruce Cu-Zn volcanogenic massive sulfide deposit, Arizona: *Economic Geology*, v. 79, p. 1880–1896.
- Leitch, C.H.B., and Lentz, D.R., 1994, The Gresens approach to mass balance constraints of alteration systems—Methods, pitfalls, examples, *in* Lentz, D.R., ed., *Alteration and alteration processes associated with ore-forming systems: Geological Association of Canada Short Course Notes*, v. 11, p. 161–192.
- Lentz, D.R., 2005, Mercury as a lithochemical exploration vectoring technique—A review of methodologies and applications, with selected VMS case histories: *Geological Association of Canada Mineral Deposits Division, The Gangee*, issue 85, p. 1, 5–11.
- Lerouge, C., Deschamps, Y., Joubert, M., Béchu, E., Fouillac, A.-M., and Castro, J.A., 2001, Regional oxygen isotope systematics of felsic volcanics—A potential exploration tool for volcanogenic massive sulphide deposits in the Iberian pyrite belt: *Journal of Geochemical Exploration*, v. 72, p. 193–210.
- Leybourne, M.I., 2007, Aqueous geochemistry in mineral exploration, *in* Goodfellow, W.D., ed., *Mineral deposits of Canada—A synthesis of major deposit-types, district metallogeny, the evolution of geological provinces, and exploration methods: Geological Association of Canada, Mineral Deposits Division, Special Publication 5*, p. 1007–1033.
- Leybourne, M.I., Boyle, R.R., and Goodfellow, W.D., 2003, Interpretation of stream water and stream sediment geochemistry in the Bathurst mining camp, New Brunswick, Canada—Application to mineral exploration, *in* Goodfellow, W.D., McCutcheon, S.R., and Peter, J.M., eds., *Massive sulfide deposits of the Bathurst mining camp, New Brunswick, and northern Maine: Economic Geology Monograph 11*, p. 741–761.
- Lydon, J.W., 1996, Characteristics of volcanogenic massive sulfide deposits—Interpretations in terms of hydrothermal convection systems and magmatic hydrothermal systems: *Instituto Tecnológico Geominero de España, Boletín Geológico y Minero*, v. 107, no. 3–4, p. 15–64.
- Massoth, G., Baker, E., Worthington, T., Lupton, J., de Ronde, C., Arculus, R., Walker, S., Nakamura, K., Ishibashi, J., Stoffers, P., Resing, J., Greene, R., and Lebon, G., 2007, Multiple hydrothermal sources along the south Tonga arc and Valu Fa Ridge: *Geochemistry, Geophysics, Geosystems*, v. 8, 26 p.
- May, E.R., and Schmidt, P.G., 1982, The discovery, geology and mineralogy of the Crandon Precambrian massive sulphide deposit, Wisconsin, *in* Hutchinson, R.W., Spence, C.D., and Franklin, J.M., eds., *Precambrian sulphide deposits: Geological Association of Canada Special Paper 25*, p. 447–480.

- McCarthy, J.H., Jr., Lambe, R.N., and Dietrich, J.A., 1986, A case study of soil gases as an exploration guide in glaciated terrain—Crandon massive sulfide deposit, Wisconsin: *Economic Geology*, v. 81, p. 408–420.
- McClenaghan, M.B., Thorleifson, L.H., and DiLabio, R.N.W., 1997, Till geochemical and indicator mineral methods in mineral exploration, in Gubins, A.G., ed., *Geophysics and geochemistry at the millennium—Proceedings of Exploration 97*, Fourth Decennial International Conference on Mineral Exploration: Toronto, GEO F/X Division of AG Information Systems, p. 233–248.
- McMartin, I., and McClenaghan, M.B., 2001, Till geochemistry and sampling techniques in glaciated shield terrain—A review, in McClenaghan, M.B., Bobrowsky, P.T., Hall, G.E.M., and Cook, S.J., eds., *Drift exploration in glaciated terrain: Geological Society of London Special Publication 185*, p. 19–43.
- Milkereit, B., Eaton, D., Wu, J., Perron, G., Salisbury, M., Berrer, E., and Morrison, G., 1996, Seismic imaging of massive sulfide deposits—Part II. Reflection seismic profiling: *Economic Geology*, v. 91, p. 829–834.
- Miller, C., Halley, S., Green, G., and Jones, M., 2001, Discovery of the West 45 volcanic-hosted massive sulfide deposit using oxygen isotopes and REE geochemistry: *Economic Geology*, v. 96, p. 1227–1237.
- Mosier, D.L., Berger, V.I., and Singer, D.A., 2009, Volcanogenic massive sulfide deposits of the world—Database and grade and tonnage models: U.S. Geological Survey Open-File Report 2009–1034, 50 p.
- Nesbitt, B.E., and Kelley, W.C., 1980, Metamorphic zonation of sulfides, oxides, and graphite in and around the orebodies at Ducktown, Tennessee: *Economic Geology*, v. 75, p. 1010–1021.
- Nykanen, V., and Ojala, V.J., 2007, Spatial analysis techniques as successful mineral-potential mapping tools for orogenic gold deposits in the northern Fennoscandian shield, Finland: *Natural Resources Research*, v. 16, p. 85–92.
- Paradis, S., Taylor, B.E., Watkinson, D.H., and Jonasson, I.J., 1993, Oxygen isotope zonation and alteration in the Noranda mining district, Abitibi greenstone belt, Quebec: *Economic Geology*, v. 88, p. 1512–1525.
- Peter, J.M., 2003, Ancient iron formations—Their genesis and use in the exploration for stratiform base metal sulphide deposits, with examples from the Bathurst mining camp, in Lentz, D.R., ed., *Geochemistry of sediments and sedimentary rocks—Evolutionary considerations to mineral deposit-forming environments: Geological Association of Canada GEOTEXT 4*, p. 145–176.
- Peter, J.M., and Goodfellow, W.D., 1996, Mineralogy, bulk and rare earth element geochemistry of massive sulphide-associated hydrothermal sediments of the Brunswick horizon, Bathurst mining camp, New Brunswick: *Canadian Journal of Earth Sciences*, v. 33, p. 252–283.
- Peter, J.M., and Goodfellow, W.D., 2003, Hydrothermal sedimentary rocks of the Heath Steele belt, Bathurst mining camp, New Brunswick—Part 3. Application of mineralogy and mineral and bulk compositions to massive sulfide exploration, in Goodfellow, W.D., McCutcheon, S.R., and Peter, J.M., eds., *Massive sulfide deposits of the Bathurst mining camp, New Brunswick, and northern Maine: Economic Geology Monograph 11*, p. 417–433.
- Peter, J.M., Goodfellow, W.D., and Doherty, W., 2003a, Hydrothermal sedimentary rocks of the Heath Steele belt, Bathurst mining camp, New Brunswick—Part 2. Bulk and rare earth element geochemistry and implications for origin, in Goodfellow, W.D., McCutcheon, S.R., and Peter, J.M., eds., *Massive sulfide deposits of the Bathurst mining camp, New Brunswick, and northern Maine: Economic Geology Monograph 11*, p. 391–415.
- Peter, J.M., Kjarsgaard, I.M., and Goodfellow, W.D., 2003b, Hydrothermal sedimentary rocks of the Heath Steele belt, Bathurst mining camp, New Brunswick—Part 1. Mineralogy and mineral chemistry, in Goodfellow, W.D., McCutcheon, S.R., and Peter, J.M., eds., *Massive sulfide deposits of the Bathurst mining camp, New Brunswick, and northern Maine: Economic Geology Monograph 11*, p. 361–390.
- Piché, M., and Jébrak, M., 2004, Normative minerals and alteration indices developed for mineral exploration: *Journal of Geochemical Exploration*, v. 82, p. 59–77.
- Piercey, S.J., 2007, An overview of the use of petrochemistry in regional exploration for volcanogenic massive sulfide (VMS) deposits, in Milkereit, B., ed., *Exploration in the new millennium—Proceedings of Exploration 07*, Fifth Decennial International Conference on Mineral Exploration: Toronto, GEO F/X Division of AG Information Systems, p. 223–246.
- Piercey, S.J., 2009, Litho-geochemistry of volcanic rocks associated with volcanogenic massive sulphide deposits and applications to exploration, in Cousens, B., and Piercey, S.J., eds., *Submarine volcanism and mineralization—Modern through ancient: Geological Association of Canada, Short Course Notes*, v. 19, p. 15–40.
- Raines, G.L., and Mihalasky, M.J., 2002, A reconnaissance method for delineation of tracts for regional-scale mineral-resource assessment based on geologic-map data: *Natural Resources Research*, v. 11, p. 241–248.

- Sangster, D.F., 1980, Quantitative characteristics of volcano-genic massive sulphide deposits—Part I. Metal content and size distribution of massive sulphide deposits in volcanic centres: Canadian Institute of Mining and Metallurgy Bulletin, v. 73, no. 814, p. 74–81.
- Singer, D.A., 1993, Basic concepts in three-part quantitative assessments of undiscovered mineral resources: Natural Resources Research, v. 2, p. 69–81.
- Singer, D.A., 2008, Mineral deposit densities for estimating mineral resources: Mathematical Geosciences, v. 40, p. 33–46.
- Singer, D.A., and Menzie, W.D., 2008, Map scale effects on estimating the number of undiscovered mineral deposits: Natural Resources Research, v. 17, p. 79–86.
- Slack, J.F., 1982, Tourmaline in Appalachian-Caledonian massive sulphide deposits and its exploration significance: Institution of Mining and Metallurgy Transactions, section B, v. 91, p. B81–B89.
- Slack, J.F., Atelsek, P.J., and Whitlow, J.W., 1990, Geochemistry of stream sediments and heavy-mineral concentrates from the Orange County copper district, east-central Vermont, chap. Q of Slack, J.F., ed., Summary results of the Glens Falls CUSMAP project, New York, Vermont, and New Hampshire: U.S. Geological Survey Bulletin 1887, 21 p.
- Spry, P.G., 2000, Sulfidation and oxidation haloes as guides in the exploration for metamorphosed massive sulfide ores, *in* Spry, P.G., Marshall, B., and Vokes, F.M., eds., Metamorphosed and metamorphogenic ore deposits: Reviews in Economic Geology, v. 11, p. 149–161.
- Spry, P.G., Peter, J.M., and Slack, J.F., 2000, Meta-exhalites as exploration guides to ore, *in* Spry, P.G., Marshall, B., and Vokes, F.M., eds., Metamorphosed and metamorphogenic ore deposits: Reviews in Economic Geology, v. 11, p. 163–201.
- Spry, P.G., and Scott, S.D., 1986, The stability of zincian spinels in sulfide systems and their potential as exploration guides for metamorphosed massive sulfide deposits: Economic Geology, v. 81, p. 1446–1463.
- Stolz, J., and Large, R.R., 1992, Evaluation of the source-rock control on precious metal grades in volcanic-hosted massive sulfide deposits from western Tasmania: Economic Geology, v. 87, p. 720–738.
- Taylor, B.E., and Slack, J.F., 1984, Tourmalines from Appalachian-Caledonian massive sulfide deposits—Textural, chemical, and isotopic relationships: Economic Geology, v. 79, p. 1703–1726.
- Taylor, B.E., and South, B.C., 1985, Regional stable isotope systematics of hydrothermal alteration and massive sulfide deposition in the West Shasta district, California: Economic Geology, v. 80, p. 2149–2163.
- Telmer, K., Pass, H.E., and Cook, S., 2002, Combining dissolved, suspended and bed load stream geochemistry to explore for volcanic massive sulfide deposits—Big Salmon Complex, northern British Columbia: Journal of Geochemical Exploration, v. 75, p. 107–121.

20. Geoenvironmental Features

By Robert R. Seal II and Nadine Piatak

20 of 21

Volcanogenic Massive Sulfide Occurrence Model

Scientific Investigations Report 2010–5070–C

U.S. Department of the Interior
U.S. Geological Survey

U.S. Department of the Interior
KEN SALAZAR, Secretary

U.S. Geological Survey
Marcia K. McNutt, Director

U.S. Geological Survey, Reston, Virginia: 2012

For more information on the USGS—the Federal source for science about the Earth, its natural and living resources, natural hazards, and the environment, visit <http://www.usgs.gov> or call 1-888-ASK-USGS.

For an overview of USGS information products, including maps, imagery, and publications, visit <http://www.usgs.gov/pubprod>

To order this and other USGS information products, visit <http://store.usgs.gov>

Any use of trade, product, or firm names is for descriptive purposes only and does not imply endorsement by the U.S. Government.

Although this report is in the public domain, permission must be secured from the individual copyright owners to reproduce any copyrighted materials contained within this report.

Suggested citation:

Seal II, R.R. and Piatak, Nadine, 2012, Geoenvironmental features in volcanogenic massive sulfide occurrence model: U.S. Geological Survey Scientific Investigations Report 2010-5070 -C, chap. 20, 18 p.

Contents

| | |
|---|-----|
| Weathering Processes | 323 |
| Sulfide Oxidation, Acid Generation, and Acid Neutralization Processes | 323 |
| Metal Cycling Associated with Efflorescent Sulfate Salts | 324 |
| Secondary Precipitation of Hydroxides and Hydroxysulfates | 324 |
| Pre-Mining Baseline Signatures in Soil, Sediment, and Water | 324 |
| Past and Future Mining Methods and Ore Treatment | 325 |
| Volume of Mine Waste and Tailings | 327 |
| Mine Waste Characteristics | 327 |
| Mineralogy | 327 |
| Acid-Base Accounting | 328 |
| Element Mobility Related to Mining in Groundwater and Surface Water | 330 |
| Pit Lakes | 334 |
| Ecosystem Issues | 335 |
| Human Health Issues | 335 |
| Climate Effects on Geoenvironmental Signatures | 335 |
| References Cited | 336 |

Figures

| | |
|--|-----|
| 20-1. Graphs showing geochemical data for waters associated with unmined massive sulfide deposits | 326 |
| 20-2. Graphs showing geochemical data for major constituents in mine drainage associated with massive sulfide deposits | 332 |
| 20-3. Graphs showing geochemical data for minor constituents in mine drainage associated with massive sulfide deposits | 333 |
| 20-4. Graphs showing geochemical data for dissolved metals in drainage associated with massive sulfide deposits | 334 |

Tables

| | |
|---|-----|
| 20-1. Selected common mineralogical characteristics of volcanogenic massive sulfide deposits with a comparison to sedimentary-exhalative deposits | 329 |
| 20-2. Environmental guidelines relevant to mineral deposits | 331 |

20. Geoenvironmental Features

By Robert R. Seal II and Nadine Piatak

Weathering Processes

Modern weathering processes associated with mine wastes from massive sulfide deposits are similar, in many respects, to those operating in the supergene environment after the initial formation of the mineral deposit. Nevertheless, some important differences exist. Acid-mine drainage is one of the most significant challenges associated with these deposits due to the abundance of pyrite, pyrrhotite, or both iron sulfides and the general lack of any significant neutralizing potential or alkalinity. The geochemistry of acid-mine drainage has been reviewed by Nordstrom and Alpers (1999a), and additional aspects of the weathering of a variety of ore and gangue minerals were discussed by Plumlee (1999). Seal and others (2001a), Seal and Hammarstrom (2003), and Seal (2004) have reviewed the geoenvironmental characteristics of volcanic-hosted massive sulfide deposits.

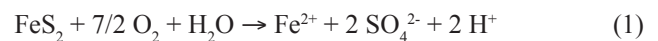
Geochemical aspects of the formation of acid-mine drainage and its burden of metals and other elements of concern can be divided into three broad topics: (1) sulfide oxidation, acid generation, and acid neutralization processes; (2) metal cycling associated with secondary efflorescent sulfate salts; and (3) secondary precipitation of hydroxides and hydroxysulfates and associated sorption of metals.

Sulfide Oxidation, Acid Generation, and Acid Neutralization Processes

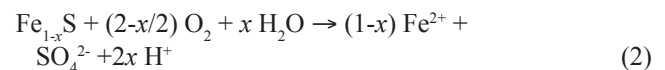
The abundance of pyrite and pyrrhotite in massive sulfide deposits dominates most aspects of the environmental behavior of these deposits and their mine wastes. The acid generated by their oxidative weathering can aggressively attack other ore and gangue minerals, thereby liberating a variety of potentially toxic elements including aluminum and manganese, which are not part of the “typical” ore assemblage of metals but instead are found in silicate and carbonate gangue minerals. These acidic, metal-laden acid-sulfate waters can adversely affect the surrounding surface- and groundwaters. Within the hydrologic system of mine workings or mine wastes, minerals and other compounds, such as lime used in flotation circuits, and even monosulfide minerals, such as sphalerite, can neutralize

acid generated by the oxidative weathering of sulfide minerals. Thus, the chemistry of drainage from a mine site is the result of the competing processes of acid generation and acid neutralization.

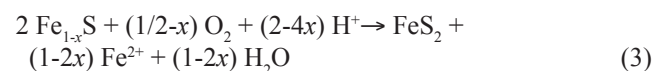
The oxidation of pyrite or pyrrhotite and other sulfide minerals proceeds with either dissolved oxygen (O_2) or dissolved ferric iron (Fe^{3+}) as the oxidizing agent. Dissolved oxygen is the most important oxidant at pH values above approximately 4, whereas ferric iron dominates below approximately 4 (Williamson and others, 2006). The aqueous oxidation of pyrite by dissolved oxygen is described by reaction 1:



The aqueous oxidation of pyrrhotite by dissolved oxygen is described by reaction 2:



where x ranges from 0.000 to 0.125. Both reactions 1 and 2 actually represent the mass action of numerous intermediate reactions. In the oxidative weathering of pyrrhotite, a common initial reaction is the oxidation of pyrrhotite to either pyrite or marcasite as described by the reaction:

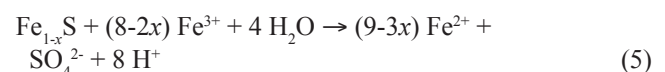


Textural evidence of marcasite replacement of pyrrhotite is common in pyrrhotitic mine wastes (Jambor, 1994, 2003; Hammarstrom and others, 2001).

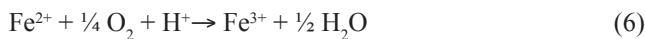
The aqueous oxidation of pyrite by ferric iron is described by reaction 4:



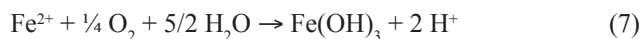
The aqueous oxidation of pyrrhotite by ferric iron is described by reaction 5:



For reactions 4 and 5, where ferric iron is the oxidant, ferrous iron must be oxidized to ferric iron to perpetuate the reaction as described by the reaction:

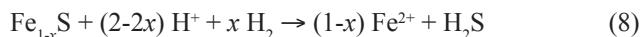


The rate of the oxidation of ferrous iron to ferric iron is greatly enhanced by the iron oxidizing bacterium *Acidithiobacillus ferrooxidans*. Singer and Stumm (1970) observed that *A. ferrooxidans* increased the rate of oxidation of ferrous iron to ferric iron by a factor of 100,000 compared to the abiotic rate. In the case of both sets of reactions for pyrite and pyrrhotite, additional acid is generated by the oxidation and hydrolysis of the aqueous ferrous iron as described by the reaction:



which also produces the orange and brown precipitates that typify acid-mine drainage.

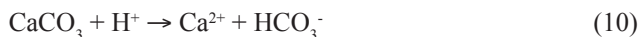
Pyrrhotite and other monosulfides, such as sphalerite, can also undergo non-oxidative dissolution under anoxic conditions when exposed to acid, as described by the respective reactions:



which, in the case of pyrrhotite, effectively decouples iron and sulfur oxidation. Both of these reactions consume acid.

Ore minerals such as sphalerite, galena, and chalcocopyrite react by similar reactions, with dissolved oxygen and ferric iron serving as oxidants. Zinc and copper tend to go into solution, but lead commonly forms secondary phases such as anglesite (PbSO_4) or cerussite (PbCO_3), depending upon the concentrations of sulfate and carbonate in solution.

Gangue minerals in the host rocks generally react to consume the acid generated by the oxidation of sulfides. Carbonate minerals, such as calcite, consume acid as described by reaction:



Under anoxic conditions, siderite will neutralize acid. However, the oxidation and hydrolysis of the resulting ferrous iron will offset the alkalinity produced. Aluminosilicate minerals such as plagioclase can consume acid, even though they are not as reactive as carbonate minerals (Plumlee, 1999; Jambor and others, 2002). The reaction of these minerals typically adds dissolved constituents such as aluminum to the water and produces secondary phases.

Metal Cycling Associated with Efflorescent Sulfate Salts

Evaporative concentration of sulfate-rich mine drainage can produce a series of highly soluble secondary sulfate salts.

Evaporative processes can operate during hot arid conditions, within mine workings or other sheltered areas, or in tailings piles beneath snow packs. Common secondary sulfate salts in mining environments include melanterite, rozenite, halotrichite, alunogen, copiapite, goslarite, and chalcantinite, among numerous others (Jambor, 1994; Jambor and others, 2000; Hammarstrom and others, 2001). Gypsum is another common secondary sulfate that can contribute dissolved solids to drainage but does not store acidity or metals. Metal-sulfate salts offer a means of temporarily sequestering acidity and metals for later dissolution during rain events or snowmelt (Jambor, 2003; Jambor and others, 2000; Hammarstrom and others, 2001). The effects of salt dissolution events can be dramatic, cycling through a watershed in a matter of hours.

Secondary Precipitation of Hydroxides and Hydroxysulfates

The oxidation of dissolved ferrous iron and neutralization of mine drainage produces a wide variety of secondary Fe or Al hydroxides and hydroxysulfates that are significantly less soluble than efflorescent sulfate salts. These phases range from compounds that are nearly amorphous to those that are well crystalline. Important Fe minerals include ferrihydrite (nominally $\text{Fe}_5\text{HO}_8 \cdot 4\text{H}_2\text{O}$), schwertmannite, jarosite, and goethite ($\alpha\text{-FeO}(\text{OH})$). Important Al phases include amorphous Al hydroxide ($\text{Al}(\text{OH})_3$), gibbsite ($\gamma\text{-Al}(\text{OH})_3$), and basaluminite ($\text{Al}_4(\text{SO}_4)(\text{OH})_{10} \cdot 4\text{H}_2\text{O}$). In mine-drainage environments, neutralization and hydrolysis are the main processes leading to the precipitation of the aluminum phases, whereas oxidation is additionally important for the precipitation of the iron phases. Jarosite tends to form in low-pH (1.5–3.0), high-sulfate (>3,000 mg/L) environments, schwertmannite in moderately acidic (pH of 3.0–4.0), moderate-sulfate (1,000–3,000 mg/L) environments, and ferrihydrite in near-neutral (pH > 5.0) environments (Bigham, 1994; Bigham and Nordstrom 2000; Stoffregen and others, 2000). Aluminum-bearing phases commonly precipitate at pH values above 4.5 (Nordstrom and Alpers, 1999a). An important aspect of the secondary iron hydroxides is their ability to sorb significant quantities of trace metals and remove them from solution. Sorption behavior is pH-dependent. Metal cations such as Pb^{2+} , Cu^{2+} , Zn^{2+} , and Cd^{2+} generally sorb to a greater extent with increasing pH, whereas most oxyanions, such as arsenate (AsO_4^{3-}) and selenate (SeO_4^{2-}), sorb to a greater extent with decreasing pH (Smith, 1999). Thus, secondary ferric hydroxides and hydroxysulfates can effectively remove metals from solution.

Pre-Mining Baseline Signatures in Soil, Sediment, and Water

Mine permitting and remediation require an estimate of pre-mining natural background conditions, particularly in

regulated media such as groundwater and surface water, soil, and sediment, to serve as a goal for post-mining reclamation. Detailed baseline geochemical characterization prior to the onset of mining is essential. However, for many abandoned mines, baseline characterization was not done prior to mining. Thus, a variety of methods have been used to estimate pre-mining backgrounds for abandoned mines (Runnells and others, 1992, 1998; Alpers and others, 1999b; Alpers and Nordstrom, 2000). Baseline data from undisturbed mineral deposits are useful for comparing and contrasting geochemical signatures among different types of massive sulfide deposits. These comparisons illustrate the importance of using a geochemically based classification of massive sulfide deposits in selecting an appropriate baseline. Mafic-siliciclastic type deposits are typically hosted by sulfide-rich black shales that are enriched in subeconomic concentrations of heavy metals and which formed through many of the same geochemical processes responsible for massive sulfide mineralization. Thus, drainage from watersheds underlain by these black shale units provides useful background data for mafic-siliciclastic type deposits (Seal and others, 1998b). Available background geochemical data include soil and stream-sediment data from a variety of deposits in Alaska, groundwater and surface-water chemistry in and around unmined bimodal-mafic type and bimodal-siliciclastic type deposits, and surface-water chemistry from watersheds underlain by sulfidic black shale host rocks for which mafic-siliciclastic type deposits are located in adjacent watersheds.

Pre-mining soil and stream sediment signatures may be useful for establishing pre-mining backgrounds. Also, soils around abandoned mine sites represent a significant sink for metals. The elemental suite and magnitude of geochemical anomalies in soil and sediment collected from undisturbed massive sulfide deposits depend upon a number of factors, including deposit type, extent of ore outcrop or overburden, climate, and topography, among others. Stream-sediment samples collected downstream from bimodal-felsic type deposits in temperate rain forest on Admiralty Island, Alaska, contain 5–10 wt% iron, as much as 10,000 mg/kg barium, hundreds to several thousand milligram per kilogram zinc, hundreds of milligram per kilogram lead, tens to hundreds of milligram per kilogram arsenic, copper, and nickel, as well as 0–20 mg/kg silver, bismuth, cadmium, mercury, molybdenum, and antimony (Kelley, 1990; Rowan and others, 1990; Taylor and others, 1992). Stream sediment geochemical signatures associated with undisturbed to variably disturbed mafic-ultramafic and mafic-siliciclastic type deposits in the Prince William Sound, Alaska, are similar to those just described. They contain 10–40 wt% iron, several hundred milligram per kilogram barium, hundreds of milligram per kilogram arsenic and zinc, tens to hundreds of milligram per kilogram lead, hundreds to thousands of milligram per kilogram copper, and 0–20 mg/kg silver, bismuth, mercury, molybdenum, and antimony (Goldfarb and others, 1995).

The available data for water associated undisturbed massive sulfide deposits span a range in pH from approximately

3 to 10 and a range of concentrations of dissolved Fe, a dominant cation, from approximately <0.02 to 300 mg/L. The availability of atmospheric oxygen and the position of the groundwater table are two of the most important factors in determining the natural weathering behavior of massive sulfide terranes. Surface waters around exposed deposits generally are more acidic and carry more dissolved Fe than those draining buried deposits (fig. 20–1A). The Alaskan sedimentary-exhalative deposits, Red Dog, Lik, and Drenchwater, and the black shales that host the Fontana and Hazel Creek mafic-siliciclastic type deposits in North Carolina are exposed at the surface, whereas the Bald Mountain (bimodal-mafic type) deposit and the Restigouche and Halfmile Lake (felsic-siliciclastic type) deposits are buried beneath glacial overburden or unmineralized rock.

The natural weathering of these host rocks can cause elements of concern for ecosystem health, such as Cu and Zn, to reach concentrations in excess of generic water-quality guidelines for the protection of aquatic life. In the Great Smoky Mountains National Park (North Carolina and Tennessee), watersheds underlain by the Anakeesta Formation, a sulfidic schist that hosts two mafic-siliciclastic type massive sulfide deposits, have dissolved concentrations of Cu and Zn that exceed generic acute toxicity water-quality guidelines (Seal and others, 1998b). Here, the biota in the ecosystem exists despite the concentrations of metals. Similarly, elements of concern for human health, such as As, also can exhibit anomalous background concentrations in groundwaters around unmined deposits. Concentrations of dissolved As reach 430 µg/L, which significantly exceed the drinking-water standards in the United States (10 µg/L), in the vicinity of the undisturbed Bald Mountain bimodal-mafic type deposit in northern Maine (Seal and others, 1998a) and near the undisturbed felsic-siliciclastic deposits in the Bathurst mining camp, New Brunswick (fig. 20–1B) (Leybourne and others, 1998). In the compiled dataset, many of the natural background waters have higher As concentrations than mine drainage; the low-pH, high-As waters from Iron Mountain (bimodal-mafic type), California, are an exception (fig. 20–1B). The higher concentrations of As in natural background waters compared to those of mine drainage are likely related to a combination of two factors. First, the near-neutral, low-Fe background waters generally remain undersaturated with respect to hydrous ferric oxide, which can sorb significant amounts of As; second, As is an oxyanion, which sorbs to greater extents at lower pH values rather than at higher values (Smith, 1999).

Past and Future Mining Methods and Ore Treatment

Mining methods and ore-beneficiation techniques significantly influence the potential environmental impacts of massive sulfide deposits. Both open-pit and underground methods have been used to mine massive sulfide deposits in historical

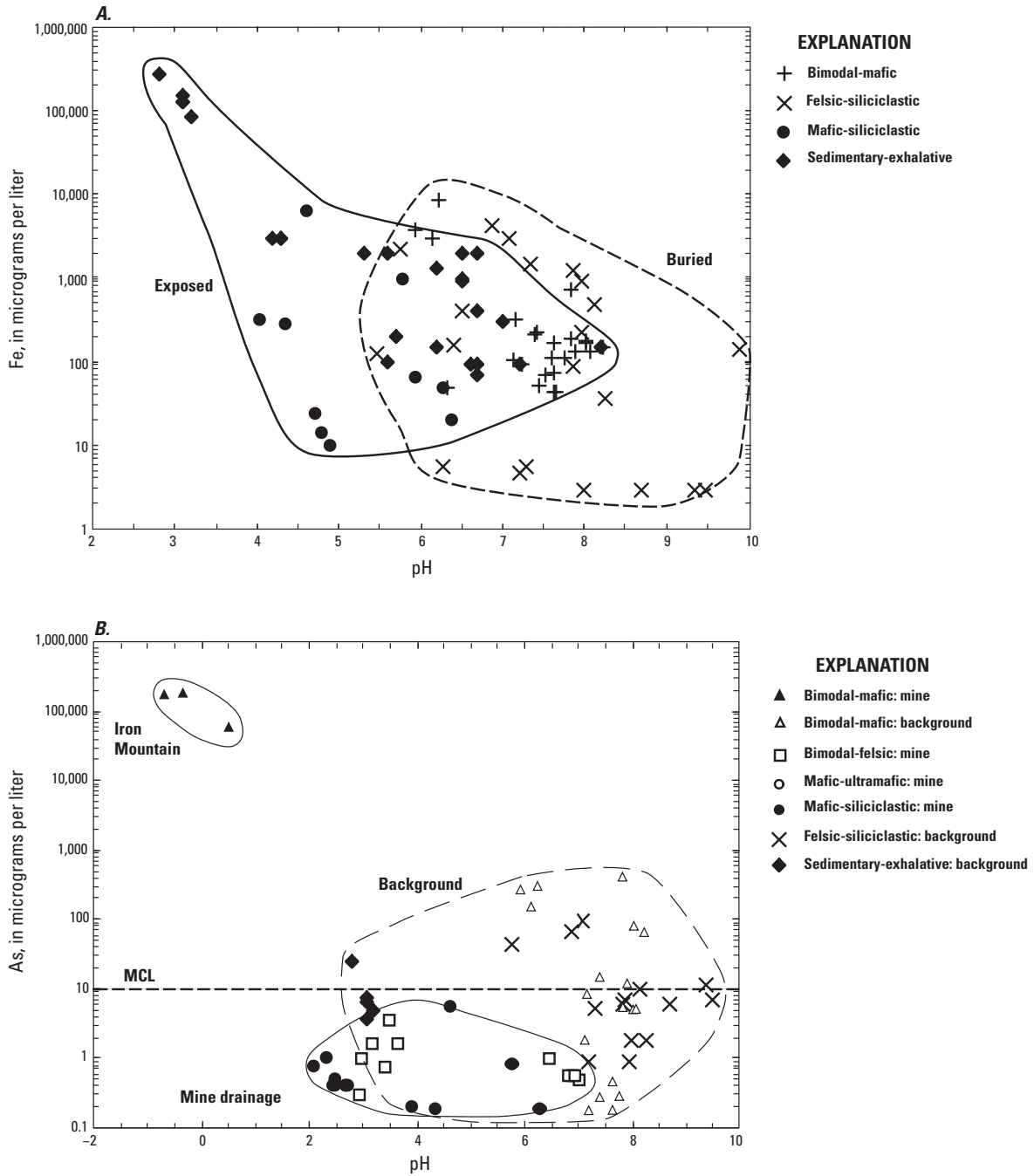


Figure 20-1. Geochemical data for waters associated with unmined massive sulfide deposits. *A*, Dissolved iron (Fe) versus pH. Dashed field indicates data from buried deposits, and solid field indicates data from deposits exposed at the surface, highlighting the importance of the availability of oxygen as a control on environmental signatures. *B*, Variation of the concentration of dissolved arsenic (As) with pH for mine drainage. Dashed field indicates natural background waters (unmined deposits), and solid field indicates mine drainage. For reference, MCL (maximum contaminant limit) is the current U.S. Environmental Protection Agency drinking-water limit. [$\mu\text{g/L}$, micrograms per liter]

and modern operations. The hydrologic differences between underground and open-pit mines are significant, especially at abandoned mines. Evaporative concentration is prominent in open pits, particularly those in semiarid to arid settings.

Mineral processing causes a number of physical and chemical changes to the ore from which the metal concentrates are produced. Most massive sulfide deposits contain a large excess of iron-sulfide minerals relative to valuable base-metal sulfide minerals. The nature of ore processing and the method of disposal of the sulfide-mineral-rich tailings and waste rocks are critical parameters that influence the scope of environmental impacts associated with mining massive sulfide deposits. Some modern mines discharge fine-grained, sulfide-rich tailings into tailings ponds underlain by impermeable linings, but historical tailings impoundments lack impermeable barriers at the base. Thus, many historical mining operations discharged tailings in a manner that has resulted in significant contamination of surface water and shallow groundwater.

Base-metal sulfide minerals are typically separated by froth flotation. Early flotation circuits generally produced copper concentrates and discharged both sphalerite and iron sulfides to tailings ponds. Some surfactants used in the process are toxic, but most are recycled and only relatively minor amounts are discharged to tailings facilities. The flotation properties of various sulfide minerals are affected by pH. Thus, base addition, typically in the form of lime (CaO) or sodium carbonate (Na_2CO_3), is a common practice to produce various sulfide-mineral concentrates; other additives to flotation circuits include potassium amyl xanthate, alcohols, ethers, pine oil, sodium cyanide (NaCN), and cupric sulfate ($\text{CuSO}_4 \cdot n\text{H}_2\text{O}$), all of which affect the flotation properties of various minerals (Biswas and Davenport, 1976). Most of these chemicals leave the sites as the tailings piles dewater; however, some may remain and continue to influence drainage chemistry. Other wastes from mineral processing can also be deposited with mill tailings. At the Kidd Creek mine, tailings from the mill are co-disposed with natrojarosite residues that are produced by the zinc processing plant (Al and others, 1994).

The fine grain size, the typically large size of tailings piles, and the addition of a variety of chemicals establish distinct geochemical environments in tailings piles. The fine grain size enhances the reactivity of the sulfide and gangue minerals by increasing surface area, but it also facilitates the formation of hardpan layers that can act as semipermeable to impermeable barriers to oxygen diffusion, thus limiting sulfide oxidation (Blowes and others 1991, 2003). Numerous studies of tailings from a variety of mineral-deposit types indicate that the pH of pore waters in the unsaturated and saturated zones of tailings piles is generally buffered by a predictable series of solid phases. Commonly, pore waters show a step-decrease in pH from 6.5–7.5, to 4.8–6.3, to 4.0–4.3, and finally to <3.5, which corresponds to buffering by calcite, siderite, $\text{Al}(\text{OH})_3$, and $\text{Fe}(\text{OH})_3$, respectively (Blowes and Ptacek, 1994; Jurjovec and others, 2002; Blowes and others, 2003). Thus, despite being a minor component of many of these mineralized

systems, carbonate minerals exert an important control on the geochemistry of anoxic pore waters in tailing piles.

Some historical massive sulfide deposits were mined for their sulfur content. Therefore, much of the sulfide waste has had major to minor amounts of the pyrite or pyrrhotite removed. Roasting of pyrite or pyrrhotite ores for the manufacture of sulfuric acid produces a hematitic calcine waste; the calcine in the Copper Basin, Tennessee, contains variable amounts of sulfate and can generate acid drainage (Moyer and others, 2002). Smelter slag is another important type of mine waste, and the reactivity of slags is significant (Parsons and others, 2001; Piatak and others, 2004). Leaching studies demonstrated that the suite of metals in leachates varies according to the compositional character of the ore (Piatak and others, 2004).

Volume of Mine Waste and Tailings

For all classes of massive sulfide deposits, mined deposits are historically in the 1 to 5 million tonnes range, but individual deposits can approach 500 million tonnes (Singer, 1986a, b; Singer and Mosier, 1986). Development of new deposits from all classes in frontier areas likely requires at least 10 million tonnes of reasonably high grade ore. Most mafic-ultramafic type deposits contain less than 15 million tonnes of ore. Most mafic-siliciclastic type deposits are also fairly small; notable exceptions include the >300 million tonne Windy Craggy, British Columbia, deposit. Bimodal-felsic type deposits, especially those of Precambrian age, can be very large, such as the world class Kidd Creek, Ontario, deposit. Because ore grades typically reach several percent at most, the tonnage of tailings is similar to the tonnage of ore. However, the amount of waste rock will vary mostly on the basis of mining method. Open-pit mines may need to strip significant amounts of subeconomic, but potentially problematic, waste rock, whereas the amount of waste rock generated by underground mines is typically less.

Mine Waste Characteristics

Mineralogy

Seafloor massive sulfide deposits are collectively defined by the fact that they formed syngenetically on or near the ancient seafloor through hot spring activity as lenslike or tabular bodies of stratiform sulfide minerals, dominantly pyrite or pyrrhotite. By definition, the deposits contain massive zones of sulfide minerals, many with sulfide mineral contents exceeding 90 vol%. Most deposits also contain extensive zones of semimassive sulfide rock (25–50 vol%) that contain economically exploitable ore. Quartz- or carbonate-rich stringer ore zones in the footwall of the massive sulfides typically contain 5–20 vol% sulfide minerals, hosted in quartz

veins and disseminated in chloritic wallrocks. The primary ore mineralogy defines the suite of heavy metals that may cause potential environmental problems. In addition to pyrite and pyrrhotite, the ore minerals chalcopyrite (CuFeS_2), sphalerite (ZnS), and galena (PbS) are commonly major constituents in these deposits and are the principal sources of elevated concentrations of Cu, Zn, and Pb in mine drainage.

Trace-element concentrations of ore minerals and accessory minerals also contribute to environmental impacts of massive sulfide deposits, even though many of these elements do not occur as distinct mineral species. For example, elevated dissolved concentrations of cadmium typically are correlated with its substitution into sphalerite. Cadmium rarely forms a discrete mineral in these types of deposits. Mercury can also be an important solid-solution component of sphalerite and tetrahedrite. Schwartz (1997) observed that sphalerite has higher Hg concentrations (4–4,680 mg/kg) in Proterozoic massive sulfide deposits than in Phanerozoic massive sulfide deposits (0.3–548 mg/kg). Arsenic commonly substitutes into pyrite in concentrations up to several weight percent, and arsenopyrite is also a common accessory mineral in some deposit types; both minerals constitute a significant source of As in some deposits. Cobalt probably resides in pyrrhotite or pyrite (Craig and Vaughan, 1990) but also occurs locally as cobaltite (CoAsS), glaucodot ($(\text{Co,Fe})\text{AsS}$), or carrollite (CuCo_2S_4). Nickel can also be an important component of pyrite and pyrrhotite. The primary mineralogical characteristics of massive sulfide deposits and associated heavy elements are summarized in table 20–1.

Various carbonate minerals, most of which contribute neutralizing potential, are associated locally with primary alteration assemblages of some of these deposit types. Calcite and ankerite ($\text{Ca}(\text{Fe,Mg})\text{CO}_3$) dominate the carbonate mineralogy. Sedimentary-exhalative deposits may have dolomitic shales in their host rocks and siderite, which has no net neutralizing potential, in their alteration assemblages. Post-mineralization deformation can introduce late calcite veinlets into the rock units surrounding these deposits, such as at the Big Mike mafic-ultramafic type deposit in Nevada, where pit waters have neutral pH.

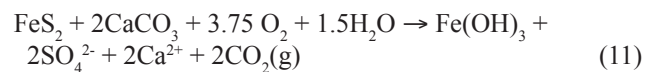
The secondary mineralogy associated with the weathering of a deposit or its mine wastes tends to sequester metals and (or) acidity on either a long-term or short-term basis. Hydrated ferric oxides can sorb metals on a somewhat refractory substrate, whereas efflorescent metal sulfate salts, such as melanterite, serve as a means of stored metals and acidity during dry periods. These salts readily dissolve during rain storm or spring melt of snow and deliver their metals and acidity to the surrounding watershed. Secondary minerals also have important implications for acid-base accounting. General secondary mineralogical features of massive sulfide deposits are summarized in table 20–1.

Secondary minerals formed in temperate climates include goethite, crystalline and amorphous silica, jarosite, a variety of metal-bearing hydroxysulfate minerals (beudantite, plumbojarosite, argentojarosite, woodhouseite, beaverite,

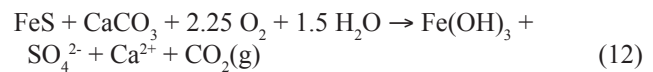
meta-aluminite, hinsdalite, and brochantite), scorodite, native gold, native silver, native bismuth, barite, anglesite, litharge, covellite, chalcocite, digenite, enargite, luzonite, and acanthite (Taylor and others, 1995). Anglesite and cerussite are the most abundant secondary lead minerals but coronadite, mimetite, nadorite, pyromorphite, and lanarkite have also been reported (Kelley and others, 1995). Secondary zinc minerals are rare, with the exception of goslarite.

Acid-Base Accounting

The primary and secondary mineralogy of the ores, their solid mine wastes, and associated rock types can affect the acid-base accounting (ABA) calculations. A series of static-test methods has been developed to predict the acid-generating potential of mine wastes as a tool to assist in waste disposal. These tests are known as acid-base accounting or ABA (Sobek and others, 1978; White and others, 1999), which is discussed in detail by Jambor (2003). Acid-base accounting is based on the stoichiometric reaction:



which is simply the sum of reactions 1 and 10 to eliminate H^+ as a constituent. It describes acid generation through the oxidation of pyrite and subsequent neutralization by calcite (Sobek and others, 1978). In the case of mafic-siliciclastic type and some sedimentary-exhalative massive sulfide deposits, pyrrhotite (Fe_{1-x}S ; where x ranges from 0.000 to 0.106) is the dominant sulfide mineral. For pyrrhotite, acid-base accounting can be approximated by the simplified stoichiometric reaction:



The net result of the proportion of CaCO_3 per unit of total S is the same as in reaction 11, but the total S per unit of solid will be lower because pyrrhotite has approximately half of the S of pyrite.

From an ABA perspective, the various types of massive sulfide deposits can differ significantly with regard to the speciation of sulfur in primary ores, host rocks, and mine wastes (table 20–1). Sulfide minerals such as pyrite, pyrrhotite, chalcopyrite, and sphalerite dominate the primary ore mineralogy of these deposits and contribute to the maximum potential acidity. Secondary metal-sulfate salts that commonly accumulate as intermediate products of sulfide oxidation also will contribute acidity (Alpers and others, 1994a; Cravotta, 1994; Hammarstrom and others, 2001). For example, melanterite ($\text{FeSO}_4 \cdot 7\text{H}_2\text{O}$), rozenite ($\text{FeSO}_4 \cdot 4\text{H}_2\text{O}$), copiapite ($\text{Fe}^{2+}\text{Fe}_4^{3+}(\text{SO}_4)_6(\text{OH})_2 \cdot 20\text{H}_2\text{O}$), and halotrichite ($\text{Fe}^{2+}\text{Al}_2(\text{SO}_4)_4 \cdot 22\text{H}_2\text{O}$), among others, are common and highly soluble; less soluble sulfate minerals such as jarosite and schwertmannite ($\text{Fe}_8\text{O}_8(\text{SO}_4)(\text{OH})_6$) also are common in mining environments (table 20–1). In contrast, the alkaline-earth sulfate minerals,

Table 20-1. Selected common mineralogical characteristics of volcanogenic massive sulfide deposits with a comparison to sedimentary-exhalative deposits.

[X, major; x, minor]

| | Mafic-ultramafic | Bimodal-mafic | Bimodal-felsic | Mafic-siliciclastic | Felsic-siliciclastic | Sedimentary-exhalative |
|------------------------------|-------------------------|----------------------|-----------------------|----------------------------|-----------------------------|-------------------------------|
| Primary sulfide minerals | | | | | | |
| Pyrite | X | X | X | X, x | X | X |
| Pyrrhotite | x | X, x | x | X | X | X, x |
| Chalcopyrite | X | X | X | X | X | x |
| Sphalerite | x | X | X | x | X | X |
| Galena | x | x | X | x | X | X |
| Arsenopyrite | | x | x | | x | |
| Tetrahedrite-tennantite | | x | x | | | x |
| Cinnabar | | | | | | x |
| Primary sulfate minerals | | | | | | |
| Anhydrite | | | X | | | X |
| Barite | | X | X | | X | X |
| Primary carbonate minerals | | | | | | |
| Calcite | x | x | x | x | x | X |
| Dolomite | | | x | x | | X |
| Ankerite | | x | | x | x | x |
| Siderite | | x | x | | x | x |
| Primary oxide minerals | | | | | | |
| Magnetite | x | x | x | | x | x |
| Hematite | x | x | x | | | |
| Secondary sulfide minerals | | | | | | |
| Marcasite | | x | x | x | | x |
| Covellite | | x | x | x | | |
| Chalcocite | x | x | | x | | |
| Enargite | | x | x | | | |
| Secondary sulfate minerals | | | | | | |
| Gypsum | | x | x | x | | x |
| Barite | | x | x | | | |
| Melanterite/rozenite | x | x | x | x | | x |
| Copiapite | | x | x | x | | |
| Halotrichite | x | | x | x | | x |
| Alunogen | | | x | x | | |
| Epsomite | x | | | x | | |
| Chalcanthite | x | | | x | | |
| Goslarite | x | x | x | x | | x |
| Anglesite | | x | x | | | x |
| Secondary carbonate minerals | | | | | | |
| Siderite | | | | | | |
| Cerussite | | | | | | x |

Table 20-1. Selected common mineralogical characteristics of volcanogenic massive sulfide deposits with a comparison to sedimentary-exhalative deposits.—Continued

[X, major; x, minor]

| | Mafic-ultramafic | Bimodal-mafic | Bimodal-felsic | Mafic-siliciclastic | Felsic-siliciclastic | Sedimentary-exhalative |
|---------------------------------|------------------|---------------|----------------|---------------------|----------------------|------------------------|
| Secondary oxyhydroxide minerals | | | | | | |
| Ferrihydrite | x | x | | x | | x |
| Goethite | x | x | | x | | x |
| Schwertmannite | x | x | | x | | |
| Jarosite | | x | | x | | |
| Amorphous Al(OH) ₃ | | | | | | |
| Basaluminite | | | x | x | | |
| Jurbanite | | | | | | |

such as barite, anhydrite, and gypsum, also are common as both primary and secondary minerals (table 20-2), but they do not contribute acidity even though their sulfur content will be reported in determinations of total sulfur. The most prominent differences in secondary sulfate-mineral speciation among mine wastes from the different types of massive sulfide deposits are in their jarosite and metal-sulfate salts, particularly in the presence or absence of chalcantite ($\text{CuSO}_4 \cdot 5\text{H}_2\text{O}$), goslarite ($\text{ZnSO}_4 \cdot 7\text{H}_2\text{O}$), Cu-Mg melanterite ($(\text{Fe,Cu,Mg})\text{SO}_4 \cdot 7\text{H}_2\text{O}$), and alunogen ($\text{Al}_2(\text{SO}_4)_3 \cdot 17\text{H}_2\text{O}$), among others. Modifications to the original ABA procedures attempt to accommodate these problems (White and others, 1999).

Net neutralization potentials for both bimodal-felsic and mafic-siliciclastic type tailings are generally net acid. Bimodal-felsic type tailings range from -142.0 to 17.2 kilograms calcium carbonate per ton (kg CaCO_3/t) (Seal and others, 2009). Net neutralization potentials for two samples of mafic-siliciclastic type deposits are -324.0 kg CaCO_3/t for coarse tailings and -282.5 kg CaCO_3/t for fine tailings (Seal and others, 2009).

Element Mobility Related to Mining in Groundwater and Surface Water

The quality of mine drainage is controlled by the geological characteristics of the mineral deposit modified by the combined effects of the mineralogy, the mining and ore-beneficiation methods used, the hydrologic setting of the mine workings and waste piles, and climate. Fewer published geochemical data for mine drainage are available for mafic-ultramafic and felsic-siliciclastic type deposits than for bimodal-felsic, mafic-siliciclastic, bimodal-mafic, and sedimentary-exhalative type deposits, for which data are available from several deposits in different climatic settings.

Mine drainage associated with massive sulfide deposits shows a general negative correlation between dissolved metals and pH for most metals, such as Fe, Al, Cu, Zn, Ni, Co, Cd,

and Pb, and sulfate (figs. 20-2, 20-3). Iron is typically the dominant cation, and sulfate is the dominant anion. The correlations among pH, metals, and sulfate reflect acid generation dominantly through the aqueous, oxidative weathering of pyrite, pyrrhotite, and associated ore sulfides. For the divalent metals and for Fe and Al, mine-drainage compositions overlap significantly with natural background compositions but extend to higher metal concentrations and lower pH values. Increases in total dissolved base metals and iron in mine drainage generally correlate with increases in pyrite content, decreases in acid neutralizing capacity, and increases in base-metal content of deposits (Plumlee, 1999). However, the presence of anoxic conditions in tailings and other waste piles may result in seepage waters that have high concentrations of Fe at near-neutral pH values because the iron is dominantly in the more soluble ferrous state than in the less soluble ferric state (Seal and others, 2001b).

The geochemistry of mine drainage from massive sulfide deposits shows clear evidence of primary controls based on deposit type, as well as mineralogical controls for individual metals. In terms of dissolved Cu and Zn, the data correlate positively, with individual deposit types falling at distinct ranges of Zn:Cu ratios, which are directly related to the primary character of the ores (fig. 20-4A). The Zn:Cu ratios (mass basis) for waters associated with the Cu-rich mafic-ultramafic type deposits range from approximately 1:10 to 10:1, whereas those associated with Cu>Zn mafic-siliciclastic type deposits range from approximately 1:10 to more than 100:1, and those associated with Zn>Cu bimodal-felsic type deposits are the highest, ranging from 1:1 to 10,000:1. Correlations between Cu and Pb are less distinct, presumably due to the saturation of Pb with respect to anglesite. Unlike Cu and Zn, the systematics of dissolved Cd and Zn are different; the fields for all massive sulfide types overlap in a range of Zn:Cd ratios (mass basis) that scatter about 100:1 (fig. 20-4B). The overlap reflects the fact that Cd occurs primarily in all massive sulfide deposits as a minor solid-solution element in sphalerite.

Table 20–2. Environmental guidelines relevant to mineral deposits.

[mg/kg, milligram per kilogram; mg/L, milligram per liter]

| Element | Human health | | | | Aquatic ecosystem | |
|-----------------|--|---------------------------------------|-------------------------------------|-------------------------------------|-------------------------------------|---------------------------------------|
| | Residential soil ¹ mg/kg | Industrial soil ¹ mg/kg | Drinking water ¹ mg/L | Drinking water ² mg/L | Acute toxicity ¹ mg/L | Chronic toxicity ¹ mg/L |
| Aluminum (Al) | 77,000 | 990,000 | 200 | | 750 | 87 |
| Arsenic (As) | 23 | 160 | 10 | 10 | 340 | 150 |
| Cadmium (Cd) | 70 | 810 | 5 | 3 | 2* | 0.25* |
| Chromium (Cr) | 280 | 1,400 | 100 | 50 | 570* | 74* |
| Copper (Cu) | 3,100 | 41,000 | 1,300 | 2,000 | 13* | 11* |
| Iron (Fe) | 55,000 | 720,000 | 300 | | | 1,000 |
| Mercury (Hg) | 6.7 | 28 | 2 | 6 | 1.4 | 0.77 |
| Manganese (Mn) | 1,800 | 23,000 | 50 | 400 | | |
| Molybdenum (Mo) | 390 | 5,100 | | 70 | | |
| Nickel (Ni) | 1,600 | 20,000 | | 70 | 470* | 52* |
| Lead (Pb) | 400 | 800 | 15 | 10 | 65* | 2.5* |
| Selenium (Se) | 390 | 5,100 | 50 | 10 | | 5 |
| Uranium (U) | 230 | 3,100 | | 15 | | |
| Zinc (Zn) | 23,000 | 310,000 | 5,000 | | 120* | 120* |

*Hardness-dependent water-quality standards; value is based on a hardness of 100 mg/L CaCO₃.

¹ U.S. Environmental Protection Agency (2006)

² World Health Organization (2008)

Cobalt also can be an important trace element in drainage from mafic-siliciclastic type mines and mine wastes. Elevated concentrations of Co (up to 7.2 mg/L) in drainage at the Elizabeth and Ely deposits are probably derived from the weathering of pyrrhotite and Co sulfides (Seal and others, 2001b).

The hydrologic setting, especially relative to the water table, is another key variable in determining the magnitude of mine drainage problems. The extent of mineralized outcrop and (or) mine-related excavations exposed to the atmosphere or oxygen-rich groundwater and the position relative to the water table are hydrologic factors that can influence significantly the intensity and scale of environmental problems related to massive sulfide deposits. Availability of dissolved oxygen is a controlling factor for the acid-generating potential of massive sulfide deposits and their wastes.

A comparison of mine drainage from pyritic ores at Iron Mountain (bimodal-mafic type) and the Penn mine (bimodal-felsic type) in California emphasizes the importance of the location of the deposit relative to the water table. Although both deposits are in similar climatic settings, Iron Mountain is mostly located above the water table; the Penn deposit, however, is mostly below the water table, but waste piles above the water table contribute to water-quality degradation (Alpers and others, 1994b, 1999a). At Iron Mountain, pH values are as low as -3.4 and concentrations of total dissolved solids exceed 100,000 mg/L (Alpers and others, 1994b; Nordstrom and Alpers, 1999b; Nordstrom and others, 2000). In contrast, pH

values of mine waters from the Penn mine vary to a low of 3.1 and total dissolved solids reach a maximum of approximately 5,500 mg/L (Alpers and others, 1999a). Mine drainage from the pyrrhotitic Elizabeth mine also emphasizes the importance of hydrologic setting. Two dominant mine-waste hydrologic settings are present at Elizabeth: one dominated by surface flow over mine wastes, and the other dominated by groundwater flow through tailings piles. In these two environments, the relationship of dissolved Fe to pH varies significantly. Surface waters show a general negative correlation of dissolved Fe, Al, Cu, and Zn, among other metals, and pH. In contrast, waters emerging from the base of the tailings piles are anoxic and near-neutral to slightly acidic (pH of 6.1–6.9) but carry amounts of dissolved Fe (14.0–904.0 mg/L) and sulfate (1,300–3,800 mg/L) that are comparable to those in the surface waters. However, dissolved concentrations of Al (<0.001–0.5 mg/L), Cu (<0.5–20 µg/L), and Zn (5.0–100.0 µg/L) are comparatively low (Seal and others, 2001b). The geochemical differences between these two environments can be related to several factors. The low concentrations of aluminum are a reflection of the near-neutral pH and the low solubility of aluminum under these conditions. In contrast, the copper concentrations are well below their theoretical maximum solubilities under these conditions, which attest to the efficiency of the ore-beneficiation technique or to the role of sorption at the oxic/anoxic interface near the top of the tailings. Oxidative weathering of pyrrhotite involving dissolved oxygen, as

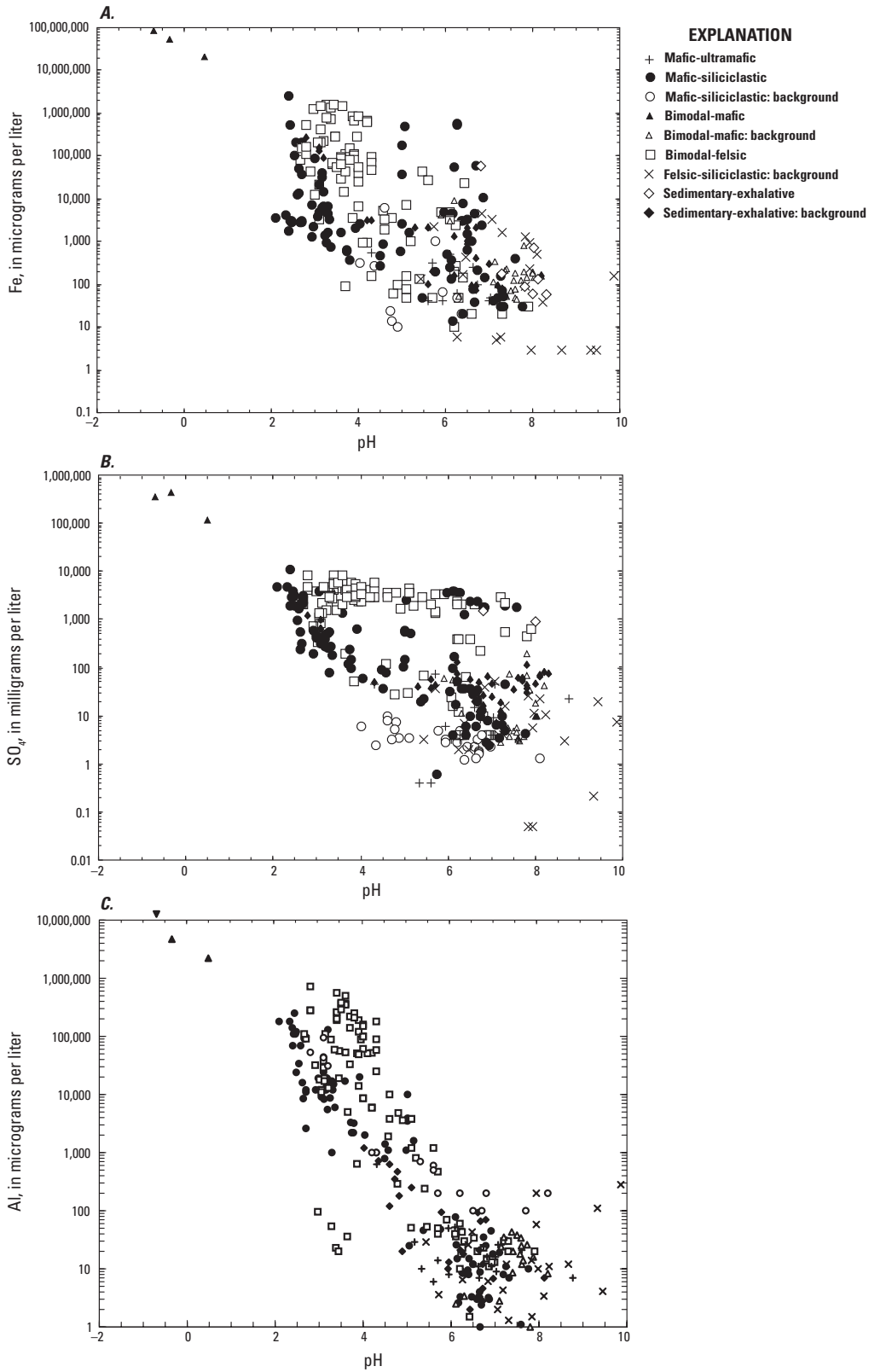


Figure 20-2. Geochemical data for major constituents in mine drainage associated with massive sulfide deposits. *A.* Iron (Fe) versus pH. *B.* Sulfate (SO₄) versus pH. *C.* Aluminum (Al) versus pH. Note the general negative correlation between pH and dissolved constituents. [$\mu\text{g/L}$, micrograms per liter; mg/L , milligrams per liter]

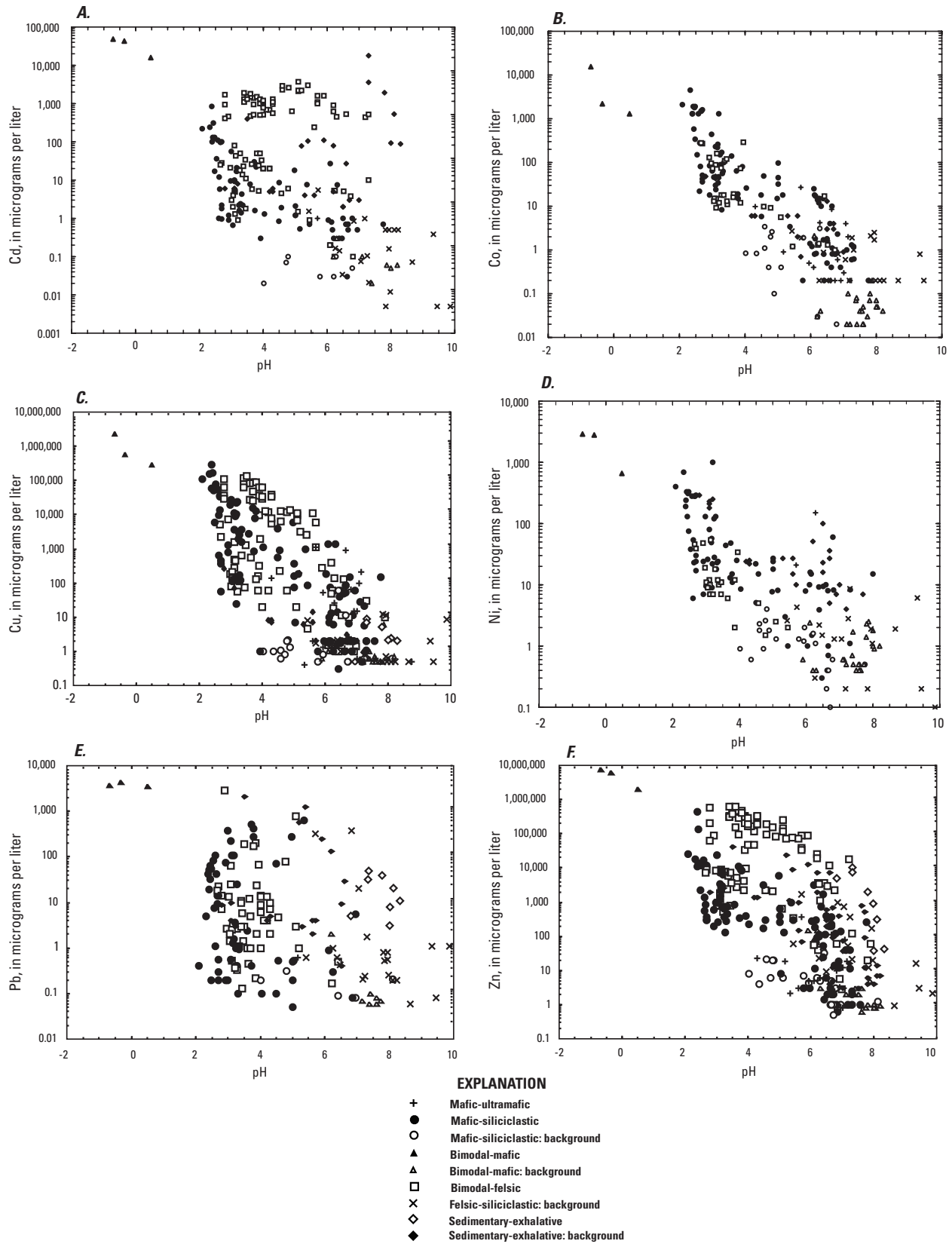


Figure 20-3. Geochemical data for minor constituents in mine drainage associated with massive sulfide deposits. *A*, Cadmium (Cd) versus pH. *B*, Cobalt (Co) versus pH. *C*, Copper (Cu) versus pH. *D*, Nickel (Ni) versus pH. *E*, Lead (Pb) versus pH. *F*, Zinc (Zn) versus pH.

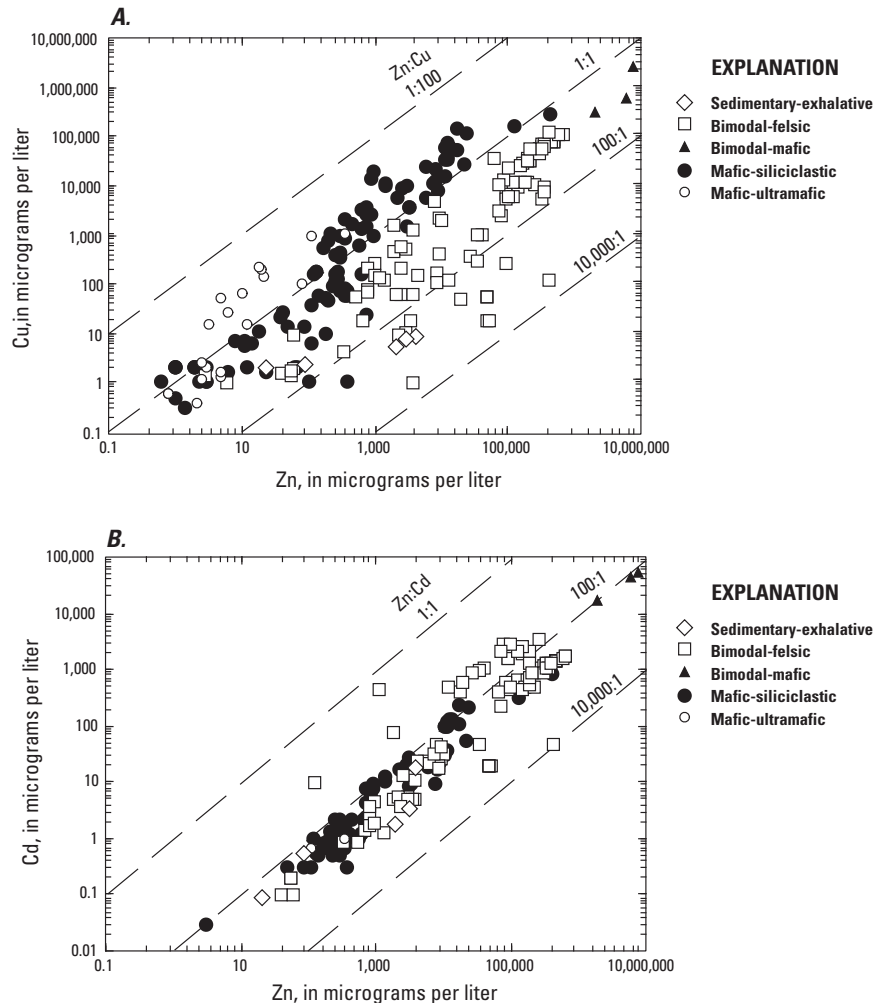


Figure 20-4. Geochemical data for dissolved metals in drainage associated with massive sulfide deposits. *A*, Copper (Cu) versus zinc (Zn). *B*, Cadmium (Cd) versus zinc. [$\mu\text{g/L}$, micrograms per liter]

described by reaction 2, develops minor acid in an oxygen-limited environment such as the subsurface of the tailings pile. The presence of minor amounts of carbonate minerals in the host rock and the addition of lime in mineral-processing circuits prior to disposal may also contribute to the near-neutral pH of groundwaters emerging from the tailings pile. Likewise, under anoxic conditions, pyrrhotite can consume acid to produce ferrous iron and H_2S (reaction 8). High concentrations of iron can be attributed to the high solubility of ferrous iron. Because of the near-neutral pH, the groundwaters flowing through the tailings do not have elevated concentrations of metals such as Al, Cu, Zn, and Cd. Sorption of divalent metals on hydrated ferric oxides in the oxidized, upper portions of the tailings pile may explain the lower concentrations of Cu, Zn, and Cd. High flotation recoveries of the ore minerals may also explain the lower concentrations of Cu. Upon emerging from the base of the tailings pile, ferrous iron in the groundwaters

undergoes rapid oxidation to Fe^{3+} , followed by hydrolysis and a concomitant drop in pH. In contrast, under oxygenated conditions, such as in the surface waters at Elizabeth, the iron commonly occurs in both valence states. Under these conditions, acidic pH values are required to carry significant concentrations of iron in the drainage.

Pit Lakes

Studies of pit lakes associated with volcanic-hosted massive sulfide deposits are limited. A small pit lake at the abandoned Elizabeth mine, a mafic-siliciclastic type deposit, in Vermont has moderately low pH and moderate total dissolved solids (Seal and others, 2006). The ephemeral pit lake at the Big Mike mine, a mafic-ultramafic type deposit, has slightly alkaline pH and low total dissolved solids (Shevenell and others, 1999).

Ecosystem Issues

Ecosystem threats are dominantly produced by acid mine drainage, which targets aquatic environments. The oxidative weathering of pyrite (FeS_2) and pyrrhotite (Fe_{1-x}S), is described by reactions 1 to 5. The lower pH values generated by the oxidation of pyrite and pyrrhotite enhance the solubility of base metals such as Cu, Zn, Cd, Co, Ni, and Pb and the ability to attack silicate-gangue minerals, thus liberating Al, Mn, and other elements. Most metals show greater solubility at lower pH values; however, aluminum and ferric iron have solubility minimums at circumneutral pH values, with greater solubility at both lower and higher pH. Once liberated, the metals and acidity can affect downstream aquatic ecosystems. Downstream effects can be localized or can extend at least 100 km from mine sites. Metal contamination can also be dispersed downstream by the erosion and transport of tailings, which subsequently release metals to the water column.

The toxicity of the metals Cd, Cr, Cu, Pb, Ni, Ag, and Zn to aquatic ecosystems is dependent on water hardness; higher concentrations of metals are needed to exceed toxicity limits at higher hardness values (U.S. Environmental Protection Agency, 2006). Hardness is a measure of the concentrations of Ca and Mg. The concentration of hardness is expressed in terms of an equivalent concentration of CaCO_3 , typically in milligrams per liter. The U.S. Environmental Protection Agency (USEPA) has presented hardness-dependent expressions for both acute (one-hour exposure) and chronic (four-day exposure) toxicity and limits independent of hardness for cyanide, Al, As, Sb, Fe, Hg, Se, and Tl (table 20–2) (U.S. Environmental Protection Agency, 2006).

Human Health Issues

Human-health impacts of massive sulfide deposits are generally associated with either the inhalation or the ingestion of metals. Ingestion may be in the form of drinking water or as particulates. The USEPA has set primary maximum contaminant levels (MCLs) for cyanide, Sb, As, Cu, Cd, Cr, Hg, and Ni, among other compounds, for drinking water (table 20–2) (U.S. Environmental Protection Agency, 2009). Groundwaters around mineral deposits, both from undisturbed and disturbed settings, can exceed drinking-water standards. For example, the concentration of dissolved As in groundwaters around the unmined Bald Mountain massive sulfide deposit in northern Maine reaches a maximum of 430 $\mu\text{g/L}$, whereas the USEPA drinking water standard is 10 $\mu\text{g/L}$ (fig. 20–1B) (Seal and others, 1998a). The unmined deposit contains minor amounts of both primary arsenopyrite and secondary enargite. Likewise, a shallow groundwater well near the abandoned Elizabeth mine in Vermont has high concentrations of Cu and Cd (Hathaway and others, 2001).

Risks are generally related to ingestion of Pb-rich mine waste through incidental contact. Studies have demonstrated that the relative bioavailability of Pb in the digestive tract

varies according to mineralogy. Lead in galena and anglesite (PbSO_4) is considered to be less bioavailable than Pb in cerussite (PbCO_3) (U.S. Environmental Protection Agency, 1999). At the Valzinco mine in central Virginia, fine-grained flotation tailings exposed to wind and water contain up to 4,000 mg/kg Pb, well in excess of USEPA residential and industrial soil criteria (400 and 750 mg/kg Pb, respectively). For bimodal-felsic type massive sulfide deposits such as Valzinco, Pb is present as galena and its weathering product, anglesite. Thus, because of the geochemical character of the bimodal-felsic type massive sulfide deposits, Pb remains speciated in solid forms that are less bioavailable. For all Pb-bearing deposits, the fine grinding required for concentration by flotation increases the risk of inhalation because of the airborne transport of Pb-bearing dust. This phenomenon is most likely to occur in semiarid to arid regions in which strong winds prevail.

Mercury risks are generally related to the consumption of Hg-contaminated fish and the contamination of drinking water. Mercury occurs as several aqueous species, with methylmercury the one of greatest environmental concern. Methylmercury is a potent neurotoxin that bioaccumulates with increasing trophic level in aquatic and terrestrial ecosystems (Gehrke and others, 2011). The primary pathway for human-health impacts is through the consumption of fish and other higher organisms in Hg-contaminated environments. The United States Food and Drug Administration issues fish-consumption advisories for Hg concentrations in fish tissue above 1,000 ng/g (wet basis). Thus, Hg derived either from past amalgamation use or from solid solution in minerals, such as sphalerite, may affect human and other animals if it becomes methylated and enters the foodweb.

In semiarid to arid areas, the human-health risks associated with Hg are more likely related to drinking-water supplies that are obtained from shallow groundwaters. The surficial weathering of mine wastes, especially during the rainy season, may liberate metals to the local groundwater. In the case of sedimentary-exhalative ores, the most likely metals of concern in drinking water are Pb, Zn, Cd, As, and Tl in addition to Hg (table 20–2).

Climate Effects on Geoenvironmental Signatures

Climate plays an especially important role in the potential environmental impact from mines that exploit massive sulfide deposits (Nordstrom, 2009). However, its effect is difficult to quantify systematically because insufficient data are available for a given deposit type in a wide spectrum of climatic settings. Nevertheless, temperature and humidity are the prime variables that control evaporation. Evaporation can be expected to limit the amount of water in semiarid to arid climates. Evaporation can concentrate solutes in all climates. Acidity and total metal concentrations in mine drainage in arid environments are typically several orders of magnitude greater

than in more temperate climates because of the concentrating effects of the evaporation of mine effluent and the resulting “storage” of metals and acidity in highly soluble metal-sulfate salt minerals. Minimal surface-water flow in these areas inhibits generation of significant volumes of highly acidic, metal-enriched drainage. Concentrated release of these stored contaminants to local watersheds may be initiated by precipitation following a dry spell. In wet climates, high water tables may reduce exposure of abandoned orebodies to oxidation and may continually flush existing tailings and mine dumps. Although metal-laden acidic mine water does form, it may be diluted to benign metal abundances within several hundred meters of mixing with a higher order stream.

The importance of climate as a variable can also be demonstrated by comparing seasonal variations in the chemistry of effluent from two abandoned mines that exploited massive sulfide deposits in the eastern United States—one with a winter-long snow pack, the Elizabeth mine in Vermont, and one without a winter-long snow pack, the Valzinco mine in Virginia. At Elizabeth, concentrations of dissolved Cu in surface waters peak during spring melt and are interpreted to reflect the dissolution and flushing of efflorescent salts or brines formed in the subsurface of the tailings pile during the winter. In contrast, concentrations of dissolved Cu in the drainage from the Valzinco mine reach a peak in the summer as the flow approaches base conditions, possibly with some evaporative concentration. The absolute differences in the peak concentrations of Cu between the Elizabeth and Valzinco mines reflect the Cu-rich character of the Elizabeth ores and the Zn-rich character of the Valzinco ores. In both settings during the summer, the concentrations of Cu and other dissolved constituents can spike because of the dissolution of efflorescent salts during rain storms.

References Cited

- Al, T.A., Blowes, D.W., and Jambor, J.L., 1994, A geochemical study of the tailings impoundment at the Falconbridge Limited, Kidd Creek division metallurgical site, Timmons, Ontario, *in* Jambor, J.L., and Blowes, D.W., eds., Environmental geochemistry of sulfide mine-wastes: Mineralogical Association of Canada Short Course Series, v. 22, p. 333–364.
- Alpers, C.N., Blowes, D.W., Nordstrom, D.K., and Jambor, J.L., 1994a, Secondary minerals and acid mine-water chemistry, *in* Jambor, J.L., and Blowes, D.W., eds., Environmental geochemistry of sulfide mine-wastes: Mineralogical Association of Canada Short Course Series, v. 22, p. 247–270.
- Alpers, C.N., Hamlin, S.N., and Hunerlach, M.P., 1999a, Hydrogeology and geochemistry of acid mine drainage in ground water in the vicinity of Penn Mine and Comanche Reservoir, Calaveras County, California—Summary report, 1993–95: U.S. Geological Survey Water-Resources Investigations Report 96–4287, 59 p.
- Alpers, C.N., and Nordstrom, D.K., 2000, Estimation of pre-mining conditions for trace metal conditions for trace metal mobility in mineralized areas—An overview, *in* International Conference on Acid Rock Drainage, 5, Denver, Colo., 21–24 May 2000, Proceedings: Littleton, Colo., Society for Mining, Metallurgy, and Exploration, p. 463–472.
- Alpers, C.N., Nordstrom, D.K., and Thompson, J.M., 1994b, Seasonal variations of Zn/Cu ratios in acid mine water from Iron Mountain, California, *in* Alpers, C.N., and Blowes, D.W., eds., Environmental geochemistry of sulfide oxidation: American Chemical Society Symposium Series 550, p. 324–344.
- Alpers, C.N., Nordstrom, D.K., Verosub, K.L., and Helm, C.M., 1999b, Paleomagnetic reversal in Iron Mountain gossan provides limits on long-term premining metal flux rates: Geological Society of America Abstracts with Programs, v. 31, p. 33.
- Bigham, J.M., 1994, Mineralogy of ochre deposits formed by sulfide oxidation, *in* Jambor, J.L., and Blowes, D.W., eds., Environmental geochemistry of sulfide mine-wastes: Mineralogical Association of Canada Short Course Series, v. 22, p. 103–132.
- Bigham, J.M., and Nordstrom, D.K., 2000, Iron and aluminum hydroxysulfates from acid sulfate waters, *in* Alpers, C.N., Jambor, J.L., and Nordstrom, D.K., eds., Sulfate minerals—Crystallography, geochemistry, and environmental significance: Reviews in Mineralogy and Geochemistry, v. 40, p. 351–404.
- Biswas, A.K., and Davenport, W.G., 1976, Extractive metallurgy of copper: New York, Pergamon, 438 p.
- Blowes, D.W., and Ptacek, C.J., 1994, Acid-neutralization mechanisms in inactive mine tailings, *in* Jambor, J.L., and Blowes, D.W., eds., Environmental geochemistry of sulfide mine-wastes: Mineralogical Association of Canada Short Course Series, v. 22, p. 271–292.
- Blowes, D.W., Ptacek, C.J., and Jurjovec, J., 2003, Mill tailings—Hydrogeology and geochemistry, *in* Jambor, J.L., Blowes, D.W., and Ritchie A.I.M., eds., Environmental aspects of mine wastes: Mineralogical Association of Canada Short Course Series, v. 31, p. 95–116.

- Blowes, D.W., Reardon, E.J., Jambor, J.L., and Cherry, J.A., 1991, The formation and potential importance of cemented layers in inactive sulfide mine tailings: *Geochimica et Cosmochimica Acta*, v. 55, no. 4, p. 965–978.
- Craig, J.R., and Vaughan, D.J., 1990, Compositional and textural variations of the major iron and base-metal sulphide minerals, *in* Gray, P.M.J., Bowyer, G.J., Castle, J.F., Vaughan, D.J., and Warner, N.A., eds., *Sulphide deposits—Their origin and processing*: London, Institute of Mining and Metallurgy, p. 1–16.
- Cravotta, C.A., III, 1994, Secondary iron-sulfate minerals as sources of sulfate and acidity—Geochemical evolution of acidic ground water at a reclaimed surface coal mine in Pennsylvania, *in* Alpers, C.N., and Blowes, D.W., eds., *Environmental geochemistry of sulfide oxidation*: American Chemical Society Symposium Series 550, p. 345–364.
- Gehrke, G.E., Blum, J.D., Slotton, D.G., and Greenfield, B.K., 2011, Mercury isotopes link mercury in San Francisco Bay forage fish to surface sediments: *Environmental Science and Technology*, v. 45, p. 1264–1270.
- Goldfarb, R.J., Nelson, S.W., Taylor, C.D., d'Angelo, W.M., and Meier, A.L., 1995, Acid mine drainage associated with volcanogenic massive sulfide deposits, Prince William Sound, Alaska, *in* Moore, T.E., and Dumoulin, J.A., eds., *Geologic studies in Alaska by the U.S. Geological Survey, 1994*: U.S. Geological Survey Bulletin 2152, p. 3–16.
- Hammarstrom, J.M., Seal, R.R., II, Ouimette, A.P., and Foster, S.A., 2001, Sources of metals and acidity at the Elizabeth and Ely mines—Geochemistry and mineralogy of solid mine waste and the role of secondary minerals in metal recycling, *in* Hammarstrom, J.M., and Seal, R.R., II, eds., *Environmental geochemistry and mining history of massive sulfide deposits in the Vermont copper belt*: Society of Economic Geologists Guidebook Series, v. 35, pt. II, p. 213–248.
- Hathaway, E.M., Lovely, W.P., Acone, S.E., and Foster, S., 2001, The other side of mining—Environmental assessment and the process for developing a cleanup approach for the Elizabeth mine, *in* Hammarstrom, J.M., and Seal, R.R., II, eds., *Environmental geochemistry and mining history of massive sulfide deposits in the Vermont copper belt*: Society of Economic Geologists Guidebook Series, v. 35, pt. II, p. 277–293.
- Jambor, J.L., 1994, Mineralogy of sulfide-rich tailings and their oxidation products, *in* Jambor, J.L., and Blowes, D.W., eds., *Environmental geochemistry of sulfide mine-wastes*: Mineralogical Association of Canada Short Course Series, v. 22, p. 59–102.
- Jambor, J.L., 2003, Mine-waste mineralogy and mineralogical perspectives of acid-base accounting, *in* Jambor, J.L., Blowes, D.W., and Ritchie, A.I.M., eds., *Environmental aspects of mine wastes*: Mineralogical Association of Canada Short Course Series, v. 31, p. 117–146.
- Jambor, J.L., Dutrizac, J.E., Groat, L.A., and Raudsepp, M., 2002, Static tests of neutralization potentials of silicate and aluminosilicate minerals: *Environmental Geology*, v. 43, p. 1–17.
- Jambor, J.L., Nordstrom, D.K., and Alpers, C.N., 2000, Metal-sulfate salts from sulfide mineral oxidation, *in* Alpers, C.N., Jambor, J.L., and Nordstrom, D.K., eds., *Sulfate minerals—Crystallography, geochemistry, and environmental significance*: Reviews in Mineralogy and Geochemistry, v. 40, p. 303–350.
- Jurjovec, J., Ptacek, C.J., and Blowes, D.W., 2002, Acid neutralization mechanisms and metal release in mine tailings—A laboratory column experiment: *Geochimica et Cosmochimica Acta*, v. 66, no. 9, p. 1511–1523.
- Kelley, K.D., 1990, Interpretation of geochemical data from Admiralty Island, Alaska—Evidence for volcanogenic massive sulfide mineralization, *in* Goldfarb, R.J., Nash, J.T., and Stoesser, J.W., eds., *Geochemical studies in Alaska by the U.S. Geological Survey, 1989*: U.S. Geological Survey Bulletin 1950, p. A1–A9.
- Kelley, K.D., Seal, R.R., II, Schmidt, J.M., Hoover, D.B., and Klein, D.P., 1995, Sedimentary-exhalative Zn-Pb-Ag deposits, *in* du Bray, E.A., ed., *Preliminary compilation of descriptive geoenvironmental mineral deposit models*: U.S. Geological Survey Open-File Report 95–851, p. 225–233.
- Leybourne, M.I., Goodfellow, W.D., and Boyle, D.R., 1998, Hydrogeochemical, isotopic, and rare earth element evidence for contrasting water-rock interactions at two undisturbed Zn-Pb massive sulfide deposits, Bathurst mining camp, N.B., Canada: *Journal of Geochemical Exploration*, v. 64, p. 237–261.
- Moyer, T.C., Dube, T.E., and Johnsen, M.G., 2002, The impacts of hardrock mining in eastern Tennessee—Integrated studies of Davis Mill Creek and the Copper Basin mine site [abs.]: *Geological Society of America Abstracts with Programs*, v. 34, p. 143–144.
- Nordstrom, D.K., 2009, Acid rock drainage and climate change: *Journal of Geochemical Exploration*, v. 100, p. 97–104.
- Nordstrom, D.K., and Alpers, C.N., 1999a, Geochemistry of acid mine waters, *in* Plumlee, G.S., and Logsdon, M.J., eds., *The environmental geochemistry of mineral deposits—Part A. Processes, techniques, and health issues*: Reviews in Economic Geology, v. 6A, p. 161–182.

- Nordstrom, D.K., and Alpers, C.N., 1999b, Negative pH, efflorescent mineralogy, and consequences for environmental restoration at the Iron Mountain Superfund site, California, *in* Smith, J.V., ed., *Geology, mineralogy, and human welfare: Proceedings of the National Academy of Science of the United States of America*, v. 96, p. 3455–3462.
- Nordstrom, D.K., Alpers, C.N., Ptacek, C.J., and Blowes, D.W., 2000, Negative pH and extremely acidic mine waters from Iron Mountain, California: *Environmental Science and Technology*, v. 34, p. 254–258.
- Parsons, M.B., Bird, D.K., Einaudi, M.T., and Alpers, C.N., 2001, Geochemical and mineralogical controls of trace element release from the Penn Mine base-metal slag dump, California: *Applied Geochemistry*, v. 16, p. 1567–1593.
- Piatak, N.M., Seal, R.R., II, and Hammarstrom, J.M., 2004, Mineralogical and geochemical controls on the release of trace elements from slag produced by base- and precious-metal smelting at abandoned mine sites: *Applied Geochemistry*, v. 19, p. 1039–1064.
- Plumlee, G.S., 1999, The environmental geology of mineral deposits, *in* Plumlee, G.S., and Logsdon, M.J., eds., *The environmental geochemistry of mineral deposits—Part A. Processes, techniques, and health issues: Reviews in Economic Geology*, v. 6A, p. 71–116.
- Rowan, E.L., Bailey, E.A., and Goldfarb, R.J., 1990, Geochemical orientation study for identification of metallic mineral resources in the Sitka quadrangle, southeastern Alaska, *in* Goldfarb, R.J., Nash, J.T., and Stoesser, J.W., eds., *Geochemical studies in Alaska by the U.S. Geological Survey, 1989: U.S. Geological Survey Bulletin 1950*, p. B1–B12.
- Runnells, D.D., Dupon, D.P., Jones, R.L., and Cline, D.J., 1998, Determination of natural background concentrations of dissolved components in water at mining, milling, and smelting sites: *Mining Engineering*, v. 50, no. 2, p. 65–71.
- Runnells, D.D., Shepherd, T.A., and Angino, E.E., 1992, Metals in water—Determining natural background concentrations in mineralized areas: *Environmental Science & Technology*, v. 26, p. 2316–2323.
- Schwartz, M.O., 1997, Mercury in zinc deposits—Economic geology of a polluting element: *International Geology Review*, v. 39, no. 10, p. 905–923.
- Seal, R.R., II, 2004, Geoenvironmental models for massive sulphide deposits with an emphasis on sedimentary lead-zinc deposits, *in* Deb, M., and Goodfellow, W.D., eds., *Sediment-hosted lead-zinc sulphide deposits: New Delhi*, Narosa Publishing House, p. 191–221.
- Seal, R.R., II, Balistrieri, L., Piatak, N.M., Garrity, C.P., Hammarstrom, J.M., and Hathaway, E.M., 2006, Processes controlling geochemical variations in the South Pit lake, Elizabeth Mine Superfund site, Vermont, USA, *in* International Conference on Acid Rock Drainage, 7, St. Louis, Mo., 26–30 March 2006, *Proceedings: Lexington, Ky., American Society of Mining and Reclamation*, p. 1936–1951.
- Seal, R.R., II, Foley, N.K., Haffner, D.P., and Meier, A.L., 1998a, Environmental geochemistry of surface and ground waters around the Bald Mountain massive sulfide deposit, northern Maine—Natural backgrounds from a mineralized, but unmined area [abs.]: *Geological Society of America Abstracts with Programs*, v. 30, p. 128.
- Seal, R.R., II, and Hammarstrom, J.M., 2003, Geoenvironmental models of mineral deposits—Examples from massive sulfide and gold deposits, *in* Jambor, J.L., Blowes, D.W., and Ritchie A.I.M., eds., *Environmental aspects of mine wastes: Mineralogical Association of Canada Short Course Series*, v. 31, p. 11–50.
- Seal, R.R., II, Hammarstrom, J.M., and Meier, A.L., 2001a, Geochemical controls on drainage from massive sulfide mines in the eastern USA, *in* Cidu, R., ed., *International Symposium on Water-Rock Interaction, 10, Villasimius, 10–15 July 2001, Proceedings: The Netherlands, A.A. Balkema, Rotterdam*, v. 2, p. 1273–1276.
- Seal, R.R., II, Hammarstrom, J.M., Southworth, C.S., Meier, A.L., Haffner, D.P., Schultz, A.P., Plumlee, G.S., Flohr, M.J.K., Jackson, J.C., Smith, S.M., and Hageman, P.L., 1998b, Preliminary report on water quality associated with the abandoned Fontana and Hazel Creek mines, Great Smoky Mountains National Park, North Carolina and Tennessee: *U.S. Geological Survey Open-File Report 98-476*, 50 p.
- Seal, R.R., II, Kornfeld, J.M., Meier, A.L., and Hammarstrom, J.M., 2001b, Geochemical settings of mine drainage in the Vermont copper belt, *in* Hammarstrom, J.M., and Seal, R.R., II, eds., *Environmental geochemistry and mining history of massive sulfide deposits in the Vermont copper belt: Society of Economic Geologists Guidebook Series*, v. 35, pt. II, p. 255–276
- Seal, R.R., II, Piatak, N.M., Levitan, D.M., Hageman, P.L., and Hammarstrom, J.M., 2009, Comparison of geochemical characteristics of modern-style mine wastes from a variety of mineral deposit types for insights into environmental challenges associated with future mining, *in* *Securing the Future and Eighth International Conference on Acid Rock Drainage, Skellefteå, Sweden, 23–26 June 2009, Proceedings: International Network for Acid Prevention*, accessed December 7, 2010, at <http://www.proceedings-stfandicard-2009.com>.

- Shevenell, L., Conors, K.A., and Henry, C.D., 1999, Controls on pit lake water quality at sixteen open-pit mines in Nevada: *Applied Geochemistry*, v. 14, p. 669–687.
- Singer, D.A., 1986a, Descriptive model of Cyprus massive sulfide, *in* Cox, D.P., and Singer, D.A., eds., *Mineral deposit models*: U.S. Geological Survey Bulletin 1693, p. 131–135.
- Singer, D.A., 1986b, Descriptive model of Kuroko massive sulfide, *in* Cox, D.P., and Singer, D.A., eds., *Mineral deposit models*: U.S. Geological Survey Bulletin 1693, p. 189–197.
- Singer, D.A., and Mosier, D.L., 1986, Grade and tonnage model of Kuroko massive sulfide, *in* Cox, D.P., and Singer, D.A., eds., *Mineral deposit models*: U.S. Geological Survey Bulletin 1693, p. 190–197.
- Singer, P.C., and Stumm, W., 1970, Acidic mine drainage—The rate-determining step: *Science*, v. 167, p. 1121–1123.
- Smith, K.S., 1999, Metal sorption on mineral surfaces—An overview with examples relating to mineral deposits, *in* Plumlee, G.S., and Logsdon, M.J., eds., *The environmental geochemistry of mineral deposits—Part A. Processes, techniques, and health issues: Reviews in Economic Geology*, v. 6A, p. 161–182.
- Sobek, A.A., Schuller, W.A., Freeman, J.R., and Smith, R.M., 1978, Field and laboratory methods applicable to overburdens and minesoils: Cincinnati, Ohio, U.S. Environmental Protection Agency Protection Technology EPA-600/2-78-054, 203 p.
- Stoffregen, R.E., Alpers, C.N., and Jambor, J.L., 2000, Alunite-jarosite crystallography, thermodynamics, and geochronology, *in* Alpers, C.N., Jambor, J.L., and Nordstrom, D.K., eds., *Sulfate minerals—Crystallography, geochemistry, and environmental significance: Reviews in Mineralogy and Geochemistry*, v. 40, p.454–480.
- Taylor, C.D., Cieutat, B.A., and Miller, L.D., 1992, A followup geochemical survey of base metal anomalies in the Ward Creek/Windfall Harbor and Gambier Bay areas, Admiralty Island S.E. Alaska, *in* Bradley, D., and Dusel-Bacon, C., eds., 1991 *Geologic Studies in Alaska*: U.S. Geological Survey Bulletin 2041, p. 70–85.
- Taylor, C.D., Zierenberg, R.A., Goldfarb, R.J., Kilburn, J.E., Seal, R.R., II, and Kleinkopf, M.D., 1995, Volcanic-associated massive sulfide deposits, *in* du Bray, E.A., ed., *Preliminary compilation of descriptive geoenvironmental mineral deposit models*: U.S. Geological Survey Open-File Report 95–851, p. 137–144.
- U.S. Environmental Protection Agency, 1999, IEUBK model bioavailability variable: U.S. Environmental Protection Agency, Office of Solid Waste and Emergency Response, EPA 540-F-00-006, accessed July 9, 2009, at <http://www.epa.gov/superfund/lead/products/sspbbioc.pdf>.
- U.S. Environmental Protection Agency, 2006, National recommended water quality criteria: U.S. Environmental Protection Agency, accessed July 9, 2009, at <http://www.epa.gov/waterscience/criteria/nrwqc-2006.pdf>.
- U.S. Environmental Protection Agency, 2009, National primary drinking water regulations: U.S. Environmental Protection Agency EPA 816-F-09-004, accessed July 9, 2009, at <http://www.epa.gov/safewater/consumer/pdf/mcl.pdf>.
- White, W.W., III, Lapakko, K.A., and Cox, R.L., 1999, Static-test methods most commonly used to predict acid-mine drainage—Practical guidelines for use and interpretation, *in* Plumlee, G.S., and Logsdon, M.J., eds., *The environmental geochemistry of mineral deposits—Part A. Processes, techniques, and health issues: Reviews in Economic Geology*, v. 6A, p. 325–338.
- Williamson, M.A., Kirby, C.S., and Rimstidt, J.D., 2006, Iron dynamics in acid mine drainage, *in* Barnhisel, R.I., ed., *International Conference on Acid Rock Drainage, 7*, St. Louis, Mo., 26–30 March 2006, *Proceedings: American Society of Mining and Reclamation*, p. 2411–2423.
- World Health Organization, 2008, *Guidelines for drinking-water quality (3d ed.)*: Geneva, Switzerland, World Health Organization Press, accessed July 9, 2009, at http://www.who.int/water_sanitation_health/dwq/gdwq3rev/en/index.html.

21. Knowledge Gaps and Future Research Directions

21 of 21

Volcanogenic Massive Sulfide Occurrence Model

Scientific Investigations Report 2010–5070–C

U.S. Department of the Interior
U.S. Geological Survey

U.S. Department of the Interior
KEN SALAZAR, Secretary

U.S. Geological Survey
Marcia K. McNutt, Director

U.S. Geological Survey, Reston, Virginia: 2012

For more information on the USGS—the Federal source for science about the Earth, its natural and living resources, natural hazards, and the environment, visit <http://www.usgs.gov> or call 1-888-ASK-USGS.

For an overview of USGS information products, including maps, imagery, and publications, visit <http://www.usgs.gov/pubprod>

To order this and other USGS information products, visit <http://store.usgs.gov>

Any use of trade, product, or firm names is for descriptive purposes only and does not imply endorsement by the U.S. Government.

Although this report is in the public domain, permission must be secured from the individual copyright owners to reproduce any copyrighted materials contained within this report.

Suggested citation:

2012, Knowledge gaps and future research directions in volcanogenic massive sulfide occurrence model:
U.S. Geological Survey Scientific Investigations Report 2010-5070-C, chap. 21, 1 p.

Contents

| | |
|--|-----|
| Supergiant Deposit Formation Processes | 345 |
| Mapping at Regional and Quadrangle Scales | 345 |
| New Modeling of Fluid Flow and Mineralization | 345 |
| Causes of Temporal and Spatial Localization and Preservation of Deposits | 345 |
| New Methods of Prospection for Concealed Deposits..... | 345 |

Chapter 21. Knowledge Gaps and Future Research Directions

This review of the state of knowledge of VMS deposits has revealed a number of areas that merit additional research. Following is a simple list of topics that deserve further attention.

Supergiant Deposit Formation Processes

- Volumes of source rock or magma required for magmatic hydrothermal and lateral secretion models of metal sources;
- Geochemical discrimination of unique igneous ore-related magmas;
- Single fluid inclusion compositions in VMS ore minerals by new techniques to define metal concentrations during ore formation and to understand magmatic vapor rather than magmatic brine transport of metals; and
- Longevity of hydrothermal systems (need for improved geochronology).

Mapping at Regional and Quadrangle Scales

- Relationships of heat and magmatic volatile producing igneous bodies to VMS deposits;
- Localization of mineralization—vertical and lateral;
- Post-ore plutons and gold rich VMS deposits;
- Ultramafic associations (komatiites); and
- Physical volcanology and facies architecture of volcanic belts.

New Modeling of Fluid Flow and Mineralization

- New programs with new capabilities—HYDROTHERM, FISHERS, TOUGHREACT, GWB, GASWORKS;
- Duration and mass transport of hydrothermal systems;
- Reactive transport and solubility change due to dissolution/precipitation;
- Effect of magmatic volatile pulses into convective systems; and
- Fluid flow into hanging wall systems.

Causes of Temporal and Spatial Localization and Preservation of Deposits

- Anoxia,
- Eruption,
- Landslides,
- Subseafloor mineralization, and
- Silica or mudstone/argillite caprock.

New Methods of Prospection for Concealed Deposits

- Heavy minerals;
- Geochemistry, new isotope systems (Fe, Cu, Zn, ³³S), laser and ion microprobe analyses;
- Distal, cryptic alteration; and
- New geophysical techniques.

Publishing support provided by:
Denver Publishing Service Center

For more information concerning this publication, contact:
Center Director, USGS Central Mineral and Environmental Resources
Science Center

Box 25046, Mail Stop 973
Denver, CO 80225
(303) 236-1562

Or visit the Central Mineral and Environmental Resources Science
Center Web site at:
<http://minerals.cr.usgs.gov/>

